UC Irvine

UC Irvine Electronic Theses and Dissertations

Title

Syntheses of Lissoclimide Analogues and the Investigation of Novel Halogen-pi Interactions & Progress Towards the Synthesis of Brasilicardin A Using a Polyene Cyclization Approach

Permalink

https://escholarship.org/uc/item/7jw463qf

Author

Supantanapong, Nantamon

Publication Date

2024

Peer reviewed|Thesis/dissertation

eScholarship.org Powered by the California Digital Library
University of California

UNIVERSITY OF CALIFORNIA,
IRVINE

Syntheses of Lissoclimide Analogues and the Investigation of Novel Halogen-pi Interactions & Progress Towards the Synthesis of Brasilicardin A Using a Polyene Cyclization Approach

DISSERTATION

submitted in partial satisfaction of the requirements
for the degree of

DOCTOR OF PHILOSOPHY

in Chemistry

by

Nantamon Supantanapong

Dissertation Committee:
Professor Christopher D. Vanderwal, Chair
Professor Scott D. Rychnovsky
Professor Vy M. Dong

2024

Chapter 1 © 2021 American Chemical Society
All other materials © 2024 Nantamon Supantanapong

DEDICATION

To

Myself and everyone I love.

TABLE OF CONTENTS

LIST OF FIGURES ..... **VI**

LIST OF SCHEMES ..... **VII**

LIST OF TABLES ..... **X**

ACKNOWLEDGEMENTS ..... **XI**

VITA ..... **XIII**

ABSTRACT OF THE DISSERTATION ..... **XV**

CHAPTER 1 INTRODUCTION TO THE LISSOCLIMIDE NATURAL PRODUCTS **1**

1.1 Isolation of Lissoclimides and Their Anticancer Activities 1

1.2 Chlorolissoclimide: A Novel Protein Synthesis Inhibitor 2

1.3 Previous Synthetic Work Towards of Lissoclimide Analogues 3

1.4 Early Approach to Dichlorolissoclimide by Vanderwal Group 6

1.5 Semisynthesis of Chlorolissoclimide and Synthesis of Lissoclimide Analogues 7

1.6 The Discovery of Novel Halogen–π Interaction 11

1.7 Synthesis of Lissoclimide Natural Products, Haterumaimide J and K, by Vanderwal Group 14

1.8 Conclusion 17

1.9 References 18

CHAPTER 2 SYNTHESIS OF LISSOCLIMIDE ANALOGUES **21**

2.1 Introduction 21

2.2 Retrosynthetic Analysis of BrL, FL, and MeL 22

2.3 C–H Fluorination of Sclareolide and Attempts Towards Methylsclareolide 22

2.3.1 C–H Fluorination of Sclareolide 24

2.3.2 Attempts Towards Methylsclareolide 28

2.4 Semi-synthesis of Fluoro- and Methyllissoclimide 30

2.5 X-ray Cocrystal Structures of Lissoclimide Derivatives and 80S Ribosome 33

2.6 Biological Activities of Lissoclimide Analogues 34

2.7 Conclusions 35
2.8 References 36
2.9 Experimental Information 39
2.9.1 General Experimental Method 39
2.9.2 Experimental Procedures and Characterization Data 40
2.9.3 Supplemental References 63

CHAPTER 3 INTRODUCTION TO BRASILICARDIN NATURAL PRODUCTS 64
3.1 Isolation and Structure Determination of Brasilicardin A 64
3.2 Biological Activity of Brasilicardin A 65
3.3 Biosynthesis of Brasilicardin A 68
3.4 Previous Attempts Towards *Trans/Syn/Trans*-Perhydrophenanthrene Skeleton 69
3.4.1 Mercury(II)-Induced Olefins Cyclization by Nishizawa et al. 69
3.4.2 Diels–Alder Cycloaddition Approach 70
3.5 Synthesis of Brasilicardin A and Analogues 71
3.5.1 Synthesis of BraA Analogue by Jung et al. 71
3.5.2 Total Synthesis of Brasilicardin A by Anada et al. 73
3.5.3 Total Synthesis of Brasilicardin A by Yoshimura and Tanino et al. 75
3.5.4 Semi-Synthesis of Brasilicardin A Using Genetic Engineering Approach 76
3.5.5 Synthesis of Brasilicardin Analogue by Vanderwal group 77
3.6 Conclusions and Motivation 78
3.7 References 79

CHAPTER 4 PROGRESS TOWARDS THE SYNTHESIS OF BRASILICARDIN A USING A POLYENE CYCLIZATION APPROACH 82
4.1 Introduction 82
4.2 Retrosynthetic Analysis of Brasilicardin A 82
4.3 Synthesis of Coupling Fragments for Polyene Substrates 84
4.3.1 Synthesis of Vinyl Iodide Fragment 84
4.3.2 Initial Attempts for Synthesis of Diene Fragment using Diels–Alder Cycloaddition 85
4.3.3 Enantioselective Diels-Alder Reactions 87
4.3.4 Successful Synthesis of Diene Fragment 89
4.3.5 Synthesis of Polyene Substrates 91
4.4 Attempted Cationic Polyene Cyclizations 93

4.4.1 Background on the Acid-Catalyzed Epoxypolyene Cyclization 93
4.4.2 Attempted Cationic Polyene Cyclization 95
4.5 Attempted Radical Polyene Cyclizations 96
4.5.1 Precedence for Proposed Radical Polyene Cyclization 97
4.5.2 Attempted Radical Polyene Cyclizations 99
4.6 Radical Polyene Cyclization of Model Alkene 102
4.7 Revised Synthetic Route Towards Epoxypolyenes 105
4.8 Future Work 106
4.9 Conclusions 108
4.10 References 109
4.11 Experimental Information 112
4.11.1 General Experimental Method 112
4.11.2 Experimental Procedures and Characterization Data 113
4.11.3 Supplemental References 153

APPENDIX A: NMR DATA FOR CHAPTER 2 154

APPENDIX B: NMR DATA FOR CHAPTER 4 204

LIST OF FIGURES

Figure 1.1 Cytotoxicity of DCL and CL against several cancer cell lines.[3] 1

Figure 1.2 Cytotoxicity of selected lissoclimide natural products and analogues against P388 cell lines. 2

Figure 1.3 CHX and LTM located in tRNA E-site. Reproduced with permission from ref 8. Copyright 2014 Springer Nature. 3

Figure 1.4 (a) Cocrystal structure of CHX (pink), LTM (cyan) and CL (yellow) located in 60S E-site. (b) Binding interactions between CL and tRNA E-site pocket. Reproduced with permission from ref 17. Copyright 2017 Springer Nature. 12

Figure 1.5 Cytotoxicity of lissoclimide-type compounds against P388, A2058, and DU145 cell lines.[17] 13

Figure 1.6 (a) Cocrystal structure of C45 (**1.73**) and 25S rRNA. (PDB:5TBW) (b) Detailed view of the synthetic C45 (**1.73**) with A-ring in a twist-boat conformation and halogen-π interaction of C2 and C3 chlorides to guanine residues. Reproduced with permission from ref 19. Copyright 2019 Oxford University Press. 14

Figure 2.1 Translation-inhibitory activities of CL and known translation inhibitors.[2] 21

Figure 2.2 Effects of C2 site-selective C–H functionalization of sclareolide.[6] 23

Figure 2.3 (a) Lissoclimides analogues bound within S. cerevisiae 80S yeast ribosome. (b) Details of the interactions of lissoclimide compounds in the binding pocket. (C-F) HatQ, MeL, FL, and BrL are located in the binding pocket of 80S ribosome.[13] 33

Figure 2.4 (a) Cytotoxicity of synthetic lissoclimides. (b)Translation-inhibitory activity of synthetic lissoclimides.[13] 35

Figure 3.1 BraA (**3.1**) and three congeners, brasilicardin B-D (**3.2-3.4**). 64

Figure 3.2 Inhibition of mouse MLR of brasilicardin derivatives.[9] 67

Figure 3.3 BraA (**3.1**) derived from [1-^{13}C]glucose.[11] 68

LIST OF SCHEMES

Scheme 1.1 Synthesis of diequatorial dichlorinated A ring by Jung group.[9] 4

Scheme 1.2 Synthesis of hatQ (**1.3**) by González group.[10] 5

Scheme 1.3 Synthesis of hatQ (**1.3**) using a key Evans aldol reaction by Chai group.[12] 6

Scheme 1.4 Attempts towards the synthesis of DCL by Vanderwal group.[14] 7

Scheme 1.5 Semisynthesis of CL using C–H chlorination approach by Vanderwal group.[15] 9

Scheme 1.6 Synthesis of strategic alkenes **1.61** and **1.62** to access hatQ (**1.3**) and lissoclimide analogues.[17] 10

Scheme 1.7 Synthesis of C18-oxygenated lissoclimide analogues.[17] 11

Scheme 1.8 (a) Terminal-epoxide-initiated cyclization by Goldsmith and Phillips.[20] (b) Our plan to synthesize hatJ (**1.8**) using epoxide-initiated π-cyclization cascade.[21] 15

Scheme 1.9 a) Synthesis of hatJ (**1.8**) and hatK (**1.9**) using terminal-epoxide-initiated bicyclization cascade.[21] b) Chlorine-bearing stereogenic center controls diastereoselectivity of π-cyclization product. 16

Scheme 2.1 Retrosynthesis of BrL, FL, and MeL. 22

Scheme 2.2 Radical-mediated C–H functionalization using amide reagent **2.6a-b**.[3-4] 23

Scheme 2.3 (a) Regioselectivity observed for the C–H fluorination of sclareolide.[7] (b) Proposed mechanism of TBADT-catalyzed C–H fluorination.[7b] 24

Scheme 2.4 C–H fluorination of sclareolide using Britton conditions.[7b] 25

Scheme 2.5 (a) Aliphatic C–H functionalization of sclareolide using amide **2.12**.[8] (b) Select conditions for C–H fluorination using Alexanian chemistry. 26

Scheme 2.6 Propose mechanism of C–H fluorination of sclareolide (**2.5**) using *O*-alkenylhydroxamate **2.12**.[8] 27

Scheme 2.7 Attempted C-H fluorination of sclareolide-derived compounds. 28

Scheme 2.8 Attempts to access methylsclareolide via (a) metallaphotoredox cross-coupling.[10] (b) Wittig reaction and hydrogenation.[10] (c) Methylation of iodosclareolide. 29

Scheme 2.9 The synthesis of methylsclareolide **2.4c** using Alexanian's C–H functionalization. 29

Scheme 2.10 Synthesis of lissoclimide derivatives. 31

Scheme 2.11 (a) Synthesis of 7-deoxylissoclimide derivatives. (b) Attempted late-stage C–H fluorination of intermediates bearing hydroxy succinimide. 32

Scheme 3.1 (a) Methanolysis of BraA (**3.1**).[4] (b) *p*-bromobenzoyl derivative **3.9**. 65

Scheme 3.2 Proposed synthetic pathway of BraA (**3.1**) by Dairi *et al*.[12] 69

Scheme 3.3 $Hg(OTf)_2$/amine complex-induced polyene cyclization.[13] 70

Scheme 3.4 Danishefsky's Diels–Alder cycloaddition approach.[14] 71

Scheme 3.5 Jung's Diels-Alder cycloadditon.[16] 71

Scheme 3.6 Synthesis of brasilogue A (**3.28**) by Jung group.[17] 72

Scheme 3.7 Preparation of trichloroacetimidate glycosyl donor (**3.33**) by Jung group.[19] 73

Scheme 3.8 Total synthesis of BrA (**3.1**) by Anada *et al*.[20] 74

Scheme 3.9 Total synthesis of BrA (**3.1**) by Yoshimura and Tanino *et al*.[22] 76

Scheme 3.10 Semi-synthesis of BraA (**3.1**) by Stegmann *et al*.[24] 77

Scheme 3.11 Vanderwal's synthesis of brasilicardin analogue (**3.65**).[25] 78

Scheme 4.1 Retrosynthesis of brasilicardin A (**4.1**). 83

Scheme 4.2 Synthesis of vinyl iodide **4.18**. 84

Scheme 4.3 Proposed synthetic route towards diene **4.22**. 86

Scheme 4.4 (a) Asymmetric Diels–Alder cycloaddition using oxazaborolidine catalyst reported by Corey and co-workers.[14] (b) Proposed enantioselective Diels–Alder to access the cycloadduct **4.21-H**. 88

Scheme 4.5 Preparation of ketone **4.32**. 90

Scheme 4.6 Completion of the synthesis of triene **4.35**. 91

Scheme 4.7 B-alkyl Suzuki–Miyaura cross-coupling of vinyl iodide **4.18** and triene **4.35**. 92

Scheme 4.8 Synthesis of epoxypolyenes **4.38** and **4.43**. 93

Scheme 4.9 (a) Cationic Cyclization of squalene 2,3-oxide by van Tamelen.[23] (b) Epoxy Trienylsilane cyclization by Coates.[24] (c) Synthesis of pentacyclic triterpene using $MeAlCl_2$ by Corey.[25] (d) Cyclization of phenyl ether **4.53** using $EtAlCl_2$.[26] 94

Scheme 4.10 $EtAlCl_2$-catalyzed polyene cyclization of epoxypolyene **4.38** and possible mechanisms. 96

Scheme 4.11 (a) Titanocene-catalyzed radical cyclization of squalene 2,3-oxide.[30] (b) Ti(III)-mediated radical cascade cyclization of epoxypolyene **4.62**.[31] (c) Preparation of tricyclic meroterpene **4.68**.[32] 98

Scheme 4.12 Example of Ti(III)-catalyzed radical cyclization of ketoepoxypolyprene **4.69**.[29] .. 99

Scheme 4.13 (a) Desired radical polyene cyclization of **4.43**. (b) Proposed catalytic cycle of the desired polyene cyclization. 100

Scheme 4.14 (a) Radical polyene cyclization of epoxypolyene **4.43** (b) Possible reaction pathway leading to unusual 5-*exo* product **4.72**. 102

Scheme 4.15 (a) Synthesis of model substrate **4.75a-b** using B-alkyl Suzuki cross coupling. (b) Preparation of protected alcohols **4.75c-d**. 103

Scheme 4.16 (a) Radical cyclization of oxabicycle **4.79**. (b) Attempted Ti(III)-mediated radical polyene cyclization to access tricyclic core of brasilicardin A. 105

Scheme 4.17 Revised synthesis of epoxypolyene **4.88**. 106

Scheme 4.18 Future work for cationic and radical polyene cyclization. 107

LIST OF TABLES

Table 3.1 Mixed lymphocyte reaction (MLR) inhibitory and *in vitro* cytotoxic activity against L1210 cells of brasilicardin A-D in comparison with cyclosporin A.[8] 66

Table 4.1 Initial attempts for Diels–Alder cycloaddition towards diene **4.2**. 86

Table 4.2 Successful Diels–Alder reaction using silyl enol ether **4.23**. 87

Table 4.3 Optimization of enantioselective Diels–Alder reaction between diene **4.23** and 2-methylacrolein (**4.20-H**). 89

Table 4.4 Conditions attempted for enone **4.33** formation. 90

Table 4.5 Radical cyclization on model systems **4.75a-e**. 104

ACKNOWLEDGEMENTS

I would like to express my sincere gratitude to my committee chair and advisor, Professor Chris Vanderwal, for your invaluable mentorship and unwavering support throughout my graduate studies at UCI. Your guidance has been essential to my growth as a researcher and as an individual. I am also particularly grateful for the opportunities you provided to improve both writing and presentation skills. Thank you for having me to present my work at conferences and Riesmanderwal joint group meetings where I had the pleasure of meeting inspiring colleagues. Your mentorship has taught me that a supportive and collaborative environment fosters exceptional scientific achievement.

I would like to thank my thesis committee members, Professor Scott Rychnovsky and Professor Vy Dong, for their guidance and support throughout my doctoral studies. I am deeply grateful for your continued guidance since my candidacy exam and 4th-year proposal. I am truly fortunate to have had the opportunity to learn from both of you and appreciate your time and dedication.

I would like to extend my heartfelt thanks to Assoc. Prof. Dr. Jumreang Tummatorn, my advisor during my Master's program at CGI, Thailand. You helped me develop essential research skills. My time in your lab was not only productive but also incredibly enjoyable. I am deeply appreciative of your belief in my abilities and your dedication to helping me reach my goals. Your generosity is deeply appreciated.

I would like to thank to Professor Daniel Seidel at the University of Florida for granting me the opportunity to join your lab as a visiting student. Your guidance and support have been invaluable, and I have learned a great deal from you and your team, especially in conducting methodology experiments. My first experience in the U.S. was immensely enjoyable, filled with wonderful memories, thanks to you and your lab.

To Dr. Zhengbo Zhu from the Seidel lab, I want to express my heartfelt gratitude. You were my first and best mentor. Thank you for allowing me to join your project and for teaching me so much about chemistry. Your encouragement to be confident, through sharing your experiences, has been incredibly helpful.

It has been a great pleasure in my life to work with talented postdocs in the Vanderwal lab, Dr. Ramakrishna Kankanala, Dr. Jonathan Chung, Dr. Fabi Hormann, Dr. Nick Magann and Dr. Ibo Celik. I deeply appreciate your help with my chemistry endeavors. Thank you for your valuable comments and answers to my numerous questions. I thoroughly enjoyed our discussions and the fun we had talking about chemistry. To me, all of you are truly inspiring.

During the 5 years I have been with the Vanderwal group, I would like to thank to my good and closest friend, Dr. Natalie Dwulet. Not only did you help me with my chemistry, but you also offered invaluable advice on both my work and various aspects of my life. Having you during my graduate school years has been a true gift. I also want to thank Dr. Scott Niman, who provided significant assistance with the Brasilicardin A project and consistently inquired about my chemistry progress. I cherish our daily lunches together and deeply value our friendship. My gratitude extends to Dr. Bonnie Pak, who worked with me on the lissoclimides synthesis. You mentored me from the very beginning of this project, and your optimism has profoundly changed my perspective on problem-solving. It was a joy working and conversing with you in the lab.

I truly appreciate the friendships I have formed with former and current members of the Vanderwal lab (Joe, Griffin, Lucas, Bonnie, Hanh, Phil, Matt, Brandon, Mira, John, Theo, Seamus, Ryan, Josh, Amber, Sebastian, Benjamin). You are wonderful people, and working in the lab has been a fun and enriching experience thanks to all of you. Thank you for sharing your chemistry knowledge and engaging in daily conversations with me.

I am deeply grateful to my friends outside the lab. First and foremost, Phan Phu and Kylie Uyeda, you are my best friends here. Thank you for your friendship and for taking me out to enjoy good food. Your support and our shared meals have always cheered me up. Graduate school wouldn't have been as joyful without the two of you. I also want to thank the Thai students at UCI. Your friendship made my life in a foreign country so much fun. Cooking, traveling, and playing board games with you were the happiest times during my graduate school years. Especially, thanks to Punyanuch Sophanpanichkul for assistance in editing my thesis. A special thanks to Gift, Kate, Kwang, and friends in Thailand, for over a decade of friendship. You have always been by my side, no matter what. Thank you for keeping in touch and for listening to all my random topics.

Lastly, I would like to thank my parents for your unconditional love. You are my team, my backup, and my biggest supporters. Thank you for believing in me and allowing me to pursue my dreams. I love you. I also want to thank all my family members for wonderful support: my grandpa, grandma, aunts, uncles, and cousins. Thank you for your love and for taking care of each other. Seeing all of you healthy and happy brings me joy. I would like to thank Dr. Darius Vrubliauskas. Thank you for always being by my side and helping me through tough times. I could not have overcome the challenges of graduate school without your help and love. Your love for chemistry, your motivation, and your hard work inspire me and keep me focused on this path.

Funding: Thai Government Scholarship and BIOTEC, Thailand.

Chapter 1 of this dissertation is reprinted with permission from Pak, B. S.; Supantanapong, N.; Vanderwal, C. D. “The Recurring Roles of Chlorine in Synthetic and Biological Studies of the Lissoclimides.” *Acc. Chem. Res.* **202**1, *54*, 1131–1142. Copyright 2021 American Chemical Society. The coauthors listed in this publication are Bonnie S. Pak and Christopher D. Vanderwal. Christopher D. Vanderwal directed and supervised research which forms the basis for the dissertation. Financial support was provided by the University of California, Irvine and NIH GM-129164.

Cite this: https://pubs.acs.org/doi/10.1021/acs.accounts.0c00866

VITA

Nantamon Supantanapong

EDUCATION:

Ph.D. Chemistry (August 2024)
University of California, Irvine
Research Advisor: Professor Christopher Vanderwal

M.Sc. Chemical Biology (April 2019)
Chulabhorn Graduate Institute, Thailand
Research Advisor: Assoc. Prof. Dr. Jumreang Tummatorn

B.Sc. Chemistry (May 2016)
Prince of Songkla University, Thailand

RESEARCH EXPERIENCE:

University of California, Irvine (2019 – 2024)
Graduate student researcher

Progress Towards the Synthesis of Brasilicardin A

- Developed coupling fragments synthesis.
- Synthesized epoxypolyene substrate containing diene and enone terminating groups with various C2 protecting groups to access the desired polycyclic products.
- Synthesized the carbon framework of brasilicardin A.
- Investigation the C2 protecting groups effecting π cyclization of model substrates.

Syntheses of Lissoclimide Analogues and the Investigation of Novel Halogen-π Interactions

- Synthesized the fluorolissoclimide and methyllissoclimide using key C–H functionalization of sclareolide.

Chulabhorn Graduate Institute (2017 – 2019)

- Assisted in synthesizing isocryptolepine-triazole adducts using azide rearrangement chemistry and click reaction.
- Synthesized benzannulated indole and benzofuran derivatives from *ortho*-alkynylarylketones and primary amine derivatives using AgOTf-catalyzed ketonization, followed by $In(OTf)_3$-catalyzed double cyclization.
- Assisted in synthesizing dihydronaphthofurans using silver-catalyzed cyclization of *ortho*-carbonylarylacetylenols

University of Florida (Sept 2018 – Feb 2019)
Visiting student

- Assisted in synthesizing polycyclic chromanes using chiral thiourea-carboxylic acid-catalyzed enantioselective [4 + 2] cycloadditions.

PUBLICATIONS:

- Pak, B. S.; Supantanapong, N.; Vanderwal, C. D. *Acc. Chem. Res.* **2021**, *54*, 1131–1142.
- Terrosu, S.; Nurullina, L.; Pak, B. S.; Supantanapong, N.; Nguyen, S.; Wu, C.; Lin, M.; Nguyen, B.; Blanchard, S. C.; Horne, D. A.; Sachs, M.; Yusupov, M.; Furche, F.; Vanderwal, C. D. *Manuscript in preparation.*
- Zhu, Z.; Odagi, M.; Supantanapong, N.; Xu, W.; Saame, J.; Kirm, H.-U.; Abboud, K. A.; Leito, I.; Seidel, D. *J. Am. Chem. Soc.* **2020**, *142*, 15252–15258.
- N. Supantanapong , P. Chuangsoongnern , J. Tummatorn , C. Thongsornkleeb and S. Ruchirawat , *Org. Chem. Front*., **2019**, *6*, 1340–1355.

TEACHING EXPERIENCE:

Organic Chemistry Teaching Assistant
University of California, Irvine (Spring 2021, Spring 2022)
Courses Taught: Chem51A, Chem51C

Laboratory Teaching Assistant
University of California, Irvine (Spring 2023, Spring 2024)
Courses Taught: Chem51LC

PRESENTATION:

- **"Syntheses of Lissoclimide Analogues and the Investigation of Novel Halogen–π Interactions"**
  August 2022 – Poster presentation at International Society of Heterocyclic Chemistry Conference (Santa Barbara, CA)

COMMUNITY INVOLVEMENT:

- LEAPS (Laboratory Experiments and Activities in the Physical Sciences) (2024)
  Department of Chemistry, University of California, Irvine

ABSTRACT OF THE DISSERTATION

Syntheses of Lissoclimide Analogues and the Investigation of Novel Halogen-pi Interactions & Progress Towards the Synthesis of Brasilicardin A Using a Polyene Cyclization Approach

Nantamon Supantanapong

Doctor of Philosophy in Chemistry

University of California, Irvine, 2024

Professor Christopher D. Vanderwal, Chair

Chapter 1 provides an overview of lissoclimide natural products and previous synthetic efforts. The isolation of lissoclimides and their anticancer properties against various cell lines are detailed. Subsequently, the mechanism of protein translation inhibition by chlorolissoclimide is discussed. Our group's previous synthetic endeavors, including the semi-synthesis of chlorolissoclimide, analogue-oriented synthesis of lissoclimide derivatives, and Lewis acid-catalyzed bicyclization to access a related natural product, are presented. In collaboration with the Yusupov, Blanchard, Furche, and Horne groups, we explored novel halogen-π dispersive interactions of chlorolissoclimide within the tRNA E-site pocket. Additionally, the anticancer activities of synthetic lissoclimides were evaluated.

Chapter 2 describes the conversion of sclareolide into fluorolissoclimide and methyllissoclimide. Selective C–H functionalization of sclareolide was achieved using an Alexanian hydroxyamide reagent to introduce fluorine and methyl groups with the desired stereochemistry at the C2 position. The mechanism underlying C–H fluorination and the structural basis for selective radical C–H modification of sclareolide were elucidated. Methylsclareolide was

subsequently synthesized through methylation of the corresponding iodinated derivative. The syntheses of fluorolissoclimide and methyllissoclimide were completed in concise 9-10 step sequences. Finally, the halogen-π interactions of these compounds, along with bromolissoclimide, chlorolissoclimide, and haterumaimide Q, were investigated within the 80S ribosomal pocket.

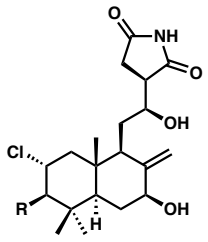
Chapter 3 commences with a description of. the isolation and structural characterization of brasilicardin A, along with its biological activities and proposed biosynthetic pathway. The complex *trans/syn/trans*-perhydrophenanthrene core of brasilicardin A has posed significant synthetic challenges, with previous total syntheses relying on Diels–Alder cyclization and intramolecular Michael addition strategies. Our group developed a novel cobalt-catalyzed MHAT-induced polycyclization approach to efficiently construct the tricyclic core of a brasilicardin analogue. Structure-activity relationship studies using SARS models highlighted the critical roles of the disaccharide, amino acid side chain, and diterpenoid core in the biological activity of brasilicardin A.

Chapter 4 details the synthesis of brasilicardin A via a polyene cyclization strategy inspired by the biosynthetic pathway. A retrosynthetic analysis identified directed hydrogenation as a key step to construct the desired perhydrophenanthrene core. Epoxypolyene intermediates were prepared via a crucial B-alkyl Suzuki–Miyaura cross-coupling reaction. Both cationic and radical cyclization pathways were explored. Cyclization of a diene-containing epoxypolyene afforded the tricyclic core of brasilicardin A. Investigation of C2 hydroxyl protection revealed that a free alcohol facilitated the desired 6-endo-trig cyclization of an enone-terminated polyene. Future work will focus on optimizing polyene substrate synthesis.

CHAPTER 1 INTRODUCTION TO THE LISSOCLIMIDE NATURAL PRODUCTS

1.1 Isolation of Lissoclimides and Their Anticancer Activities

The lissoclimide natural products are marine alkaloids produced by shell-less mollusks. These compounds possess a labdane core structure bearing unusual succinimide moiety. In the early 1990s, Malochet-Grivois and co-workers isolated dichlorolissoclimide (DCL) (**1.1**) and chlorolissoclimide (CL) (**1.2**) from *Lissoclinum voeltzkowi* Michaelson, and elucidated their structures[1–2] (**Figure 1.1**). The succinimide-bearing labdane core was found to possess A-ring chloride substituents. CL and DCL were reported to inhibit four cancer cell lines: P388 murine leukemia cell lines, non-small cell lung cancer (NSCLC), epidermoid carcinoma (KB) cells, and doxorubicin-resistant P388 (P388/R).[3]



	IC_{50} (ng/mL)			
	P388	**NSCLC**	**KB**	**P388/R**
DCL (**1.1**): R = Cl	1	9	14	300
CL (**1.2**): R = H	1.7	10	52	200

Figure 1.1 Cytotoxicity of DCL and CL against several cancer cell lines.[3]

Later, the Ueda and Schmitz groups isolated haterumaimides A–Q and 3ß-hydroxy chlorolissoclimide from the ascidian *Lissoclinum sp*. collected from Hateruma Island, from mollusks *Pleurobranchus albiguttatus* and *P. forskali*.[4] The structure-activity relationships (SARs) between DCL, CL and haterumaimides against P388 cells, as reported by Ueda and co-workers, indicated that allylic hydroxyl group at C7, imide N–H, C12 hydroxyl group and chlorine atom at C2 contributed to the anti-tumor activity[5] (**Figure 1.2**). Moreover, oxygenation at C18 could potentiate anti-P388 cell activity of hatJ against P388 cells exhibiting higher cytotoxicity than DCL and CL.

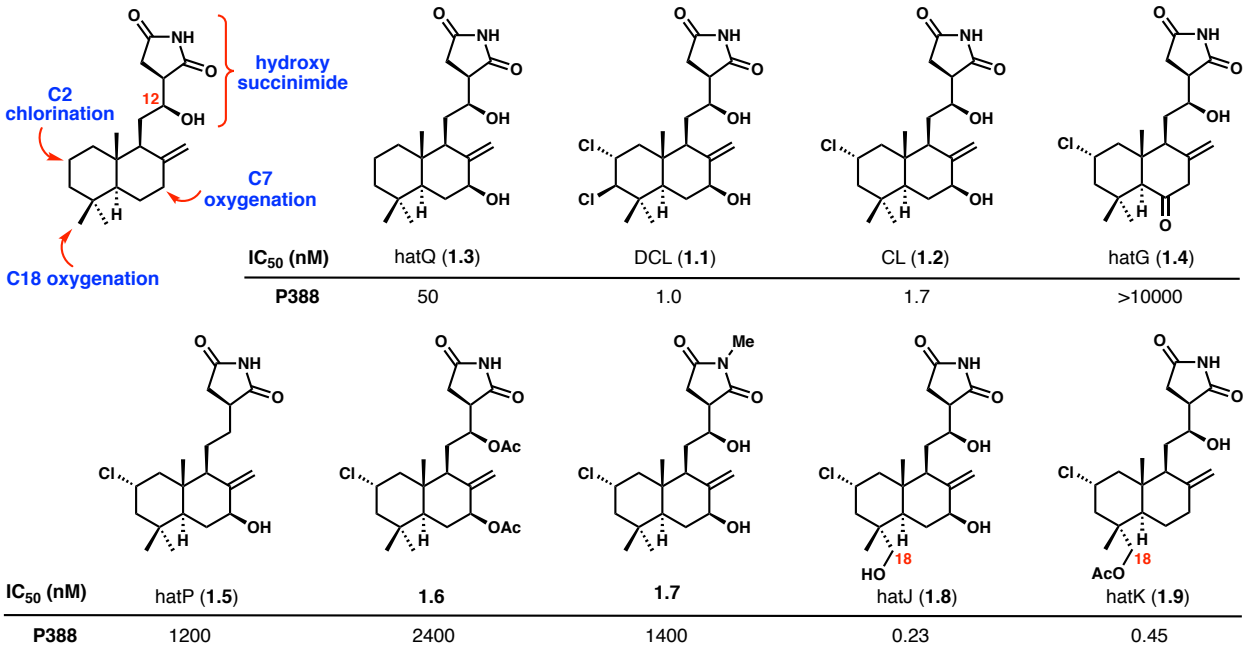


Figure 1.2 Cytotoxicity of selected lissoclimide natural products and analogues against P388 cell lines.

1.2 Chlorolissoclimide: A Novel Protein Synthesis Inhibitor

Due to the higher rate of proliferation of cancer cells compared to normal cells, the inhibition of protein synthesis in cancer cells is an important mechanism for the anti-cancer activity of natural products and synthetic molecules.[6] In the laboratory, the most widely used translation inhibitor in eukaryotic cells is the glutarimide natural product, cycloheximide (CHX).[7] Pelletier's group discovered CL and DCL as new inhibitors of eukaryotic translation and found it had same mechanism of action as CHX.[6] In vitro translation assays of Krebs-2 cell extracts demonstrated that CL could inhibit protein synthesis more potently than DCL with an IC_{50} of CL = 0.7 µM and an IC_{50} of DCL = 1.25 µM. The structural similarity of CL and CHX was noted by Pelletier, who related the succinimide moiety of lissoclimides and the glutarimide of CHX. Also, eEF1A- and eEF2-dependent assays indicated that CL could inhibit eEF2-mediated translocation of ribosome and cause the stabilization of polysomes on the mRNA templates in the same manner as CHX.

Also, CL was proven to not disturb the delivery of aminoacyl-tRNA at A-site and peptidyl transferase enzyme at P-site of the ribosome. Later, Yusupov *et al.* investigated the cocrystal structure of CHX and lactimidomycin (LTM), another glutarimide translation inhibitor, with eukaryotic 80S ribosomes to support that CHX and LTM were located at E-site tRNA of large subunit ribosomes (**Figure 1.3**).[8] Lastly, Yusupov group also confirmed that CHX binds at the 3'-CCA end of the E-site tRNA.

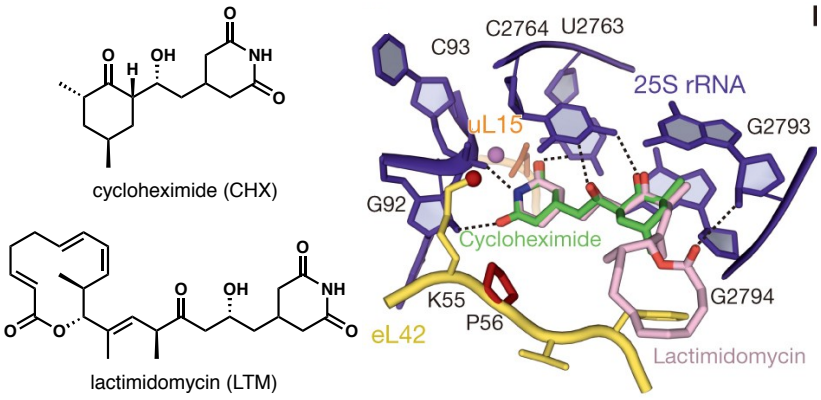
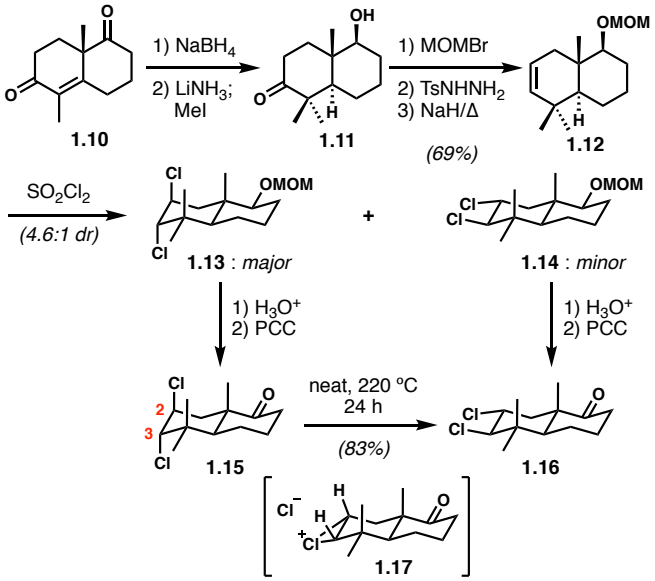


Figure 1.3 CHX and LTM located in tRNA E-site. Reproduced with permission from ref 8. Copyright 2014 Springer Nature.

1.3 Previous Synthetic Work Towards of Lissoclimide Analogues

Jung and co-workers attempted to synthesize the challenging vicinal *trans*-diequatorial dichloride found in DCL[9] (**Scheme 1.1**). Alkene **1.12** was prepared from dimethyloctalone **1.10** via reductive methylation, followed by Shapiro reaction of ketone **1.11**. Chlorination of **1.12** using thionyl chloride gave the undesired kinetically-favored dichlorinated **1.13** as a major product in a ratio of diaxial chlorides **1.13** to diequatorial chlorides **1.14**, 4.6:1. It was shown that compound **1.15** could be converted to the desired diequatorial isomer **1.16** under thermal conditions. The mechanism of rearrangement was proposed to occur through a chloronium ion intermediate **1.17**, where the 2β chloride atom in **1.15** attacked the 3α carbon atom from the bottom. However, no further efforts toward DCL were reported by Jung.

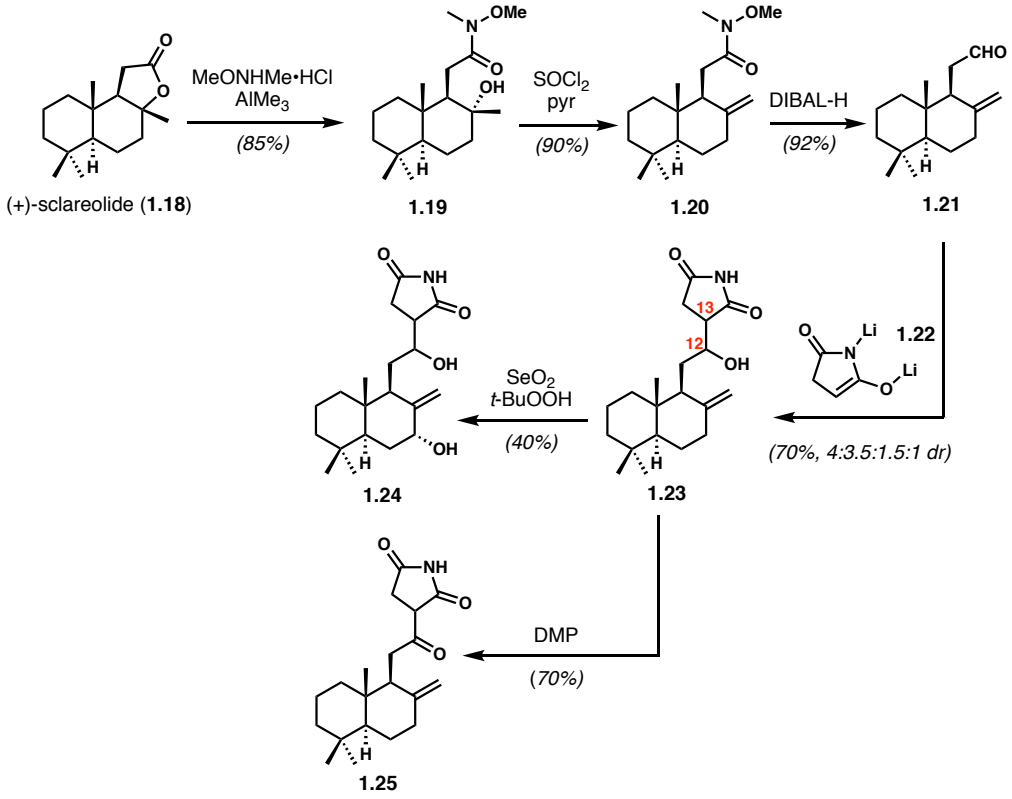
Scheme 1.1 Synthesis of diequatorial dichlorinated A ring by Jung group.[9]



The lissoclimide derivatives, ketone **1.23** and 7-*epi*-haterumaimide **1.24** were successfully synthesized by González and co-workers[10] (**Scheme 1.2**). In this synthesis, commercially available (+)-sclareolide (**1.18**) containing the decalin ring system with the desired stereochemistry of the core was used as starting material. First, the lactone in sclareolide was converted to the corresponding Weinreb amide **1.19**. The elimination of tertiary alcohol **1.19** yielded exocyclic alkene **1.20**, which underwent DIBAL-H reduction to provide aldehyde **1.21**. This preparation of aldehyde **1.21** was reported in Boukouvalas's (+)-zerumin B synthesis.[11] The key aldol reaction between **1.21** and **1.22** gave product **1.23** in 50% as a mixture of four diastereomers at C12 and C13 in ratios of 4.5:3.5:1.5:1. Unfortunately, the authors claimed that the diastereomeric mixture could not be resolved via chromatographic techniques, so the stereochemistry was not assigned. Next, the mixture of four diastereomers **1.23** was subjected to selenium dioxide oxidation and provided a 1:1 mixture of diastereomers of 7-*epi*-heterumaimide **1.24** at C12 and C13. The oxidation at C12 provided ketone derivative **1.25** as a 1:1 mixture of diastereomers at C13. Lastly, the *in vitro* antitumor activity of synthetic lissoclimide analogues **1.23**, **1.24**, and **1.25** was

investigated. The mixture of compounds **1.23** showed the highest cytotoxicity against Jurkat leukemia cells with CC_{50} of 4.3 ± 1 μg/mL and HeLa cancer cell lines with CC_{50} of 4.5 ± 1.2 μg/mL, along with the highest selectivity index (SI) with 6.7 for Jurkat cells and 6.5 for HeLa cells.

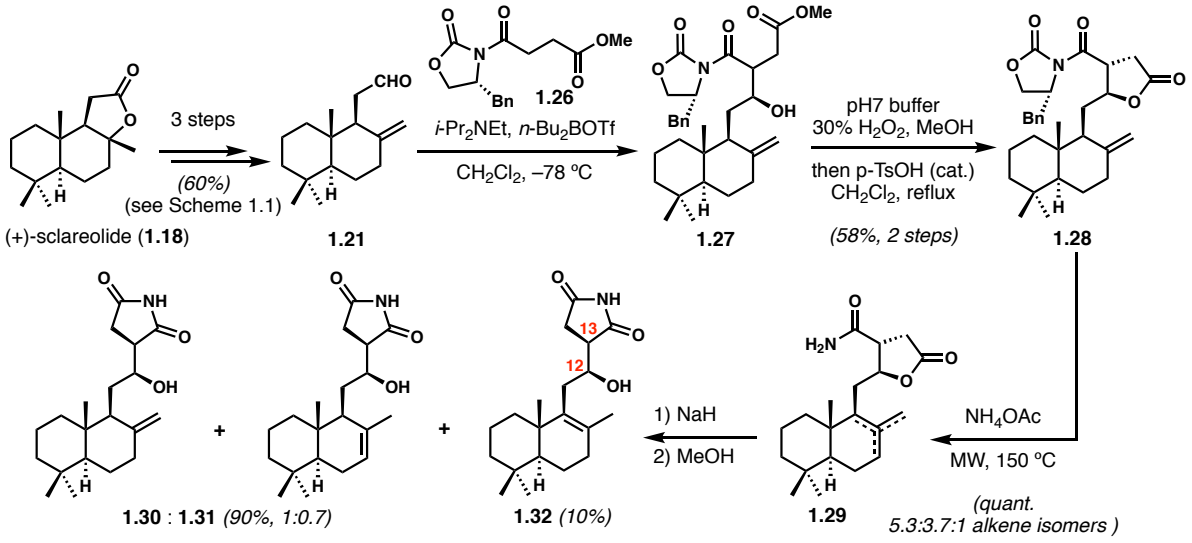
Scheme 1.2 Synthesis of hatQ (**1.3**) by González group.[10]



Chai's group utilized an asymmetric boron-mediated aldol using Evans' auxiliary to address the issue of stereoselectivity at C12 and C13[12] (**Scheme 1.3**). Aldehyde **1.21** was prepared from sclareolide in three steps as described by González.[10] The *syn*-selective aldol addition of **1.21** with chiral oxazolidinone **1.26** set the C12 and C13 stereocenters while in situ lactonization of **1.27** using catalytic amounts of *p*-toluenesulfonic acid furnished the desired lactone **1.28** in 58% yield. The succinimide formation of **1.28** was found to require forcing conditions. Treatment of compound **1.28** with excess ammonium acetate under microwave irradiation at 150 °C resulted in removal of the auxiliary and isomerization of the exocyclic alkene. Next, the resulting mixture

1.29 was subjected to imidation under basic conditions forming 90% of regioisomers **1.30** and **1.31** and 10% of **1.32**. Lastly, Chai and co-workers determined the stereochemistry of C12 and C13 of esters derived from compound **1.32** using NOE correlation experiments. Although the Evans aldol reaction secured the desired C12/C13 configurations, conversion to the succinimide was plagued by alkene isomerization.

Scheme 1.3 Synthesis of hatQ (**1.3**) using a key Evans aldol reaction by Chai group.[12]

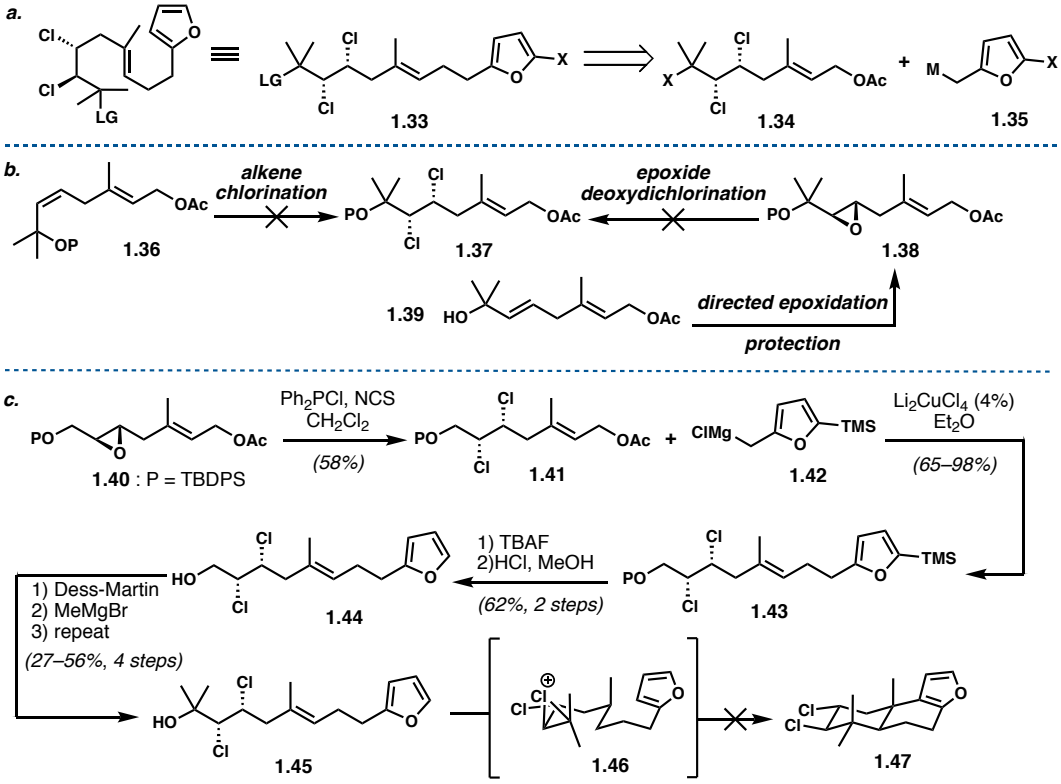


1.4 Early Approach to Dichlorolissoclimide by Vanderwal Group

The Vanderwal group attempted to synthesize the DCL decalin framework via a chloronium-induced cyclization (**Scheme 1.4a**).[11-14] Cyclization precursor **1.33** could be conveniently accessed via copper-catalyzed allylic/benzylic coupling of fragments **1.34** and **1.35**.[13] The furan group was chosen as the preferred terminating group for the pi-cyclization because it could serve as a precursor for functional groups required to install the succinimide moiety. Dichlorination of alkene **1.36** and deoxydichlorination of epoxide **1.38** proved challenging due to the steric hindrance of the adjacent fully substituted carbon atom (**Scheme 1.4b**). Therefore, the synthesis of bicyclic **1.47** began with deoxydichlorination of the epoxide **1.40** to provide allylic

acetate **1.41**, which then underwent a copper-catalyzed coupling reaction with furanylmethyl Grignard reagent **1.42** to yield alkene **1.43**. After deprotection of silyl groups and iterative DMP oxidation and methyl Grignard addition, the cyclization precursor **1.45** was obtained. Despite extensive efforts using various reaction conditions to effect ionization of the tertiary alcohol, the cationic π-cyclization of **1.45** was not successful (**Scheme 1.4c**).

Scheme 1.4 Attempts towards the synthesis of DCL by Vanderwal group.[14]

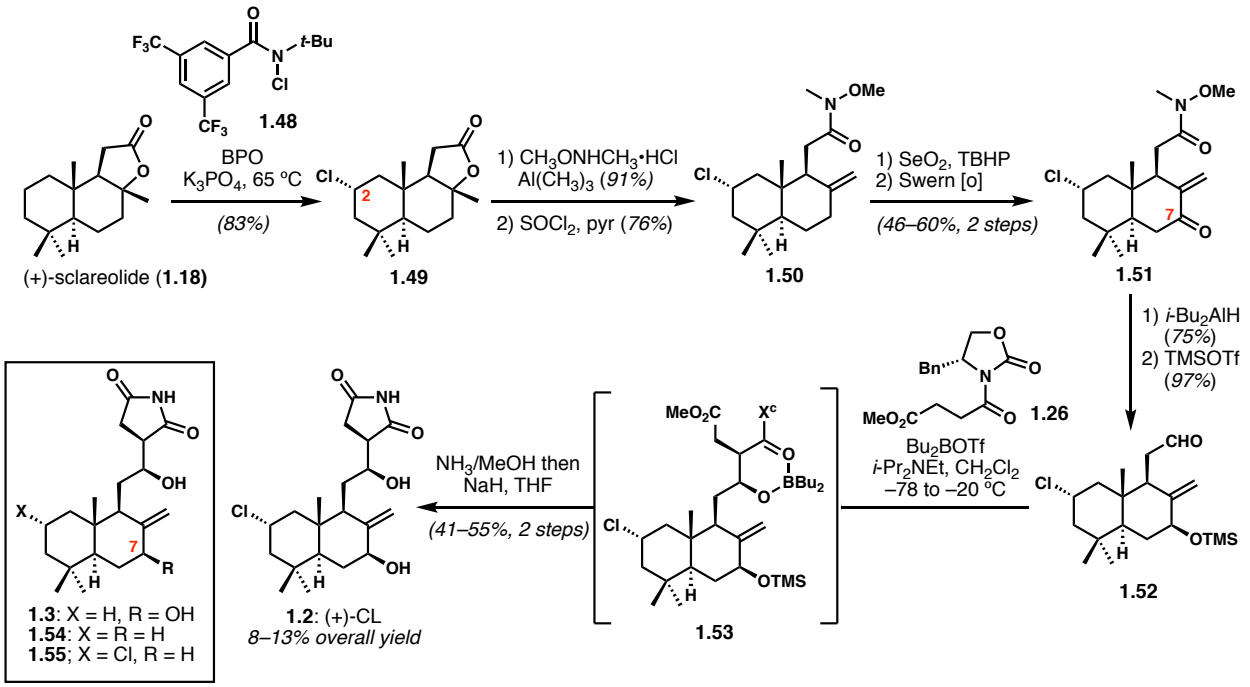


1.5 Semisynthesis of Chlorolissoclimide and Synthesis of Lissoclimide Analogues

Among the lissoclimide natural products, CL possesses potent cytotoxicity against various cancer cell lines (**Figure 1.1**). Therefore, the Vanderwal group aimed to synthesize CL using a new approach involving selective C–H functionalization of sclareolide (**1.18**), C–H oxygenation at C7, and succinimide installation as key steps[15] (**Scheme 1.5**). For the key C2 chlorination, they first utilized manganese porphyrin-catalyzed radical C–H chlorination, as reported by Groves and

co-workers.[16] (not shown) However, the desired C2 equatorial chloride **1.49** was obtained as a mixture of regioisomers along with C3 chlorosclareolide in moderate yield. Therefore, they then applied radical C–H chlorination of sclareolide using *N*-chloroamide **1.48**, a reagent that was under development by the Alexanian group; together, our groups optimized this reaction to guide effective C2 chlorination. *N*-Chloroamide **1.48** underwent radical initiation in the presence of Bz_2O_2 (BPO) as a radical initiator, which presumably afforded a key amidyl radical to abstract C2 hydrogen atom on sclareolide (**1.18**). The desired C2 equatorial chlorosclareolide **1.49** was furnished in 83% yield with good regio- and stereoselectivity. Aldehyde **1.52** was synthesized as reported in part in works of Boukouvalas[11], González[10] and Chai[12]. C2-Chorosclareolide **1.49** was converted to Weinreb amide **1.50**, followed by dehydration of the tertiary alcohol. Next, alkene **1.50** was converted to ketone **1.51** via selenium dioxide-mediated oxidation followed by Swern oxidation. They then used double reduction of compound **1.51** to afford the aldehyde **1.52** with the desired stereochemistry at the C7 hydroxyl group. The conditions for Evans asymmetric aldol addition were optimized to solve the issues of lactonization after aldol addition and alkene isomerization.[12] The corresponding aldehyde **1.52** was subjected to asymmetric aldol addition with the boron enolate of imide **1.26**. This afforded aldolate **1.53** which was prone to lactonization during aqueous workup. Without workup, **1.53** was exposed to methanolic ammonia, followed by NaH to provide 41-55% yield of CL (**1.2**) without undesired lactone as reported in Chai's work. Chlorolissoclimide, haterumaimide Q (**1.3**), 7-deoxyhaterumaimide Q (**1.54**), and 7-deoxychlorolissoclimide (**1.55**) were efficiently synthesized using this synthetic sequence.

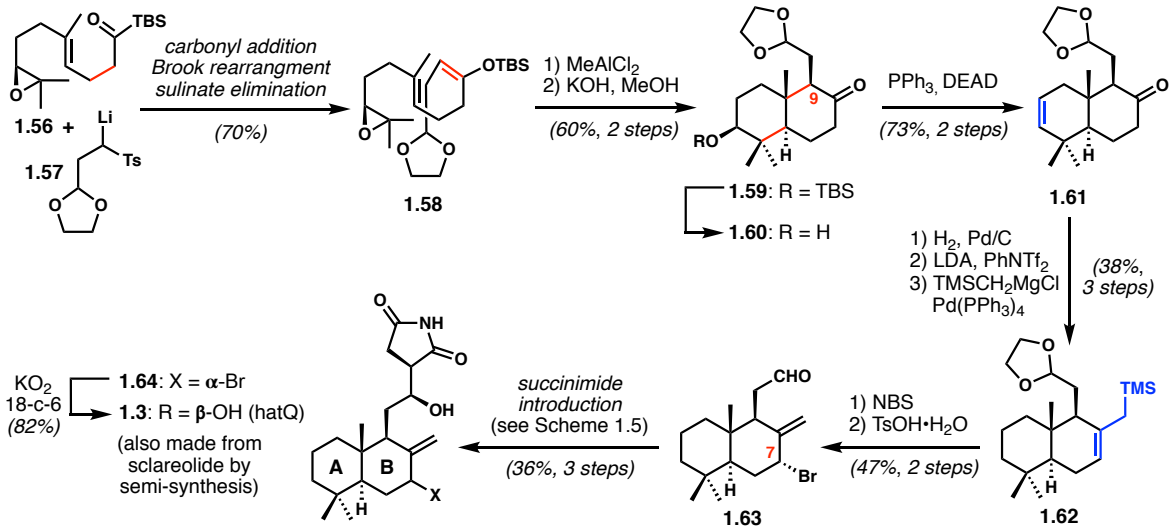
Scheme 1.5 Semisynthesis of CL using C–H chlorination approach by Vanderwal group.[15]



Although CL, hat Q and two C7-deoxy lissoclimide derivatives could be synthetized from sclareolide (**1.18**) using our semisynthetic strategy, other modifications of the labdane core remained challenging. Therefore, our group designed an analogue-oriented synthesis of lissoclimides using a polyene cyclization approach (**Scheme 1.6**).[17] Polyene **1.58** could be produced from acylsilane **1.56** and lithiated sulfone **1.57** in one step through carbonyl addition, triggering Brook rearrangement and elimination of a tosyl group, as developed in similar systems by Corey and co-workers.[18] Compound **1.58** with TBS enoxysilane terminating group was subjected to Lewis acid-catalyzed cationic polyene cyclization, followed by epimerization at C9 to form the desired *trans*-decalin **1.59**. After deprotection of TBS group, secondary alcohol **1.60** was eliminated under Mitsunobu conditions to form alkene **1.61**. The alkene on the A-ring could be functionalized via various reactions, such as, dichlorination to give diaxial dichlorinated product or hydrogenation to give a saturated derivative. Ketone **1.61** was converted to allylsilane

1.62 through enolate triflation and Pd-catalyzed Kumada cross coupling with (trimethylsilyl)methylmagnesium chloride. The resulting allylsilane **1.62** was useful for B-ring functionalization, where the next step involved bromination and hydrolysis of dioxolane **1.62** to give aldehyde **1.63**. The synthetic sequence of boron-mediated aldol addition and succinimide formation yielded the lissoclimide derivative **1.64** in 36% over 3 steps. Hat Q (**1.3**) was also synthesized from the hydrolysis of allylic bromide **1.64**.

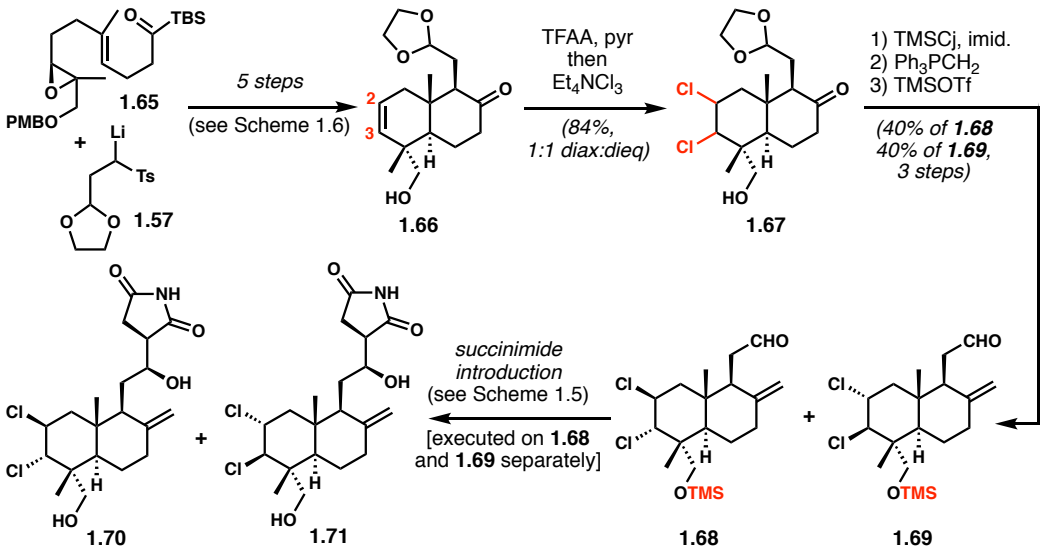
Scheme 1.6 Synthesis of strategic alkenes **1.61** and **1.62** to access hatQ (**1.3**) and lissoclimide analogues.[17]



Our group next investigated the synthesis of C18-oxygenated lissoclimide-type compounds, exemplified by hatJ (**1.8**) (**Scheme 1.7**), to evaluate this route's potential for generating lissoclimide analogues. The previous described five-step synthesis was applied to convert acylsilane **1.65** and organolithium reagent **1.57** into alkene **1.66**. Interestingly, dichlorination of cyclohexene **1.66** yielded a 1:1 ratio of diaxial and diequatorial dichlorides (compound **1.67**). Notably, the presence of a primary alcohol pendant group in **1.67**, compared to the usual methyl group at C18, resulted in partial diequatorial dichlorination. Wittig reaction of ketones **1.68** and **1.69** furnished olefins **1.70** and **1.71**. The succinimide moiety was then

introduced independently to each aldehyde (**1.68** and **1.69**) to afford the final lissoclimide analogues **1.70** and **1.71**.

Scheme 1.7 Synthesis of C18-oxygenated lissoclimide analogues.[17]



1.6 The Discovery of Novel Halogen–π Interaction

Previously, Yusupov and co-workers had investigated the binding interactions of 16 small-molecule ribosomal inhibitors including the glutarimide-containing cycloheximide (CHX) and lactimidomycin (LTM), with the eukaryotic 80S ribosome using X-ray cocrystallography.[8] These studies revealed that CHX and LTM block deacylated tRNA from binding the E-site. Our group collaborated with the Yusupov group to analyze the X-ray cocrystal structures of the synthetic CL and lissoclimide analogues (e.g. **1.54**, **1.55**, **1.70**, **1.71**) with the *Saccharomyces* 80S ribosome. Their analysis showed that CL occupies the same binding pocket as CHX and LTM at E-site of 60S ribosomal subunit[17] (**Figure 1.4a**). Furthermore, they identified a novel halogen-π dispersive interaction between a chlorine substituent on the decalin core of CL and the aromatic ring system of guanine residue G-2794 within the 60S E-site (**Figure 1.4b**). This interaction has a distance of 3.2 Å. In collaboration with the Furche group at UCI, the interaction energy between the chlorine

atom and the guanine ring was calculated using PBE-D3 calculations, which yielded a value of 1.1 kcal/mol. Subsequently, the computed interaction energy of C2 halogen substituents on lissoclimide core was investigated computationally. This analysis revealed an expected trend of increasing interaction energy in the order F < Cl < Br.

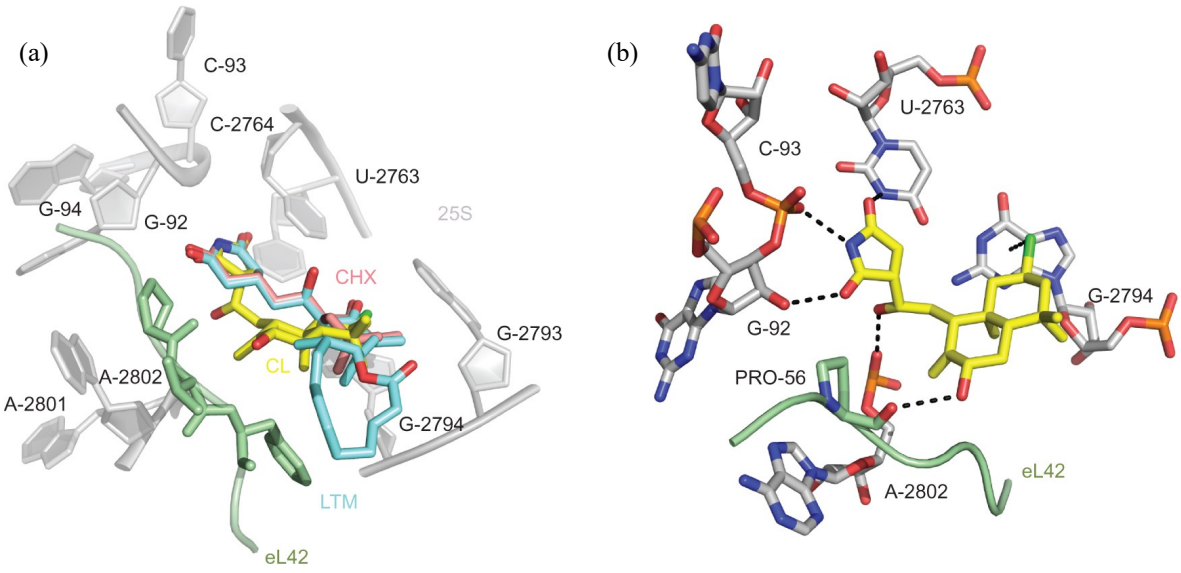
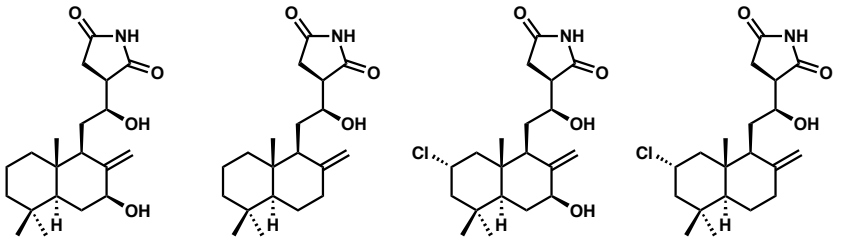


Figure 1.4 (a) Cocrystal structure of CHX (pink), LTM (cyan) and CL (yellow) located in 60S E-site. (b) Binding interactions between CL and tRNA E-site pocket. Reproduced with permission from ref 17. Copyright 2017 Springer Nature.

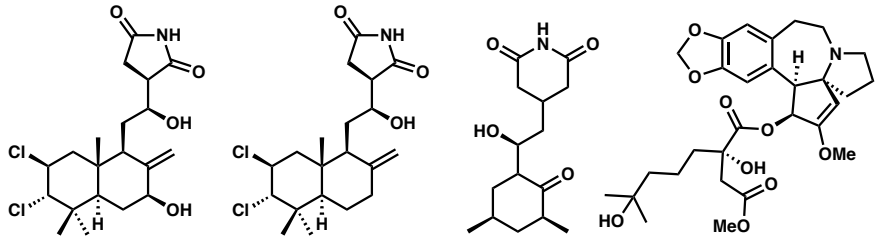
Our group then evaluated the anticancer activity of synthetic lissoclimide analogues, CL (**2**) , hatQ (**3**), and derivatives, against leukemia (P388), prostate (DU145) and melanoma (A2058) cell lines[17] (**Figure 1.5**). Structure-activity relationship (SAR) studies suggested that C7-hydroxy and C2-chlorine substituents play a significant role in antitumor activity. This is evidenced by the increasing cytotoxicity observed in the order: derivative **1.54** < derivative **1.55** < CL (**1.2**). Notably, CL (**1.2**) exhibited the most potent inhibitory effect on the proliferation of P388 cancer cells among the tested lissoclimide analogues, with cytotoxicity in the nanomolar range. Interestingly, compound **1.72** containing dichloride atoms displayed greater cytotoxicity than CL

(**1.2**) against A2058 cells. Similarly, the C45 derivative **1.73** without C7 hydroxyl group exhibited higher cytotoxicity compared to CL (**1.2**) against DU145 cells. Because **1.72** and **1.73** bear axial chlorides, we expected them to possess poor binding affinity and thus exhibit low cytotoxicity.

Figure 1.5 Cytotoxicity of lissoclimide-type compounds against P388, A2058, and DU145 cell lines.[17]



	hat Q: **1.3**	**1.54**	CL: **1.2**	**1.55**
P388 (μM)	0.20	0.43	0.06	0.32
A2058 (μM)	2.34	1.91	0.25	0.63
DU145 (μM)	1.49	1.91	0.49	1.13



	1.72	**1.73**	CHX	Homoharingtonine
P388 (μM)	0.46	0.14	5.6	0.05
A2058 (μM)	0.18	0.97	>10	0.17
DU145 (μM)	0.57	0.37	>10	0.23

Mobley and co-workers investigated the docked structure of C45 (**1.73**) in the 80S ribosomal E-site using computational methods.[19] Their analysis revealed a conformational change in the A-ring of C45 (**1.73**) from the expected chair conformation to a twist-boat conformation within the ribosomal pocket (**Figure 1.6a**). Additionally, C45 (**1.73**) does not engage with eL42 protein because it does not have the C7 hydroxyl group on the B-ring. Furthermore, the twist-boat conformation oriented the chlorides in a pseudo-equatorial arrangement, permitting the halogen-

π interactions of the C2- and C3-dichlorides with the aromatic guanines. (**Figure 1.6b**). This finding was corroborated by the Yusupov group's X-ray cocrystal structure of C45 (**1.73**) with the ribosomal E-site. The structure confirmed the twist-boat conformation of the A-ring and identified a significant halogen-π interaction between the two chlorine atoms of C45 (**1.73**) and guanines G2793 and G2794 of the 60S ribosomal RNA, potentially contributing to its anticancer activity.

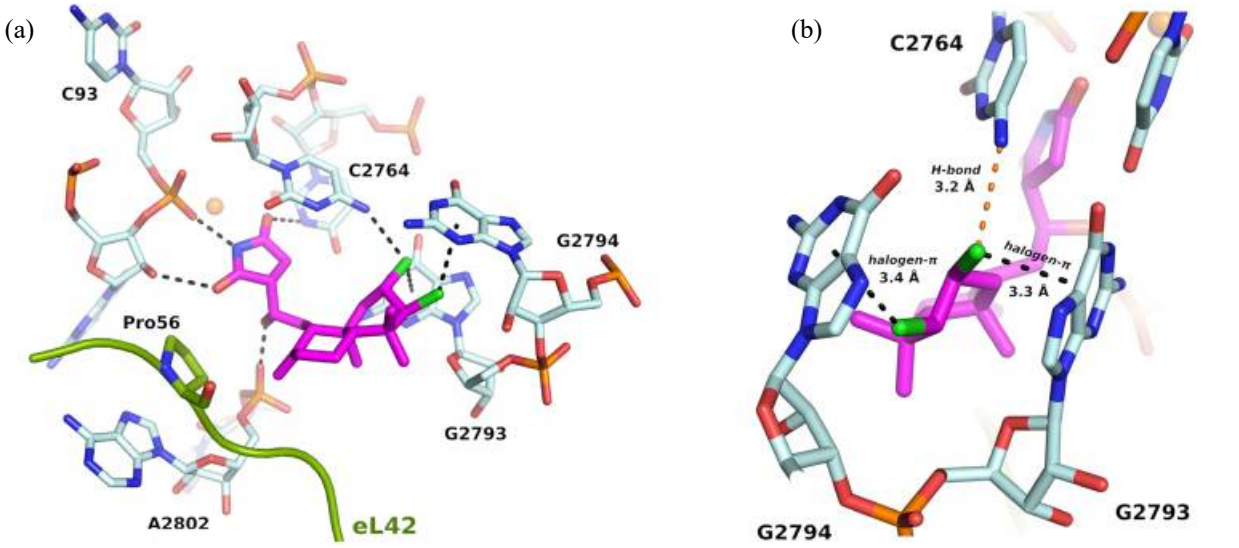


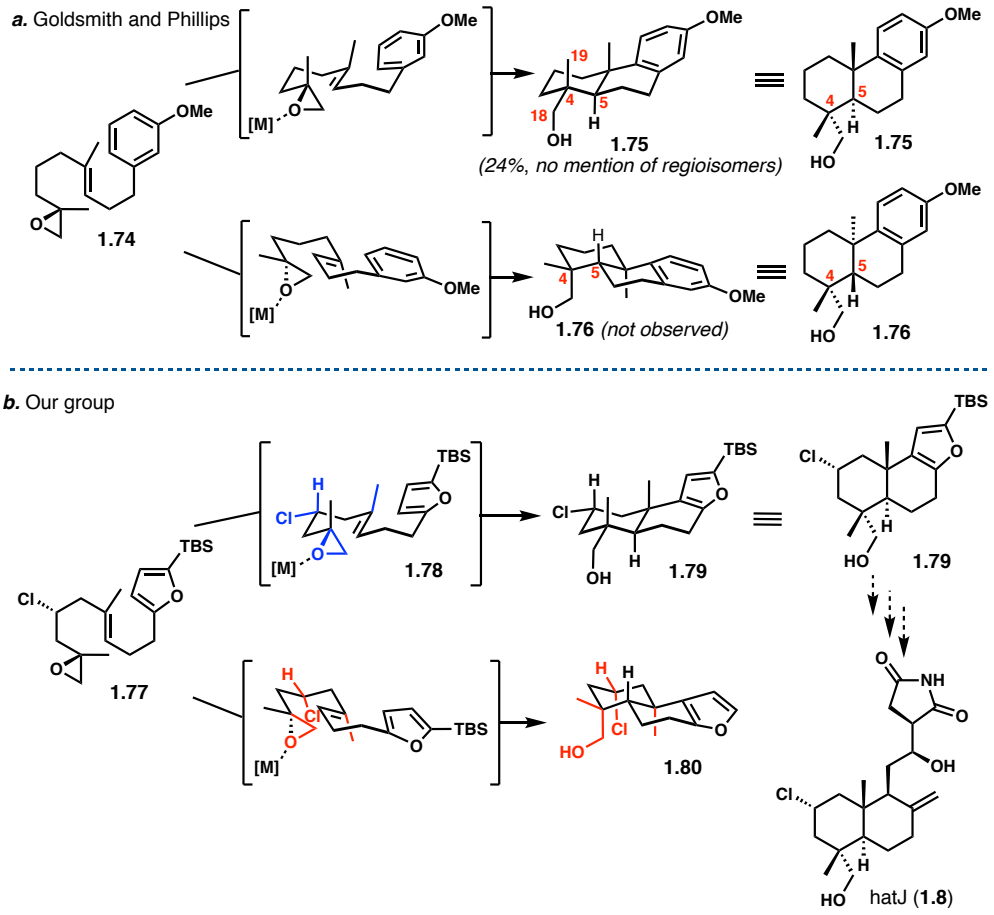
Figure 1.6 (a) Cocrystal structure of C45 (**1.73**) and 25S rRNA. (PDB:5TBW) (b) Detailed view of the synthetic C45 (**1.73**) with A-ring in a twist-boat conformation and halogen-π interaction of C2 and C3 chlorides to guanine residues. Reproduced with permission from ref 19. Copyright 2019 Oxford University Press.

1.7 Synthesis of Lissoclimide Natural Products, Haterumaimide J and K, by Vanderwal Group

The successful semisynthesis strategy and analogue-oriented synthesis developed by the Vanderwal group produced CL, hatQ, and lissoclimide analogues. HatJ (**1.8**), with its C18 hydroxyl group and exceptional anti-P388 activity[5], inspired our group to explore a π-cyclization approach to obtain the desired decalin core and to achieve the C18 oxidation present in hatJ (**1.8**). Our group planned to use a substrate with a terminal epoxide as an initiator, which is an uncommon precursor for epoxide-initiated polycyclizations. In 1969, Goldsmith and Phillips reported a

terminal-epoxide-initiated π-bicyclization approach (**Scheme 1.8a**), where epoxyolefin **1.74** cyclized to give *trans*-decalin **1.75** in 24% yield.[20] This work exemplifies polycyclization favoring equatorial C18 oxygenation with the desired C4/C5 relative configuration; however, it was unknown if the mass balance of the reaction included other stereoisomers.

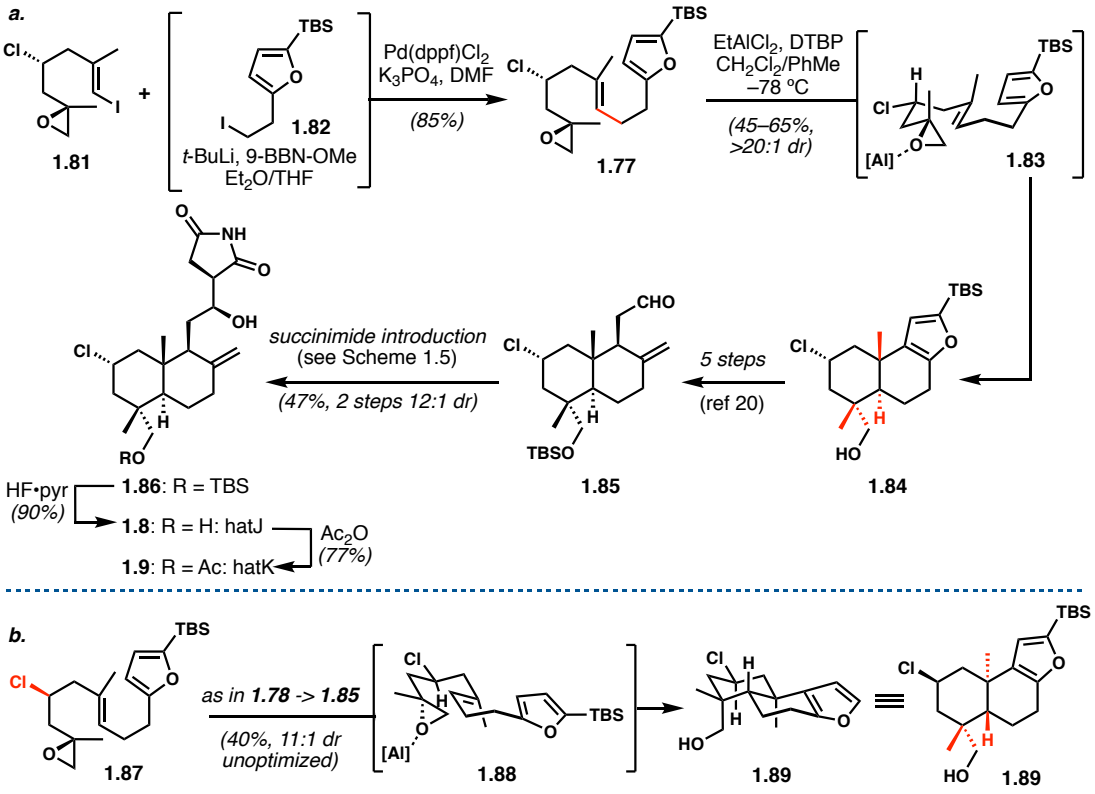
Scheme 1.8 (a) Terminal-epoxide-initiated cyclization by Goldsmith and Phillips.[20] (b) Our plan to synthesize hatJ (**1.8**) using epoxide-initiated π-cyclization cascade.[21]



To synthesize hatJ (**1.8**), our group planned to employ a substrate containing terminal epoxide, C2 chloride, and a furan terminating group in a Lewis acid-mediated π-cyclization (**Scheme 1.8b**).[21] The equatorial C2 chlorine atom was expected to direct the stereochemical outcome of the π-cyclization, potentially leading to the desired bicyclic core structure. Based on our hypothesis, the unique cyclization precursor **1.77**, bearing a terminal epoxide and an equatorial

C2 chlorine, would preferentially react via a transition state (**1.78**) to afford the formation of a single stereoisomer **1.79**, corresponding to hatJ (**1.8**).

Scheme 1.9 a) Synthesis of hatJ (**1.8**) and hatK (**1.9**) using terminal-epoxide-initiated bicyclization cascade.[21] b) Chlorine-bearing stereogenic center controls diastereoselectivity of π-cyclization product.



Our previous graduate student, Dr. Sharon Michalak, commenced the synthesis of hatJ (**1.8**) with a Suzuki–Miyaura cross-coupling reaction between vinyl iodide **1.81** and furan-containing alkyl iodide **1.82** (**Scheme 1.9**). Subsequent treatment of chloroepoxide **1.77** with ethylaluminum dichloride as a Lewis acid catalyst promoted a cationic cyclization reaction. This reaction afforded a single diastereomer of the bicyclic product **1.84**, featuring C18 (equatorial) oxygenation, through the proposed reactive conformation **1.83**. Furan moiety in **1.84** was then converted to aldehyde **1.85** in five steps. This process involved oxidative ring opening, *in situ* carboxylate methylation, and diastereoselective hydrogenation. The resulting aldehyde **1.85** served

as a substrate for asymmetric aldol addition followed by deprotection of the TBS group, ultimately yielding hatJ (**1.8**). HatK (**1.9**) was synthesized via acetylation of hatJ (**1.8**). Interestingly, investigation of the cyclization reaction using diastereomer **1.87** revealed a preference for C19 (axial) oxygenation. This resulted in the formation of *trans*-decalin **1.89** as the major product with a 11:1 diastereomeric ratio.

1.8 Conclusion

The potent cytotoxicity of DCL and CL against various cancer cell lines and their unique chlorine and succinimide-containing structure motivated prior research into the synthesis of compounds in this natural product class. The groups of González and Chai were the first to make use of sclareolide in semi-synthetic approaches of lissoclimides; however, they encountered challenges with diastereoselectivity, leading to mixtures of diastereomers at C12 and C13. Our group showed that sclareolide could serve as a viable precursor for the semisynthesis of CL. Through collaboration with the Alexanian group, we employed their *N*-chloroamide reagent to introduce an equatorial C2 chlorine atom onto sclareolide. Our group also developed the conditions for Evans aldol addition to install a hydroxy succinimide moiety as a single diastereomer at C12 and C13. This nine-step sequence successfully yielded CL. Subsequently, our group devised an analogue-oriented synthesis strategy to access strategically valuable intermediates, enabling further modification of the A- and B-rings on the lissoclimide core structure. This approach facilitated the preparation of a diverse library of lissoclimide derivatives for biological evaluation. Finally, our group focused on the synthesis of hatJ, which possesses a C18 hydroxyl group. To achieve this, our group employed a terminal-epoxide-initiated bicyclization strategy where the C2 chlorine atom directed the stereochemical outcome of the cyclization.

Our research has demonstrated the critical role of the C2 chlorine atom in lissoclimide binding to the ribosome. We observed that the C2-chlorine atom in CL participates in a halogen-π dispersive interaction with guanine residues within the 80S ribosome. This interaction has been identified as a major contributor to the anticancer activity of CL. Therefore, we aim to investigate the role of halogen-π interactions in the anticancer activity of lissoclimide derivatives, with the goal of enhancing the biological activity of compounds in this family. We hypothesize that a stronger halogen-π interaction may correlate with higher cytotoxicity of lissoclimide derivatives. This hypothesis is supported by computational modeling by the Furche group, which suggests that the strength of halogen-π interactions between C2 substituents and aromatic guanines increases in the order F < Cl < Br. To test this hypothesis, we will synthesize lissoclimide analogues containing C2-fluorine and C2-bromine substituents and evaluate their halogen-π interactions within the ribosomal pocket.

1.9 References

1. Malochet-Grivois, C.; Cotelle, P.; Biard, J.F.; Hénichart, J.P.; Debitus, C.; Roussakis, C.; Verbist, J.F. *Tetrahedron Lett.* **1991**, *32*, 6701–6702.
2. Malochet-Grivois, C.; Roussakis, C.; Robillard, N.; Biard, J.F.; Riou, D.; Debitus, C.; Verbist, J.F. *Anticancer Drug Des.* **1992**, *7*, 493–502.
3. Biard, J.F.; Malochet-Grivois, C.; Roussakis, C.; Cotelle, P.; Hénichart, J.P.; Debitus, C.; Verbist, J.F. *Nat. Prod. Lett.* **1994**, *4*, 43–50.
4. (a) Uddin, M. J.; Kokubo, S.; Suenaga, K.; Ueda, K.; Uemura, D. *Heterocycles* **2001**, *54*, 1039. (b) Uddin, M. J.; Kokubo, S.; Suenaga, K.; Ueda, K.; Uemura, D. *J. Nat. Prod.* **2001**, 64, 1169. (c) Uddin, M. J.; Kokubo, S.; Suenaga, K.; Ueda, K.; Uemura, D. The World Chemistry Congress, Brisbane, Australia, 2001, abstract, PFD25, p 562. (d) Uddin, M. J.;

Kokubo, S.; Suenaga, K.; Ueda, K.; Uemura, D. *Chem. Lett*. **2002**, *10*, 1028. (e) Fu, X.; Palomar, A. J.; Hong, E. P.; Schmitz, F. J.; Valeriote, F. A. *J. Nat. Prod*. **2004**, *67*, 1415.

5. Uddin, J.; Ueda, K.; Siwu, E. R. O.; Kita, M.; Uemura, D. *Bioorg. Med. Chem*. **2006**, *14*, 6954–6961.
6. Robert, F.; Hao, H. Q.; Donia, M.; Merrick, W. C.; Hamann, M. T.; Pelletier, J. *RNA* **2006**, *12*, 717–725.
7. Schneider-Poetsch, T.; Ju, J.; Eyler, D. E.; Dang, Y.; Bhat, S.; Merrick, W. C.; Green, R.; Shen, B.; Liu, J. O. *Nat. Chem. Biol*. **2010**, *6*, 209–217.
8. Garreau de Loubresse, N.; Prokhorova, I.; Holtkamp, W.; Rodnina, M. V.; Yusupova, G.; Yusupov, M. *Nature* **2014**, *513*, 517–522.
9. Jung, M. E.; Gomez, A. V. *Tetrahedron Lett*. **1993**, *34*, 2891–2894.
10. González, M. A.; Romero, D.; Zapata, B.; Betancur-Galvis, L. *Lett. Org. Chem*. **2009**, *6*, 289–292.
11. Boukouvalas, J.; Wang, J.-X.; Marion, O.; Ndzi, B. *J. Org. Chem*. **2006**, *71*, 6670.
12. Nguyen, T. M.; Vu, N. Q.; Youte, J.-J.; Lau, J.; Cheong, A.; San Ho, Y.; Tan, B. S.W.; Yoganathan, K.; Butler, M. S.; Chai, C. L.L. Tetrahedron 2010, 66, 9270–9276.
13. (a) Szklarski, A. R. PhD Dissertation, University of California, Irvine, 2013. (b) Könst, K. A. PhD Dissertation, University of California, Irvine, 2016. (c) Michalak, S. E. PhD Dissertation, University of California, Irvine, 2019.
14. Review on the lissoclimides: Pak, B. S.; Supantanapong, N.; Vanderwal, C. D. *Acc. Chem. Res*. **2021**, *54*, 1131–1142.

15. Quinn, R. K.; Könst, Z. A.; Michalak, S. E.; Schmidt, Y.; Szklarski, A. R.; Flores, A. R.; Nam, S.; Horne, D. A.; Vanderwal, C. D.; Alexanian, E. J. *J. Am. Chem. Soc*. **2016**, *138*, 696–702.

16. Liu, W.; Groves, J. T. *J. Am. Chem. Soc*. **2010**, *132*, 12847–12849.

17. Konst, Z. A.; Szklarski, A. R.; Pellegrino, S.; Michalak, S. E.; Meyer, M.; Zanette, C.; Cencic, R.; Nam, S.; Voora, V. K.; Horne, D. A.; Pelletier, J.; Mobley, D. L.; Yusupova, G.; Yusupov, M.; Vanderwal, C. D. *Nat. Chem.* **2017**, *9*, 1140–1149.

18. Corey, E. J.; Luo, G.; Lin, L. S. *J. Am. Chem. Soc*. **1997**, *119*, 9927–9928.

19. Pellegrino, S.; Meyer, M.; Könst, Z. A.; Holm, M.; Voora, V. K.; Kashinskaya, D.; Zanette, C.; Mobley, D. L.; Yusupova, G.; Vanderwal, C. D.; Blanchard, S. C.; Yusupov, M. *Nucleic Acids Res.* **2019**, 47, 3223–3232.

20. Goldsmith, D. J.; Phillips, C. F. *J. Am. Chem. Soc*. **1969**, *91*, 5862–5870.

21. Michalak, S. E.; Nam, S.; Kwon, D. M.; Horne, D. A.; Vanderwal, C. D. *J. Am. Chem. Soc*. **2019**, *141*, 9202–9206.

CHAPTER 2 SYNTHESIS OF LISSOCLIMIDE ANALOGUES

2.1 Introduction

Uddin and co-workers have demonstrated that C2 chlorination, the presence of the C7 hydroxy group, and hydroxy succinimide moiety of lissoclimide analogues are all crucial for their activity against P388 leukemia cells (**Figure 2.1**).[1] The anticancer activity of chlorolissoclimide (CL) is thought to arise from its demonstrated ability to suppress protein synthesis in eukaryotic cells. CL exhibits inhibitory activity comparable to cycloheximide (CHX) and homoharringtonine, both of which are eukaryotic translation inhibitors (**Figure 2.1**).[2] Furthermore, it has been shown that CL shares the same binding pocket with CHX and lactimidomycin (LTM) at the E-site ribosome. Detailed studies of the binding interactions between CL and the 80S ribosome revealed a novel and unusual halogen-π interaction between C2-chlorine atom of CL and guanine G-2794 at the binding-site. Computational modelling predicted that a bromine at C2 would exhibit the strongest halogen-π interaction with the guanine residue, followed by chlorine and fluorine atoms. Therefore, this work focuses on modifying the C2 position of the lissoclimide. Specifically, we aimed to synthesize Bromolissoclimide (BrL), fluorolissoclimide (FL), and methyllissoclimide (MeL) to gain deeper understanding of the halogen-π interaction of lissoclimide derivatives and their relationship to the inhibition of translation.

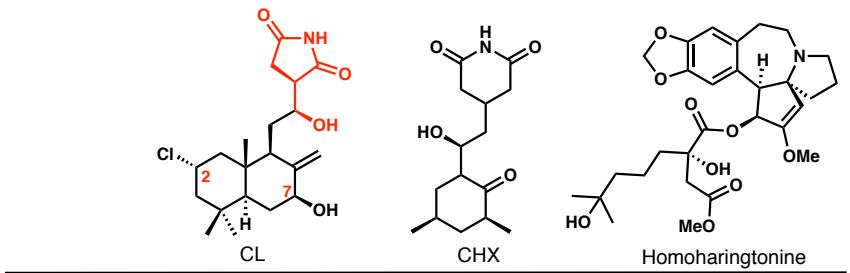
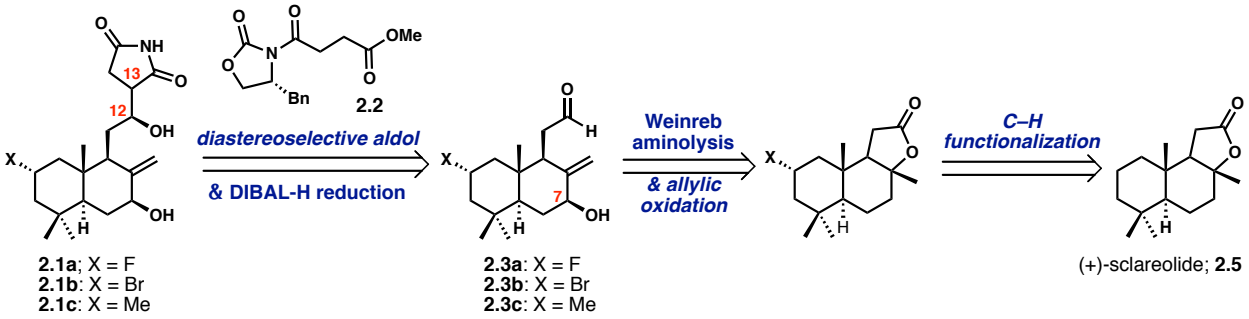


Figure 2.1 Translation-inhibitory activities of CL and known translation inhibitors.[2]

2.2 Retrosynthetic Analysis of BrL, FL, and MeL

In order to rapidly access analogues, we elected to the semisynthetic approach by Vanderwal group. This synthesis delivers CL as a single diastereomer in 9 steps, with an overall yield of 8-13%.[2] We planned to synthesize FL (**2.1a**), BrL (**2.1b**), and MeL (**2.1c**) by leveraging this route which starts from commercially available sclareolide (**2.5**) (**Scheme 2.1**). Lissoclimide analogues (**2.1a-c**), could be obtained via formation of the hydroxy succinimide functional group from the requisite chain, installed by a diastereoselective aldol addition of aldehyde **2.3a-c** with the Evans auxiliary **2.2**. The C7 hydroxyl group of compound **2.3a-c** could be introduced through allylic oxidation of the intermediate **2.4a-c**. The key intermediate **2.4a-e**, with various C2 substituents, would be prepared from sclareolide **2.5** utilizing C–H functionalization chemistry developed by Alexanian *et al.*

Scheme 2.1 Retrosynthesis of BrL, FL, and MeL.

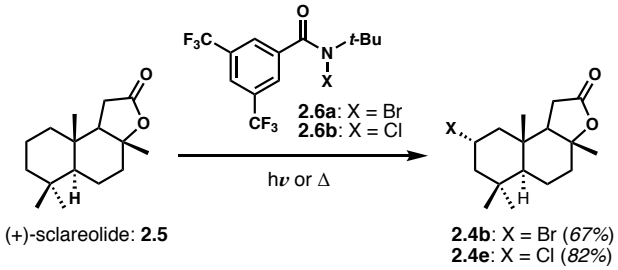


2.3 C–H Fluorination of Sclareolide and Attempts Towards Methylsclareolide

Alexanian and coworkers developed *N*-bromoamide reagent **2.6a** in 2014 for the C–H bromination of aliphatic compounds, including terpenoid sclareolide (**2.5**) (**Scheme 2.2**).[3] Our group in collaboration with Alexanian group, subsequently demonstrated efficient C–H chlorination of sclareolide (**2.5**) on a multi-gram scale using *N*-chloroamide **2.6b**, affording chlorosclareolide (**2.4e**).[4] The reactivity of amide reagents **2.6a-b** for C–H functionalization was

thoroughly explored by the Alexanian group.[3-5] The research also revealed that *N*-*t*Bu amidyl radial generated from *N*-halomides **2.6a-b** could selectively abstract hydrogen atoms from aliphatic molecules regioselectivity controlled through a combination of steric and electronic effects. 2,6-Bis-trifluoromethyl of *N*-*t*Bu amide **2.6a-b** also enhanced the sterically dictated selectivity in C–H bromination and chlorination. Building upon this success, we sought to achieve selective C–H fluorination at the C2 position of sclareolide to synthesize the target molecule, fluorosclareolide (FL).

Scheme 2.2 Radical-mediated C–H functionalization using amide reagent **2.6a-b**.[3-4]



The structure of sclareolide plays a crucial role in directing radical C–H halogenations, with the C2 position being the most electron rich (**Figure 2.2**). Firstly, the inductive effect of the lactone deactivates the B and C rings, with higher the electron density at C2 and C3 (**2.5**). Secondly, C2 experiences less steric hindrance compared to C3 or C1 due to the absence of adjacent quaternary carbons. Additionally, the equatorial α-C–H at C2 is more accessible for radical abstraction as it avoids 1,3-diaxial interactions with the axial C–H bonds and the A-ring methyl groups. Finally, the C2 methylene exhibits a stronger hyperconjugation effect compared to the methyl groups, further enhancing its reactivity.

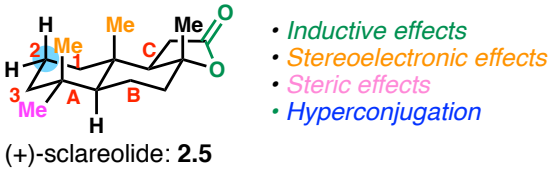
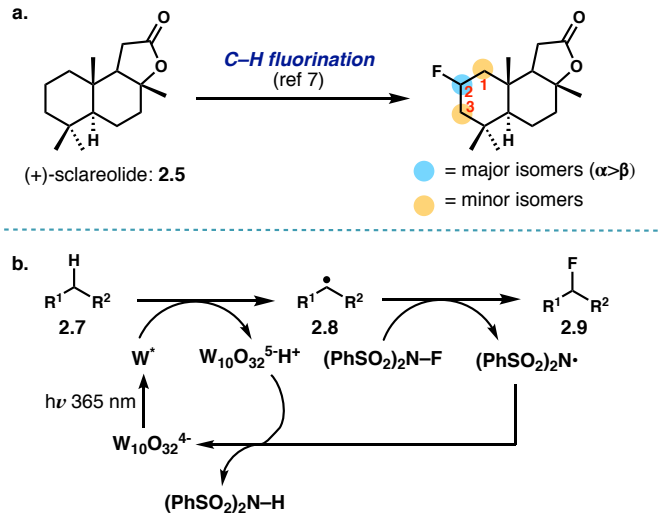


Figure 2.2 Effects of C2 site-selective C–H functionalization of sclareolide.[6]

2.3.1 C–H Fluorination of Sclareolide

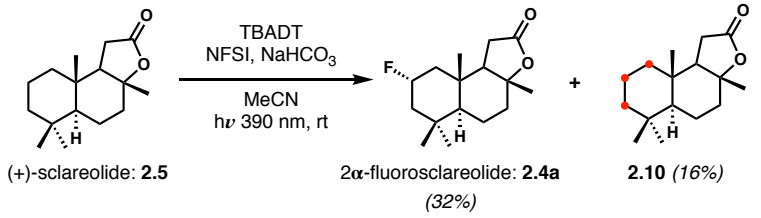
The field of sclareolide (**2.5**) C–H fluorination has witnessed significant exploration by various research groups (**Scheme 2.3a**).[7] Groves and co-workers pioneered the use of a manganese porphyrin catalyst for oxidative aliphatic C–H fluorination of sclareolide.[7a] Metal-free approaches for sp^3–H fluorination have also been reported, with Chen[7c] and Tang[7e] achieving success. Additionally, Britton and coworkers demonstrated the efficient abstraction of a hydrogen atom from the aliphatic carbon of sclareolide using a tetrabutylammonium salt of decatungstate (TBADT) under UV light irradiation (**Scheme 2.3b**).[7b] The proposed mechanism involves excitation of TBADT to its excited state (W*) upon UV light exposure, which engages in hydrogen atom abstraction from sclareolide (**2.6**) to form the carbon radical intermediate (**2.7**). *N*-Fluorobenzenesulfonimide (NFSI) then serves as the fluorine atom source, converting the radical to the desired alkyl fluoride product (**2.8**). Finally, a hydrogen atom transfer (HAT) from a nitrogen-centered radical regenerates the decatungstate anion ($W_{10}O_{32}^{4-}$).

Scheme 2.3 (a) Regioselectivity observed for the C–H fluorination of sclareolide.[7] (b) Proposed mechanism of TBADT-catalyzed C–H fluorination.[7b]



Based upon Britton's work[7b] , we adopted TBADT catalyst, prepared in a single step from tetrabutylammonium bromide and sodium tungstate dihydrate, as the photocatalyst for C–H fluorination of sclareolide (**2.5**) (**Scheme 2.4**). The reaction employed NFSI as the fluorine source under UV light irradiation (λ = 390 nm). To mitigate the generation of hydrofluoric acid and its associated acetamide by-product, a catalytic amount of $NaHCO_3$ was included. While the desired 2α-fluorosclareolide (**2.4a**) was obtained as the major product with a combined yield of 32% (isolated and NMR), the reaction also afforded a mixture of 2β-fluorosclareolide and regioisomers at C1 and C3 (**2.10**) in a total yield of 16%. This reaction was also problematic for material throughout as gram scale reactions did not proceed to completion. Attempts to improve regio- and stereoselectivity by varying the UV light wavelength (440 nm and 450 nm) or employing visible light proved unsuccessful (data not shown). These findings corroborate previous reports on the inherent challenges associated with achieving a regio- and stereoselective C–H fluorination of sclareolide, prompting us to explore alternative reaction conditions.

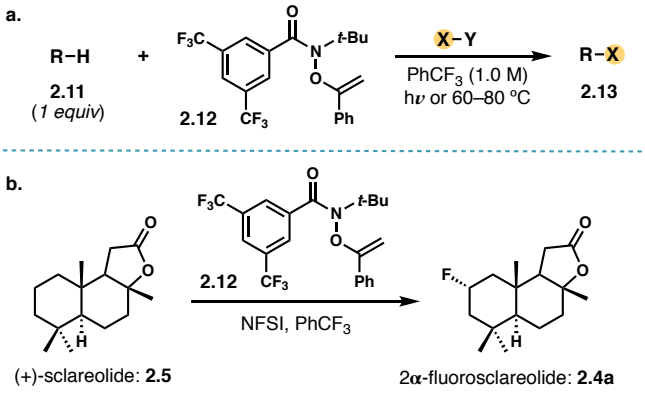
Scheme 2.4 C–H fluorination of sclareolide using Britton conditions.[7b]



The Alexanian group recently introduced a method for site-selective aliphatic C–H functionalization of linear and cyclic substrates **2.11** using an *O*-alkenylhydroxamate **2.12** which proceeds via a radical chain transfer cascade (**Scheme 2.5a**).[8] This versatile approach allows for the incorporation of various halogens through the use of distinct radical-trapping reagents (Cl_4C, Cl_3CBr, $F_{13}C_6I$, and NFSI). Inspired by this work, we envisioned that C–H fluorination of sclareolide (**2.5**) with *O*-alkenylhydroxamate **2.12** and *N*-fluorobenzenesulfonimide (NSFI) could

achieve selective formation of the desired 2α-fluorosclareolide (**2.4a**) as a single diastereomer (**Scheme 2.5b**) based upon regioselectivity of C-H chlorination and bromination in Scheme 2.2. Following Alexanian's procedure, we prepared the requisite reagent **2.12**. Employing blue LEDs (λ = 440 nm) for overnight irradiation, the C–H fluorination reaction significantly improved the yield of 2α-fluorosclareolide (**2.4a**) to 49% compared to the TBADT-catalyzed approach (entry 1). However, scaling up the reaction under identical irradiation conditions resulted in only 50% conversion of sclareolide, with a product yield of 31% for **2.4a** (entry 2). This decrease is attributed to limited light penetration in the larger reaction volume. Finally, heating the fluorination reaction at 70 °C overnight provided 2α-fluorosclareolide **2.4a** in a moderate yield (entry 3).

Scheme 2.5 (a) Aliphatic C–H functionalization of sclareolide using amide **2.12**.[8] (b) Select conditions for C–H fluorination using Alexanian chemistry.

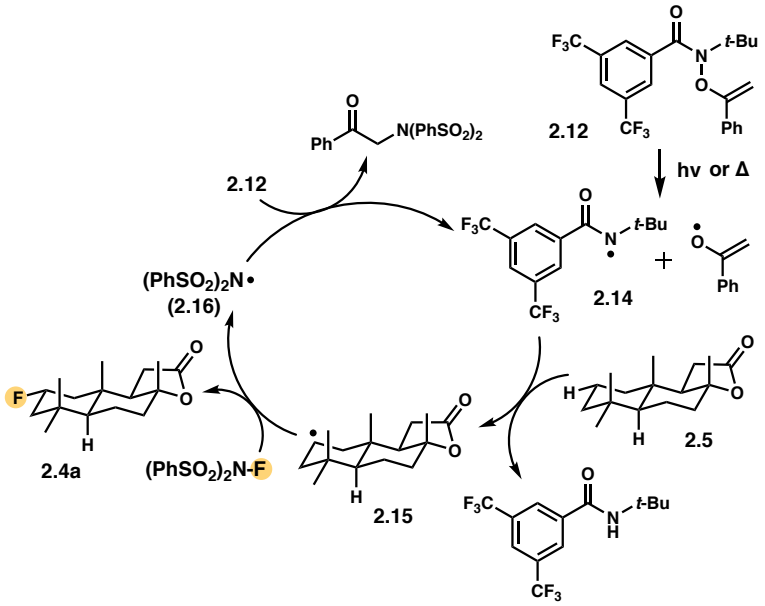


Entry	(+)-Sclareolide	Conditions	Yields
1	0.05 mmol	hν 440 nm, rt	49% (full conversion)
2	4.0 mmol	hν 440 nm, rt	31% (50% conversion)
3	0.1 mmol	70 °C	48% (full conversion)

The C–H fluorination of sclareolide (**2.5**) mediated by *O*-alkenylhydroxamate **2.12** proceeds via a radical chain mechanism (**Scheme 2.6**). This reaction is initiated by visible light irradiation or mild heating to generate the amidyl radical **2.14** from **2.12**. Radical **2.14** selectively abstracts a hydrogen atom at the α-position of C2 in sclareolide (**2.5**), forming carbon-centered

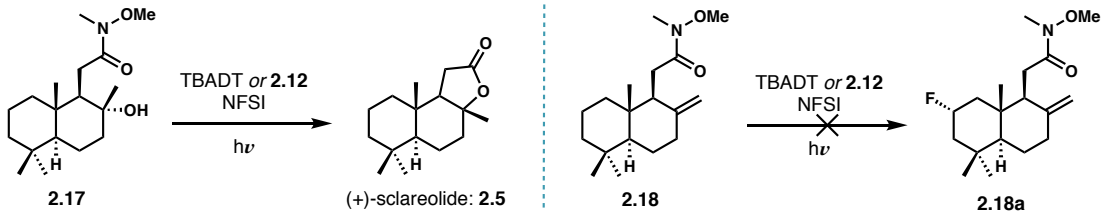
radical **2.15**. In a key chain transfer step, radical **2.15** efficiently captures fluorine from NFSI, introducing a fluorine atom at C2 to yield the desired product, 2α-fluorosclareolide (**2.4a**). Finally, the sulfonimide radical **2.16** is able to regenerate the amidyl radical **2.14** closing the catalytic cycle.

Scheme 2.6 Propose mechanism of C–H fluorination of sclareolide (**2.5**) using *O*-alkenylhydroxamate **2.12**.[8]



To probe the generality of the C–H fluorination method, we investigated the reaction with compounds **2.17** and **2.18** using both TBADT and Alexanian's amide reagent **2.12** (**Scheme 2.7**). Interestingly, analysis of the crude product by proton NMR revealed the presence of sclareolide (**2.5**). This observation highlights the importance of the sclareolide's lactone moiety as an electron-withdrawing group to predispose the system for halogenation. In its absence, the C–H fluorination of alkene **2.18** using the alkenylhydroxamate reagent **2.12** resulted in the recovery of starting material (**2.18**). Similarly, TBADT/NFSI-mediated fluorination of **2.17** yielded only trace amounts of the desired product in the crude mixture. These findings collectively demonstrate that sclareolide (**2.5**) serves as the most effective precursor for the radical-mediated C–H halogenation approach described in this study.

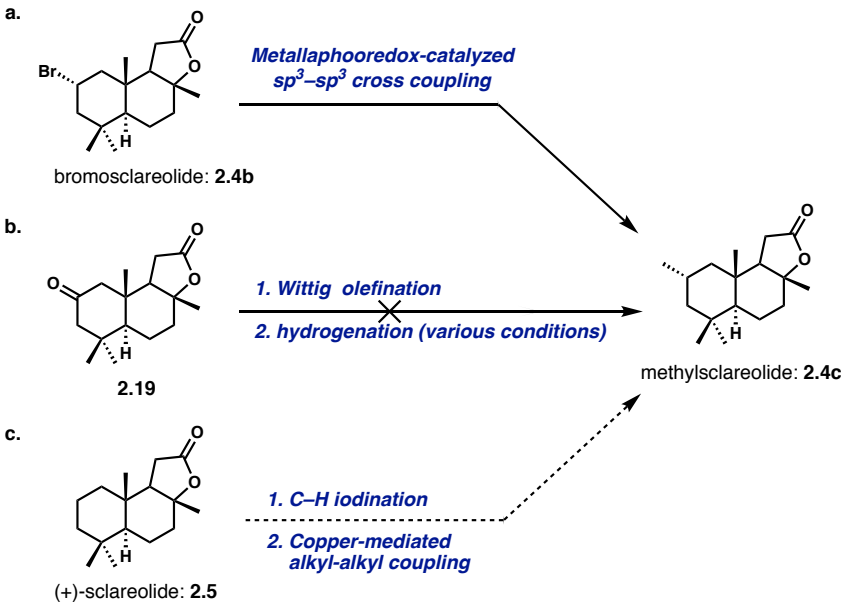
Scheme 2.7 Attempted C-H fluorination of sclareolide-derived compounds.



2.3.2 Attempts Towards Methylsclareolide

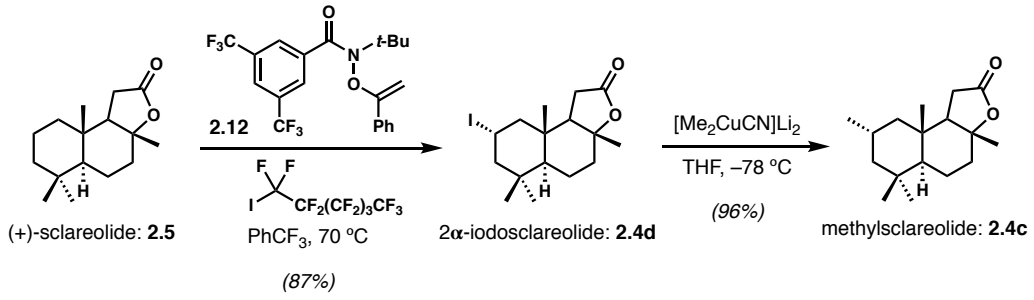
The synthesis of methylsclareolide (**2.4c**) was explored through various approaches (**Scheme 2.8**). Initially, Dr. Bonnie Pak investigated a metallaphotoredox-catalyzed cross-coupling method reported by MacMillan and co-workers for the conversion of bromosclareolide (**2.4b**) to methylsclareolide (**2.4c**) (**Scheme 2.8a**).[9] This reaction employed an Ir(III) photocatalyst and Ni(II) catalyst to afford the desired product **2.4c** as a single diastereomer with 45% yield and retention of C2 stereochemistry.[10] However, scaling up this method to gram quantities proved problematic. As an alternative strategy, Dr. Bonnie Pak also explored the Baran group's electrochemical C–H oxidation approach to obtain decagram quantities of 2-oxo-sclareolide (**2.19**) from sclareolide (**2.5**) (**Scheme 2.8b**).[11] Subsequent Wittig methylation of ketone **2.19** followed by HAT-mediated hydrogenation was envisioned to yield methylsclareolide (**2.4c**). Unfortunately, the hydrogenation step was not selective for the desired isomer, and isolation of the compound in pure form. To address this hurdle, we devised an additional strategy utilizing Alexanian's chemistry for methylation of iodosclareolide, targeting methylated analogue **2.4c** (**Scheme 2.8c**).[7]

Scheme 2.8 Attempts to access methylsclareolide via (a) metallaphotoredox cross-coupling.[10] (b) Wittig reaction and hydrogenation.[10] (c) Methylation of iodosclareolide.



Based on the work of Alexanian *et al.*, who demonstrated C–H iodination of various substrates using *O*-alkenylhydroxamate (**2.12**) and perfluorohexyl iodide ($F_{13}C_6I$)[8], we achieved regioselective and stereoselective C–H iodination of sclareolide (**2.5**) at 70 °C. This reaction, following Alexanian's procedure, afforded a single diastereomer of iodosclareolide (**2.4d**) in excellent yield (87%) (**Scheme 2.9**). Subsequent treatment of the isolated iodosclareolide (**2.4d**) with Gilman reagent (Me_2CuLi) facilitated a radical methylation reaction, successfully yielding the desired methylsclareolide (**2.4c**) in high yield with retention of stereochemistry at the C2 position.

Scheme 2.9 The synthesis of methylsclareolide **2.4c** using Alexanian's C–H functionalization.



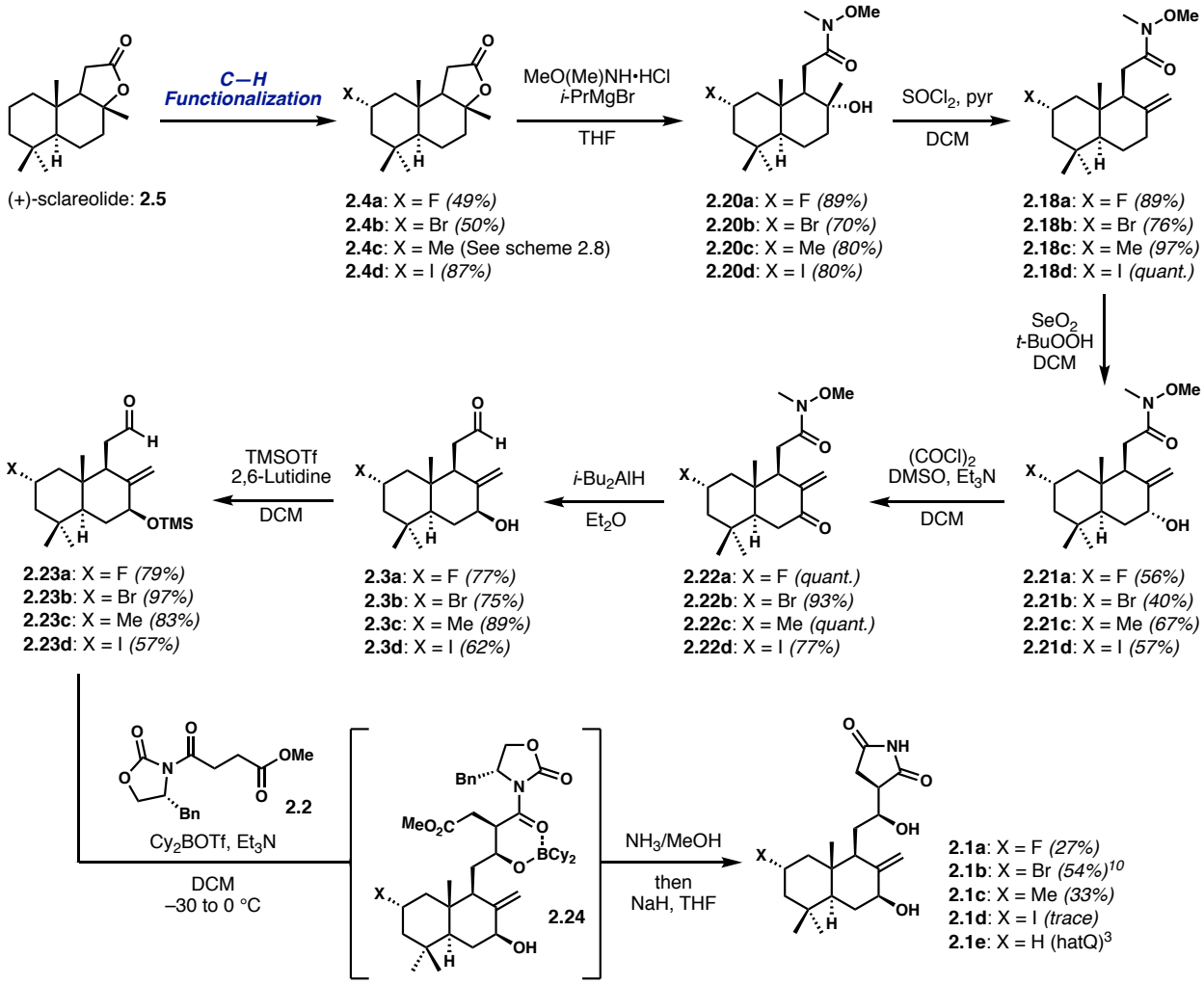
2.4 Semi-synthesis of Fluoro- and Methyllissoclimide

Leveraging the C2-functionalized sclareolide intermediates **2.4a-d**, we employed the established approach to obtain the target compounds FL (**2.1a**), BrL (**2.1b**), MeL (**2.1c**), and potentially IL (**2.1d**) (**Scheme 2.10**). Given our successful C–H iodination of sclareolide (**2.5**) to yield iodosclareolide (**2.4d**), we envisioned its incorporation into the synthesis of IL (**2.1d**). The reaction sequence commenced with the conversion of compounds **2.4a-d** to the corresponding Weinreb amides **2.20a-d** via *N,O*-dimethylhydroxylamine/*i*PrMgBr in good yields. Subsequent treatment of the tertiary alcohols **2.20a-d** with thionyl chloride and base facilitated alkene formation via elimination to arrive at compounds **2.18a-d**. Allylic oxidation of **2.18a-d** using selenium dioxide followed by Swern oxidation of the resulting alcohols **2.21a-d** introduced the ketone at C7. Enone intermediates **2.22a-d** were then converted to the corresponding allylic alcohols **2.3a-d** and aldehydes through DIBAL-H reduction, with concomitant amide-to-aldehyde conversion. To protect the secondary alcohols **2.3a-d**, a trimethylsilyl (TMS) group was introduced.

The stereochemistry at C12 and C13 of the lissoclimide analogues **2.1a-e** was established through a key Evans asymmetric aldol addition. Initial attempts by Dr. Bonnie Pak sought to utilize dibutyl boron triflate and Hünig's base, as previously reported in the CL semi-synthesis.[10] However, this resulted in variable diastereoselectivity at C12 and C13. To address this challenge, we switched to dicyclohexyl boron triflate and triethylamine for the aldol addition. After optimization, the reaction conditions were established, requiring enolate formation at 0 °C and subsequent aldol addition at –30 °C. This optimized procedure afforded a single diastereomer of the aldol products **2.1a-d** via intermediate **2.24**, with the TMS group being cleaved in this step. Cleavage of the imide moiety with ammonia in methanol, followed by installation of the hydroxy

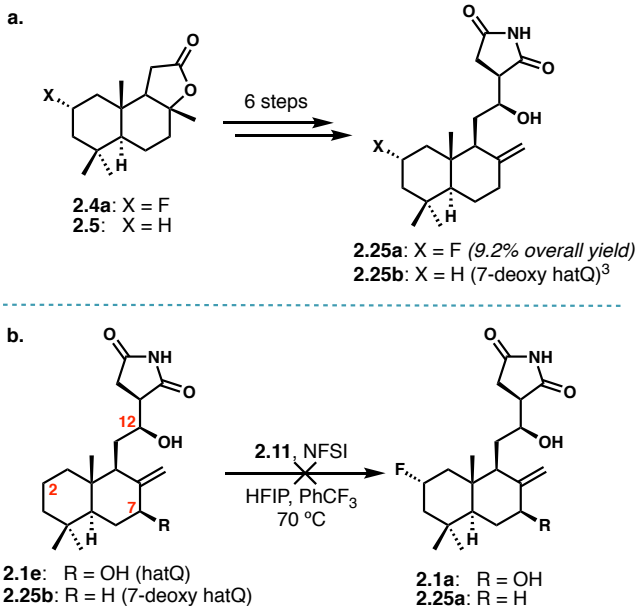
succinimide group under basic conditions, furnished the desired products FL (**2.1a**), BrL (**2.1b**)[10] (performed by Dr. Bonnie Pak), MeL (**2.1c**), and hatQ[4] (**2.1e**). Unfortunately, the Evans aldol reaction with aldehyde **2.23d** proved unsuccessful for IL (**2.1d**) synthesis, possibly due to cleavage of the C–I bond under the reaction conditions.

Scheme 2.10 Synthesis of lissoclimide derivatives.



Our semi-synthetic approach offered flexibility for the synthesis of analogues lacking the C7 hydroxyl group. By omitting the Riley oxidation, and Swern oxidation steps, we obtained 7-deoxygenated FL (**2.25a**) and 7-deoxygeanted hatQ (**2.25b**) (**Scheme 2.11a**). Furthermore, we explored a streamlined approach involving late-stage halogenation of readily available hatQ derivatives (**Scheme 2.11b**). This strategy aimed to reduce the overall number of synthetic steps. On the basis of work by Alexanian, we hypothesized that hexafluoroisopropanol (HFIP) could participate in hydrogen bonding with the hydroxy groups at C7 and C12, deactivating some of the electron rich C–H bonds in this part of lissoclimide molecule and directing C–H fluorination to C2 on the A-ring. Unfortunately, this approach did not yield the desired fluorinated products (**2.1a** and **2.25a**) under the tested conditions.

Scheme 2.11 (a) Synthesis of 7-deoxylissoclimide derivatives. (b) Attempted late-stage C–H fluorination of intermediates bearing hydroxy succinimide.



2.5 X-ray Cocrystal Structures of Lissoclimide Derivatives and 80S Ribosome

In collaboration with the Yusupov group, Dr. Salvatore Terrosu investigated the binding interactions of halogenated lissoclimide derivatives (FL, CL, and BrL), methyllissoclimide (MeL), and hatQ with the *S. cerevisiae* 80S ribosome. Consistent with previous findings for CL[4], all four lissoclimide derivatives bound to the CCA-end of the E-site tRNA within the 60S large ribosomal subunit (**Figure 2.3a**).

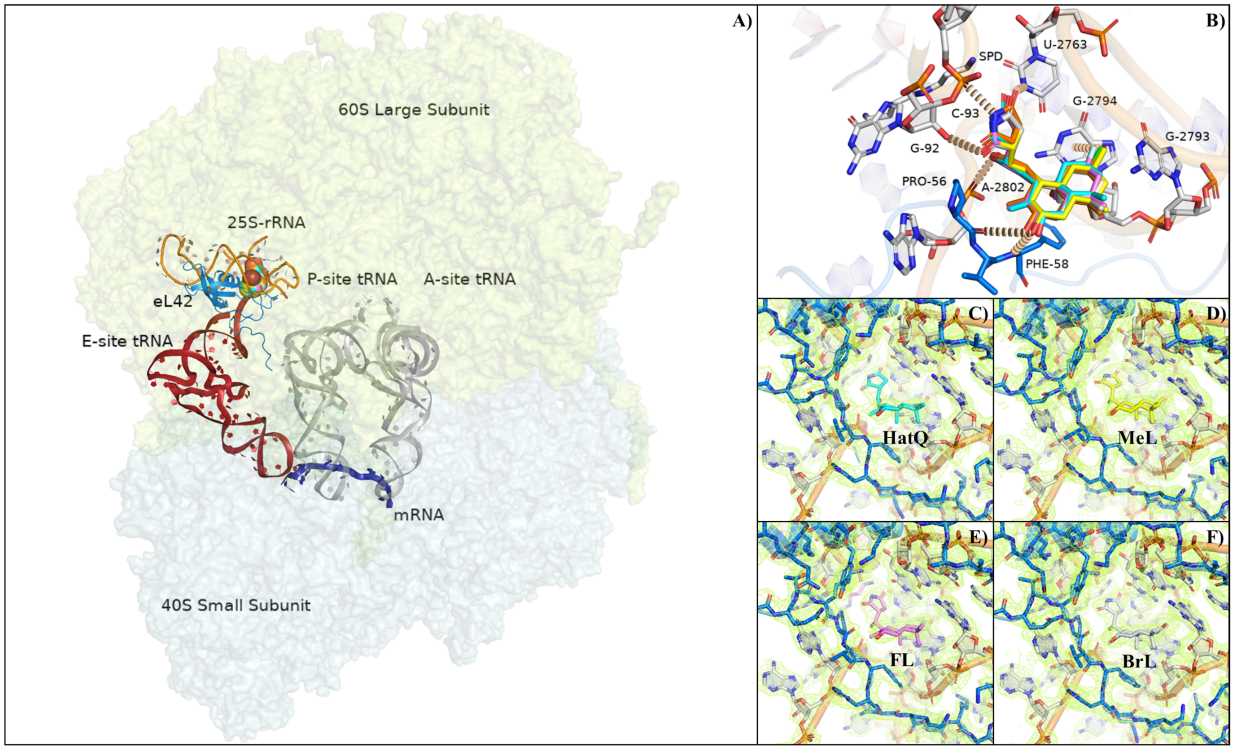


Figure 2.3 (a) Lissoclimides analogues bound within S. cerevisiae 80S yeast ribosome. (b) Details of the interactions of lissoclimide compounds in the binding pocket. (C-F) HatQ, MeL, FL, and BrL are located in the binding pocket of 80S ribosome.[13]

While exhibiting slight variations, their binding interactions shared three key features (**Figure 2.3b**). First, the hydroxy succinimide moiety formed hydrogen bonds with C-93, G-92, U-2763, and Pro-56 of ribosomal protein eL42. Second, a hydrogen bond formed between the C7 hydroxyl group and Phe-58 of eL42. Third, the C2 substituents engaged in halogen-π dispersion interactions with the guanine nucleobase G-2794. The distances between the C2 substituents and

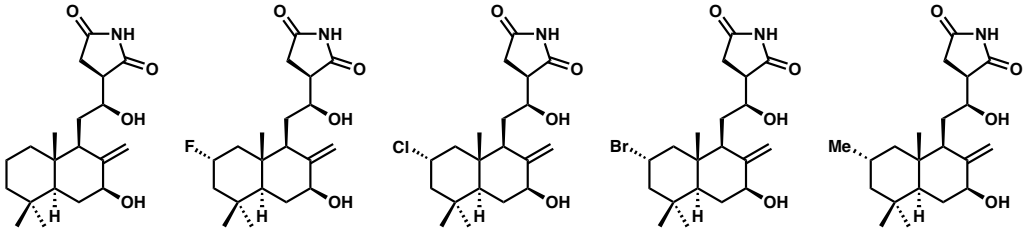
G-2794 were measured (**Figure 2.3c-f**). Due to the absence of a halogens at C2, a halogen-π interaction was not observed for hatQ (**2.1e**). The C2-halogen (methyl) bond length followed the trend F < Cl < Br = Me (3.1 Å, 3.4 Å, 3.6 Å, 3.6 Å, respectively), reflecting the increasing size of the halogen atoms. The lack of a heavy atom at C2 in hatQ (**2.1e**) positioned the decalin core closer to G2793 and G2794, resulting in a longer distance between the C7-OH group and eL42.

2.6 Biological Activities of Lissoclimide Analogues

To investigate the potential link between the observed ribosome binding interactions and biological activity, David Horne and colleagues at City of Hope assessed the anti-tumor activity of hatQ (**2.1e**), FL (**2.1a**), CL, BrL (**2.1b**), and MeL (**2.1c**) against melanoma (A2058) and prostate (DU145) cancer cell lines (**Figure 2.4a**).[13] The trend in anti-tumor activity was observed as follows: hatQ < MeL < BrL < FL < CL, indicating a possible correlation between the strength of the halogen-π interaction and cytotoxicity. However, CL displayed the most potent activity against both cancer cell lines. This finding suggests that the presence of the halogen-π interaction did not align consistently with computational modeling and cytotoxicity data. Although BrL, with its high polarizability, was expected to have the strongest halogen-π interaction, it was actually less cytotoxic compared to those of fluorine (F) and chlorine (Cl), and exhibited less anti-tumor activity. Additionally, the lack of a C2 substituent in hatQ resulted in the weakest anti-cancer effect. Furthermore, translation inhibition assays were performed by the Sachs using rabbit reticulocytes to corroborate the investigation (**Figure 2.4b**). CL and FL (**2.1a**) exhibited similar translation inhibitory activity, aligning with their potent anti-cancer effects and lowest IC_{50} values. Interestingly, MeL (**2.1c**) displayed translation inhibition comparable to BrL (**2.1b**), despite lacking a halogen-π interaction. This suggests that other factors beyond this specific interaction might contribute to MeL's activity. Finally, hatQ (**2.1e**) demonstrated the weakest ability to

suppress protein synthesis, further supporting the potential role of the halogen-π interaction in the mechanism of action.

a.



	hat Q: **2.1e**	FL: **2.1a**	CL	BrL: **2.1b**	MeL: **2.1c**
A2058 (μM)	1.2	0.17	0.029	0.24	0.68
DU145 (μM)	7.1	0.32	0.079	1.1	3.6

b.

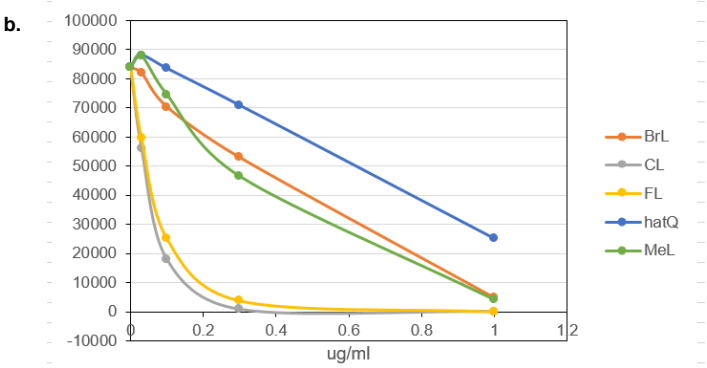


Figure 2.4 (a) Cytotoxicity of synthetic lissoclimides. (b)Translation-inhibitory activity of synthetic lissoclimides.[13]

2.7 Conclusions

Based on previous work demonstrating CL's potent protein suppression activity akin to known translation inhibitors like cycloheximide (CHX) and harringtonine[2], our collaborative studies identified a crucial halogen-π interaction between the C2-chloride of CL and amino acids within the 80S ribosomal E-site. Computational predictions suggested a trend of increasing binding interaction energy for C2-substituents in the order F < Cl < Br.[12] In this study, we synthesized FL, BrL, MeL, and 7-deoxygenated lissoclimide analogues to gain deeper insights into the binding modes of these C2-derivatives. The key synthetic step involved C–H functionalization of sclareolide using Alexanian's alkenylhydroxamate reagent, enabling the selective introduction of

the desired C2-halogenated sclareolide diastereomer. X-ray cocrystallography studies revealed the role of halogen-π interactions between synthetic lissoclimides and the eukaryotic ribosome. We observed that C2-bound heavy atoms (F, Cl, Br, Me) play a critical role in maintaining the distance between the lissoclimide and ribosomal protein eL42. Increasing size of halogen atoms was observed to diminish the length of halogen-π interactions in the sequence F < Cl < Br. Additionally, the hydroxy succinimide and C7-OH groups were, in every case, found to be essential for positioning FL, CL, BrL, MeL, and hatQ within the ribosomal pocket. While CL remained the most potent compound against A2058 and DU145 cancer cell lines, both CL and FL exhibited similar translation inhibition in rabbit reticulocyte assays. Interestingly, although the halogen-π interaction distances between C2-substituents and G-2794 did not directly correlate with overall biological activity (BrL not being the most bioactive), our findings significantly contribute to the understanding of how lissoclimide functional groups interact with the ribosome. Importantly, these results suggest that the halogen-π interaction is not the sole determinant of translation inhibitory activity within the lissoclimide family of compounds.

2.8 References

1. Uddin, J.; Ueda, K.; Siwu, E. R. O.; Kita, M.; Uemura, D. *Bioorg. Med. Chem*. **2006**, *14*, 6954–6961.
2. Konst, Z. A.; Szklarski, A. R.; Pellegrino, S.; Michalak, S. E.; Meyer, M.; Zanette, C.; Cencic, R.; Nam, S.; Voora, V. K.; Horne, D. A.; Pelletier, J.; Mobley, D. L.; Yusupova, G.; Yusupov, M.; Vanderwal, C. D. *Nat. Chem.* **2017**, *9*, 1140–1149.
3. Schmidt, V. A.; Quinn, R. K.; Brusoe, A. T.; Alexanian, E. J. *J. Am. Chem. Soc*. **2014**, *136*, 14389–14392.

4. Quinn, R. K.; Könst, Z. A.; Michalak, S. E.; Schmidt, Y.; Szklarski, A. R.; Flores, A. R.; Nam, S.; Horne, D. A.; Vanderwal, C. D.; Alexanian, E. J. *J. Am. Chem. Soc*. **2016**, *138*, 696–702.
5. Tierney, M. M.; Crespi, S.; Ravelli, D.; Alexanian, E. J. *J. Org. Chem*. **2019**, *84*, 12983–12991.
6. (a) Newhouse, T.; Baran, P.S. *Angew. Chem. Int. Ed*. **2011**, *50*, 3362–3374. (b) Chen, M. S.; White, M. C. *Science* **2010**, *327*, 566–571.
7. Select examples of 2-fluorination of sclareolide: (a) Liu, W.; Huang, X.; Cheng, M.-J.; Nielsen, R. J.; Goddard, W. A., III; Groves, J. T. *Science* **2012**, *337*, 1322–1325. (b) Halperin, S. D.; Fan, H.; Chang, S.; Martin, R. E.; Britton, R. *Angew. Chem., Int. Ed*. **2014**, *53*, 4690–4693. (c) Xia, J.-B.; Ma, Y.; Chen, C. *Org. Chem. Front*. **2014**, *1*, 468–472. (d) J.-B. Xia, C. Zhu and C. Chen, *Chem. Commun*., **2014**, *50*, 11701–11704. (e) Zhang, X.; Guo, S.; Tang, P. *Org. Chem. Front*. **2015**, *2*, 806–810. (f) S. Min, B. Park, J. Nedsaengtip, S. Hyeok Hong, *Adv. Synth. Catal*. **2022**, *364*, 1975–1981.
8. Fazekas, T. J.; Alty, J. W.; Neidhart, E. K.; Miller, A. S.; Leibfarth, F. A.; Alexanian, E. J. *Science* **2022**, *375*, 545–550.
9. Smith, R. T.; Zhang, X.; Rincón, J. A.; Agejas, J.; Mateos, C.; Barberis, M.; García-Cerrada, S.; de Frutos, O.; MacMillan, D. W. C. *J. Am. Chem. Soc*. **2018**, *140*, 17433–17438.
10. Pak, B. S. PhD Dissertation, University of California, Irvine, 2023.
11. Kawamata, Y.; Yan, M.; Liu, Z.; Bao, D-H.; Chen, J.; Starr, J. T.; Baran, P. S. *J. Am. Chem. Soc.* **2017**, *139*, 7448–7451.
12. Pak, B. S.; Supantanapong, N.; Vanderwal, C. D. *Acc. Chem. Res*. **2021**, *54*, 1131–1142.

13. (4) Terrosu, S.; Nurullina, L.; Supantanapong, N.; Pak, B. S.; Nguyen, S.; Holm, M.; Wu, C.; Lin, M; Horne, D. A.; Sachs, M.; Blanchard, S. C.; Yusupov, M.; Vanderwal, C. D. *Manuscript in preparation.*

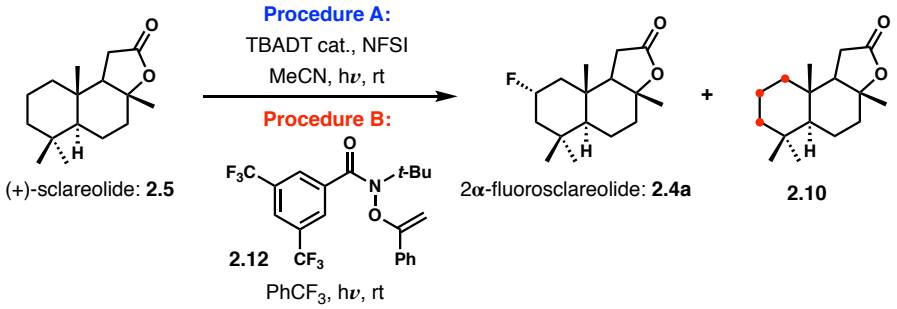
2.9 Experimental Information

2.9.1 General Experimental Method

All reactions were performed in oven–dried or flame–dried glassware under an atmosphere of dry argon unless otherwise noted. Reaction solvents including dichloromethane (CH_2Cl_2, Fisher, HPLC Grade), hexanes (Fisher, HPLC Grade), diethyl ether (Et_2O, Fisher, BHT stabilized, HPLC Grade), benzene (C_6H_6, Fisher, HPLC Grade), tetrahydrofuran (THF, Fisher, HPLC Grade), and toluene ($PhCH_3$, Fisher, HPLC Grade), methanol (MeOH, Fisher, low water Grade) were dried by percolation through a column packed with neutral alumina and a column packed with Q5 reactant, a supported copper catalyst for scavenging oxygen, under a positive pressure of argon. Solvents for workup and chromatography were: hexanes (Fisher or EMD, ACS Grade), EtOAc (Fisher, ACS Grade), dichloromethane (CH_2Cl_2, Fisher, ACS Grade), diethyl ether (Fisher, ACS Grade), methanol (MeOH, Fisher). Argon gas (5.0 grade, AR 5.0UH-T, Praxair) was dispensed from size T cylinders. Column chromatography was performed using EMD Millipore 60 Å (0.040–0.063 mm) mesh silica gel (SiO_2). Analytical and preparatory thin-layer chromatography was performed on Merck silica gel 60 F254 TLC plates. Visualization was accomplished with UV (254 or 210 nm), and *p*-anisaldehyde, potassium permanganate, or ceric ammonium molybdate stain solutions and heat as developing agents. Chloroform-d ($CDCl_3$, D 99.8%, DLM-7) was purchased from Cambridge Isotope Laboratories. K_2CO_3 (anhydrous, 99%, Alfa Aesar), $NaHCO_3$ (ACS grade, Fisher), NaOH (ACS grade, Macron or Fisher), $Na_2S_2O_3$ (ACS grade, Fisher), triethylamine (Et_3N, EMD, CaH_2) and pyridine (Alfa Aesar, CaH_2), were distilled from the indicated drying agents prior to use. Proton and carbon magnetic resonance spectra (^{1}H NMR and ^{13}C NMR) were recorded at 298 K on a Bruker CRYO500 (500 MHz, ^{1}H; 125 MHz, ^{13}C) spectrometer with solvent resonance as the internal standard (^{1}H NMR: $CHCl_3$ at 7.26 ppm, ^{13}C NMR: $CDCl_3$ at 77.16 ppm).

^{1}H NMR data are reported as follows: chemical shift, multiplicity (app = apparent, s = singlet, d = doublet, t = triplet, q = quartet, dd = doublet of doublets, ddd = doublet of doublet of doublets, dddd = doublet of doublet of doublet of doublets, dtt = doublet of triplet of triplets, td = triplet of doublets, tdd = triplet of doublet of doublets, qd = quartet of doublets, m = multiplet, br s = broad singlet), coupling constants (Hz), and integration. High resolution mass spectra (HRMS) were recorded on a Waters LCT Premier spectrometer using ESI-TOF (electrospray ionization-time of flight) and data are reported in the form of (m/z).

2.9.2 Experimental Procedures and Characterization Data



(3a*R*,5a*S*,8*S*,9a*S*)-8-Fluoro-3a,6,6,9a-tetramethyldecahydronaphtho[2,1-*b*]furan-2(1*H*)-one (**2.4a**): **Procedure A**: To a flame–dried vial containing sclareolide (**2.5**) (3.0 g, 12 mmol, 1.0 equiv), *N*-fluorobenzenesulfonimide (4.5 g, 14 mmol, 1.2 equiv), TBADT catalyst[1] (0.80 g, 0.20 mmol, 2.0 mol%), and $NaHCO_3$ (0.1 g, 1.2 mmol, 10 mol%) was added MeCN (6.0 mL). The reaction mixture was purged with argon for 10 minutes (using a balloon) and irradiated using two 390 nm lights at ambient temperature (cooled by a fan). After 34 hours, satd. aq. $NaHCO_3$ (40 mL) was added and the aqueous phase was extracted with CH_2Cl_2 (3 x 15 mL). The combined organic extracts were dried over Na_2SO_4 and concentrated *in vacuo*. The crude residue was purified by column chromatography (SiO_2, 40:8:1 hexanes/CH_2Cl_2/EtOAc and then 40:8:1.4 hexanes/EtOAc/CH_2Cl_2) to afford 2α-fluorosclareolide (**2.4a**) (1.0 g, 32% yield, *spectral data in*

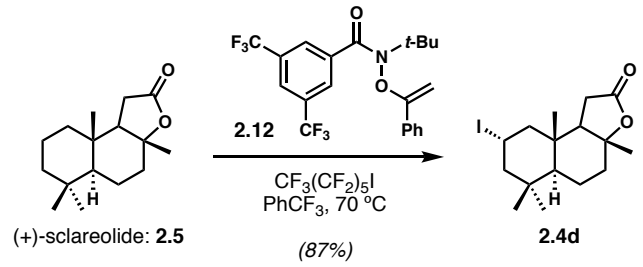
agreement with those reported in the literature[1]) as a white solid and separately a mixture of regio- and diastereomers of fluorosclareolide (**2.10**) (516.2 mg, 16% yield) as a white solid.

Procedure B: Prepared according to a known literature procedure[2], using sclareolide (**2.5**) (25 mg, 0.10 mmol, 1.0 equiv), *N*-fluorobenzenesulfonimide (86 mg, 0.20 mmol, 2.0 equiv), and vinylhydroxyamide reagent **2.12** (63 mg, 0.20 mmol, 2.0 equiv). The crude product was purified by flash column chromatography (SiO_2, 5% EtOAc in hexanes) to afford 2α-fluorosclareolide (**2.4a**) (13 mg, 48% yield, >20:1 *dr*) as a white solid.

^{1}H NMR (500 MHz, $CDCl_3$) δ 4.84 (dtt, J = 48.0, 11.3, 4.7 Hz, 1H), 2.45 (dd, J = 16.1, 14.8 Hz, 1H), 2.28 (dd, J = 16.1, 6.5 Hz, 1H), 2.11 (dt, J = 12.0, 3.3 Hz, 1H), 2.06 – 1.97 (m, 3H), 1.92 (ddt, J = 14.3, 3.9, 3.1 Hz, 1H), 1.71 (td, J = 12.6, 4.1 Hz, 1H), 1.43 – 1.36 (m, 2H), 1.34 (s, 3H), 1.19 (dd, J = 21.6, 10.8 Hz, 1H), 1.13 (dd, J = 12.7, 2.6 Hz, 1H), 1.00 (s, 3H), 0.96 (s, 3H), 0.90 (s, 3H).

^{13}C NMR (125 MHz, $CDCl_3$) δ 176.2, 87.8 (d, $J_{C\text{-}F}$ = 168.0 Hz), 86.0, 58.9, 56.2 (d, $J_{C\text{-}F}$ = 2.1 Hz), 48.0 (d, $J_{C\text{-}F}$ = 16.0 Hz), 45.4 (d, $J_{C\text{-}F}$ = 17.4 Hz), 38.5, 37.6 (d, $J_{C\text{-}F}$ = 11.9 Hz), 35.1 (d, $J_{C\text{-}F}$ = 12.3 Hz), 33.4, 28.8, 21.9, 21.8, 20.3, 16.3.

HRMS (ES+) m/z calc'd for $C_{16}H_{25}FO_2Na$ $[M+Na]^+$: 291.1736, found 291.1724.



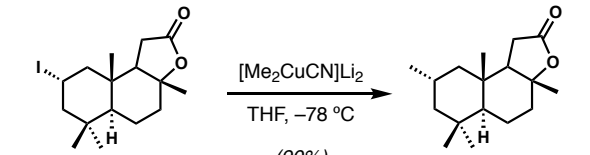
(3a*R*,5a*S*,8*S*,9a*S*,9b*R*)-8-iodo-3a,6,6,9a-tetramethyldecahydronaphtho[2,1-*b*]furan-2(1*H*)-one (**2.4d**): Prepared according to a known literature procedure[2], using sclareolide (**2.5**) (0.38 g,

1.5 mmol, 1.0 equiv), perfluorohexyl iodide (1.3 mL, 6.0 mmol, 4.0 equiv), and hydroxyamide reagent (**2.12**) (0.97 g, 2.3 mmol, 1.5 equiv), which was added degassed $PhCF_3$ (1.9 mL). The mixture was heated at 70 °C and stirred overnight. Then, the volatiles were removed *in vacuo* and the crude residue was purified by flash column chromatography (SiO_2, 8:1:1 Hexanes/EtOAc/CH_2Cl_2) to afford iodosclareolide (**2.4d**) (0.49 g, 87% yield, *spectral data in agreement with those reported in the literature*[2]) as a white solid.

^{1}H NMR (500 MHz, $CDCl_3$) δ 4.57 (tt, *J* = 12.7, 3.9 Hz, 1H), 2.41 (app tt, *J* = 15.4 Hz, 1H), 2.29 – 2.23 (m, 2H), 2.19 (app d, *J* = 12.1 Hz, 1H), 2.10 (app dt, *J* = 11.9, 3.1 Hz, 1H), 2.01 (dd, *J* = 14.7, 6.5 Hz, 1H), 1.95 – 1.86 (m, 2H), 1.78 – 1.67 (m, 2H), 1.39 – 1.30 (m, 4H), 1.19 (dd, *J* = 12.7, 2.5 Hz, 1H), 0.96 (s, 3H), 0.93 (s, 3H), 0.89 (s, 3H).

^{13}C NMR (125 MHz, $CDCl_3$) δ 176.1, 85.9, 58.5, 55.8, 55.7, 53.1, 39.8, 38.6, 37.7, 32.8, 28.7, 22.8, 21.8, 21.1, 20.6, 15.5.

HRMS (ES+) m/z calc'd for $C_{16}H_{25}IO_2Na$ $[M+Na]^+$: 399.0797, found 399.0797.



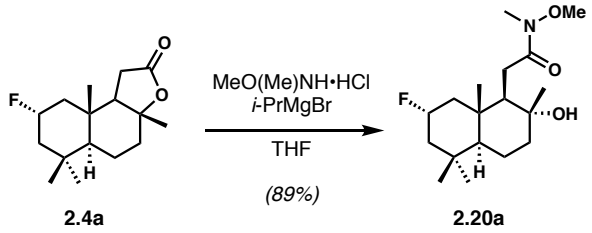
2α-iodosclareolide: **2.4d** methylsclareolide: **2.4c**

(3a*R*,5a*S*,8*S*,9a*S*,9b*R*)-3a,6,6,8,9a-pentamethyldecahydronaphtho[2,1-*b*]furan-2(1*H*)-one (**2.4c**): Prepared according to a known literature procedure[2], using iodosclareolide **2.4d** (10 mg, 0.03 mmol, 1.0 equiv), CuCN (24 mg, 0.27 mmol, 10 equiv), and methyllithium (1.2 M in Et_2O, 0.44 mL, 0.53 mmol, 20 equiv). The crude product was purified by flash column chromatography (SiO_2, 30% EtOAc in hexanes) to afford methylsclareolide (**2.4c**) (6.7 mg, 96%, *spectral data in agreement with those reported in the literature*[2]) as white crystals.

^{1}H NMR (500 MHz, $CDCl_3$) δ 2.41 (dd, *J* = 16.2, 14.8 Hz, 1H), 2.24 (dd, *J* = 16.2, 6.5 Hz, 1H), 2.08 (dt, *J* = 11.9, 3.3 Hz, 1H), 1.95 (dd, *J* = 14.8, 6.5 Hz, 1H), 1.89 (ddt, *J* = 14.3, 7.0, 3.0 Hz, 1H), 1.85 – 1.76 (m, 1H), 1.69 (td, *J* = 12.5, 4.2 Hz, 1H), 1.46 – 1.39 (m, 2H), 1.37 (app dd, *J* = 14.1, 3.6 Hz, 1H), 1.33 (s, 3H), 0.99 (dd, *J* = 12.6, 2.7 Hz, 1H), 0.92 (s, 3H), 0.89 (s, 3H), 0.87 (d, *J* = 6.4 Hz, 3H), 0.84 (s, 3H), 0.68 (t, *J* = 12.2 Hz,1H).

^{13}C NMR (125 MHz, $CDCl_3$) δ 177.0, 86.5, 59.3, 56.6, 51.6, 48.6, 38.8, 36.9, 33.9, 33.4, 28.9, 23.9, 22.7, 21.8, 21.7, 20.6, 16.0.

HRMS (ES+) m/z calc'd for $C_{17}H_{28}O_2$ $[M+Na]^+$: 287.1987, found 287.1984.



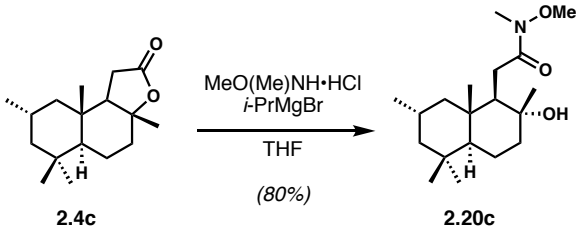
2.4a 2.20a

2-((1*R*,2*R*,4a*S*,7*S*,8a*S*)-7-fluoro-2-hydroxy-2,5,5,8a-tetramethyldecahydronaphthalen-1-yl)-*N*-methoxy-*N*-methylacetamide (**2.20a**): To a cooled (–40 °C) suspension of *N,O*-dimethylhydroxylamine hydrochloride (0.51 g, 5.2 mmol, 2.8 equiv) in THF (9.8 mL) was added *i*–PrMgBr (3.0 M in 2-methyltetrahydrofuran, 3.4 mL, 10 mmol, 5.4 equiv). After stirring for 15 minutes, lactone **2.4a** (0.50 g, 1.9 mmol, 1.0 equiv) in THF (2.5 mL) was added dropwise over 10 minutes while keeping the cooling bath temperature at –40 °C. The reaction mixture was stirred at –40 °C for 1 hour, slowly warmed to –10 °C and quenched with satd. aq. NH_4Cl (3 mL). After warming to ambient temperature, the phases were separated and the aqueous phase was extracted with EtOAc (3 x 20 mL). The combined organic extracts were dried over Na_2SO_4, filtered and concentrated *in vacuo.* The crude product was purified by flash column chromatography (SiO_2, 50% EtOAc in hexanes) to afford amide **2.20a** (0.55 g, 89%) as a white solid.

^{1}H NMR (500 MHz, $CDCl_3$) δ 4.77 (dtt, *J* = 48.3, 11.5, 4.6 Hz, 1H), 3.73 (s, 3H), 3.19 (s, 3H), 2.64 – 2.58 (m, 2H), 2.48 (dd, *J* = 16.8, 6.6, Hz, 1H), 2.07 – 2.05 (m, 2H), 1.96 (dt, *J* = 12.7, 3.2 Hz, 1H), 1.93 – 1.91 (m, 1H), 1.73 – 1.70 (m, 1H), 1.48 (td, *J* = 13.1, 3.8, Hz, 1H), 1.37 – 1.23 (m, 2H), 1.16 (s, 3H), 1.14 – 108 (m, 2H), 0.99 (s, 3H), 0.88 (s, 3H), 0.85 (s, 3H).

^{13}C NMR (125 MHz, $CDCl_3$) δ 175.7, 88.5 (d, $J_{C\text{-}F}$ = 166.6 Hz), 72.5, 61.3, 55.9, 55.3 (d, $J_{C\text{-}F}$ = 1.8 Hz), 47.5 (d, $J_{C\text{-}F}$ = 15.7 Hz), 45.1 (d, $J_{C\text{-}F}$ = 16.7 Hz), 44.1, 40.3 (d, $J_{C\text{-}F}$ = 11.2 Hz), 35.0 (d, $J_{C\text{-}F}$ = 12.2 Hz), 33.5, 27.0, 23.5, 22.3, 20.1, 16.8.

HRMS (ES+) m/z calc'd for $C_{18}H_{32}FNO_3Na$ $[M+Na]^+$: 352.2264, found 352.2277.



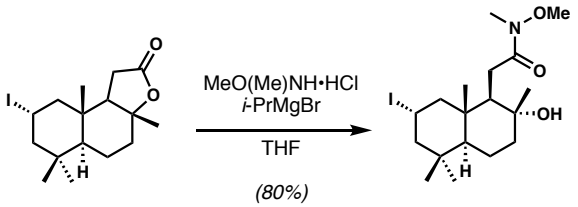
2.4c 2.20c

2-((1*R*,2*R*,4a*S*,7*S*,8a*S*)-2-hydroxy-2,5,5,7,8a-pentamethyldecahydronaphthalen-1-yl)-*N*-methoxy-*N*-methylacetamide (**2.20c**): Lactone **2.4c** (66 mg, 0.25 mmol, 1.0 equiv) was subjected to the reaction conditions described for the preparation of **2.19a**. The crude product was purified by flash column chromatography (SiO_2, 50% EtOAc in hexanes) to afford amide **2.20c** (64 mg, 80%) as a white solid.

^{1}H NMR (500 MHz, $CDCl_3$) δ 3.73 (s, 3H), 3.19 (s, 3H), 2.59 (app d, *J* = 16.4 Hz,1H), 2.49 – 2.44 (m, 2H), 1.96 – 1.92 (m, 2H), 1.75 – 1.68 (m, 2H), 1.51 (app d, *J* = 12.5 Hz, 1H), 1.45 (td, *J* = 13.0, 3.7 Hz, 1H), 1.37 (app d, *J* = 11.9 Hz, 1H), 1.27 (ddd, *J* = 26.0, 13.4, 3.1 Hz, 1H), 1.16 (s, 3H), 0.96 (dd, *J* = 12.2, 2.0 Hz, 1H), 0.88 (s, 3H),0.85 – 0.83 (m, 6H), 0.80 (s, 3H), 0.62 (t, *J* = 12.3 Hz, 1H).

^{13}C NMR (125 MHz, $CDCl_3$) δ 73.1, 61.4, 56.5, 55.7, 51.1, 48.4, 44.7, 39.4, 34.1, 33.6, 27.1, 24.1, 23.5, 23.0, 22.2, 20.6, 16.8.

HRMS (ES+) m/z calc'd for $C_{19}H_{35}NO_3Na$ $[M+Na]^+$: 348.2515, found 348.2531.



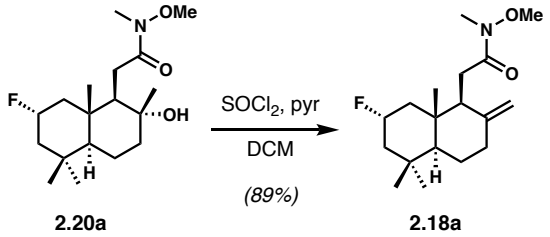
2.4d **2.20d**

2-((1*R*,2*R*,4a*S*,7*S*,8a*S*)-2-hydroxy-7-iodo-2,5,5,8a-tetramethyldecahydronaphthalen-1-yl)-N-methoxy-N-methylacetamide (**2.20d**): Lactone **2.4d** (50 mg, 0.13 mmol, 1.0 equiv) was subjected to the reaction conditions described for the preparation of **2.20a**. The crude product was purified by flash column chromatography (SiO_2, 80% EtOAc in hexanes to 100% EtOAc) to afford amide **2.20d** (47 mg, 80%) as a white solid.

^{1}H NMR (500 MHz, $CDCl_3$) δ 4.56 (tt, *J* = 12.8, 3.9 Hz, 1H), 3.74 (s, 3H), 3.21 (s, 3H), 2.54 (d, *J* = 16.8 Hz, 1H), 2.46 (dd, *J* = 16.4, 6.8 Hz, 1H), 2.31 (d, *J* = 12.3 Hz, 1H), 2.20 (ddd, *J* = 13.0, 3.8, 1.8 Hz, 1H), 2.01 (dd, *J* = 6.4, 3.7 Hz, 1H), 1.95 (dt, *J* = 12.7, 3.7 Hz, 1H), 1.89 (t, *J* = 13.0 Hz, 1H), 1.74 – 1.65 (m, 2H), 1.56 (br s, 1H), 1.46 (td, *J* = 13.0, 3.9 Hz, 1H), 1.28 – 1.20 (m, 1H), 1.16 – 1.12 (m, 4H), 0.92 (s, 3H), 0.88 (s, 3H), 0.84 (s, 3H).

^{13}C NMR (150 MHz, $CDCl_3$) δ 72.8, 61.4, 56.0, 55.4, 54.8, 53.1, 44.3, 42.6, 37.7, 33.0, 27.1, 25.4, 23.6, 21.6, 20.5, 16.2.

HRMS (ES+) m/z calc'd for $C_{18}H_{32}INO_3Na$ $[M+Na]^+$: 460.1325, found 460.1332.

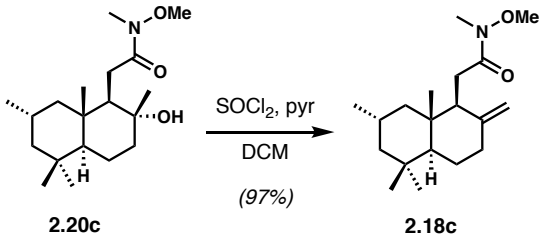


2-((1*S*,4a*S*,7*S*,8a*S*)-7-fluoro-5,5,8a-trimethyl-2-methylenedecahydronaphthalen-1-yl)-*N*-methoxy-*N*-methylacetamide (**2.18a**): To a solution of alcohol **2.20a** (95 mg, 0.29 mmol, 1.0 equiv) in CH_2Cl_2 (2.0 mL) was added pyridine (47 µL, 0.58 mmol, 2.0 equiv) and the resulting mixture was cooled to –78 °C. Then, a solution of $SOCl_2$ (0.1 mL, 1.4 mmol, 5.0 equiv) and pyridine (0.19 mL, 2.4 mmol, 8.3 equiv) in CH_2Cl_2 (3.0 mL) was added dropwise to the alcohol **2.20a** containing flask (over 10 minutes, at –78 °C). After stirring for 1 hour at –78 °C, the reaction was quenched with satd. aq. $NaHCO_3$ (3 mL) and warmed to ambient temperature. The phases were separated and the aqueous layer was extracted with CH_2Cl_2 (3 x 10 mL). The combined organic extracts were washed with brine, dried over $MgSO_4$, filtered and concentrated *in vacuo.* The crude product was purified by flash column chromatography (SiO_2, 10% EtOAc in hexanes) to afford exocyclic alkene **2.18a** (80 mg, 89%) as a white solid.

^{1}H NMR (500 MHz, $CDCl_3$) δ 4.79, 4.75 (dtt, *J* = 48.6, 11.6, 4.4 Hz, 1H), 4.49 (s, 1H), 3.37 (s, 3H), 3.16 (s, 3H), 2.74 (dd, *J* = 15.7, 10.3 Hz, 1H), 2.60 (app d, *J* = 10.8 Hz, 1H), 2.41 – 2.38 (m, 2H), 2.18 – 2.11 (m, 1H), 2.07 (dddd, *J* = 11.5, 6.9, 4.2, 2.1 Hz, 1H), 1.93 (dddd, *J* = 12.6, 6.5, 4.4, 2.2 Hz, 1H), 1.76 – 1.73 (m, 1H), 1.38 (dd, *J* = 22.1, 11.7 HZ, 1H), 1.35 – 1.26 (m, 3H), 0.99 (s, 3H), 0.87 (s, 3H), 0.78 (s, 3H).

^{13}C NMR (125 MHz, $CDCl_3$) δ 174.2, 148.5, 107.2, 89.1 (d, $J_{C\text{-}F}$ = 166.9 Hz), 61.5, 54.5 (d, $J_{C\text{-}F}$ = 2.1 Hz), 51.6, 47.7 (d, $J_{C\text{-}F}$ = 15.6 Hz), 45.0 (d, $J_{C\text{-}F}$ = 16.7 Hz), 40.6 (d, $J_{C\text{-}F}$ = 11.1 Hz), 37.3, 35.4 (d, $J_{C\text{-}F}$ = 12.0 Hz), 33.8, 27.4, 23.6, 22.8, 15.8.

HRMS (ES+) m/z calc'd for $C_{18}H_{30}FNO_2Na$ $[M+Na]^+$: 334.2158, found 334.2155.



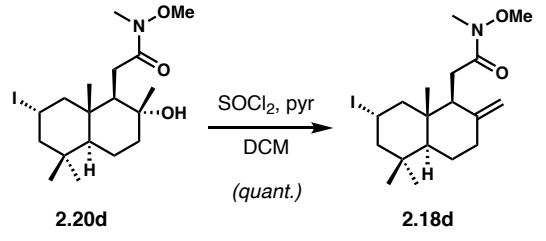
2.20c **2.18c**

***N*-methoxy-*N*-methyl-2-((1*S*,4a*S*,7*S*,8a*S*)-5,5,7,8a-tetramethyl-2-methylenedecahydronaphthalen-1-yl)acetamide** (**2.18c**): Alcohol **2.20c** (64 mg, 0.20 mmol, 1.0 equiv) was subjected to the reaction conditions described for the preparation of **2.18a**. The crude product was purified by flash column chromatography (SiO_2, 50% EtOAc in hexanes) to afford alkene **2.18c** (59 mg, 97%) as a colorless oil.

^{1}H NMR (500 MHz, $CDCl_3$) δ 4.74 (d, *J* = 1.1 Hz, 1H), 4.44 (s, 1H), 3.73 (s, 3H), 3.16 (s, 3H), 2.70 (dd, *J* = 15.6, 10.5 Hz, 1H), 2.49 (app d, *J* = 10.5 Hz, 1H), 2.44 – 2.37 (m, 2H), 2.14 (td, *J* = 13.1, 5.1 Hz, 1H), 1.74 (ddt, *J* =12.9, 5.3, 2.6 Hz, 1H), 1.71 – 1.16 (m, 1H), 1.55 (app d, *J* = 12.5 Hz, 1H), 1.38 (ddd, *J* = 13.1, 3.0, 2.0 Hz, 1H), 1.32 (qd, *J* = 13.0, 4.3 Hz, 1H), 1.18 (dd, *J* = 12.6, 2.6 Hz, 1H), 0.88 (s, 3H), 0.87 – 0.85 (m, 4H), 0.84 – 0.82 (m, 4H), 0.74 (s, 3H).

^{13}C NMR (125 MHz, $CDCl_3$) δ 149.8, 106.1, 61.5, 54.8, 51.9, 51.2, 48.1, 39.6, 37.7, 34.3, 33.8, 27.3, 24.8, 24.0, 23.2, 22.5, 15.6.

HRMS (ES+) m/z calc'd for $C_{19}H_{33}NO_2$ $[M+Na]^+$: 330.2409, found 330.2412.



2.20d **2.18d**

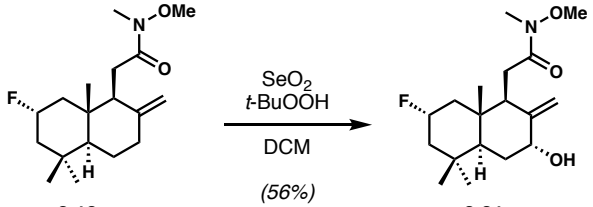
2-((1*S*,4a*S*,7*S*,8a*S*)-7-iodo-5,5,8a-trimethyl-2-methylenedecahydronaphthalen-1-yl)-*N*-methoxy-*N*-methylacetamide (**2.18d**): Alcohol **2.20d** (31 mg, 70 μmol, 1.0 equiv) was subjected

to the reaction conditions described for the preparation of **2.18a**. The crude product was purified by flash column chromatography (SiO_2, 30% EtOAc in hexanes) to afford alkene **2.18d** (30 mg, quant.) as a colorless oil.

^{1}H NMR (500 MHz, $CDCl_3$) δ 4.77 (d, *J* = 1.0 Hz, 1H), 4.55 (tt, *J* = 12.9, 3.8 Hz, 1H), 4.47 (s, 1H), 3.73 (s, 3H), 3.17 (s, 3H), 2.71 – 2.66 (m, 1H), 2.58 (d, *J* = 10.2 Hz, 1H), 2.41 – 2.33 (m, 2H), 2.22 (ddd, *J* = 13.1, 3.9, 2.1 Hz, 1H), 2.18 – 2.11 (m, 1H), 1.98 – 1.88 (m, 2H), 1.73 – 1.69 (m, 1H), 1.55 – 1.53 (m, 1H), 1.35 – 1.31 (m, 1H), 1.29 – 1.25 (m, 1H), 0.93 (s, 3H), 0.86 (s, 3H), 0.78 (s, 3H).

^{13}C NMR (125 MHz, $CDCl_3$) δ 176.1, 148.5, 107.1, 61.6, 55.6, 53.8, 52.8, 51.5, 42.8, 38.0, 37.3, 33.1, 27.3, 26.4, 23.9, 22.0, 15.0.

HRMS (ES+) m/z calc'd for $C_{18}H_{30}INO_2H$ $[M+H]^+$: 420.1400, found 420.1400.



2.18a **2.21a**

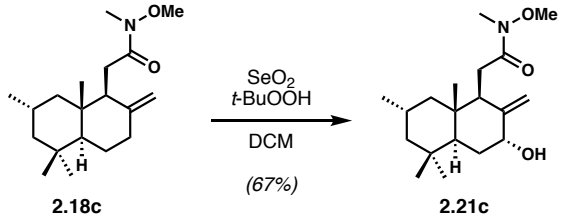
2-((1*R*,3*R*,4a*S*,7*S*,8a*S*)-7-fluoro-3-hydroxy-5,5,8a-trimethyl-2-methylenedecahydronaphthalen-1-yl)-*N*-methoxy-*N*-methylacetamide (**2.21a**): To an ice-cold solution of selenium dioxide (39 mg, 0.35 mmol, 0.60 equiv) in CH_2Cl_2 (5.5 mL) was added *t*-butyl hydroperoxide (5.5 M in nonane, 0.69 mL, 3.8 mmol, 6.5 equiv). After stirring at 0 ºC for 30 minutes, a solution of alkene **2.18a** (0.18 g, 0.58 mmol, 1.0 equiv) in CH_2Cl_2 (3.5 mL) was added dropwise and the reaction was allowed to room temperature. After 16 hours, satd. aq. Na_2SO_3 (5 mL) was added and the mixture was diluted with water (5 mL). The phases were separated and the aqueous layer was extracted with CH_2Cl_2 (3 x 20 mL). The combined organic extracts were washed

with brine, dried over $MgSO_4$, filtered and concentrated *in vacuo.* The crude product was purified by flash column chromatography (SiO_2, 50% EtOAc in hexanes to 100% EtOAc) to afford allylic alcohol **2.21a** (0.11 g, 56%) as a white foam.

^{1}H NMR (500 MHz, $CDCl_3$) δ 5.01 (s, 1H), 4.76 (dtt, *J* = 48.6, 11.6, 4.4 Hz, 1H), 4.61 (s, 1H), 4.37 (t, *J* = 2.7 Hz, 1H), 3.73 (s, 3H), 3.16 (s, 3H), 3.07 (app d, *J* = 10.8 Hz, 1H), 2.70 (dd, *J* = 15.6, 11.4 Hz, 1H), 2.44 (dd, *J* = 16.2, 3.2 Hz, 1H), 2.10 – 2.06 (m, 1H), 1.96 – 1.89 (m, 3H), 1.84 (dd, *J* = 13.2, 2.7 Hz, 1H), 1.51 – 1.34 (m, 3H), 1.00 (s, 3H), 0.87 (s, 3H), 0.76 (s, 3H).

^{13}C-NMR (125 MHz, $CDCl_3$) δ 173.9, 149.8, 110.4, 89.1 (d, $J_{C\text{-}F}$ = 167.1 Hz), 73.3, 61.5, 47.7 (d, $J_{C\text{-}F}$ = 15.6 Hz), 46.8 ($J_{C\text{-}F}$ = 2.1 Hz), 46.2, 44.7 ($J_{C\text{-}F}$ = 17.0 Hz), 40.8 ($J_{C\text{-}F}$ = 11.3 Hz), 35.0 ($J_{C\text{-}F}$ = 11.3 Hz), 33.5, 30.0, 27.0, 22.7, 14.9.

HRMS (ES+) m/z calc'd for $C_{18}H_{30}FNO_3Na$ $[M+Na]^+$: 350.2108, found 350.2108.



2.18c 2.21c

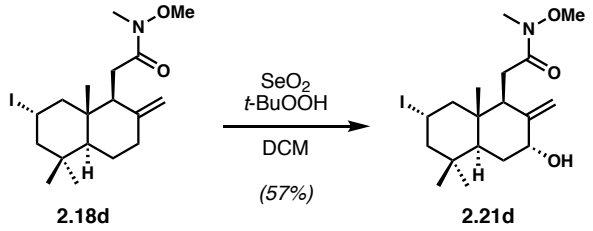
2-((1*R*,3*R*,4a*S*,7*S*,8a*S*)-3-hydroxy-5,5,7,8a-tetramethyl-2-methylenedecahydronaphthalen-1-yl)-*N*-methoxy-*N*-methylacetamide (**2.21c**): Alkene **2.18c** (13 mg, 40 μmol, 1.0 equiv) was subjected to the reaction conditions described for the preparation of **2.21a**. The crude product was purified by flash column chromatography (SiO_2, 50% EtOAc in hexanes to 100% EtOAc) to afford alcohol **2.21c** (9.4 mg, 67%) as a colorless oil.

^{1}H NMR (500 MHz, $CDCl_3$) δ 4.97 (s, 1H), 4.58 (s, 1H), 4.36 (t, *J* = 2.7 Hz, 1H), 3.73 (s, 3H), 3.16 (s, 3H), 2.96 (app d, *J* = 10.6 Hz, 1H), 2.66 (dd, *J* = 15.9, 10.9 Hz, 1H), 2.46 (dd, *J* = 16.1, 3.2 Hz, 1H), 1.91 (dt, *J* = 13.9, 2.6 Hz, 1H), 1.79 (br s, 1H), 1.73 – 1.65 (m, 2H), 1.56 – 1.49 (m,

2H), 1.41 (app dt, *J* = 13.0, 2.2 ,1H), 1.25 (app s, 1H), 0.90 (s, 3H), 0.87 (d, *J* = 6.5 Hz, 3H), 0.82 (s, 3H), 0.72 (s, 3H).

^{13}C NMR (125 MHz, $CDCl_3$) δ 174.6, 150.9, 109.5, 73.8, 61.5, 51.2, 47.8, 47.1, 46.5, 39.8, 33.8, 33.5, 30.4, 26.9, 24.9, 23.2, 22.4, 14.7.

HRMS (ES+) m/z calc'd for $C_{19}H_{33}NO_3H$ $[M+H]^+$: 324.2539, found 324.2523.



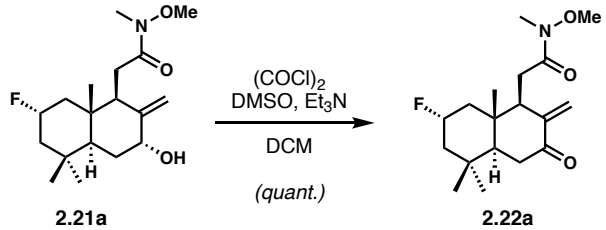
2.18d **2.21d**

2-((1*R*,3*R*,4a*S*,7*S*,8a*S*)-3-hydroxy-7-iodo-5,5,8a-trimethyl-2-methylenedecahydronaphthalen-1-yl)-*N*-methoxy-*N*-methylacetamide (**2.21d**): Alkene **2.18d** (30 mg, 70 µmol, 1.0 equiv) was subjected to the reaction conditions described for the preparation of **2.21a**. The crude product was purified by flash column chromatography (SiO_2, 80% EtOAc in hexanes to 100% EtOAc) to afford alcohol **2.21d** (18 mg, 57%) as a colorless oil.

^{1}H NMR (500 MHz, $CDCl_3$) δ 5.00 (s, 1H), 4.60 (s, 1H), 4.54 (t, *J* = 12.8, 3.7 Hz, 1H), 4.37 – 4.36 (m, 1H), 3.74 (s, 3H), 3.16 (s, 3H), 3.06 (d, *J* = 10.3 Hz, 1H), 2.68 – 2.62 (m, 1H), 2.41 – 2.34 (m, 2H), 2.25 – 2.22 (m, 1H), 2.01 – 1.85 (m, 5H), 1.50 – 1.43 (m, 1H), 0.94 (s, 3H), 0.86 (s, 3H), 0.76 (s, 3H).

^{13}C NMR (125 MHz, $CDCl_3$) δ 149.8, 110.3, 73.3, 61.6, 55.5, 52.5, 46.1, 46.0, 42.9, 37.5, 32.8, 30.3, 26.9, 26.1, 21.9, 14.1.

HRMS (ES+) m/z calc'd for $C_{18}H_{30}INO_3H$ $[M+H]^+$: 436.1349, found 436.1362.



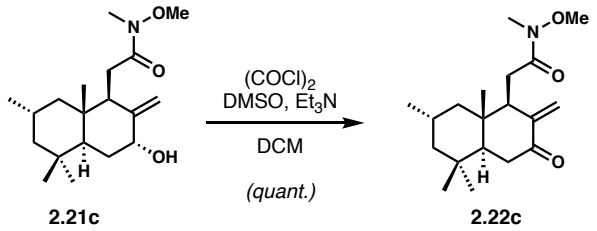
2.21a **2.22a**

2-((1*R*,4a*S*,7*S*,8a*S*)-7-fluoro-5,5,8a-trimethyl-2-methylene-3-oxodecahydronaphthalen-1-yl)-*N*-methoxy-*N*-methylacetamide (**2.22a**): Allylic alcohol **2.21a** (9.0 mg, 30 µmol, 1.0 equiv) was dried by azeotropic distillation from benzene (2 x 0.5 mL) and placed *in vacuo* for 30 minutes. Next, a flamed–dried round bottom flask containing oxalyl chloride (2.0 M in CH_2Cl_2, 40 µL, 70 µmol, 2.5 equiv) in CH_2Cl_2 (0.23 mL) was cooled to –78 °C. DMSO (10 µL, 0.14 mmol, 5.0 equiv) was added to this flask and the reaction was stirred at –78 °C for 30 minutes. Alcohol **2.21a** was dissolved in CH_2Cl_2 (0.46 mL) and added dropwise (over 10 minutes) to the solution of chloro(dimethyl)sulfonium chloride. The reaction was stirred at –78 °C for 1 hour and Et_3N (40 µL, 0.29 mmol, 10 equiv) was added dropwise. The suspension was slowly warmed to 0 °C and stirred for 50 minutes. The mixture was diluted with hexanes (0.14 mL) and sat. aq. NH_4Cl (0.14 mL) before warming to room temperature. Next, 1:1 EtOAc:Hexanes (0.54 mL) and water (0.54 mL) were added, the phases were separated and the aqueous layer was extracted with EtOAc (3 x 5.0 mL). The combined organic extracts were washed with brine, dried over Na_2SO_4, filtered and concentrated *in vacuo.* The crude product was purified by flash column chromatography (SiO_2, 50% EtOAc in hexanes) to afford ketone **2.22a** (9.0 mg, quant.) as a viscous colorless oil.

^{1}H NMR (500 MHz, $CDCl_3$) δ 6.00 (d, *J* = 2.5 Hz, 1H), 5.12 (d, *J* = 2.3 Hz, 1H), 4.79 (dtt, *J* = 48.3, 15.9, 4.3 Hz, 1H), 3.73 (s, 3H), 3.18 (s, 3H), 3.02 – 3.00 (m, 1H), 2.68 – 2.57 (m, 3H), 2.27 (dd, *J* = 17.9, 14.1 Hz, 1H), 2.17 – 2.15 (m, 1H), 2.03 – 1.97 (m, 1H), 1.71 (dd, *J* = 14.0, 4.6 Hz, 1H),1.43 (dd, *J* = 21.4, 11.8 Hz, 1H), 1.37 (dd, *J* = 16.5, 6.4 Hz, 1H), 0.98 (s, 3H), 0.93 (s, 3H), 0.89 (s, 3H).

^{13}C NMR (125 MHz, $CDCl_3$) δ 200.8, 147.0, 121.2, 88.3 (d, $J_{C\text{-}F}$ = 168.2 Hz), 61.6, 50.2 (d, $J_{C\text{-}F}$ = 1.9 Hz), 50.0, 47.4 (d, $J_{C\text{-}F}$ = 16.1 Hz), 44.6 (d, $J_{C\text{-}F}$ = 17.8 Hz), 39.1 (d, $J_{C\text{-}F}$ = 11.6 Hz), 37.6, 35.3 (d, $J_{C\text{-}F}$ = 12.1 Hz), 32.7, 29.2, 22.0, 15.6.

HRMS (ES+) m/z calc'd for $C_{18}H_{28}FNO_3Na$ $[M+Na]^+$: 348.1951, found 348.1950.



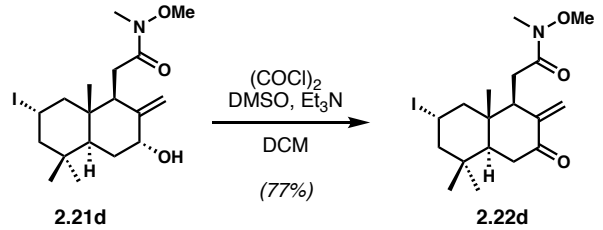
2.21c **2.22c**

***N*-methoxy-*N*-methyl-2-((1*R*,4a*S*,7*S*,8a*S*)-5,5,7,8a-tetramethyl-2-methylene-3-oxodecahydronaphthalen-1-yl)acetamide** (**2.22c**): Alcohol **2.21c** (22 mg, 70 μmol, 1.0 equiv) was subjected to the reaction conditions described for the preparation of **2.22a**. The crude product was purified by flash column chromatography (SiO_2, 30% EtOAc in hexanes) to afford ketone **2.22c** (22 mg, quant.) as a colorless oil.

^{1}H NMR (500 MHz, $CDCl_3$) δ 5.94 (d, *J* = 2.4 Hz, 1H), 5.05 (d, *J* = 2.2 Hz, 1H), 3.74 (s, 3H), 3.18 (s, 3H), 2.90 – 2.88 (m, 1H), 2.65 – 2.60 (m, 3H), 2.30 (dd, *J* = 17.8, 14.1 Hz, 1H), 1.79 – 1.69 (m, 1H), 1.66 – 1.59 (m, 2H), 1.46 (app d, *J* = 13.1 Hz, 1H), 0.91 – 0.87 (m, 11H), 0.85 (s, 3H).

^{13}C NMR (125 MHz, $CDCl_3$) δ 202.0, 173.8, 148.0, 120.1, 61.6, 50.7, 50.6, 50.4, 47.7, 38.1, 37.9, 34.3, 32.7, 29.1, 24.5, 23.0, 21.7, 15.3.

HRMS (ES+) m/z calc'd for $C_{19}H_{31}NO_3H$ $[M+H]^+$: 322.2382, found 322.2370.

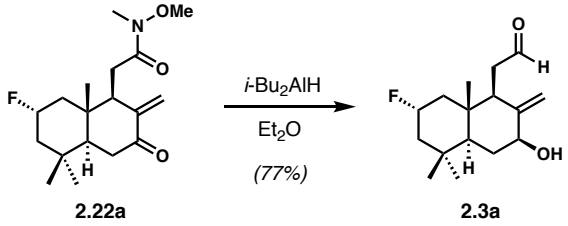


2.21d **2.22d**

2-((1*R*,4a*S*,7*S*,8a*S*)-7-iodo-5,5,8a-trimethyl-2-methylene-3-oxodecahydronaphthalen-1-yl)-*N*-methoxy-*N*-methylacetamide (**2.22d**): Alcohol **2.21d** (18 mg, 40 μmol, 1.0 equiv) was subjected to the reaction conditions described for the preparation of **2.22a**. The crude product was purified by flash column chromatography (SiO_2, 50% EtOAc in hexanes) to afford ketone **2.22d** (14 mg, 77%, 80% purity) as a colorless oil.

^{1}H NMR (500 MHz, $CDCl_3$) δ 5.98 (d, *J* = 2.3 Hz, 1H), 5.10 (d, *J* = 2.0 Hz, 1H), 4.52 (tt, *J* =12.9, 3.4 Hz, 1H), 3.75 (s, 3H), 3.20 (s, 3H), 3.00 – 2.98 (m, 1H), 2.63 – 2.56 (m, 2H), 2.50 – 2.42 (m, 2H), 2.31 – 2.22 (m, 2H), 2.00– 1.91 (m, 2H), 1.76 (dd, *J* = 13.9, 4.5 Hz, 1H), 0.93 – 0.92 (m, 6H), 0.89 (s, 3H).

HRMS (ES+) m/z calc'd for $C_{18}H_{28}INO_3H$ $[M+H]^+$: 434.1192, found 434.1202.



2.22a **2.3a**

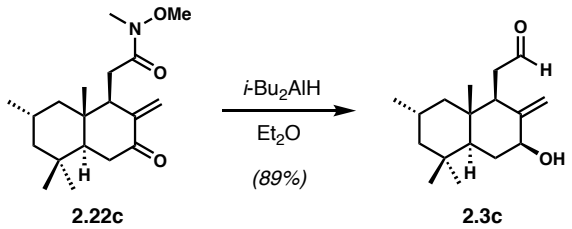
2-((1*R*,3*S*,4a*S*,7*S*,8a*S*)-7-fluoro-3-hydroxy-5,5,8a-trimethyl-2-methylenedecahydronaphthalen-1-yl)acetaldehyde (**2.3a**): Enone **2.22a** (80 mg, 0.24 mmol, 1.0 equiv) in an oven-dried round bottom flask was dried by azeotropic distillation from benzene (2 x 1 mL) and dissolved in Et_2O (4.9 mL). To the solution of enone **2.22a** in Et_2O was cooled to –78 °C and slowly added *i*-Bu_2AlH (1.0 M in toluene, 0.98 mL, 1.0 mmol, 4.0 equiv) along the side

of the flask (over 10 minutes). After stirring for 30 minutes, the reaction was slowly warmed to –40 °C and stirred at that temperature. After 1 hour, the reaction was warmed to –10 °C, diluted with EtOAc (2.5 mL) and quenched with NaOH (1.0 M in water, 2.5 mL) and water (2.5 mL). The biphasic solution was allowed to room temperature. The phases were separated and the aqueous layer was extracted with EtOAc (3 x 15 mL). The combined organic extracts were washed with brine, dried over Na_2SO_4, filtered and concentrated *in vacuo.* The crude product was purified by flash column chromatography (SiO_2, 20% EtOAc in hexanes) to afford alcohol **2.3a** (51 mg, 77%) as a white foam.

^{1}H NMR (500 MHz, $CDCl_3$) δ 9.67 (app d, J = 2.8 Hz, 1H), 5.25 (s, 1H), 4.77 (dtt, J = 48.3, 11.3, 4.3 Hz, 1H), 4.63 (s, 1H), 4.14 – 4.10 (m, 1H), 2.65 (ddd, J = 16.9, 11.0, 2.9 Hz, 1H), 2.50 (dd, J = 17.0, 3.6 Hz, 1H), 2.43 (app d, J = 10.8 Hz, 1H), 2.14 – 2.11 (m, 1H), 2.07 – 2.04 (m, 1H), 2.00 – 1.96 (m, 1H), 1.80 (br s, 1H),1.42 (d, J = 11.4 Hz, 1H), 1.37 (d, J = 11.8 Hz, 1H), 1.30 – 1.29 (m, 1H), 1.27 – 1.22 (m, 1H), 1.03 (s, 3H), 0.89 (s, 3H), 0.76 (s, 3H).

^{13}C-NMR (125 MHz, $CDCl_3$) δ 201.8, 149.5, 106.1, 88.6 (d, $J_{C\text{-}F}$ = 168.0 Hz), 73.2, 52.3 (d, $J_{C\text{-}F}$ = 2.1 Hz), 48.8, 47.6 (d, $J_{C\text{-}F}$ = 16.0 Hz), 45.1 (d, $J_{C\text{-}F}$ = 17.4 Hz), 40.2 (d, $J_{C\text{-}F}$ = 11.2 Hz), 39.7, 35.2 (d, $J_{C\text{-}F}$ = 12.1 Hz), 33.7, 32.8, 22.7, 15.6.

HRMS (ES+) m/z calc'd for $C_{16}H_{25}FO_2Na$ $[M+Na]^+$: 291.1736, found 291.1736.



2.22c **2.3c**

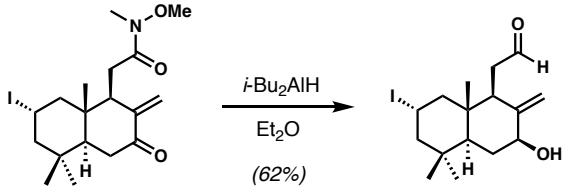
2-((1*R*,3*S*,4a*S*,7*S*,8a*S*)-3-hydroxy-5,5,7,8a-tetramethyl-2-methylenedecahydronaphthalen-1-yl)acetaldehyde (**2.3c**): Enone **2.22c** (22 mg, 70 µmol, 1.0 equiv) was subjected to the reaction

conditions described for the preparation of **2.3a**. The crude product was purified by flash column chromatography (SiO_2, 30% EtOAc in hexanes) to afford aldehyde **2.3c** (16 mg, 89%) as a colorless oil.

^{1}H NMR (500 MHz, $CDCl_3$) δ 9.65 (app d, *J* = 3.0 Hz, 1H), 5.20 (s, 1H), 4.59 (s, 1H), 4.10 (dd, *J* = 10.5, 5.0 Hz, 1H), 2.62 – 2.49 (m, 2H), 2.30 (dd, *J* = 10.6, 3.3 Hz, 1H), 2.14 (ddd, *J* = 12.0, 5.6, 2.1 Hz, 1H), 1.74 – 1.68 (m, 2H), 1.57 – 1.51 (m, 2H), 1.45 (app dd, *J* = 13.2, 2.0 Hz, 1H), 1.30 (dd, *J* = 24.2, 11.9 Hz, 1H), 1.20 (dd, *J* = 13.0, 2.0 Hz, 1H), 0.93 (s, 3H), 0.88 (d, *J* = 6.5 Hz, 3H), 0.84 (s, 3H), 0.74 – 0.69 (m, 4H).

^{13}C NMR (125 MHz, $CDCl_3$) δ 202.8, 150.6, 105.1, 73.6, 52.7, 51.1, 49.2, 48.2, 39.7, 39.4, 34.2, 33.7, 33.5, 24.9, 23.0, 22.4, 15.4.

HRMS (ES+) m/z calc'd for $C_{17}H_{28}O_2Na$ $[M+Na]^+$: 287.1987, found 287.1974.

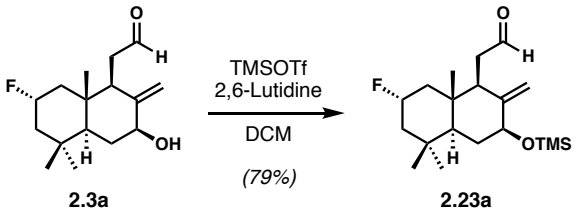


2-((1R,3S,4aS,7S,8aS)-3-hydroxy-7-iodo-5,5,8a-trimethyl-2-methylenedecahydronaphthalen-1-yl)acetaldehyde (**2.3d**): Enone **2.22d** (14 mg, 70 μmol, 1.0 equiv) was subjected to the reaction conditions described for the preparation of **2.3a**. The crude product was purified by flash column chromatography (SiO_2, 20% EtOAc in hexanes) to afford aldehyde **2.3d** (7.4 mg, 62%, 80% purity) as a colorless oil.

^{1}H NMR (500 MHz, $CDCl_3$) δ 9.66 (s, 1H), 5.23 (s, 1H), 4.21 (s, 1H), 4.51 (tt, *J* = 12.6, 3.7 Hz, 1H), 4.13 – 4.09 (m, 1H), 2.65 – 2.54 (m, 2H), 2.45 (dd, *J* = 17.0, 3.3 Hz, 1H), 2.40 – 2.38 (m,

1H), 2.33 – 2.25 (m, 1H), 2.27 – 2.25 (m, 1H), 2.10 (dd, J = 11.4, 4.4 Hz, 1H), 1.94 (t, J = 13.1 Hz, 2H), 1.79 (t, J = 12.5 Hz, 2H), 0.97 (s, 3H), 0.88 (s, 3H), 0.75 (s, 3H).

^{13}C NMR (125 MHz, $CDCl_3$) δ 201.7, 149.5, 106.0, 73.1, 55.4, 52.8, 51.7, 48.5, 42.2, 39.4, 37.7, 33.2, 33.0, 24.5, 21.9, 14.8.



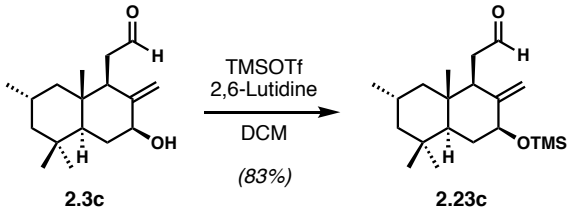
2.3a **2.23a**

2-((1*R*,3*S*,4a*S*,7*S*,8a*S*)-7-fluoro-5,5,8a-trimethyl-2-methylene-3-((trimethylsilyl)oxy)decahydro-naphthalen-1-yl)acetaldehyde (**2.23a**): A solution of alcohol **2.3a** (4.8 mg, 20 μmol, 1.0 equiv) in CH_2Cl_2 (0.3 mL) was cooled to –78 °C. Then, stock solutions of 2,6-lutidine (1.0 M in CH_2Cl_2, 107 μL, 0.11 mmol, 6.0 equiv) and TMSOTf (1.0 M in CH_2Cl_2, 90 μL, 90 μmol, 5.0 equiv) were added sequentially. The reaction was stirred at –78 °C for 1 hour and then Et_3N (40 μL) followed by MeOH (40 μL) were added. The mixture was warmed to room temperature then diluted with 10% EtOAc in hexanes (2 mL) and water (1 mL). The phases were separated and the aqueous layer was extracted with EtOAc (3 x 5 mL). The combined organic extracts were washed with brine, dried over $MgSO_4$, filtered and concentrated *in vacuo.* The crude product was purified by flash column chromatography (pH7 SiO_2, 5% EtOAc in hexanes) to afford aldehyde **2.23a** (5.0 mg, 79%, 90% pure) as a colorless oil.

^{1}H NMR (500 MHz, $CDCl_3$) δ 9.65 (app d, J = 2.7 Hz, 1H), 5.26 (s, 1H), 4.76 (dtt, J = 48.4, 11.4, 4.4 Hz, 1H), 4.59 (s, 1H), 4.03 – 4.01 (m, 1H), 2.65 – 2.59 (m, 1H), 2.46 (dd, J = 16.9, 3.5 Hz, 1H), 2.41 (app d, J = 10.8 Hz, 1H), 2.05 – 2.02 (m, 1H), 2.00 – 1.92 (m, 1H), 1.39 – 1.31 (m, 2H), 1.26 – 1.17 (m, 2H), 1.02 (s, 3H), 0.87 (s, 3H), 0.75 (s, 3H), 0.14 (s, 9H).

^{13}C NMR (125 MHz, $CDCl_3$) δ 202.0, 148.7, 107.2, 88.7 (d, $J_{C\text{-}F}$ = 167.8 Hz), 73.7, 52.4 (d, $J_{C\text{-}F}$ = 1.9 Hz), 49.0, 47.6 (d, $J_{C\text{-}F}$ = 15.9 Hz), 45.2 (d, $J_{C\text{-}F}$ = 17.2 Hz), 40.2 (d, $J_{C\text{-}F}$ = 11.1 Hz), 39.7, 35.1 (d, $J_{C\text{-}F}$ = 12.1 Hz), 33.7, 33.6, 22.7, 15.6, 0.03.

HRMS (ES+) m/z calc'd for $C_{19}H_{33}FO_2SiNa$ $[M+Na]^+$: 363.2132, found 363.2130.

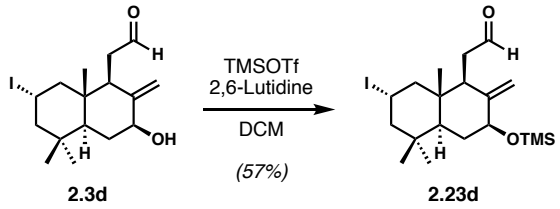


2-((1*R*,3*S*,4a*S*,7*S*,8a*S*)-5,5,7,8a-tetramethyl-2-methylene-3-((trimethylsilyl)oxy)decahydronaphthalen-1-yl)acetaldehyde (**2.23c**): Alcohol **2.3c** (9.5 mg, 40 μmol, 1.0 equiv) was subjected to the reaction conditions described for the preparation of **2.23a**. The crude product was purified by flash column chromatography (30% EtOAc in hexanes) to afford silyl enol ether **2.23c** (10 mg, 83%) as a colorless oil.

^{1}H NMR (500 MHz, $CDCl_3$) δ 9.63 (app d, *J* = 2.3 Hz, 1H), 5.22 (s, 1H), 4.55 (s, 1H), 4.02 (dd, *J* = 11.1, 5.5 Hz, 1H), 2.59 – 2.53 (m, 1H), 2.48 (dd, *J* = 16.7, 3.9 Hz, 1H), 2.27 (dd, *J* = 10.5, 3.6 Hz, 1H), 1.94 (ddd, *J* = 12.4, 5.4 , 2.4 Hz, 1H), 1.73 – 1.68 (m, 1H), 1.55 (app s, 1H), 1.51 (app d, *J* = 12.5 Hz, 1H), 1.44 (ddd, *J* = 13.2, 3.0, 2.0 Hz, 1H), 1.36 (td, *J* = 12.7, 11.3 Hz, 1H), 1.16 (dd, *J* = 13.0, 2.4 Hz, 1H), 0.91 (s, 3H), 0.88 (d, *J* = 6.5 Hz, 3H), 0.83 (s, 3H), 0.72 – 0.68 (m, 4H), 0.14 (s, 9H).

^{13}C NMR (125 MHz, $CDCl_3$) δ 203.1, 149.8, 106.2, 74.1, 52.8, 51.1, 49.4, 48.4, 39.8, 39.4, 34.2, 34.1, 33.6, 24.9, 23.1, 22.4, 15.4, 1.2.

HRMS (ES+) m/z calc'd for $C_{20}H_{36}O_2SiNa$ $[M+Na]^+$: 359.2382, found 359.2385.

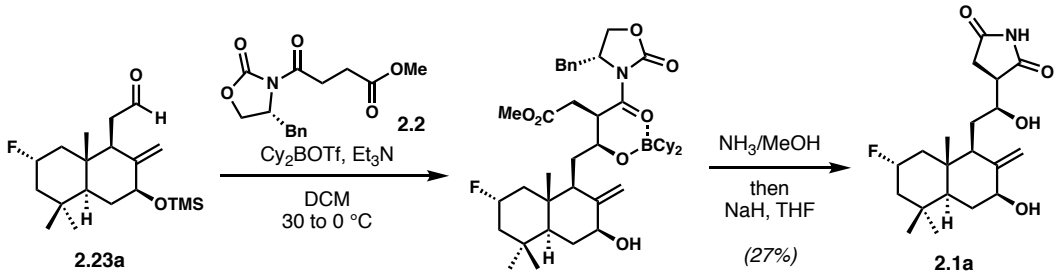


2-((1*R*,3*S*,4a*S*,7*S*,8a*S*)-7-iodo-5,5,8a-trimethyl-2-methylene-3-((trimethylsilyl)oxy)decahydronaphthalen-1-yl)acetaldehyde (**2.23d**): Alcohol **2.3d** (7.4 mg, 20 μmol, 1.0 equiv) was subjected to the reaction conditions described for the preparation of **2.23a**. The crude product was purified by flash column chromatography (30% EtOAc in hexanes) to afford silyl enol ether **2.23d** (5.0 mg, 57%, 90% pure) as a colorless oil.

^{1}H NMR (500 MHz, $CDCl_3$) δ 9.64 (d, *J* = 2.9 Hz, 1H), 5.25 (s, 1H), 4.57 (s, 1H), 4.51 (tt, *J* = 12.8, 3.9 Hz, 1H), 4.02 – 4.00 (m, 1H), 2.60 (ddd, *J* = 16.7, 11.0, 3.0 Hz, 1H), 2.42 (dd, *J* = 16.7, 3.4 Hz, 1H), 2.38 – 2.36 (m, 1H), 2.32 – 2.30 (m, 1H), 2.26 (ddd, *J* = 13.1, 3.6, 1.9 Hz, 1H), 1.93 (t, *J* = 10.7 Hz, 1H), 1.78 (t, *J* = 12.5 Hz, 1H), 0.95 (s, 3H), 0.87 (s, 3H), 0.74 (s, 3H), 0.13 (s, 12H).

^{13}C NMR (125 MHz, $CDCl_3$) δ 201.9, 148.7, 107.1, 73.6, 55.5, 53.0, 51.8, 48.7, 42.2, 39.5, 37.7, 34.0, 33.0, 24.8, 21.8, 14.8, 0.04.

HRMS (Cl+) m/z calc'd for C19H33IO2Si $[M+]^+$: 448.1295, found 448.1277.



(*R*)-3-((*S*)-2-((1*R*,3*S*,4a*S*,7*S*,8a*S*)-7-fluoro-3-hydroxy-5,5,8a-trimethyl-2-methylenedecahydronaphthalen-1-yl)-1-hydroxyethyl)pyrrolidine-2,5-dione (**2.1a**):

Oxazolidinone **2.2** (41 mg, 0.14 mmol, 2.2 equiv) was dried by azeotropic distillation from benzene (2 x 0.50 mL) and placed *in vacuo* for 30 minutes. CH_2Cl_2 (0.69 mL) was added under an argon atmosphere and the solution was cooled to 0 ºC. Then, Cy_2BOTf (1.0 M in CH_2Cl_2, 0.16 mL, 0.16 mmol, 2.5 equiv) was added dropwise and the resulting solution was stirred for 30 minutes. Et_3N (1.0 M in CH_2Cl_2, 0.23 mL, 0.22 equiv, 3.5 equiv) was added at 0 °C and the mixture was stirred for 30 minutes. Then, the reaction vial was cooled to –30 °C and aldehyde **2.23a** (22 mg, 64 µmol, 1.0 equiv) was added dropwise. The reaction was stirred for 35 minutes then warmed to 0 °C and stirred at that temperature for 42 hours. The resulting orange solution was treated with pH 7 buffer (0.5 mL) and MeOH (0.5 mL). The phases were separated and the aqueous phase was extracted with CH_2Cl_2 (3 x 5.0 mL). Combined organic extracts were dried over $MgSO_4$, and concentrated *in vacuo* to give crude aldol product as a yellow oil.

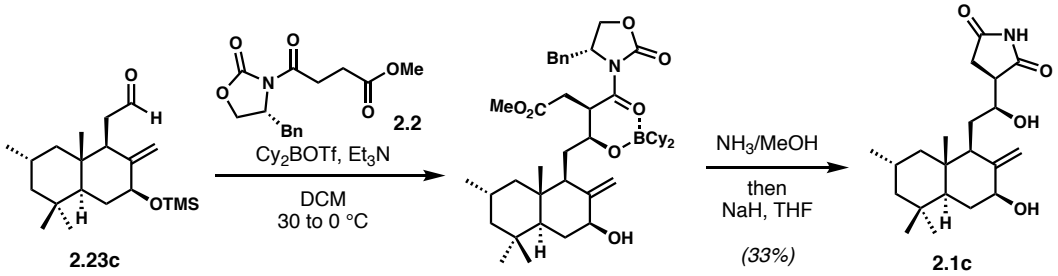
The crude aldol product was dried by azeotropic distillation from benzene (2 x 0.5 mL) and placed *in vacuo* for 30 minutes. A solution of NH_3 (2.0 M in methanol, 1.0 mL) was added to the vial containing the crude aldol product and the reaction was stirred at ambient temperature overnight. The solution was concentrated to dryness *in vacuo* and dried further by azeotropic distillation from benzene (2 x 0.5 mL). The resulting crude mixture was re-dissolved in THF (2.0 mL) and NaH (60% suspension in mineral oil, 21 mg, 0.51 mmol, 8.0 equiv) was added at ambient temperature. The reaction was stirred for 15 minutes, then treated with 1.0 M HCl (1.0 mL) followed by water (2.0 mL). The phases were separated and the aqueous phase was extracted with EtOAc (3 x 5.0 mL). The combined organic extracts were dried over $MgSO_4$, filtered and concentrated *in vacuo.* The crude product was purified by flash column chromatography (SiO_2, 8:1:1:1 toluene/EtOH/CH_2Cl_2/EtOAc) to give 90% pure product. This product was further purified

by preparative thin layer chromatography (8:4:1 EtOAc/Hexanes/CH_2Cl_2) to afford pure fluorolissoclimide (**2.1a**) (6.3 mg, 27%) as a white solid.

^{1}H NMR (600 MHz, $CDCl_3$) δ 8.43 (br s, 1H), 5.33 (s, 1H), 4.91 (s, 1H), 4.78 (dtt, *J* = 48.2, 11.4, 4.5 Hz, 1H), 4.32 (app t, *J* = 6.0 Hz, 1H), 4.01 (dd, *J* = 10.9, 5.3 Hz, 1H), 2.91 – 2.89 (m, 1H), 2.87 – 2.83 (m, 1H), 2.67 (dd, *J* = 17.8, 9.1 Hz, 1H), 2.18 – 2.17 (m, 1H), 2.11 (ddd, *J* = 12.0, 5.2, 1.8 Hz, 1H), 1.99 – 1.97 (m, 1H), 1.84 (ddd, *J* = 14.4, 11.0, 5.0 Hz, 1H), 1.64 – 1.60 (m, 1H), 1.36 (dd, *J* = 22.9, 11.6 Hz, 1H), 1.29 – 1.23 (m, 1H), 1.18 (dd, *J* = 13.0, 1.8 Hz, 1H), 1.07 (dd, *J* = 21.4, 11.3 Hz, 1H), 1.01 (s, 3H), 0.87 (s, 3H), 0.73 (s, 3H).

^{13}C NMR (150 MHz, $CDCl_3$) δ 179.6, 177.0, 149.6, 105.5, 88.8 (d, $J_{C\text{-}F}$ = 166.6 Hz), 73.5, 68.9, 52.7 (d, $J_{C\text{-}F}$ = 1.9 Hz), 51.7, 47.6 (d, $J_{C\text{-}F}$ = 15.8 Hz), 46.8, 44.9 (d, $J_{C\text{-}F}$ = 17.1 Hz), 41.0 (d, $J_{C\text{-}F}$ = 11.0 Hz), 35.2 (d, $J_{C\text{-}F}$ = 12.1 Hz), 33.7, 33.1, 29.5, 29.4, 22.6, 15.4.

HRMS (ES+) m/z calc'd for $C_{20}H_{30}FO_4Na$ $[M+Na]^+$: 390.2057, found 390.2054.



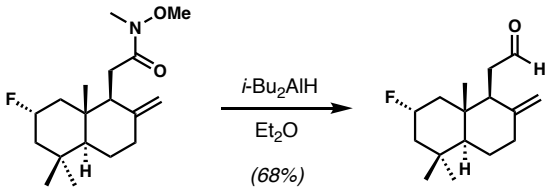
(*R*)-3-((*S*)-1-hydroxy-2-((1*R*,3*S*,4a*S*,7*S*,8a*S*)-3-hydroxy-5,5,7,8a-tetramethyl-2-methylenedecahydronaphthalen-1-yl)ethyl)pyrrolidine-2,5-dione (**2.1c**): Aldehyde **2.23c** (10 mg, 30 μmol, 1.0 equiv) was subjected to the reaction conditions described for the preparation of fluorolissoclimide **2.1a**. The crude product was purified by flash column chromatography (30% EtOAc in hexanes). This product was further purified by preparative thin layer chromatography

(8:1:1:1 toluene/EtOH/CH_2Cl_2/EtOAc) to afford methyllissoclimide **2.1c** (3.6 mg, 33%) as a white solid.

^{1}H NMR (500 MHz, $CDCl_3$) δ 8.26 (br s, 1H), 5.29 (s, 1H), 4.87 (s, 1H), 4.34 (t, *J* = 12.8 Hz, 1H), 3.99 (dd, *J* = 11.1, 5.2 Hz, 1H), 2.92 – 2.85 (m, 2H), 2.65 (dd, *J* = 16.9, 8.2 Hz, 1H), 2.13 – 2.10 (m, 1H), 1.83 – 1.77 (m, 1H), 1.76 – 1.69 (m, 1H), 1.67 – 1.63 (m, 2H), 1.60 (br s, 1H), 1.49 – 1.42 (m, 3H), 1.31 – 1.24 (m, 1H), 1.06 (dd, *J* = 12.9, 2.4 Hz, 1H), 0.90 (s, 3H), 0.89 (d, *J* = 6.5 HZ, 3H), 0.82 (s, 3H), 0.69 (s, 3H), 0.54 (t, *J* = 12.0 Hz, 1H).

^{13}C NMR (125 MHz, $CDCl_3$) δ 179.5, 176.9, 150.7, 104.5, 73.9, 69.1, 53.1, 52.1, 51.1, 48.2, 46.8, 40.2, 34.2, 33.8, 33.7, 29.5, 29.1, 24.9, 23.2, 22.3, 15.3.

HRMS (ES+) m/z calc'd for $C_{21}H_{33}NO_4$ $[M+Na]^+$: 386.2307, found 386.2309.



2.18a **S1**

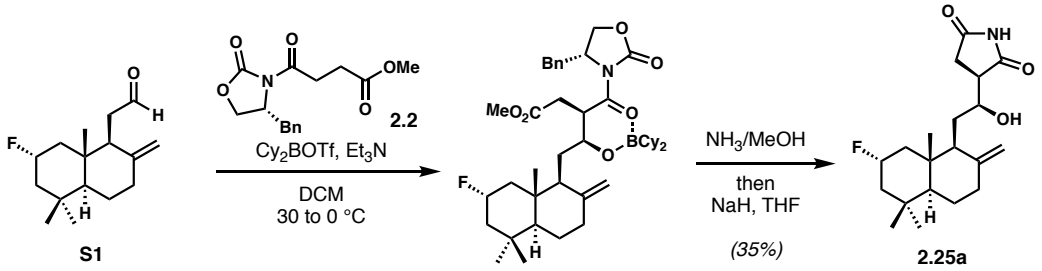
2-((1*S*,4a*S*,7*S*,8a*S*)-7-fluoro-5,5,8a-trimethyl-2-methylenedecahydronaphthalen-1-yl)acetaldehyde (**S1**): Amide **2.18a** (70 mg, 0.22 mmol, 1.0 equiv) was subjected to the reaction conditions described for the preparation of **2.3a**. The crude product was purified by flash column chromatography (SiO2, 10% EtOAc/Hexanes) to give the desired product of 90% purity. This product was further purified by preparative thin layer chromatography (18:1:1 Hexanes/EtOAc/CH_2Cl_2) to afford pure aldehyde **S1** (39 mg, 68%) as a colorless oil.

^{1}H NMR (500 MHz, $CDCl_3$) δ 9.65 (app d, *J* = 3.2 Hz, 1H), 4.88 (s, 1H), 4.76 (dtt, *J* = 48.5, 11.5, 4.4 Hz, 1H), 4.44 (s, 1H), 2.56 (ddd, *J* = 17.5, 12.0, 3.1 Hz, 1H), 2.47 – 2.42 (m, 3H), 2.13 – 2.04 (m, 2H), 1.96 (dddd, *J* = 12.1, 6.1, 4.7, 2.0 Hz, 1H), 1.77 (dddd, *J* = 12.7, 5.5, 2.7, 2.3 Hz, 1H),

1.39 (dd, J = 22.3, 11.6 Hz, 1H), 1.33 (dd, J = 12.8, 4.2 Hz, 1H), 1.29 – 1.23 (m, 2H), 1.00 (s, 3H), 0.88 (s, 3H), 0.76 (s, 3H).

^{13}C NMR (125 MHz, $CDCl_3$) δ 202.6, 147.3, 109.4, 88.8 (d, $J_{C\text{-}F}$ = 167.4 Hz), 54.7 (d, $J_{C\text{-}F}$ = 2.0 Hz), 50.8, 47.7 (d, $J_{C\text{-}F}$ = 15.7 Hz), 45.3 (d, $J_{C\text{-}F}$ = 17.0 Hz), 40.5 (d, $J_{C\text{-}F}$ = 11.1 Hz), 39.9, 37.2, 35.4 (d, $J_{C\text{-}F}$ = 12.0 Hz), 33.8, 23.4, 22.8, 15.6.

HRMS (Cl+) m/z calc'd for $C_{16}H_{25}FONa$ $[M+NH_4]^+$: 270.2233, found 270.2220.



(*R*)-3-((*S*)-2-((1*S*,4a*S*,7S,8a*S*)-7-fluoro-5,5,8a-trimethyl-2-methylenedecahydronaphthalen-1-yl)-1-hydroxyethyl)pyrrolidine-2,5-dione (**2.25a**): Aldehyde **S1** (12 mg, 50 μmol, 1.0 equiv) was subjected to the reaction conditions described for the preparation of fluorolissoclimide (**2.1a**). The crude product was purified by flash column chromatography (SiO_2, 5:5:1 Hexanes/EtOAc/CH_2Cl_2) to afford C7–deoxy–fluorolissoclimide **2.25a** (5.9 mg, 35%) as a white solid.

^{1}H NMR (500 MHz, $CDCl_3$) δ 7.98 (br s, 1H), 4.98 (s, 1H), 4.84 – 4.68 (m, 2H), 4.36 (t, J = 6.2 Hz, 1H), 2.93 – 2.85 (m, 2H), 2.68 (dd, J = 17.1, 8.5 Hz, 1H), 2.47 – 2.43 (m, 1H), 2.22 – 2.17 (m, 1H), 2.04 – 2.00 (m, 1H), 1.98 – 1.93 (m, 1H), 1.79 – 1.73 (m, 2H), 1.69 (app d, J = 10.8 Hz, 1H), 1.63 – 1.59 (m, 2H), 1.34 – 1.27 (m, 2H), 1.14 – 1.07 (m, 2H), 0.99 (s, 3H), 0.86 (s, 3H), 0.74 (s, 3H).

^{13}C NMR (125 MHz, $CDCl_3$) δ 178.9, 176.5, 147.8, 108.8, 88.9 (d, $J_{C\text{-}F}$ = 167.4 Hz), 69.4, 55.2 (d, $J_{C\text{-}F}$ = 1.5 Hz), 53.8, 47.7 (d, $J_{C\text{-}F}$ = 15.7 Hz), 46.9, 45.2 (d, $J_{C\text{-}F}$ = 16.8 Hz), 41.5 (d, $J_{C\text{-}F}$ = 10.8 Hz), 38.0, 35.4 (d, $J_{C\text{-}F}$ = 12.0 Hz), 33.8, 29.6, 29.5, 23.8, 22.7, 15.4.

HRMS (ES+) calculated for $C_{20}H_{30}FNO_3Na$ $[M+Na]^+$: 374.2108, found 374.2123.

2.9.3 Supplemental References

1. Halperin, S. D.; Fan, H.; Chang, S.; Martin, R. E.; Britton, R. *Angew. Chem. Int. Ed*. **2014**, *53*, 4690–4693.
2. Fazekas, T. J.; Alty, J. W.; Neidhart, E. K.; Miller, A. S.; Leibfarth, F. A.; Alexanian, E. J. *Science* **2022**, *375*, 545–550.
3. Lipshutz, B. H.; Wilhelm, R. S.; Floyd, D. M. *J. Am. Chem. Soc.* **1981**, *103*, 7672– 7674.

CHAPTER 3 INTRODUCTION TO BRASILICARDIN NATURAL PRODUCTS

3.1 Isolation and Structure Determination of Brasilicardin A

Brasilicardin A (BraA) (**3.1**) is a tricyclic terpenoid that was isolated from *Nocardia brasiliensis* IFM-0406, a pathogenic actinomycete strain, by Kobayashi *at al.* in 1996 (**Figure 3.1**).[1] Mikami and co-workers reported the fermentation of this bacteria to produce BraA (**3.1**) at 60 mg/liter, as detected by HPLC.[2] Brasilicardins B-D (**3.2-3.4**) were also isolated alongside BraA (**3.1**) by Kobayashi *et al*.[3]

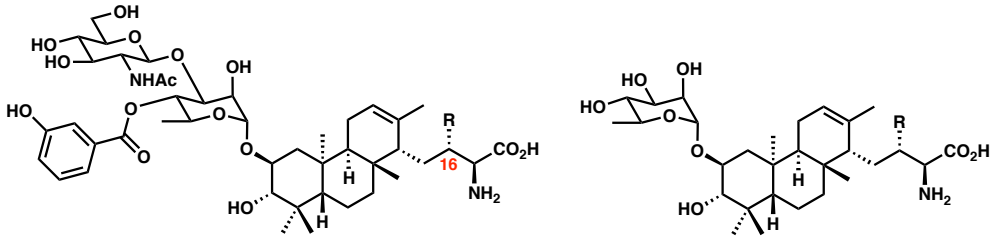
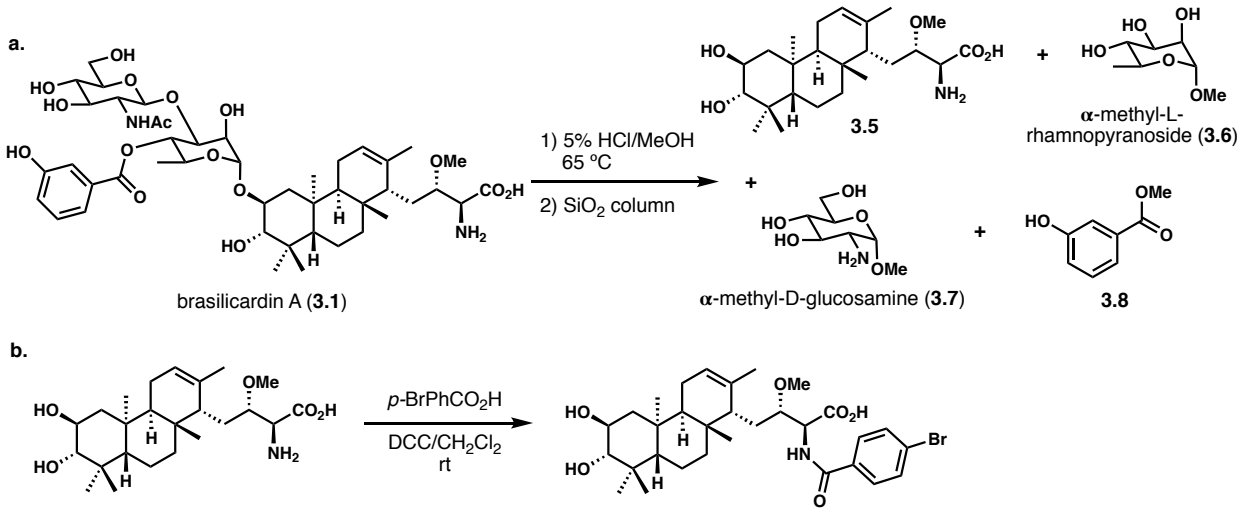


Figure 3.1 BraA (**3.1**) and three congeners, brasilicardin B-D (**3.2-3.4**).

The chemical structure of BraA (**3.1**), characterized by the Kobayashi group, features an unusual *trans/syn/trans*-perhydrophenanthrene skeleton with an amino acid side chain as well as a rhamnose/*N*-acetylglucosamine disaccharide motif (**Figure 3.1a**).[4] Kobayashi and co-workers elucidated the structure of this perhydrophenanthrene core using ^{1}H, ^{13}C and 2D NMR spectroscopy. BraA (**3.1**) underwent methanolysis to afford aglycone **3.5**, methyl α-methyl-L-rhamnopyranoside (**3.6**), methyl α-methyl-D-glucosamine (**3.7**), and methyl 3-hydroxybenzoate (**3.8**) fragments. GC-MS and amino acid analysis were used to identify L-rhamnose (**3.6**) and glucosamine (**3.7**). Optical rotation was used to assign the absolute configurations of compounds **3.6** and **3.7**. Finally, aglycone **3.5** was derivatized to *p*-bromobenzoyl derivative **3.9** for X-ray crystallographic analysis (**Scheme 3.1b**).

Scheme 3.1 (a) Methanolysis of BraA (**3.1**).[4] (b) *p*-bromobenzoyl derivative **3.9**.



3.2 Biological Activity of Brasilicardin A

Mikami *et al.* first investigated the immunosuppressive activity of BraA (**3.1**) using a mixed lymphocyte reaction (MLR) assay in mice.[2] BraA (**3.1**) significantly suppressed the proliferation of mouse lymphocytes with an IC_{50} value of 0.057 μg/ml. This effect was more potent compared to cyclosporin A[5] (IC_{50} = 0.15 μg/ml), a widely used immunosuppressant for organ transplantation. Subsequently, Mikami and co-workers explored the mechanism of action of BraA (**3.1**), specifically whether it inhibited interleukin 2 (IL-2) signaling, a pathway known to be targeted by cyclosporin A. Interestingly, BraA (**3.1**) did not suppress IL-2 expression, but rather slowed the rate of lymphocyte proliferation. Surprisingly, at a concentration of 0.25 μg/ml, BraA (**3.1**) increased cell production.

Mikami *et al*. also evaluated the *in vitro* cytotoxicity of BraA (**3.1**) against various cell lines.[2] The observed toxicity ranged from 5.6 to 100 μg/ml, depending on the cell type, and was comparable to that of cyclosporin A, another clinically important immunosuppressant. Notably, BraA (**3.1**) exhibited low toxicity in mice at a dose of 100 mg/kg, which was lower than the LD_{50}

of cyclosporin A (107 mg/kg)[6]. Furthermore, they found that BraA (**3.1**) lacked antimicrobial and antifungal activity against gram-positive and gram-negative bacteria, fungi, and yeast. Interestingly, among various cell lines, BraA (**3.1**) displayed selective cytotoxicity against P388 leukemia cells resistant to adriamycin (P388/ADR), with an IC_{50} value of 0.078 μg/ml, which was more potent than adriamycin (IC_{50} = 1.0 μg/ml).[7] A preliminary study by Kobayashi *et al.* suggested that BraA (**3.1**) inhibits P388 cells by promoting G1-phase cell cycle arrest, ultimately leading to apoptosis.

Kobayashi and co-workers investigated the structure-activity relationships (SARs) between brasilicardin A-D (**3.1**-**3.4**) with respect to immunosuppressive activity and cytotoxicity against murine lymphoma L1210 cells (**Table 3.1**).[8] They compared the inhibitory effects of brasilicardin B-D (**3.2**-**3.4**) on mouse lymphocyte proliferation to those of previously reported BraA (**3.1**) and cyclosporin A. BraA (**3.1**) exhibited the most potent immunosuppressive activity among the tested compounds, including cyclosporin A. The absence of the C16 methoxy group, *N*-acetylglucosamine, and/or benzoyl moieties in brasilicardin B-D (**3.2**-**3.4**) resulted in diminished immunosuppressive activity in mouse mixed lymphocyte reaction (MLR) assay. Brasilicardin D (**3.4**) lacked immunosuppressive activity altogether (IC_{50} >10 g/ml). The methoxy group C16 appeared to be critical for the cytotoxicity of BraA (**3.1**) and its congeners, as brasilicardin B (**3.2**) and D (**3.4**) displayed no cytotoxicity against L1210 cells.

Table 3.1 Mixed lymphocyte reaction (MLR) inhibitory and *in vitro* cytotoxic activity against L1210 cells of brasilicardin A-D in comparison with cyclosporin A.[8]

Compounds	IC_{50} (μg/mL)	
	MLR	L1210
3.1	0.057	1.2
3.2	2.5	>10
3.3	2.5	7.8
3.4	>10	>10
Cyclosporin A	0.15	Not tested

Kobayashi next investigated the effects of modifying the amino acid of BraA (**3.1**) with various substituents, such as methyl (**3.10**) and benzyl (**3.11**) groups (**Figure 3.2**).[9] The immunosuppressive activity in a MLR assay and the cytotoxicity of these compounds against eight cancer cell lines were then evaluated. BraA (**3.1**) exhibited the greatest cytotoxicity among the tested derivative. The bulky benzyl group in compound **3.11** significantly reduced its cytotoxicity. Only compound **3.10** displayed higher inhibitory activity of mouse MLR and cytotoxicity than BraA (**3.1**) against human colon adenocarcinoma (DLD-1) and human lung non-small cell carcinoma (Lu65). Finally, derivatives lacking the glucosamine and benzoate moieties (**3.12** and **3.13**) showed no immunosuppressive activity and low cytotoxicity against cancer cell lines.

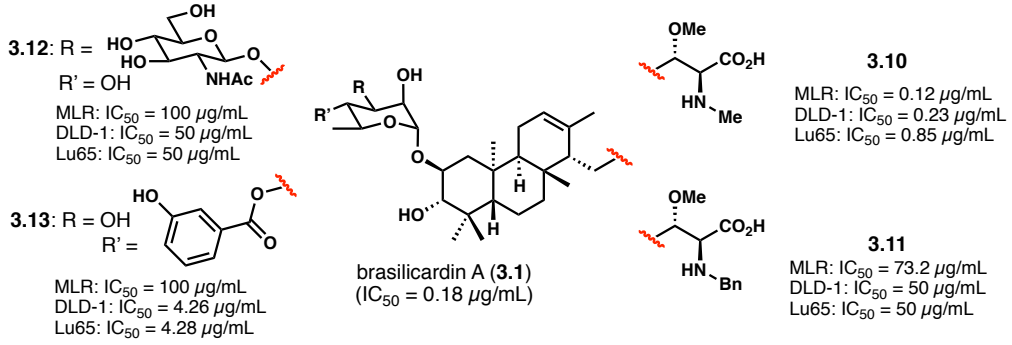


Figure 3.2 Inhibition of mouse MLR of brasilicardin derivatives.[9]

BraA (**3.1**) was previously reported to exhibit immunosuppressive activity distinct from cyclosporin A. To understand the mechanism by which BraA (**3.1**) suppresses the immune system in a MLR assay, Usui *et al.* investigated its molecular target for inducing G_1 cell cycle arrest in a mouse T cell lymphoma cell line.[10] They discovered that BraA (**3.1**) utilizes an amino acid to interact with the substrate binding site of system L. The amino acid transporter system L is a plasma membrane protein responsible for the cellular uptake of large neutral amino acids possessing branched or aromatic side chains. Inhibition of system L disrupts amino acid metabolism and arrests cell cycle progression, particularly at the G1 phase. Consequently, it was

concluded that the immunosuppressive activity of BraA (**3.1**) stems from the inhibition of the amino acid transporter system L, a mechanism different from cyclosporin A, which targets IL-2 signaling.

3.3 Biosynthesis of Brasilicardin A

The biosynthetic pathway of the aglycon of BraA (**3.1**) was investigated by Kobayashi *et al.* (**Figure 3.3**).[11] *N. brasiliensis* IFM 0406 cultures were incubated with [1-^{13}C]-labeled glucose, and 25 mg of BraA (**3.1**) was isolated from 1 liter of culture broth. ^{13}C NMR analysis of BraA (**3.1**) revealed the presence of a perhydrophenanthrene core, which was proposed to be derived from geranylgeranyl phosphate and an amino acid side chain (C16-C18) formed from [3-^{13}C]pyruvate, and thus doubly labeled IPP.

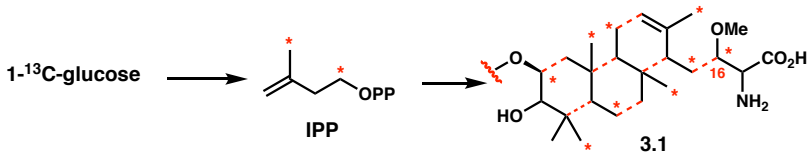
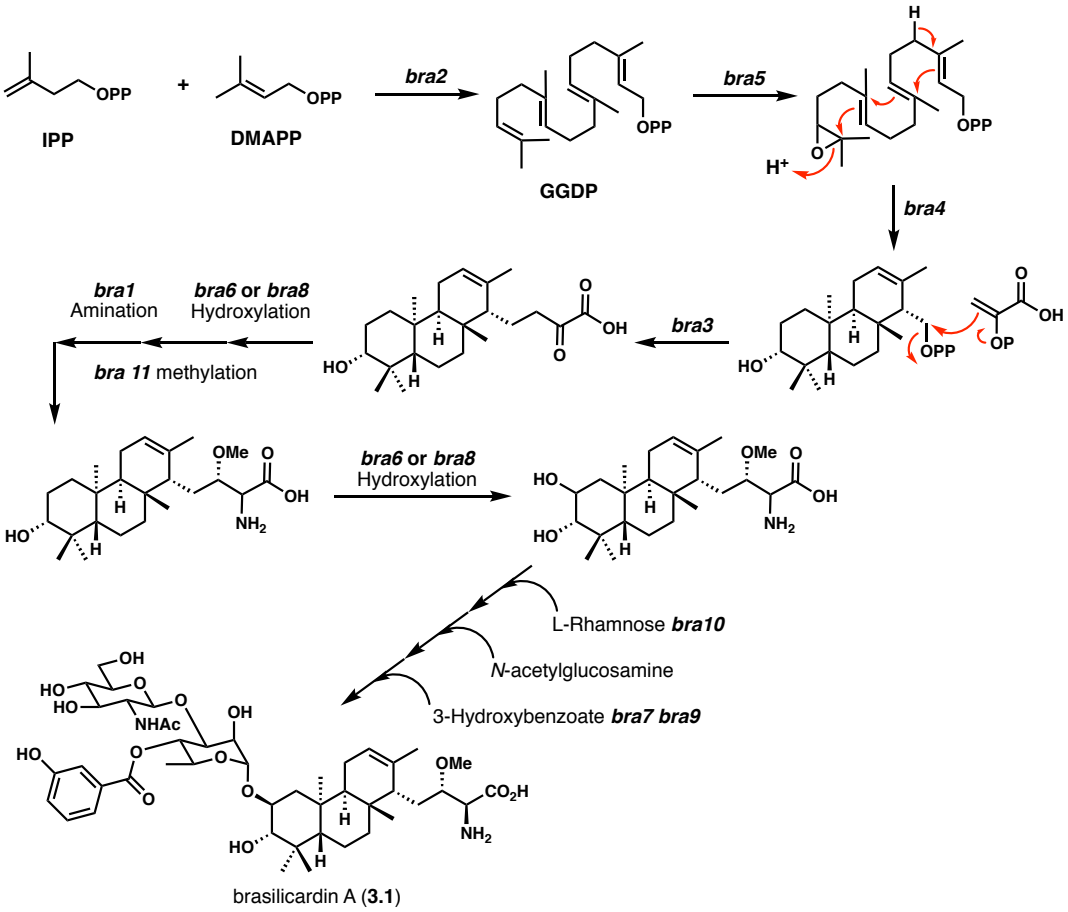


Figure 3.3 BraA (**3.1**) derived from [1-^{13}C]glucose.[11]

In 2008, Dairi *et al.* employed a cloning experiment to investigate the biosynthetic gene cluster of BrA (**3.1**) (**Scheme 3.2**).[12] They successfully cloned the *gapps 1* gene, which encodes geranylgeranyl diphosphate synthase (GGPPS), an enzyme involved in precursor production for BraA synthesis. Sequence analysis of *ggpps 1* revealed the presence of 11 genes putatively responsible for BraA (**3.1**) biosynthesis. The proposed biosynthetic pathway of BraA (**3.1**) begins with the formation of geranylgeranyl diphosphate from common diterpenoid precursors, as suggested by the identification of the *bra2* gene encoding the GGPPS enzyme. FAD-epoxidase, encoded by the *bra5* gene, is predicted to be involved in the cyclization step, leading to the formation of a tricyclic perhydrophenanthrene skeleton. Prenyltransferase (*bra3*) and subsequent

genes are thought to be responsible for amino acid installation: *bra1* for amination, *bra6* or *bra8* for hydroxylation, and *bra11* for methylation. *Bra6* or *bra8* genes are also implicated in the oxidation of C2 of the tricyclic intermediate. Finally, tailoring genes responsible for the incorporation of L-rhamnose (*bra10*) and 3-hydroxybenzoate (*bra7* and *bra9*) were identified, although the gene for the *N*-acetylglucosamine moiety was not detected.

Scheme 3.2 Proposed synthetic pathway of BraA (**3.1**) by Dairi *et al*.[12]



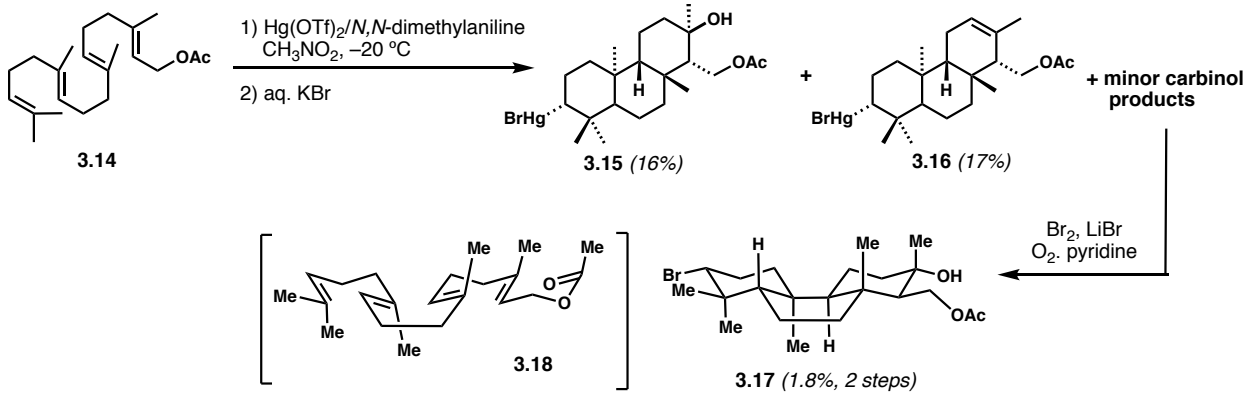
3.4 Previous Attempts Towards *Trans/Syn/Trans*-Perhydrophenanthrene Skeleton

3.4.1 Mercury(II)-Induced Olefins Cyclization by Nishizawa et al.

Nishizawa *et al*. reported that a mercury(II)triflate/amine complex-promoted the polyene cyclization of (*E*,*E*)-geranylgeranyl acetate (**3.14**) (**Scheme 3.3**).[13] The cyclization reaction yielded

tricyclic compounds **3.15** and **3.16** as major products, along with unidentified minor compounds. Subsequently, the mixture of minor product was brominated to afford crystalline compound **3.17** (1.8% yield over two steps), which had likely been formed via chair/boat/chair transition state **3.18**. Notably, compound **3.17** possesses an *trans/syn/trans*-perhydrophenanthrene skeleton. This work demonstrates the potential of biomimetic cyclization for the formation of the BraA (**3.1**) diterpenoid backbone.

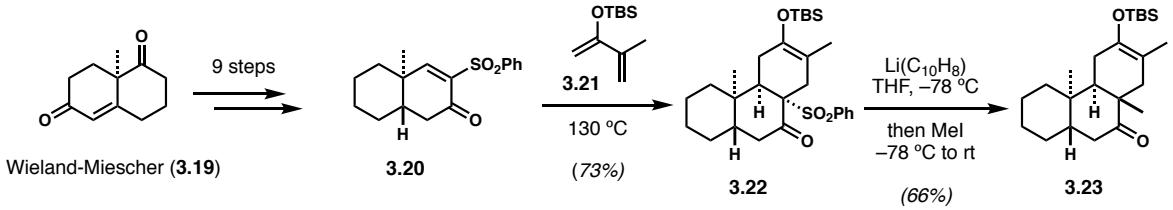
Scheme 3.3 $Hg(OTf)_2$/amine complex-induced polyene cyclization.[13]



3.4.2 Diels–Alder Cycloaddition Approach

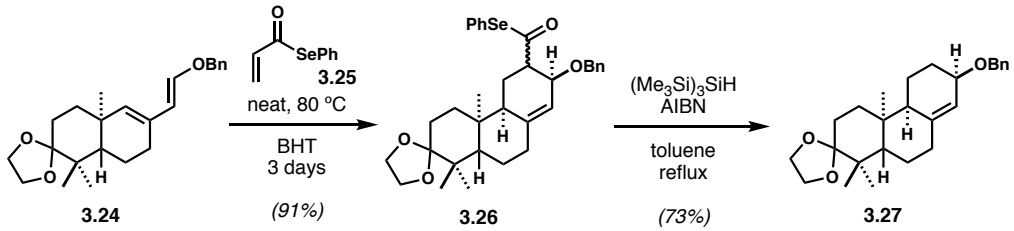
Danishefsky *et al.* developed an efficient method for the synthesis of *trans/syn/trans*-perhydrophenanthrene tricyclic rings (**Scheme 3.4**).[14] Their approach established the bicyclic compound **3.20** bearing *anti*-relative stereochemistry at the AB ring from Wieland–Miescher ketone **3.19** via 9 synthetic steps. The key step involved the Diels–Alder cycloaddition of ketosulfone **3.20** and silyl enol ether **3.21** to generate cycloaddition product **3.22** with boat conformer of ring B. Subsequent treatment of this adduct **3.22** with lithium naphthalenide ($LiC_{10}H_8$) and methyl iodide afforded the methylated product **3.23** bearing the desired *anti* BC ring junction.

Scheme 3.4 Danishefsky's Diels–Alder cycloaddition approach.[14]



Jung group developed the Diels–Alder cycloaddition of diene **3.24** and phenyl selenoacrylate **3.25**[15] to form the ring C of the perhydrophenanthrene core (**Scheme 3.5**).[16] After 3 days, the cycloaddition between diene **3.24** and dienophile **3.25** gave a mixture of *endo* and *exo* cycloadducts **3.26** in 90% yield as a single regioisomer. Compound **3.26** was then subjected to deselenylation/decarboxylation to afford the tricyclic product **3.27** in 73% yield.

Scheme 3.5 Jung's Diels-Alder cycloadditon.[16]



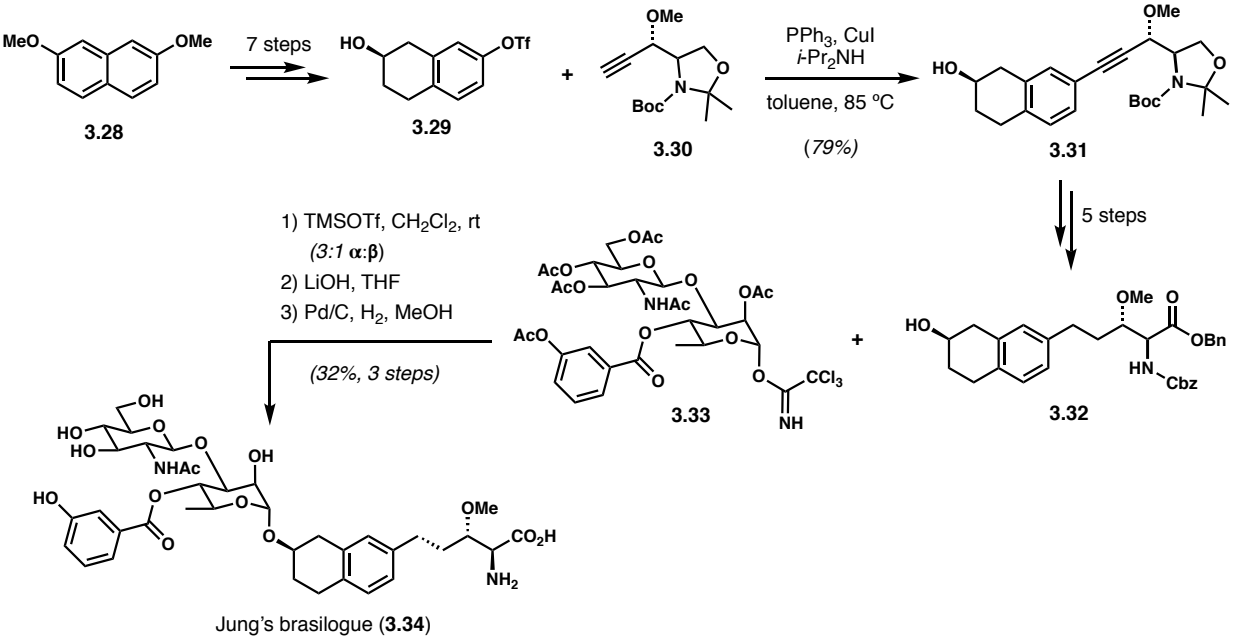
3.5 Synthesis of Brasilicardin A and Analogues

3.5.1 Synthesis of BraA Analogue by Jung et al.

Building on the SAR study by Kobayashi group, which revealed the importance of the sugar moiety and amino acid side chain for the immunosuppressive activity of BraA (**3.1**), the Jung group designed brasilicardin A analogue **3.34** containing a more accessible tetrahydronaphthalene core structure (**Scheme 3.6**).[17] They proposed that analogue **3.34** would maintain a similar orientation and distance between sugar and amino acid structures as in BraA (**3.1**), thereby preserving immunosuppressive activity. The synthesis of analogue **3.34** commenced with the formation of substituted tetralin **3.29** from 2,7-dimethoxynaphthlene (**3.28**) through 7 step sequence involving dissolving metal reduction and Noyori asymmetric reduction. Subsequently,

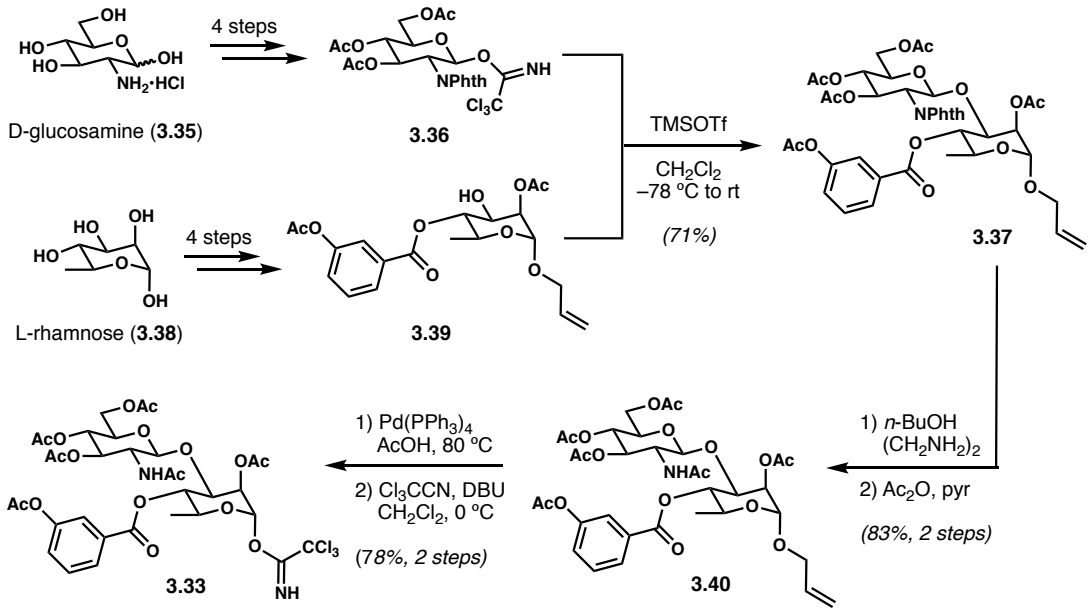
the Sonogashira coupling of aryl triflate **3.29** and alkyne **3.30** derived from D-serine[18], yielded aryl alkyne **3.31**. The amino acid carbon skeleton of compound **3.32** was then constructed from coupling product **3.31** in 5 steps including alkyne reduction, acetonide opening, and chemoselective TEMPO-catalyzed oxidation of primary alcohol. Alcohol **3.32** underwent trimethyl silyltrifluoromethanesulfonate (TMSOTf)-mediated glycosylation with trichloroacetimidate **3.33**, developed in Jung group[19], followed by protecting group removal to produce brasilicardin A analogue **3.34**. Compound **3.34** was then evaluated for its immunosuppressive potential in human T cells alongside BraA (**3.1**) and cyclosporin A. BraA (**3.1**) exhibited the most potent inhibition of T cell proliferation, with an effective concentration of 25 nM. Cyclosporin A demonstrated activity at 100 nM. Conversely, synthetic analogue **3.34** showed no suppressive effect on T cell proliferation even at concentrations as high as 400 nM. Therefore, the tetralin core in analogue **3.34**, despite potentially retaining the spatial arrangement between the sugar and amino acid groups, was not be able to substitute for the perhydrophenanthrene core of BraA (**3.1**) in terms of preserving immunosuppressive activity.

Scheme 3.6 Synthesis of brasilogue A (**3.28**) by Jung group.[17]



The previously mentioned disaccharide **3.33** was prepared from a key disaccharide **3.37** (**Scheme 3.7**).[19] Disaccharide **3.37** could be synthesized through TMSOTf-catalyzed coupling of 2-phthalimido-2-deoxyglucose donor **3.36** and glycosyl acceptor **3.39**. Imine **3.36** was prepared from D-glucosamine **3.35** in 4 steps. Coupling fragment **3.39** was obtained from L-rhamnose **3.38** in 4 steps. The coupling product **3.37** was deprotected by removing the phthaloyl group, followed by acylation to furnish *N*-acetylglucosamine **3.40** in 83% yield in 2 steps. Finally, a palladium catalyst was employed to remove the allyl group of **3.40**, yielding the secondary alcohol. This alcohol intermediate was subsequently treated with trichloroacetonitrile and 1,8-diazabicyclo[5.4.0]undec-7-ene (DBU) to afford the desired trichloroacetimidate **3.33**.

Scheme 3.7 Preparation of trichloroacetimidate glycosyl donor (**3.33**) by Jung group.[19]

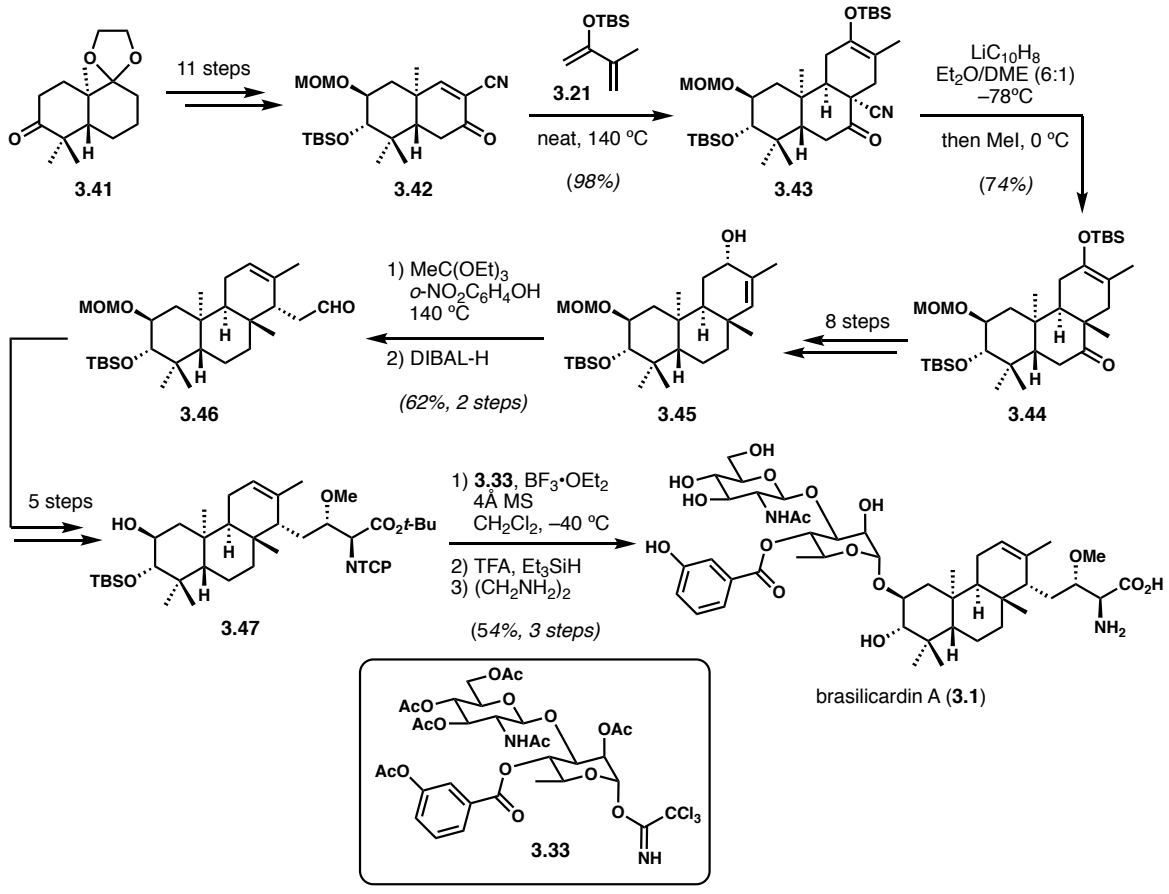


3.5.2 Total Synthesis of Brasilicardin A by Anada et al.

Anada *et al.* achieved the first total synthesis of BraA (**3.1**) (**Scheme 3.8**).[20] The synthesis involved the formation of α-cyano-α,β-enone **3.42** from a known bicyclic precursor **3.41**[21] derived from Wieland–Miescher ketone. Enone **3.42** underwent Diels–Alder cycloaddition with diene **3.22**

to generate tricyclic product **3.43**. Anada group then optimized the reductive methylation of α-cyanoketone **3.43** to obtain the desired C-methylated ketone **3.44**. Silyl enol ether **3.44** was converted to allylic alcohol **3.45** in an 8-step sequence. Allylic alcohol **3.45** was then transformed into aldehyde **3.46** via Johnson–Claisen rearrangement and subsequent DIBAL-H reduction. The installation of the amino acid side chain of compound **3.47** was accomplished in 5 steps, utilizing a key chiral-auxiliary directed *anti*-aldol addition. Secondary alcohol **3.47** was subsequently treated with Jung's trichloroacetimidate **3.33** and BF_3•OEt_2 to generate α-glycoside. Finally, removal of *tert*-butyl, TBS, and tetrachlorophthaloyl (TCP) groups yielded BraA (**3.1**) in 31 steps from starting material **3.41**.

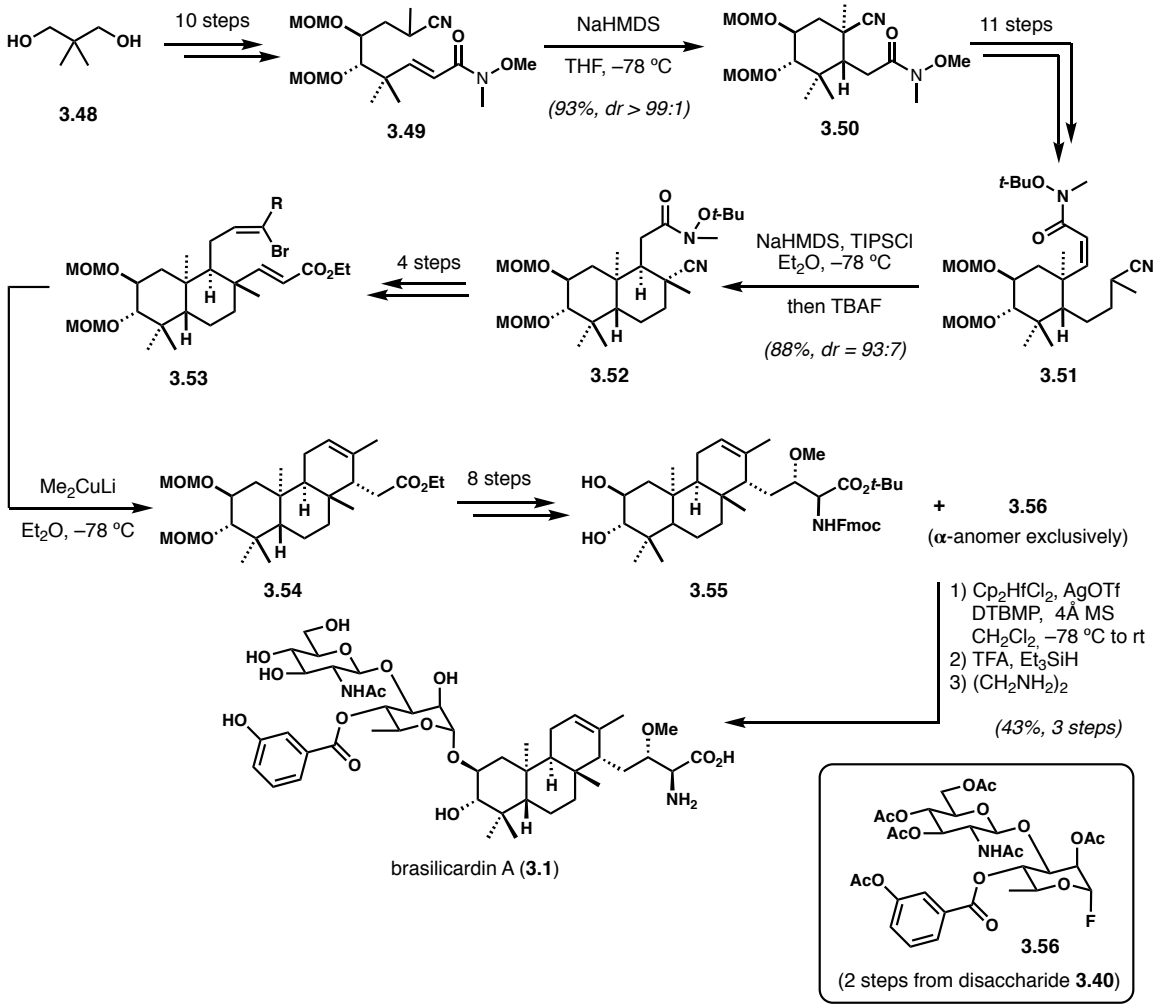
Scheme 3.8 Total synthesis of BrA (**3.1**) by Anada *et al*.[20]



3.5.3 Total Synthesis of Brasilicardin A by Yoshimura and Tanino et al.

The synthesis of BraA (**3.1**) by Yoshimura and Tanino *et al*. was achieved through a 39-step linear sequence utilizing key intramolecular Michael addition reactions.[22] They initiated the process by converting the starting material, 2,2-dimethylpropane-1,3-diol (**3.48**), into Weinreb amide **3.49** via a 10-step sequence. Subsequent treatment of nitrile **3.49** with sodium hexamethyldisilazide (NaHMDS) facilitated intramolecular 1,4-addition, yielding cyclohexane **3.50**. Alkyl nitrile **3.50** was then subjected to an 11-step sequence encompassing DIBAL-H reduction, cyano group introduction, *Z*-selective Horner–Wadsworth–Emmons (HWE) olefination, and amidation to furnish methylamide **3.51**. This amide **3.51** served as a precursor for the second intramolecular Michael addition, forming the B ring of **3.52**. Ring C formation was introduced through the intramolecular conjugate addition of 1,1-dibromoalkene **3.53**, derived from amide **3.52**. The corresponding tricyclic product **3.54** was obtained as a single diastereomer exhibiting the desired *trans/syn/trans* -perhydrophenanthrene ring system. The amino acid moiety was incorporated into compound **3.54** through an 8-step sequence, utilizing asymmetric dihydroxylation. Initial attempts to glycosylate diol **3.52** with Jung's trichloroacetimidate donor **3.33** resulted in a mixture of regioisomers and substrate decomposition. To address this, Yoshimura and Tanino *et al.* developed the fluoride donor **3.56**, derived from disaccharide **3.40** (the same intermediate used for Jung's donor **3.33**). Employing the metallocene-based activator $Cp_2HfCl_2/AgOTf$[23], glycosylation of aglycone **3.55** with fluoride **3.56** afforded the α-glycoside product with high regio- and anomeric selectivity. Finally, removal of the TBS and TCP protecting groups yielded the target compound, BraA (**3.1**) in 39 linear steps from diol **3.48**.

Scheme 3.9 Total synthesis of BrA (**3.1**) by Yoshimura and Tanino *et al*.[22]

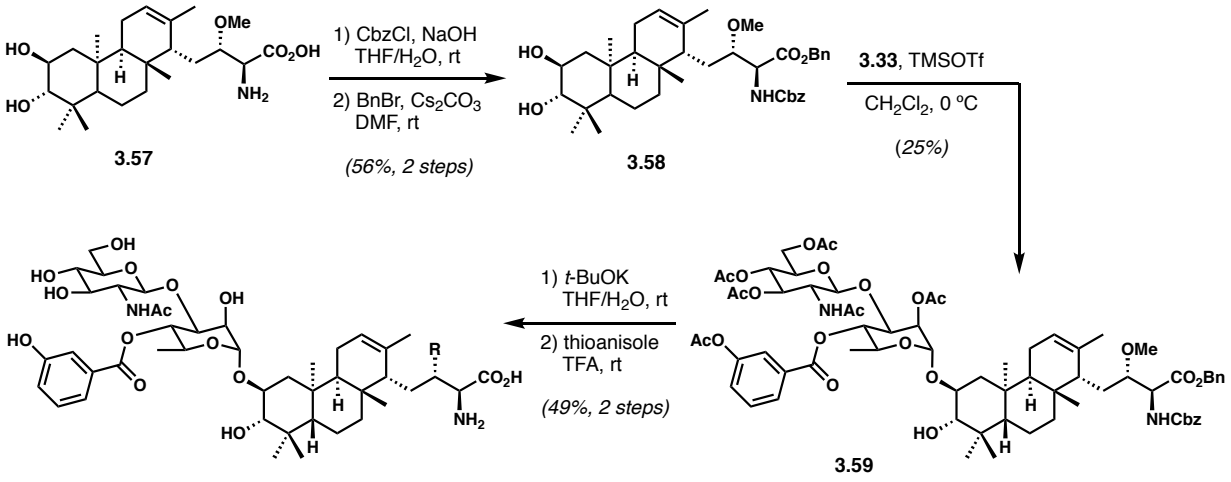


3.5.4 Semi-Synthesis of Brasilicardin A Using Genetic Engineering Approach

Stegmann *et al*. (2021) explored heterologous expression of the BraA biosynthetic gene cluster in over 70 actinomycete hosts, primarily yielding aglycone brasilicardin E (BraE) (**3.57**).[24] This approach facilitated gram-scale BraE (**3.57**) production, reaching 1,151 mg/L from *S. griseus*:bcaAB01 (pRHAMO) after 12 days. To synthesize the immunosuppressive BraA (**3.1**), BraE (**3.57**) was subjected to semi-synthesis (**Scheme 3.10**). The amino group was protected with carboxybenzyl (Cbz), followed by benzyl (Bn) protection of the carboxylic acid. Glycosylation of diol **3.58** preferentially yielded the C2-regioisomer **3.59** (25%). Subsequent removal of acetyl and

benzoyl groups, and Cbz cleavage using thioanisole and TFA, afforded BraA (**3.1**) with a 7% overall yield over five steps.

Scheme 3.10 Semi-synthesis of BraA (**3.1**) by Stegmann *et al*.[24]

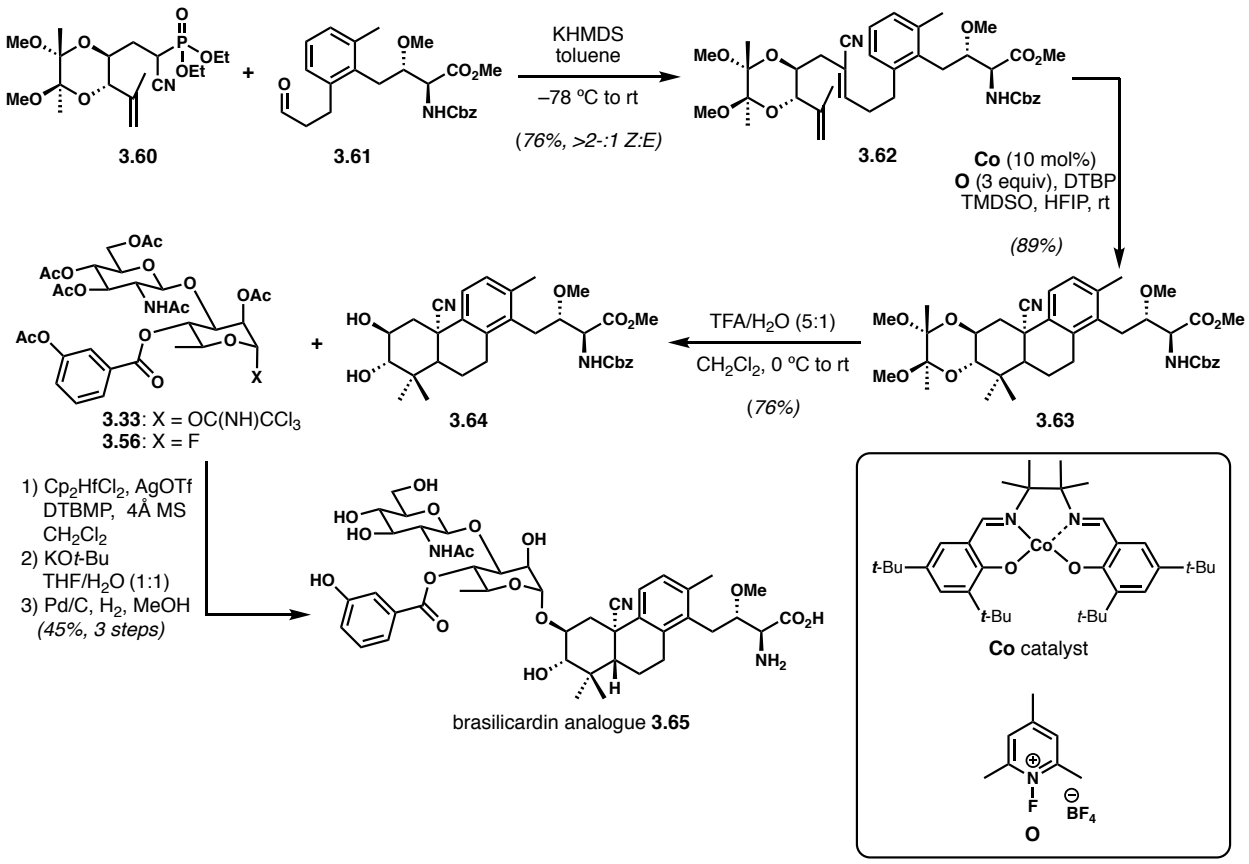


3.5.5 Synthesis of Brasilicardin Analogue by Vanderwal group

Brasilicardin analogue **3.65** was synthesized in 17 linear steps by our previous graduate student, Dr. Scott Niman. A key cobalt-catalyzed MHAT-induced radical bicyclization transformed diene **3.62** into tricyclic compound **3.63** (**Scheme 3.11**).[25] Diene **3.62** was accessed through a HWE olefination of cyanophosphonate **3.60** with aldehyde **3.61**.[26] Glycosylation of diol **3.64** to install the sugar moiety proved challenging. While Jung's trichloroacetimidate **3.33** afforded an inseparable mixture of anomers at C2, the peracetyl glycosyl fluoride **3.56** developed by Yoshimura and Tanino provided the desired glycoside product with high regio- and stereoselectivity. Deprotection of protecting groups afforded BraA analogue **3.65** in 45% yield over three steps. To assess the immunosuppressive potential of compound **3.65**, its effects on cell cycle progression and mTOR signaling were evaluated in IL-2-dependent CTLL-2 cells. Unlike rapamycin, a known mTOR inhibitor, brasilicardin analogue **3.65** did not induce cell cycle arrest or inhibit mTOR downstream effectors, including elF4E-binding protein-1 and ribosomal S6.

These findings underscore the critical role of the diterpenoid core structure in mediating immunosuppressive activity.

Scheme 3.11 Vanderwal's synthesis of brasilicardin analogue (**3.65**).[25]



3.6 Conclusions and Motivation

BraA (**3.1**), a polycyclic terpenoid natural product, was isolated from *Nocardia brasiliensis*, and potently inhibits immune response in the mouse MLR assay (IC_{50} = 0.057 μg/mL). Mechanistic studies revealed that BraA (**3.1**) suppresses cell cycle progression at the G1 phase by inhibiting amino acid transport system L. Its unique *trans/syn/trans*-perhydrophenanthrene core, adorned with a disaccharide and an amino acid moieties, was elucidated through X-ray crystallography of a brominated aglycone derivative. Structure-activity relationship (SAR) studies underscored the importance of the diterpene scaffold, sugar unit, and

amino acid side chain for immunosuppressive activity. Biosynthetic investigations, including gene cluster analysis and precursor labeling, support a non-mevalonate pathway for BraA (**3.1**) biosynthesis.

The disaccharide and amino acid components of BraA (**3.1**) have been successfully synthesized by previous research groups. However, constructing the complex *trans/syn/trans*-perhydrophenanthrene core has proven challenging, as exemplified by the synthetic efforts of Danishefsky and Jung. While fermentation of *Nocardia brasiliensis* can produce BraA (**3.1**), insufficient quantities limit comprehensive biological evaluation. Total syntheses by Anada, Yoshimura, and Tanino, requiring over 30 linear steps, and a semi-synthetic approach from brasilicardin E have been reported; however, they do not provide a platform for extensive analog synthesis. Furthermore, no existing synthetic route incorporates biomimetic strategies. To address these challenges, our group aims to develop a bioinspired cyclization approach to efficiently construct the *trans/syn/trans*-perhydrophenanthrene core of BraA (**3.1**). This strategy is expected to streamline the synthesis and enable the preparation of analogs for further medicinal chemistry investigations.

3.7 References

1. Shigemori, H.; Tanaka, Y.; Yazawa, K.; Mikami, Y.; Kobayashi, J. *Tetrahedron* **1996**, *52*, 9031–9034.
2. Komaki, H.; Nemoto, A.; Tanaka, Y.; Takagi, H.; Yazawa, K.; Mikami, Y.; Shigemori, H.; Kobayashi, J.; Ando, A.; Nagata, Y. *J. Antibiot. (Tokyo)* **1999**, *52*, 13–19.
3. Komatsu, K.; Tsuda, M.; Tanaka, Y.; Mikami, Y.; Kobayashi, J. *Bioorg. Med. Chem.* **2005**, *13*, 1507–1513.

4. Shigemori, H.; Komaki, H.; Yazawa, K.; Mikami, Y.; Nemoto, A.; Tanaka, Y.; Sasaki, T.; In, Y.; Ishida, T.; Kobayashi, J.; *J. Org. Chem*. **1998**, 63, 6900–6904.
5. White, D. J. G. *Drugs* **1982**, *24*, 322–334.
6. Borel, J. F.; Feurer, C.; Magnée, C.; Stähelin, H. *Immunology*, **1977**, *32*, 1017–1025.
7. Komaki, H.; Tanaka, Y.; Yazawa, K.; Takagi, H.; Ando, A.; Nagata, Y.; Mikami, Y. *J. Antibiot.* **2000**, *53*, 75–77.
8. Komatsu, K.; Tsuda, M.; Shiro, M.; Tanaka, Y.; Mikami, Y.; Kobayashi, J. *Bioorg. Med*. *Chem*. **2004**, *12*, 5545–5551.
9. Komatsu, K.; Tsuda, M.; Tanaka, Y.; Mikami, Y.; Kobayashi, J. *Bioorg. Med. Chem*., **2005**, *13*, 1507–1513.
10. Usui, T.; Nagumo, Y.; Watanabe, A.; Kubota, T.; Komatsu, K.; Kobayashi, J.; Osada, H. *Chem Biol*, **2006**, *13*, 1153–1160.
11. Shigemori, H.; Komaki, H.;Yazawa, K.; Mikami, Y.; Nemoto, A.; Tanaka, Y.; Kobayashi J. *Tetrahedron Lett*., **1999**, *40*, 4353–4354.
12. Hayashi, Y.; Matsuura, N.; Toshima, H.; Itoh, N.; Ishikawa, J.; Mikami, Y.; Dairi, T. *J. Antibiot. (Tokyo)* **2008**, *61*, 164–174.
13. Nishizawa, M.; Takenaka, H.; Hirotsu, K.; Higuchi, T.; Hayashi, Y. *J. Am. Chem. Soc.* **1984**, *106*, 4290–4291.
14. Coltart, D. M.; Danishefsky, S. J. *Org. Lett.* **2003**, *5*, 1289–1292.
15. Tiecco, M.; Testaferri, K.; Temperini, A.; Bagnoli, L.; Marini, F.; Santi, C.; Terlizzi, R.; *Eur. J. Org. Chem*. **2004**, 3447–3458.

16. Jung, M. E.; Perez, F.; Regan, C. F.; Yi, S. W.; Perron, Q. *Angew. Chem. Int. Ed.* **2013**, *52*, 2060–2062.

17. Jung, M. E.; Chamberlain, B. T.; Koch, P.; Niazi, K. R. *Org. Lett.* **2015**, *17*, 3608–3611.

18. Herold, P. *Helv. Chim. Acta* **1988**, *71*, 354–362.

19. Jung, M. E.; Koch, P. *Org. Lett*. **2011**, *13*, 3710–3713.

20. Anada, M.; Hanari, T.; Kakita, K.; Kurosaki, Y.; Katsuse, K.; Sunadoi, Y.; Jinushi, Y.; Takeda, K.; Matsunaga, S.; Hashimoto, S. *Org. Lett.* **2017**, *19*, 5581–5584.

21. Hagiwara, H.; Uda, H. *J. Org. Chem*. *1988*, 53, 2308–2311.

22. Yoshimura, F.; Itoh, R.; Torizuka, M.; Mori, G.; Tanino, K. *Angew. Chem. Int. Ed*. **2018**, *57*, 17161–17167.

23. K. Suzuki, H. Maeta, T. Matsumoto, *Tetrahedron Lett*. **1989***, 30*, 4853–4856.

24. Botas, A.; Eitel, M.; Schwarz, P. N.; Buchmann, A.; Costales, P.; Núñez, L. E.; Cortés, J.; Morís, F.; Krawiec, M.; Wolański, M.; Gust, B.; Rodriguez, M.; Fischer, W.-N.; Jandeleit, B.; Zakrzewska- Czerwińska, J.; Wohlleben, W.; Stegmann, E.; Koch, P.; Méndez, C.; Gross, H. *Angew. Chem. Int. Ed*. **2021**, *60*, 13536–13541.

25. Niman, S. W.; Buono, R.; Fruman, D. A.; Vanderwal, C. D. *Org. Lett.* **2023**, *25*, 3451–3455.

26. Niman, S. W. PhD Dissertation, University of California, Irvine, 2023.

CHAPTER 4 PROGRESS TOWARDS THE SYNTHESIS OF BRASILICARDIN A USING A POLYENE CYCLIZATION APPROACH

4.1 Introduction

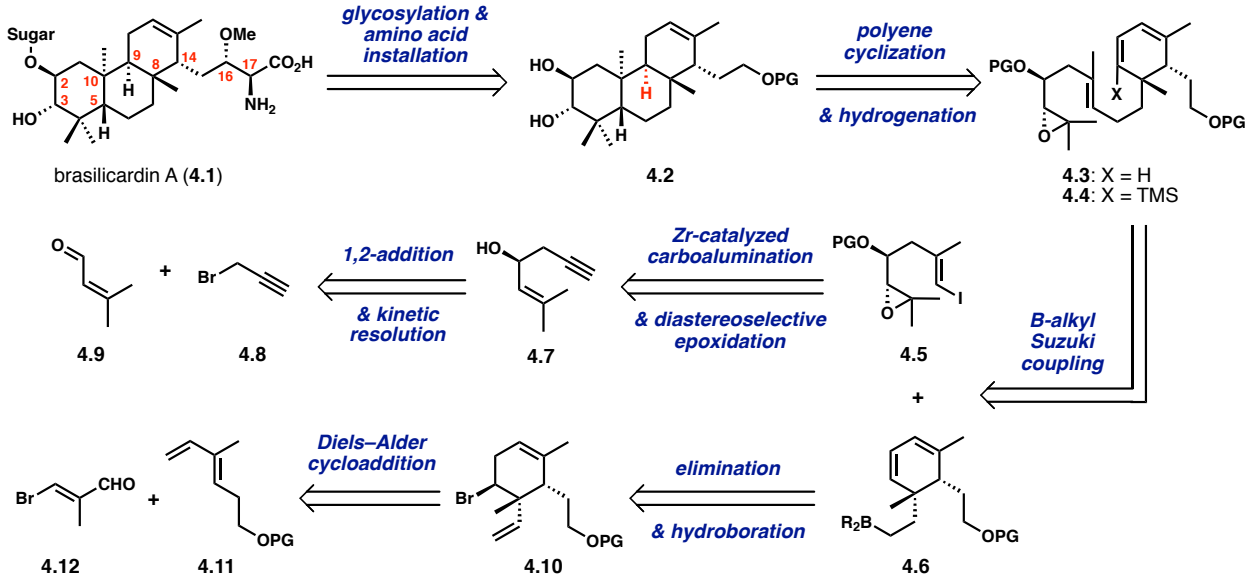
Brasilicardin A was chosen as a target molecule due to its unique structure, which possesses an *trans/syn/trans*-perhydrophenanthrene skeleton, and because it exhibits potent immunosuppressive activity (see Chapter 3). Our group has successfully synthesized several terpenoid natural products using polyene cyclizations of substrates with aromatic terminating groups.[1] In this work, we aimed to develop a novel synthesis of brasilicardin A's perhydrophenanthrene core using an unprecedented diene-terminated polyene cyclization. We investigated both cationic and radical-based conditions for the polycyclization reaction.

4.2 Retrosynthetic Analysis of Brasilicardin A

The retrosynthetic analysis of brasilicardin A (**4.1**) commences with installation of the sugar moiety and the amino acid side chain, which was reported earlier in Jung's[2], Anada's[3] and Yoshimura's[4] works (**Scheme 4.1**). Alternatively, the amino acid could be installed via an aldol reaction, using an aldehyde derived from the protected primary alcohol **4.2**. The key step in our approach involves a polyene cyclization to form the *trans/syn/trans*-perhydrophenanthrene core, a characteristic structural element of brasilicardin A (**4.1**). This reaction has not been previously reported, and we planned to investigate it under both cationic and radical conditions with epoxy-triene **4.3** or its silylated analog **4.4**. Importantly, we hypothesized that a directed hydrogenation of an endocyclic alkene may be required to install the central, boat conformed ring. Notably, we chose to preinstall the methyl bearing quaternary center in hopes of biasing the second ring closure to occur from the face opposite to the larger alkyl group – generating the desired diastereomeric tricycle **4.2**. Depending on the mechanistic pathway, one could envision several different outcomes

for the polyene cyclization in terms of alkene positioning in the final product. For example, if a radical cyclization was employed with the diene substrate **4.3**, the product(s) might possess only one alkene. Alternatively, if we obtained a diene bearing product via a cationic polyene cyclization, we hoped to be able to direct a selective, kinetically controlled hydrogenation of the endocyclic alkene using the pendent alkoxy moiety in the side chain.

Scheme 4.1 Retrosynthesis of brasilicardin A (**4.1**).



The polyene substrate **4.3** could be synthesized via a B-alkyl Suzuki–Miyaura cross-coupling reaction between vinyl iodide **4.5** and cyclohexadiene **4.6**. Vinyl iodide **4.5** could be synthesized using a zirconium-catalyzed methylalumination and hydroxyl-directed epoxidation of alkyne **4.7**. Intermediate **4.7** could be obtained from the propargylation of propargyl bromide **4.8** with 3-methylcrotonaldehyde (**4.9**). Finally, diene **4.6** may be derived from the elimination of cyclohexyl bromide **4.10**, which could be synthesized via a Diels–Alder cycloaddition between diene **4.11** and 2-bromoacrolein (**4.12**), followed by hydroboration of the exocyclic alkene. Based on previous reports[5], we anticipated that the [4+2]-cycloaddition would furnish the desired *endo*

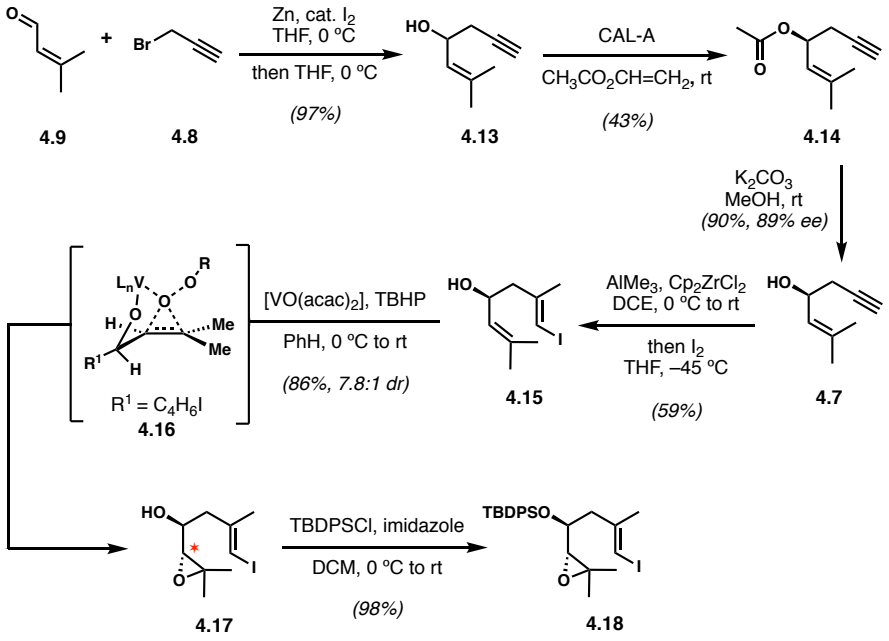
adduct as the predominant isomer and that the use of an appropriate catalyst may provide enantioenriched material.

4.3 Synthesis of Coupling Fragments for Polyene Substrates

4.3.1 Synthesis of Vinyl Iodide Fragment

The synthesis of fragment **4.18** began with the Zn-catalyzed propargylation of 3-methylcrotonaldehyde (**4.9**) to form racemic allylic alcohol **4.13** (**Scheme 4.2**). The desired enantiomer of allylic alcohol (**4.7**) was subsequently isolated in a 43% yield after 52% conversion following an enzymatic kinetic resolution of the racemic mixture (**4.13**) using Lipase A from Candida antarctica (CAL-A)[6] . The resolution provided acetate ester **4.14**, which was hydrolyzed with potassium carbonate in methanol to afford the secondary alcohol **4.7** in an 89% enantiomeric excess. The absolute configuration of compound **4.7** was established using Mosher ester analysis with (*S*)-(–)-α-methoxy-α-(trifluoromethyl)phenylacetic acid ((–)-MTPA), and later corroborated with X-ray crystallographic analysis.

Scheme 4.2 Synthesis of vinyl iodide **4.18**.



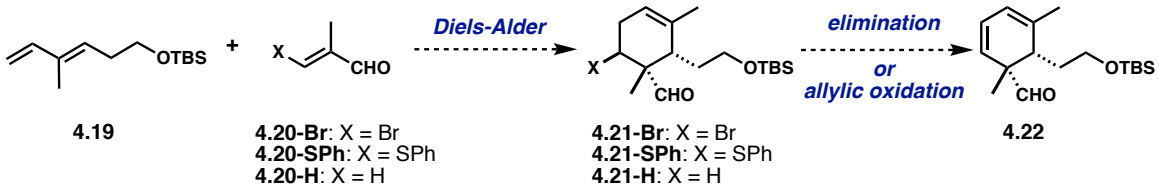
Treatment of alkyne **4.7** with zirconocene dichloride and trimethylaluminum generated a carboaluminated intermediate, which was then quenched with iodine to yield *cis*-addition product **4.15**. It was observed that a longer reaction time during the methylalumination step resulted in a higher yield of the vinyl iodide product **4.15**. Next, a vanadium-catalyzed asymmetric epoxidation of alkene **4.15** was performed using $VO(acac)_2$ and *tert*-butyl hydroperoxide (TBHP). This diastereoselective epoxidation of allylic alcohol **4.15** afforded a 7.8:1 dr mixture favoring the desired diastereomer **4.17** through the *threo* transition state **4.16**.[7] Finally, alcohol **4.17** was protected with a tert-butyldiphenylsilyl (TBDPS) group to form fragment **4.18**. The TBDPS group was chosen due to its stability and UV light absorption properties, facilitating the handling of the compound in subsequent steps.

4.3.2 Initial Attempts for Synthesis of Diene Fragment using Diels–Alder Cycloaddition

This work proposes a synthetic route to diene **4.22** via Diels–Alder cycloaddition between diene **4.19** and methacrolein derivatives **4.20** (**Scheme 4.3**). We expected cycloadducts **4.21** to undergo elimination reactions as a method of forming alkene **4.22**. We anticipate obtaining endo adducts **4.21**, where the aldehyde and enoxysilane groups reside on the same face of the molecule. Williard *et al*. previously reported a Diels–Alder cycloaddition between isoprene and β-chloromethacrolein under thermal conditions in toluene to generate the corresponding cycloaddition product.[8] In our study, attempts to synthesize β-chloromethacrolein from aldehyde **4.20-Br** through halogen exchange[9] or from chlorination of methacrolein **4.20-H**, followed by elimination with various bases, were unsuccessful (data not shown). Diene **4.19** was prepared in three steps from commercially available ethyl sorbate.[10] The synthesis of 3-bromoacrolein **4.20-Br** involved bromination of methacrolein followed by elimination with 1,8-

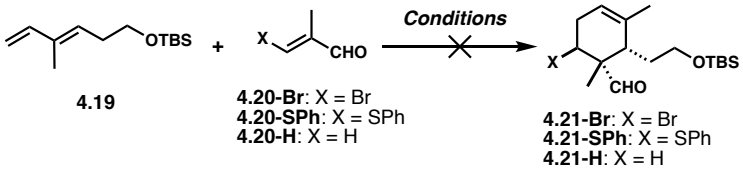
diazabicyclo[5.4.0]undec-7-ene (DBU).[11] Finally, treatment of bromomethacrolein **4.20-Br** with sodium thiophenolate afforded aldehyde **4.20-SPh**.[12]

Scheme 4.3 Proposed synthetic route towards diene **4.22**.



We first investigated the feasibility of a [4+2] cycloaddition between 2-bromomethacrolein (**4.20-Br**) and diene **4.19** (Table **4.1**). Thermal conditions using BHT as a radical scavenger and propylene oxide as an acid scavenger were employed under solvent free conditions and at evaluated temperatures (entries 1-3). However, these reactions did not yield the desired cyclohexane product **4.21-Br**. Similarly, Lewis acid-promoted [4+2] cycloadditions using various Lewis acids resulted in decomposition or no reaction (entries 4-7). We further explored the reactivity of the dienophile by subjecting aldehydes **4.20-SPh** and **4.20-H** to diene **4.19** (entries 8-9). These reactions also did not produce any desired products.

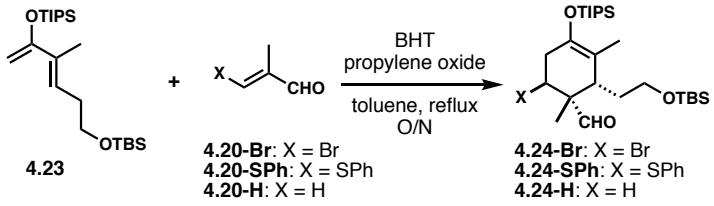
Table 4.1 Initial attempts for Diels–Alder cycloaddition towards diene **4.2**.



Entry	X	Conditions	Results
1	Br	BHT, propylene oxide, toluene, 150 °C, O/N	no reaction
2	Br	BHT, propylene oxide, 150 °C, O/N	decomposition
3	Br	BHT, propylene oxide, MW 200 °C, xylene, 30 min	decomposition
4	Br	BF_3•Et_2O, CH_2Cl_2, –78 °C to rt, O/N	decomposition
5	Br	$AlCl_3$, PhMe, rt, O/N	no reaction
6	Br	$EtAlCl_2$, CH_2Cl_2, rt, O/N	no reaction
7	Br	TMSOTf, CH_2Cl_2, –78 °C to rt, O/N	no reaction
8	SPh	BHT, propylene oxide, toluene, reflux, O/N	no reaction
9	H	BHT, propylene oxide, toluene, 150 °C, O/N	no reaction

In order to increase the nucleophilicity of the diene, we synthesized diene **4.23** incorporating a triisopropylsilyloxy (TIPSO) group as an electron-donating substituent (**Table 4.2**). Unfortunately, reactions with dienophiles **4.20-Br** and **4.20-SPh** were unsuccessful (entries 1-2). Conversely, the Diels–Alder cycloaddition between triisopropylsiloxy diene **4.23** and commercially available 2-methylacrolein (**4.20-H**) afforded endo cyclohexene **4.24-H** in 81% yield under thermal conditions (entry 3).

Table 4.2 Successful Diels–Alder reaction using silyl enol ether **4.23**.



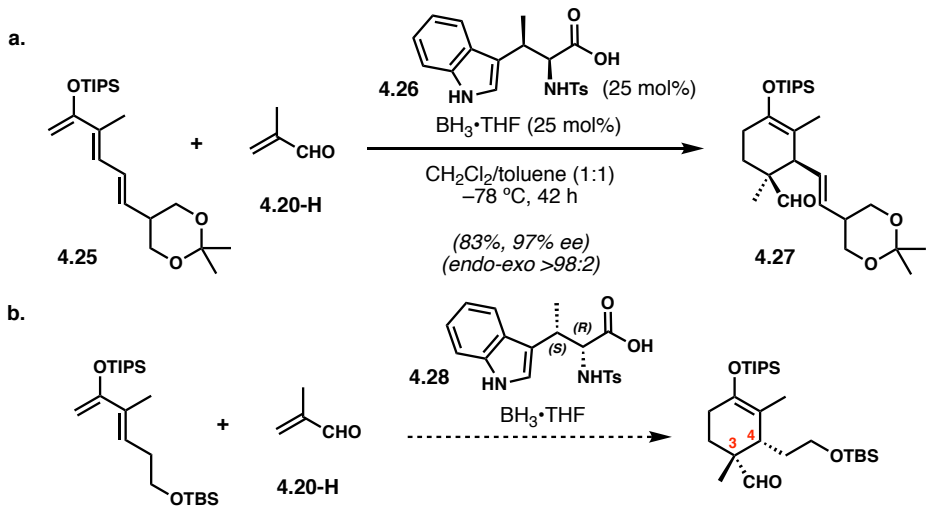
Entry	X	Results
1	Br	trace
2	SPh	no reaction
3	H	81%

4.3.3 Enantioselective Diels-Alder Reactions

The thermal [4+2] cycloaddition of diene **4.23** with dienophile **4.20-H** was successful, affording cycloadduct **4.24-H** in good yield (**Table 4.2**). However, the product **4.24-H** was obtained as a racemic mixture. Synthesizing a single enantiomer of the Diels–Alder product would improve the efficiency of our synthetic route by minimizing the number of diastereomers formed in subsequent convergent steps. Corey and Hong reported the enantioselective Diels–Alder cycloaddition of a diene with 2-methylacrolein (**4.20-H**) using (*R*)-(+)-*o*-tolyl-CBS-oxazaborolidine as a chiral catalyst in 2006.[13] Using this method, we obtained 79% of the target product **4.29** with 59% ee (see experimental section). Corey and co-workers described an asymmetric Diels–Alder reaction using tryptophan-derived oxazaborolidine catalyst **4.26** (**Scheme**

4.4a).[14] This catalyst afforded the desired enantiomer **4.27** with 97% ee from the cycloaddition of precursors **4.25** and methacrolein (**4.20-H**). Their study also showed that TIPS enoxysilane **4.25** resulted in higher enantioselectivity compared to the *tert*-butyldimethylsiloxy (TBS) analogue. In our research, we aimed to obtain the (3*R*,4*S*)-enantiomer **4.29**, which has the opposite configuration at C3 and C4 compared to the product obtained by Corey *et al*. (**Scheme 4.4b**). To achieve this, we planned to use the enantiomer of catalyst **4.26**, (*S*)-β-methyl-catalyst **4.28**. We then attempted to synthesize tosylated catalyst **4.28** through a seven-step sequence.[15] Unfortunately, attempts to resolve the racemic mixture of the catalyst precursor to obtain the desired catalyst **4.28** were unsuccessful.

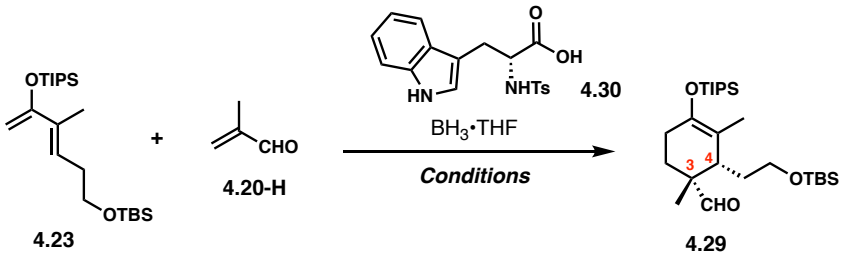
Scheme 4.4 (a) Asymmetric Diels–Alder cycloaddition using oxazaborolidine catalyst reported by Corey and co-workers.[14] (b) Proposed enantioselective Diels–Alder to access the cycloadduct **4.21-H**.



Because the synthesis of (*S*)-β -methyl-catalyst **4.28** proved to be challenging, we adopted a simpler strategy. We synthesized catalyst **4.30** in a single step via tosylation of commercially available D-tryptophan (**Table 4.3**).[16] Tosyl-D-tryptophan **4.30** was then treated with borane tetrahydrofuran complex to generate the oxazaborolidine catalyst *in situ*. The desired (3*R*,4*S*)-enantiomer **4.29** was obtained with acceptable enantioselectivity (76-78% ee) through the

enantioselective Diels–Alder reaction of TIPS enoxysilane **4.23** with methacrolein (**4.20-H**). We observed that the reaction was slow and incomplete when toluene was used as the solvent (entries 1-2). Conversely, increasing the amount of the *in situ* oxazaborolidine catalyst led to a higher yield of product **4.29** (entry 3).

Table 4.3 Optimization of enantioselective Diels–Alder reaction between diene **4.23** and 2-methylacrolein (**4.20-H**).

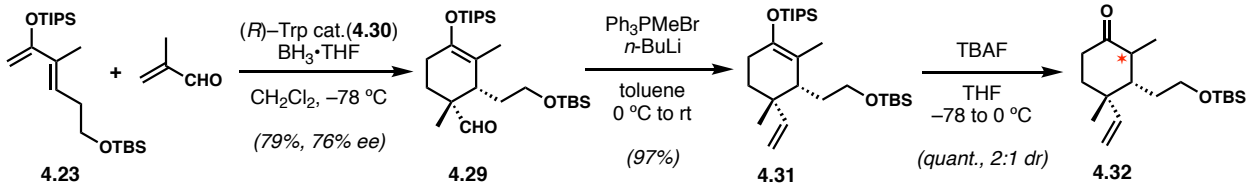


Entry	Conditions	Yield	%ee
1	**4.30** (40 mol%), BH_3THF (20 mol%) CH_2Cl_2/toluene (1:1), –78 °C, 48 h	61% (19% recovered **4.23**)	78%
2	**4.30** (40 mol%), BH_3THF (20 mol%) CH_2Cl_2, –78 °C, O/N	71%	78%
3	**4.30** (40 mol%), BH_3THF (40 mol%) CH_2Cl_2, –78 °C, 20 h	79%	76%

4.3.4 Successful Synthesis of Diene Fragment

The enantioenriched cyclohexene **4.29** from the Diels–Alder cycloaddition served as an important intermediate for the synthesis of the diene fragment needed for convergent fragment coupling. Wittig olefination of aldehyde **4.29** yielded alkene **4.31** (**Scheme 4.5**). Desilylation of the TIPS enoxysilane **4.31** using one equivalent of tetrabutylammonium fluoride (TBAF) selectively cleaved the TIPS group, affording ketone **4.32** as a mixture of diastereomers (2:1 dr). The order of these reaction steps was crucial. We discovered that performing the Wittig reaction before deprotection of the TIPS group was necessary to avoid an intramolecular aldol addition reaction between the enoxy silane and the aldehyde. This undesired side reaction led to the formation of pinane-like by-products.

Scheme 4.5 Preparation of ketone **4.32**.



We then attempted to oxidize cyclohexanone **4.32** to enone **4.33** using various methods (**Table 4.4**). Initially, we treated ketone **4.32** with phenylselenyl bromide and base for selenation, forming the α-phenylseleno ketone.[17] Subsequent oxidation with hydrogen peroxide generated a selenoxide intermediate, which underwent intramolecular elimination to yield the desired α,β-unsaturated ketone **4.33** in 55% yield (entry 1). However, this reaction proved to be irreproducible. Therefore, we explored an alternative approach involving a two-step dehydrogenation of ketone **4.32**: first through silylation followed by Saegusa-Ito dehydrogenation using $Pd(OAc)_2$ as catalyst under an oxygen atmosphere[18] (entry 2). Finally, employing the palladium-catalyzed Saegusa–Ito oxidation of the trimethylsilyl enol ether intermediate with dimethyl sulfoxide (DMSO) as a solvent provided a higher yield of the corresponding cyclohexenone **4.33** (entry 3).

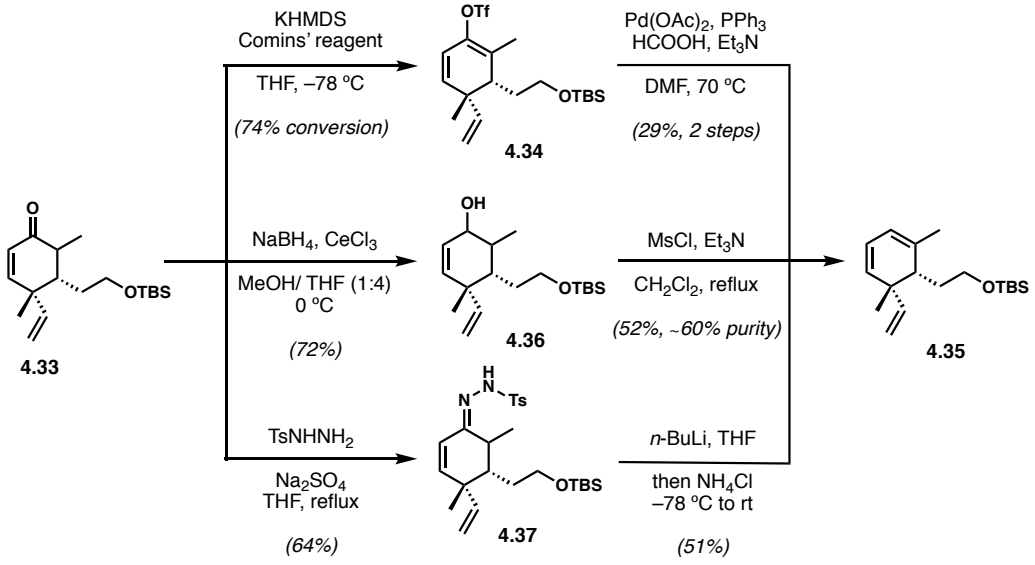
Table 4.4 Conditions attempted for enone **4.33** formation.



Entry	Conditions	Yield
1	LiHMDS, PhSeBr, THF, –78 to 0 °C then H_2O_2, THF/CH_2Cl_2, O_2 to rt	55%
2	LDA, TMSCl, THF, –78 °C then $Pd(OAc)_2$ (1 equiv), MeCN, rt	29%
3	LiHMDS, TMSCl, THF, 0 °C to rt then $Pd(OAc)_2$ (2 equiv), DMSO, O_2, 40 °C	86%

Our initial approach to synthesize the target triene fragment **4.35** (**Scheme 4.6**) involved the palladium-catalyzed reduction of alkenyl triflate **4.34,**[19] which was prepared in one step from α,β-unsaturated ketone **4.33**. However, this two-step sequence afforded triene **4.35** in low yield. Alternatively, Luche reduction of enone **4.33** yielded allylic alcohol **4.36** in good yield.[20] Subsequent mesylation and elimination of **4.36** under reflux conditions provided cyclohexadiene **4.35** along with several unidentified impurities. We then investigated the Shapiro reaction of tosylhydrazone **4.37** for the synthesis of **4.35**.[21] Treatment of **4.37** with excess lithium hydride (LiH) resulted in the formation of **4.35** in very low yield (not shown). Fortunately, employing n-butyllithium (*n*-BuLi) in place of LiH provided the desired triene fragment **4.35** in 51% yield.

Scheme 4.6 Completion of the synthesis of triene **4.35**.

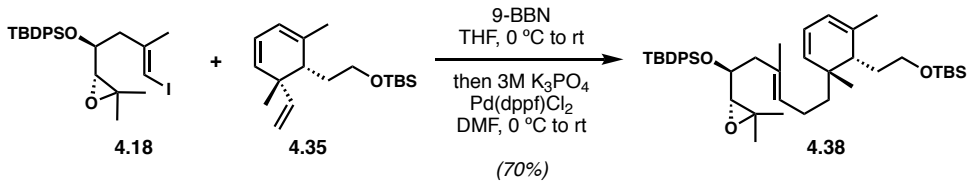


4.3.5 Synthesis of Polyene Substrates

Following the successful synthesis of fragments **4.18** and **4.35**, we employed B-alkyl Suzuki–Miyaura cross-coupling to prepare epoxypolyene **4.38** (**Scheme 4.7**).[1d,22] Treatment of triene **4.33** with 9-borabicyclo[3.3.1]nonane (9-BBN) at room temperature resulted in the selective formation of the terminal alkyl borane intermediate and subsequent B-alkyl Suzuki coupling of

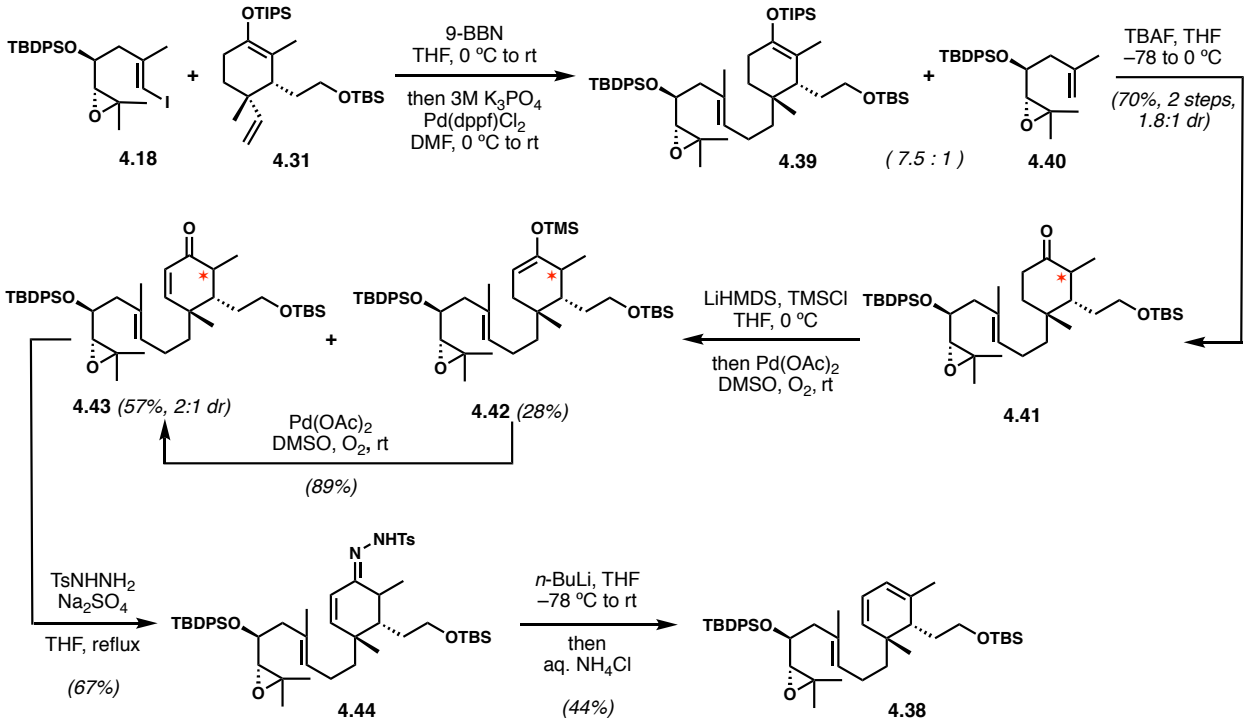
this intermediate with the vinyl iodide **4.18** afforded the desired coupling product **4.38** in 70% yield.

Scheme 4.7 B-alkyl Suzuki–Miyaura cross-coupling of vinyl iodide **4.18** and triene **4.35**.



Alternatively, we envisioned that the polyene substrate **4.43**, containing a cyclohexenone terminal group, would be advantageous for radical-mediated polyene cyclization (**Scheme 4.8**). The synthesis of epoxypolyene **4.43** began with a B-alkyl Suzuki-Miyaura cross-coupling reaction between vinyl iodide **4.18** and the alkyl borane derived from olefin **4.31**. The coupling product **4.39** was obtained along with alkene **4.40**, posing challenges during purification. To address this, we performed a desilylation reaction on the TIPS enoxysilane **4.39** using TBAF, affording ketone **4.41** in a combined yield of 70% over two steps. Next, we aimed to introduce the α,β-unsaturated ketone functionality by Saegusa–Ito oxidation of the kinetically generated enoxysilane **4.42**, similar to the approach used for enone **4.33**. However, this reaction was less efficient on a larger scale, resulting in a moderate yield of the desired α,β-unsaturated ketone **4.43** as a mixture of diastereomers (2:1 dr) along with unreacted enoxysilane **4.42** (28% recovery). Fortunately, the recovered enoxysilane **4.42** was relatively stable and could be resubjected to the oxidative conditions. Although the diastereomers of **4.43** were separable by column chromatography, we proceeded with the mixture for the subsequent hydrazone formation and Shapiro reaction with *n*-BuLi. This reaction sequence furnished the previously synthesized diene polyene substrate **4.38**.

Scheme 4.8 Synthesis of epoxypolyenes **4.38** and **4.43**.

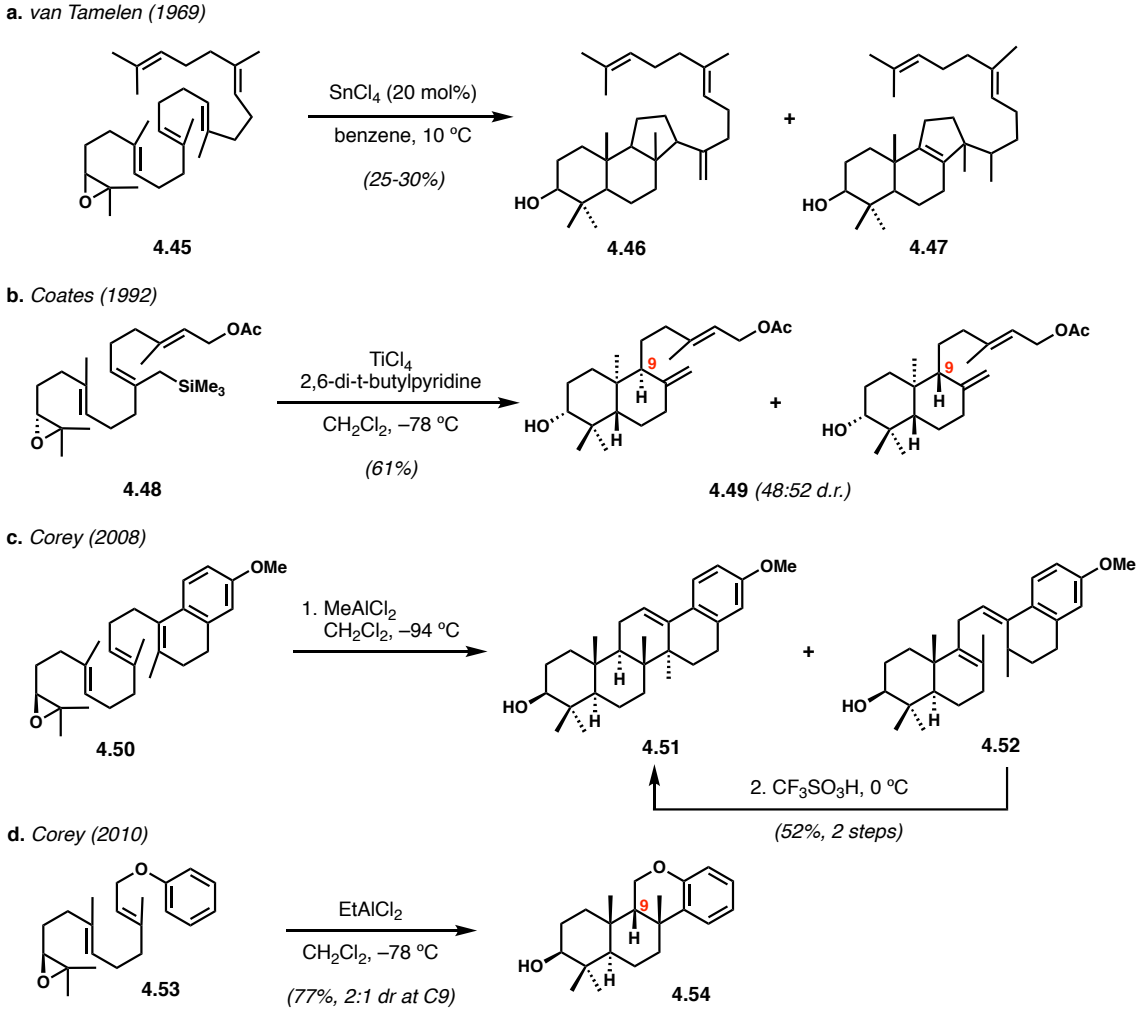


4.4 Attempted Cationic Polyene Cyclizations

4.4.1 Background on the Acid-Catalyzed Epoxypolyene Cyclization

As previously noted during the retrosynthetic analysis of brasilicardin A, the proposed polyene cyclization involving a diene terminator remains unexplored. Hence, establishing a precedent for the Lewis acid-catalyzed polyene cyclization of epoxypolyenes containing terminating alkenes would be advantageous for investigating reaction conditions. To support this concept, we reviewed prior Lewis acid-mediated cyclization reactions using various catalysts and substrates.

Scheme 4.9 (a) Cationic Cyclization of squalene 2,3-oxide by van Tamelen.[23] (b) Epoxy Trienylsilane cyclization by Coates.[24] (c) Synthesis of pentacyclic triterpene using $MeAlCl_2$ by Corey.[25] (d) Cyclization of phenyl ether **4.53** using $EtAlCl_2$.[26]



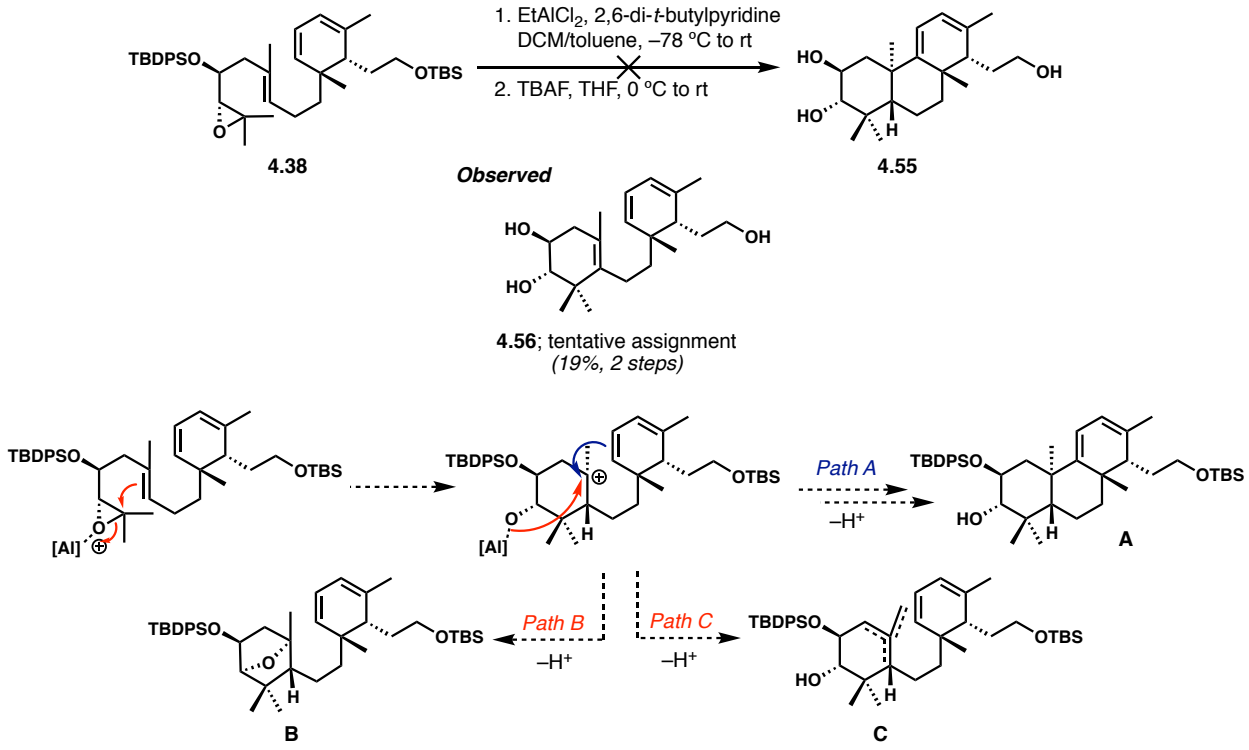
In their pioneering studies, Van Tamelen and co-workers showed that the treatment of squalene 2,3-oxide (**4.45**) with tin(IV) chloride ($SnCl_4$) afforded a mixture of tricyclic compounds **4.46** and **4.47** in 25-30% yield (**Scheme 4.9a**).[23] Later, Coates *et al*. demonstrated that the trimethylsilyl group could stabilize a tertiary carbocation intermediate resulting after the second cyclization, leading to enhanced cyclization efficiency.[24] The epoxide-initiated cationic polyene cyclization of epoxytrienylsilane **4.48** using titanium tetrachloride ($TiCl_4$) resulted in bicyclic products **4.49** as a mixture of diastereomers at C9 (**Scheme 4.9b**).[24] Corey and Surendra reported

a two-stage acid-catalyzed cyclization of epoxytriene **4.50** in the presence of a styryl terminator using methylaluminum dichloride ($MeAlCl_2$) to form pentacycle **4.51** along with bicycle **4.52** (**Scheme 4.9c**).[25] Triflic acid was then employed to convert byproduct **4.52** to the desired product **4.51** via a [1,5]-hydride shift mechanism. Finally, Corey and Shenvi achieved the selective synthesis of 9β-H product **4.54** (2:1 dr at C9) through the ethylaluminum dichloride ($EtAlCl_2$)-catalyzed polyene cyclization of phenyl ether **4.53** (**Scheme 4.9d**).[26] As a whole, these results demonstrate that arenes and olefins can serve as terminating groups in polyene cyclizations, which in turn suggests that use of cyclic and acyclic dienes could also be viable.

4.4.2 Attempted Cationic Polyene Cyclization

Our first approach to synthesizing the brasilicardin A core structure involved Lewis acid-mediated polyene cyclization.[26] However, our initial attempt at cyclization of precursor **4.38** with $EtAlCl_2$ did not yield the desired 6/6/6 tricyclic compound **4.55** via the proposed Path A reaction mechanism (**Scheme 4.10**). Instead, we isolated the monocyclic product **4.56** in 19% yield over two steps through a proposed monocyclization mechanism (Path C) and we did not observe bridged oxabicycle **B** from Path B. We postulate that closure of the second ring is kinetically outcompeted by deprotonation to quench the carbocation intermediate. One reason why the C–C bond formation is slower is likely the fact that the B-ring is required to adopt a boat-like conformation. This hypothesis could be supported by previous study of the cationic polyene cyclization using bismuth triflate ($BiOTf_3$) as a catalyst.[27] Given these results, we elected to investigate radical-based conditions to affect the key polycyclization.

Scheme 4.10 $EtAlCl_2$-catalyzed polyene cyclization of epoxypolyene **4.38** and possible mechanisms.



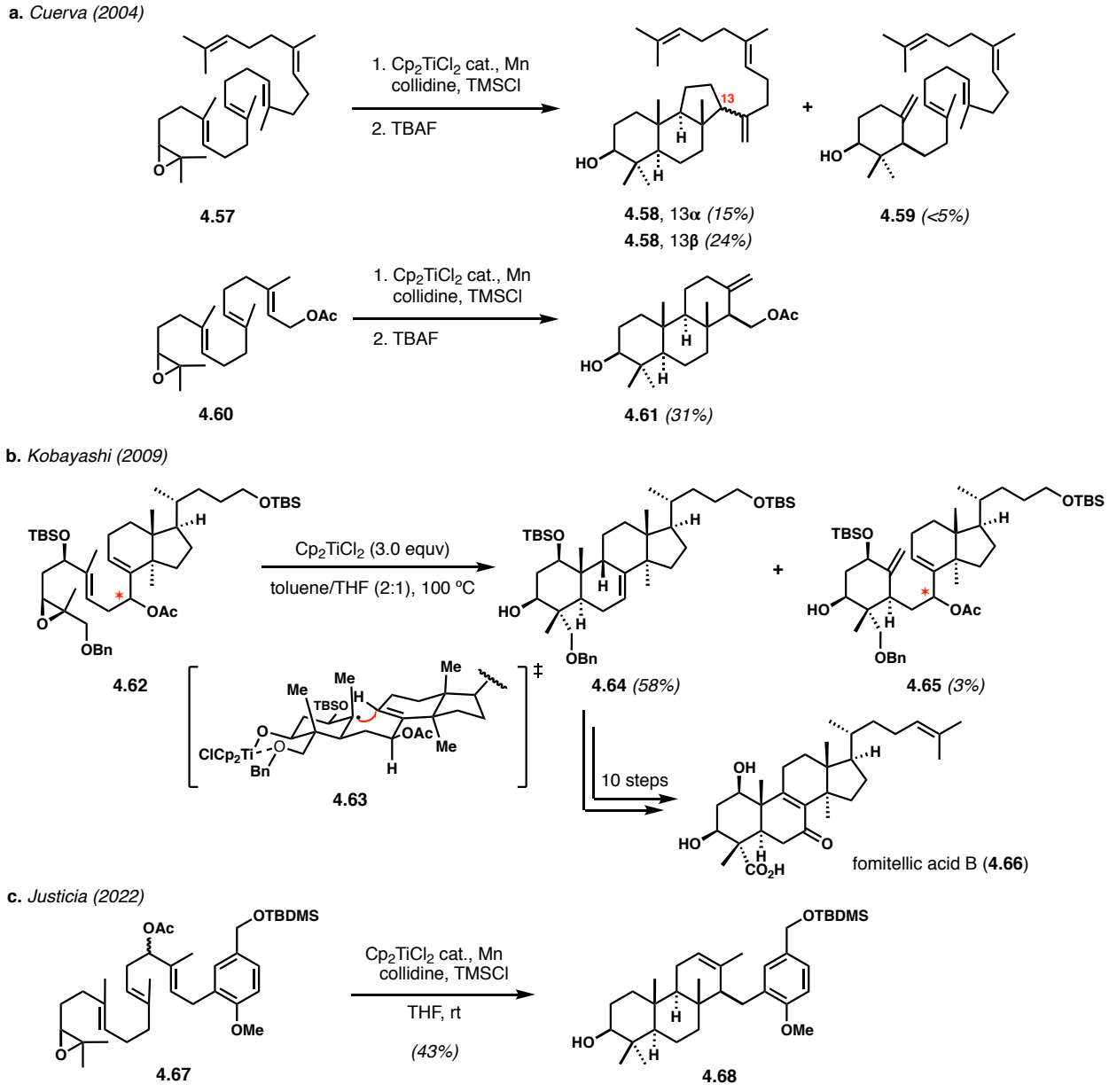
4.5 Attempted Radical Polyene Cyclizations

Titanocene(III) complexes derived from reduction of titanocene dichloride (Cp_2TiCl_2) have been widely used for radical cascade cyclizations of epoxypolyene substrates.[28] In this study, following the unsuccessful attempt at acid-induced polyene cyclization of the diene-terminated polyene **4.38**, we investigated radical-mediated polyene cyclization using Cp_2TiCl_2. As described previously, we also synthesized epoxyolefin **4.43** with a cyclohexenone terminal group. We envisioned that rendering the terminating group electron-deficient could help facilitate the final ring closure, thus we chose to investigate this substrate **4.43** in the titanocene-mediated polyene cyclization.[29]

4.5.1 Precedence for Proposed Radical Polyene Cyclization

We then studied literature examples demonstrating the feasibility of radical-based cyclizations using titanocene(III) reagents for the synthesis of polycyclic frameworks. Cuerva *et al*. previously reported the use of titanocene(III) to promote radical polyene cyclization of 2,3-oxidosqualene **4.57** bearing an alkene terminal group (**Scheme 4.11a**).[30] This approach afforded a mixture of diastereomers (**4.58**) at C13 via 5-*exo*-trig cyclization, along with trace amounts of alcohol **4.59** (**Scheme 4.11a**). In the same study, Cuerva *et al*. showed that epoxypolyene **4.60** underwent Ti(III)-catalyzed radical polyene cyclization to form tricycle **4.61** with an exocyclic alkene following β-elimination (**Scheme 4.11a**). Kobayashi *et al*. demonstrated a similar approach for the synthesis of fomitellic acid B (**4.66**) (**Scheme 4.11b**).[31] Polyene **4.62**, containing an allyl acetate moiety, underwent two 6-*endo* cyclizations using Cp_2TiCl_2 to form tricyclic **4.64** and monocycle **4.65** via a *trans*-fused chair/boat-like transition state (**4.63**) with subsequent elimination of the acetate group (**Scheme 4.11b**). Finally, a similar radical polyene cyclization with acetate elimination was also reported for the synthesis of a makassaric acid derivative (**Scheme 4.11c**).[32]

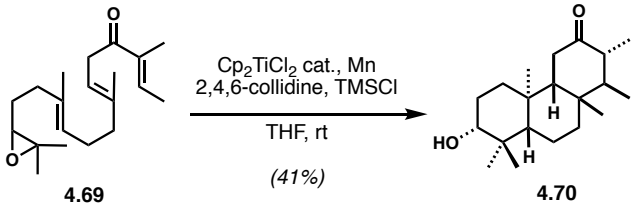
Scheme 4.11 (a) Titanocene-catalyzed radical cyclization of squalene 2,3-oxide.[30] (b) Ti(III)-mediated radical cascade cyclization of epoxypolyene **4.62**.[31] (c) Preparation of tricyclic meroterpene **4.68**.[32]



Most of the previous examples showcased unactivated alkene terminators until Cuerva *et al*. reported the titanocene(III)-catalyzed reductive cyclization of ketoepoxypolyprene **4.69** (**Scheme 4.12**) in 2014.[29] This cascade constructed the congested tricyclic framework of **4.70** in a respectable 41% yield. Mechanistic studies revealed that the C-ring preferentially underwent *cis*

ring closure due to a lower energy transition state, leading to the *cis*-fused decalin product. The presence of an internal α,β-unsaturated ketone in compound **4.69** serves as a precedent for our investigation into the use of polyene substrate **4.43**, which possesses a cyclohexenone terminal group.

Scheme 4.12 Example of Ti(III)-catalyzed radical cyclization of ketoepoxypolyprene **4.69**.[29]



4.69 **4.70**

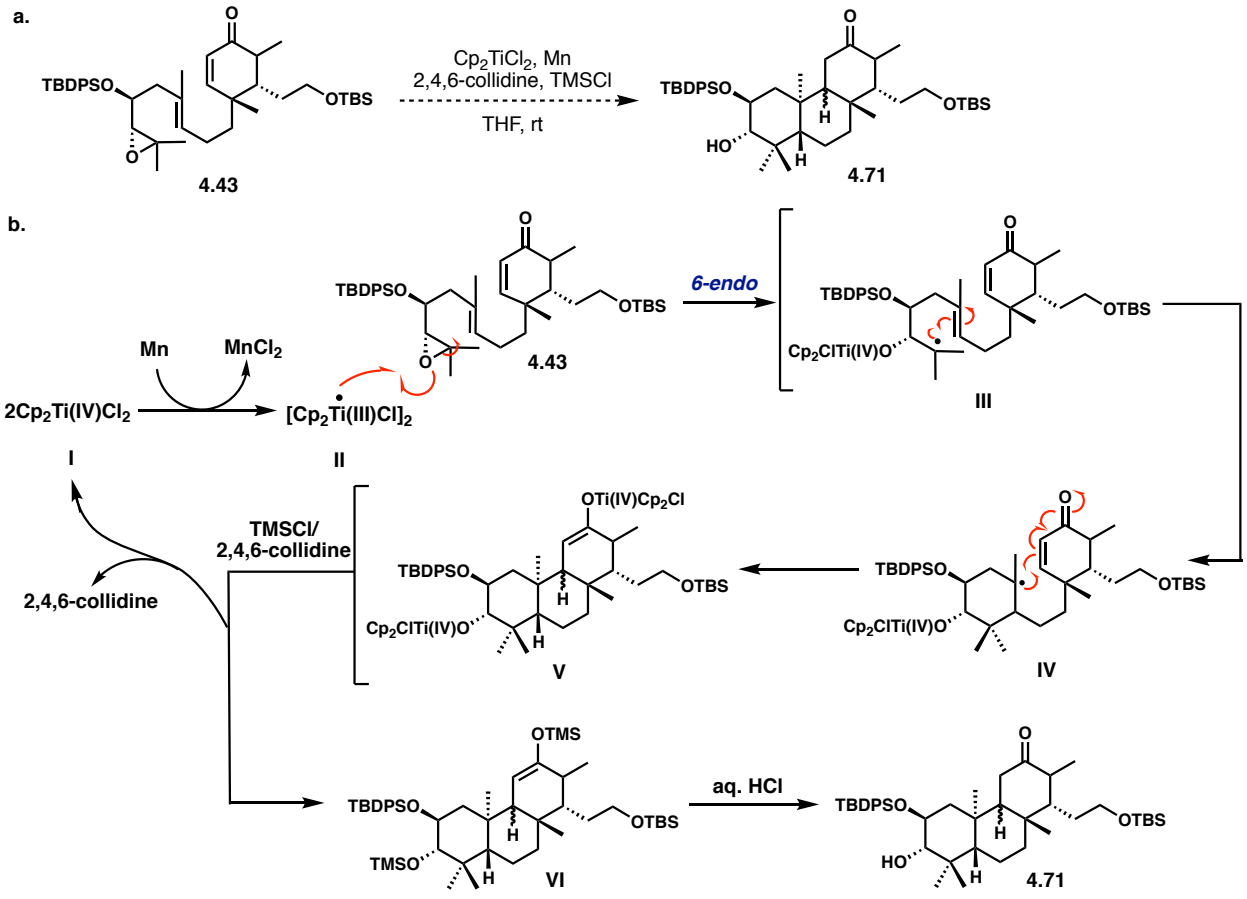
As a whole, these works highlight that using various alkenes as terminating groups in radical polyene cyclizations can be fruitful. We speculate that a diene might also be a suitable if not superior acceptor for the final cyclization due to greater delocalization in the penultimate radical intermediate. Given that our diene **4.38** is cyclic and also bears an adjacent quaternary center, it is difficult to predict the efficiency of such a radical cyclization *a priori*. As articulated previously, there are no examples in the literature of cyclic dienes being utilized as terminating groups in radical or polar polyene cyclizations. Nevertheless, our main focus at this stage was to evaluate enone bearing substrates in our polyene cyclization approach to BraA (**4.1**). We postulated that the polarity-matched nature of the intermediate involved in the second ring closure could at the very least favor tricyclic framework formation.

4.5.2 Attempted Radical Polyene Cyclizations

We hypothesized that the titanocene(III)-catalyzed radical polyene cyclization of the novel C2-oxygenated polyene **4.43** would potentially afford the desired tricyclic product **4.71** (**Scheme 4.13a**). The proposed catalytic cycle is based on established mechanistic data from the Cuerva and Barrero groups (**Scheme 4.13b**).[29-30,33] The reaction is initiated by the reduction of titanocene

dichloride (**I**) by manganese to form the titanocene monochloride dimer (**II**). The titanocene(III) complex subsequently transfers an electron to **4.43**, resulting in epoxide opening and the generation of tertiary radical **III**. This β-titanoxy radical **III** undergoes a 6-*endo*-trig cyclization to form monocyclic radical **IV**, which then undergoes further cyclization to form intermediate **V**. The Ti(IV) enolate **V** is then exposed to a combination of trimethylsilyl chloride (TMSCl) and 2,4,6-collidine to regenerate Cp_2TiCl_2 for the next catalytic cycle, while concurrently forming enoxysilane **VI**. The final desired tricyclic product **4.71** is isolated following standard acidic workup.

Scheme 4.13 (a) Desired radical polyene cyclization of **4.43**. (b) Proposed catalytic cycle of the desired polyene cyclization.

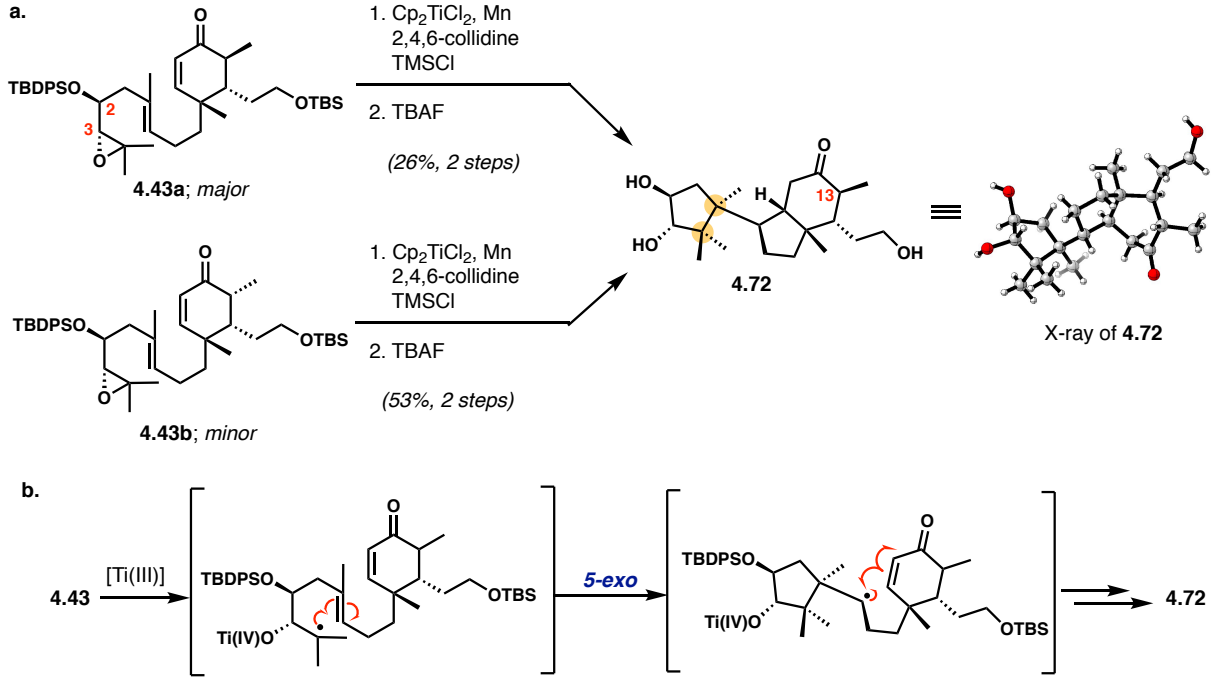


In continuation of **Scheme 4.8**, we successfully isolated two diastereomers of enone **4.43**. The major diastereomer was assumed to be ketone **4.43a** due to the less sterically encumbered equatorial methyl group. Subsequently, both diastereomers (**4.43a** and **4.43b**) were subjected to titanocene(III)-catalyzed radical cyclization to afford products that were isolated and characterized independently (**Scheme 4.14a**). The reaction conditions employed were similar to those reported in previous literature[29,31] with slight modifications in the amount of reagents used. However, column chromatography and preparative thin-layer chromatography failed to purify the cyclization product due to the presence of unidentified impurities. To address this issue and obtain crystals suitable for X-ray diffraction studies, the cyclization product was subjected to TBAF deprotection. This deprotection step was undertaken with the expectation that intermolecular hydrogen bonding may provide for more crystalline material. Unexpectedly, the crystal structure analysis revealed the product to be **4.72**, a 5/6 fused bicyclic skeleton, which differed from the structure proposed in **Scheme 4.13**. Interestingly, tricycle **4.72** was isolated from the radical cyclization, regardless of the diastereomer employed (**4.43a** or **4.43b**). We suspect that TBAF acts as a base, promoting the epimerization of the C13 methyl group from the α to the β isomer.

This unexpected cyclization outcome is attributed to the presence of the bulky *tert*-butyldiphenylsilyl ether at C2 of epoxypolyene **4.43**. At this point, it remains unclear why this steric effect is thought to favor a 5-*exo*-trig cyclization of the A-ring, leading to the formation of a vicinal quaternary centers instead of the usual 6-*endo* process observed in previous studies (**Scheme 4.14b**)[29-32]. It is important to note that our group has previously reported radical polyene cyclization with C2 oxygenation where only the expected decalin products were observed.[1a-c] One tentative rationale could be that the protected C2 alcohol chelates the titanium metal center along with the C3 alkoxy group in an intramolecular fashion, enforcing a conformation favoring 5-*exo*-

trig cyclization. These results prompted us to perform a model study examining the influence of the C2 alcohol protecting group on the mode of the first ring closure.

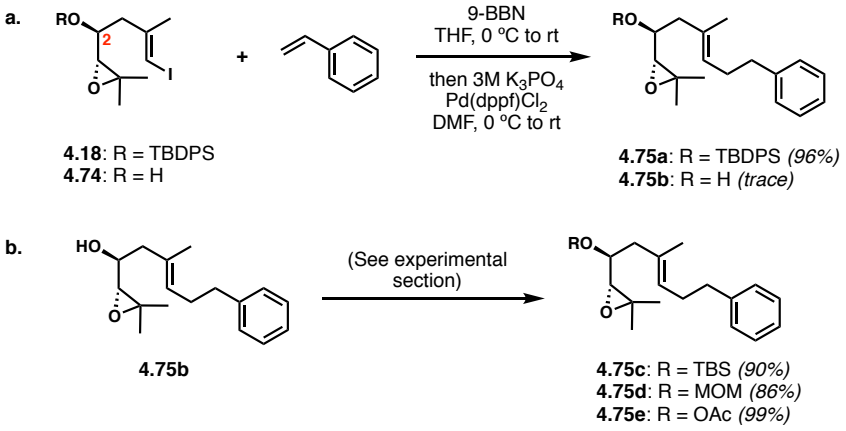
Scheme 4.14 (a) Radical polyene cyclization of epoxypolyene **4.43** (b) Possible reaction pathway leading to unusual 5-*exo* product **4.72**.



4.6 Radical Polyene Cyclization of Model Alkene

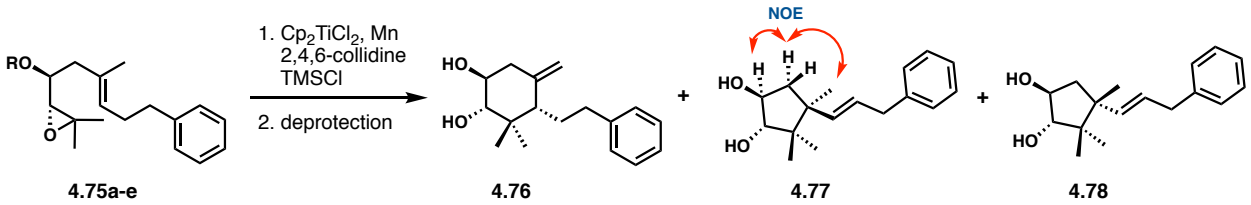
It was hypothesized that a less bulky protecting group at C2 might favor the desired 6-*endo*-trig cyclization pathway. Model substrates **4.75a** and **4.75b** were synthesized via B-alkyl Suzuki cross-coupling of vinyl iodides **4.18** and **4.74**, respectively, with styrene (**Scheme 4.15a**). However, only trace amounts of the desired secondary alcohol **4.75b** were obtained using carbinol **4.35b** in the coupling reaction. The carbinol **4.75b** was successfully obtained via TBAF-mediated deprotection of the TBDPS ether **4.75a** (see experimental section). Subsequently, various epoxyalkenes **4.75c-e** bearing different substituents were synthesized from secondary alcohol **4.75b** using appropriate protection conditions (**Scheme 4.15b**) (see experimental section).

Scheme 4.15 (a) Synthesis of model substrate **4.75a-b** using B-alkyl Suzuki cross coupling. (b) Preparation of protected alcohols **4.75c-d**.



Next, we investigated the titanocene(III)-promoted radical cyclization of model alkenes **4.75a-e**, followed by deprotection of the resulting products (**Table 4.5**). For these studies, the desired product was a cyclohexane **4.76** with an exocyclic alkene moiety. The reaction of TBDPS ether **4.75a** resulted in a mixture of 5-*exo* cyclization products (**4.77** and **4.78**) (entry 1) after radical cyclization and desilylation. The structure of the major 5-membered ring product (**4.77**) was determined using 2D NOESY NMR analysis. The NOE correlations between assigned protons are shown in **Table 4.5**. Subsequently, the reaction was performed with TBS ether substrate **4.75b**, which has less steric hindrance compared to the TBDPS group, however the desired cyclohexene **4.76** was not obtained (entry 2). The C2 silyl group was then varied by replacing it with a methoxymethyl (MOM) ether in **4.75c** and acetate in **4.75d**. While the desired product **4.76** was successfully obtained in these reactions (entries 3-4), undesired pentacyclic products **4.77** and **4.78** were also formed. Finally, the reaction was carried out with the alcohol substrate **4.75e**. Gratifyingly, this reaction yielded the desired exocyclic alkene **4.76** as a single regioisomer in 59% isolated yield (entry 5). This result suggests that a hydroxyl group at the C2 position favors the 6-*endo*-trig cyclization pathway, which we hoped to apply in our synthesis.

Table 4.5 Radical cyclization on model systems **4.75a-e**.



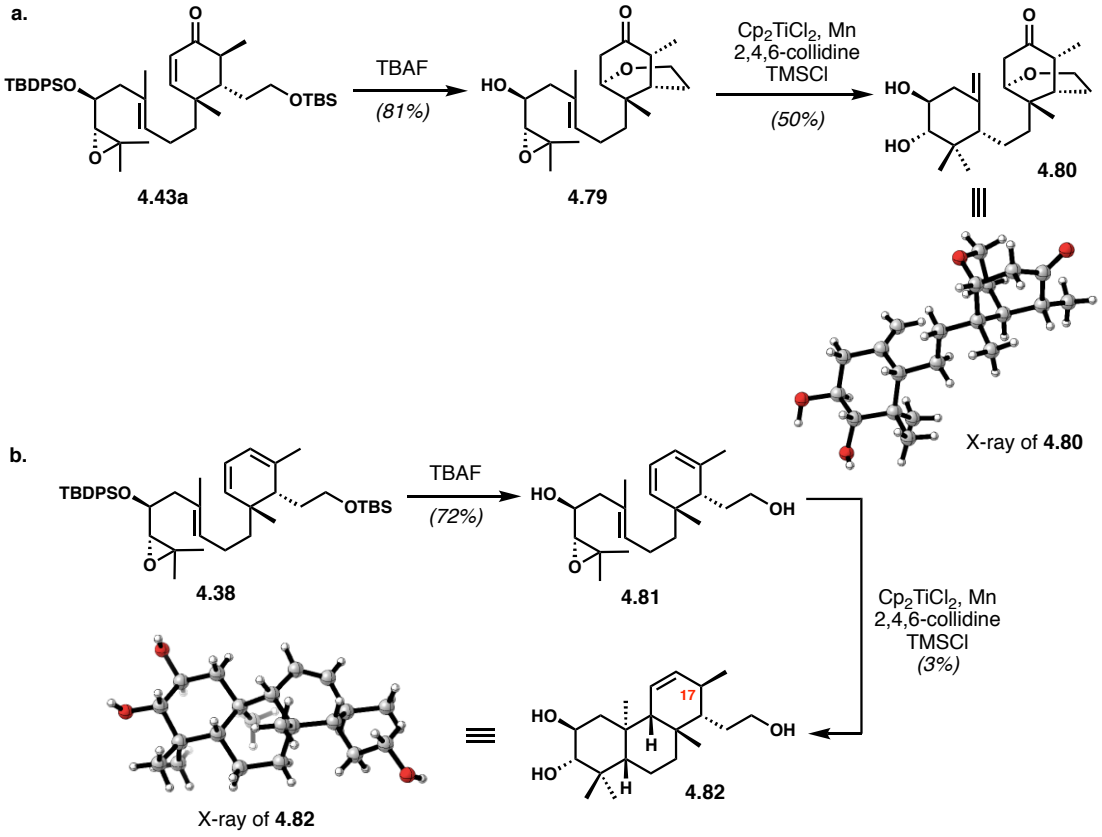
4.75a-e 4.76 4.77 4.78

Entry	R	Yield (2 steps)		
		4.76	4.77	4.78
1	TBDPS	–	32%	14%
2	TBS	–	49%	30%
3	MOM	24%	39%	19%
4	Ac	35%	39%	24%
5	H	59%	–	–

With the polyenes **4.38** and **4.43** in hand, we elected to deprotect the C2 silylethers and form the corresponding C2 hydroxy groups (**Scheme 4.16**). However, during the attempted deprotection, the more labile primary OTBS pendent group was preferentially removed. Interestingly, the desilylation of compound **4.43a** resulted in the formation of oxabicycle **4.79** via intramolecular oxa-Michael cyclization. Subsequently, epoxyalkene **4.79** was subjected to the radical cyclization, affording monocycle **4.80**. The structure of **4.80** was confirmed by X-ray crystallography (**Scheme 4.16a**). In a noteworthy reaction, we attempted the cyclization with **4.81,** which yielded the tricyclic compound **4.82** in 3% isolated yield. The X-ray crystal structure of **4.82** was subsequently obtained (**Scheme 4.16b**). Structural analysis revealed that **4.82** possesses a *trans*/*anti*/*cis*-perhydrophenanthrene core with unexpected regiochemistry of the internal alkene in the ring C. This tricyclic product **4.82** represents not only the first example of a radical polyene cyclization terminating with a diene but also illustrates an unusual reduction to a 1,2-disubstituted alkene instead of the exocyclic alkene as observed in previous studies.[33] These findings support

our hypothesis that the presence of a C2 hydroxy group is crucial for promoting the 6-*endo*-trig cyclization mode in this reaction.

Scheme 4.16 (a) Radical cyclization of oxabicycle **4.79**. (b) Attempted Ti(III)-mediated radical polyene cyclization to access tricyclic core of brasilicardin A.

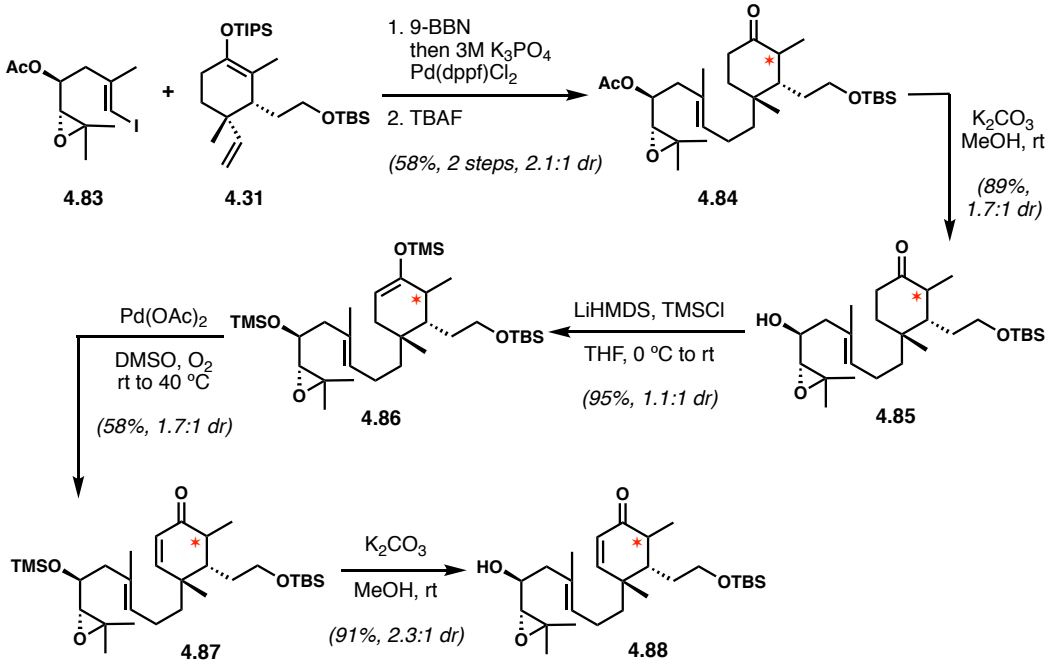


4.7 Revised Synthetic Route Towards Epoxypolyenes

Given the significance of the C2-OH group in our radical cyclization, we refined our synthesis of epoxypolyene substrates intended for Ti(III)-mediated radical polyene cyclization (**Scheme 4.17**). The synthetic route towards epoxypolyene **4.88** began with a B-alkyl Suzuki cross-coupling reaction between vinyl iodide **4.83** and Diels–Alder adduct **4.31**. Subsequent TIPS deprotection afforded ketone **4.84** in 58% yield over two steps. The order of the synthetic steps was crucial, as the removal of the acetate protecting group from **4.84** must precede Saegusa–Ito

oxidation. Silylation of ketone **4.84** to form the corresponding TMS enoxysilane proved challenging in the presence of the acetate group. After acetate hydrolysis with potassium carbonate in methanol and TMS silylation, we obtained the desired enoxysilane **4.86** in 95% yield. Next, Saegusa–Ito oxidation of compound **4.86** afforded enone **4.87** in 58% yield. Finally, removal of the TMS group under basic conditions revealed the desired epoxypolyene **4.88**.

Scheme 4.17 Revised synthesis of epoxypolyene **4.88**.

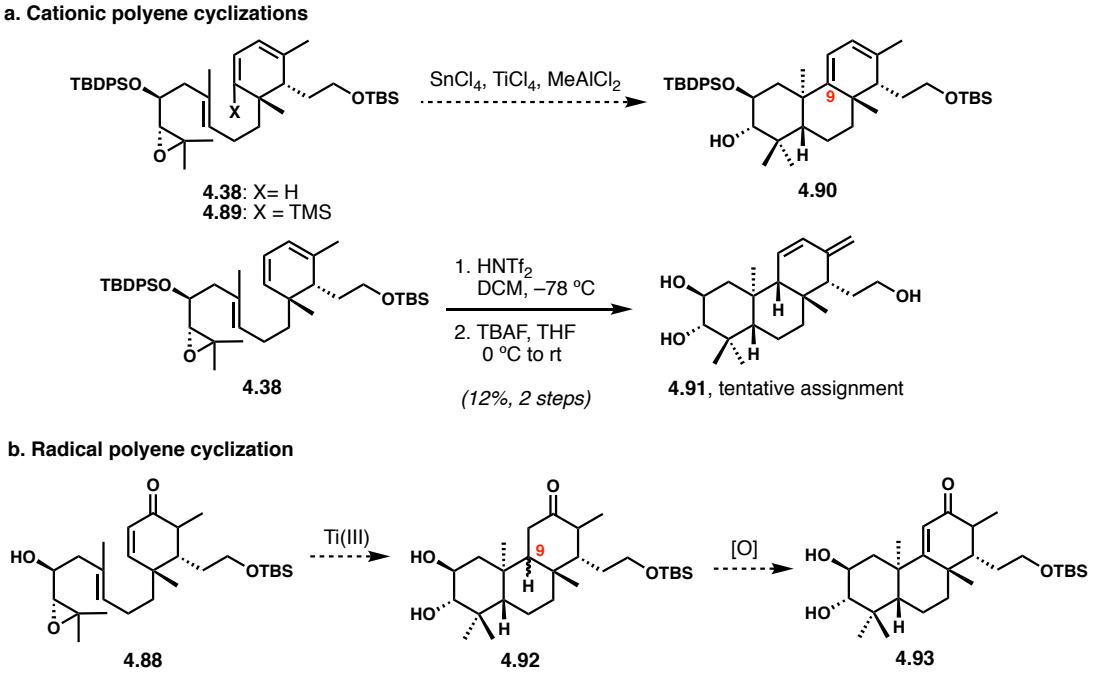


4.8 Future Work

Our future plan is to develop a concise approach to the *trans*/*syn*/*trans*-perhydrophenanthrene core of brasilicardin A (**4.1**) by employing cationic and radical polyene cyclization strategies. Investigations of the acid-catalyzed polyene cyclization with diene-terminating substrate (**4.38**) will be carried out using various Lewis acids, such as $SnCl_4$, $TiCl_4$, and $MeAlCl_2$ (**Scheme 4.18a**).[24-26] The preliminary study of using Brønsted acid for polar polyene cyclization of epoxypolyene **4.38** provided the tentatively assigned tricyclic **4.91** bearing an

exocyclic alkene on the C ring. We will also synthesize a polyene substrate **4.89** containing an alkenyl TMS group to improve the cationic polyene cyclization by stabilizing the penultimate cationic intermediate. We propose establishing the desired stereochemistry at C9 with directed hydrogenation (C9 in **4.90**) utilizing the side-chain hydroxyl group. Building upon our achievement in synthesizing the tricyclic product **4.82** and preparing the epoxypolyene **4.38**, we intend to scale up Ti(III)-mediated radical polyene cyclization of these substrates. Our focus will be on screening reaction conditions to enhance the yield of the target product **4.92.** Additionally, we will probe the possibility of achieving the desired C9 stereochemistry directly via the key cascade cyclization (**Scheme 4.18b**). The oxidation of **4.92** would be necessary if product **4.92** is obtained with the undesired C9 stereochemistry, requiring a kinetically controlled reduction to forge the strained tricyclic ring system.

Scheme 4.18 Future work for cationic and radical polyene cyclization.



4.9 Conclusions

The cross-coupling fragments, vinyl iodide **4.18**, enoxysilane **4.31**, and diene **4.35**, were successfully synthesized. Vinyl iodide **4.18** was prepared through a concise six-step sequence involving a key enzymatic kinetic resolution and diastereoselective epoxidation. The oxazaborolidine-catalyzed enantioselective Diels–Alder reaction using tosylated D-tryptophan was optimized to afford the desired cycloadduct **4.29** in good yield and reasonable enantioselectivity. The desired enantiomer of the Diels–Alder product was employed for the synthesis of fragments **4.31** and **4.35** via Saegusa–Ito oxidation and Shapiro reaction. Subsequently, we investigated the B-alkyl Suzuki–Miyaura cross-coupling reaction between the vinyl iodide and alkene fragments to synthesize the desired epoxypolyenes. We found that polyene substrate with a cyclohexadiene terminating group could be synthesized using the same reaction sequence employed for the cyclohexenone-bearing fragments.

Our attempts to forge the desired tricyclic framework via a Lewis acid-catalyzed cationic polyene cyclization with $EtAlCl_2$ were unsuccessful. Therefore, we explored radical polycyclizations mediated by low-valent Ti, generated *in situ* by reduction of Cp_2TiCl_2. We discovered that the presence of C2 substituents, particularly the bulky TBDPS group, favored 5-*exo*-trig cyclization, leading to the formation of the unusual bicyclic ketone **4.72**. To investigate the effect of the C2 protecting group on the cyclization mode, we prepared model alkenes **4.75a-e** and subjected them to Ti(III)-mediated radical cyclization. We found that the C2-hydroxyl group was required to form the desired six-membered ring product. This observation was further supported by the radical polyene cyclization of real system precursors, oxabicyclic alcohol **4.79** and epoxypolyene **4.81**. The X-ray crystal structure of the cyclized products confirmed the formation of the 6/6/6 tricyclic core, demonstrating a proof of concept for our synthetic proposal

to brasilicardin A for the first time. In conclusion, we have successfully synthesized the key cross-coupling fragments and established a strategy for the construction of the brasilicardin A core utilizing a radical polyene cyclization approach. Future efforts will focus on optimizing the reaction conditions for scaling up the current route and developing an approach to obtain the desired stereochemistry at C9 of the tricyclic core.

4.10 References

1. Polyene cyclization by Vanderwal group; (a) Niman, S. W.; Buono, R.; Fruman, D. A.; Vanderwal, C. D. *Org. Lett*. **2023**, *25*, 3451–3455. (b) Vrubliauskas D.; Vanderwal C. D. *Angew. Chem. Int. Ed*. **2020**, *59*, 6115. (c) Vrubliauskas, D.; Groß, B.; Vanderwal, C. D. *J. Am. Chem. Soc*. **2021**, *143*, 2944–2952. (d) Michalak, S. E.; Nam, S.; Kwon, D. M.; Horne, D. A.; Vanderwal, C. D. *J. Am. Chem. Soc*. **2019**, *141*, 9202–9206.
2. Jung, M. E.; Chamberlain, B. T.; Koch, P.; Niazi, K. R. *Org. Lett.* **2015**, *17*, 3608–3611.
3. Anada, M.; Hanari, T.; Kakita, K.; Kurosaki, Y.; Katsuse, K.; Sunadoi, Y.; Jinushi, Y.; Takeda, K.; Matsunaga, S.; Hashimoto, S. *Org. Lett*. **2017**, *19*, 5581–5584.
4. Yoshimura, F.; Itoh, R.; Torizuka, M.; Mori, G.; Tanino, K. *Angew. Chem. Int. Ed*. **2018**, *57*, 17161–17167.
5. (a) Brandes, E.; Grieco, P. A.; Garner, P. *J. Chem. Soc., Chem. Commun.*, **1988**, *7*, 500–502. (b) Liang, D.; Zou, Y.; Wang, Q.; Goeke, A. *J. Org. Chem.* **2014**, *79*, 6726–6731.
6. Sawama, Y.; Sawama, Y.; Krause, N. *Org. Biomol. Chem*., **2008**, *6*, 3573–3579.
7. (a) Adam, W.; Wirth, T. *Acc. Chem. Res.* **1999,** *32*, 703–710. (b) Adam, W.; Mitchell, C. M.; Saha-Möller, C. R. *J. Org. Chem.* **1999,** *64,* 3699–3707.
8. Williard, P. G.; De Laszlo, S. E. *J. Org. Chem.* **1985**, *50*, 3738–3749.
9. Koukal, P.; Ulč, J.; Nečas, D.; Kotora, M. *Eur. J. Org. Chem*. **2016**, 2110–2114.

10. (a) Shing, T. K. M.; Tang, Y. *Tetrahedron* **1990**, *46*, 2187–2194. (b) Deng, J.; Zhou, S.; Zhang, W.; Li, J.; Li, R.; Li, A. *J. Am. Chem. Soc*. **2014**, *136*, 8185–8188.
11. Niman, S. W. PhD Dissertation, University of California, Irvine, 2023.
12. Serra, S.; Fuganti, C. *Tetrahedron: Asymmetry* **2001**, *12*, 2191–2196.
13. Hong, S.; Corey, E. J. *J. Am. Chem. Soc.* **2006**, *128*, 1346–1352.
14. Corey, E. J.; Guzman-Perez, A.; Loh, T.-P. *J. Am. Chem. Soc*. **1994**, *116*, 3611–3612.
15. (a) Sawai, Y.; Mizuno, M.; Ito, T.; Kawakami, J.-i.; Yamano M. Tetrahedron **2009**, *65*, 7122–7128. (b) Zipfel, H. F.; Carreira, E. M. *Org. Lett*. **2014**, *16*, 2854–2857.
16. Corey, E. J.; Loh, T. P. *J. Am. Chem. Soc*. **1991**, *113*, 8966–8967.
17. Fu, L.; Lin, Q.-X.; Liby, K. T.; Sporn, M. B.; Gribble, G. W. *Org. Biomol. Chem*. **2014**, *12*, 5192–5200.
18. (a) Esposito, A.; Giovanni, C.; De Fenza, M.; Talarico, G.; Chino, M.; Palumbo, G.; Guaragna, A.; D'Alonzo, D. *Chem. Eur. J*. **2020**, *26*, 2597–2601. (b) Yu, B.; Jiang, T.; Quan, W.; Li, J.; Pan, X.; She, X. *Org. Lett*. **2009**, *11*, 629–632.
19. Wang, H.; Regan, C. J.; Codelli, J. A.; Romanato, P.; Puchlopek-Dermenci, A. L. A.; Reisman, S. E. *Org. Lett*. **2017**, *19*, 1698–1701.
20. Zhang, W.; Ding, M.; Li, J.; Guo, Z.; Lu, M.; Chen, Y.; Liu, L.; Shen, Y.-H.; Li, A. *J. Am. Chem. Soc*. **2018**, *140*, 4227–423.
21. (a) Taspinar, Ö.; Wilczek, T.; Erver, J.; Breugst, M.; Neudörfl, J.-M.; Schmalz, H.-G. *Chem. Eur. J*. **2020**, *26*, 4256–4260. (b) Tahara, T.; Streit, U.; Pelish, H. E.; Shair, M. D. *Org. Lett*. **2017**, *19*, 1538–1541.
22. Elkhayat, Z.; Safir, I.; Retailleau, P.; Arseniyadis, S. Org. Lett. 2007, 9, 4841–4844.

23. (a) Van Tamelen, E. E.; Sharpless, K. B. *J. Am. Chem. Soc*. **1969**, *91*, 1848–1849. (b) Van Tamelen, E. E.; Willett, J.; Schwartz, M.; Nadeau, R. *J. Am. Chem. Soc*., **1996**, *88*, 5937–5938.

24. Yee, N. K. N.; Coates, R. M. *J. Org. Chem.* **1992**, *57*, 4598–4608.

25. Surendra, K.; Corey, E. J. *J. Am. Chem. Soc*. **2008**, *130*, 8865–8869.

26. Shenvi, R. A.; Corey, E. J. *Org.Lett.* **2010**, *12*, 3548–3551.

27. Castillo, A.; Quilez Del Moral, J. F.; Barrero, A. F. *Nat. Prod. Commun.*, **2017**, *12*, 657–658.

28. Morcillo ,S. P.; Miguel , D.; Campana , A. G.; Alvarez de Cienfuegos, L.; Justicia, J.; Cuerva , J. M. *Org. Chem. Front.*, **2014**, *1*, 15–33.

29. Morcillo, S. P.;Miguel, D.; Resa, S.; Martín-Lasanta, A.; Millań, A.; Choquesillo-Lazarte, D.; García-Ruiz, J. M.; Mota, A. J.; Justicia, J.; Cuerva, J. M. *J. Am. Chem. Soc.* **2014**, *136*, 6943−6951.

30. Justicia, J.; Rosales, A.; Buñuel, E.; Oller-López, J. L.; Valdivia, M.; Haïdour, A.; Oltra, J. E.; Barrero, A. F.; Cárdenas, D. J.; Cuerva, J. M. *Chem. Eur. J.* **2004**, *10*, 1778–1788.

31. Yamaoka, M.; Nakazaki, A.; Kobayashi, S. *Tetrahedron Lett*, **2009**, *50*, 6764–6768.

32. Rosales, J.; Cabrera, G.; Justicia, J. *Molecules* **2022**, *27*, 2400.

33. González-Delgado, J. A.; Escobar, G.; Arteaga, J. F.; Barrero, A. F. *Molecules* **2014**, *19*, 1748–1762.

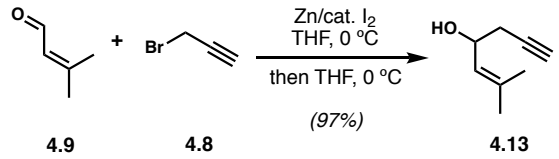
4.11 Experimental Information

4.11.1 General Experimental Method

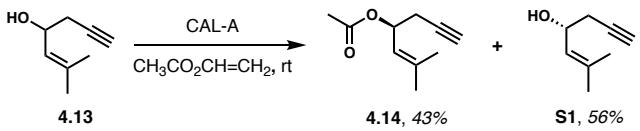
All reactions were performed in oven–dried or flame–dried glassware under an atmosphere of dry argon unless otherwise noted. Reaction solvents including dichloromethane (CH_2Cl_2, Fisher, HPLC Grade), hexanes (Fisher, HPLC Grade), diethyl ether (Et_2O, Fisher, BHT stabilized, HPLC Grade), benzene (C_6H_6, Fisher, HPLC Grade), tetrahydrofuran (THF, Fisher, HPLC Grade), and toluene ($PhCH_3$, Fisher, HPLC Grade), methanol (MeOH, Fisher, low water Grade), 1,2-dichloroethane (DCE, Fisher, HPLC Grade), dimethylformamide (DMF, Fisher, HPLC Grade) were dried by percolation through a column packed with neutral alumina and a column packed with Q5 reactant, a supported copper catalyst for scavenging oxygen, under a positive pressure of argon. Solvents for workup and chromatography were: hexanes (Fisher or EMD, ACS Grade), EtOAc (Fisher, ACS Grade), dichloromethane (CH_2Cl_2, Fisher, ACS Grade), and diethyl ether (Fisher, ACS Grade). Argon gas (5.0 grade, AR 5.0UH-T, Praxair) was dispensed from size T cylinders. Column chromatography was performed using EMD Millipore 60 Å (0.040–0.063 mm) mesh silica gel (SiO_2). Analytical and preparatory thin-layer chromatography was performed on Merck silica gel 60 F254 TLC plates. Visualization was accomplished with UV (254 or 210 nm), and *p*-anisaldehyde, potassium permanganate, or ceric ammonium molybdate stain solutions and heat as developing agents. Chloroform-d ($CDCl_3$, D 99.8%, DLM-7) was purchased from Cambridge Isotope Laboratories. K_2CO_3 (anhydrous, 99%, Alfa Aesar), $NaHCO_3$ (ACS grade, Fisher), NaOH (ACS grade, Macron or Fisher), $Na_2S_2O_3$ (ACS grade, Fisher), triethylamine (Et_3N, EMD, CaH_2) and pyridine (Alfa Aesar, CaH_2), were distilled from the indicated drying agents prior to use. Proton and carbon magnetic resonance spectra (^1H NMR and ^{13}C NMR) were recorded at 298 K on a Bruker CRYO500 (500 MHz, ^1H; 125 MHz, ^{13}C) spectrometer with solvent

resonance as the internal standard (^{1}H NMR: $CHCl_3$ at 7.26 ppm, ^{13}C NMR: $CDCl_3$ at 77.16 ppm). ^{1}H NMR data are reported as follows: chemical shift, multiplicity (app = apparent, s = singlet, d = doublet, t = triplet, q = quartet, dd = doublet of doublets, ddd = doublet of doublet of doublets, dddd = doublet of doublet of doublet of doublets, dtt = doublet of triplet of triplets, td = triplet of doublets, tdd = triplet of doublet of doublets, qd = quartet of doublets, m = multiplet, br s = broad singlet), coupling constants (Hz), and integration. High resolution mass spectra (HRMS) were recorded on a Waters LCT Premier spectrometer using ESI-TOF (electrospray ionization-time of flight) and data are reported in the form of (m/z).

4.11.2 Experimental Procedures and Characterization Data



6-methylhept-5-en-1-yn-4-ol (**4.13**): Prepared according to a known literature procedure[1], using 3-methyl-2-butenal (**4.9**) (0.91 mL, 9.5 mmol, 1.0 equiv), propargyl bromide (1.9 mL, 18 mmol, 1.9 equiv), zinc activated by HCl (1.5 g, 23 mmol, 2.4 equiv), and iodine (0.20 g, 0.79 mmol, 0.080 mmol). The crude product was purified by flash column chromatography (SiO_2, 20% EtOAc in hexanes) to afford alcohol (**4.13**) (1.1 g, 97% yield, *spectral data are in agreement with that reported in literature*[1]) as a yellow oil.

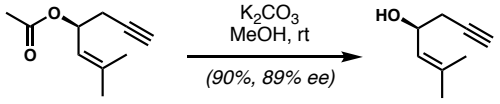


(*S*)-6-methylhept-5-en-1-yn-4-yl acetate (**4.14**): Prepared according to a known literature procedure[2], using alcohol **4.13** (6.5 g, 53 mmol, 1.0 equiv), *Candida antarctica* lipase A (CAL-A)

(0.65 g, 10 % wt.), and vinyl acetate (29 mL). The reaction mixture was stirred at room temperature for 1 hour 45 minutes. The crude product was purified by flash column chromatography (SiO_2, 10% EtOAc in hexanes) to afford alcohol **4.13** (3.8 g, 43% yield) as a light yellow oil and alkene **S1** (3.7 g, 56%) as a yellow oil.

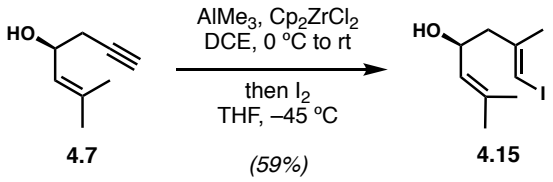
^{1}H NMR (500 MHz, $CDCl_3$) δ 5.60 (dt, *J* = 9.1,6.1 Hz, 1H), 5.22 – 5.20 (m, 1H), 2.47 (ddd, *J* = 6.0, 2.5, 1.7 Hz, 2H), 2.04 (s, 3H), 1.96 (t, *J* = 2.6 Hz, 1H), 1.73 (s, 6H).

^{13}C NMR (125 MHz, $CDCl_3$) δ 170.5, 138.9, 122.1, 79.8, 70.2, 69.1, 25.8, 25.1, 21.3, 18.7.



4.14 **4.7**

(*S*)-6-methylhept-5-en-1-yn-4-ol (**4.7**): To a solution of acetate **4.14** (3.8 g, 23 mmol, 1.0 equiv) in MeOH (230 mL) was added K_2CO_3 (16 g, 11 mmol, 5.0 equiv) at room temperature. The reaction mixture was stirred for 90 min then diluted with water (80 mL), CH_2Cl_2 (80 mL), and brine (80 mL). The phases were separated and the aqueous layer was extracted with CH_2Cl_2 (3 x 130 mL). The combined organic extracts were washed with brine, dried over $MgSO_4$, filtered and concentrated *in vacuo.* The crude product was purified by flash column chromatography (SiO_2, 20% EtOAc in hexanes) to afford allylic alcohol **4.7** (2.8 g, 90%, , *spectral data are in agreement with that reported in literature*[1]) as a light yellow oil. The product **4.7** had 89% ee as determined by NMR analysis of the Mosher ester.

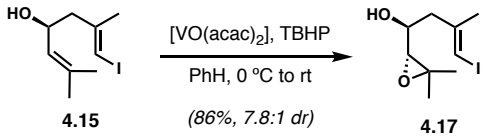


(*S*,*E*)-1-iodo-2,6-dimethylhepta-1,5-dien-4-ol (**4.15**): A three-neck 250 mL round bottom flask was equipped with an addition funnel and then charged with Cp_2ZrCl_2 (2.5 g, 8.4 mmol, 1.0 equiv). The flask was evacuated and refilled with dry argon gas three times. DCE (34 mL) was added into the reaction flask. Me_3Al (2.0 M in toluene, 21 mL, 42 mmol, 5.0 equiv) was added dropwise using the addition funnel at room temperature under an atmosphere of argon. The resulting yellow solution was stirred for 20 minutes at this temperature. Next, the reaction was cooled to 0 ºC and a solution of alkyne **4.7** (1.0 g, 8.4 mmol, 1.0 equiv, dried by azeotropic distillation from benzene) in DCE (34 mL) was added dropwise. The resulting mixture was warmed to room temperature and stirred for 48 hours. The reaction was cooled to –45 ºC and a solution of iodine (2.8 g, 10.9 mmol, 1.3 equiv) in THF (34 mL) was added dropwise. After stirring for 1 hour at –45 ºC, the reaction was quenched with 10% aq. Na_2CO_3 (67 mL). The phases were separated and the aqueous layer was extracted with CH_2Cl_2 (4 x 30 mL). The combined organic extracts were washed with brine, dried over Na_2SO_4, filtered and concentrated *in vacuo.* The crude product was purified by flash column chromatography (pH7 SiO_2, 5% EtOAc in hexanes to 10% EtOAc in hexanes) to afford vinyl iodide **4.15** (1.3 g, 59%) as a light yellow oil.

^{1}H NMR (500 MHz, $CDCl_3$) δ 6.00 (s, 1H), 5.14 (d, J = 8.5 Hz, 1H), 4.48 (td, J = 8.3, 5.1 Hz, 1H), 2.44 (dd, J = 13.5, 8.2 Hz, 1H), 2.32 (dd, J = 13.5, 4.7 Hz, 1H), 1.88 (s, 3H), 1.72 (s, 3H), 1.68 (s, 3H), 1.51 (br s, 1H).

^{13}C NMR (125 MHz, $CDCl_3$) δ 144.7, 136.0, 127.0, 77.6, 66.5, 47.6, 25.9, 24.4, 18.4.

HRMS [ES+] m/z calc'd for $C_9H_{14}I$ $[M+H-H_2O]^+$: 249.0140, found 249.0147.



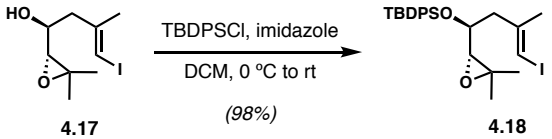
4.15 4.17

(*S*,*E*)-1-((*R*)-3,3-dimethyloxiran-2-yl)-4-iodo-3-methylbut-3-en-1-ol (**4.17**): Allylic alcohol **4.15** (1.2 g, 4.6 mmol, 1.0 equiv) was dried by azeotropic distillation from benzene (3 x 1.0 mL) and dissolved in benzene (230 mL). To a cooled (0 ºC) solution of allylic alcohol **4.17** in benzene was added $VO(acac)_2$ (0.25 g, 0.92 mmol, 0.20 equiv) and TBHP (5.5 M in nonane, 1.3 mL, 6.9 mmol, 1.5 equiv). The resulting mixture was warmed to room temperature and stirred for 1 hour. The reaction was quenched with 10% w/v aq. $Na_2S_2O_3$ (230 mL). The phases were separated and the aqueous layer was extracted with EtOAc (3 x 140 mL). The combined organic extracts were washed with brine, dried over $MgSO_4$, filtered and concentrated *in vacuo.* The crude product was purified by flash column chromatography (SiO_2, 10% EtOAc in hexanes to 20% EtOAc in hexanes) to afford epoxyolefin **4.17** (1.1 g, 86%, 7.8:1 dr) as a light yellow oil.

^{1}H NMR (500 MHz, $CDCl_3$) δ 6.07 (s, 1H), 3.61 (q, *J* = 7.1 Hz, 1H), 2.69 (d, *J* = 7.9 Hz, 1H), 2.56 (dd, *J* = 13.8, 7.2 Hz, 1H), 2.42 (dd, *J* = 13.8, 6.3 Hz, 1H), 2.15 (br s, 1H), 1.89 (s, 3H), 1.32 (s, 3H), 1.28 (s, 3H).

^{13}C NMR (125 MHz, $CDCl_3$) δ 143.5, 78.0, 68.8, 67.4, 60.0, 44.0, 25.0, 24.7, 19.5.

HRMS [ES+] m/z calc'd for $C_9H_{15}IO_2Na$ $[M+Na]^+$: 305.0015, found 305.0015.



4.17 4.18

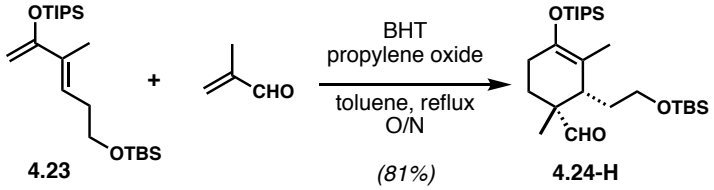
***tert*-butyl(((*S*,*E*)-1-((*R*)-3,3-dimethyloxiran-2-yl)-4-iodo-3-methylbut-3-en-1-yl)oxy)diphenylsilane** (**4.18**): To a solution of alcohol (19 mg, 66 µmol, 1.0 equiv) in CH_2Cl_2 at 0 ºC was added imidazole (18 mg, 0.26 mmol, 4.0 equiv) and TBDPSCl (41 µL, 0.16 mmol, 2.4

equiv). The reaction mixture was stirred at room temperature overnight before quenching with water (700 μL). The phases were separated and the aqueous layer was extracted with EtOAc (3 x 1.5 mL). The combined organic extracts were washed with brine, dried over Na_2SO_4, filtered and concentrated *in vacuo.* The crude product was purified by flash column chromatography (pH7 SiO_2, 5% Et_2O in hexanes) to afford enoxysilane **4.18** (34 mg, 98%) as a colorless oil.

^{1}H NMR (500 MHz, $CDCl_3$) δ 7.73 – 7.70 (m, 4H), 7.45 – 7.36 (m, 6H), 5.84 (a, 1H), 3.53 (td, *J* = 8.1, 6.0 Hz, 1H), 2.79 (d, *J* = 5.7 Hz, 1H), 2.40 – 2.31 (m, 2H), 1.41 (s, 3H), 1.25 (s, 3H), 1.09 (s, 9H), 0.95 (s, 3H).

^{13}C NMR (125 MHz, $CDCl_3$) δ 143.4, 136.3, 136.2, 134.2, 133.4, 129.84, 129.80, 127.7, 127.6, 78.1, 71.1, 67.8, 58.9, 45.5, 27.1, 24.9, 24.3, 19.8, 19.5.

HRMS (Cl+) m/z calc'd for $C_{21}H_{24}IO_3Si$ $[M+tBu]^+$: 463.0590, found 463.0609.

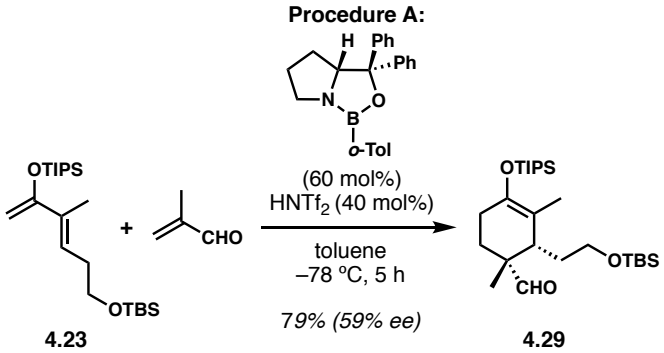


(1*R*,2*S*)-2-(2-((*tert*-butyldimethylsilyl)oxy)ethyl)-1,3-dimethyl-4-((triisopropylsilyl)oxy)cyclohex-3-ene-1-carbaldehyde (**4.24-H**): To a flame-dried vial containing enoxysilane (0.12 g, 0.31 mmol, 1.0 equiv) in toluene (620 μL) was added methacrolein (0.13 mL, 1.5 mmol, 5.0 equiv), propylene oxide (2 drops), and butylated hydroxytoluene (BHT) (6.7 mg, 31 μmol, 0.10 equiv) at room temperature. The reaction mixture was refluxed overnight. The solution was then concentrated *in vacuo*. The crude product was purified by flash column chromatography (pH7 SiO_2, 5% CH_2Cl_2 in hexanes to 10% CH_2Cl_2 in hexanes) to afford cycloadduct **4.24-H** (0.12 g, 81%) as a yellow oil.

^{1}H NMR (600 MHz, $CDCl_3$) δ 9.59 (s, 1H), 3.56 (qt, *J* = 10.2, 6.6 Hz, 2H), 2.13 – 2.10 (m, 3H), 1.86 (dt, *J* = 13.4, 9.0 Hz, 1H), 1.69 (s, 3H), 1.58 – 1.47 (m, 3H), 1.16 – 1.08 (m, 24H), 0.89 (s, 9H), 0.033 (s, 6H).

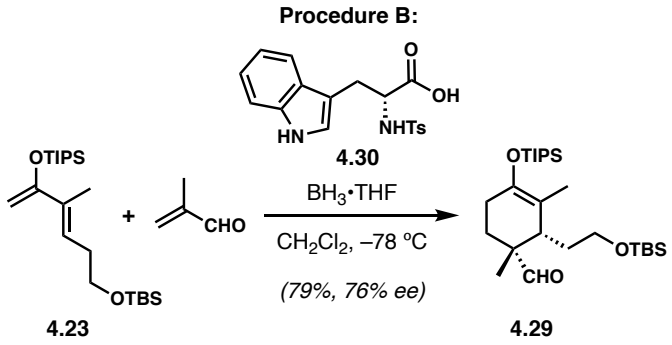
^{13}C NMR (150 MHz, $CDCl_3$) δ 206.5, 142.8, 112.2, 62.4, 48.6, 42.2, 36.6, 26.6, 26.1, 24.1, 19.2, 18.4, 18.3, 18.2, 16.6, 13.3, -5.19.

HRMS (ES+) m/z calc'd for $C_{26}H_{52}O_3Si_2Na$ $[M+Na]^+$: 491.3353, found 491.3347.

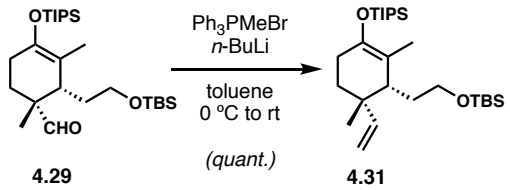


(1*R*,2*S*)-2-(2-((*tert*-butyldimethylsilyl)oxy)ethyl)-1,3-dimethyl-4-((triisopropylsilyl)oxy)cyclohex-3-ene-1-carbaldehyde (**4.29**): **Procedure A**: Enoxysilane **4.23** (40 mg, 0.10 mmol, 1.0 equiv) was dried by azeotropic distillation from benzene (3 x 100 µL) and placed *in vacuo* for 30 minutes. To a cooled (–20 ºC) (*R*)-Me-Corey–Bakshi–Shibata catalyst (0.50 M in toluene, 0.12 mL, 60 µmol, 0.60 equiv) was added a stock solution of $NHTf_2$ (0.15 M, in toluene, 0.27 mL, 40 µmol, 0.40 equiv). After stirring for 40 minutes, the resulting solution was cooled to –78 ºC. Then, a solution of enoxysilane **4.23** in toluene (400 µL) followed by methacrolein (40 µL, 0.50 mmol, 5.0 equiv) were added slowly, down the side of the reaction vial. The reaction was stirred at –78 ºC for 5 hours before quenching with Et_3N (100 µL). Next, the solution was then concentrated *in vacuo*. The crude product was purified by flash column chromatography (pH7 SiO_2, 20% CH_2Cl_2 in hexanes) to afford cycloadduct **4.29** (37 mg, 79%,

*spectral data are in agreement with that reported in **4.24-H***) as a colorless oil. The product **4.29** had 59% ee as determined by NMR analysis of the Mosher ester.



Procedure B: Enoxysilane **4.23** (0.10 g, 0.25 mmol, 1.0 equiv) was dried by azeotropic distillation from benzene (3 x 200 µL) and placed *in vacuo* for 30 minutes. To a suspension of catalyst **4.30** (36 mg, 0.10 mmol, 0.40 equiv) in CH_2Cl_2 (2.5 mL) was added BH_3•THF (1.0 M in THF, 0.10 mL, 0.10 mmol, 0.40 equiv) at room temperature. The mixture was stirred for 15 minutes before cooling to –78 ºC. Then, methacrolein (0.10 mL, 1.3 mmol, 5.0 equiv) was added dropwise. A precooled solution of enoxysilane **4.23** in CH_2Cl_2 (2.5 mL) at –78 ºC was added dropwise down the side of vial. After stirring for 20 hours, the reaction mixture was added Et_3N (150 µL) followed by satd. aq. $NaHCO_3$ (150 µL) and warmed to room temperature. The solution was then concentrated *in vacuo*. The resulting crude residue was dissolved in EtOAc (500 µL) and dried over Na_2SO_4. The slurry was filtered and washed with EtOAc (3 x 500 µL). The filtrate was concentrated *in vacuo*. The crude product was purified by flash column chromatography (pH7 SiO_2, 20% CH_2Cl_2 in hexanes) to afford cycloadduct **4.29** (93 mg, 79%, *spectral data are in agreement with that reported in **4.24-H***) as a colorless oil. The product **4.29** had 76% ee as determined by NMR analysis of the Mosher ester.

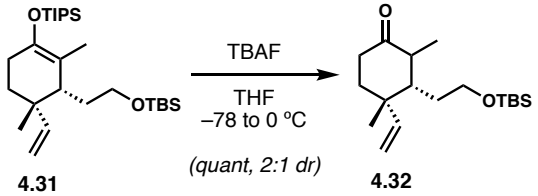


***tert*-butyl(2-((1*R*,6*S*)-2,6-dimethyl-3-((triisopropylsilyl)oxy)-6-vinylcyclohex-2-en-1-yl)ethoxy)dimethylsilane** (**4.31**): Methyltriphenylphosphonium bromide (1.4 g, 3.9 mmol, 2.5 equiv) was dried by azeotropic distillation from benzene (3 x 2.0 mL) and placed *in vacuo* for 5 hours. Aldehyde **4.29** (0.73 g, 1.6 mmol, 1.0 equiv) was dried by azeotropic distillation from benzene (3 x 0.6 mL) and placed *in vacuo* for 30 minutes. A cooled (–78 ºC) suspension of Methyltriphenylphosphonium bromide in THF (24 mL) was treated with *n*-BuLi (1.5 M in hexanes, 2.4 mL, 3.6 mmol, 2.3 equiv). The mixture was warmed to room temperature and stirred for 1 hour. Then the reaction was cooled to –78 ºC and a solution aldehyde **4.29** in THF (10 mL) was added. The reaction mixture was warmed to room temperature and stirred for 20 hours before quenching with satd. aq. NH_4Cl (14 mL). The phases were separated and the aqueous phase was extracted with CH_2Cl_2 (3 x 20 mL). The combined organic extracts were washed with brine, dried over Na_2SO_4, filtered and concentrated *in vacuo.* The crude product was purified by flash column chromatography (pH7 SiO_2, 10% CH_2Cl_2 in hexanes) to afford alkene **4.31** (0.70 g, 97%) as a colorless oil.

^{1}H NMR (600 MHz, $CDCl_3$) δ 5.85 (dd, *J* = 17.6, 10.9 Hz, 1H), 4.96 (dd, *J* = 10.9, 1.2 Hz, 1H), 4.91 (dd, *J* = 17.6, 1.1 Hz, 1H), 3.60 – 3.53 (m, 2H), 2.17 – 2.06 (m, 2H), 1.70 (ddd, *J* = 12.8, 11.0, 7.0 Hz, 1H), 1.65 (s, 3H), 1.63 – 1.57 (m, 2H), 1.47 – 1.39 (m, 2H), 1.17 – 1.08 (m, 21H), 1.00 (s, 3H), 0.89 (s, 9H), 0.033 (s, 6H).

^{13}C NMR (150 MHz, $CDCl_3$) δ 147.7, 142.1, 113.7, 111.0, 63.7, 45.8, 38.8, 36.1, 28.5, 27.5, 26.2, 24.8, 18.5, 18.30, 18.28, 16.4, 13.3, -5.04.

HRMS (Cl+) m/z calc'd for $C_{27}H_{54}O_2Si_2$ $[M]^+$: 466.3662, found 466.3664.

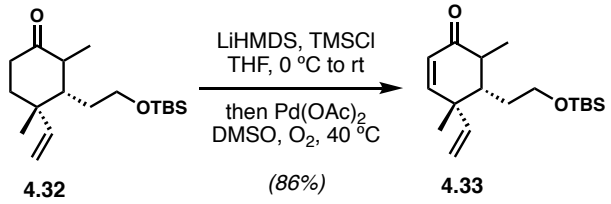


(3*S*,4S)-3-(2-((*tert*-butyldimethylsilyl)oxy)ethyl)-2,4-dimethyl-4-vinylcyclohexan-1-one (**4.32**): To a stirred solution of enoxysilane **4.31** (0.70 g, 1.5 mmol, 1.0 equiv) in THF (10 mL) at –78 ºC was added TBAF (1.0 M in THF, 1.6 mL, 1.6 mmol, 1.1 equiv). The reaction mixture was warmed to 0 ºC, stirred for 30 minutes, and quenched with satd. aq. NH_4Cl (16 mL). The phases were separated and the aqueous phase was extracted with EtOAc (3 x 16 mL). The combined organic extracts were washed with brine, dried over Na_2SO_4, filtered and concentrated *in vacuo.* The crude product was purified by flash column chromatography (pH7 SiO_2, 5% EtOAc in hexanes) to afford ketone **4.32** (0.48 g, quant.) as a light yellow oil.

^{1}H NMR (500 MHz, $CDCl_3$) δ 6.19 (dd, *J* = 17.5, 11.0 Hz, 2H), 5.88 (dd, *J* = 17.6, 10.9 Hz, 1H), 5.24 (d, *J* = 11.0 Hz, 2H), 5.19 (d, *J* = 17.6 Hz, 2H), 5.03 (d, *J* = 10.9 Hz, 1H), 4.94 (d, *J* = 17.7 Hz, 1H), 3.63 – 3.58 (m, 2H), 3.52 – 3.42 (m, 4H), 2.87 (quintet, *J* = 6.4 Hz, 1H), 2.55 (td, *J* = 14.3, 6.0 Hz, 2H), 2.47 – 2.40 (m, 1H), 2.38 – 2.25 (m, 5H), 2.00 – 1.93 (m, 3H), 1.83 – 1.76 (m, 2H), 1.73 – 1.63 (m, 4H), 1.59 (s, 1H), 1.48 – 1.40 (m, 3H), 1.33 – 1.32 (m, 4H), 1.25 – 1.17 (m, 3H), 1.09 (s, 6H), 1.07 (s, 3H), 1.01 – 1.00 (m, 4H), 0.88 – 0.87 (m, 27 H), 0.036 (s, 12H), 0.016 (s, 6H).

^{13}C NMR (125 MHz, $CDCl_3$) δ 213.6, 213.1, 146.7, 141.0, 115.2, 111.8, 63.71, 63.69, 50.0, 47.9, 47.7, 44.5, 40.7, 40.3, 39.3, 38.3, 37.7, 34.5, 31.9, 30.3, 27.2, 26.1, 25.7, 18.48, 18.47, 12.66, 12.63, -5.15.

HRMS [ES+] m/z calc'd for $C_{18}H_{34}O_2SiNa$ $[M+Na]^+$: 333.2226, found 333.2227.



4.32 4.33

(4*R*,5*S*)-5-(2-((*tert*-butyldimethylsilyl)oxy)ethyl)-4,6-dimethyl-4-vinylcyclohex-2-en-1-one (**3.33**): Ketone **4.32** (0.14 g, 0.45 mmol, 1.0 equiv) was dried by azeotropic distillation from benzene (3 x 0.7 mL) and placed *in vacuo* for 30 minutes. To a cooled (0 ºC) solution of ketone **4.32** in THF (4.5 mL) was added a stock solution of LiHMDS (0.70 M in THF, 1.3 mL, 0.90 mmol, 2.0 equiv). The reaction mixture was stirred for 30 minutes before adding a stock solution of TMSCl (0.70 M in THF, 1.3 mL, 0.90 mmol, 2.0 equiv) and continued stirring at 0 ºC for 20 minutes. Then, the reaction was warmed to room temperature over 10 minutes and stirred for 50 minutes. The reaction mixture was filtered through a pad of neutral Al_2CO_3, the pad was washed with THF (3 x 1.3 mL), and the filtrate was concentrated *in vacuo*. The crude TMS enoxysilane was used for the next step directly.

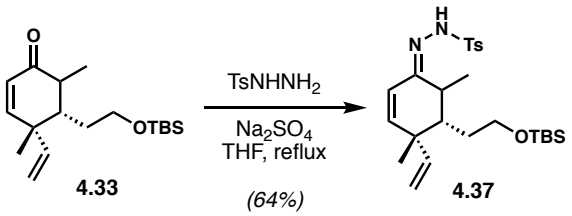
To a solution of the TMS enoxysilane in DMSO (4.5 mL) was added $Pd(OAc)_2$ (0.20 g, 0.90 mmol, 2.0 equiv). Next, O_2 gas was bubbled through the reaction solution for 10 minutes before allowing the reaction to stir at room temperature overnight under a balloon atmosphere of oxygen. TLC analysis indicated incomplete conversion so the reaction was heated to 40 ºC and stirred for 2 hours. After complete consumption of starting material, water (6.0 mL) was added. The phases were separated and the aqueous phase was extracted with CH_2Cl_2 (3 x 6.0 mL). The combined organic extracts were washed with brine, dried over Na_2SO_4, filtered and concentrated

in vacuo. The crude product was purified by flash column chromatography (SiO_2, 50% CH_2Cl_2 in hexanes) to afford enone **4.33** (0.12 g, 86%) as a yellow oil.

^{1}H NMR (600 MHz, $CDCl_3$) δ 6.68 (d, *J* = 10.2 Hz, 1H), 6.47 (d, *J* = 10.0 Hz, 2H), 5.97 (d, *J* = 10.0 Hz, 2H), 5.94 (d, *J* = 10.3 Hz, 1H), 5.90 – 5.81 (m, 3H), 5.19 (d, *J* = 10.5 Hz, 2H), 5.12 (d, *J* = 10.8 Hz, 1H), 5.09 – 5.03 (m, 3H), 3.67 (ddd, *J* = 9.8, 8.4, 5.0 Hz, 2H), 3.58 – 3.49 (m, 4H), 2.71 – 2.70 (m, 1H), 2.32 (dq, *J* = 13.6, 6.8 Hz, 2H), 1.97 – 1.96 (m, 1H), 1.79 (dtd, *J* = 14.5, 8.0, 2.2 Hz, 2H), 1.71 – 1.66 (m, 1H), 1.62 (ddd, *J* = 14.6, 6.0, 2.0 Hz, 2H), 1.51 – 1.48 (m, 1H), 1.45 – 1.40 (m, 2H), 1.28 (s, 3H), 1.25 (s, 6H), 1.14 (d, *J* = 6.8 Hz, 6H), 1.11 (d, *J* = 7.2 Hz, 3H), 0.88 – 0.86 (m, 27 H), 0.034 – 0.017 (m, 18 H).

^{13}C NMR (150 MHz, $CDCl_3$) δ 202.1, 156.1, 138.5, 127.3, 116.8, 63.4, 46.2, 44.1, 43.9, 42.5, 33.3, 26.09, 26.06, 25.3, 18.44, 18.41, 13.0, 12.5, –5.17, -5.18, -5.21.

HRMS (ES+) m/z calc'd for $C_{18}H_{32}O_2Si_2Na$ $[M+Na]^+$: 331.2069, found 331.2067.



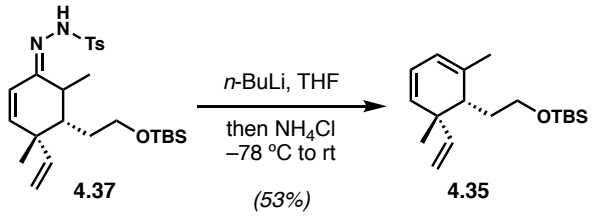
***N*'-((4*R*,5*S*,*Z*)-5-(2-((*tert*-butyldimethylsilyl)oxy)ethyl)-4,6-dimethyl-4-vinylcyclohex-2-en-1-ylidene)-4-methylbenzenesulfonohydrazide** (**4.37**): Enone **4.33** (29 mg, 95 μmol, 1.0 equiv) was dried by azeotropic distillation from benzene (3 x 0.1 mL) and placed *in vacuo* for 30 minutes. *P*-Toluenesulfonyl hydrazide ($TsNHNH_2$) (35 mg, 0.19 mmol, 2.0 equiv) was added in one portion to a vigorously stirred enone **4.33** (29 mg, 95 μmol, 1.0 equiv) and Na_2SO_4 (17.2 mg) in THF (950 μL) at room temperature under an atmosphere of argon. The reaction mixture was stirred for 19 hours at reflux before cooling to room temperature and concentrating *in vacuo*. The resulting crude

residue was purified by flash column chromatography (pH7 SiO_2, 100% hexanes to 20% EtOAc in hexanes) to afford tosylhydrazone **4.37** (29 mg, 64%) as a yellow oil.

^{1}H NMR (500 MHz, $CDCl_3$) δ 7.87 – 7.84 (m, 4H), 7.30 – 7.29 (m, 4H), 6.27 (dd, J = 10.1, 6.3 Hz, 1H), 6.09 (dd, J = 17.8, 10.3 Hz, 1H), 5.96 – 5.68 (m, 3H), 5.10 – 5.05 (m, 1H), 5.02 – 4.92 (m, 3H), 3.69 – 3.40 (m, 4H), 2.77 – 2.66 (m, 1H), 2.41 – 2.32 (m, 7H), 1.78 – 1.59 (m, 4H), 1.40 – 1.34 (m, 2H), 1.24 – 1.18 (m, 1H), 1.08 – 1.04 (m, 6H), 0.98 – 0.97 (m, 2H), 0.93 – 0.90 (m, 4H), 0.87 – 0.83 (m, 18H), 0.08 – -0.026 (m, 14H).

^{13}C NMR (125 MHz, $CDCl_3$) δ 158.7, 156.4, 144.0, 143.9, 143.8, 143.0, 135.6, 135.4, 129.7, 129.5, 129.41, 129.36, 128.2, 128.0, 124.6, 116.2, 114.8, 114.1, 63.6, 61.0, 45.7, 43.8, 41.9, 41.6, 37.6, 32.9, 29.7, 29.2, 28.0, 27.0, 26.1, 26.0, 25.1, 21.7, 18.3, 14.8, 14.0, 10.9, -5.17, -5.23.

HRMS (ES+) m/z calc'd for $C_{25}H_{40}N_2O_3SSiH$ $[M+H]^+$: 477.2607, found 477.2590.



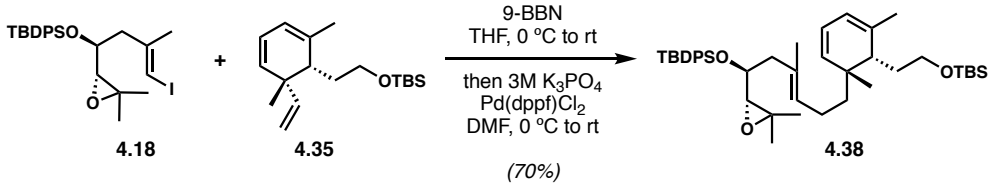
***tert*-butyl(2-((1*S*,6*R*)-2,6-dimethyl-6-vinylcyclohexa-2,4-dien-1-yl)ethoxy)dimethylsilane** (**4.35**): Tosylhydrazone **4.37** (15 mg, 32 µmol, 1.0 equiv) was dried by azeotropic distillation from benzene (3 x 0.1 mL) and placed *in vacuo* for 30 minutes. To a solution of tosylhydrazone **4.37** in THF (640 µL) at –78 ºC was added *n*-BuLi (1.5 M in hexanes, 50 µL, 67 µmol, 2.1 equiv). The warmed to room temperature and stirred overnight. TLC analysis indicated incomplete conversion so the reaction was cooled to –78 ºC and *n*-BuLi (1.5 M in hexanes, 90 µL, 0.13 mmol, 4.2 equiv) was added. After stirring for 46 hours at room temperature, TLC analysis indicated complete consumption of the starting material and the reaction was quenched with satd. aq. NH_4Cl (50 µL)

and added water (400 μL). The phases were separated and the aqueous phase was extracted with Et_2O (3 x 0.2 mL). The combined organic extracts were washed with brine, dried over Na_2SO_4, filtered and concentrated *in vacuo.* The crude product was purified by flash column chromatography (pH7 SiO_2, 100% hexanes to 5% Et_2O in hexanes) to afford diene **4.35** (5.0 mg, 53%) as a colorless oil.

^{1}H NMR (600 MHz, $CDCl_3$) δ 5.84 – 5.79 (m, 2H), 5.61 (d, *J* = 4.3 Hz, 1H), 5.57 (d, *J* = 9.6 Hz, 1H), 5.11 (d, *J* = 17.5 Hz, 1H), 5.05 (d, *J* = 10.7 Hz, 1H), 3.61 – 3.52 (m, 2H), 1.83 – 1.80 (m, 4H), 1.74 – 1.69 (m, 1H), 1.52 – 1.46 (m, 1H), 1.05 (s, 3H), 0.88 (s, 9H), 0.017 (s, 6H).

^{13}C NMR (150 MHz, $CDCl_3$) δ 144.6, 139.4, 130.3, 123.4, 117.9, 112.1, 61.8, 45.6, 42.1, 32.6, 29.9, 26.1, 25.0, 23.7, -5.03, -5.09.

HRMS (Cl+) m/z calc'd for $C_{18}H_{32}OSi$ $[M]^+$: 292.222, found 292.2226.



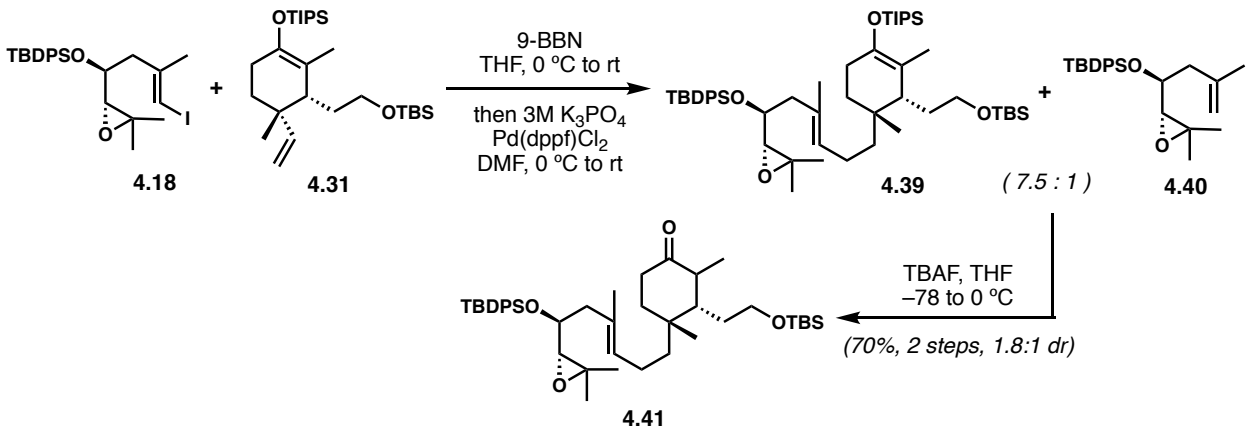
***tert*-butyl(((*S*,*E*)-6-((1*R*,6*S*)-6-(2-((*tert*-butyldimethylsilyl)oxy)ethyl)-1,5-dimethylcyclohexa-2,4-dien-1-yl)-1-((*R*)-3,3-dimethyloxiran-2-yl)-3-methylhex-3-en-1-yl)oxy)diphenylsilane** (**4.38**): Vinyl iodide **4.18** (0.11 g, 0.21 mmol, 1.0 equiv) and alkene **4.35** (69 mg, 0.24 mmol, 1.1 equiv) were separately dried by azeotropic distillation from benzene (3 x 0.1 mL) and placed *in vacuo* for 30 minutes. To alkene **4.35** in THF (3.4 mL) at 0 ºC was added 9-BBN (0.50 M in THF, 0.94 mL, 0.47 mmol, 2.2 equiv), under an atmosphere of argon. The reaction was warmed to room temperature and stirred for 1 hour. TLC analysis indicated incomplete conversion so the reaction was cooled to 0 ºC and 9-BBN (0.50 M in THF, 3.8 mL, 1.9 mmol, 8.8 equiv) was added. After

stirring at room temperature for 2 hours, TLC analysis indicated complete consumption of the starting material and the reaction was cooled to 0 ºC. Aq. K_3PO_4 (3.0 M, 0.56 mL, 7.8 equiv) was added and the resulting mixture was warmed to room temperature. After 10 minutes, $Pd(dppf)Cl_2•CH_2Cl_2$ (52 mg, 64 μmol, 0.30 equiv) was added, followed by the addition of a solution of **4.18** in DMF (3.1 mL). After stirring for 17 hours, the reaction was diluted with brine (3.2 mL), hexanes (4.6 mL), and water (3.2 mL). The phases were separated and the aqueous phase was extracted with EtOAc (3 x 2.1 mL). The combined organic extracts were washed with brine, dried over $MgSO_4$, filtered and concentrated *in vacuo.* The crude product was purified by flash column chromatography (pH7 SiO_2, 100% hexanes to 2% EtOAc in hexanes) to afford diene **4.38** (0.11 g, 70%) as a yellow oil.

^{1}H NMR (600 MHz, $CDCl_3$) δ 7.75 – 7.72 (m, 4H), 7.41 – 7.35 (m, 6H), 5.71 (dd, *J* = 9.2, 5.0 Hz, 1H), 5.59 (d, *J* = 3.9 Hz, 1H), 5.23 (d, *J* = 9.3 Hz, 1H), 5.03 (d, *J* = 6.7 Hz, 1H), 3.57 – 3..53 (m, 3H), 2.81 (d, *J* = 8.4 Hz, 1H), 2.16 – 2.12 (m, 3H), 1.90 – 1.75 (m, 9H), 1.59 – 1.57 (m, 1H), 1.44 – 1.36 (m, 2H), 1.24 (s, 3H), 1.09 (s, 9H), 0.95 (s, 3H), 0.93 (s, 3H), 0.88 (s, 9H), 0.015 (s, 6H).

^{13}C NMR (150 MHz, $CDCl_3$) δ 139.6, 136.4, 136.2, 134.6, 134.1, 133.8, 130.3, 129.7, 128.5, 127.55, 127.51, 122.7, 118.4, 71.8, 68.3, 61.5, 58.9, 43.7, 37.3, 37.2, 31.1, 27.1, 26.1, 25.0, 24.4, 22.4, 22.2, 19.9, 19.6, 18.4, 16.6, 14.3, -5.08, -5.13, -5.17.

HRMS [ES+] m/z calc'd for $C_{43}H_{66}O_3SiNa$ $[M+Na]^+$: 709.4448, found 709.4453.



***tert*-butyl(((*S*,*E*)-6-((1*R*,2*R*)-2-(2-((*tert*-butyldimethylsilyl)oxy)ethyl)-1,3-dimethyl-4-((triisopropylsilyl)oxy)cyclohex-3-en-1-yl)-1-((*R*)-3,3-dimethyloxiran-2-yl)-3-methylhex-3-en-1-yl)oxy)diphenylsilane** (**4.39**): Vinyl iodide **4.18** (0.36 g, 0.70 mmol, 1.0 equiv) and alkene **4.31** (0.36 g, 0.76 mmol, 1.1 equiv) were separately dried by azeotropic distillation from benzene (3 x 0.1 mL) and placed *in vacuo* for 30 minutes. To a cooled (0 ºC) solution of alkene **4.31** in THF (11 mL) was added 9-BBN (0.50 M in THF, 6.1 mL, 3.1 mmol, 4.4 equiv). The reaction was stirred at room temperature for 2 hours, then cooled to 0 ºC and aq. K_3PO_4 (3.0 M, 1.8 mL, 7.8 equiv) was added. The resulting mixture was stirred for 10 minutes, then $Pd(dppf)Cl_2 \bullet CH_2Cl_2$ (0.17 g, 0.21 mmol, 0.30 equiv) and a solution of **4.18** in DMF (7.0 mL) were added. After stirring for 18 hours, the reaction was diluted with brine (10 mL), hexanes (15 mL), and water (10 mL). The phases were separated and the aqueous phase was extracted with EtOAc (3 x 6.9 mL). The combined organic extracts were washed with brine, dried over $MgSO_4$, filtered and concentrated *in vacuo.* The crude product was purified by flash column chromatography (pH7 SiO_2, 3% EtOAc in hexanes) to afford a mixture of epoxypolyene **4.39** and alkene **4.40** in a 7.5 : 1 ratio. **^{1}H NMR** (500 MHz, $CDCl_3$) δ 7.74 – 7.71 (m, 4H), 7.41 – 7.34 (m, 6H), 5.01 (t, *J* = 6.2 Hz, 1H), 3.64 – 3.50 (m, 3H), 2.80 (d, *J* = 8.4 Hz, 1H), 2.18 – 2.06 (m, 3H), 2.01 – 2.00 (m, 1H), 1.84 – 1.80 (m,

2H), 1.71 – 1.61 (m, 6H), 1.50 – 1.46 (m, 1H), 1.44 – 1.36 (m, 1H), 1.23 – 1.19 (m, 7H), 1.10 – 1.08 (m, 3H), 0.04 (d, J = 2.9 Hz, 3H), 0.89 – 0.86 (m, 12H), 0.041 – 0.023 (m, 6H).

^{13}C NMR (150 MHz, $CDCl_3$) δ 142.7, 136.4, 136.2, 134.7, 133.8, 130.0, 129.7, 129.6, 128.9, 128.5, 127.54, 127.51, 113.7, 71.8, 68.3, 63.1, 58.84, 58.82, 46.1, 45.3, 39.7, 35.3, 34.8, 30.8, 27.7, 27.2, 26.1, 25.0, 23.1, 22.2, 19.9, 19.6, 18.5, 18.29, 18.28, 17.3, 16.6, 13.3, -5.06, -5.08, -5.10.

HRMS [ES+] m/z calc'd for $C_{52}H_{88}O_4Si_3Na$ $[M+Na]^+$: 883.5888, found 883.5891.

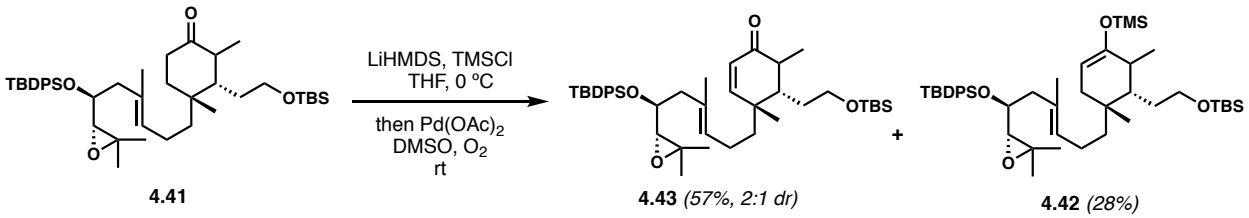
(3*S*,4*R*)-3-(2-((*tert*-butyldimethylsilyl)oxy)ethyl)-4-((*S*,*E*)-6-((tert-butyldiphenylsilyl)oxy)-6-((*R*)-3,3-dimethyloxiran-2-yl)-4-methylhex-3-en-1-yl)-2,4-dimethylcyclohexan-1-one (**4.41**): The mixture of **4.39** and **4.40** (0.57 g, 0.66 mmol) in THF (11 mL) at –78 ºC was added TBAF (1.0 M in THF, 0.72 mL, 0.73 mmol, 1.1 equiv). The reaction mixture was warmed to 0 ºC, stirred for 40 minutes, and treated with satd. aq. NH_4Cl satd. aq. (22 mL). The phases were separated and the aqueous phase was extracted with EtOAc (3 x 22 mL). The combined organic extracts were washed with brine, dried over Na_2SO_4, filtered and concentrated *in vacuo.* The crude product was purified by flash column chromatography (pH7 SiO_2, 5% EtOAc in hexanes) to afford ketone **4.41** (0.38 g, 70%) over 2 steps as a light yellow oil.

^{1}H NMR (600 MHz, $CDCl_3$) δ 7.74 – 7.71 (m, 4H), 7.41 – 7.35 (m, 6H), 5.06 – 5.00 (m, 1H), 3.63 – 3.51 (m, 2H), 3.49 – 3.44 (m, 1H), 2.84 – 2.79 (m, 1H), 2.27 – 2.21 (m, 2H), 2.19 – 2.11 (m, 2H), 1.89 – 1.73 (m, 3H), 1.55 – 1.45 (m, 2H), 1.39 – 1.28 (m, 2H), 1.27 – 1.15 (m, 9H), 1.14 – 1.08 (m, 10H), 1.00 – 0.97 (m, 3H), 0.94 – 0.91 (m, 3H), 0.89 – 0.86 (m, 9H), 0.042 – 0.0047 (s, 6H).

^{13}C NMR (125 MHz, $CDCl_3$) δ 213.8, 213.0, 136.39, 136.36, 136.2, 134.6, 133.7, 133.6, 130.8, 130.6, 129.71, 129.68, 129.60, 129.57, 128.1, 128.0, 127.51, 127.45, 71.8, 71.7, 68.2, 63.84, 63.80, 58.7, 58.6, 51.3, 47.2, 46.8, 46.0, 45.9, 44.7, 40.0, 37.9, 37.8, 36.6, 36.5, 36.2, 34.4, 34.0, 30.5,

29.5, 27.1, 27.0, 26.1, 25.8, 25.7, 25.0, 23.6, 22.6, 22.3, 19.9, 19.8, 19.64, 19.56, 18.5, 16.7, 16.5, 13.1, 12.9, -5.14. -5.19.

HRMS [ES+] m/z calc'd for $C_{43}H_{68}O_4Si_2Na$ $[M+Na]^+$: 727.4554, found 727.4554.

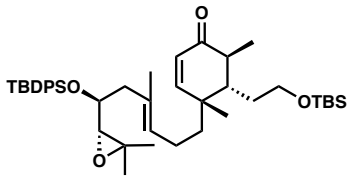


4.41 **4.43** *(57%, 2:1 dr)* **4.42** *(28%)*

(4*R*,5*S*)-5-(2-((tert-butyldimethylsilyl)oxy)ethyl)-4-((*S*,*E*)-6-((tert-butyldiphenylsilyl)oxy)-6-((*R*)-3,3-dimethyloxiran-2-yl)-4-methylhex-3-en-1-yl)-4,6-dimethylcyclohex-2-en-1-one (**4.43**): Ketone **4.41** (62 mg, 88 µmol, 1.0 equiv) was dried by azeotropic distillation from benzene (3 x 0.1 mL) and placed *in vacuo* for 30 minutes. To a cooled (0 ºC) solution of ketone **4.41** in THF (1.8 mL) was added a stock solution of LiHMDS (0.20 M in THF, 0.88 mL, 0.18 mmol, 2.0 equiv). The reaction was stirred for 10 minutes at this temperature, a stock solution of TMSCl (0.20 M in THF, 0.88 mL, 0.18 mmol, 2.0 equiv) was added dropwise and the mixture was stirred for 20 minutes at 0 ºC. Next, the reaction was warmed to room temperature and stirred for 30 minutes. At this point, TLC analysis indicated complete consumption of starting material and the reaction was filtered through a pad of Al_2O_3, the pad was washed with THF, and the volatiles were removed *in vacuo*. The crude enoxysilane crude product was taken up in DMSO (500 µL) and O_2 gas was bubbled through the mixture for 20 minutes. Then, $Pd(OAc)_2$ (59 mg, 0.26 mmol, 3.0 equiv) was added and the reaction was stirred at room temperature under a balloon atmosphere of oxygen for 41 hours. Next, water (1.2 mL) and EtOAc (1.2 mL) were added and the phases were separated and the aqueous phase was extracted with EtOAc (3 x 1.0 mL). The combined organic extracts were washed with brine, dried over Na_2SO_4, filtered and concentrated *in vacuo.* The crude

product was purified by flash column chromatography (SiO_2, 5% EtOAc in hexanes) to afford a mixture of enones **4.43a** and **4.43b** in a 2 : 1 ratio (35 mg, 57%) as a yellow oil and enoxysilane **4.42** (19 mg, 28%) as a colorless oil.

Major diastereomer-less polar compound:



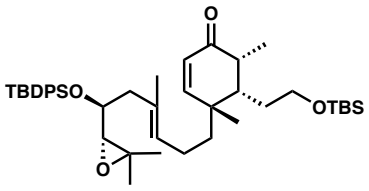
4.43a; *major*

^{1}H NMR (600 MHz, $CDCl_3$) δ 7.73 – 7.70 (td, *J* = 8.9, 1.6 Hz, 4H), 7.40 – 7.34 (m, 6H), 6.65 (d, *J* = 10.1 Hz, 1H), 5.90 (d, *J* = 10.1 Hz, 1H), 4.96 (t, *J* = 6.7 Hz, 1H), 3.68 (ddd, *J* = 9.8, 8.7, 4.1 Hz, 1H), 3.55 – 3.48 (m, 2H), 2.81 (d, *J* = 8.3 Hz, 1H), 2.32 (dq, *J* = 13.4, 6.7 Hz, 1H), 2.15 – 2.08 (m, 2H), 1.95 – 1.88 (m, 1H), 1.79 – 1.74 (m, 2H), 1.51 (ddd, *J* = 12.7, 6.4, 2.0 Hz, 1H), 1.47 – 1.39 (m, 2H), 1.27 – 1.23 (m, 4H), 1.18 – 1.15 (m, 6H), 1.07 (s, 9H), 1.05 (s, 3H), 0.95 (s, 3H), 0.89 (s, 9H), 0.045 (d, *J* = 4.8 Hz, 6H).

^{13}C NMR (150 MHz, $CDCl_3$) δ 201.9, 158.9, 136.4, 136.2, 134.6, 133.6, 131.1, 129.7, 129.6, 127.8, 127.51, 127,48, 126.9, 71.1, 68.2, 63.7, 58.6, 47.0, 45.9, 43.8, 39.6, 35.2, 33.2, 27.1, 27.0, 26.1, 25.5, 23.3, 19.8, 19.6, 18.4, 17.8, 16.5, 13.4, 12.4, -5.14, -5.15.

HRMS [ES+] m/z calc'd for $C_{43}H_{66}O_4Si_2Na$ $[M+Na]^+$: 725.4398, found 725.4398.

Minor diastereomer-less polar compound:



4.43b; *minor*

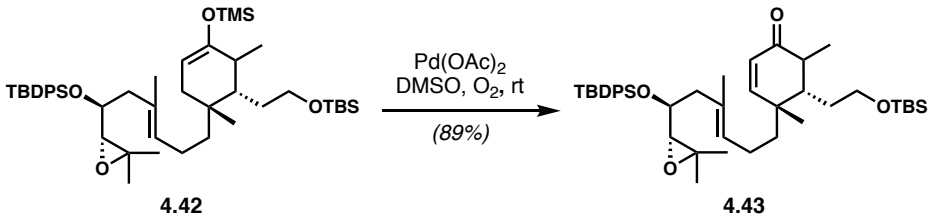
^{1}H NMR (600 MHz, $CDCl_3$) δ 7.74 – 7.71 (m, 4H), 7.41 – 7.39 (m, 2H), 7.37 – 7.35 (m, 4H), 6.57 (d, *J* = 10.2 Hz, 1H), 5.83 (d, *J* = 10.2 Hz, 1H), 5.00 (t, *J* = 6.3 Hz, 1H), 3.58 – 3.49 (m, 3H), 2.80 (d, *J* = 8.4 Hz, 1H), 2.15 – 2.12 (m, 2H), 1.94 – 1.87 (m, 3H), 1.70 – 1.64 (m, 1H), 1.44 – 1.41 (m, 3H), 1.24 – 1.23 (m, 6H), 1.19 (s, 3H), 1.13 (d, *J* = 7.1 Hz, 3H), 1.08 (s, 10H), 0.95 (s, 3H), 0.86 (s, 9H), 0.0135 (s, 6H).

^{13}C NMR (150 MHz, $CDCl_3$) δ 136.4, 136.2, 134.6, 133.7, 131.2, 129.6, 127.6, 127.54, 126.7, 71.7, 68.2, 62.3, 58.7, 46.0, 44.8, 42.6, 39.6, 37.9, 29.7, 27.1, 27.0, 26.1, 25.0, 22.4, 19.9, 19.6, 18.4, 16.6, 13.6, -5.17, -5.19.

***tert*-butyl(((1*S*,*E*)-6-((1*R*,6*S*)-6-(2-((*tert*-butyldimethylsilyl)oxy)ethyl)-1,5-dimethyl-4-((trimethylsilyl)oxy)cyclohex-3-en-1-yl)-1-((*R*)-3,3-dimethyloxiran-2-yl)-3-methylhex-3-en-1-yl)oxy)diphenylsilane** (**4.42**):

^{1}H NMR (600 MHz, $CDCl_3$) δ 7.74 – 7.71 (m, 4H), 7.41 – 7.34 (m, 6H), 5.00 (t, *J* = 6.0 Hz, 1H), 4.67 – 7.65 (m, 1H), 3.60 – 3.50 (m, 3H), 2.79 (d, *J* = 8.4 Hz, 1H), 2.17 – 2.09 (m, 1H), 1.89 – 1.66 (m, 5H), 1.23 – 1.20 (m, 7H), 1.08 – 1.05 (m, 14H), 1.02 – 1.00 (m, 2H), 0.930 – 0.925 (m, 3H), 0.89 – 0.87 (m, 13H), 0.17 – 0.15 (m, 9H), 0.052 – 0.045 (m, 6H).

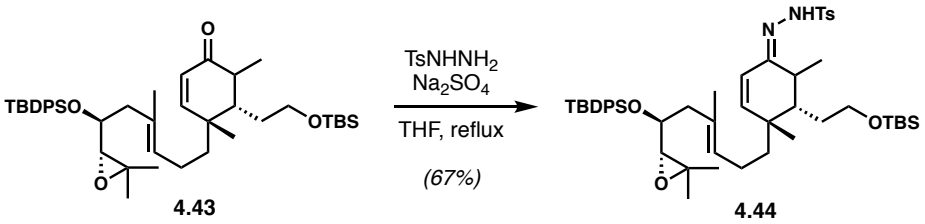
HRMS [ES+] m/z calc'd for $C_{46}H_{76}O_4Si_3Na$ $[M+Na]^+$: 799.4949, found 799.4950.



4.42 **4.43**

(4*R*,5*S*)-5-(2-((*tert*-butyldimethylsilyl)oxy)ethyl)-4-((*S*,*E*)-6-((*tert*-butyldiphenylsilyl)oxy)-6-((*R*)-3,3-dimethyloxiran-2-yl)-4-methylhex-3-en-1-yl)-4,6-dimethylcyclohex-2-en-1-one (**4.43**): A solution of enoxysilane **4.42** (0.18 g, 0.23 mmol, 1.0 equiv) in DMSO (1.1 mL) was

bubbled with O_2 gas for 20 minutes. Then, $Pd(OAc)_2$ (0.15 g, 0.68 mmol, 3.0 equiv) was added and the reaction was stirred at room temperature for 2 days under an atmosphere of oxygen. After complete consumption of starting material, water (3.1 mL) was added to the reaction mixture. The phases were separated and the aqueous phase was extracted with EtOAc (3 x 2.5 mL). The combined organic extracts were washed with brine, dried over Na_2SO_4, filtered and concentrated *in vacuo.* The crude product was purified by flash column chromatography (pH 7 SiO_2, 5% EtOAc in hexanes) to afford enone **4.43** (0.14 g, 89%) as a colorless oil.

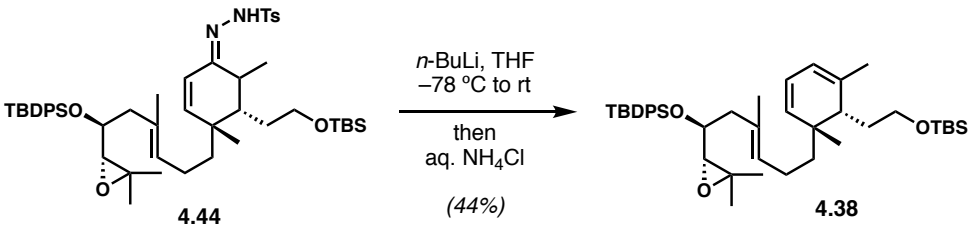


***N'*-((4*R*,5S,*Z*)-5-(2-((*tert*-butyldimethylsilyl)oxy)ethyl)-4-((*S*,*E*)-6-((*tert*-butyldiphenylsilyl)oxy)-6-((*R*)-3,3-dimethyloxiran-2-yl)-4-methylhex-3-en-1-yl)-4,6-dimethylcyclohex-2-en-1-ylidene)-4-methylbenzenesulfonohydrazide** (**4.44**): Enone **4.43** (16 mg, 23 μmol, 1.0 equiv) was dried by azeotropic distillation from toluene (3 x 0.1 mL) and placed *in vacuo* for 30 minutes. To a solution of enone **4.43** (16 mg, 23 μmol) in THF (500 μL) was added Na_2SO_4 (4.2 mg), $TsNHNH_2$ (8.6 mg, 46 μmol, 2.0 equiv) and the mixture was stirred at reflux. After 4 hours the volatiles were removed in vacuo and the crude product was purified by flash column chromatography (pH7 SiO_2, 20% EtOAc in hexanes) to afford tosylhydrazone **4.44** (13 mg, 67%) as a white foam.

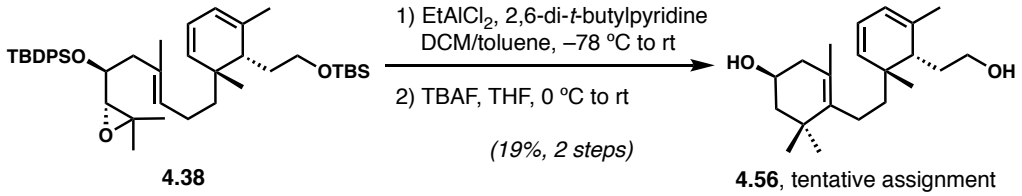
^{1}H NMR (600 MHz, $CDCl_3$) δ 7.87 – 7.84 (m, 2H), 7.72 – 7.68 (m, 3H), 7.38 – 7.29 (m, 9H), 6.13 – 6.09 (m, 1H), 4.97 – 4.91 (m, 1H), 3.64 – 3.41 (m, 3H), 2.79 – 2.77 (m, 1H), 2.42 – 2.36 (m, 4H), 2.13 – 2.10 (m, 2H), 1.83 – 1.79 (m, 1H), 1.73 – 1.67 (m, 2H), 1.58 (br s, 1H), 1.40 – 1.33

(m, 2H), 1.22 – 1.18 (m, 3H), 1.17 – 1.16 (m, 2H), 0.94 – 0.91 (m, 3H), 0.88 – 0.84 (m, 10H), 0.035 – (-0.028) (m, 6H).

HRMS [ES+] m/z calc'd for $C_{50}H_{74}N_2O_5SSi_2Na$ $[M+Na]^+$: 893.4755, found 893.4761.



***tert*-butyl(((*S*,*E*)-6-((1*R*,6*S*)-6-(2-((*tert*-butyldimethylsilyl)oxy)ethyl)-1,5-dimethylcyclohexa-2,4-dien-1-yl)-1-((*R*)-3,3-dimethyloxiran-2-yl)-3-methylhex-3-en-1-yl)oxy)diphenylsilane** (**4.38**): Tosylhydrazone **4.44** (5.0 mg, 6.0 μmol, 1.0 equiv) was dried by azeotropic distillation from toluene (3 x 0.1 mL) and placed *in vacuo* for 30 minutes. To a mixture of tosylhydrazone in THF (300 μL) at –78 ºC was added *n*-BuLi (1.2 M in hexanes, 30 μL, 36 μmol, 6.0 equiv). The reaction was warmed to room temperature and stirred for 17 hours. Next, the reaction was quenched with satd. aq. NH_4Cl (30 μL) and water (30 μL). The phases were separated, the organic phase was dried over Na_2SO_4, filtered and concentrated *in vacuo.* The crude product was purified by flash column chromatography (pH7 SiO_2, 10% EtOAc in hexanes) to afford epoxypolyene **4.38** (1.8 mg, 44%) as a colorless oil.



(*S*)-4-(2-((1*R*,6*S*)-6-(2-hydroxyethyl)-1,5-dimethylcyclohexa-2,4-dien-1-yl)ethyl)-3,5,5-trimethylcyclohex-3-en-1-ol (**4.56**): Epoxypolyene **4.38** (36 mg, 52 μmol, 1.0 equiv) was dried by azeotropic distillation from toluene (3 x 0.2 mL) and placed *in vacuo* for 30 minutes. To a solution of epoxypolyene **4.38** in a mixture of CH_2Cl_2/toluene (6:1) (1.3 mL) was added 2,6-di-*t*-butylpyridine (0.6 μL, 2.6 μmol, 0.05 equiv) at room temperature. The solution was cooled to –78 ºC and $EtAlCl_2$ (0.11 mL, 0.10 mmol, 2.0 equiv) was added down the side of the flask. After stirring at –78 ºC for 16 hours, to the reaction mixture was added Et_3N (40 μL) and MeOH (80μ) sequentially. The mixture was warmed to 0 ºC and quenched with satd. aq. Rochelle salt (1.2 mL). The biphasic mixture was vigorously stirred for 20 minutes. The phases were separated and the aqueous phase was extracted with Et_2O (3 x 5.1 mL). The combined organic phases were washed with brine, dried over $MgSO_4$, filtered and concentrated *in vacuo.* The crude product was purified by flash column chromatography (pH 7 SiO_2, 3% EtOAc in hexanes to 5% EtOAc in hexanes) to afford the silyl ether of **4.56** (30 mg) which was subjected to desilylation in the next step.

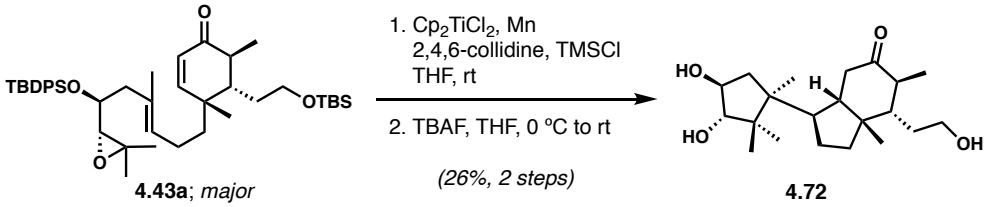
The silyl ether of **4.56** (30 mg, 44 μmol, 1.0 equiv.) was dissolved in THF (880 μL), cooled to 0 ºC, and TBAF (1.0 M in THF, 0.13 mL, 0.13 mmol, 3.0 equiv) was added. The reaction mixture warmed to room temperature and stirred for 40 minutes. Then a solution of satd. aq. NH_4Cl (440 μL) was added. The phases were separated and the aqueous phase was extracted with EtOAc (3 x 440 μL). The combined organic extracts were washed with brine, dried over Na_2SO_4, filtered and concentrated *in vacuo.* The crude product was purified by flash column chromatography (SiO_2, 50% EtOAc in hexanes) to give 70% pure product. This product was further purified by preparative

plate chromatography (70% EtOAc in hexanes) to afford monocyclic product **4.56** (3.4 mg, 19%, 80% purity) over 2 steps as a colorless oil.

^{1}H NMR (600 MHz, $CDCl_3$) δ 5.78 – 5.76 (m, 1H), 5.65 (s, 1H), 5.35 (d, J = 9.3 Hz, 1H), 4.11 (s, 1H), 3.64 – 3.61 (m, 2H), 3.11 (d, *J* = 9.5 Hz, 1H), 2.52 (s, 1H), 2.40 – 2.36 (m, 2H), 2.29 – 2.23 (m, 2H), 2.08 – 2.06 (m, 1H), 2.01 – 2.00 (m, 1H), 1.97 (dd, *J* = 15.7, 2.8 Hz, 2H), 1.83 (s, 3H), 1.60 (s, 3H), 1.47 – 1.43 (m, 2H), 1.11 (d, *J* = 6.8 Hz, 1H), 1.03 (s, 3H), 0.97 (s, 3H), 0.92 (s, 3H).

^{13}C NMR (150 MHz, $CDCl_3$) δ 139.0, 133.9, 131.7, 124.0, 123.1, 119.0, 80.3, 73.5, 61.5, 46.2, 44.7, 44.2, 38.7, 37.1, 31.0, 29.9, 24.3, 22.6, 16.1, 15.6, 8.82.

HRMS [ES+] m/z calc'd for $C_{21}H_{34}O_3Na$ $[M+Na]^+$: 357.2406, found 357.2402.



4.43a; *major* **4.72**

(3*R*,3a*S*,6*S*,7*S*,7a*R*)-3-((1*S*,3*S*,4*S*)-3,4-dihydroxy-1,2,2-trimethylcyclopentyl)-7-(2-hydroxyethyl)-6,7a-dimethyloctahydro-5*H*-inden-5-one (**4.72**): Epoxypolyene **4.43a** (47 mg, 67 μmol, 1.0 equiv) was dried by azeotropic distillation from toluene (3 x 0.1 mL) and placed *in vacuo* for 30 minutes. THF, 2,4,6-collidine, and TMSCl were degassed for 20 minutes, 10 minutes, and 30 seconds, respectively. A round bottom flask was charged with Cp_2TiCl_2 (0.1 g, 0.40 mmol, 6.0 equiv) and Mn powder (89 mg, 1.6 mmol, 24 equiv). The flask was evacuated and backfilled with argon gas three times. Then, deoxygenated THF (4.0 mL) was added to the flask at room temperature. The reaction mixture was stirred at this temperature for 15 minutes until the solution turned lime green. Next, the premixed solution of epoxypolyene **4.43a** and deoxygenated 2,4,6-collidine (0.13 mL, 0.94 mmol, 14 equiv) in THF (1.4 mL) was added, followed by deoxygenated

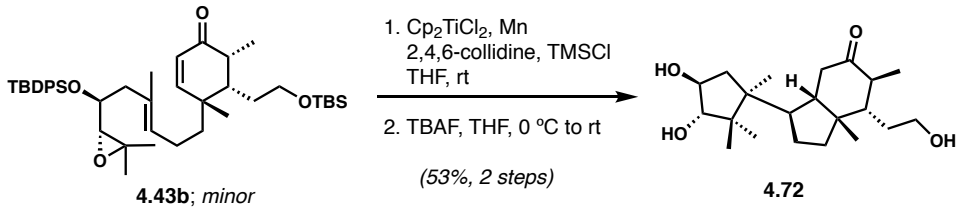
TMSCl (70 μL, 0.54 mmol, 8.0 equiv). The reaction mixture turned cloudy green and was stirred for 22 hours at room temperature. Then the reaction was cooled to 0 ºC, diluted with EtOAc (5.3 mL), and aq. 1.0 M HCl (2.6 mL) was added. The phases were separated and the aqueous phase was extracted with EtOAc (3 x 2.6 mL). The combined organic extracts were washed with brine, dried over $MgSO_4$, filtered and concentrated *in vacuo.* The crude product was purified by flash column chromatography (pH7 SiO_2, 10% EtOAc in hexanes) to give 85% pure silyl ether of **4.72** (14 mg).

The silyl ether of **4.72** (14 mg, 20 μmol, 1.0 equiv) was dissolved in THF (500 μL), cooled to 0 ºC, TBAF (1.0 M in THF, 60 μL, 60 μmol, 6.0 equiv) was added. The reaction mixture was stirred at room temperature for 19 hours then water (870 μL) was added. The phases were separated and the aqueous phase was extracted with EtOAc (3 x 870 μL). The combined organic extracts were washed with brine, dried over $MgSO_4$, filtered and concentrated *in vacuo.* The crude product was purified by flash column chromatography (pH7 SiO_2, 5% MeOH in EtOAc to 10% MeOH in EtOAc) to give 80% pure product (8.3 mg). This product was further purified by preparative plate chromatography (5% MeOH in EtOAc) to afford compound **4.72** (6.3 mg, 26%) over 2 steps as a white solid.

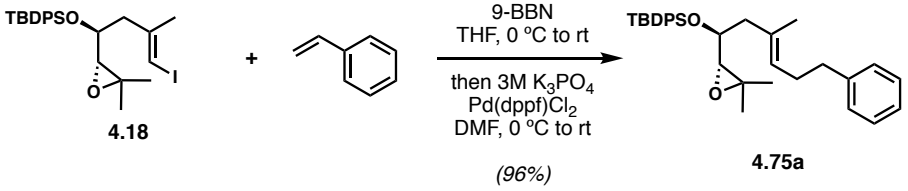
^{1}H NMR (600 MHz, CD_3OD) δ 4.02 (dt, *J* = 9.2, 6.2 Hz, 1H), 3.68 (d, *J* = 5.6 Hz, 1H), 3.63 – 3.56 (m, 2H), 2.87 (dd, *J* = 12.7, 8.5 Hz, 1H), 2.14 (d, *J* = 12.7 Hz, 1H), 2.06 – 1.98 (m, 2H), 1.84 – 1.77 (m, 2H), 1.70 – 1.66 (m, 1H), 1.65 – 1.55 (m, 4H), 1.44 – 1.37 (m, 1H), 1.35 – 1.29 (m, 2H), 1.15 (d, *J* = 7.1 Hz, 3H), 1.12 (s, 3H), 0.97 (s, 3H), 0.96 (s, 3H), 0.84 (s, 3H).

^{13}C NMR (150 MHz, CD_3OD) δ 220.8, 87.8, 78.3, 63.5, 54.0, 48.0, 47.8, 46.6, 46.2, 43.4, 43.1, 35.8, 33.3, 29.7, 28.2, 23.2, 22.6, 20.5, 17.0.

HRMS [ES+] m/z calc'd for $C_{21}H_{36}O_4Na$ $[M+Na]^+$: 375.2511, found 375.2510.



(3*R*,3a*S*,6*S*,7*S*,7a*R*)-3-((1*S*,3*S*,4*S*)-3,4-dihydroxy-1,2,2-trimethylcyclopentyl)-7-(2-hydroxyethyl)-6,7a-dimethyloctahydro-5*H*-inden-5-one (**4.72**): Epoxypolyene **4.43b** (48 mg, 68 μmol, 1.0 equiv) was subjected to the reaction conditions described for the preparation of **4.72**. After TBAF deprotection step, the crude product was purified by flash column chromatography (pH7 SiO_2, 5% MeOH in EtOAc to 10% MeOH in EtOAc) to afford compound **4.72** (13 mg, 53%, 85% purity) over 2 steps as a white solid. This product was further crystalized by slow evaporation a mixture of $CDCl_3$/MeOH (10:1) over 48 hours to produce a crystal of **4.72** suitable for X-ray diffraction studies.



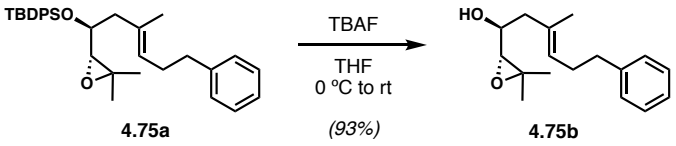
***tert*-butyl(((*S*,*E*)-1-((*R*)-3,3-dimethyloxiran-2-yl)-3-methyl-6-phenylhex-3-en-1-yl)oxy)diphenylsilane** (**4.75a**): Vinyl iodide **4.18** (91 mg, 0.17 mmol, 1.0 equiv) and styrene (30 μL, 0.23 mmol, 1.3 equiv) were subjected to the reaction conditions described for the preparation of **4.39**. The crude product was purified by flash column chromatography (pH7 SiO_2, 2% EtOAc) to afford epoxyolefin **4.75a** (84 mg, 96%) as a colorless oil.

^{1}H NMR (600 MHz, $CDCl_3$) δ 7.73 (t, *J* = 8.1 Hz, 4H), 7.43 – 7.39 (m, 2H), 7.38 – 7.35 (m, 4H), 7.28 – 7.25 (m, 3H), 7.18 (d, *J* = 7.4 Hz, 1H), 7.14 (d, *J* = 7.5 Hz, 2H), 5.11 (t, *J* = 6.8 Hz, 1H),

3.55 – 3.51 (m, 1H), 2.80 (d, *J* = 8.4 Hz, 1H), 2.54 (t, *J* = 15.9 Hz, 2H), 2.20 – 2.14 (m, 4H), 1.21 (s, 6H), 1.09 (s, 9H), 0.93 (s, 3H).

^{13}C NMR (150 MHz, $CDCl_3$) δ 142.2, 136.4, 136.2, 134.6, 133.7, 131.2, 129.7, 129.6, 128.43, 128.40, 127.53, 127.51, 127.4, 125.9, 71.8, 68.2, 58.7, 46.0, 35.9, 30.2, 27.1, 24.9, 19.8, 19.6, 16.6.

HRMS [ES+] m/z calc'd for $C_{33}H_{42}O_2SiNa$ $[M+Na]^+$: 521.2852, found 521.2858.

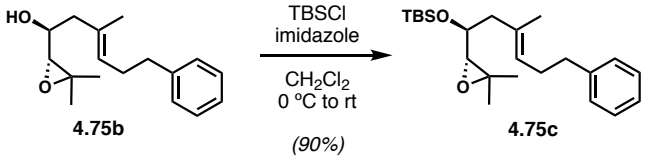


(*S*,*E*)-1-((*R*)-3,3-dimethyloxiran-2-yl)-3-methyl-6-phenylhex-3-en-1-ol (**4.75b**): To a solution of silyl ether **4.75a** (50 mg, 0.10 mmol, 1.0 equiv) in THF (2.0 mL) at 0 ºC was added TBAF (1.0 M in THF, 0.30 mL, 0.30 mmol, 3.0 equiv). The reaction mixture stirred at room temperature for 16 hours then water (3.0 mL) was added. The phases were separated and the aqueous phase was extracted with EtOAc (3 x 2.0 mL). The combined organic extracts were washed with brine, dried over $MgSO_4$, filtered and concentrated *in vacuo.* The crude product was purified by flash column chromatography (SiO_2, 30% EtOAc in hexanes to 50% EtOAc in hexanes) to afford alcohol **4.75b** (24 mg, 93%) as a colorless oil.

^{1}H NMR (500 MHz, $CDCl_3$) δ 7.27 (t, *J* = 7.5 Hz, 2H), 7.20 – 7.17 (m, 3H), 5.31 (t, *J* = 6.8 Hz, 1H), 3.53 (td, *J* = 7.9, 5.8 Hz, 1H), 2.70 – 2.66 (m, 3H), 2.36 (td, *J* = 7.3, 3.0 Hz, 2H), 2.27 (dd, *J* = 13.5, 7.9 Hz, 1H), 2.18 (dd, *J* = 13.3, 5.7 Hz, 1H), 1.99 (br s, 1H), 1.59 (s, 3H), 1.29 (s, 3H), 1.27 (s, 3H).

^{13}C NMR (125 MHz, $CDCl_3$) δ 142.0, 131.2, 128.51, 128.47, 128.0, 126.0, 68.9, 67.6, 59.2, 44.5, 35.9, 30.1, 25.0, 19.5, 16.5.

HRMS [ES+] m/z calc'd for $C_{17}H_{24}O_2Na$ $[M+Na]^+$: 283.1674, found 283.1667.

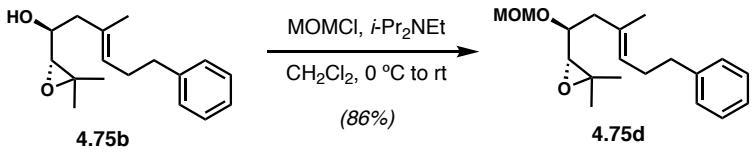


***tert*-butyl(((*S*,*E*)-1-((*R*)-3,3-dimethyloxiran-2-yl)-3-methyl-6-phenylhex-3-en-1-yl)oxy)dimethylsilane** (**4.75c**): To a solution of alcohol **4.75b** (8.8 mg, 34 μmol, 1.0 equiv) in CH_2Cl_2 (680 μL) at 0 ºC was added imidazole (9.2 mg, 0.14 mmol, 4.0 equiv) followed by TBSCl (13 mg, 85 μmol, 2.5 equiv). The reaction stirred at room temperature for 20 hours the water (340 μL) was added. The phases were separated and the aqueous phase was extracted with EtOAc (3 x 340 μL). The combined organic extracts were washed with brine, dried over Na_2SO_4, filtered and concentrated *in vacuo.* The crude product was purified by flash column chromatography (pH7 SiO_2, 10% EtOAc in hexanes to 50% EtOAc in hexanes) to afford silyl ether **4.75c** (11 mg, 90%) as a colorless oil.

^{1}H NMR (600 MHz, $CDCl_3$) δ 7.28 (t, *J* = 7.5 Hz, 2H), 7.20 – 7.18 (m, 3H), 5.26 (t, *J* = 6.8 Hz, 1H), 3.52 (q, *J* = 7.3 Hz, 1H), 2.67 – 2.64 (m, 3H), 2.32 (q, *J* = 7.8 Hz, 2H), 2.21 (dd, *J* = 13.3, 7.1 Hz, 1H), 2.14 (dd, *J* = 13.1, 5.3 Hz, 1H), 1.61 (s, 3H), 1.26 (s, 3H), 1.22 (s, 3H), 0.90 (s, 9H), 0.11 (s, 3H), 0.0446 (s, 3H).

^{13}C NMR (150 MHz, $CDCl_3$) δ 142.3, 131.5, 128.5, 128.4, 127.4, 125.9, 71.4, 68.3, 58.6, 45.6, 36.1, 30.3, 26.0, 25.0, 19.9, 18.3, 17.0, -4.18, -4.91.

HRMS [ES+] m/z calc'd for $C_{23}H_{35}O_2SiNa$ $[M+Na]^+$: 397.2539, found 397.2539.

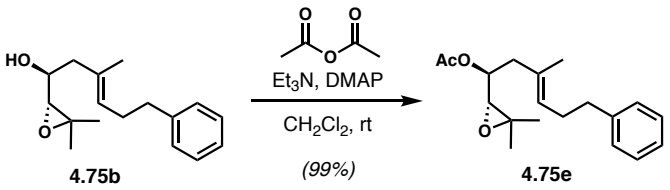


(*R*)-3-((*S*,*E*)-1-(methoxymethoxy)-3-methyl-6-phenylhex-3-en-1-yl)-2,2-dimethyloxirane (**4.75d**): To a solution of alcohol **4.75b** (15 mg, 60 μmol, 1.0 equiv) in CH_2Cl_2 (1.0 mL) at 0 ºC was added *i*-Pr_2Net (30 μL, 0.18 mmol, 3.0 equiv) followed by MOMCl (10 μL, 0.14 mmol, 2.4 equiv). The reaction warmed to room temperature and stirred for 17 hours then satd. aq. $NaHCO_3$ (30 μL), EtOAc (600 μL) and H_2O (100 μL) were added sequentially. The phases were separated and the aqueous phase was extracted with EtOAc (3 x 500 μL). The combined organic extracts were washed with brine, dried over Na_2SO_4, filtered and concentrated *in vacuo.* The crude product was purified by flash column chromatography (pH7 SiO_2, 20% EtOAc in hexanes) to afford methoxymethyl ether **4.75d** (15 mg, 86%) as a colorless oil.

^{1}H NMR (500 MHz, $CDCl_3$) δ 7.29 – 7.26 (m, 2H), 7.19 (d, *J* = 7.3 Hz, 3H), 5.31 (t, *J* = 6.8 Hz, 1H), 4.86 (d, *J* = 6.7 Hz, 1H), 4.61 (d, *J* = 6.6 Hz, 1H), 3.53 (q, *J* = 7.1 Hz, 1H), 3.36 (s, 3H), 2.73 (d, *J* = 8.3 Hz, 1H), 2.65 (t, *J* = 7.8 Hz, 2H), 2.35 – 2.29 (m, 3H), 2.17 (dd, *J* = 13.5, 5.6 Hz, 1H), 1.64 (s, 3H), 1.27 (s, 3H), 1.24 (s, 3H).

^{13}C NMR (125 MHz, $CDCl_3$) δ 142.2, 131.4, 128.5, 128.4, 127.5, 126.0, 95.4, 74.3, 67.1, 57.3, 55.5, 43.1, 36.0, 30.2, 24.9, 19.7, 16.7.

HRMS [ES+] m/z calc'd for $C_{19}H_{28}O_3Na$ $[M+Na]^+$: 327.1936, found 327.1945.

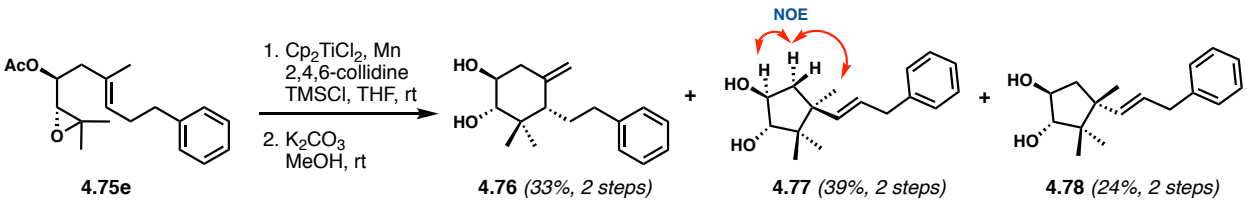


(*S*,*E*)-1-((*R*)-3,3-dimethyloxiran-2-yl)-3-methyl-6-phenylhex-3-en-1-yl acetate (**4.75e**): To a solution of alcohol **4.75b** (14 mg, 55 µmol, 1.0 equiv) in CH_2Cl_2 (1.0 mL) was added acetic anhydride (30 µL, 0.31 mmol, 5.7 equiv), Et_3N (60 µL, 0.43 mmol, 7.8 equiv), and DMAP (1.4 mg, 11 µmol, 0.20 equiv). After stirring for 17 hours at room temperature, the reaction was quenched with water (30 µL), dried over Na_2SO_4, filtered and concentrated *in vacuo.* The crude product was purified by flash column chromatography (SiO_2, 20% EtOAc in hexanes) to afford acetate **4.75e** (17 mg, 99%) as a colorless oil.

^{1}H NMR (500 MHz, $CDCl_3$) δ 7.29 – 7.26 (m, 2H), 7.18 (d, *J* = 4 Hz, 3H), 5.27 (t, *J* = 6.9 Hz, 1H), 4.82 (q, *J* = 7.3 Hz, 1H), 2.78 (d, *J* = 8.7 Hz, 1H), 2.64 (t, *J* = 7.8 Hz, 2H), 2.36 – 2.29 (m, 3H), 2.23 (dd, *J* = 13.3, 6.3 Hz, 1H), 2.03 (s, 3H), 1.63 (s, 3H), 1.29 – 1.27 (m, 6H).

^{13}C NMR (125 MHz, $CDCl_3$) δ 170.3, 142.0, 130.5, 128.5, 128.1, 126.0, 72.0, 64.8, 59.0, 42.5, 35.9, 30.1, 24.8, 21.2, 19.6, 16.7.

HRMS [ES+] m/z calc'd for $C_{19}H_{26}O_3Na$ $[M+Na]^+$: 325.1780, found 325.1788.



(1S,2S,4S)-3,3-dimethyl-5-methylene-4-phenethylcyclohexane-1,2-diol (**4.76**): Epoxyolefin **4.47e** (16 mg, 52 µmol, 1.0 equiv) was subjected to the Ti(III)-mediated radical cyclization conditions described for the preparation of **4.72**. Next, to the cyclization products in MeOH (1.0

mL) was added K_2CO_3 (35 mg, 0.25 mmol, 5.0 equiv). After stirring for 1 hour, to the reaction was added water (160 μL), CH_2Cl_2 (160 μL), and brine (160 μL). The phases were separated and the aqueous phase was extracted with EtOAc (3 x 500 μL). The combined organic extracts were washed with brine, dried over $MgSO_4$, filtered and concentrated *in vacuo.* The crude residue was purified by preparative thin-layer chromatography (eluting with 60% EtOAc in hexanes) to afford monocyclic products; **4.76** (4.5 mg, 33%), **4.77** (5.3 mg, 39%), and **4.78** (3.3 mg, 24%) over 2 steps as colorless oils.

^{1}H NMR (600 MHz, $CDCl_3$) δ 7.29 (t, *J* = 7.4 Hz, 2H), 7.20 – 7.17 (m, 3H), 5.08 (s, 1H), 4.85 (s, 1H), 3.52 – 3.48 (m, 1H), 3.12 (d, *J* = 9.2 Hz, 1H), 2.85 – 2.81 (m, 1H), 2.66 (dd, *J* = 12.1, 5.2 Hz, 1H), 2.47 – 2.42 (m, 1H), 2.14 (br s, 2H), 2.04 (dd, *J* = 11.6, 6.8 Hz, 1H), 1.87 – 1.82 (m, 1H), 1.78 – 1.73 (m, 2H), 1.06 (s, 3H), 0.642 (s, 3H).

^{13}C NMR (150 MHz, $CDCl_3$) δ 143.9, 142.8, 128.52, 128.45, 126.0, 110.7, 82.7, 72.3, 50.7, 43.5, 40.1, 34.8, 26.9, 25.6, 14.5.

HRMS [ES+] m/z calc'd for $C_{17}H_{24}O_2Na$ $[M+Na]^+$: 283.1674, found 283.1677.

(1S,2S,4S)-3,3,4-trimethyl-4-((E)-3-phenylprop-1-en-1-yl)cyclopentane-1,2-diol (**4.77**):

^{1}H NMR (600 MHz, $CDCl_3$) δ 7.29 – 7.26 (m, 2H), 7.20 – 7.17 (m, 3H), 5.66 – 5.57 (m, 2H), 4.11 (dt, *J* = 9.6, 4.6 Hz, 1H), 3.79 (d, *J* = 6.0 Hz, 1H), 3.37 (d, *J* = 6.2 Hz, 2H), 2.04 (dd, *J* = 14.3, 9.8 Hz, 1H), 1.86 (br s, 1H), 1.79 (dd, *J* = 14.3, 4.7 Hz, 1H), 1.74 (br s, 1H), 0.99 (s, 3H), 0.88 (s, 3H), 0.83 (s, 3H).

^{13}C NMR (150 MHz, $CDCl_3$) δ 141.1, 139.2, 128.6, 128.5, 126.2, 126.1, 87.2, 77.7, 46.3, 46.1, 42.7, 39.5, 22.5, 22.3, 17.9.

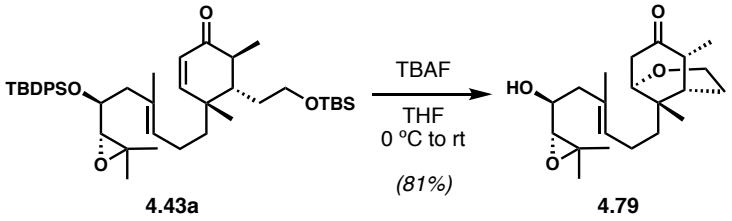
HRMS [ES+] m/z calc'd for $C_{17}H_{24}O_2Na$ $[M+Na]^+$: 283.1674, found 283.1816.

(1S,2S,4R)-3,3,4-trimethyl-4-((E)-3-phenylprop-1-en-1-yl)cyclopentane-1,2-diol (**4.78**):

^{1}H NMR (600 MHz, $CDCl_3$) δ 7.30 – 7.28 (m, 2H), 7.21 – 7.16 (m, 3H), 5.58 – 5.47 (m, 2H), 4.11 – 4.08 (m, 1H), 3.89 (d, *J* = 5.9 Hz, 1H), 3.37 (d, *J* = 6.5 Hz, 2H), 2.42 (dd, *J* = 14.1, 9.9 Hz, 1H), 1.43 (dd, *J* = 14.2, 3.9 Hz, 1H), 1.11 (s, 3H), 0.92 (s, 3H), 0.79 (s, 3H).

^{13}C NMR (150 MHz, $CDCl_3$) δ 141.1, 138.0, 128.6, 128.5, 126.6, 126.1, 87.2, 77.7, 46.2, 43.3, 39.5, 24.7, 21.3, 18.8.

HRMS [ES+] m/z calc'd for $C_{17}H_{24}O_2Na$ $[M+Na]^+$: 283.1674, found 283.1668.

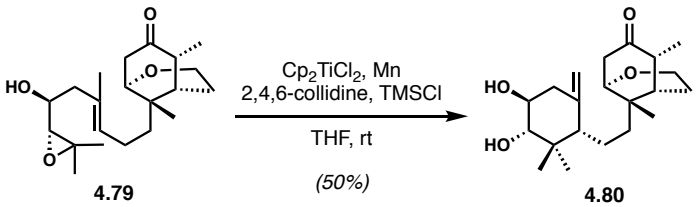


(1*R*,5*S*,6*S*,9*S*)-9-((*S*,*E*)-6-((*R*)-3,3-dimethyloxiran-2-yl)-6-hydroxy-4-methylhex-3-en-1-yl)-6,9-dimethyl-2-oxabicyclo[3.3.1]nonan-7-one (**4.79**): Enoxysilane **4.43a** (58 mg, 82 μmol, 1.0 equiv) was subjected to the reaction conditions described for the preparation of **4.75b**. The crude product was purified by flash column chromatography (pH7 SiO_2, 70% EtOAc in hexanes) to afford oxabicycle **4.79** (23 mg, 81%) as a colorless oil.

^{1}H NMR (600 MHz, $CDCl_3$) δ 5.32 (br s, 1H), 3.78 (s, 1H), 3.64 (dd, *J* = 13.2, 6.3 Hz, 1H), 3.60 – 3.56 (m, 1H), 3.34 (td, *J* = 13.4, 2.6 Hz, 1H), 2.76 – 2.73 (m, 1H), 2.71 – 2.63 (m, 2H), 2.29 (dd, *J* = 13.4, 8.0 Hz, 1H), 2.22 – 2.16 (m, 2H), 2.04 – 1.95 (m, 4H), 1.92 (br s, 1H), 1.67 (s, 3H), 1.54 (d, *J* = 14.2 Hz, 1H), 1.38 – 1.23 (m, 7H), 1.15 – 1.12 (m, 6H).

^{13}C NMR (150 MHz, $CDCl_3$) δ 212.7, 130.7, 128.6, 77.4, 69.0, 67.7, 59.3, 57.5, 44.5, 43.7, 43.3, 40.7, 36.8, 36.5, 25.0, 22.1, 21.8, 21.4, 19.5, 16.6, 13.3.

HRMS [ES+] m/z calc'd for $C_{21}H_{34}O_4Na$ $[M+Na]^+$: 373.2355, found 373.2347.

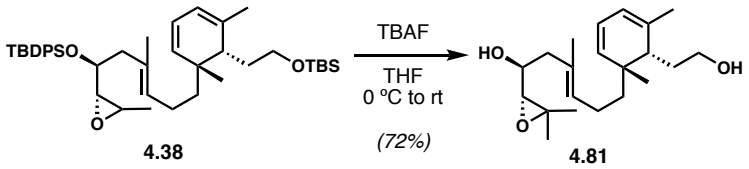


(1*R*,5*S*,6*R*,9*S*)-9-(2-((1*S*,3*S*,4*S*)-3,4-dihydroxy-2,2-dimethyl-6-methylenecyclohexyl)ethyl)-6,9-dimethyl-2-oxabicyclo[3.3.1]nonan-7-one (**4.80**): Epoxyolefin **4.79** (18 mg, 51 μmol, 1.0 equiv) was subjected to the reaction conditions described for the preparation of **4.72**. The crude was purified by preparative thin-layer chromatography (3% MeOH in EtOAc) to afford monocyclic **4.76** (4.5 mg, 50%) as a white solid. This product was crystalized by slow evaporation a mixture of $CDCl_3$/MeOH (10:1) over 48 hours to produce crystal of **4.80** suitable for X-ray diffraction studies.

^{1}H NMR (600 MHz, CD_3OD) δ 3.80 – 3.78 (m, 1H), 3.61(dd, *J* = 13.0, 6.4 Hz, 1H), 3.40 (ddd, *J* = 11.4, 9.3, 5.4 Hz, 1H), 3.35 (s, 1H), 3.07 (d, *J* = 9.2 Hz, 1H), 2.94 – 2.87 (m, 2H), 2.58 (dd, *J* = 12.2, 5.4 Hz, 1H), 2.51 (dd, *J* = 18.4, 1.9 Hz, 1H), 2.19 (td, *J* = 13.7, 5.2 Hz, 1H), 2.14 – 2.07 (m, 1H), 2.03 – 1.95 (m, 2H), 1.74 (d, *J* = 10.1 Hz, 1H), 1.65 – 1.60 (m, 1H), 1.56 – 1.48 (m, 2H), 1.47 – 1.41 (m, 1H), 1.35 – 1.33 (m, 1H), 1.31 – 1.29 (m, 1H), 1.18 (s, 3H), 1.13 – 1.12 (m, 6H), 1.05 – 1.01 (m, 2H), 0.91 – 0.86 (m, 1H), 0.67 (s, 2H).

^{13}C NMR (150 MHz, CD_3OD) δ 215.5, 146.7, 109.8, 83.2, 79.0, 73.1, 58.5, 54.1, 45.0, 44.8, 44.4, 42.3, 41.7, 38.0, 37.5, 26.2, 22.5, 21.9, 19.4, 15.1, 13.5.

HRMS [ES+] m/z calc'd for $C_{21}H_{34}O_4Na$ $[M+Na]^+$: 373.2355, found 373.2351.

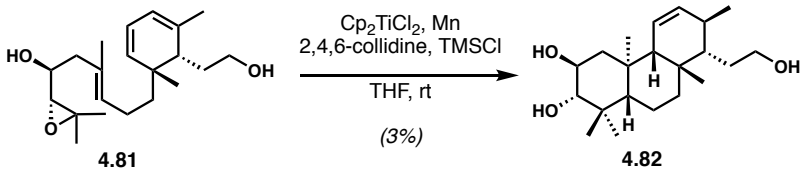


(*S*,*E*)-1-((*R*)-3,3-dimethyloxiran-2-yl)-6-((1*R*,6*S*)-6-(2-hydroxyethyl)-1,5-dimethylcyclohexa-2,4-dien-1-yl)-3-methylhex-3-en-1-ol (**4.81**): Diene **4.38** (34 mg, 50 μmol, 1.0 equiv) was subjected to the reaction conditions described for the preparation of **4.75b**. The crude product was purified by flash column chromatography (pH7 SiO_2, 30-50% EtOAc in hexanes) to afford epoxypolyene **4.81** (12 mg, 72%) as a colorless oil.

^{1}H NMR (600 MHz, $CDCl_3$) δ 5.75 (dd, *J* = 9.3, 5.0 Hz, 1H), 5.65 (d, *J* = 3.4 Hz, 1H), 5.33 (d, *J* = 9.4 Hz, 1H), 5.29 – 5.23 (m, 2H), 3.69 –3.65 (m, 1H), 3.63 – 3.60 (m, 1H), 3.59 – 3.52 (m, 2H), 2.71 (d, *J* = 7.9 Hz, 1H), 3.31 – 2.27 (m, 1H), 2.22 – 2.18 (m, 1H), 1.87 – 1.85 (m, 1H), 1.83 (s, 3H), 1.73 – 1.70 (m, 1H), 1.66 (s, 3H), 1.54 (td, *J* = 13.5, 4.5 Hz, 1H), 1.36 – 1.32 (m, 5H), 1.29 (s, 3H), 1.02 – 0.99 (m, 5H).

^{13}C NMR (150 MHz, $CDCl_3$) δ 138.9, 134.0, 130.4, 129.1, 118.9, 69.0, 67.8, 61.4, 59.4, 44.6, 44.5, 37.4, 37.2, 30.9, 25.0, 24.2, 22.7, 22.4, 19.6, 16.6.

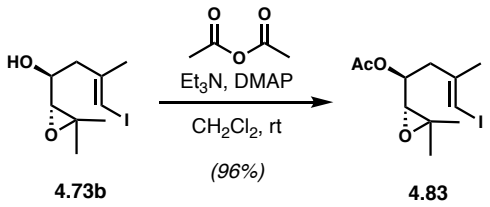
HRMS [ES+] m/z calc'd for $C_{21}H_{34}O_3Na$ $[M+Na]^+$: 357.2406, found 357.2402.



(2*S*,3*S*,4a*R*,4b*R*,7*R*,8*S*,8a*S*,10a*S*)-8-(2-hydroxyethyl)-1,1,4a,7,8a-pentamethyl-1,2,3,4,4a,4b,7,8,8a,9,10,10a-dodecahydrophenanthrene-2,3-diol (**4.82**): Epoxypolyene **4.43b** (9 mg, 26 μmol, 1.0 equiv) was subjected to the reaction conditions described for the preparation of **4.72**. The crude product was purified by flash column chromatography (pH7 SiO_2, 50% EtOAc

in hexanes) to give 50% pure product. This product was further purified by preparative thin-layer chromatography (50% EtOAc in hexanes) to afford tricycle **4.82** (0.30 mg, 3.4%) as a white film. This product was crystalized by slow evaporation a mixture of CH_2Cl_2/MeOH (10:1) over 48 hours to produce crystal of **4.82** suitable for X-ray diffraction studies.

^{1}H NMR (500 MHz, $CDCl_3$) δ 5.67 – 5.63 (m, 1H), 5.56 – 5.50 (m, 1H), 3.68 – 3.63 (m, 2H), 3.56 – 3.53 (m, 1H), 3.05 – 3.03 (m, 1H), 2.13 – 2.10 (m, 2H), 2.03 – 2.00 (m, 2H), 1.93 – 1.90 (m, 2H), 1.83 – 1.78 (m, 2H), 1.76 – 1.75 (m, 1H), 1.69 – 1.61 (m, 2H), 1.14 – 1.12 (m, 2H), 1.09 (d, *J* = 6.8 Hz, 3H), 1.01 (s, 6H), 0.96 – 0.94 (m, 2H), 0.89 (s, 3H), 0.85 (s, 3H).



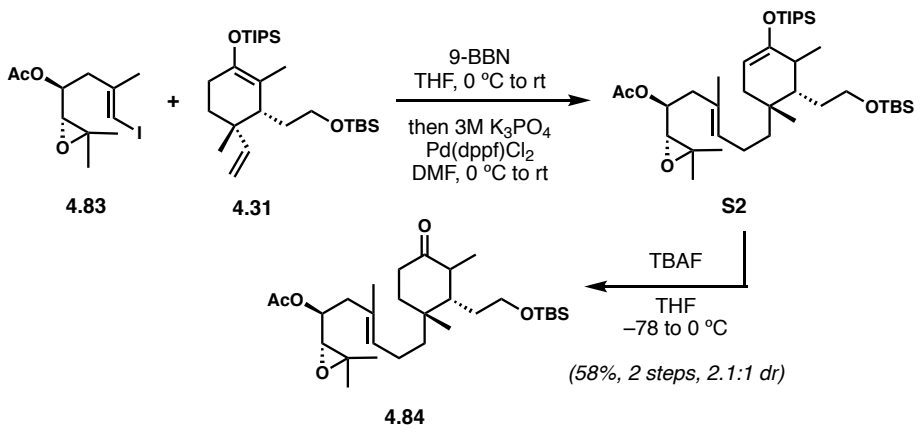
4.73b **4.83**

(*S*,*E*)-1-((*R*)-3,3-dimethyloxiran-2-yl)-4-iodo-3-methylbut-3-en-1-yl acetate (**4.83**): Alcohol **4.73b** (1.2 g, 4.2 mmol, 1.0 equiv) was subjected to the reaction conditions described for the preparation of **4.75e**. The crude product was purified by flash column chromatography (pH7 SiO_2, 20% EtOAc in hexanes) to afford acetate **4.83** (1.3 g, 96%) as a colorless oil.

^{1}H NMR (600 MHz, $CDCl_3$) δ 6.05 (s, 1H), 4.81 (q, *J* = 7.4 Hz, 1H), 2.78 (d, *J* = 8.7 Hz, 1H), 2.60 (dd, *J* = 13.4, 6.6 Hz, 1H), 2.47 (dd, *J* = 13.5, 6.9 Hz, 1H), 2.07 (s, 3H), 1.89 (s, 3H), 1.31 (s, 3H), 1.29 (s, 3H).

^{13}C NMR (150 MHz, $CDCl_3$) δ 170.3, 142.7, 78.6, 71.1, 64.4, 59.2, 42.1, 24.8, 24.5, 21.2, 19.6.

HRMS [ES+] m/z calc'd for $C_{11}H_{17}IO_3Na$ $[M+Na]^+$: 347.0120, found 347.0128.



(1*S*,*E*)-6-((1*R*,2*S*)-2-(2-((*tert*-butyldimethylsilyl)oxy)ethyl)-1,3-dimethyl-4-oxocyclohexyl)-1-((*R*)-3,3-dimethyloxiran-2-yl)-3-methylhex-3-en-1-yl acetate (**4.84**): Acetate **4.83** (0.11 g, 0.34 mmol, 1.0 equiv) and alkene **4.31** (0.19 g, 0.41 mmol, 1.2 equiv) were subjected to the reaction conditions described for the preparation of **4.39** to provide compound **S2** (0.13 g, 90% purity), which was purified by flash column chromatography (pH7 SiO_2, 15-20% EtOAc in hexanes). Next, compound **S2** was subjected to the reaction conditions described for the preparation of **4.41**. The crude product was purified by flash column chromatography (pH7 SiO_2, 10% EtOAc in hexanes) to afford epoxyolefin **4.84** (0.10 mg, 58%) over 2 steps as a colorless oil.

^{1}H NMR (600 MHz, $CDCl_3$) δ 5.26 – 5.19 (m, 1H), 4.85 – 4.80 (m, 1H), 3.64 – 3.60 (m, 1H), 3.52 – 3.45 (m, 1H), 2.80 – 2.78 (m, 1H), 2.36 – 2.28 (m, 3H), 2.33 (dd, *J* = 13.4, 6.4 Hz, 1H), 2.05 – 2.04 (m, 3H), 2.01 – 2.00 (m, 1H), 1.94 – 1.89 (m, 1H), 1.83 – 1.79 (m, 1H), 1.72 – 1.56 (m, 5H), 1.50 – 1.39 (m, 1H), 1.37 – 1.25 (m, 10H), 1.22 – 1.16 (m, 1H), 1.06 – 1.00 (m, 3H), 0.97 (s, 2H), 0.88 – 0.86 (m, 9H), 0.034 – 0.016 (m, 6H).

^{13}C NMR (150 MHz, $CDCl_3$) δ 213.8, 213.0, 190.3, 130.1, 129.9, 129.0, 128.9, 71.99, 71.96, 64.83, 74.79, 63.81, 63.77, 59.01, 58.96, 51.3, 47.2, 46.8, 44.7, 42.58, 42.56, 40.0, 37.9, 37.8, 36.7, 36.5, 36.2, 34.4, 34.0, 30.7, 29.5, 26.1, 25.8, 24.8, 23.6, 22.7, 22.4, 21.3, 19.69. 19.67, 18.5, 16.7, 16.6, 13.2, 13.0.

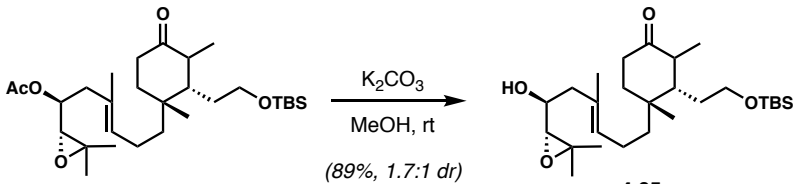
HRMS [ES+] m/z calc'd for $C_{29}H_{52}O_5SiNa$ $[M+Na]^+$: 531.3481, found 531.3501.

(1*S*,*E*)-6-((1*R*,2*S*)-2-(2-((*tert*-butyldimethylsilyl)oxy)ethyl)-1,3-dimethyl-4-oxocyclohexyl)-1-((*R*)-3,3-dimethyloxiran-2-yl)-3-methylhex-3-en-1-yl acetate (S2):

^{1}H NMR (600 MHz, $CDCl_3$) δ 5.20 (t, *J* = 6.8 Hz, 1H), 4.82 (dt, *J* = 8.0, 6.9 Hz, 1H), 3.66 – 3.58 (m, 2H), 2.79 (d, *J* = 8.8 Hz, 1H), 2.34 (dd, *J* = 13.7, 6.5 Hz, 1H), 2.23 (dd, *J* = 13.7, 6.5 Hz, 1H), 2.12 – 2.06 (m, 4H), 2.02 – 1.93 (m, 3H), 1.76 – 1.70 (m, 1H), 1.66 – 1.65 (m, 7H), 1.54 – 1.49 (m, 1H), 1.45 – 1.40 (m, 1H), 1.303 – 1.298 (m, 6H), 1.161 – 1.07 (m, 24H), 0.90 (s, 3H), 0.89 (s, 9H), 0.0035 (s, 6H).

^{13}C NMR (150 MHz, $CDCl_3$) δ 170.4, 142.7, 129.8, 129.3, 113.7, 72.1, 64.9, 63.1, 59.1, 45.4, 42.7, 39.8, 35.3, 34.9, 30.8, 27.7, 26.2, 24.9, 23.2, 22.4, 21.3, 19.7, 18.5, 18.31, 18.29, 17.3, 16.7, 13.4, -5.09, -5.11.

HRMS [ES+] m/z calc'd for C38H72O5SiH $[M+H]^+$: 655.4996, found 665.4972.



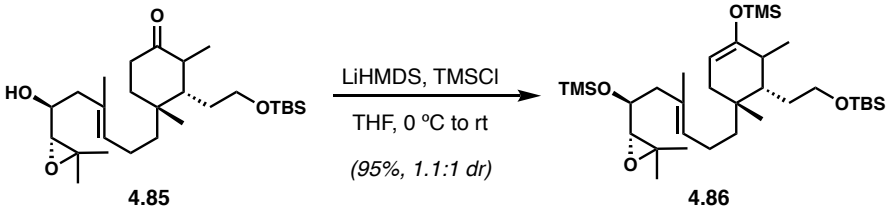
(3*S*,4*R*)-3-(2-((*tert*-butyldimethylsilyl)oxy)ethyl)-4-((*S*,*E*)-6-((*R*)-3,3-dimethyloxiran-2-yl)-6-hydroxy-4-methylhex-3-en-1-yl)-2,4-dimethylcyclohexan-1-one (**4.85**): To acetate **4.84** (11 mg, 21 μmol, 1.0 equiv) in MeOH (430 μL) was added K_2CO_3 (15 mg, 0.11 mmol, 5.0 equiv) and the mixture was stirred at room temperature for 1 hour. Then, water (70 μL), CH_2Cl_2 (70 μL) and brine (70 μL) were added. The phases were separated and the aqueous phase was extracted with EtOAc (3 x 500 μL). The combined organic extracts were washed with brine, dried over $MgSO_4$,

filtered and concentrated *in vacuo.* The crude residue was purified by flash column chromatography (pH7 SiO_2, 30-50% EtOAc in hexanes) to afford epoxyolefin **4.85** (8.8 mg, 89%) as a colorless oil.

^{1}H NMR (600 MHz, $CDCl_3$) δ 5.29 – 5.24 (m, 1H), 3.62 – 3.45 (m, 3H), 2.71 – 2.70 (m, 1H), 2.38 – 2.19 (m, 4H), 2.08 – 1.93 (m, 4H), 1.82 – 1.80 (m, 1H), 1.69 – 1.49 (m, 5H), 1.43 – 1.25 (m, 10H), 1.20 – 1.16 (m, 1H), 1.05 – 0.97 (m, 5H), 0.88 – 0.86 (m, 9H), 0.031 – 0.014 (m, 6H).

^{13}C NMR (150 MHz, $CDCl_3$) δ 213.8, 213.0, 130.9, 130.6, 128.8, 128.69, 128.66, 69.9, 68.9, 67.69, 67.66, 63.82, 63.80, 59.4, 51.4, 47.1, 46.8, 44.7, 44.5, 44.4, 40.1, 37.92, 37.87, 36.7, 36.6, 36.2, 34.5, 34.0, 30.8, 29.5, 26.1, 25.8, 25.0, 23.6, 22.7, 22.4, 19.5, 18.5, 16.64, 16.57, 13.1, 13.0, -5.15, -5.19.

HRMS [ES+] m/z calc'd for $C_{27}H_{50}O_4SiNa$ $[M+Na]^+$: 489.3376, found 489.3374.



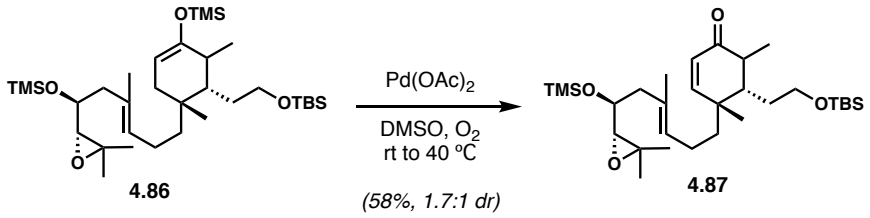
(3*S*,4*R*)-3-(2-((*tert*-butyldimethylsilyl)oxy)ethyl)-4-((*S*,*E*)-6-((*R*)-3,3-dimethyloxiran-2-yl)-4-methyl-6-((trimethylsilyl)oxy)hex-3-en-1-yl)-2,4-dimethylcyclohexan-1-one (**4.86**): Ketone **4.87** (23 mg, 49 μmol, 1.0 equiv) was dried by azeotropic distillation from benzene (3 x 0.5 mL) and placed *in vacuo* for 30 minutes. To a cooled (0 ºC) solution of ketone **4.85** in THF (980 μL) under an atmosphere of argon was added a stock solution of LiHMDS (0.20 M in THF, 0.98 mL, 0.20 mmol, 4.0 equiv). The reaction was stirred for 10 minutes then, a stock solution of TMSCl (0.20 M in THF, 0.98 mL, 0.20 mmol, 4.0 equiv) was added dropwise and the mixture was stirred for 30 minutes at 0 ºC. Next, the reaction was warmed to room temperature and stirred for 1 hour.

The reaction was filtered through a pad of Al_2O_3, the pad was washed with THF, and the volatiles were removed *in vacuo*. The crude product was purified by flash column chromatography (pH7 SiO_2, 10% EtOAc in hexanes) to afford enoxysilane **4.86** (28 mg, 95%) as a colorless oil.

^{1}H NMR (600 MHz, $CDCl_3$) δ 5.16 (t, J = 6.9 Hz, 1H), 4.68 – 4.67 (m, 1H), 3.63 – 3.56 (m, 2H), 3.53 – 3.46 (m, 1H), 2.66 – 2.64 (m, 1H), 2.20 – 2.17 (m, 1H), 2.14 – 2.10 (m, 2H), 1.87 – 1.80 (m, 1H), 1.79 – 1.69 (m, 1H), 1.62 – 1.60 (m, 3H), 1.53 – 1.48 (m, 1H), 1.47 – 1.35 (m, 1H), 1.273 – 1.266 (m, 3H), 1.23 – 1.14 (m, 4H), 1.08 – 1.01 (m, 3H), 0.93 – 0.92 (m, 2H), 0.89 – 0.88 (m, 9H), 0.17 – 0.16 (m, 11H), 0.12 – 0.10 (m, 11H), 0.045 – 0.031 (m, 6H).

^{13}C NMR (150 MHz, $CDCl_3$) δ 153.3, 153.2, 151.7, 130.45, 130.41, 129.0, 128.8, 102.5, 101.31, 101.25, 71.7, 71.6, 68.2, 64.09, 64.06, 62.6, 58.8, 47.6, 45.5, 42.8, 39.3, 35.3, 35.23, 35.18, 34.8, 34.5, 34.0, 29.4, 29.2, 26.2, 26.1, 25.7, 25.1, 24.6, 22.67, 22.66, 19.89, 19.86, 18.53, 18.51, 17.5, 17.1, 16.9, 14.4, 5.59, 0.49, 0.45, 0.40, -0.33, -5.05, -5.09, -5.11.

HRMS [ES+] m/z calc'd for $C_{33}H_{66}O_4Si_3Na$ $[M+Na]^+$: 633.4167, found 633.4172.



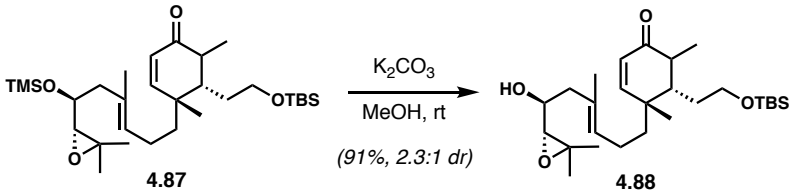
(4*R*,5*S*)-5-(2-((*tert*-butyldimethylsilyl)oxy)ethyl)-4-((*S*,*E*)-6-((*R*)-3,3-dimethyloxiran-2-yl)-4-methyl-6-((trimethylsilyl)oxy)hex-3-en-1-yl)-4,6-dimethylcyclohex-2-en-1-one (**4.87**): A solution of enoxysilane **4.86** (26 mg, 42 μmol, 1.0 equiv) in DMSO (1.0 mL) was bubbled with O_2 for 20 minutes then $Pd(OAc)_2$ (28 mg, 0.13 mmol, 3.0 equiv) was added. The reaction was stirred at 40 ºC under an atmosphere of oxygen for 16 hours. TLC analysis indicated incomplete conversion so $Pd(OAc)_2$ (20 mg, 84 μmol, 2.0 equiv) was added and the mixture was heated to 50

ºC for 1 hour. After complete consumption of starting material, water (550 µL) and EtOAc (550 µL) were added. The phases were separated and the aqueous phase was extracted with EtOAc (3 x 420 µL). The combined organic extracts were washed with brine, dried over Na_2SO_4, filtered and concentrated *in vacuo.* The crude product was purified by flash column chromatography (pH7 SiO_2, 5-10% EtOAc in hexanes) to afford enone **4.87** (13 mg, 58%) as a yellow oil.

^{1}H NMR (600 MHz, $CDCl_3$) δ 6.73 – 6.62 (m, 1H), 5.93 – 5.84 (m, 1H), 5.2 – 5.1 (m, 1H), 3.71 – 3.57 (m, 1H), 3.56 – 3.46 (m, 2H), 2.80 – 2.64 (m, 1H), 2.39 (sextet, J = 7.1 Hz, 1H), 2.22 – 2.16 (m, 1H), 2.14 – 2.04 (m, 2H), 1.98 – 1.90 (m, 1H), 1.85 – 1.80 (m, 1H), 1.75 – 1.60 (m, 4H), 1.57 – 1.54 (m, 1H), 1.49 – 1.42 (m, 2H), 1.28 – 1.23 (m, 8H), 1.17 – 1.15 (m, 4H), 0.88 – 0.87 (m, 9H), 0.12 – 0.11 (m, 9H), 0.041 – 0.020 (m, 6H).

^{13}C NMR (150 MHz, $CDCl_3$) δ 202.7, 202.0, 159.0, 156.9, 131.7, 131.62, 131.57, 127.84, 127.81, 127.6, 127.0, 126.7, 71.63, 71.58, 68.0, 63.6, 62.3, 58.72, 58.71, 47.1, 45.32, 45.25, 43.8, 42.6, 39.7, 39.6, 38.1, 35.4, 33.2, 29.8, 29.7, 26.09, 26.07, 25.6, 25.1, 23.4, 22.6, 19.84, 19.81, 18.5, 18.4, 17.1, 17.0, 13.6, 13.4, 0.39, -5.14, -5.15, -5.17, -5.20.

HRMS [ES+] m/z calc'd for $C_{30}H_{56}O_4SiNa$ $[M+Na]^+$: 559.3615, found 559.3638.



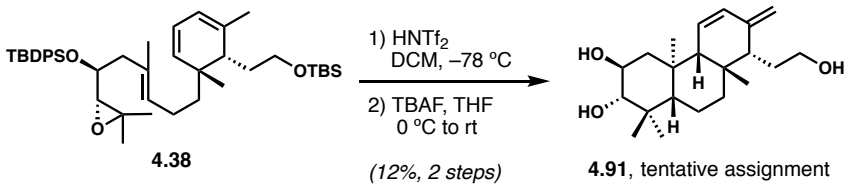
(4*R*,5*S*)-5-(2-((*tert*-butyldimethylsilyl)oxy)ethyl)-4-((*S*,*E*)-6-((*R*)-3,3-dimethyloxiran-2-yl)-6-hydroxy-4-methylhex-3-en-1-yl)-4,6-dimethylcyclohex-2-en-1-one (**4.89**):): Enoxysilane **4.88** (12 mg, 22 µmol, 1.0 equiv) was subjected to the reaction conditions described for the preparation

of **4.85**. The crude product was purified by flash column chromatography (pH7 SiO_2, 30% EtOAc in hexanes) to afford alcohol **4.89** (9.5 mg, 91%) as a colorless oil.

^{1}H NMR (600 MHz, $CDCl_3$) δ 6.73 – 6.62 (m, 1H), 5.93 – 5.84 (m, 1H), 5.25 – 5.20 (m, 1H), 3.71 – 3.67 (m, 1H), 3.60 – 3.49 (m, 2H), 2.80– 2.69 (m, 1H), 2.42 – 2.37 (m, 1H), 2.30 – 2.24 (m, 1H), 2.19 (td, *J* = 16.0, 5.5 Hz, 1H), 2.15 – 2.09 (m, 1H0, 2.00 – 1.90 (m, 2H), 1.85 – 1.80 (m, 1H), 1.72 – 1.67 (m, 1H), 1.65 – 1.60 (m, 3H), 1.57 – 1.54 (m, 1H), 1.50 – 1.43 (m, 2H), 1.31 – 1.30 (m, 3H), 1.29 – 1.28 (m, 3H), 1.25 (s, 1H), 1.17 – 1.15 (m, 5H), 0.88 – 0.87 (m, 9H), 0.041 – 0.021 (m, 6H).

^{13}C NMR (150 MHz, $CDCl_3$) δ 202.6, 202.0, 158.9, 158.8, 131.2, 128.5, 128.4, 128.2, 127.0, 126.8, 68.93, 68.89, 67.63, 67.61, 63.6, 62.4, 59.38, 59.36, 47.1, 44.9, 44.5, 44.4, 43.9, 42.6, 39.7, 39.6, 38.1, 35.4, 33.2, 29.8, 29.7, 26.1, 25.63, 25.59, 25.0, 23.4, 22.5, 19.6, 19.5, 18.5, 18.4, 16.7, 16.62, 16.58, 13.6, 13.40, 13.36, -5.15, -5.16, -5.20.

HRMS [ES+] m/z calc'd for $C_{27}H_{48}O_4SiNa$ $[M+Na]^+$: 487.3220, found 487.3214.



(2*S*,3S,4a*R*,4b*R*,8*S*,8a*S*,10a*S*)-8-(2-hydroxyethyl)-1,1,4a,8a-tetramethyl-7-methylene-1,2,3,4,4a,4b,7,8,8a,9,10,10a-dodecahydrophenanthrene-2,3-diol (**4.38**): Epoxypolyene **4.38** (21 mg, 30 μmol, 1.0 equiv) was dried by azeotropic distillation from benzene (3 x 0.5 mL) and placed *in vacuo* for 30 minutes. To a cooled (–78 ºC) solution of epoxypolyene **4.38** in CH_2Cl_2 (1.0 mL) was added a solution of $HNTf_2$ (17 mg, 60 μmol, 2.0 equiv) in CH_2Cl_2 (1.0 mL), dropwise. After stirring at –78 ºC for 2 hours, Et_3N (100 μL) and EtOAc (840 μL) were added.

The reaction was warmed to room temperature and the volatiles were removed *in vacuo*. The crude was further purified by preparative plate chromatography to give 80% pure product.

The product (7.1 mg, 10 μmol, 1.0 equiv) obtained above was dissolved in THF (500 μL), cooled to 0 ºC, and TBAF (1.0 M in THF, 30 μL, 30 μmol, 3.0 equiv) was added. The reaction mixture warmed to room temperature and stirred for 40 minutes then satd. aq. NH_4Cl (440 μL) was added. The phases were separated and the aqueous phase was extracted with EtOAc (3 x 440 μL). The combined organic extracts were washed with brine, dried over Na_2SO_4, filtered and concentrated *in vacuo.* The crude product was purified by preparative plate chromatography (70% EtOAc in hexanes) to afford tricyclic **4.91** (1.2 mg, 12%, 90% purity) over 2 steps as a white solid.

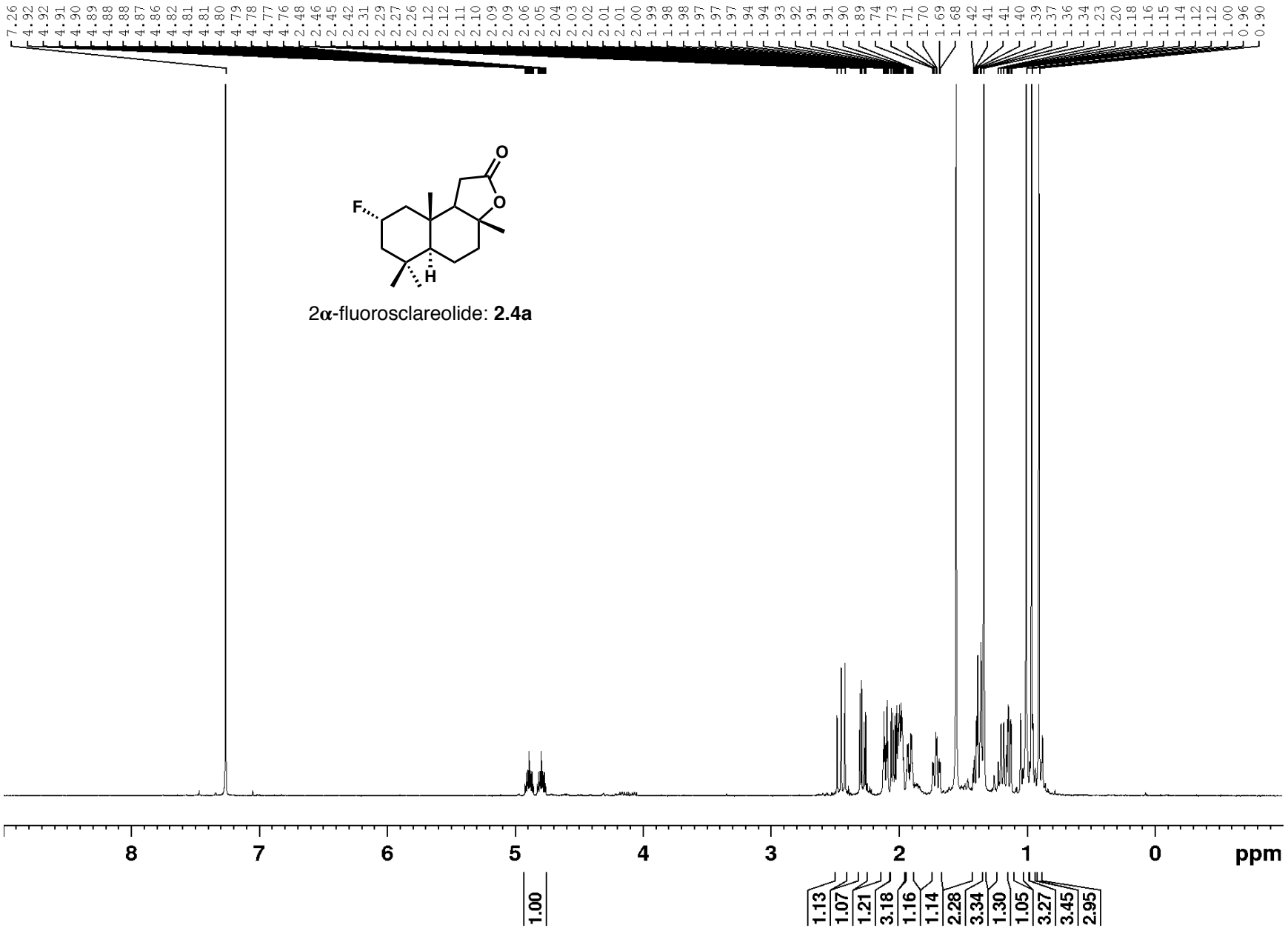
^{1}H NMR (600 MHz, $CDCl_3$) δ 5.53 – 5.50 (m, 1H), 5.45 – 5.43 (m, 1H), 4.99 (s, 1H), 4.70 (s, 1H), 3.67 – 3.60 (m, 3H), 3.48 (ddd, *J* = 11.4, 9.4, 5.3 Hz, 1H), 3.12 (d, *J* = 9.2 Hz, 1H), 2.61 (dd, *J* = 12.2, 5.3 Hz, 1H), 2.12 – 2.10 (m, 2H), 2.02 – 2.00 (m, 1H), 1.98 – 1.97 (m, 1H), 1.92 (br s, 1H), 1.83 – 1.78 (m, 2H), 1.71 – 1.67 (m, 1H), 1.43 (d, *J* = 5.7, Hz, 2H), 1.37 – 1.34 (m, 2H), 1.09 (s, 3H), 0.56 (s, 3H), 0.65 (s, 3H).

HRMS [ES+] m/z calc'd for $C_{21}H_{34}O_3Na$ $[M+Na]^+$: 357.2406, found 357.2392.

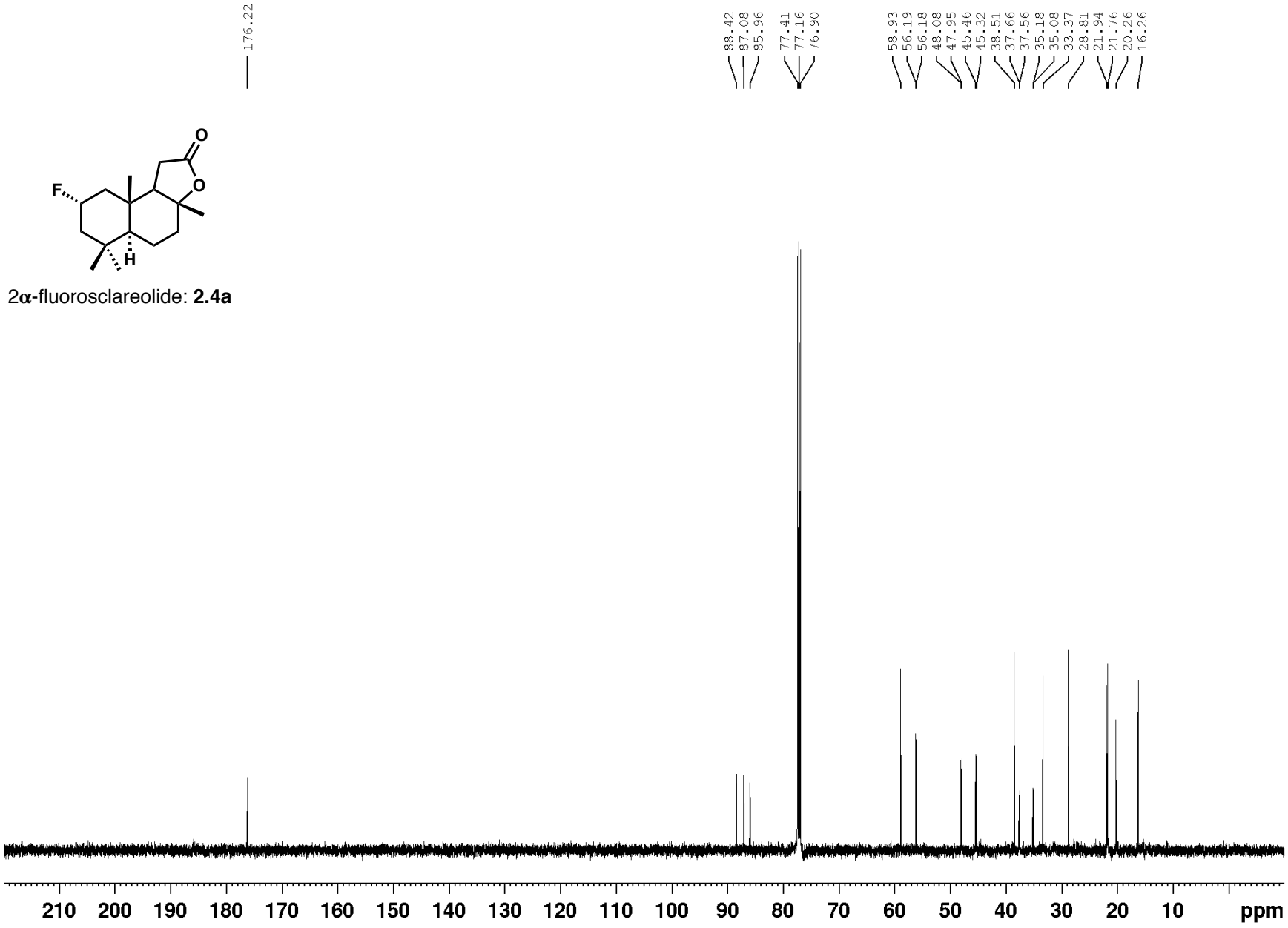
4.11.3 Supplemental References

1. Mun, B.; Kim, S.; Yoon, H.; Kim, K. H.; Lee, Y. *J. Org. Chem*. **2017**, *82*, 6349–6357.
2. Sawama, Y.; Sawama, Y.; Krause, N. *Org. Biomol. Chem*., **2008**, *6*, 3573–3579.

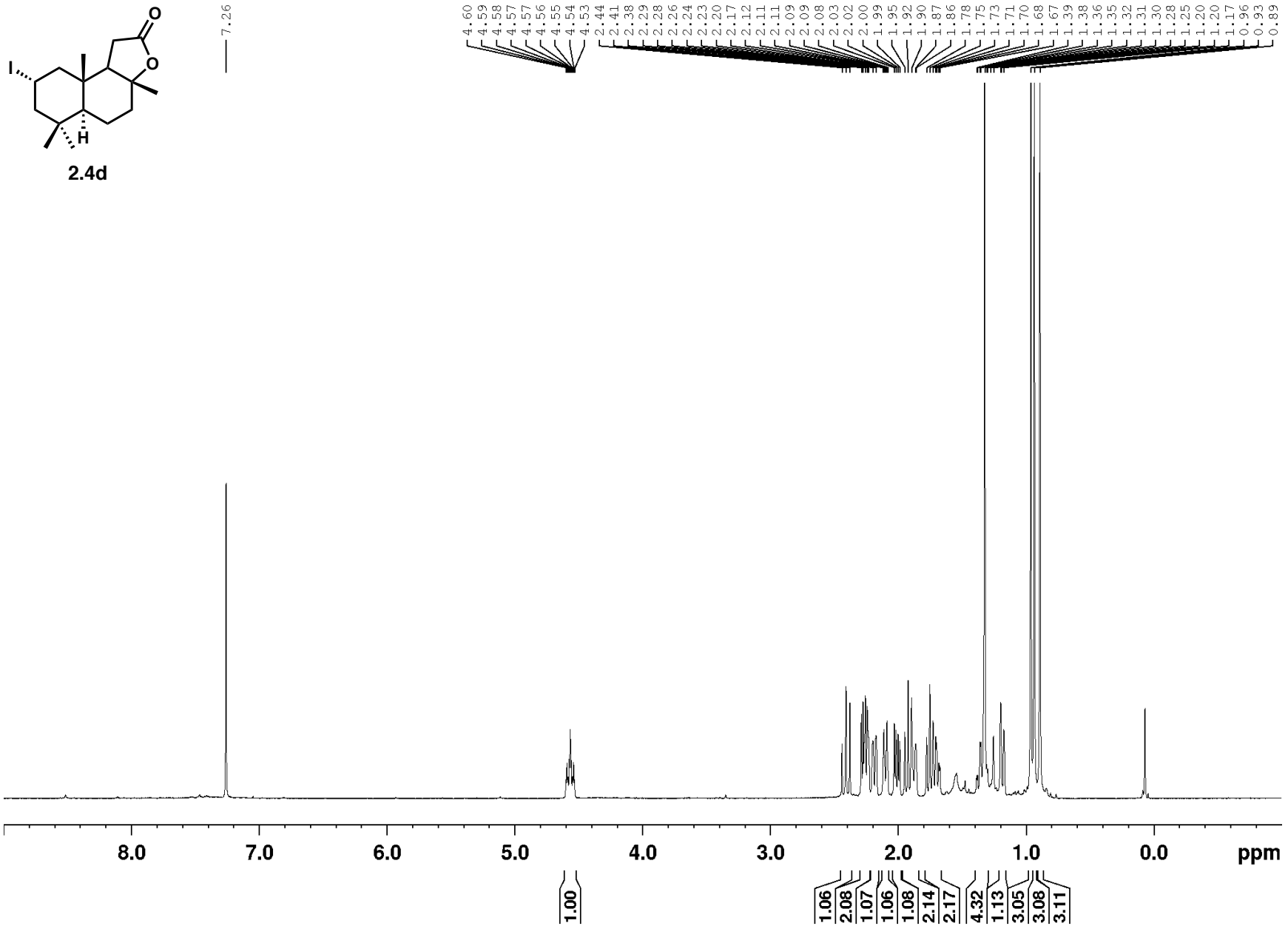
APPENDIX A: NMR DATA FOR CHAPTER 2

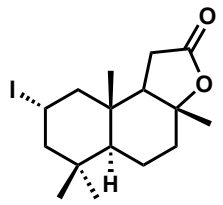


2α-fluorosclareolide: **2.4a**



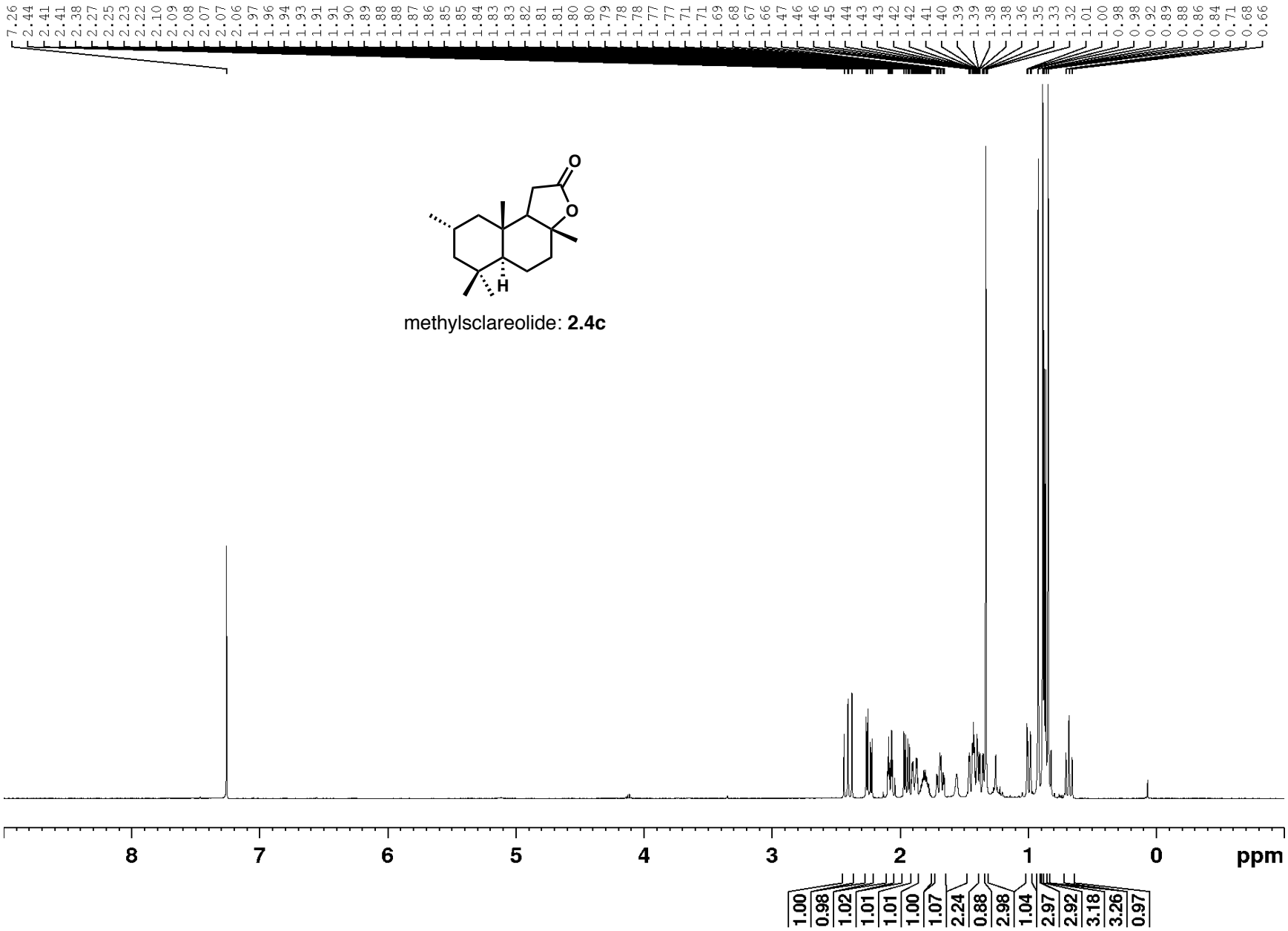
2α-fluorosclareolide: **2.4a**


O
O
I
H
2.4d
7.26
4.60
4.59
4.58
4.57
4.57
4.56
4.55
4.54
4.53
2.44
2.41
2.38
2.29
2.28
2.26
2.24
2.23
2.20
2.17
2.12
2.11
2.11
2.09
2.09
2.08
2.03
2.02
2.00
1.99
1.95
1.92
1.90
1.87
1.86
1.78
1.75
1.73
1.71
1.70
1.68
1.67
1.39
1.38
1.36
1.35
1.32
1.31
1.30
1.28
1.25
1.20
1.20
1.17
0.96
0.93
0.89
8.0
7.0
6.0
5.0
4.0
3.0
2.0
1.0
0.0
ppm
1.00
1.06
2.08
1.07
1.06
1.08
2.14
2.17
4.32
1.13
3.05
3.08
3.11

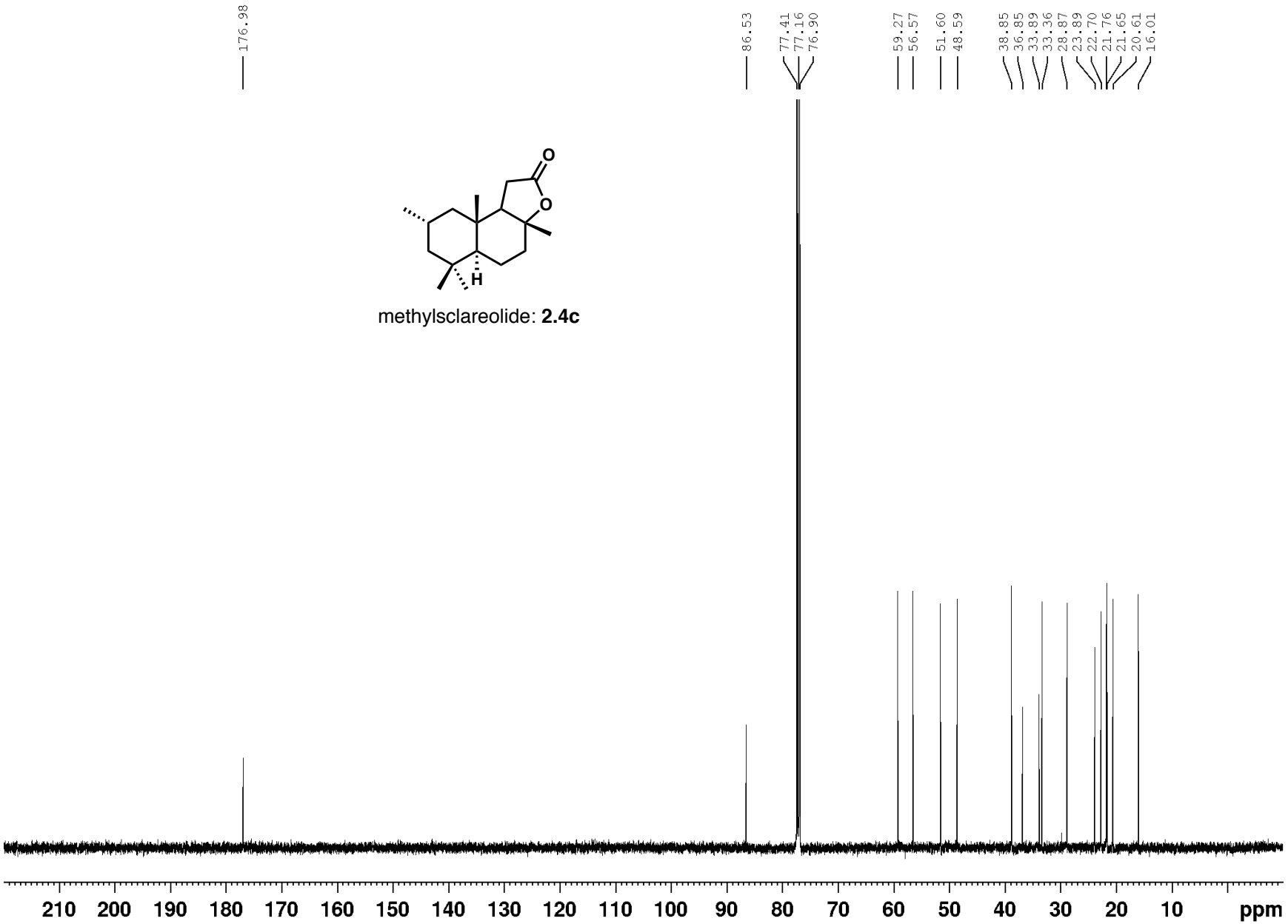

O
I
O
H

2.4d

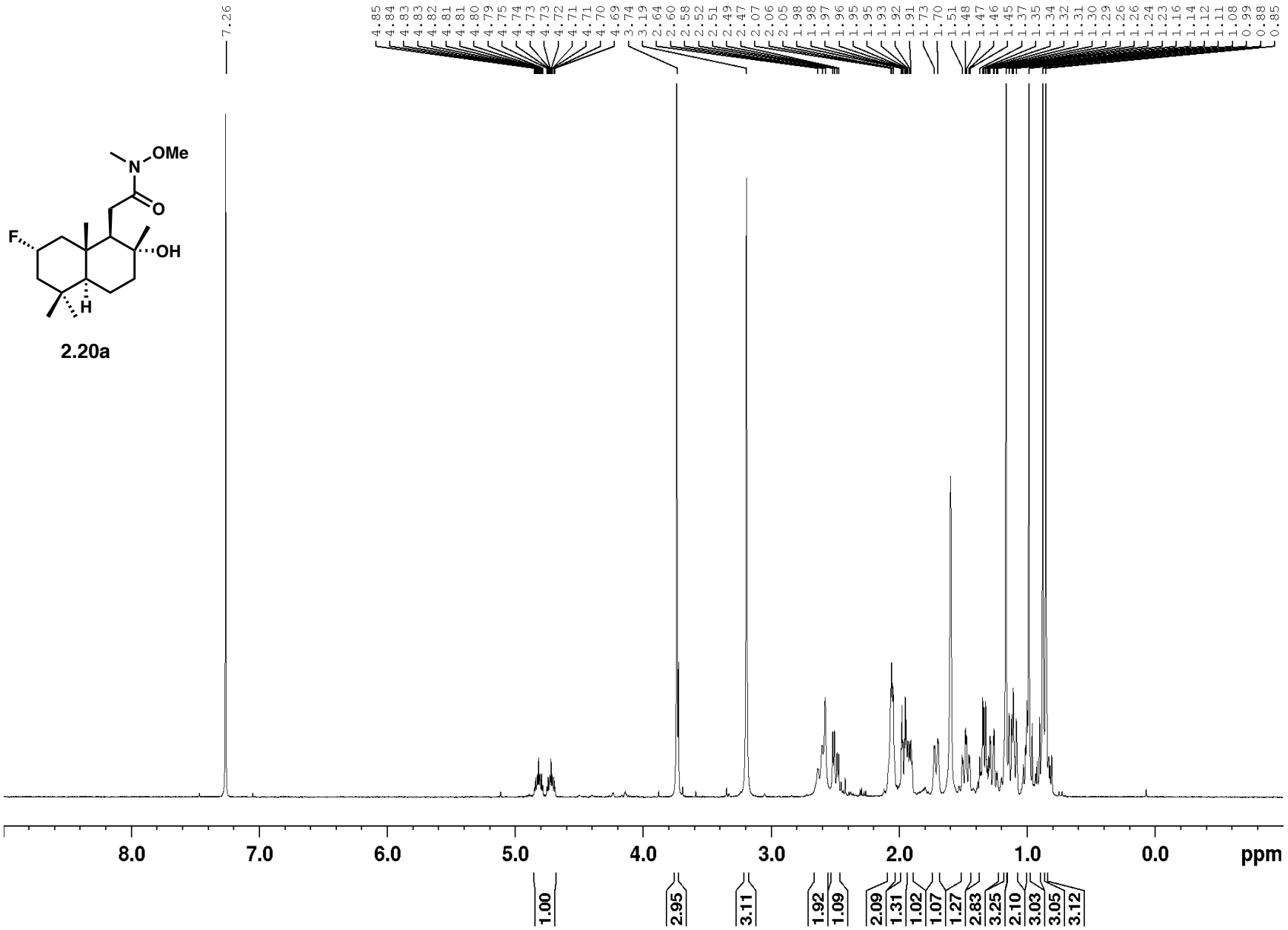
176.09
85.88
77.41
77.16
76.90
58.51
55.77
55.67
53.14
39.82
38.56
37.68
32.79
28.70
22.85
21.77
21.13
20.58
15.47
210 200 190 180 170 160 150 140 130 120 110 100 90 80 70 60 50 40 30 20 10 ppm



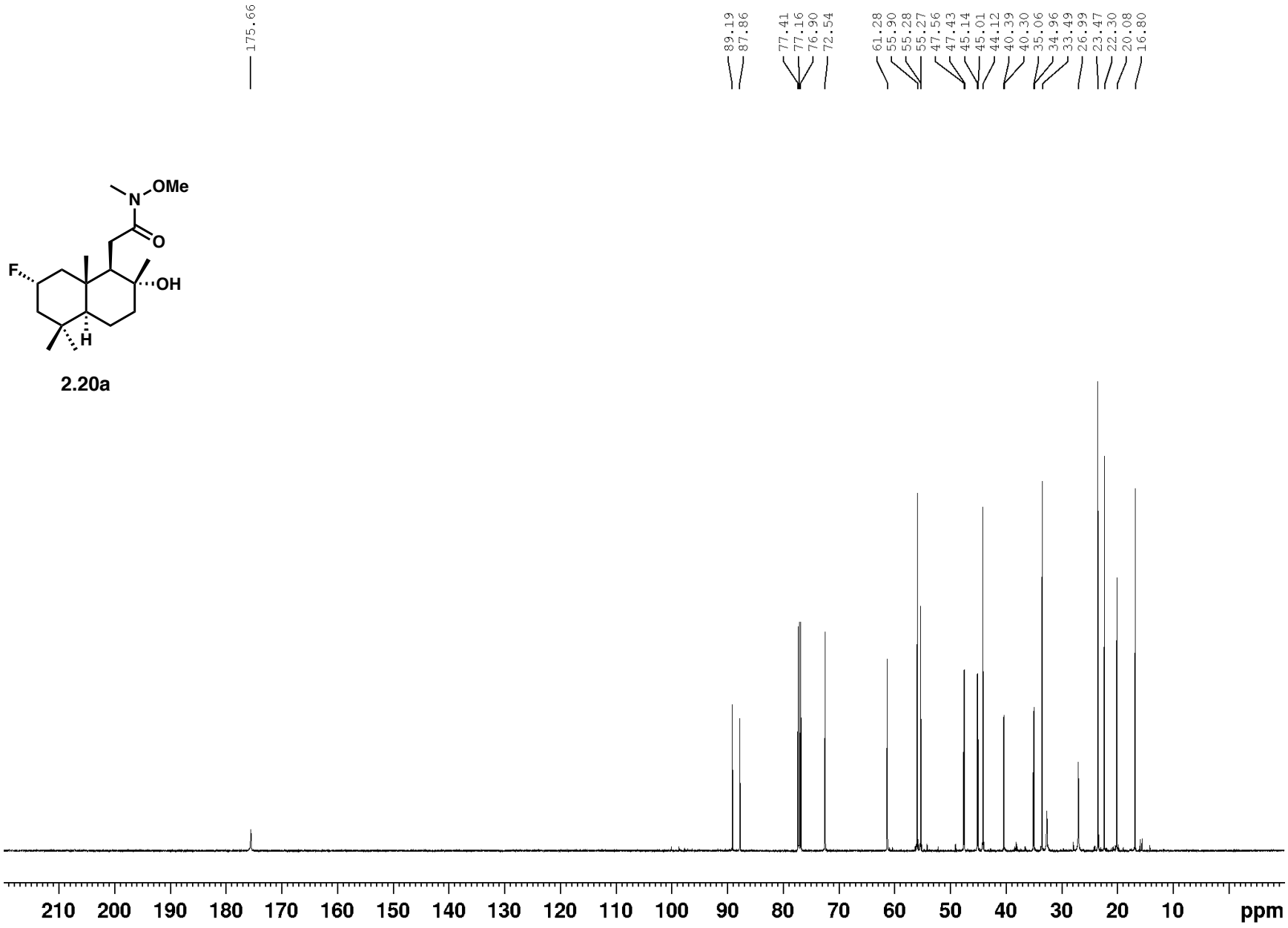
methylsclareolide: **2.4c**



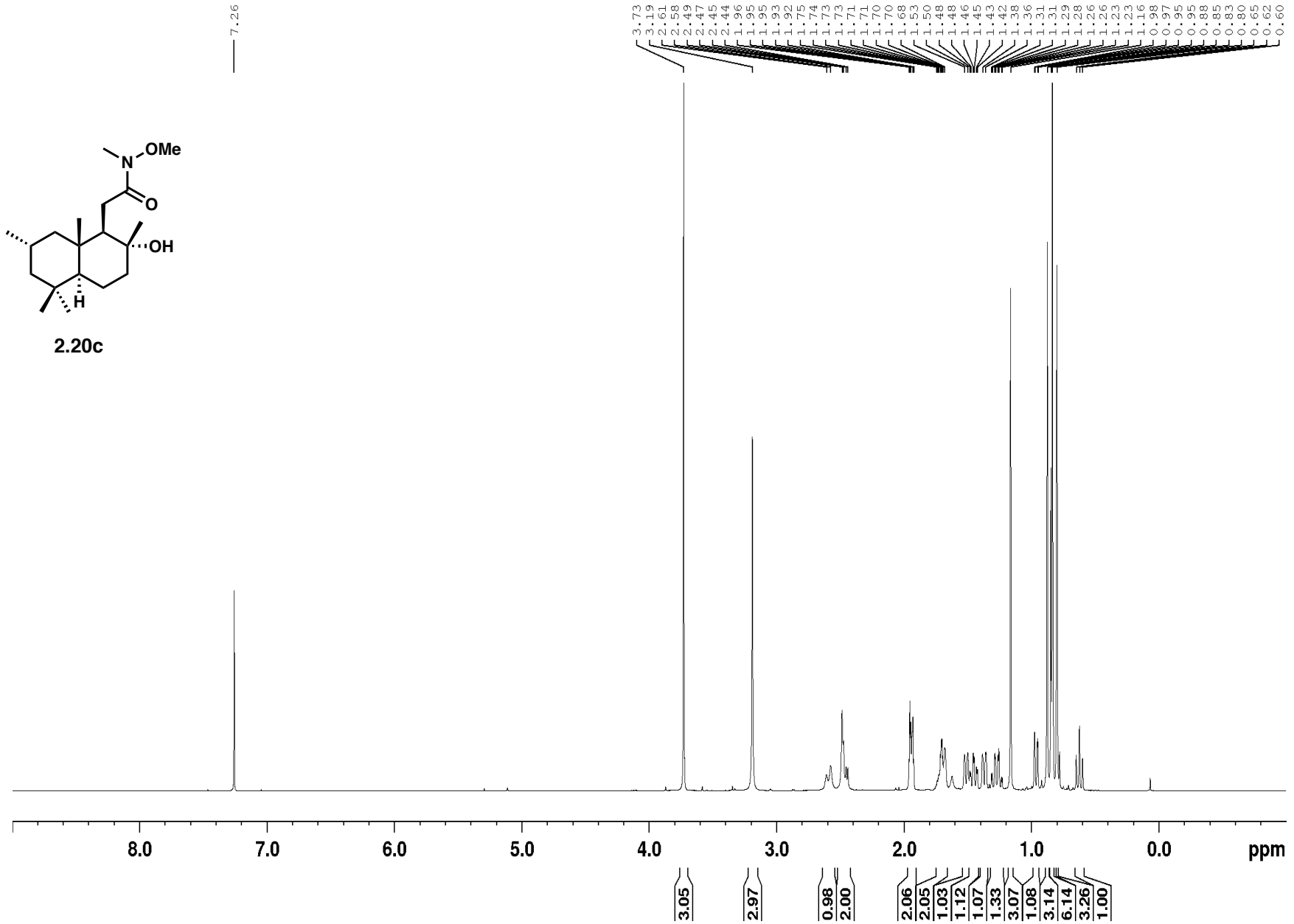
methylsclareolide: **2.4c**


7.26
4.85 4.84 4.83 4.83 4.82 4.81 4.81 4.80 4.79 4.75 4.74 4.73 4.73 4.72 4.71 4.71 4.70 4.69
3.74 3.19 2.64 2.60 2.58 2.52 2.51 2.49 2.47 2.07 2.06 2.05 1.98 1.98 1.97 1.96 1.95 1.95 1.93 1.92 1.91 1.73 1.70 1.51 1.48 1.47 1.46 1.45 1.37 1.35 1.34 1.32 1.31 1.30 1.29 1.26 1.26 1.24 1.23 1.16 1.14 1.12 1.11 1.08 0.99 0.88 0.85
N
OMe
O
F
OH
H
8.0
7.0
6.0
5.0
4.0
3.0
2.0
1.0
0.0
ppm
1.00
2.95
3.11
1.92
1.09
2.09
1.31
1.02
1.07
1.27
2.83
3.25
2.10
3.03
3.05
3.12

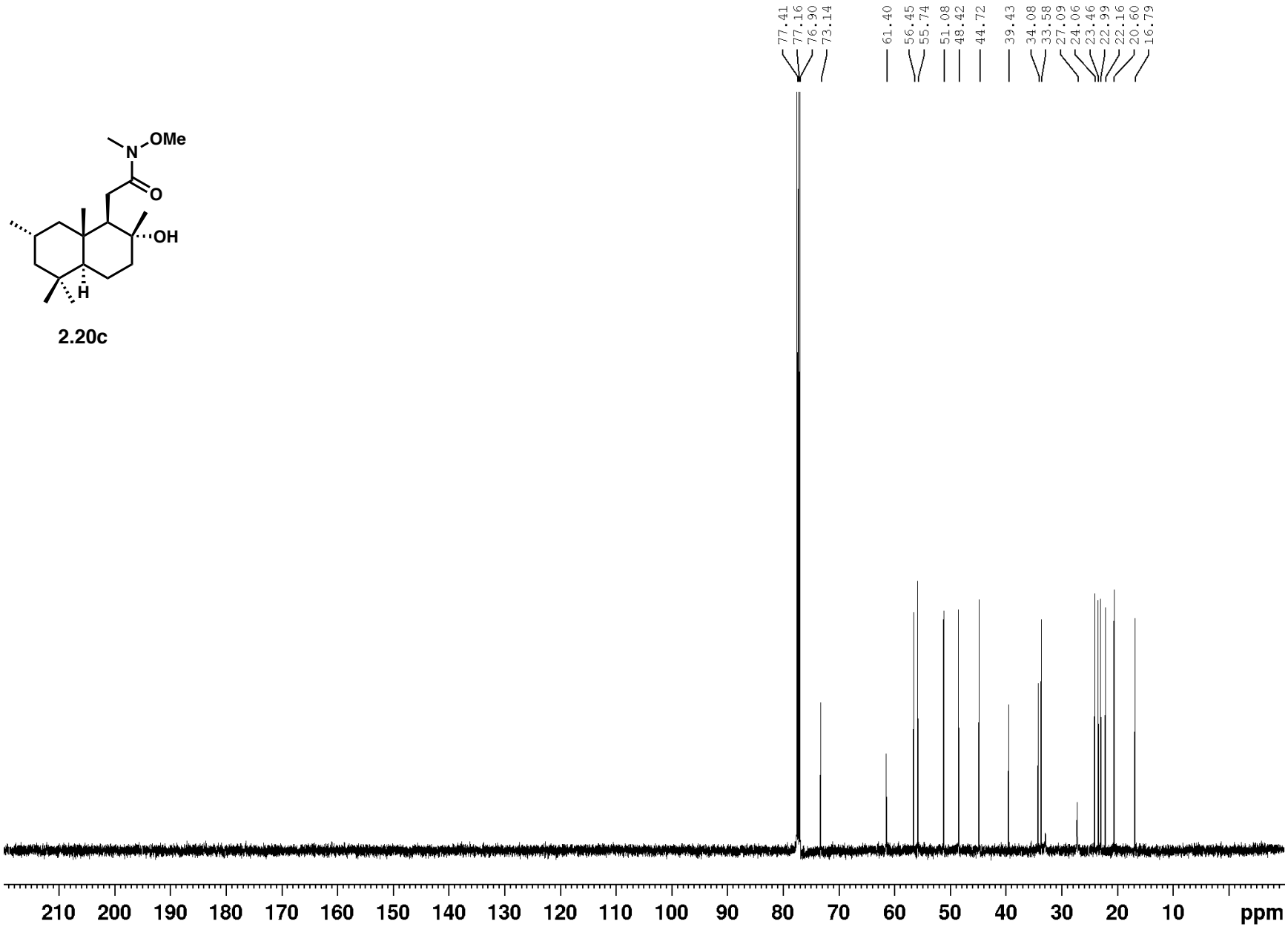
2.20a


175.66
89.19
87.86
77.41
77.16
76.90
72.54
61.28
55.90
55.28
55.27
47.56
47.43
45.14
45.01
44.12
40.39
40.30
35.06
34.96
33.49
26.99
23.47
22.30
20.08
16.80
N
OMe
O
F
OH
H
210
200
190
180
170
160
150
140
130
120
110
100
90
80
70
60
50
40
30
20
10
ppm

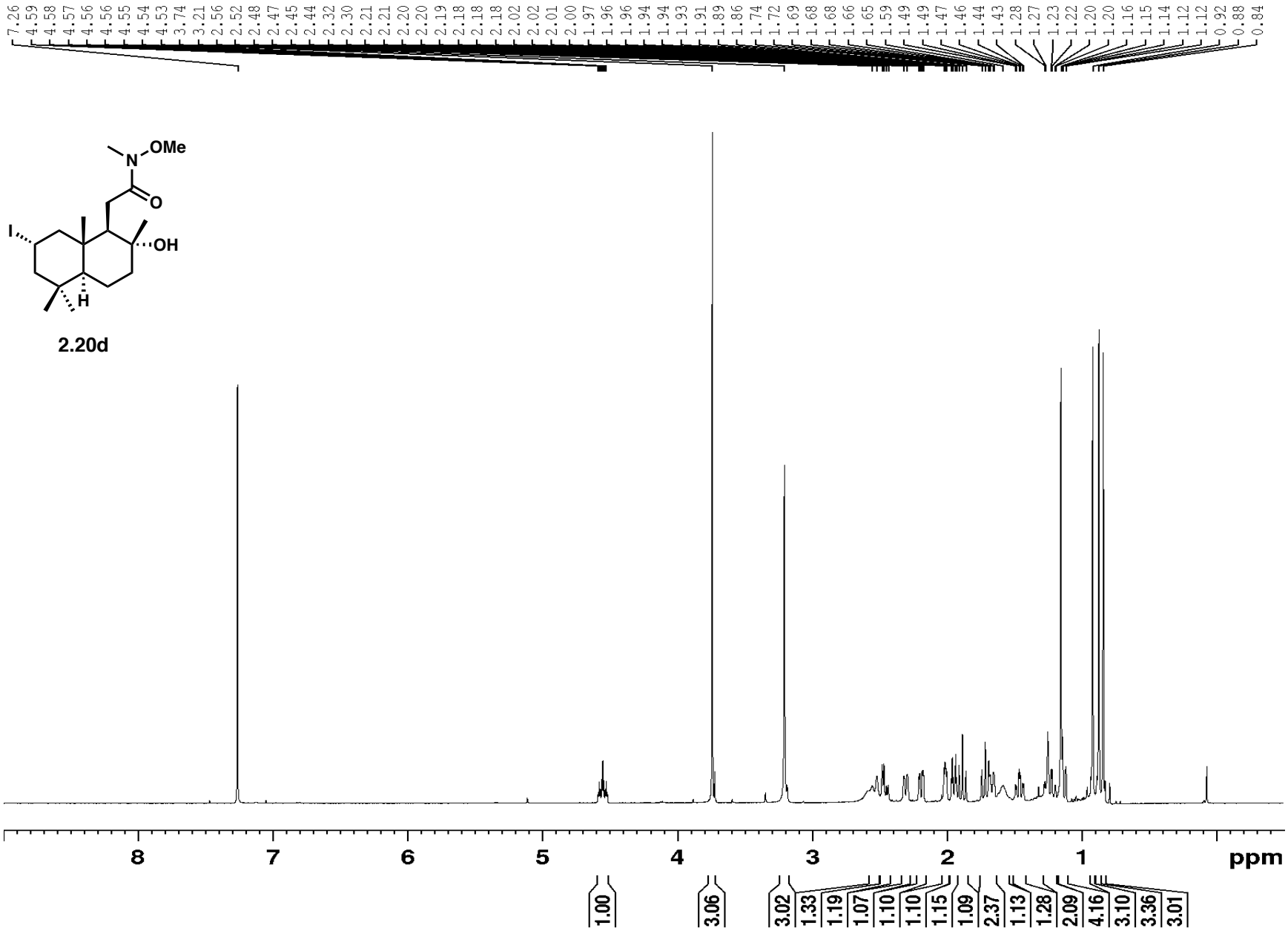
2.20a

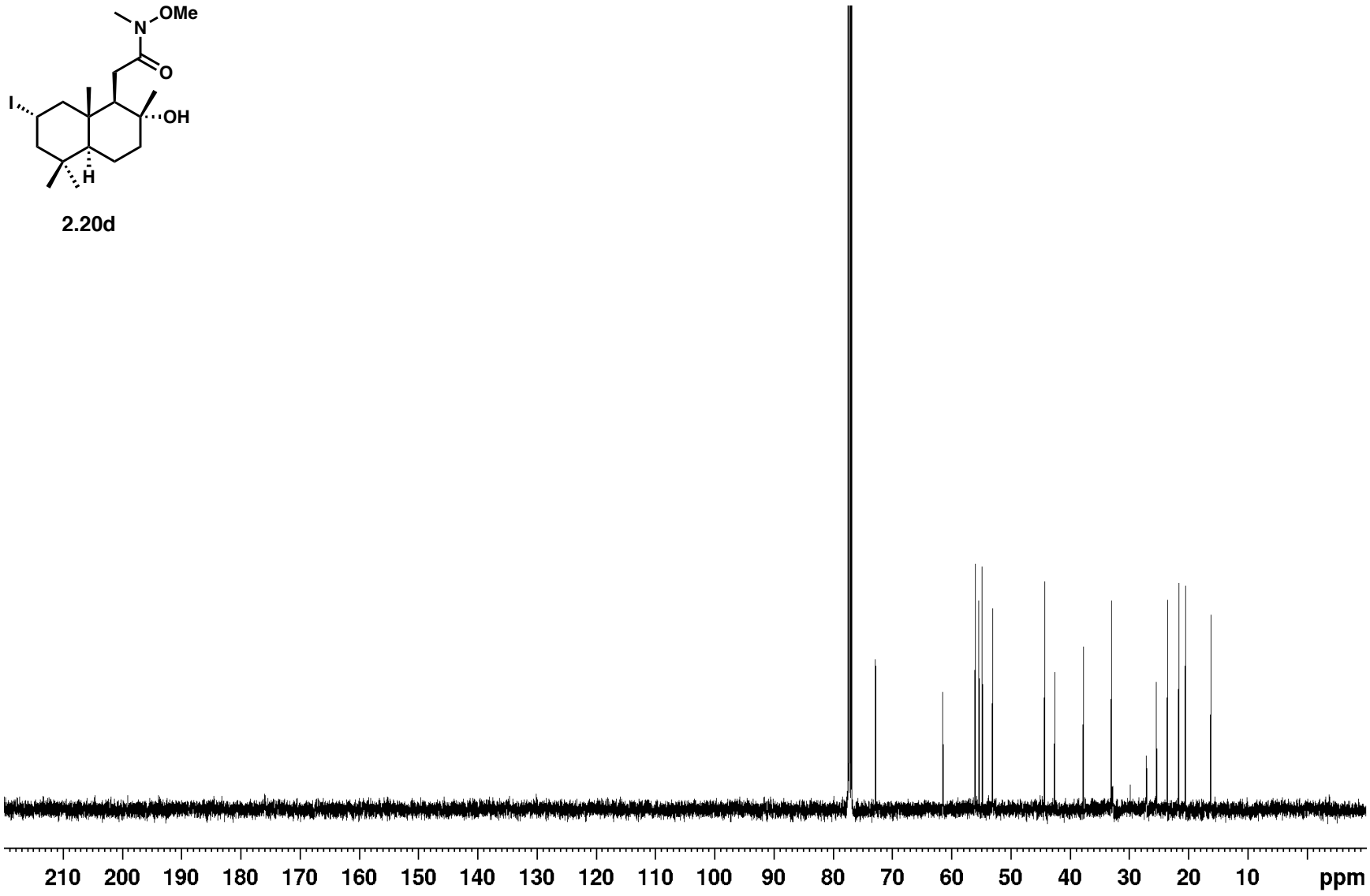

7.26
3.73
3.19
2.61
2.58
2.49
2.47
2.45
2.44
1.96
1.95
1.95
1.93
1.92
1.75
1.74
1.73
1.73
1.71
1.71
1.70
1.70
1.68
1.53
1.50
1.48
1.48
1.46
1.45
1.43
1.42
1.38
1.36
1.31
1.31
1.29
1.28
1.26
1.26
1.23
1.23
1.16
0.98
0.97
0.95
0.95
0.88
0.85
0.83
0.80
0.65
0.62
0.60
N
OMe
O
OH
H
8.0
7.0
6.0
5.0
4.0
3.0
2.0
1.0
0.0
ppm
3.05
2.97
0.98
2.00
2.06
2.05
1.03
1.12
1.07
1.33
3.07
1.08
3.14
6.14
3.26
1.00

2.20c

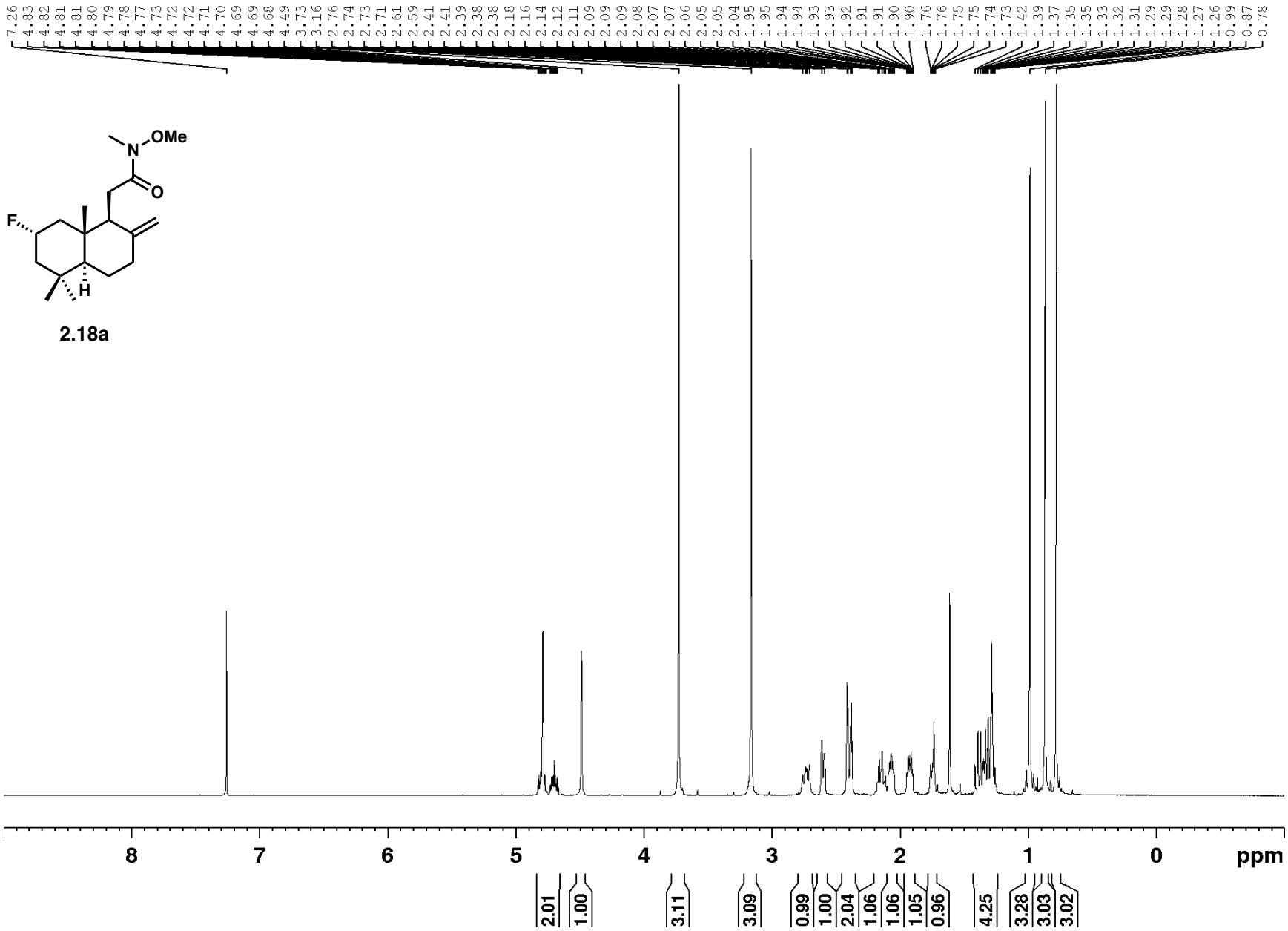

77.41
77.16
76.90
73.14
61.40
56.45
55.74
51.08
48.42
44.72
39.43
34.08
33.58
27.09
24.06
23.46
22.99
22.16
20.60
16.79
N
OMe
O
OH
H
210 200 190 180 170 160 150 140 130 120 110 100 90 80 70 60 50 40 30 20 10 ppm

2.20c

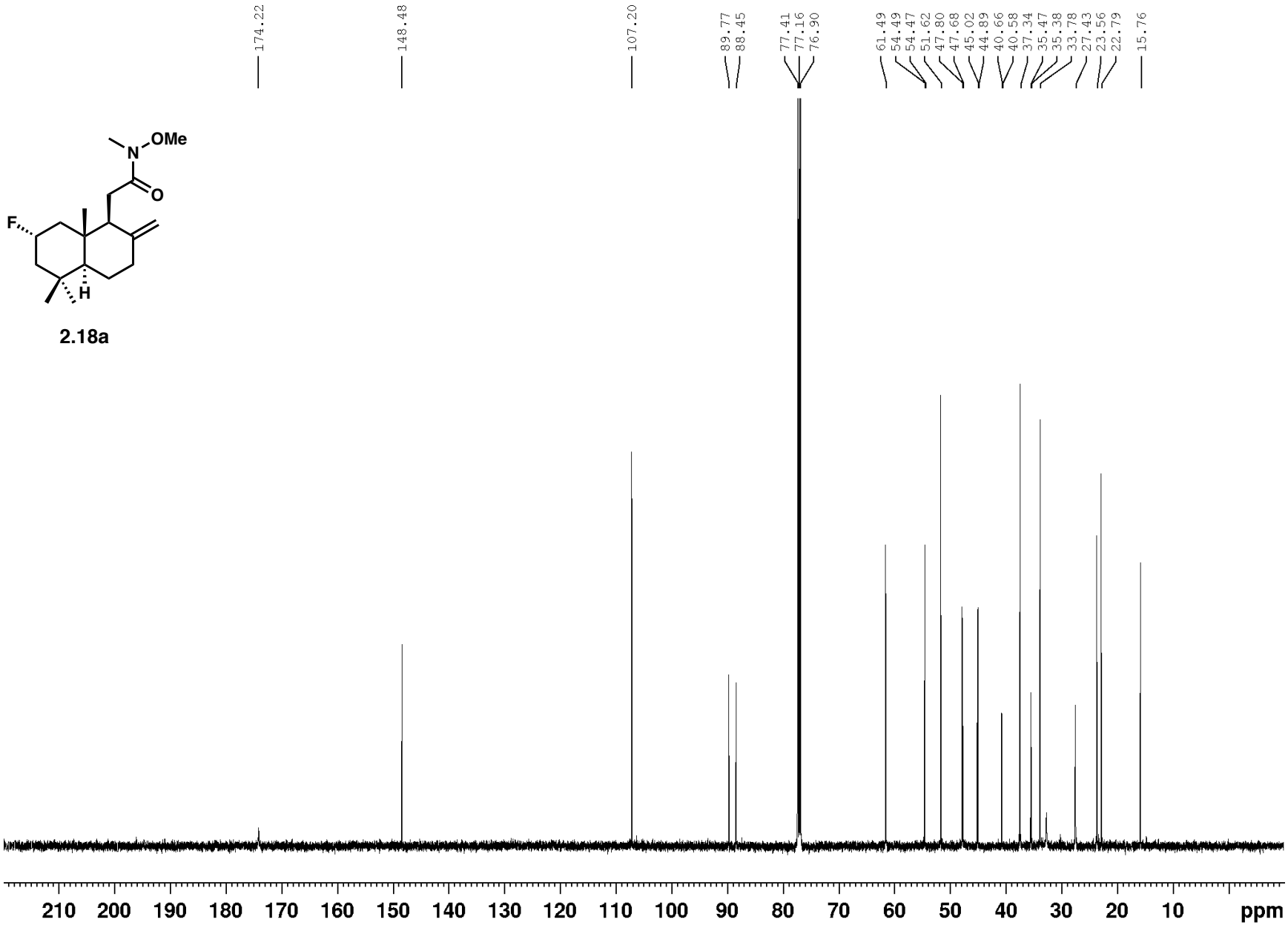

7.26
4.59
4.58
4.57
4.56
4.56
4.55
4.54
4.53
3.74
3.21
2.56
2.52
2.48
2.47
2.45
2.44
2.32
2.30
2.21
2.21
2.20
2.20
2.19
2.18
2.18
2.18
2.02
2.02
2.01
2.00
1.97
1.96
1.96
1.94
1.94
1.93
1.91
1.89
1.86
1.74
1.72
1.69
1.68
1.68
1.66
1.65
1.59
1.49
1.49
1.47
1.46
1.44
1.43
1.28
1.27
1.23
1.22
1.20
1.20
1.16
1.15
1.14
1.12
1.12
0.92
0.88
0.84
N
OMe
O
I
OH
H
2.20d
8
7
6
5
4
3
2
1
ppm
1.00
3.06
3.02
1.33
1.19
1.07
1.10
1.10
1.15
1.09
2.37
1.13
1.28
2.09
4.16
3.10
3.36
3.01


77.41
77.16
76.90
72.83
61.48
56.02
55.37
54.82
53.06
44.25
42.59
37.75
33.00
27.11
25.43
23.55
21.62
20.53
16.17
N
OMe
O
I
OH
H
210
200
190
180
170
160
150
140
130
120
110
100
90
80
70
60
50
40
30
20
10
ppm

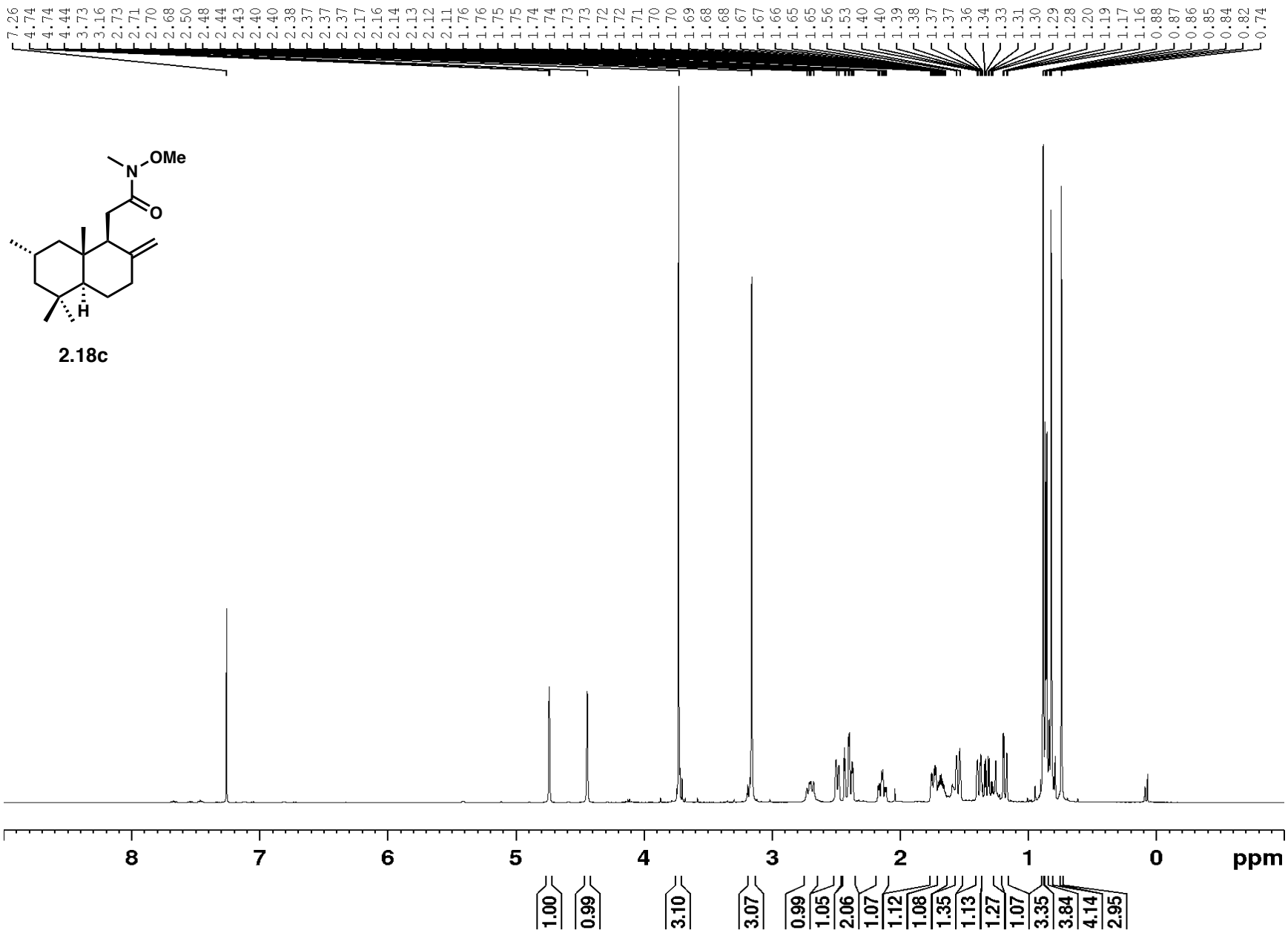
2.20d


7.26
4.83
4.82
4.81
4.81
4.80
4.79
4.78
4.77
4.73
4.72
4.72
4.71
4.70
4.69
4.69
4.68
4.49
3.73
3.16
2.76
2.74
2.73
2.71
2.61
2.59
2.41
2.41
2.39
2.38
2.38
2.18
2.16
2.14
2.12
2.11
2.09
2.09
2.09
2.08
2.07
2.07
2.06
2.05
2.05
2.04
1.95
1.95
1.94
1.94
1.93
1.93
1.92
1.91
1.91
1.90
1.90
1.76
1.76
1.75
1.75
1.74
1.73
1.42
1.39
1.37
1.35
1.35
1.33
1.32
1.31
1.29
1.29
1.28
1.27
1.26
0.99
0.87
0.78
N
OMe
O
F
H
8
7
6
5
4
3
2
1
0
ppm
2.01
1.00
3.11
3.09
0.99
1.00
2.04
1.06
1.06
1.05
0.96
4.25
3.28
3.03
3.02

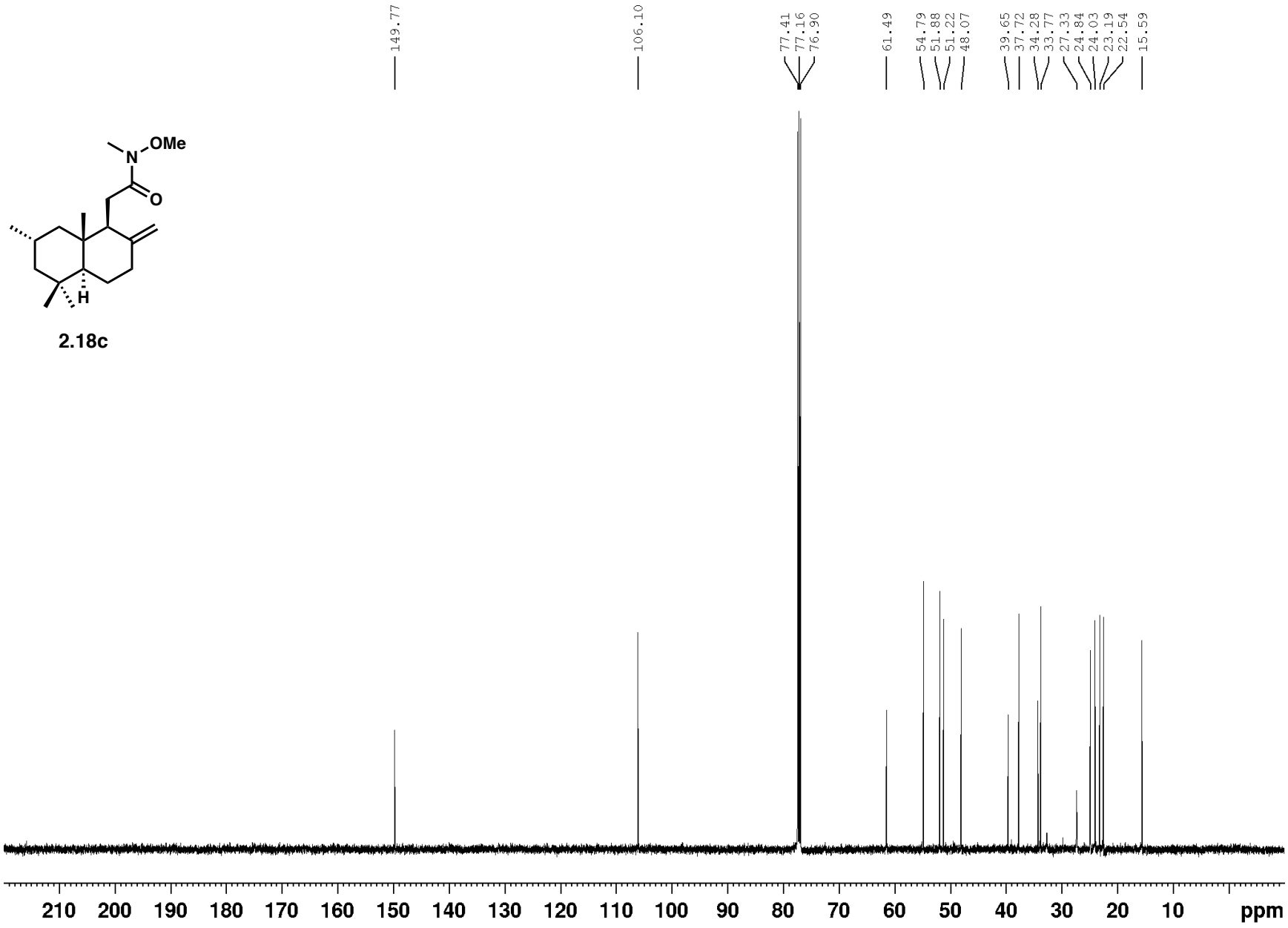
2.18a


174.22
148.48
107.20
89.77
88.45
77.41
77.16
76.90
61.49
54.49
54.47
51.62
47.80
47.68
45.02
44.89
40.66
40.58
37.34
35.47
35.38
33.78
27.43
23.56
22.79
15.76
N
OMe
O
F
H
210
200
190
180
170
160
150
140
130
120
110
100
90
80
70
60
50
40
30
20
10
ppm

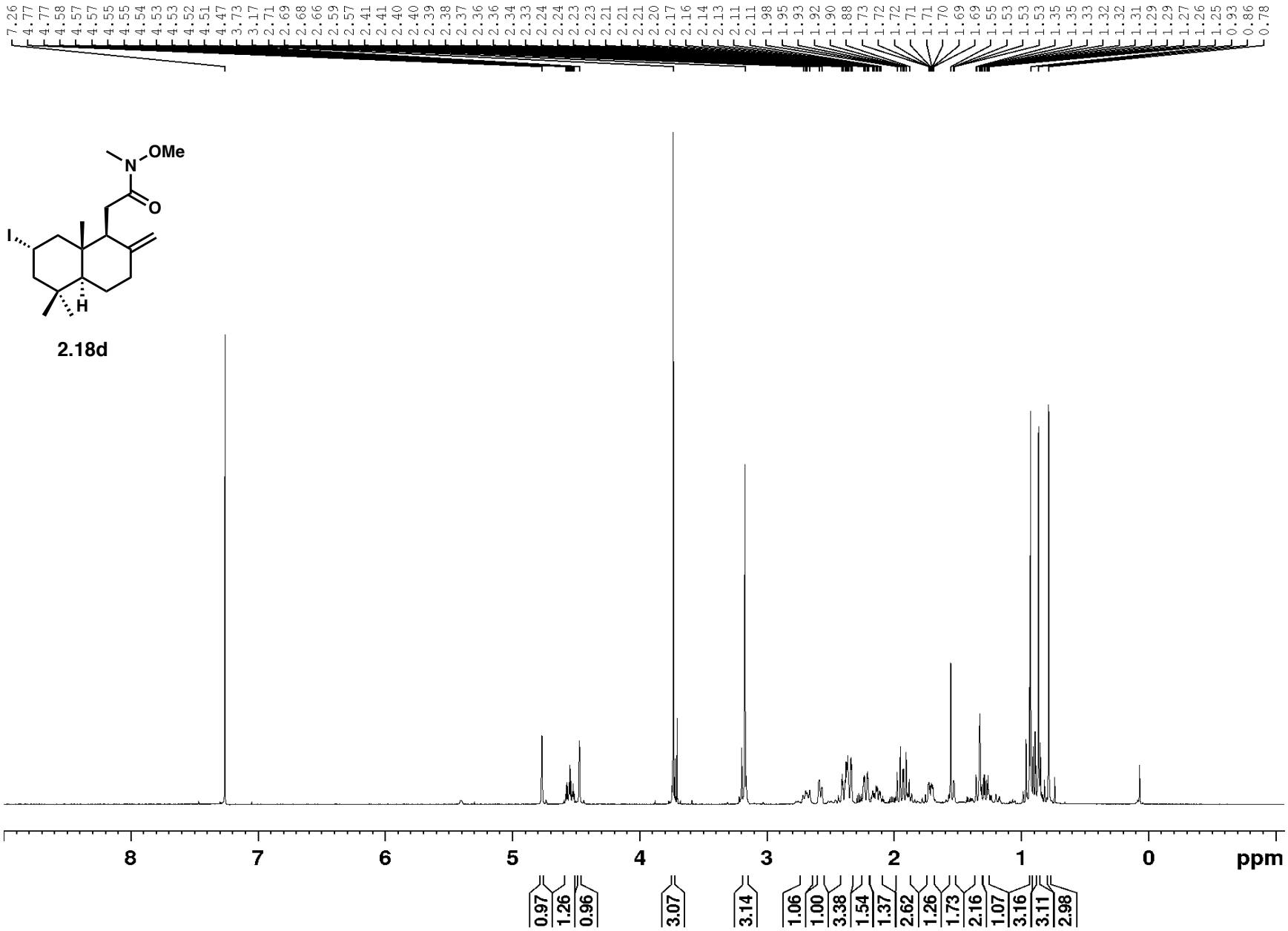
2.18a

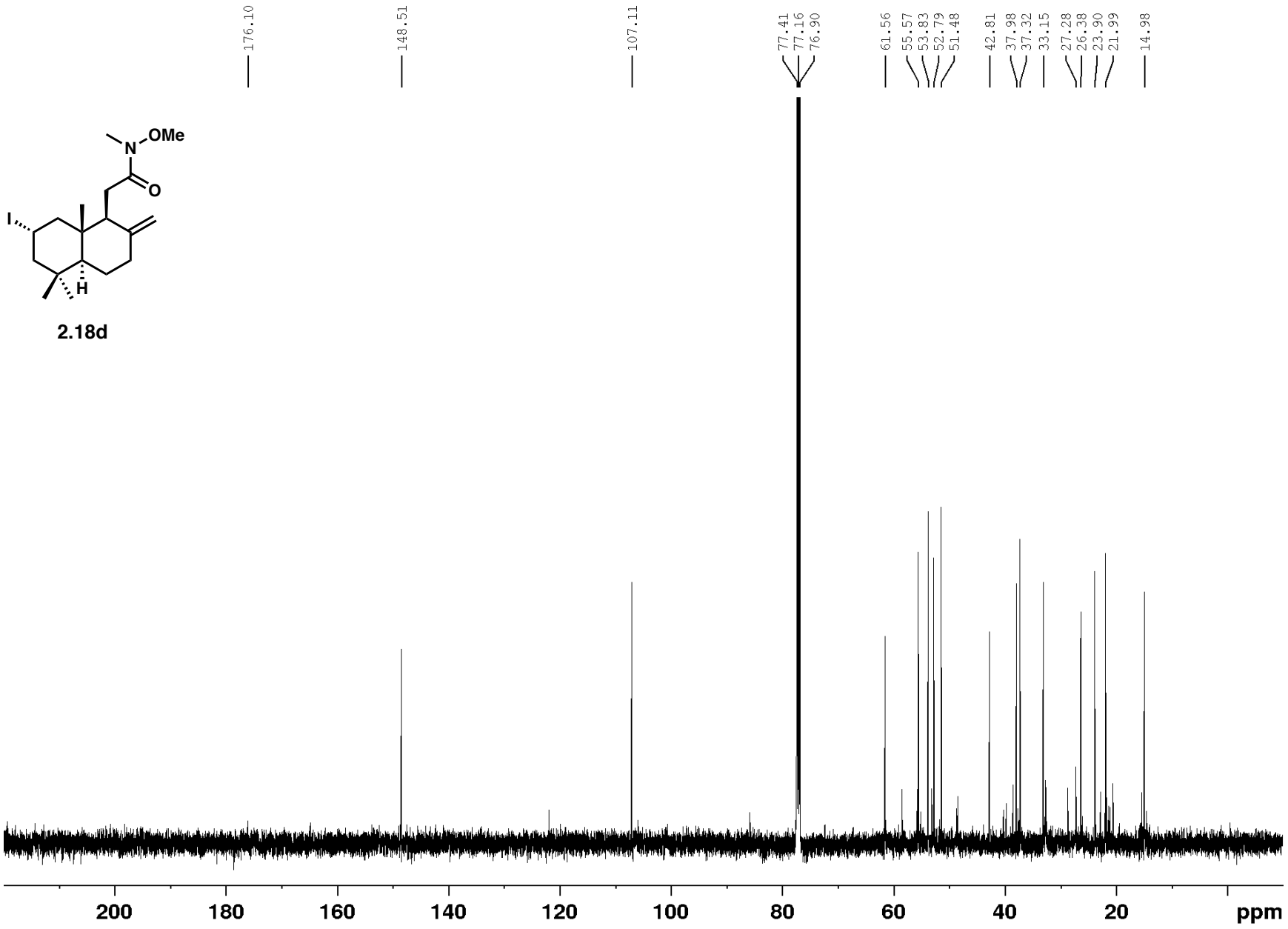

7.26
4.74
4.74
4.44
3.73
3.16
2.73
2.71
2.70
2.68
2.50
2.48
2.44
2.43
2.40
2.40
2.38
2.37
2.37
2.37
2.17
2.16
2.14
2.13
2.12
2.11
1.76
1.76
1.75
1.75
1.74
1.74
1.73
1.73
1.72
1.72
1.71
1.70
1.70
1.69
1.68
1.68
1.67
1.67
1.66
1.65
1.65
1.56
1.53
1.40
1.40
1.39
1.38
1.37
1.37
1.36
1.34
1.33
1.31
1.30
1.29
1.28
1.20
1.19
1.17
1.16
0.88
0.87
0.86
0.85
0.84
0.82
0.74
N
OMe
O
H
8
7
6
5
4
3
2
1
0
ppm
1.00
0.99
3.10
3.07
0.99
1.05
2.06
1.07
1.12
1.08
1.35
1.13
1.27
1.07
3.35
3.84
4.14
2.95

2.18c

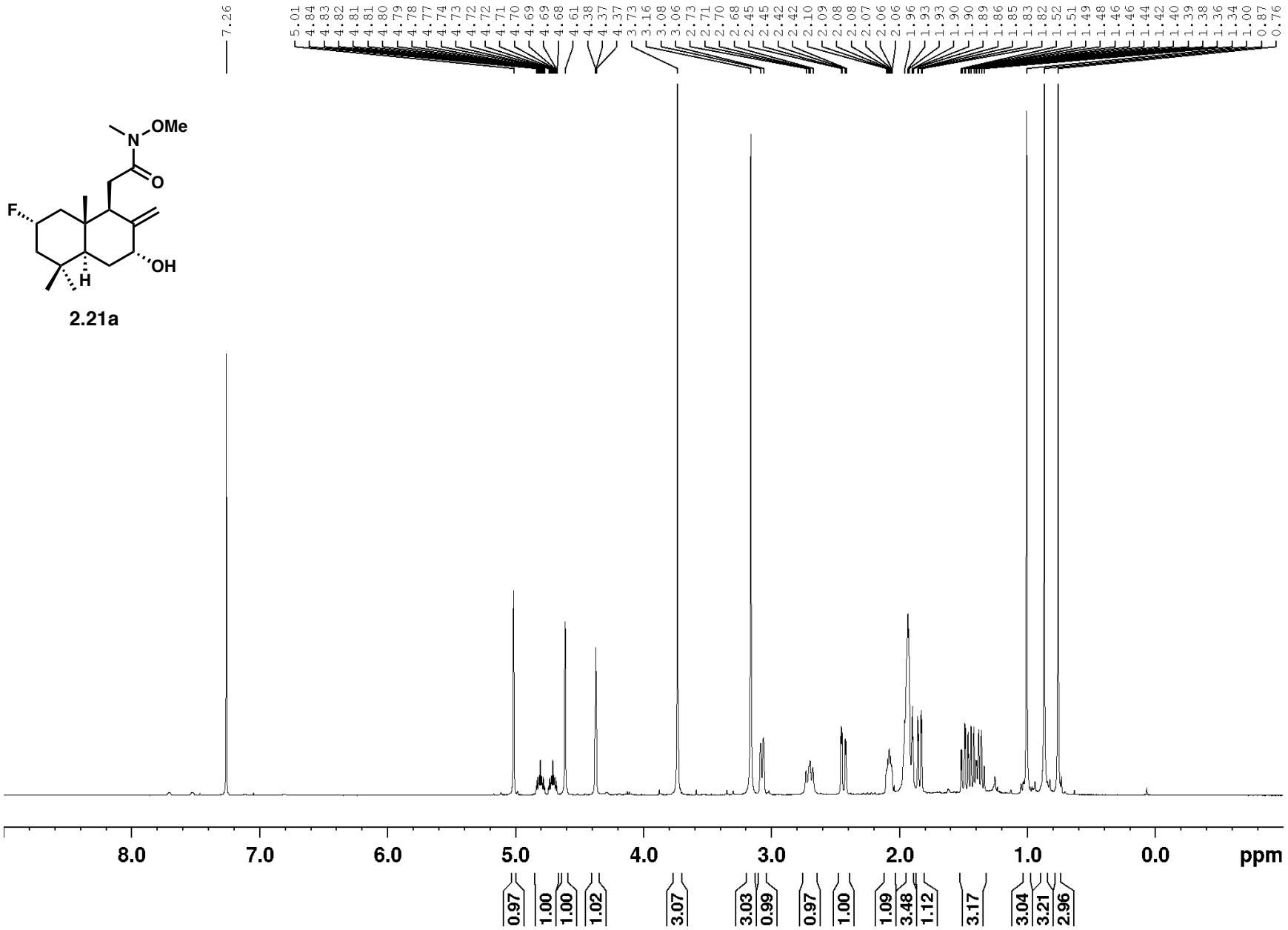

149.77
106.10
77.41
77.16
76.90
61.49
54.79
51.88
51.22
48.07
39.65
37.72
34.28
33.77
27.33
24.84
24.03
23.19
22.54
15.59
N
OMe
O
H
210 200 190 180 170 160 150 140 130 120 110 100 90 80 70 60 50 40 30 20 10 ppm

2.18c

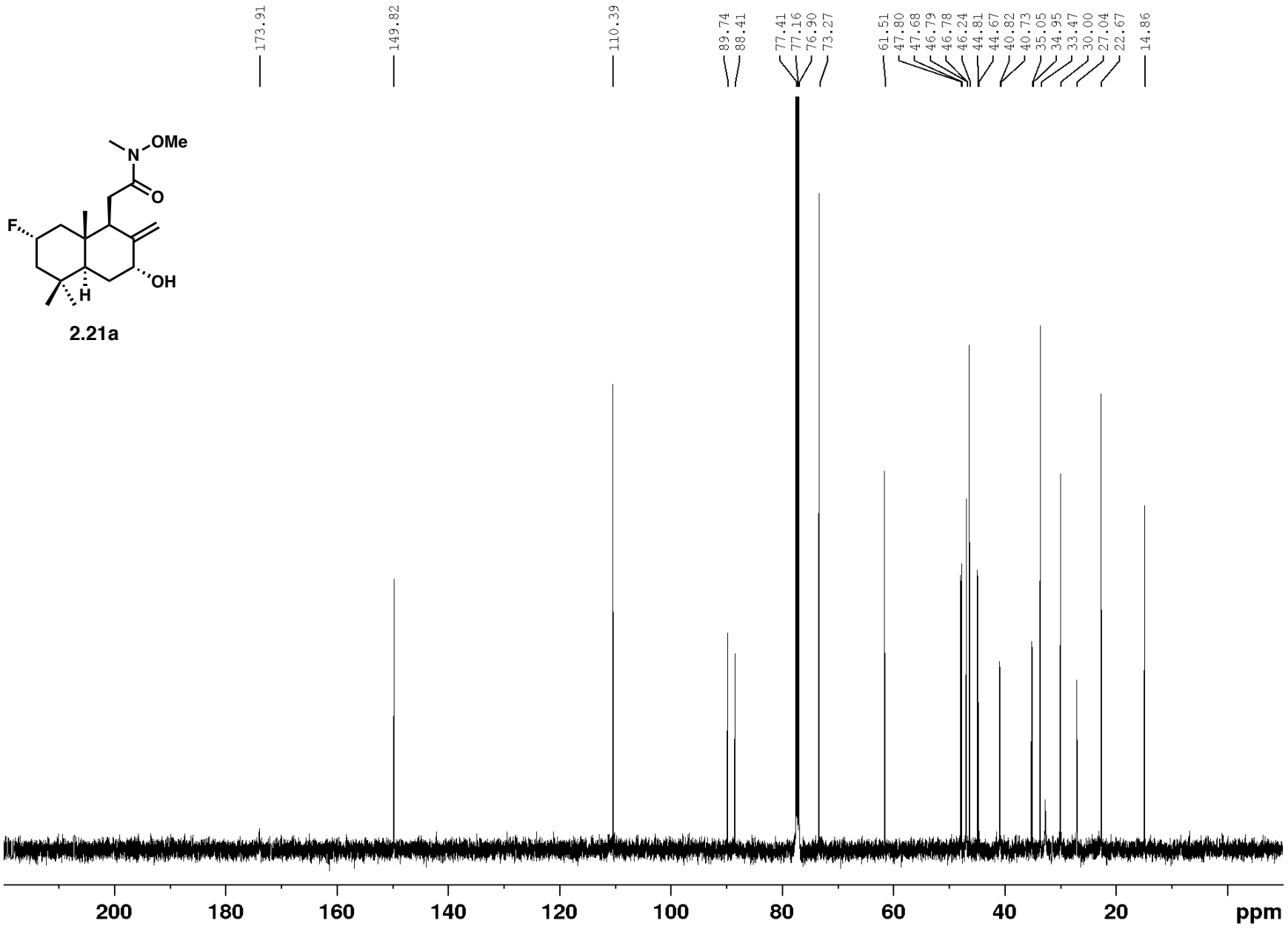

7.26 4.77 4.77 4.58 4.57 4.57 4.55 4.55 4.54 4.53 4.53 4.52 4.51 4.47 3.73 3.17 2.71 2.69 2.68 2.66 2.59 2.57 2.41 2.41 2.40 2.40 2.39 2.38 2.37 2.36 2.36 2.34 2.33 2.24 2.24 2.23 2.23 2.21 2.21 2.21 2.20 2.17 2.16 2.14 2.13 2.11 2.11 1.98 1.95 1.93 1.92 1.90 1.88 1.73 1.72 1.72 1.71 1.71 1.70 1.69 1.69 1.55 1.53 1.53 1.53 1.35 1.35 1.33 1.32 1.32 1.31 1.29 1.29 1.27 1.26 1.25 0.93 0.86 0.78
OMe
N
O
I
H
2.18d
8
7
6
5
4
3
2
1
0
ppm
0.97
1.26
0.96
3.07
3.14
1.06
1.00
3.38
1.54
1.37
2.62
1.26
1.73
2.16
1.07
3.16
3.11
2.98


176.10
148.51
107.11
77.41
77.16
76.90
61.56
55.57
53.83
52.79
51.48
42.81
37.98
37.32
33.15
27.28
26.38
23.90
21.99
14.98
N
OMe
O
I
H
200
180
160
140
120
100
80
60
40
20
ppm

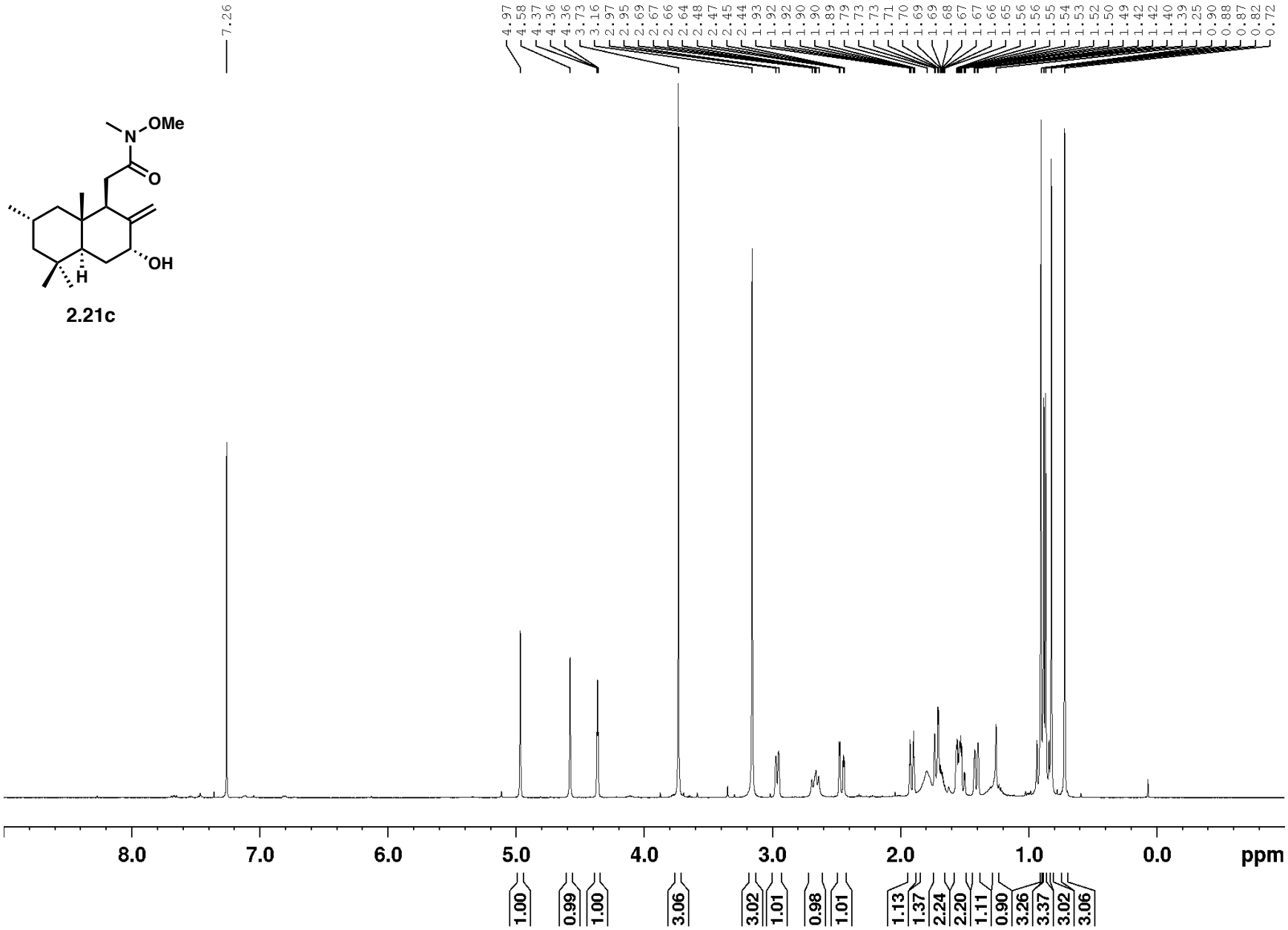
2.18d


7.26
5.01
4.84
4.83
4.82
4.81
4.81
4.80
4.79
4.78
4.77
4.74
4.73
4.72
4.72
4.71
4.70
4.69
4.69
4.68
4.61
4.38
4.37
4.37
3.73
3.16
3.08
3.06
2.73
2.71
2.70
2.68
2.45
2.45
2.42
2.42
2.10
2.09
2.08
2.08
2.07
2.06
2.06
1.96
1.93
1.93
1.90
1.90
1.89
1.86
1.85
1.83
1.82
1.52
1.51
1.49
1.48
1.46
1.46
1.44
1.42
1.40
1.39
1.38
1.36
1.34
1.00
0.87
0.76
N
OMe
O
F
OH
H
8.0
7.0
6.0
5.0
4.0
3.0
2.0
1.0
0.0
ppm
0.97
1.00
1.00
1.02
3.07
3.03
0.99
0.97
1.00
1.09
3.48
1.12
3.17
3.04
3.21
2.96

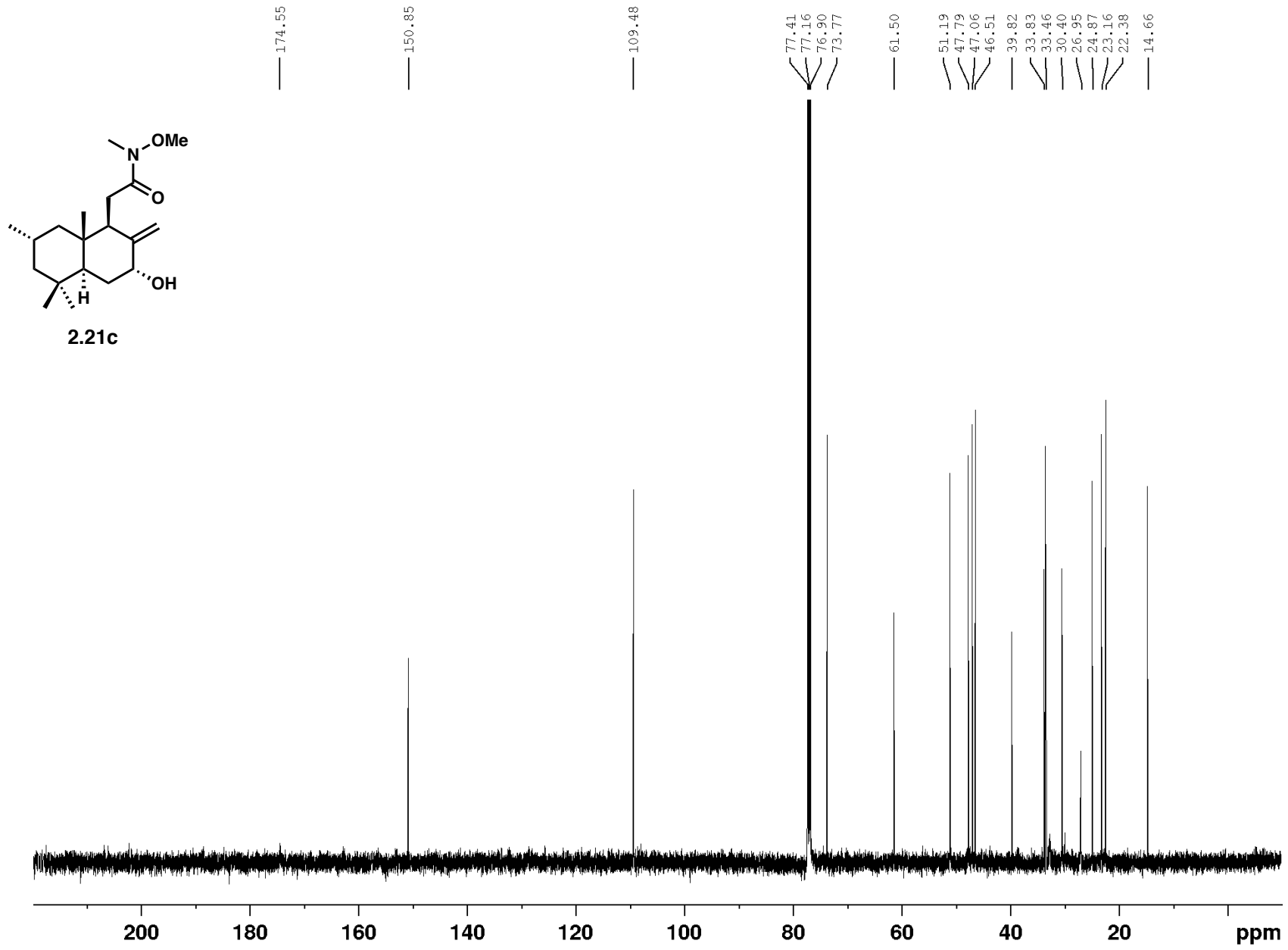
2.21a

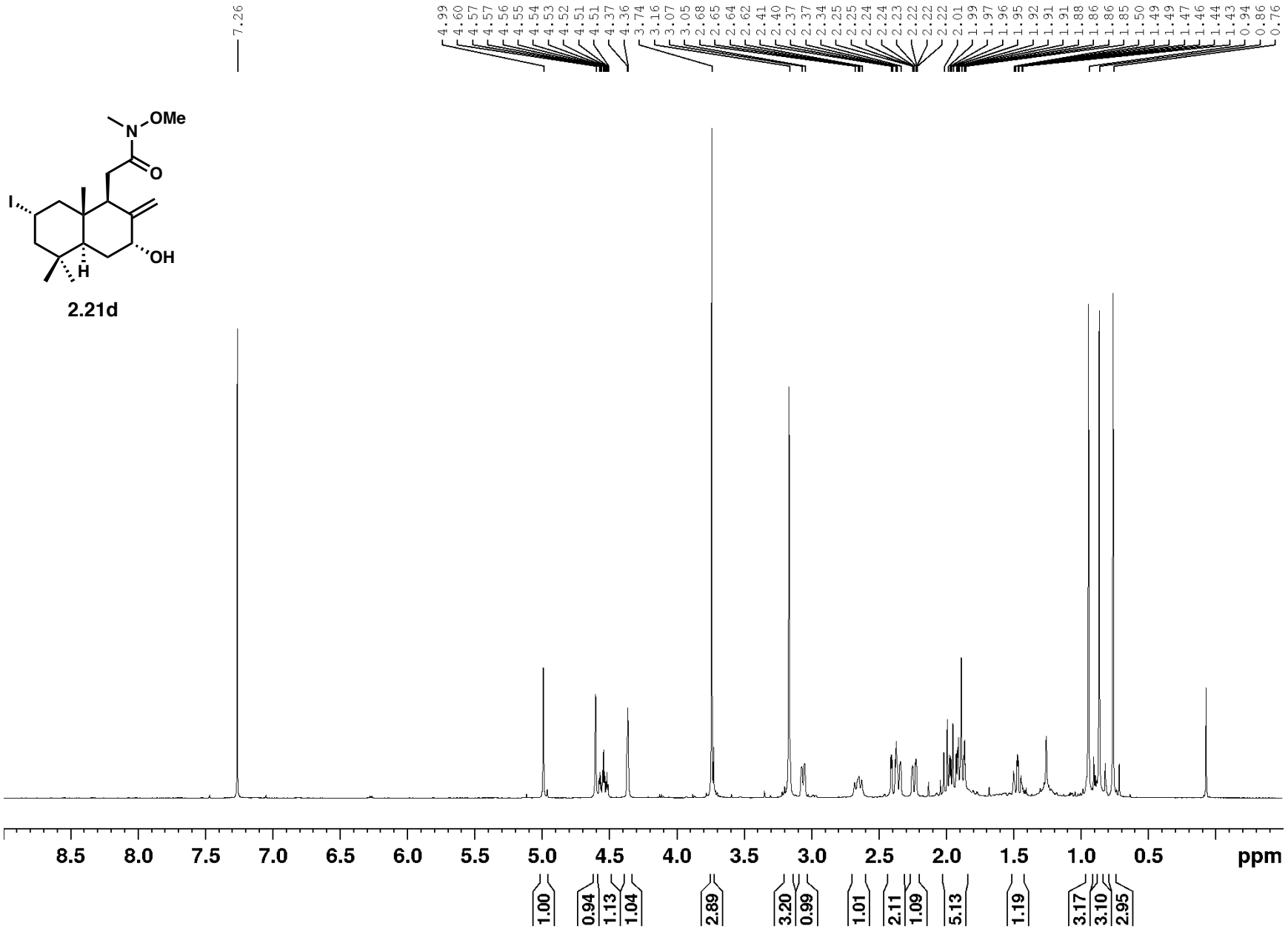

173.91
149.82
110.39
89.74
88.41
77.41
77.16
76.90
73.27
61.51
47.80
47.68
46.79
46.78
46.24
44.81
44.67
40.82
40.73
35.05
34.95
33.47
30.00
27.04
22.67
14.86
N
OMe
O
F
OH
H
200
180
160
140
120
100
80
60
40
20
ppm

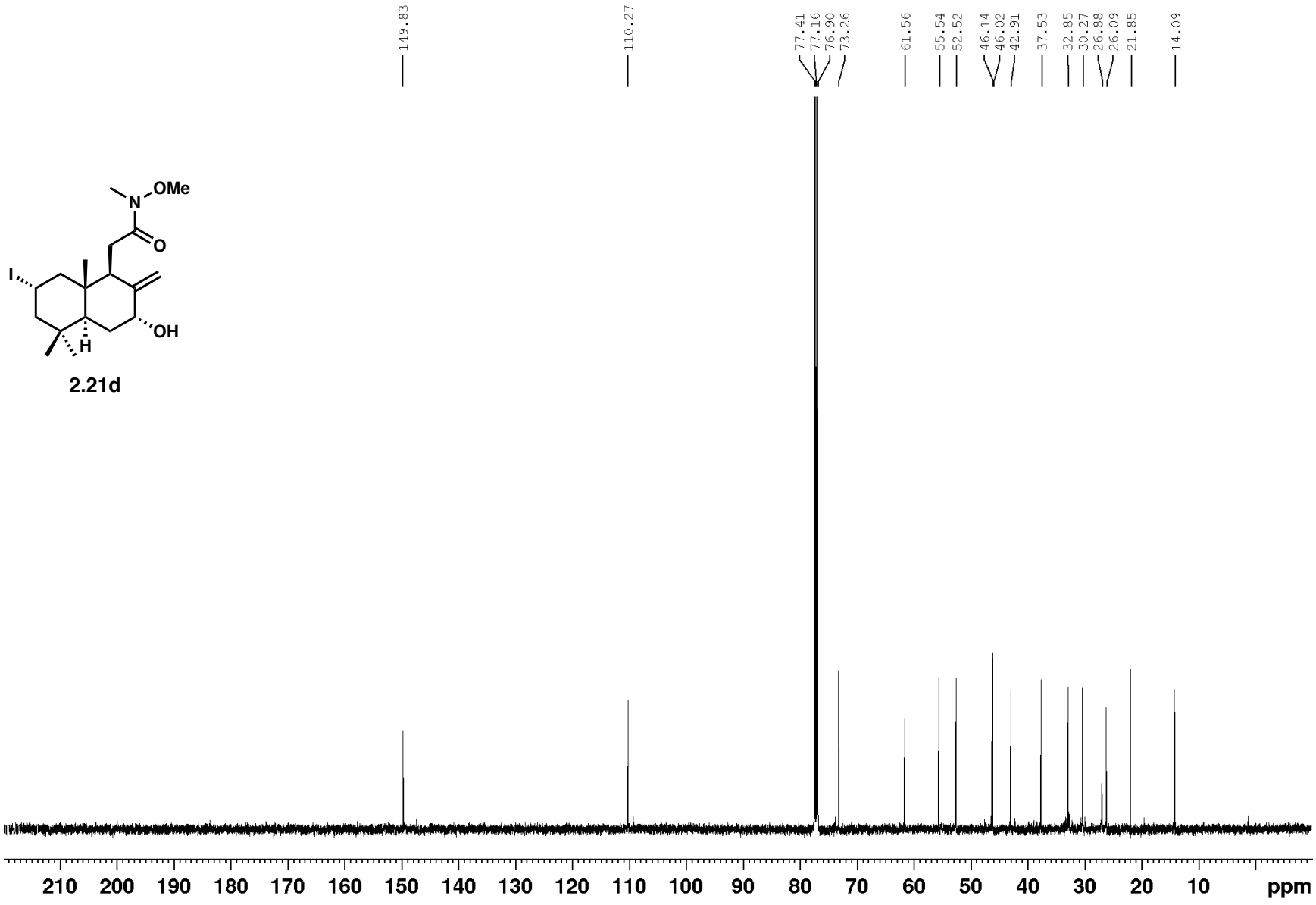
2.21a

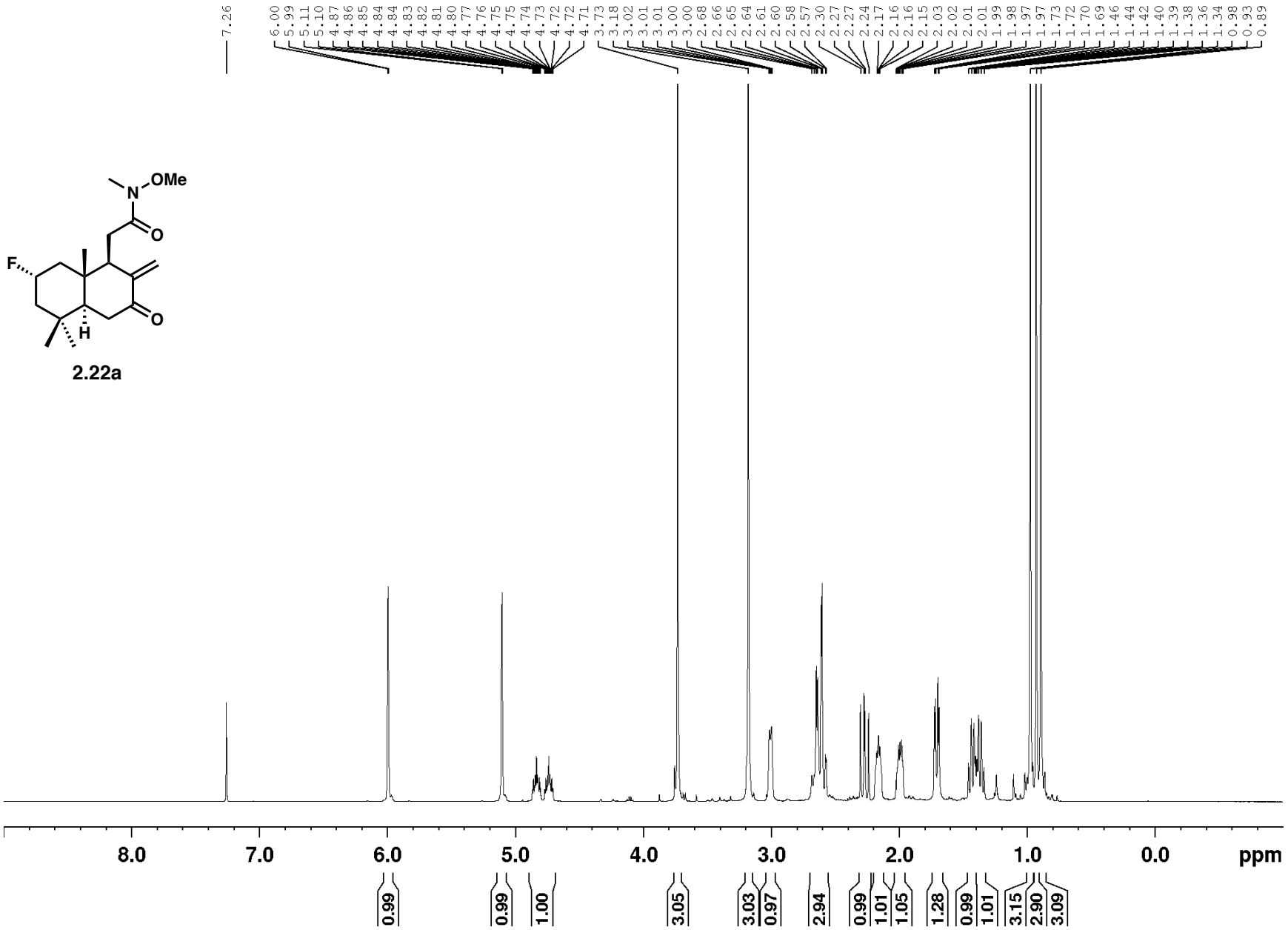

7.26
4.97
4.58
4.37
4.36
4.36
3.73
3.16
2.97
2.95
2.69
2.67
2.66
2.64
2.48
2.47
2.45
2.44
1.93
1.92
1.92
1.90
1.90
1.89
1.79
1.73
1.73
1.71
1.70
1.69
1.69
1.68
1.67
1.67
1.66
1.65
1.56
1.56
1.55
1.54
1.53
1.52
1.50
1.49
1.42
1.42
1.40
1.39
1.25
0.90
0.88
0.87
0.82
0.72
N
OMe
O
OH
H
8.0
7.0
6.0
5.0
4.0
3.0
2.0
1.0
0.0
ppm
1.00
0.99
1.00
3.06
3.02
1.01
0.98
1.01
1.13
1.37
2.24
2.20
1.11
0.90
3.26
3.37
3.02
3.06

2.21c

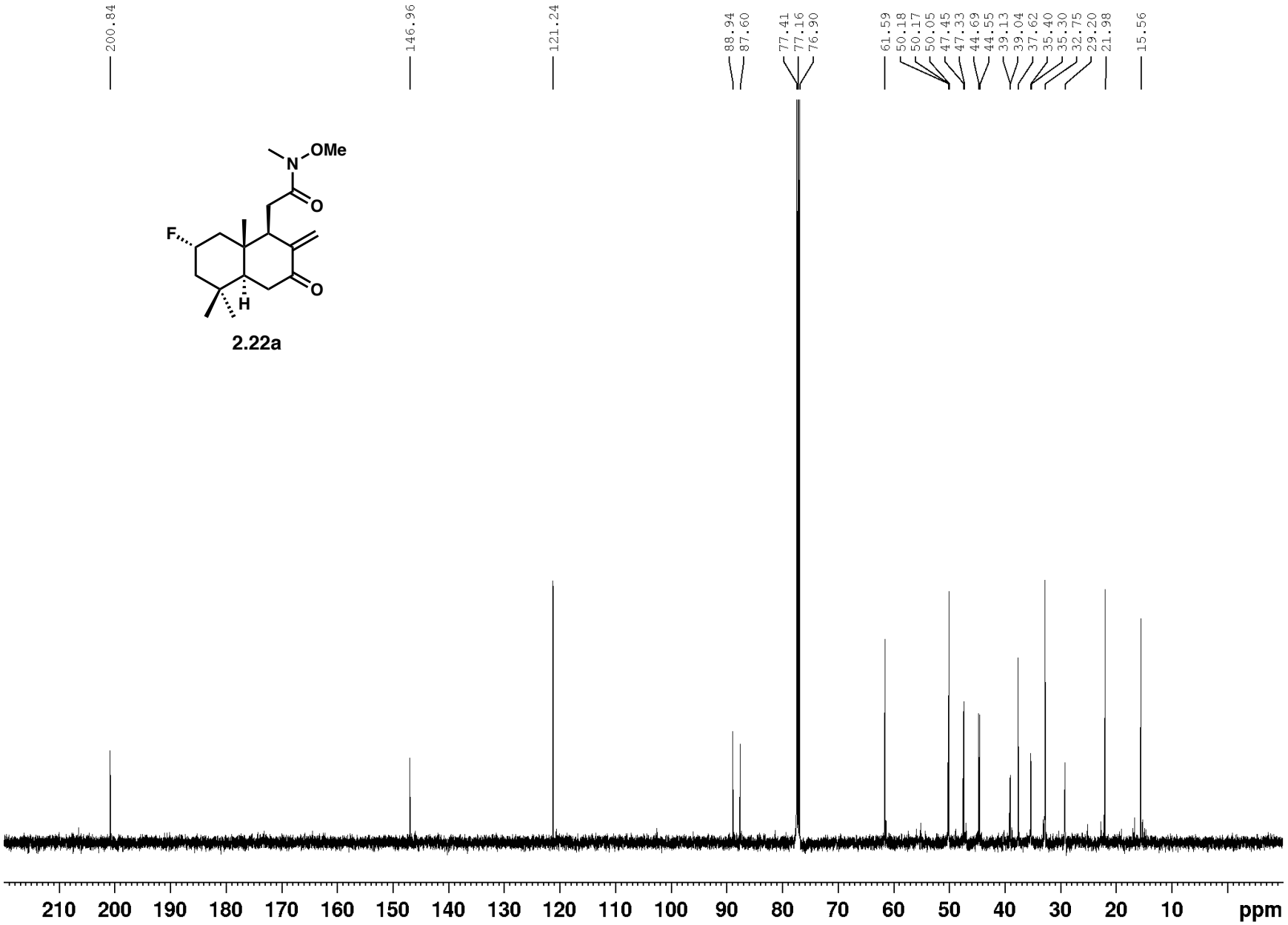

174.55
150.85
109.48
77.41
77.16
76.90
73.77
61.50
51.19
47.79
47.06
46.51
39.82
33.83
33.46
30.40
26.95
24.87
23.16
22.38
14.66
N
OMe
O
OH
H
2.21c
200
180
160
140
120
100
80
60
40
20
ppm


7.26
4.99
4.60
4.57
4.57
4.56
4.55
4.54
4.53
4.52
4.51
4.51
4.37
4.36
3.74
3.16
3.07
3.05
2.68
2.65
2.64
2.62
2.41
2.40
2.37
2.37
2.34
2.25
2.25
2.24
2.24
2.23
2.22
2.22
2.22
2.01
1.99
1.97
1.96
1.95
1.92
1.91
1.91
1.88
1.86
1.86
1.85
1.50
1.49
1.49
1.47
1.46
1.44
1.43
0.94
0.86
0.76
N
OMe
O
I
OH
H
2.21d
8.5
8.0
7.5
7.0
6.5
6.0
5.5
5.0
4.5
4.0
3.5
3.0
2.5
2.0
1.5
1.0
0.5
ppm
1.00
0.94
1.13
1.04
2.89
3.20
0.99
1.01
2.11
1.09
5.13
1.19
3.17
3.10
2.95

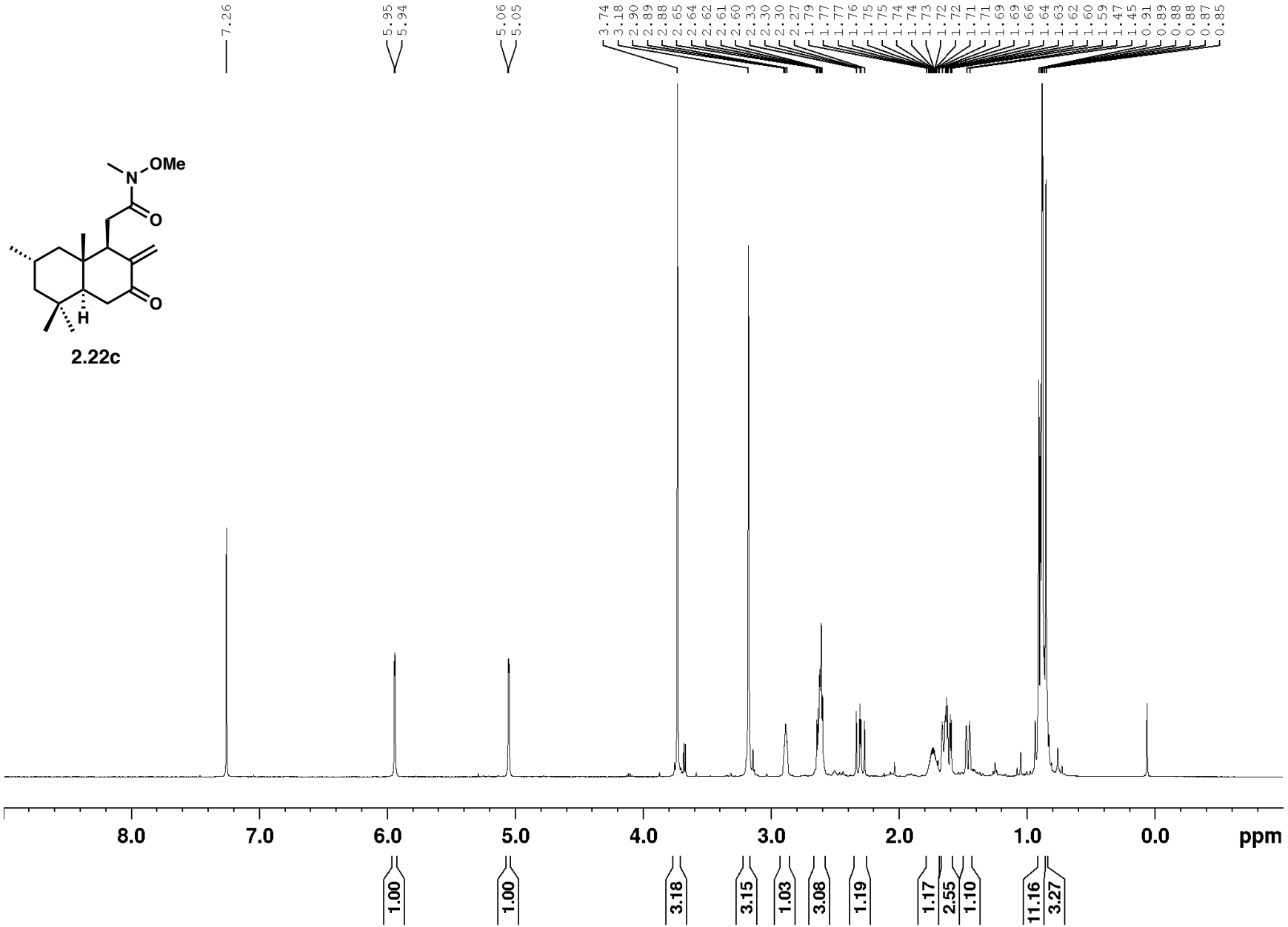

149.83
110.27
77.41
77.16
76.90
73.26
61.56
55.54
52.52
46.14
46.02
42.91
37.53
32.85
30.27
26.88
26.09
21.85
14.09
N
OMe
O
I
OH
H
2.21d
210 200 190 180 170 160 150 140 130 120 110 100 90 80 70 60 50 40 30 20 10 ppm


7.26
6.00
5.99
5.11
5.10
4.87
4.86
4.85
4.84
4.84
4.84
4.83
4.82
4.81
4.80
4.77
4.76
4.75
4.75
4.74
4.73
4.72
4.72
4.71
3.73
3.18
3.02
3.01
3.01
3.00
3.00
2.68
2.66
2.65
2.64
2.61
2.60
2.58
2.57
2.30
2.27
2.27
2.24
2.17
2.16
2.16
2.15
2.03
2.02
2.01
2.01
1.99
1.98
1.97
1.97
1.73
1.72
1.70
1.69
1.46
1.44
1.42
1.40
1.39
1.38
1.36
1.34
0.98
0.93
0.89
N
OMe
O
F
O
H
8.0
7.0
6.0
5.0
4.0
3.0
2.0
1.0
0.0
ppm
0.99
0.99
1.00
3.05
3.03
0.97
2.94
0.99
1.01
1.05
1.28
0.99
1.01
3.15
2.90
3.09

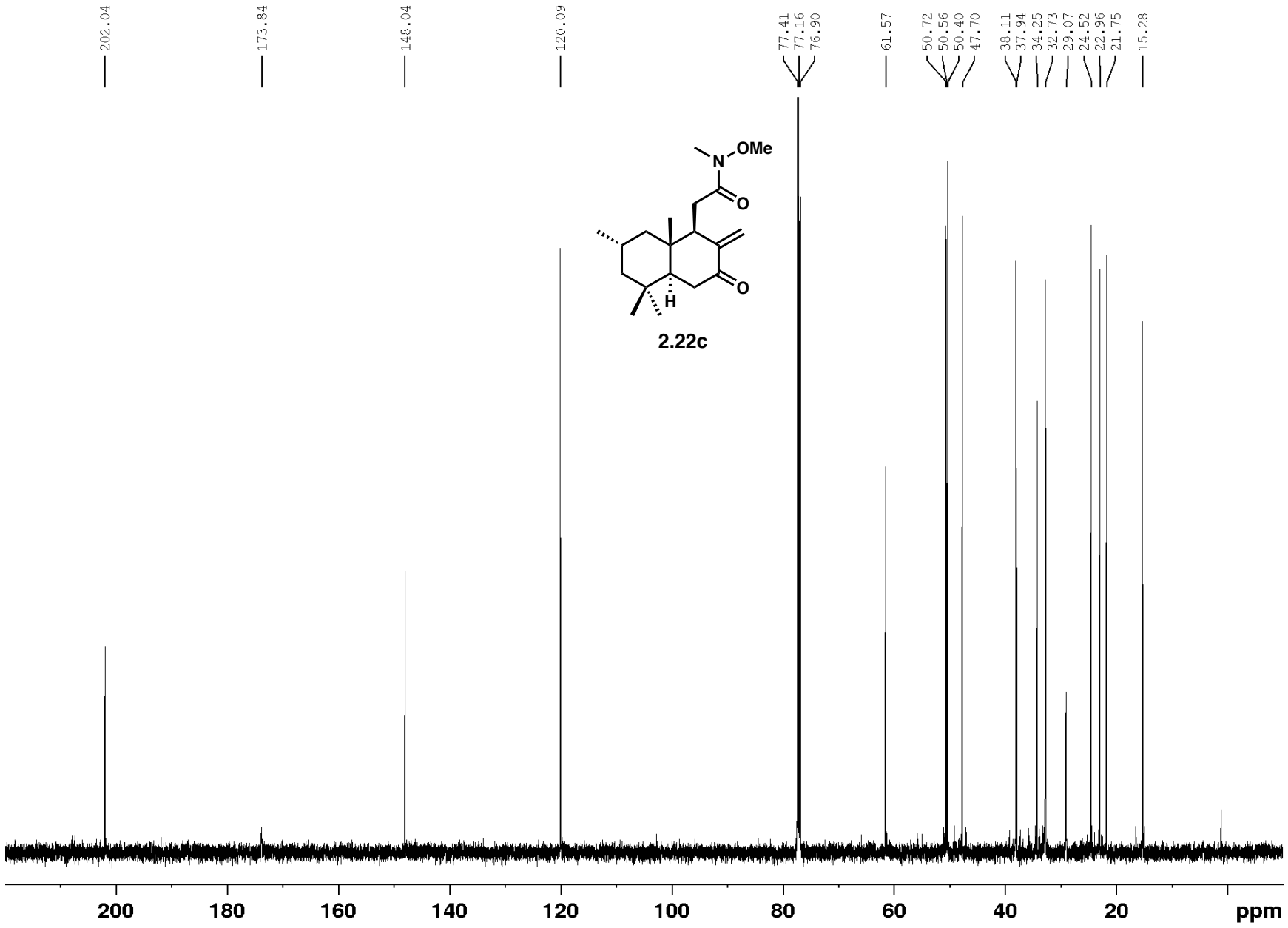
2.22a

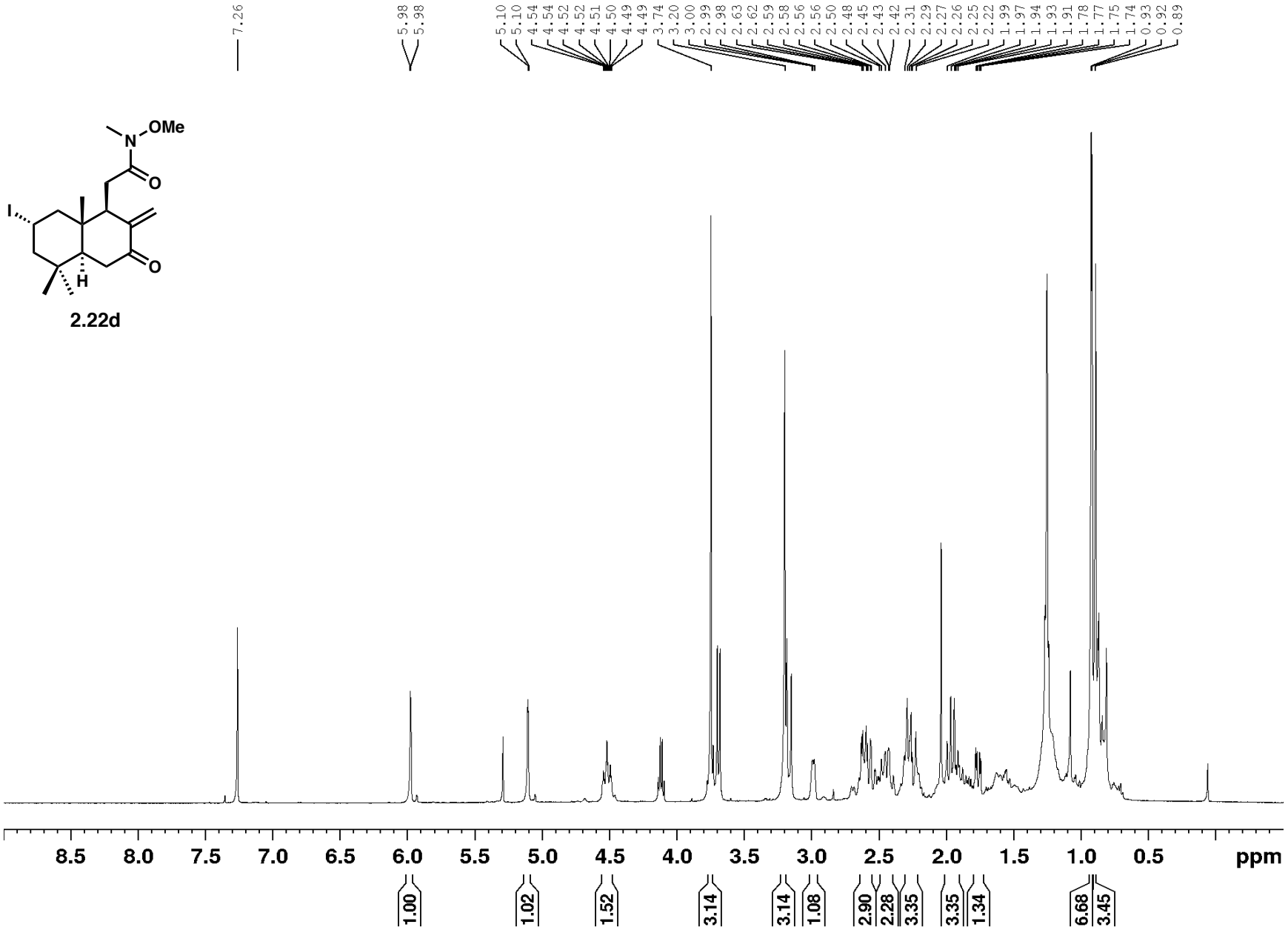

200.84
146.96
121.24
88.94
87.60
77.41
77.16
76.90
61.59
50.18
50.17
50.05
47.45
47.33
44.69
44.55
39.13
39.04
37.62
35.40
35.30
32.75
29.20
21.98
15.56
N
OMe
O
F
O
H
210
200
190
180
170
160
150
140
130
120
110
100
90
80
70
60
50
40
30
20
10
ppm

2.22a

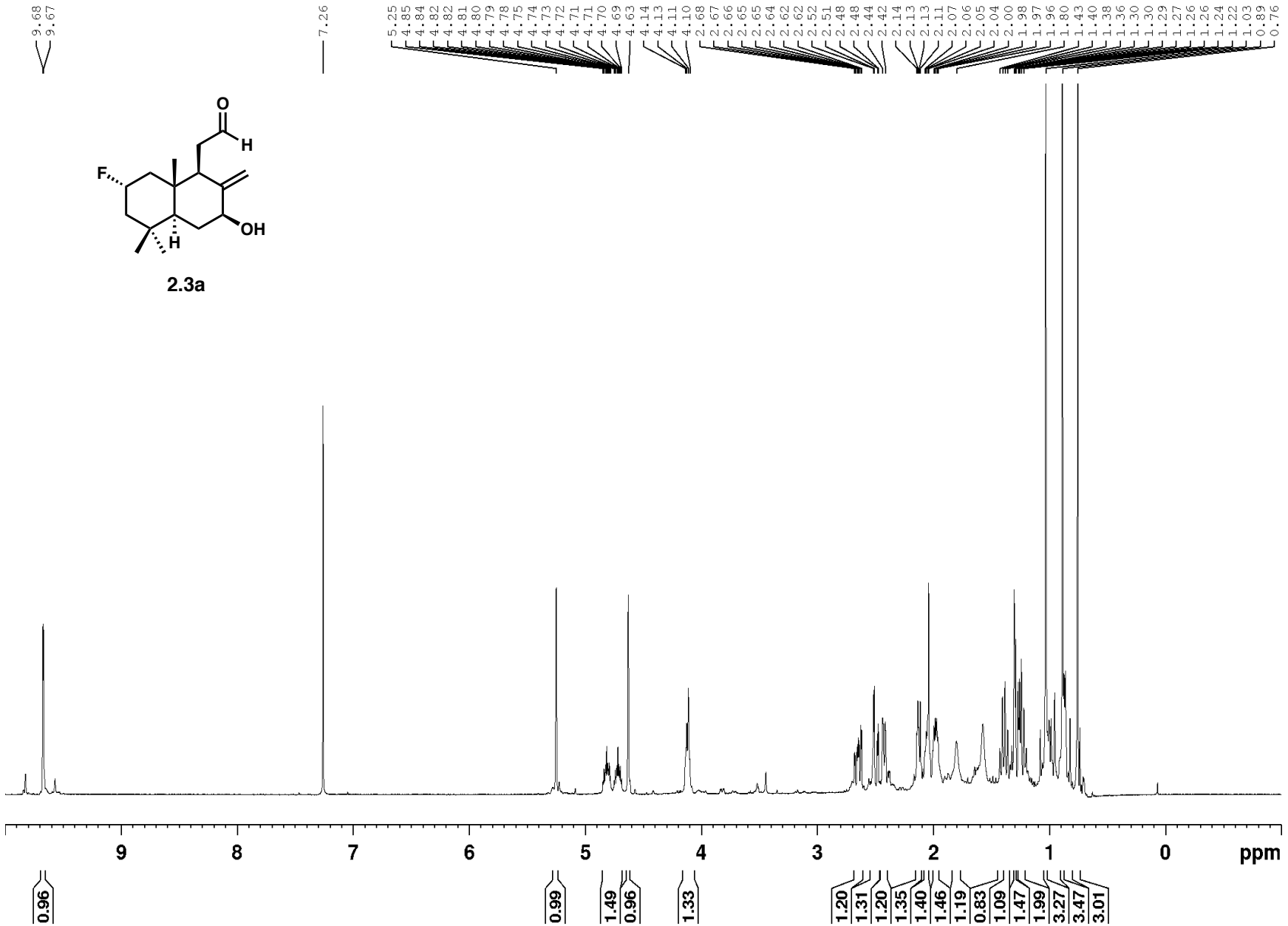

7.26
5.95
5.94
5.06
5.05
3.74
3.18
2.90
2.89
2.88
2.65
2.64
2.62
2.61
2.60
2.33
2.30
2.30
2.27
1.79
1.77
1.77
1.76
1.75
1.75
1.74
1.74
1.73
1.72
1.72
1.71
1.71
1.69
1.69
1.66
1.64
1.63
1.62
1.60
1.59
1.47
1.45
0.91
0.89
0.88
0.88
0.87
0.85
N
OMe
O
O
H
8.0
7.0
6.0
5.0
4.0
3.0
2.0
1.0
0.0
ppm
1.00
1.00
3.18
3.15
1.03
3.08
1.19
1.17
2.55
1.10
11.16
3.27

2.22c

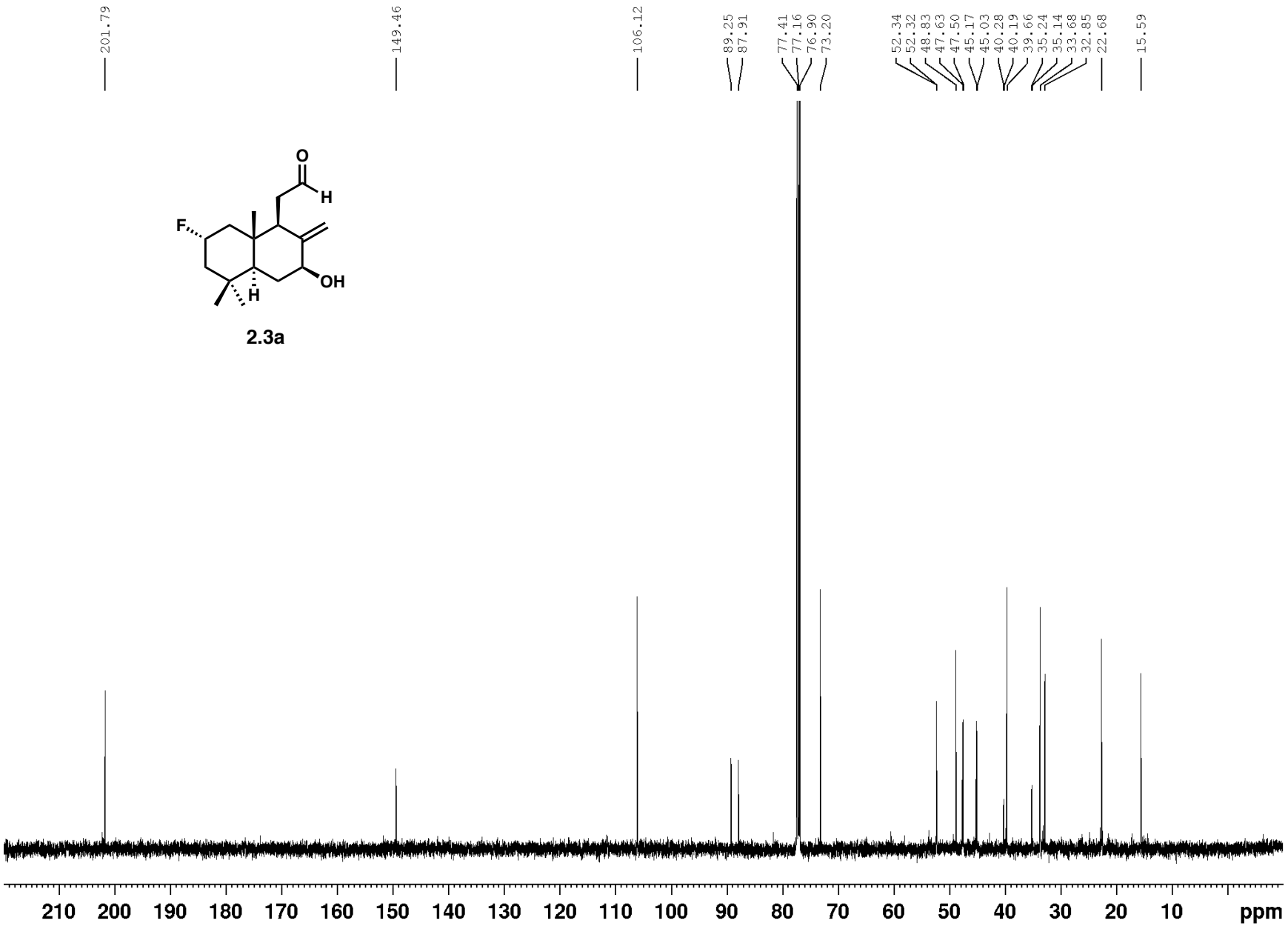

202.04
173.84
148.04
120.09
77.41
77.16
76.90
61.57
50.72
50.56
50.40
47.70
38.11
37.94
34.25
32.73
29.07
24.52
22.96
21.75
15.28
N
OMe
O
O
H
2.22c
200
180
160
140
120
100
80
60
40
20
ppm


7.26
5.98
5.98
5.10
5.10
4.54
4.54
4.52
4.52
4.52
4.51
4.50
4.49
4.49
3.74
3.20
3.00
2.99
2.98
2.63
2.62
2.59
2.58
2.56
2.56
2.50
2.48
2.45
2.43
2.42
2.31
2.29
2.27
2.26
2.25
2.22
1.99
1.97
1.94
1.93
1.91
1.78
1.77
1.75
1.74
0.93
0.92
0.89
N
OMe
O
I
O
H
8.5
8.0
7.5
7.0
6.5
6.0
5.5
5.0
4.5
4.0
3.5
3.0
2.5
2.0
1.5
1.0
0.5
ppm
1.00
1.02
1.52
3.14
3.14
1.08
2.90
2.28
3.35
3.35
1.34
6.68
3.45

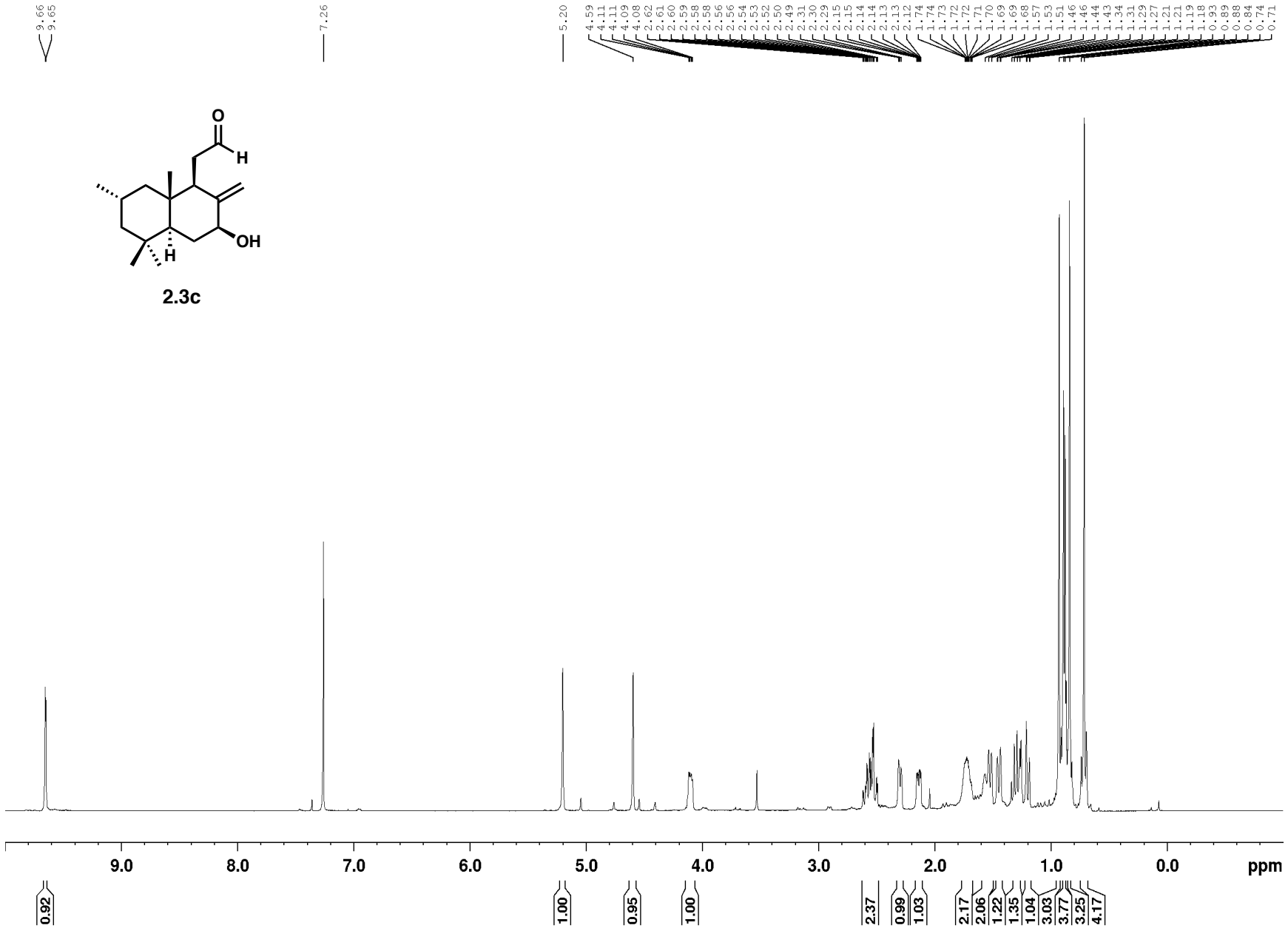
2.22d


9.68
9.67
7.26
5.25
4.85
4.84
4.82
4.82
4.81
4.80
4.79
4.78
4.75
4.74
4.73
4.72
4.71
4.71
4.70
4.69
4.63
4.14
4.13
4.11
4.10
2.68
2.67
2.66
2.65
2.65
2.64
2.62
2.62
2.52
2.51
2.48
2.48
2.44
2.42
2.14
2.13
2.13
2.11
2.07
2.06
2.05
2.04
2.00
1.98
1.97
1.96
1.80
1.43
1.40
1.38
1.36
1.30
1.30
1.29
1.27
1.26
1.26
1.24
1.22
1.03
0.89
0.76
O
H
F
OH
H
9
8
7
6
5
4
3
2
1
0
ppm
0.96
0.99
1.49
0.96
1.33
1.20
1.31
1.20
1.35
1.40
1.46
1.19
0.83
1.09
1.47
1.99
3.27
3.47
3.01

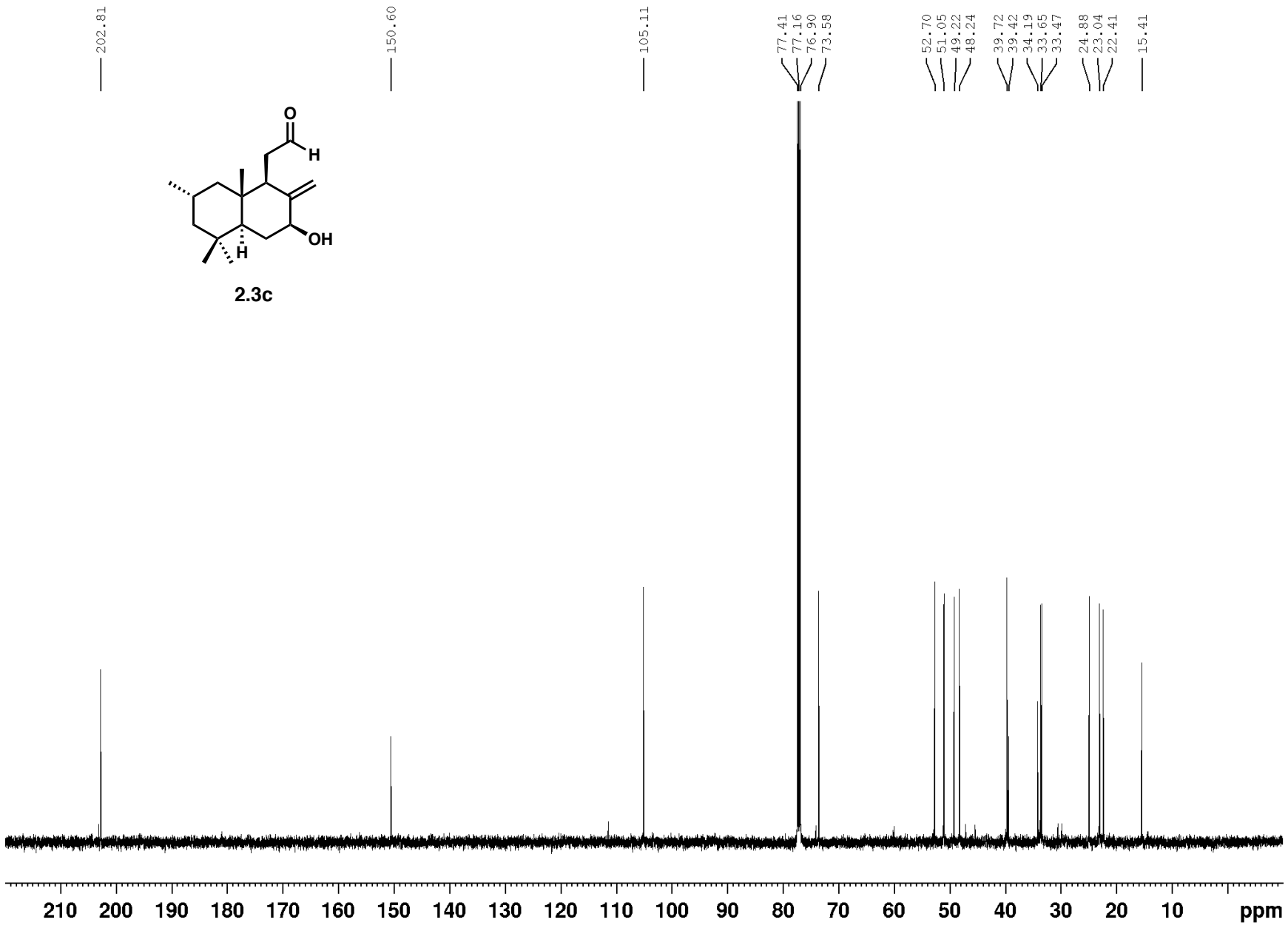
2.3a

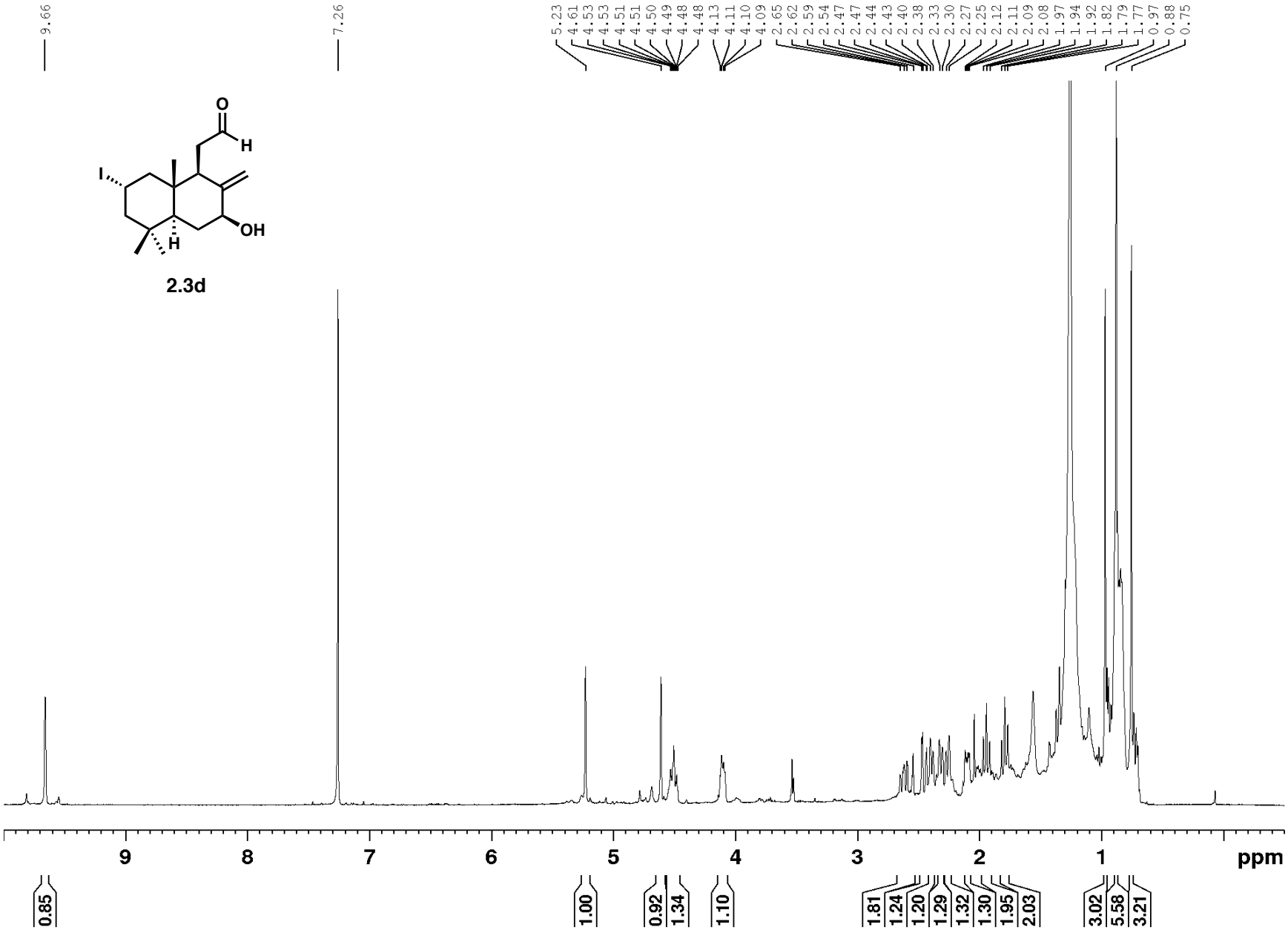

201.79
149.46
106.12
89.25
87.91
77.41
77.16
76.90
73.20
52.34
52.32
48.83
47.63
47.50
45.17
45.03
40.28
40.19
39.66
35.24
35.14
33.68
32.85
22.68
15.59
O
H
F
OH
H
210
200
190
180
170
160
150
140
130
120
110
100
90
80
70
60
50
40
30
20
10
ppm

2.3a

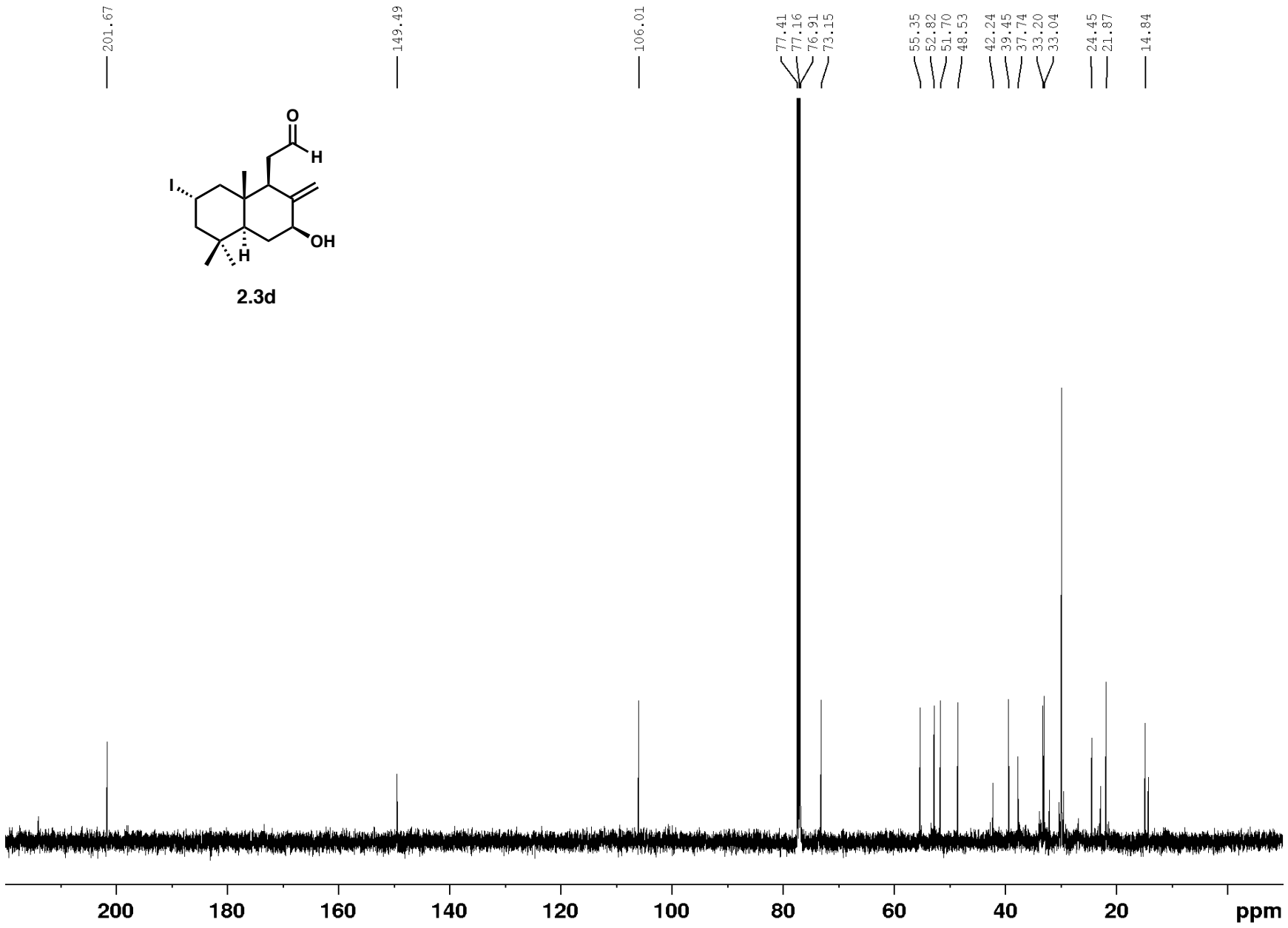

9.66
9.65
7.26
5.20
4.59
4.11
4.11
4.09
4.08
2.62
2.61
2.60
2.59
2.58
2.58
2.56
2.56
2.54
2.53
2.52
2.50
2.49
2.31
2.30
2.29
2.15
2.15
2.14
2.14
2.13
2.13
2.12
1.74
1.74
1.73
1.72
1.72
1.71
1.70
1.69
1.69
1.68
1.57
1.53
1.51
1.46
1.46
1.44
1.43
1.34
1.31
1.29
1.27
1.21
1.21
1.19
1.18
0.93
0.89
0.88
0.84
0.74
0.71
O
H
OH
H
9.0
8.0
7.0
6.0
5.0
4.0
3.0
2.0
1.0
0.0
ppm
0.92
1.00
0.95
1.00
2.37
0.99
1.03
2.17
2.06
1.22
1.35
1.04
3.03
3.77
3.25
4.17

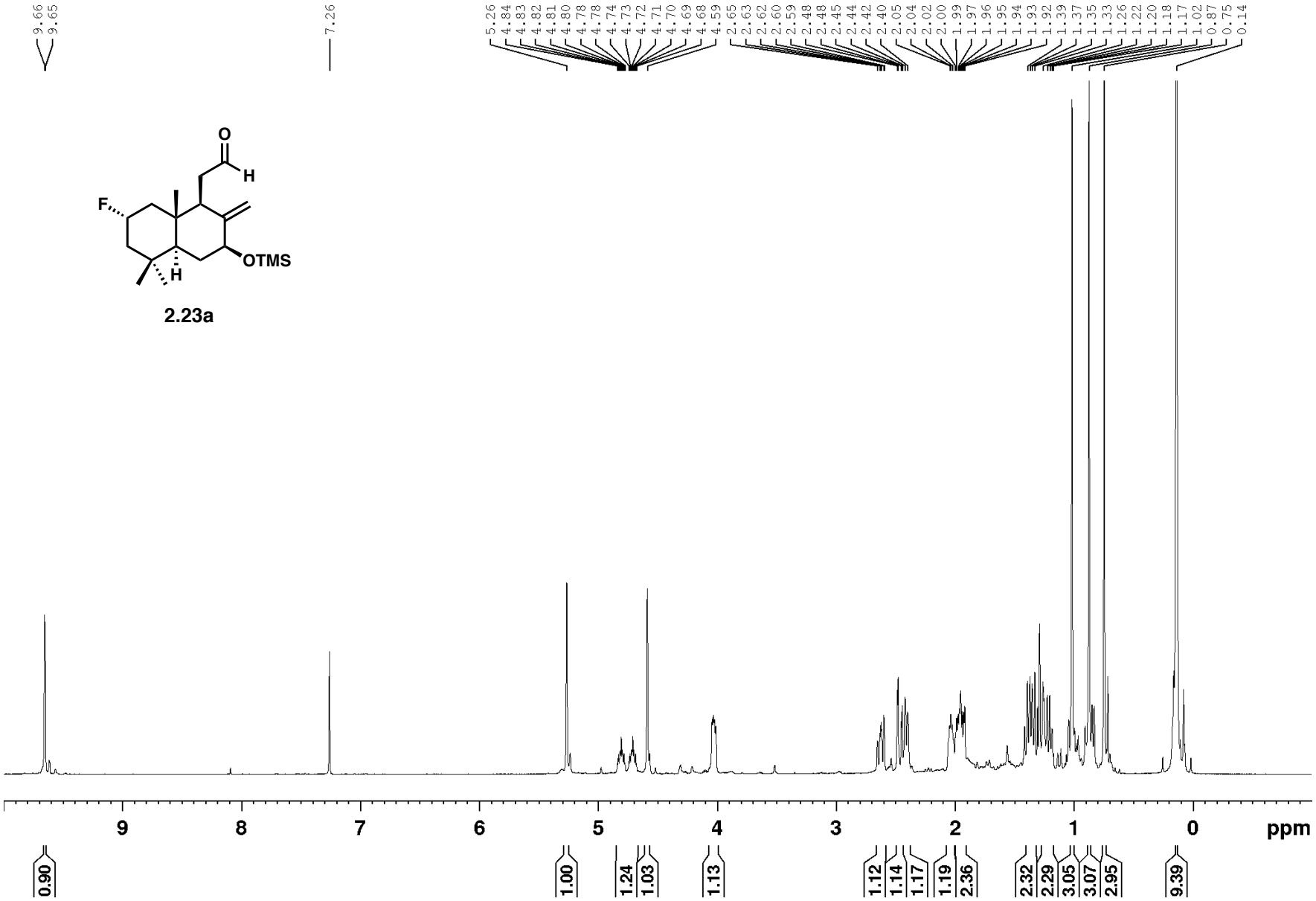
2.3c


202.81
150.60
105.11
77.41
77.16
76.90
73.58
52.70
51.05
49.22
48.24
39.72
39.42
34.19
33.65
33.47
24.88
23.04
22.41
15.41
O
H
OH
H
2.3c
210 200 190 180 170 160 150 140 130 120 110 100 90 80 70 60 50 40 30 20 10 ppm

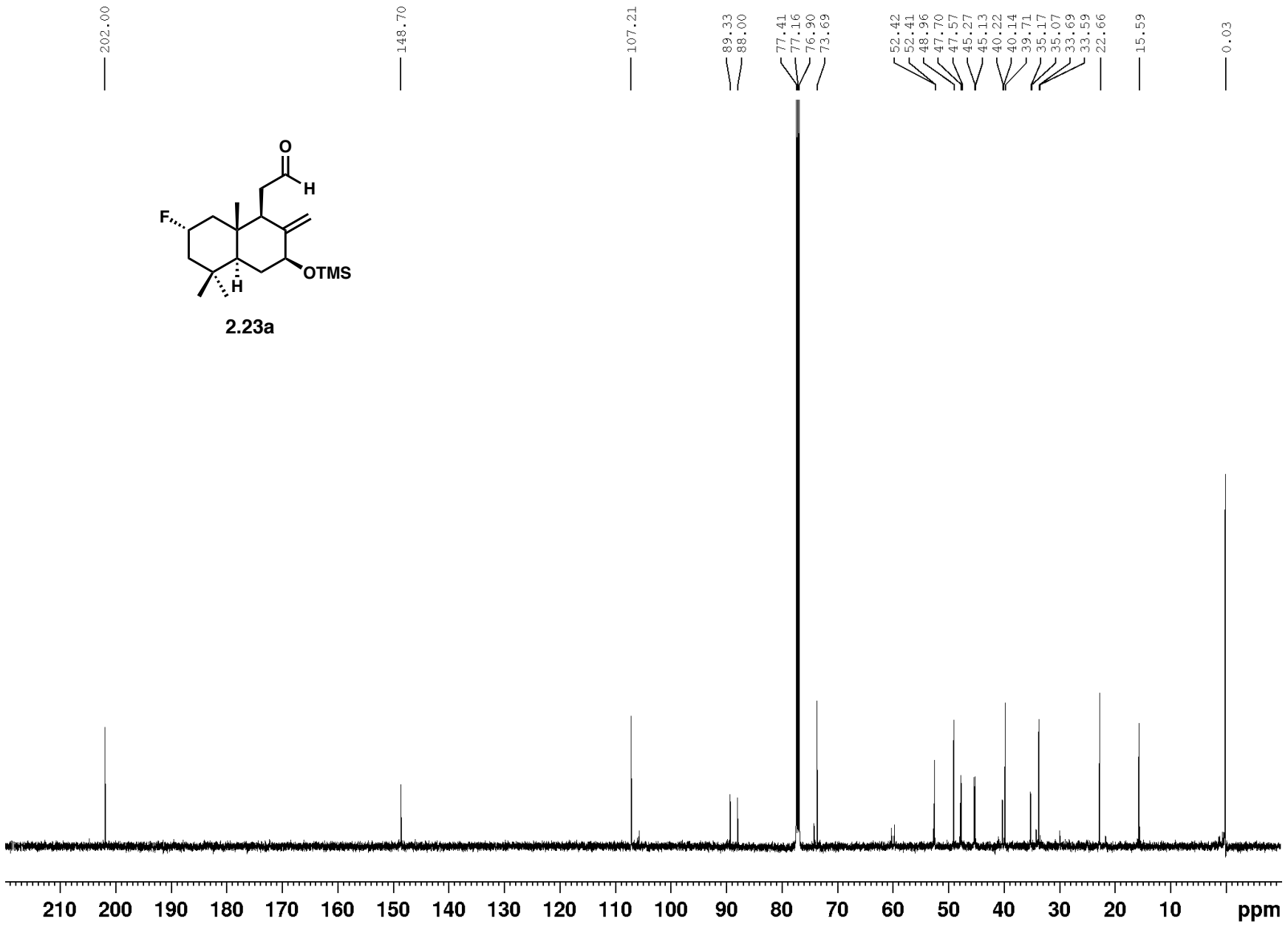

9.66
7.26
5.23
4.61
4.53
4.53
4.51
4.51
4.50
4.49
4.48
4.48
4.13
4.11
4.10
4.09
2.65
2.62
2.59
2.54
2.47
2.47
2.44
2.43
2.40
2.38
2.33
2.30
2.27
2.25
2.12
2.11
2.09
2.08
1.97
1.94
1.92
1.82
1.79
1.77
0.97
0.88
0.75
O
H
I
OH
H
9
8
7
6
5
4
3
2
1
ppm
0.85
1.00
0.92
1.34
1.10
1.81
1.24
1.20
1.29
1.32
1.30
1.95
2.03
3.02
5.58
3.21

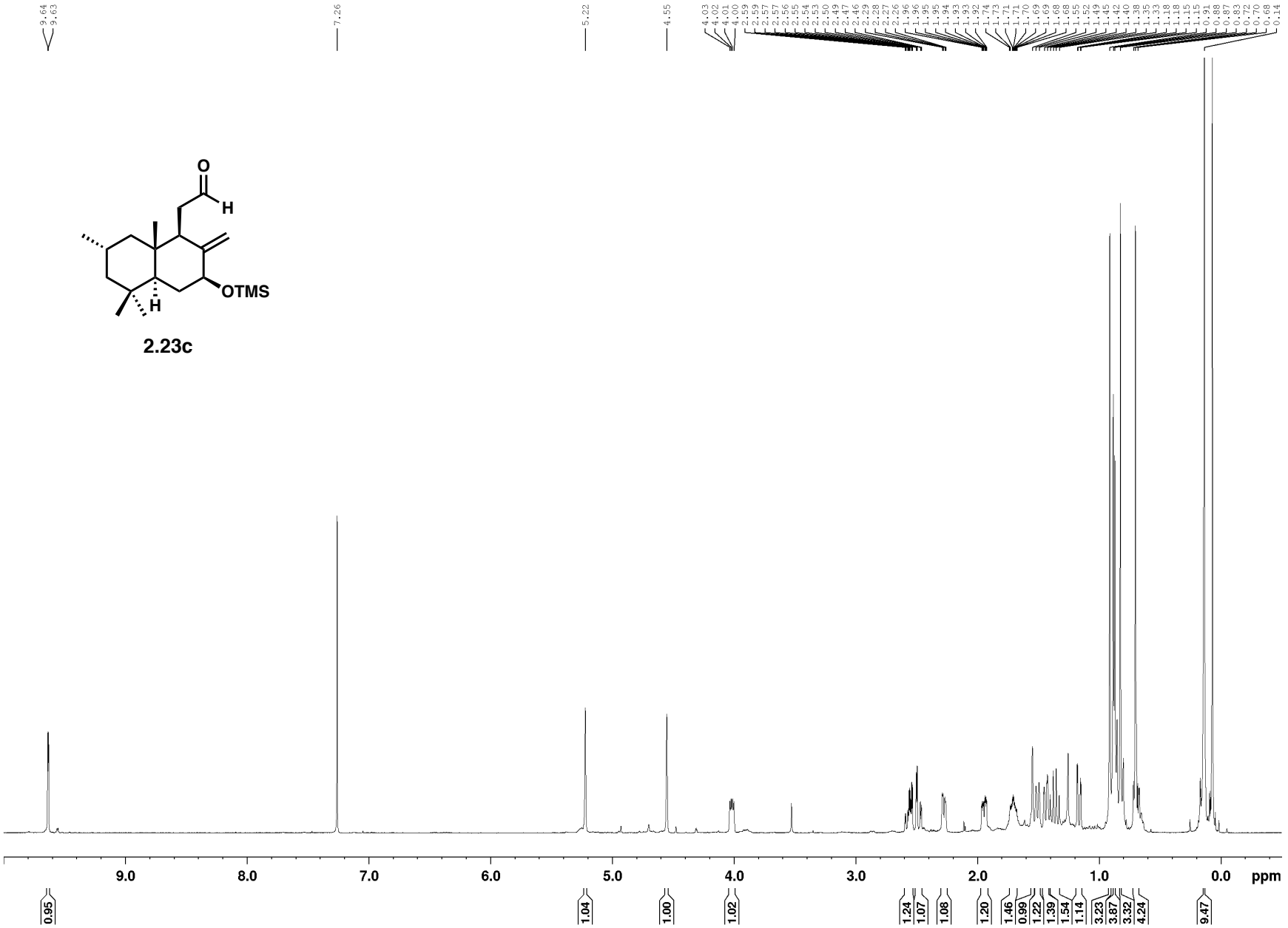
2.3d


201.67
149.49
106.01
77.41
77.16
76.91
73.15
55.35
52.82
51.70
48.53
42.24
39.45
37.74
33.20
33.04
24.45
21.87
14.84
O
H
I
OH
H
2.3d
200
180
160
140
120
100
80
60
40
20
ppm

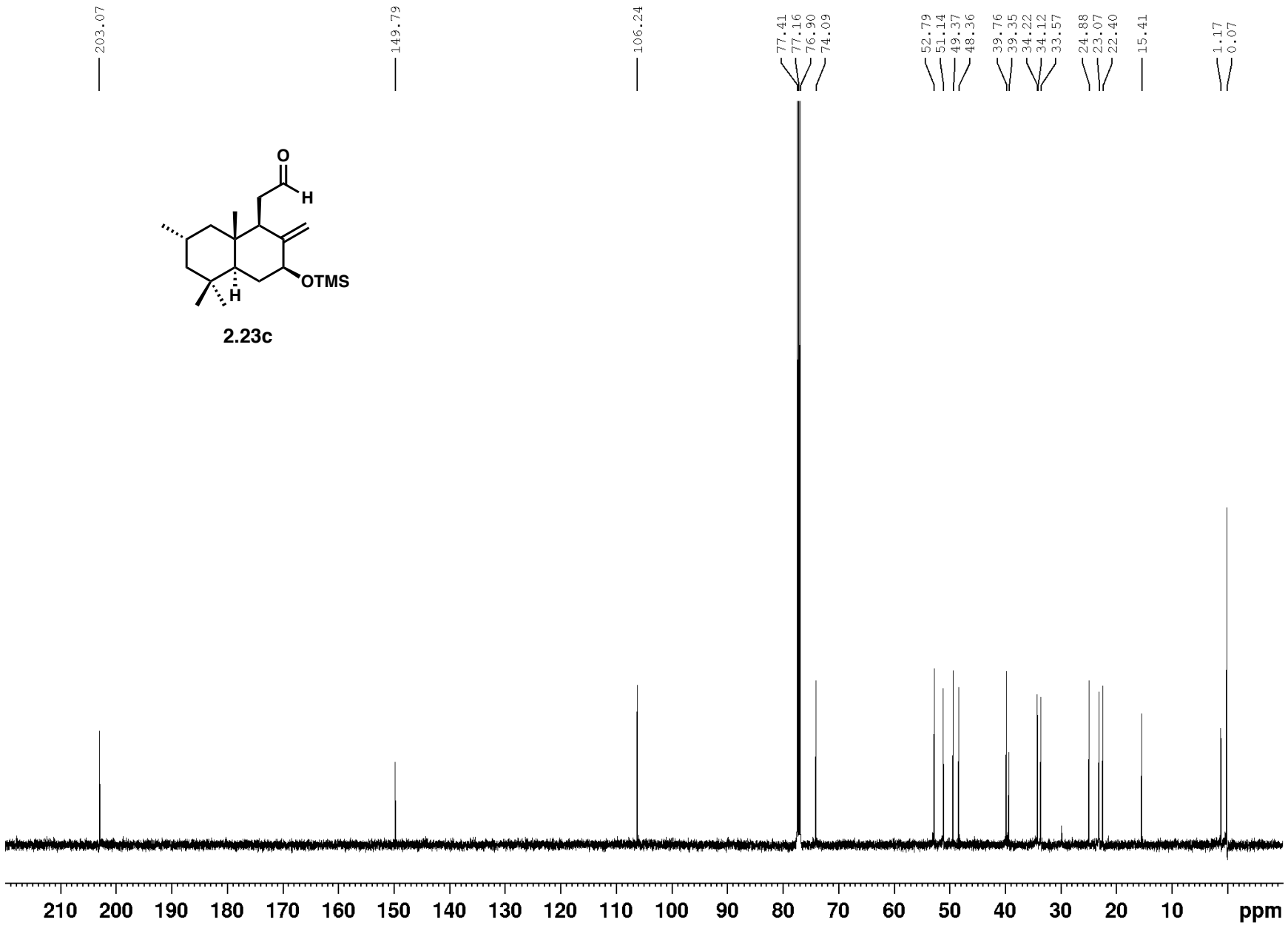

9.66
9.65
7.26
5.26
4.84
4.83
4.82
4.81
4.80
4.78
4.78
4.74
4.73
4.72
4.71
4.70
4.69
4.68
4.59
2.65
2.63
2.62
2.60
2.59
2.48
2.48
2.45
2.44
2.42
2.40
2.05
2.04
2.02
2.00
1.99
1.97
1.96
1.95
1.94
1.93
1.92
1.39
1.37
1.35
1.33
1.26
1.22
1.20
1.18
1.17
1.02
0.87
0.75
0.14
O
H
F
OTMS
H
9
8
7
6
5
4
3
2
1
0
ppm
0.90
1.00
1.24
1.03
1.13
1.12
1.14
1.17
1.19
2.36
2.32
2.29
3.05
3.07
2.95
9.39

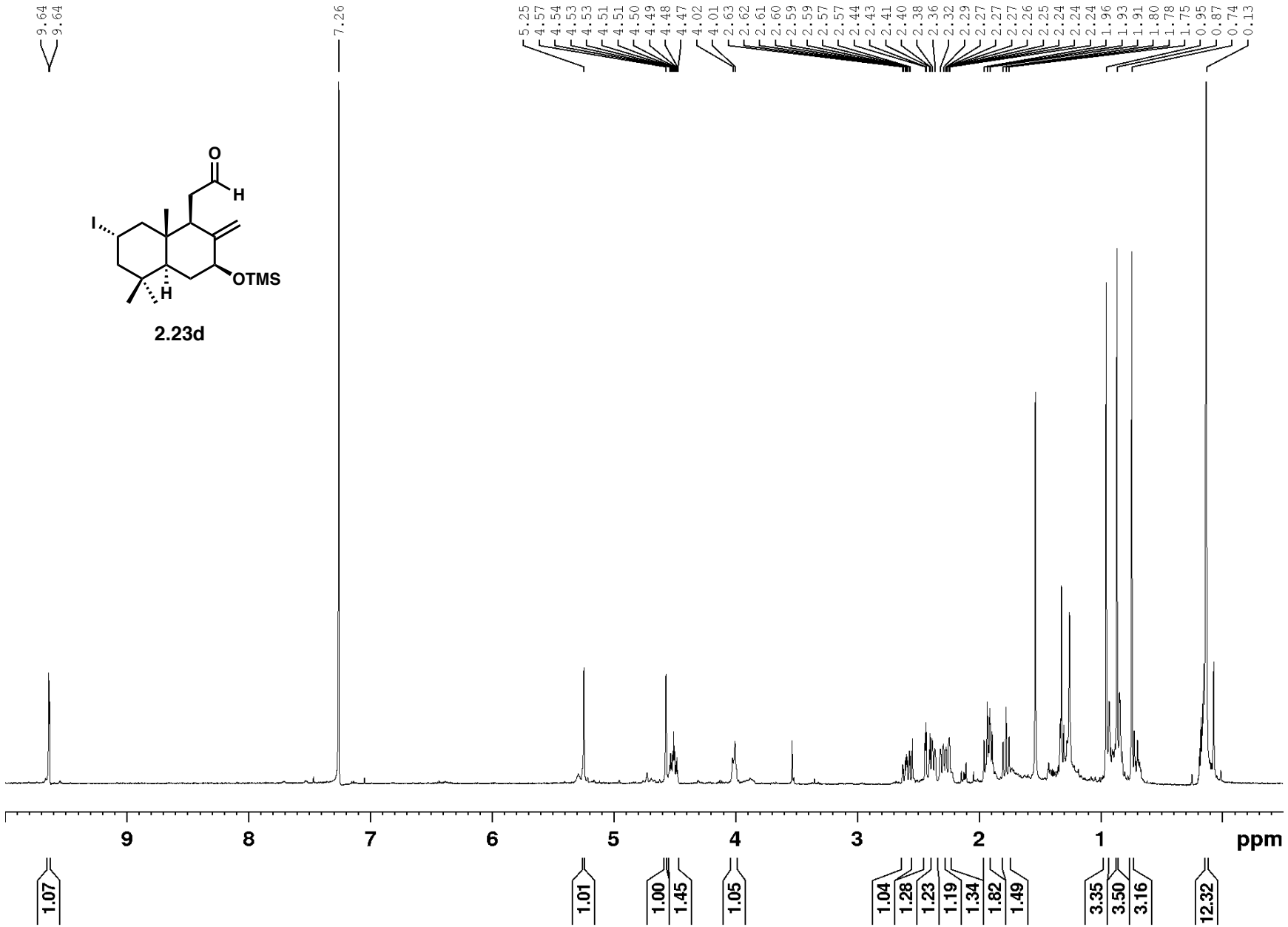
2.23a

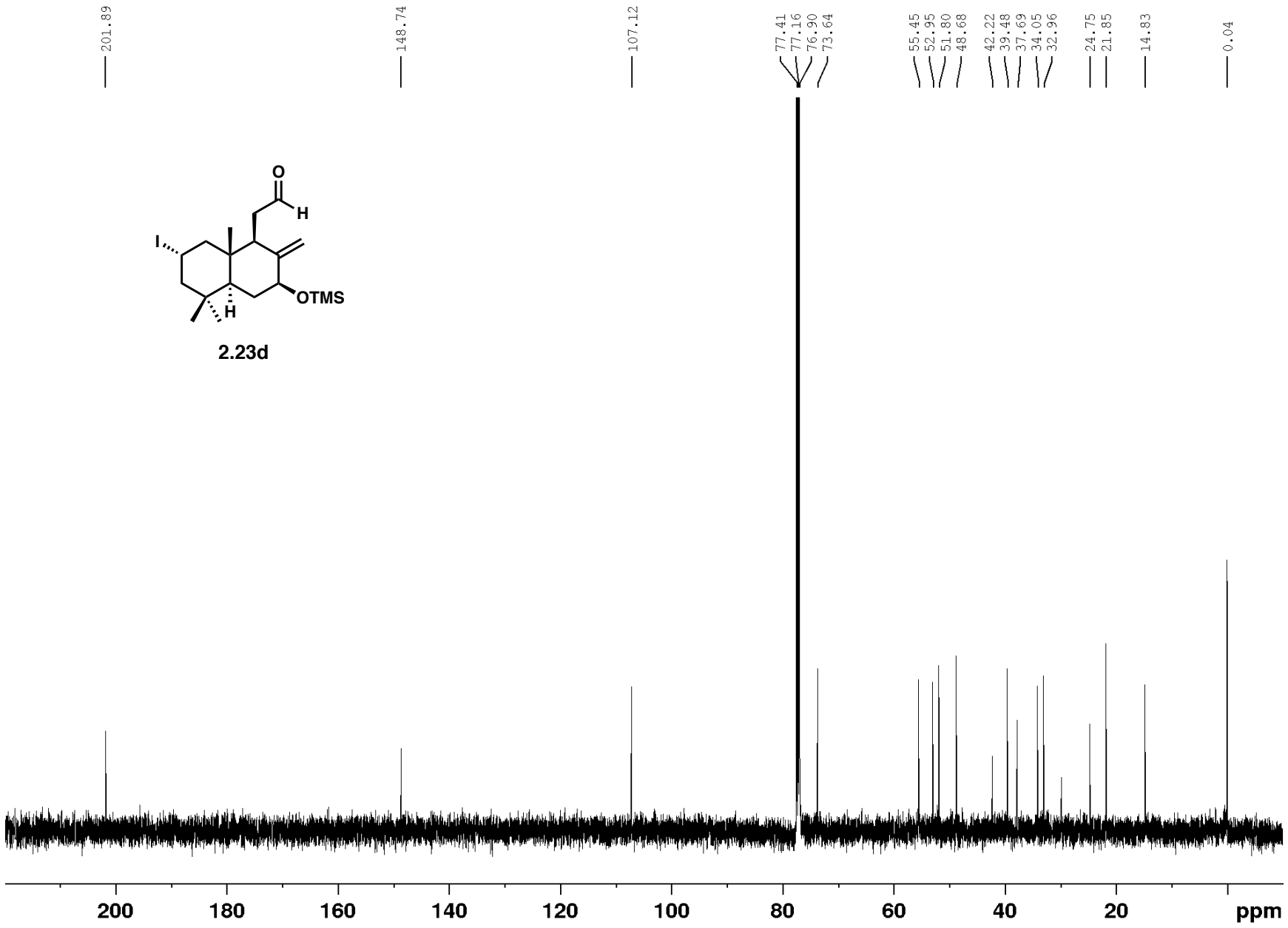

202.00
148.70
107.21
89.33
88.00
77.41
77.16
76.90
73.69
52.42
52.41
48.96
47.70
47.57
45.27
45.13
40.22
40.14
39.71
35.17
35.07
33.69
33.59
22.66
15.59
0.03
O
H
F
OTMS
H
2.23a
210
200
190
180
170
160
150
140
130
120
110
100
90
80
70
60
50
40
30
20
10
ppm


9.64
9.63
7.26
5.22
4.55
4.03
4.02
4.01
4.00
2.59
2.59
2.57
2.57
2.56
2.55
2.54
2.53
2.50
2.49
2.47
2.46
2.29
2.28
2.27
2.26
1.96
1.96
1.95
1.95
1.94
1.93
1.93
1.92
1.74
1.73
1.71
1.71
1.70
1.69
1.69
1.68
1.68
1.55
1.52
1.49
1.45
1.42
1.40
1.38
1.35
1.33
1.18
1.18
1.15
1.15
0.91
0.88
0.87
0.83
0.72
0.70
0.68
0.14
O
H
OTMS
H
9.0
8.0
7.0
6.0
5.0
4.0
3.0
2.0
1.0
0.0
ppm
0.95
1.04
1.00
1.02
1.24
1.07
1.08
1.20
1.46
0.99
1.22
1.39
1.54
1.14
3.23
3.87
3.32
4.24
9.47

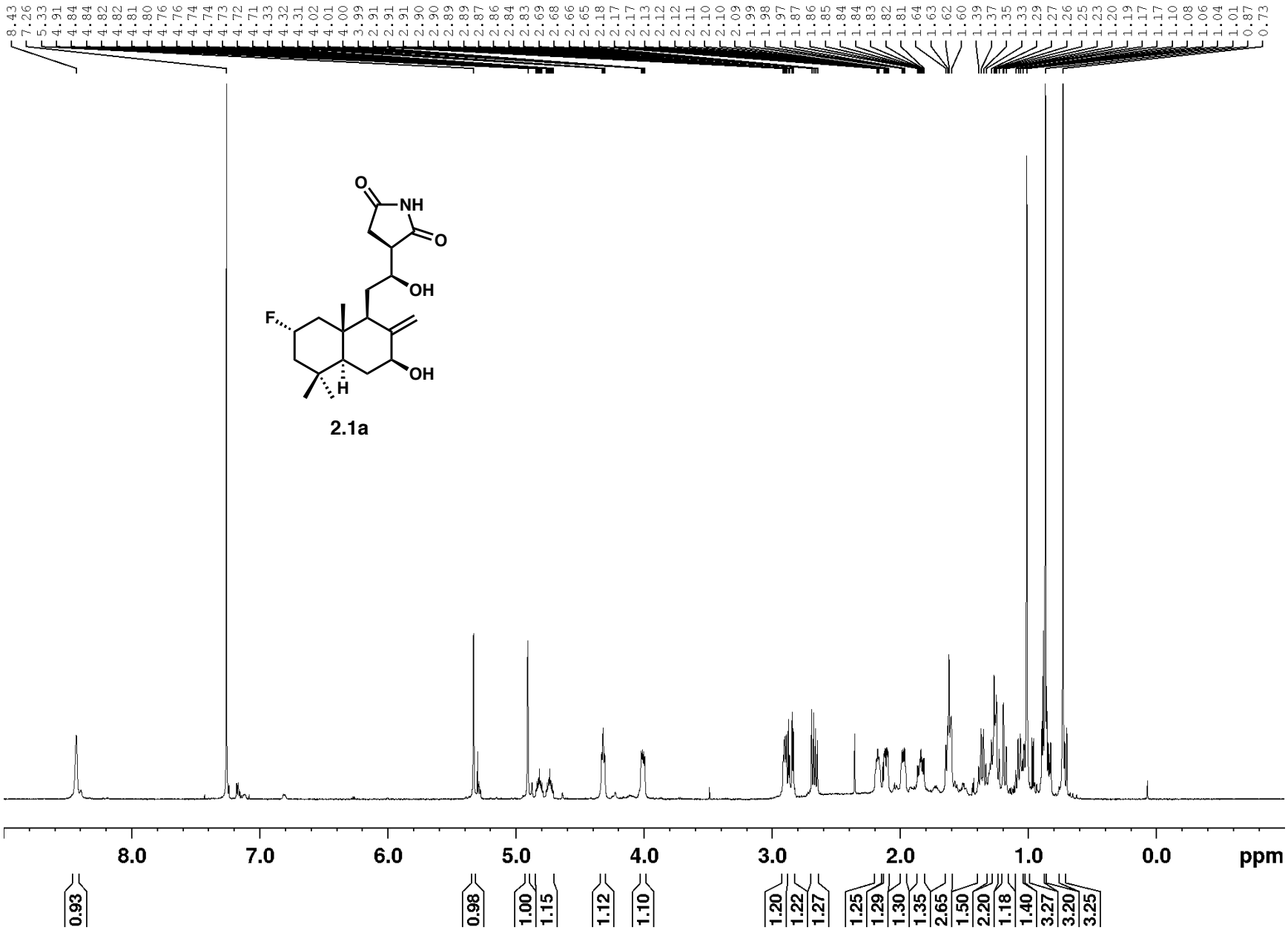
2.23c

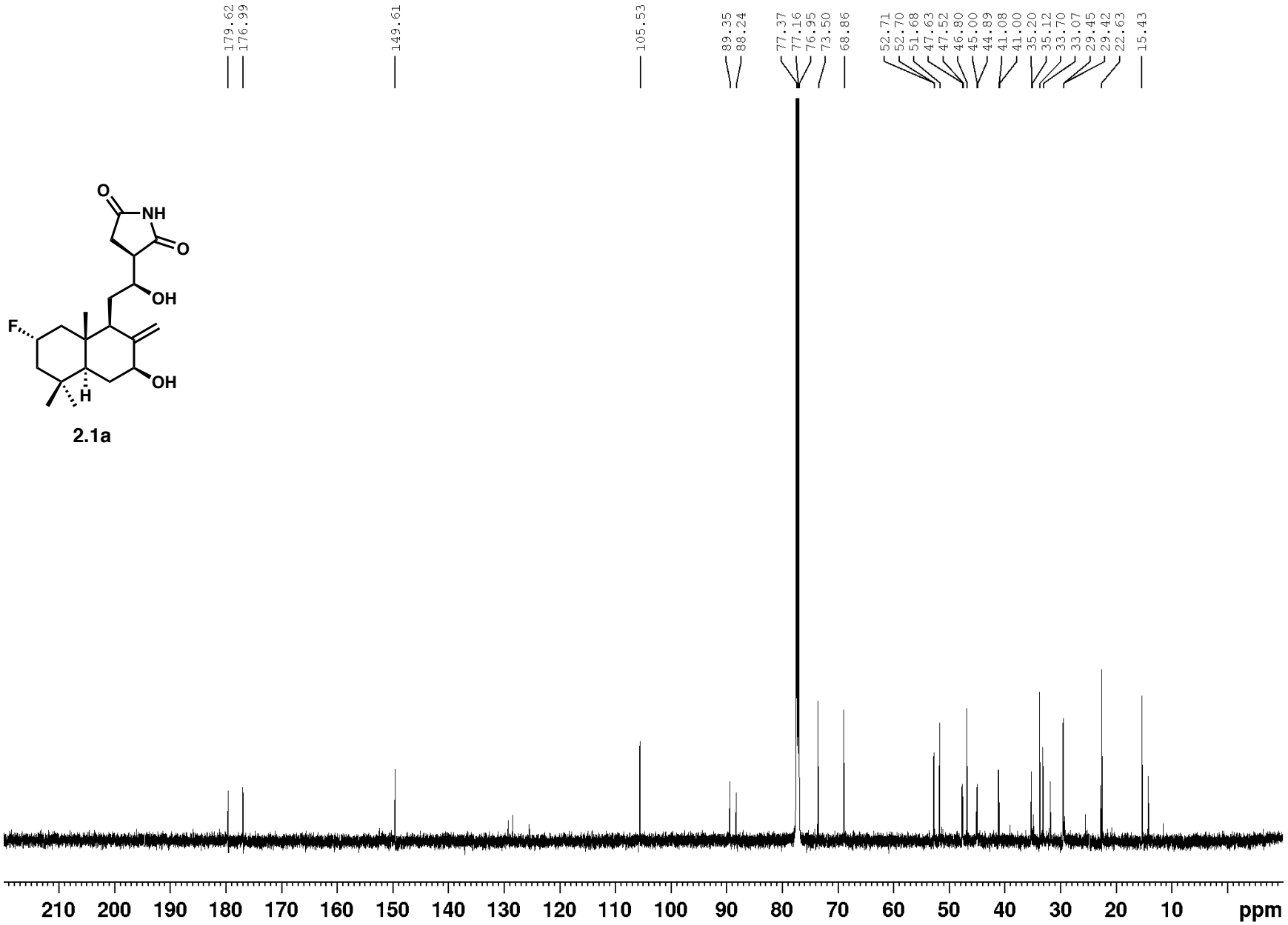

203.07
149.79
106.24
77.41
77.16
76.90
74.09
52.79
51.14
49.37
48.36
39.76
39.35
34.22
34.12
33.57
24.88
23.07
22.40
15.41
1.17
0.07
O
H
OTMS
H
2.23c
210 200 190 180 170 160 150 140 130 120 110 100 90 80 70 60 50 40 30 20 10 ppm


9.64
9.64
7.26
5.25
4.57
4.54
4.53
4.53
4.51
4.51
4.50
4.49
4.48
4.47
4.02
4.01
2.63
2.62
2.61
2.60
2.59
2.59
2.57
2.57
2.44
2.43
2.41
2.40
2.38
2.36
2.32
2.29
2.27
2.27
2.27
2.26
2.25
2.24
2.24
2.24
1.96
1.93
1.91
1.80
1.78
1.75
0.95
0.87
0.74
0.13
O
H
I
OTMS
H
2.23d
9
8
7
6
5
4
3
2
1
ppm
1.07
1.01
1.00
1.45
1.05
1.04
1.28
1.23
1.19
1.34
1.82
1.49
3.35
3.50
3.16
12.32

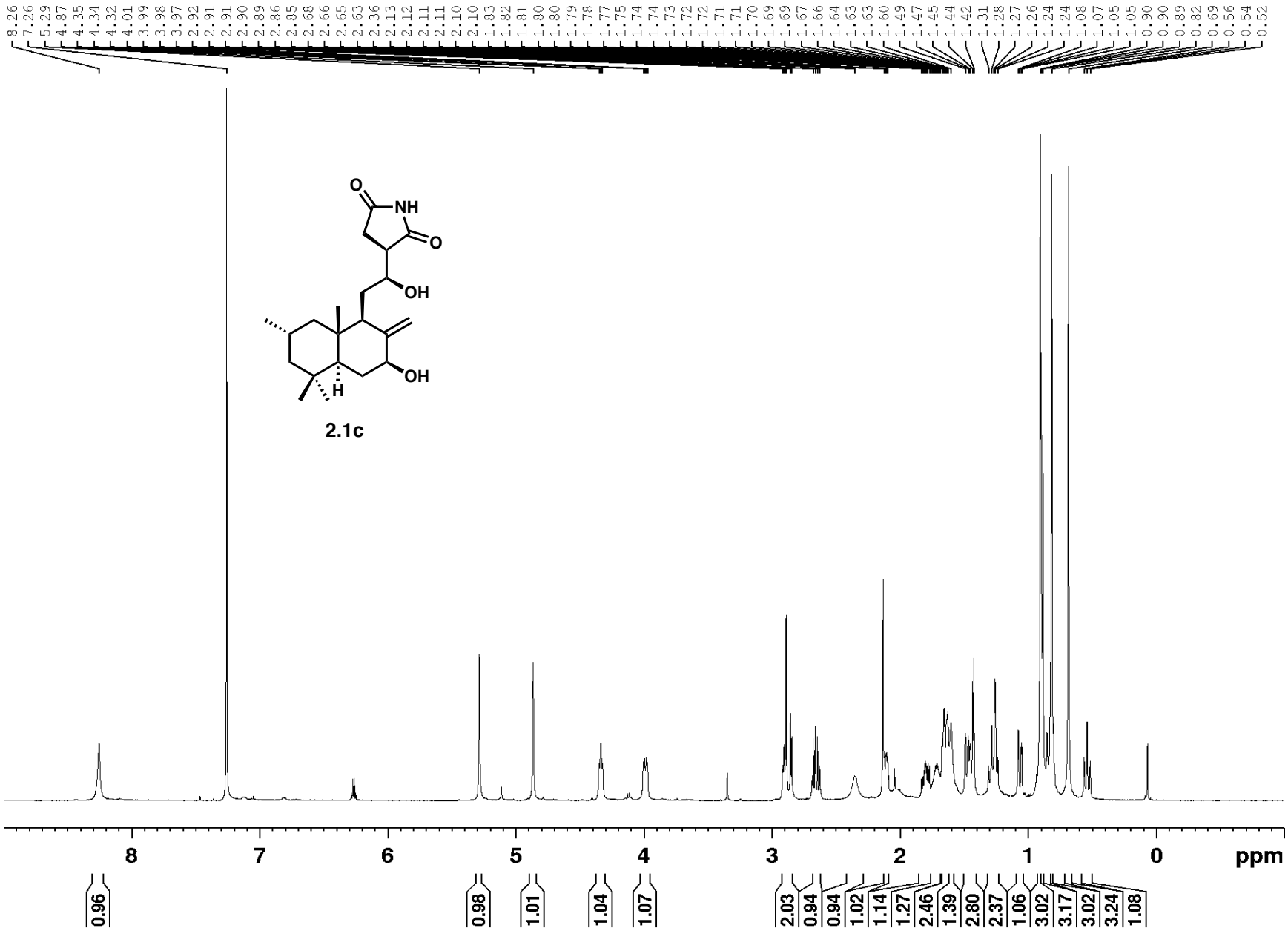

201.89
148.74
107.12
77.41
77.16
76.90
73.64
55.45
52.95
51.80
48.68
42.22
39.48
37.69
34.05
32.96
24.75
21.85
14.83
0.04
O
H
I
OTMS
H
200
180
160
140
120
100
80
60
40
20
ppm

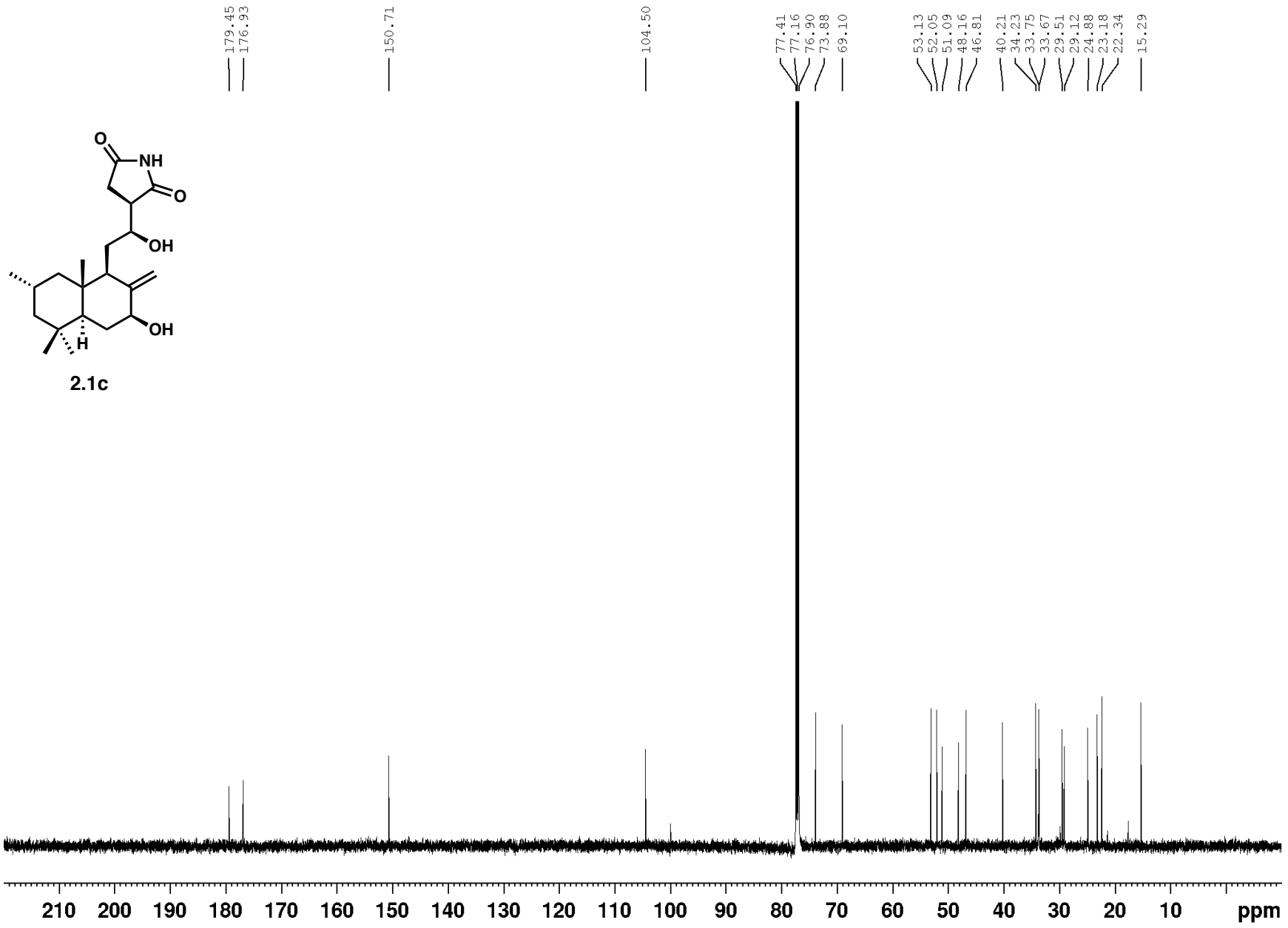
2.23d

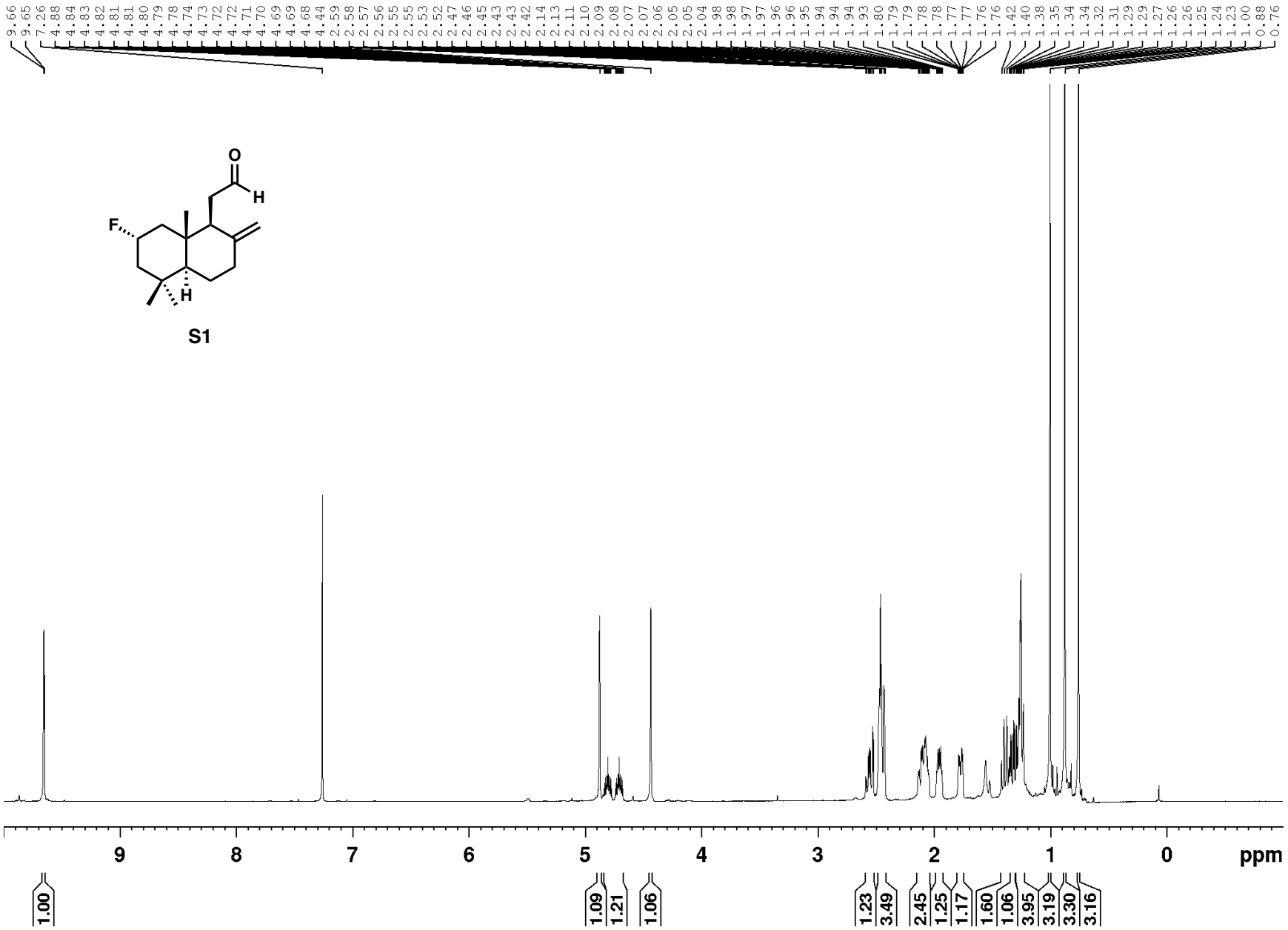

8.43 7.26 5.33 4.91 4.84 4.84 4.82 4.82 4.81 4.80 4.76 4.76 4.74 4.74 4.73 4.72 4.71 4.33 4.32 4.31 4.02 4.01 4.00 3.99 2.91 2.91 2.91 2.90 2.90 2.89 2.89 2.87 2.86 2.84 2.83 2.69 2.68 2.65 2.18 2.17 2.17 2.13 2.12 2.12 2.11 2.10 2.10 2.09 1.99 1.98 1.97 1.87 1.86 1.85 1.84 1.84 1.83 1.82 1.81 1.64 1.63 1.62 1.60 1.39 1.37 1.35 1.33 1.29 1.27 1.26 1.25 1.23 1.20 1.19 1.17 1.17 1.10 1.08 1.06 1.04 1.01 0.87 0.73
O
NH
O
OH
F
OH
H
2.1a
8.0
7.0
6.0
5.0
4.0
3.0
2.0
1.0
0.0
ppm
0.93
0.98
1.00
1.15
1.12
1.10
1.20
1.22
1.27
1.25
1.29
1.30
1.35
2.65
1.50
2.20
1.18
1.40
3.27
3.20
3.25

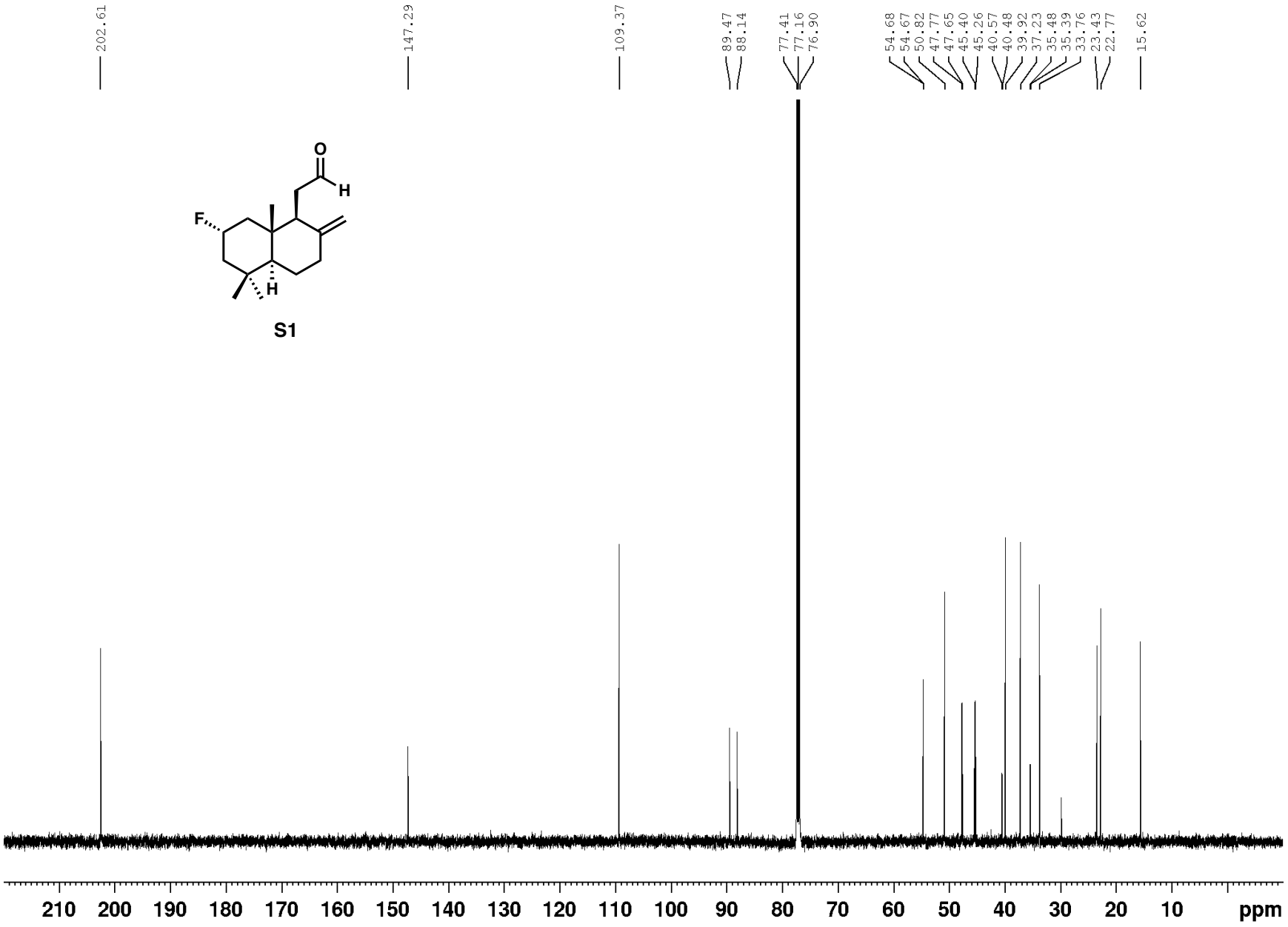

179.62
176.99
149.61
105.53
89.35
88.24
77.37
77.16
76.95
73.50
68.86
52.71
52.70
51.68
47.63
47.52
46.80
45.00
44.89
41.08
41.00
35.20
35.12
33.70
33.07
29.45
29.42
22.63
15.43
O
NH
O
OH
F
OH
H
210 200 190 180 170 160 150 140 130 120 110 100 90 80 70 60 50 40 30 20 10 ppm

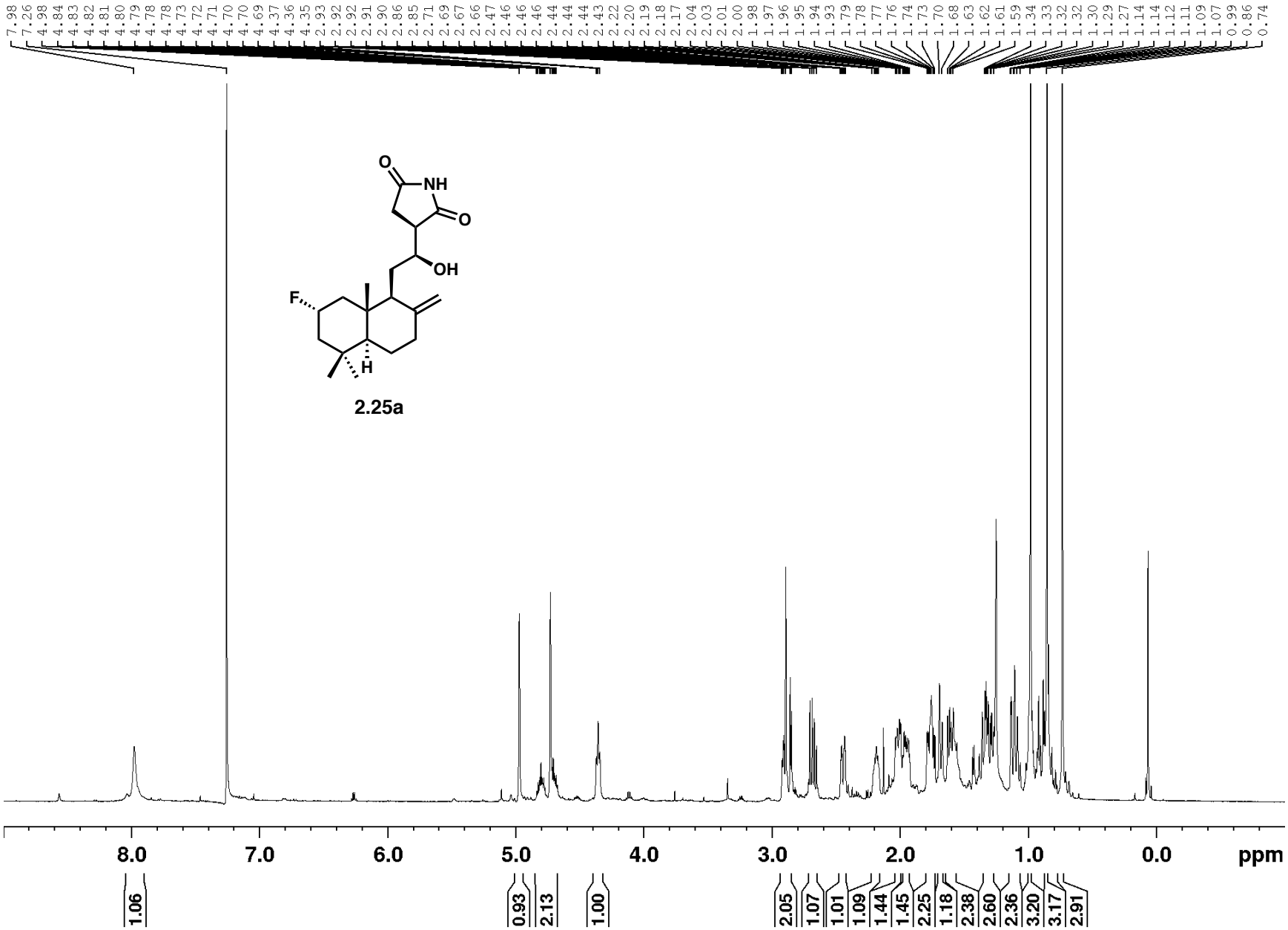
2.1a

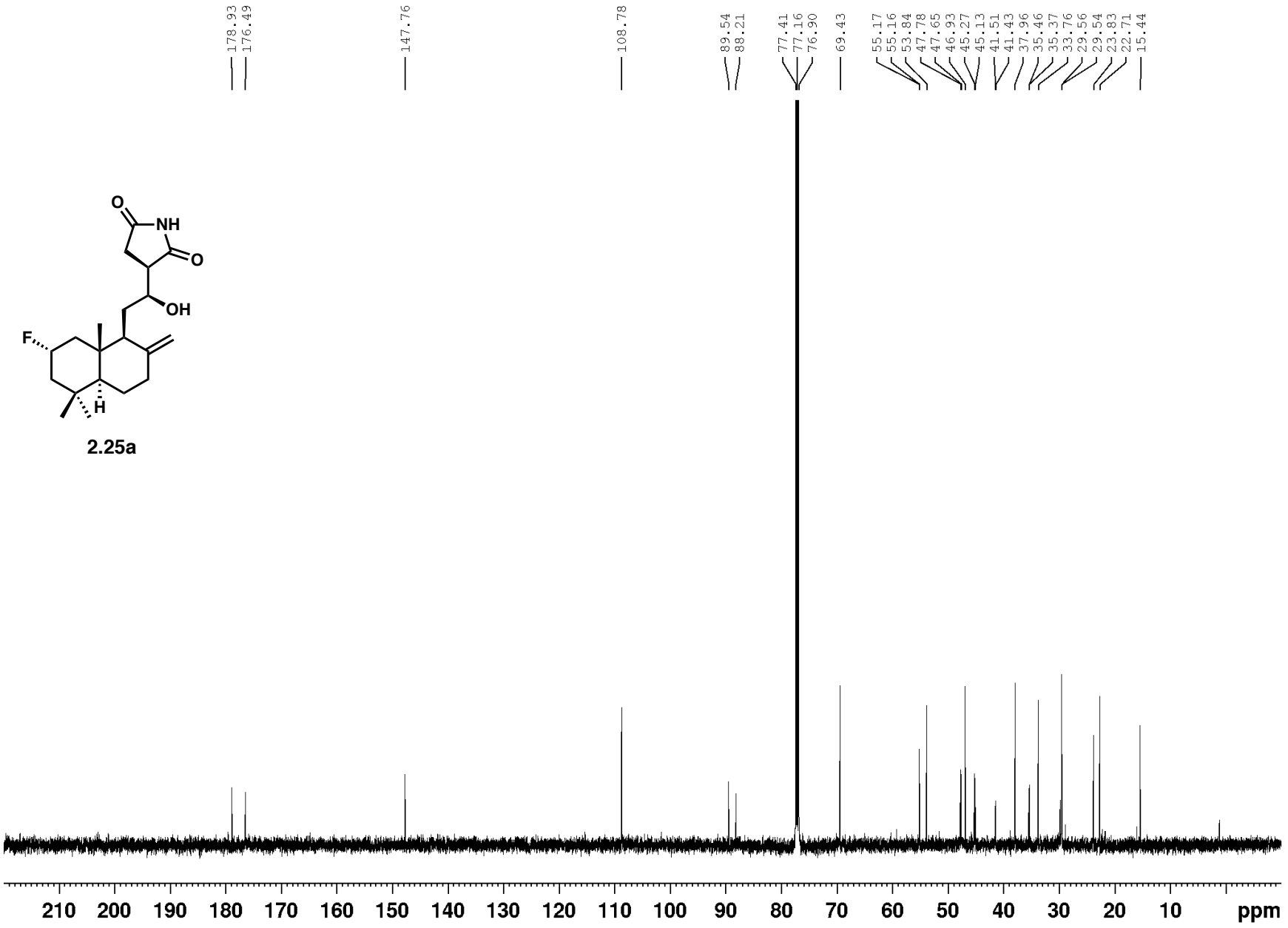

8.26 7.26 5.29 4.87 4.35 4.34 4.32 4.01 3.99 3.98 3.97 2.92 2.91 2.91 2.90 2.89 2.86 2.85 2.68 2.66 2.65 2.63 2.36 2.13 2.12 2.11 2.11 2.10 2.10 1.83 1.82 1.81 1.80 1.80 1.79 1.78 1.77 1.75 1.74 1.74 1.73 1.72 1.72 1.71 1.71 1.70 1.69 1.69 1.67 1.66 1.64 1.63 1.63 1.60 1.49 1.47 1.45 1.44 1.42 1.31 1.28 1.27 1.26 1.24 1.24 1.08 1.07 1.05 1.05 0.90 0.90 0.89 0.82 0.69 0.56 0.54 0.52
O
NH
O
OH
OH
H
2.1c
8
7
6
5
4
3
2
1
0
ppm
0.96
0.98
1.01
1.04
1.07
2.03
0.94
0.94
1.02
1.14
1.27
2.46
1.39
2.80
2.37
1.06
3.02
3.17
3.02
3.24
1.08


179.45
176.93
150.71
104.50
77.41
77.16
76.90
73.88
69.10
53.13
52.05
51.09
48.16
46.81
40.21
34.23
33.75
33.67
29.51
29.12
24.88
23.18
22.34
15.29
O
NH
O
OH
OH
H
2.1c
210 200 190 180 170 160 150 140 130 120 110 100 90 80 70 60 50 40 30 20 10 ppm


9.66 9.65 7.26 4.88 4.84 4.83 4.82 4.81 4.81 4.80 4.79 4.78 4.74 4.73 4.72 4.72 4.71 4.70 4.69 4.69 4.68 4.44 2.59 2.58 2.57 2.56 2.55 2.55 2.53 2.52 2.47 2.46 2.45 2.43 2.43 2.42 2.14 2.13 2.11 2.10 2.09 2.08 2.07 2.07 2.06 2.05 2.05 2.04 1.98 1.98 1.97 1.97 1.96 1.96 1.95 1.94 1.94 1.94 1.93 1.80 1.79 1.79 1.78 1.78 1.77 1.77 1.76 1.76 1.42 1.40 1.38 1.35 1.34 1.34 1.32 1.31 1.29 1.29 1.27 1.26 1.26 1.25 1.24 1.23 1.00 0.88 0.76
O
H
F
H
S1
9
8
7
6
5
4
3
2
1
0
ppm
1.00
1.09
1.21
1.06
1.23
3.49
2.45
1.25
1.17
1.60
1.06
3.95
3.19
3.30
3.16

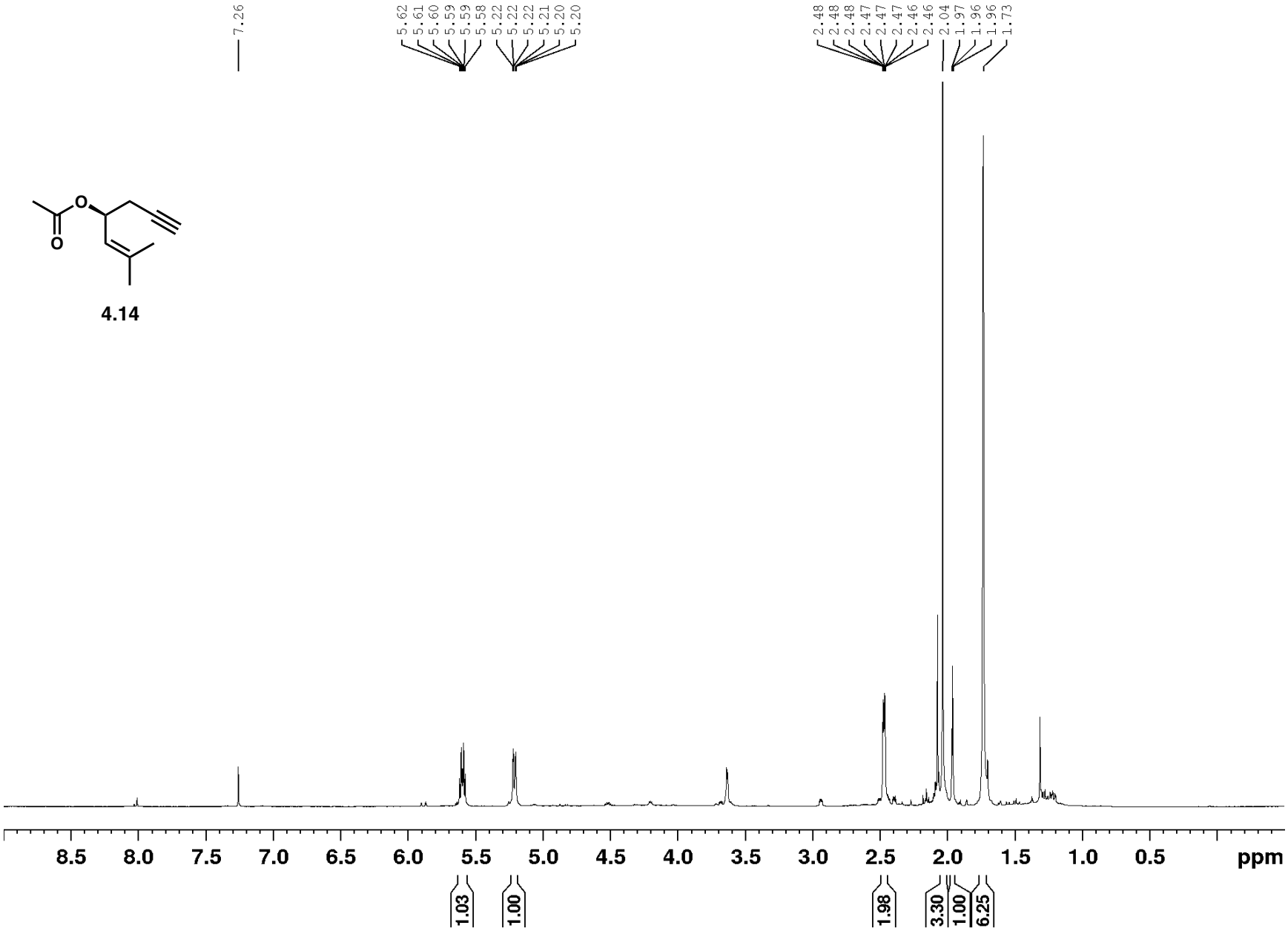

202.61
147.29
109.37
89.47
88.14
77.41
77.16
76.90
54.68
54.67
50.82
47.77
47.65
45.40
45.26
40.57
40.48
39.92
37.23
35.48
35.39
33.76
23.43
22.77
15.62
O
H
F
H
S1
210
200
190
180
170
160
150
140
130
120
110
100
90
80
70
60
50
40
30
20
10
ppm

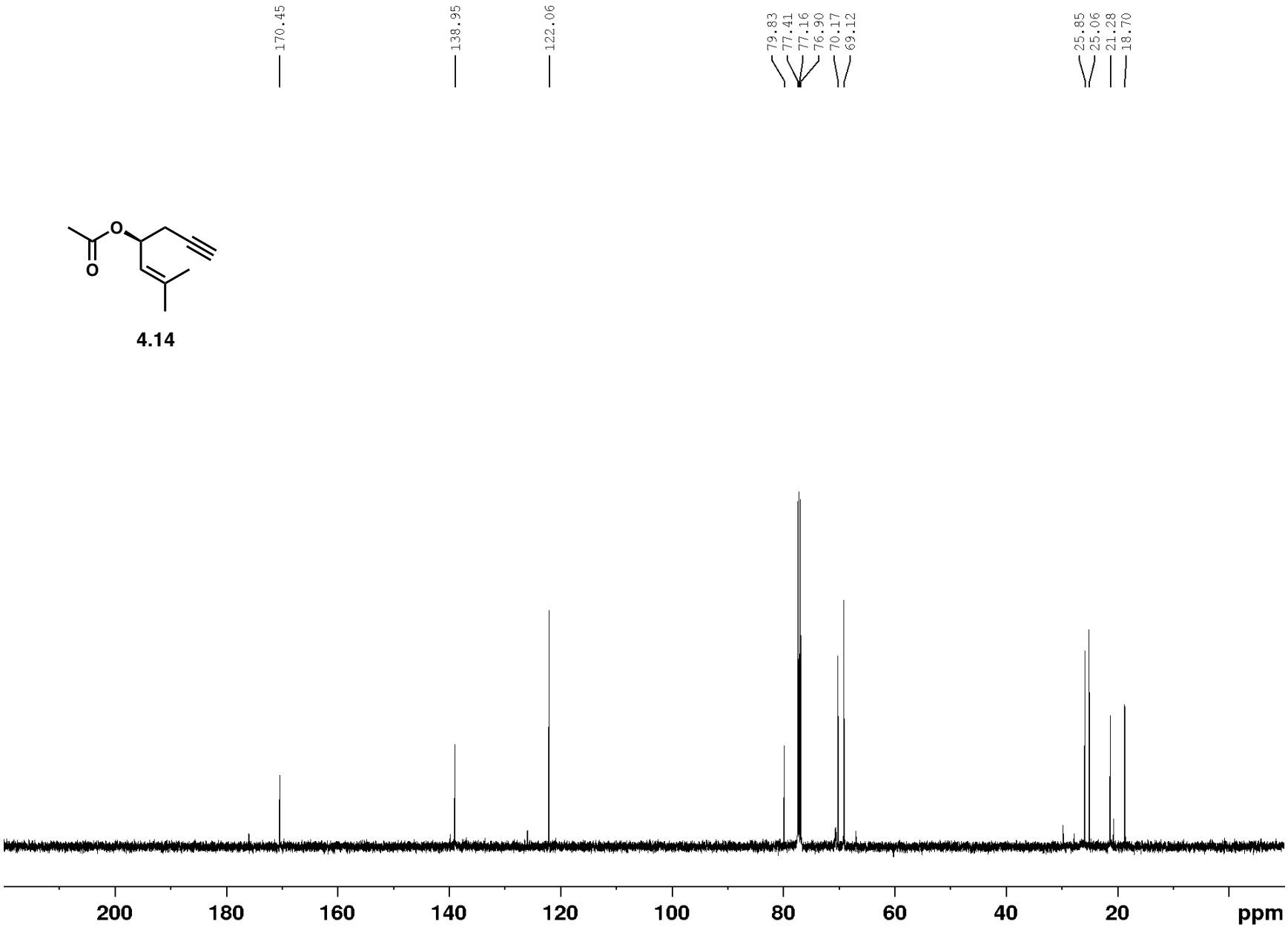

7.98 7.26 4.98 4.84 4.83 4.82 4.81 4.80 4.79 4.78 4.78 4.73 4.72 4.71 4.70 4.70 4.69 4.37 4.36 4.35 2.93 2.92 2.92 2.91 2.90 2.86 2.85 2.71 2.69 2.67 2.66 2.47 2.46 2.46 2.46 2.44 2.44 2.44 2.43 2.22 2.20 2.19 2.18 2.17 2.04 2.03 2.01 2.00 1.98 1.97 1.96 1.95 1.94 1.93 1.79 1.78 1.77 1.76 1.74 1.73 1.70 1.68 1.63 1.62 1.61 1.59 1.34 1.33 1.32 1.32 1.30 1.29 1.27 1.14 1.14 1.12 1.11 1.09 1.07 0.99 0.86 0.74
O
NH
O
OH
F
H
2.25a
8.0
7.0
6.0
5.0
4.0
3.0
2.0
1.0
0.0
ppm
1.06
0.93
2.13
1.00
2.05
1.07
1.01
1.09
1.44
1.45
2.25
1.18
2.38
2.60
2.36
3.20
3.17
2.91


178.93
176.49
147.76
108.78
89.54
88.21
77.41
77.16
76.90
69.43
55.17
55.16
53.84
47.78
47.65
46.93
45.27
45.13
41.51
41.43
37.96
35.46
35.37
33.76
29.56
29.54
23.83
22.71
15.44
O
NH
O
OH
F
H
210
200
190
180
170
160
150
140
130
120
110
100
90
80
70
60
50
40
30
20
10
ppm

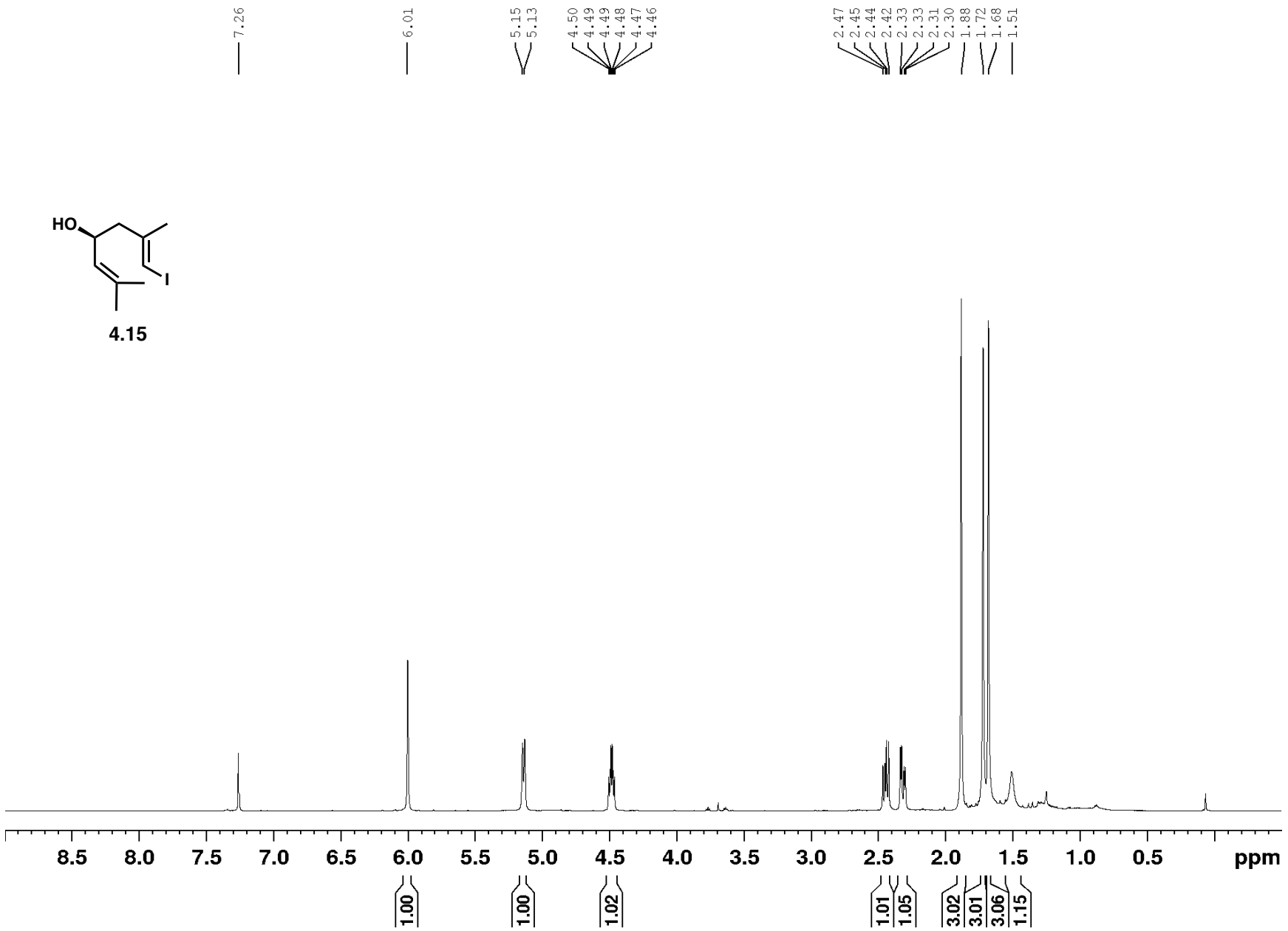
2.25a

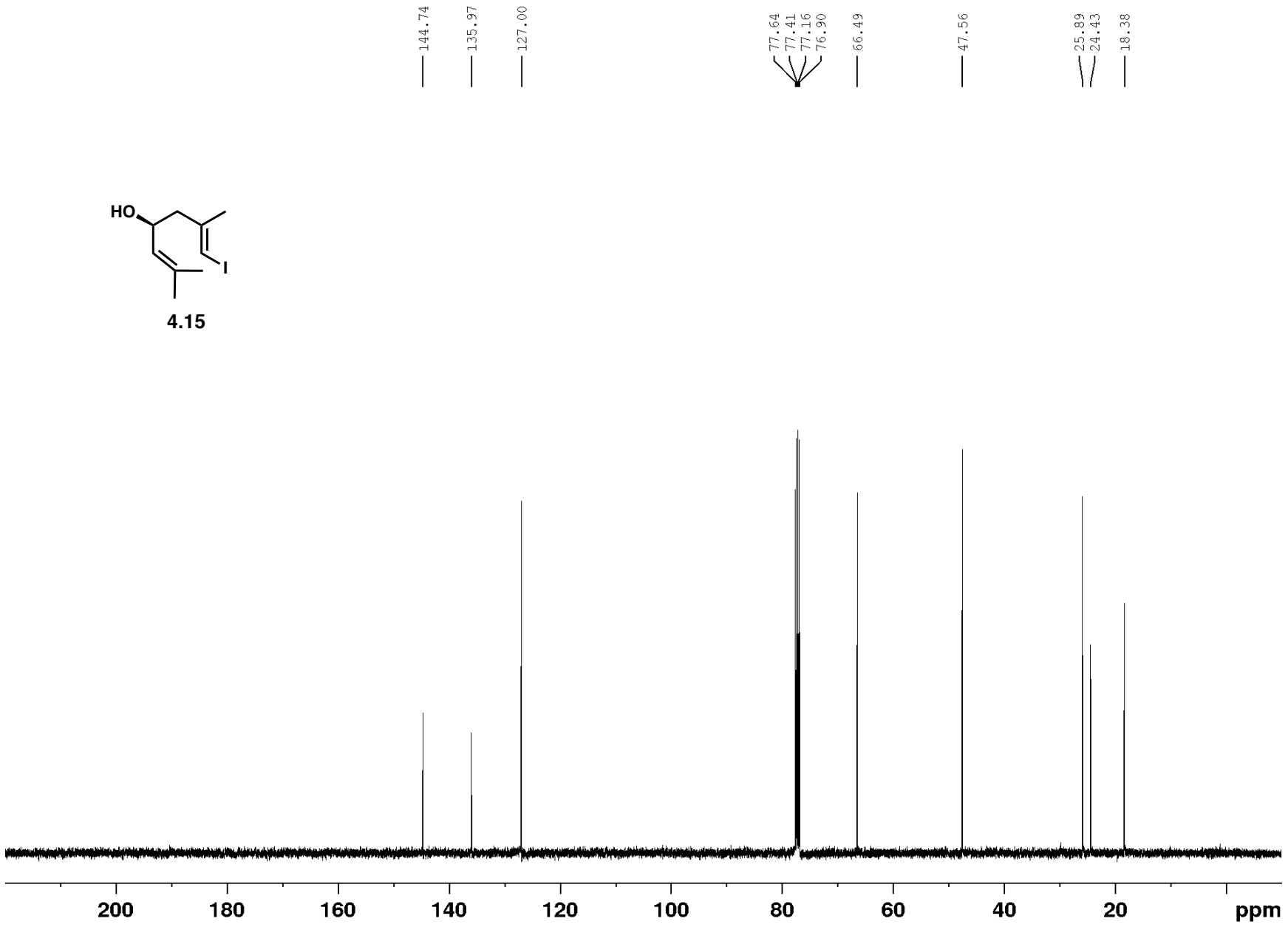
APPENDIX B: NMR DATA FOR CHAPTER 4

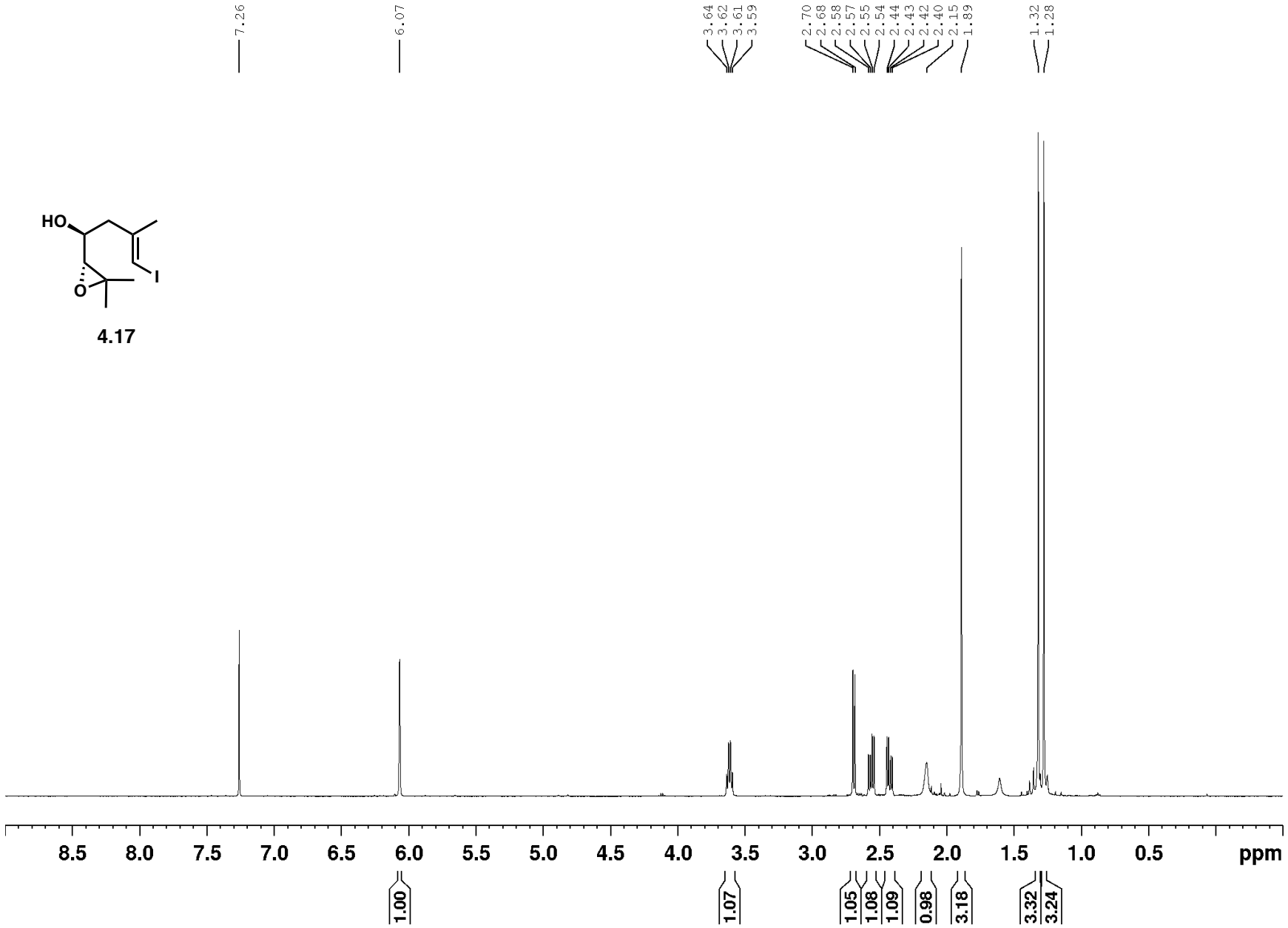

7.26
5.62
5.61
5.60
5.59
5.59
5.58
5.22
5.22
5.22
5.21
5.20
5.20
2.48
2.48
2.48
2.47
2.47
2.47
2.46
2.46
2.04
1.97
1.96
1.96
1.73
O
O
4.14
8.5
8.0
7.5
7.0
6.5
6.0
5.5
5.0
4.5
4.0
3.5
3.0
2.5
2.0
1.5
1.0
0.5
ppm
1.03
1.00
1.98
3.30
1.00
6.25

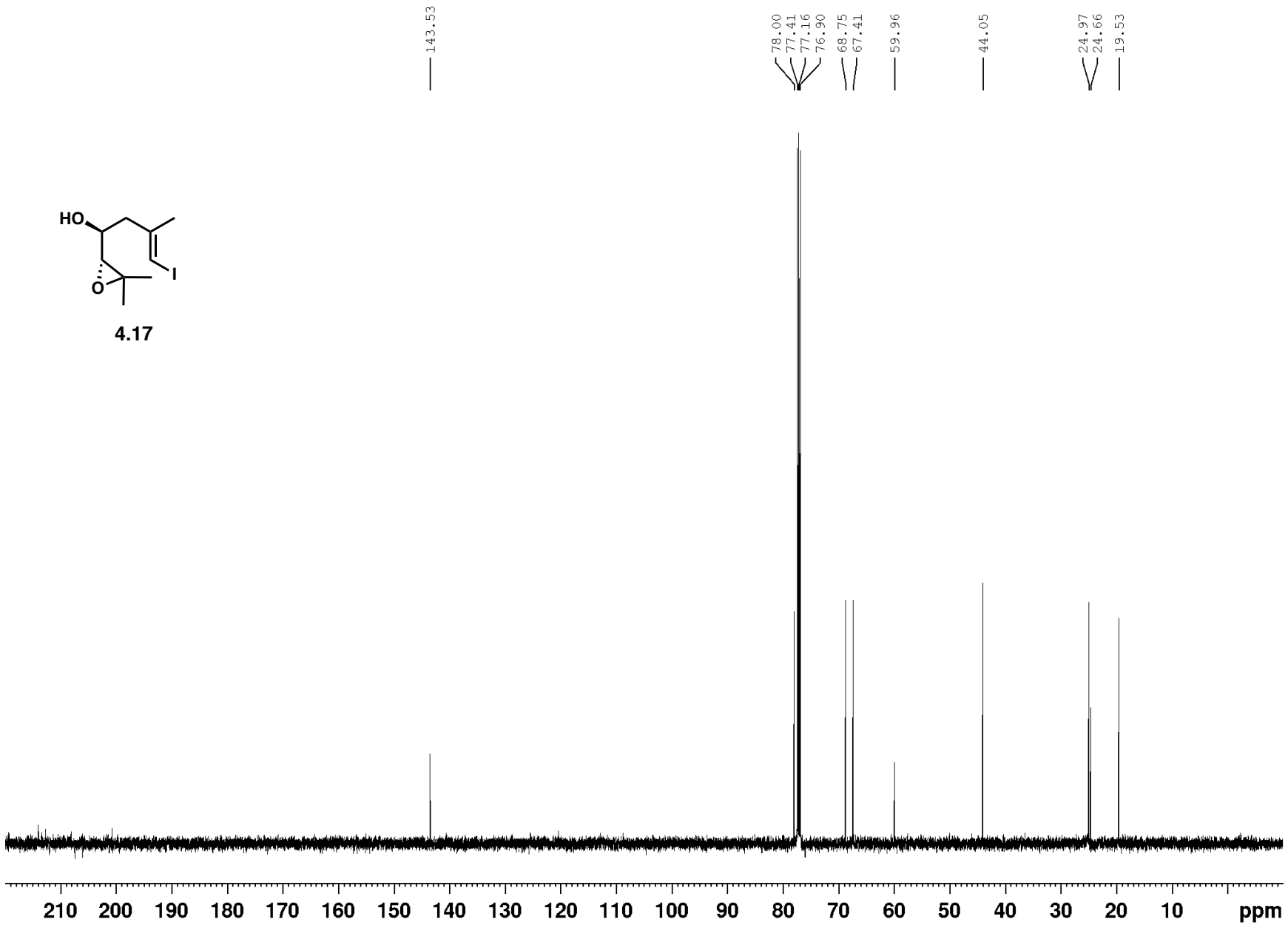

170.45
138.95
122.06
79.83
77.41
77.16
76.90
70.17
69.12
25.85
25.06
21.28
18.70
O
O
200
180
160
140
120
100
80
60
40
20
ppm

4.14

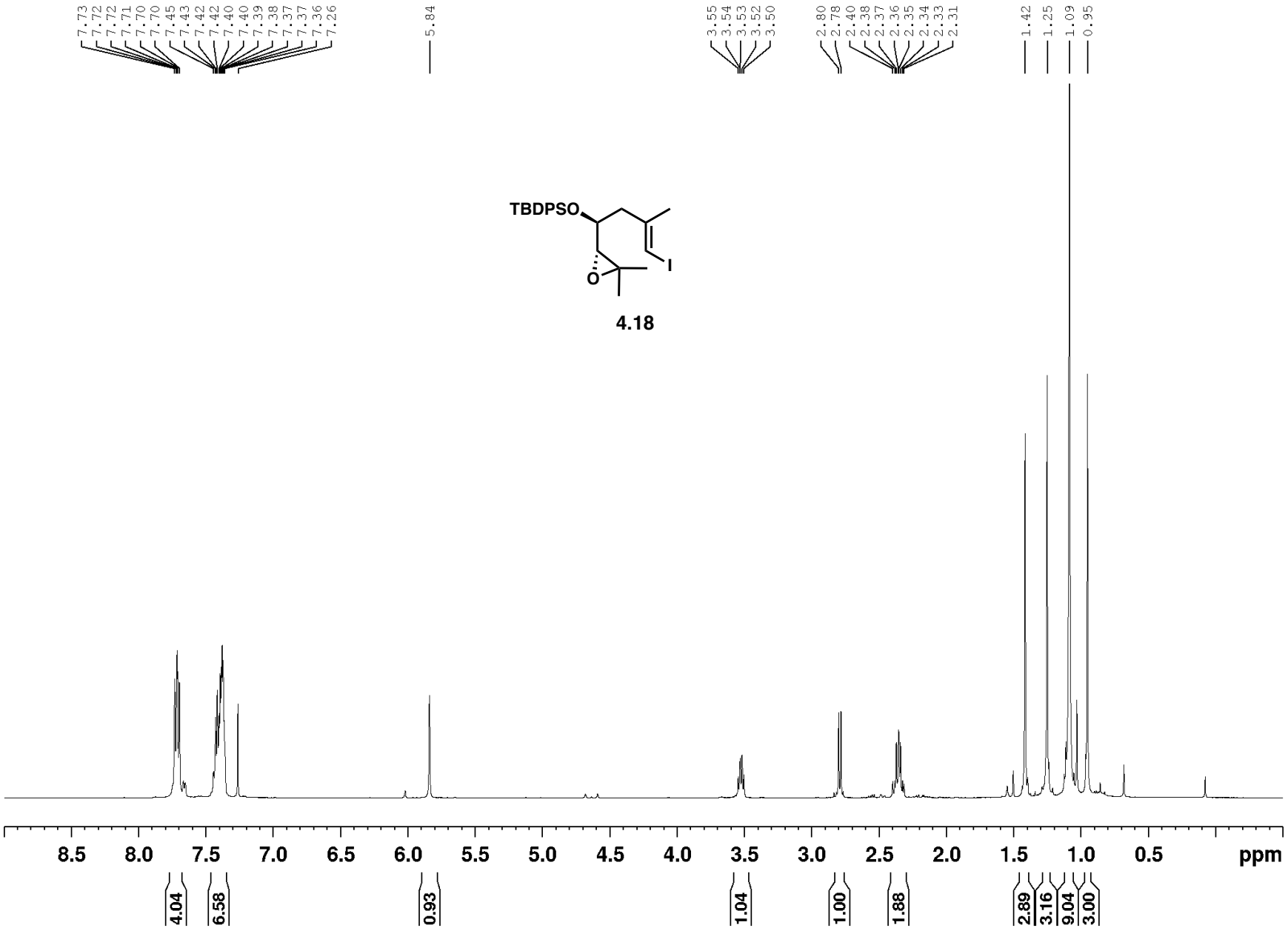

7.26
6.01
5.15
5.13
4.50
4.49
4.49
4.48
4.47
4.46
2.47
2.45
2.44
2.42
2.33
2.33
2.31
2.30
1.88
1.72
1.68
1.51
HO
I
4.15
8.5
8.0
7.5
7.0
6.5
6.0
5.5
5.0
4.5
4.0
3.5
3.0
2.5
2.0
1.5
1.0
0.5
ppm
1.00
1.00
1.02
1.01
1.05
3.02
3.01
3.06
1.15

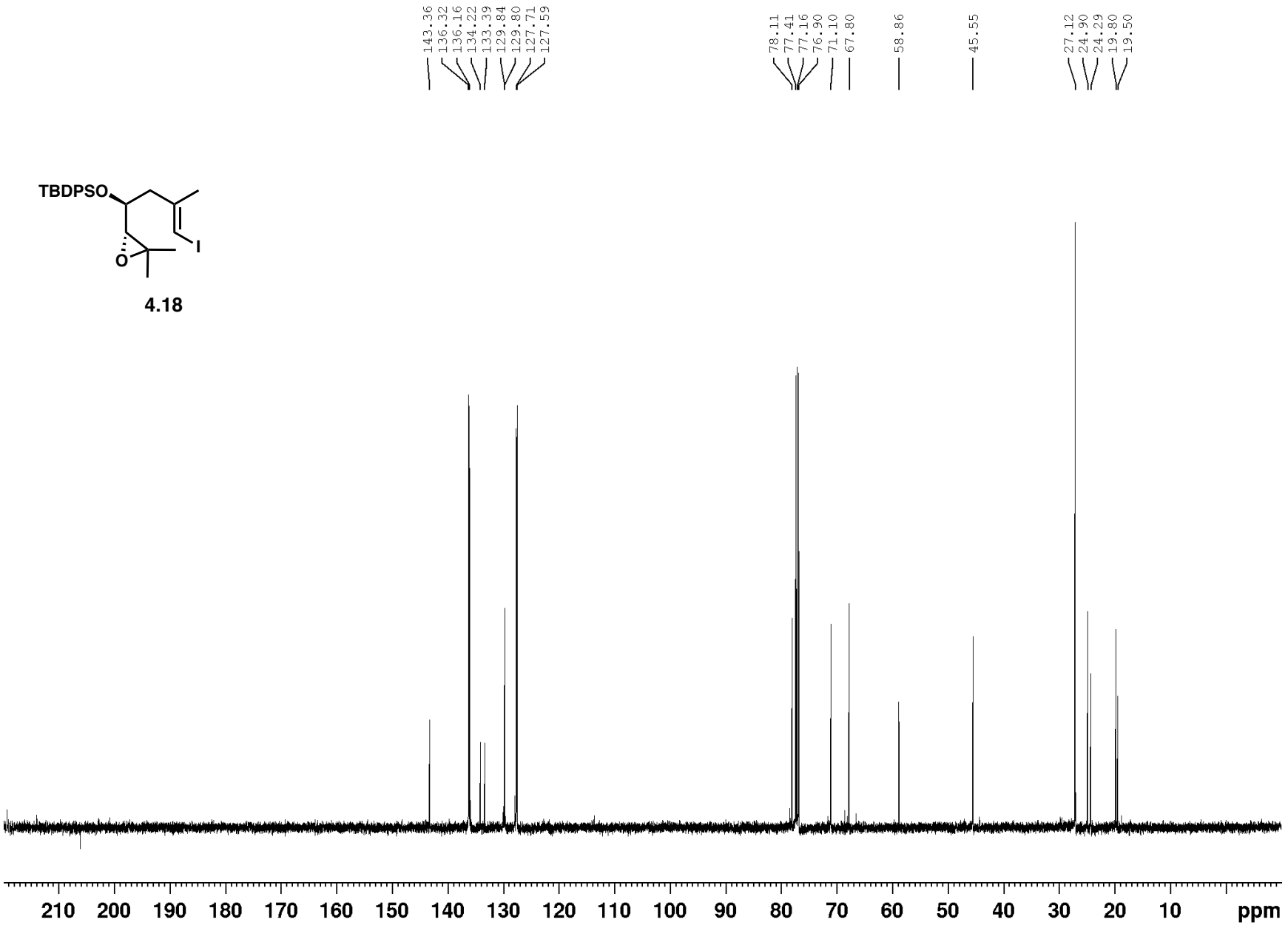

144.74
135.97
127.00
77.64
77.41
77.16
76.90
66.49
47.56
25.89
24.43
18.38
HO
I
4.15
200
180
160
140
120
100
80
60
40
20
ppm

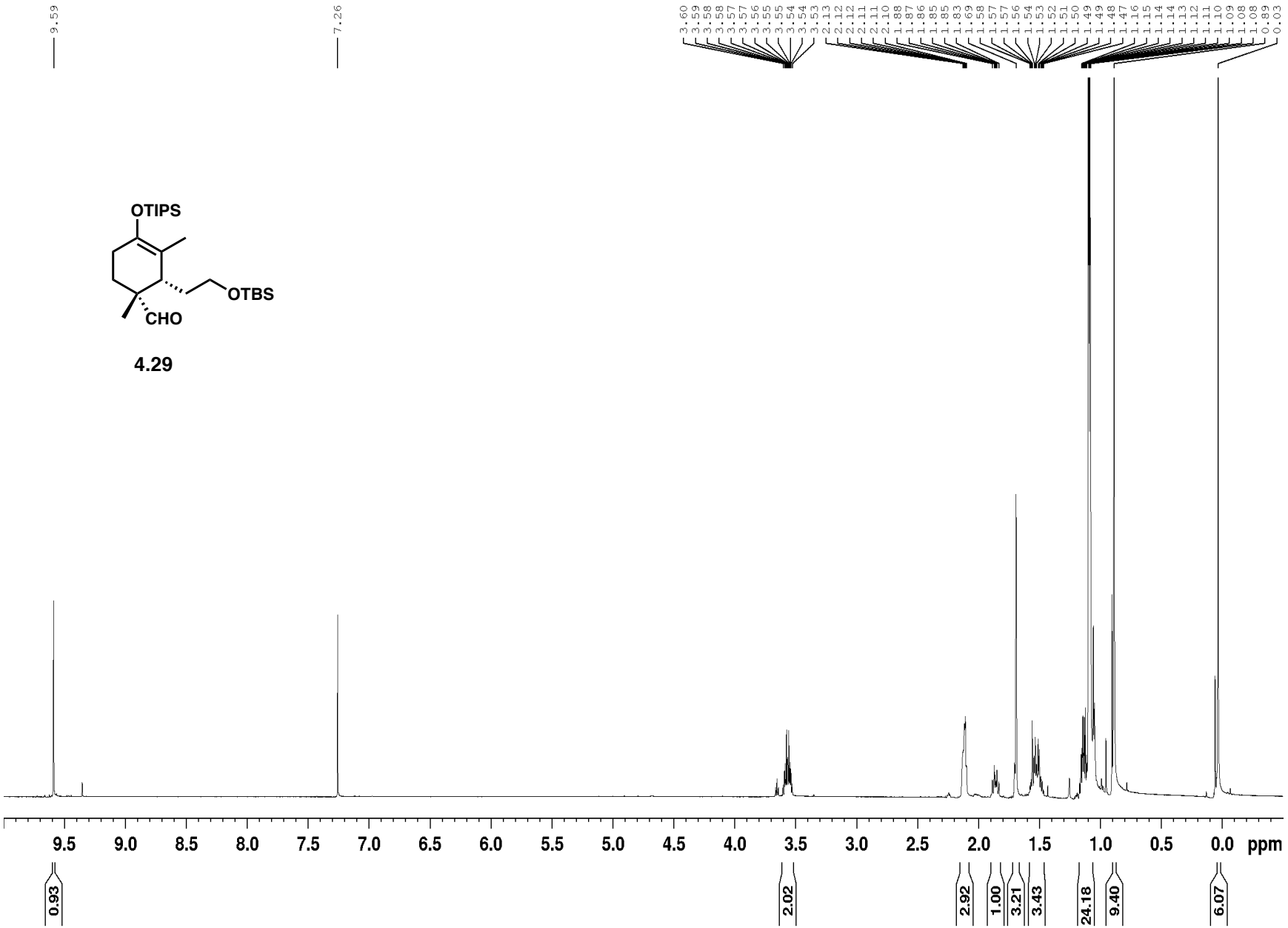

7.26
6.07
3.64
3.62
3.61
3.59
2.70
2.68
2.58
2.57
2.55
2.54
2.44
2.43
2.42
2.40
2.15
1.89
1.32
1.28
HO
O
I
4.17
8.5
8.0
7.5
7.0
6.5
6.0
5.5
5.0
4.5
4.0
3.5
3.0
2.5
2.0
1.5
1.0
0.5
ppm
1.00
1.07
1.05
1.08
1.09
0.98
3.18
3.32
3.24

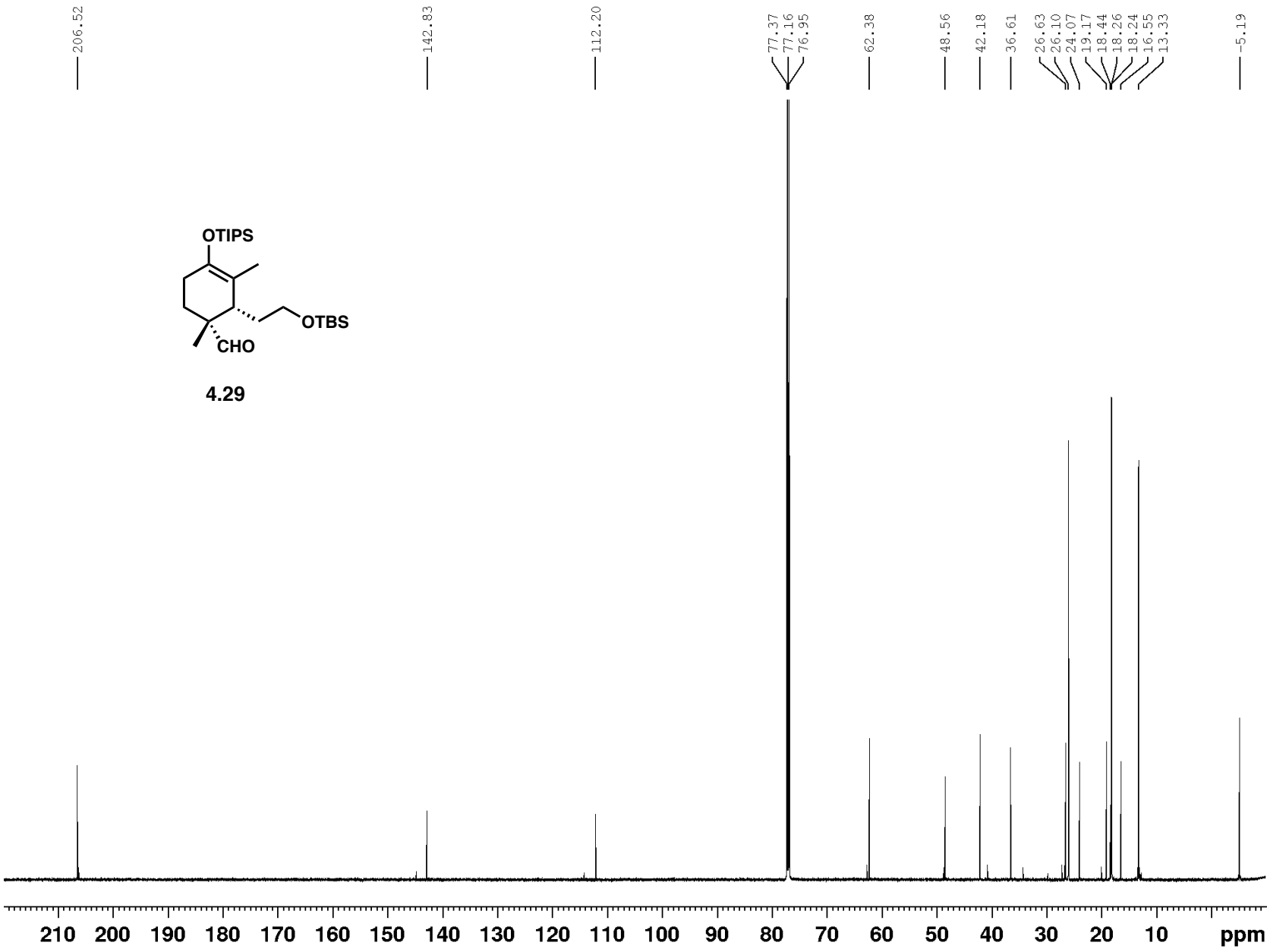

143.53
78.00
77.41
77.16
76.90
68.75
67.41
59.96
44.05
24.97
24.66
19.53
HO
O
I
210 200 190 180 170 160 150 140 130 120 110 100 90 80 70 60 50 40 30 20 10 ppm

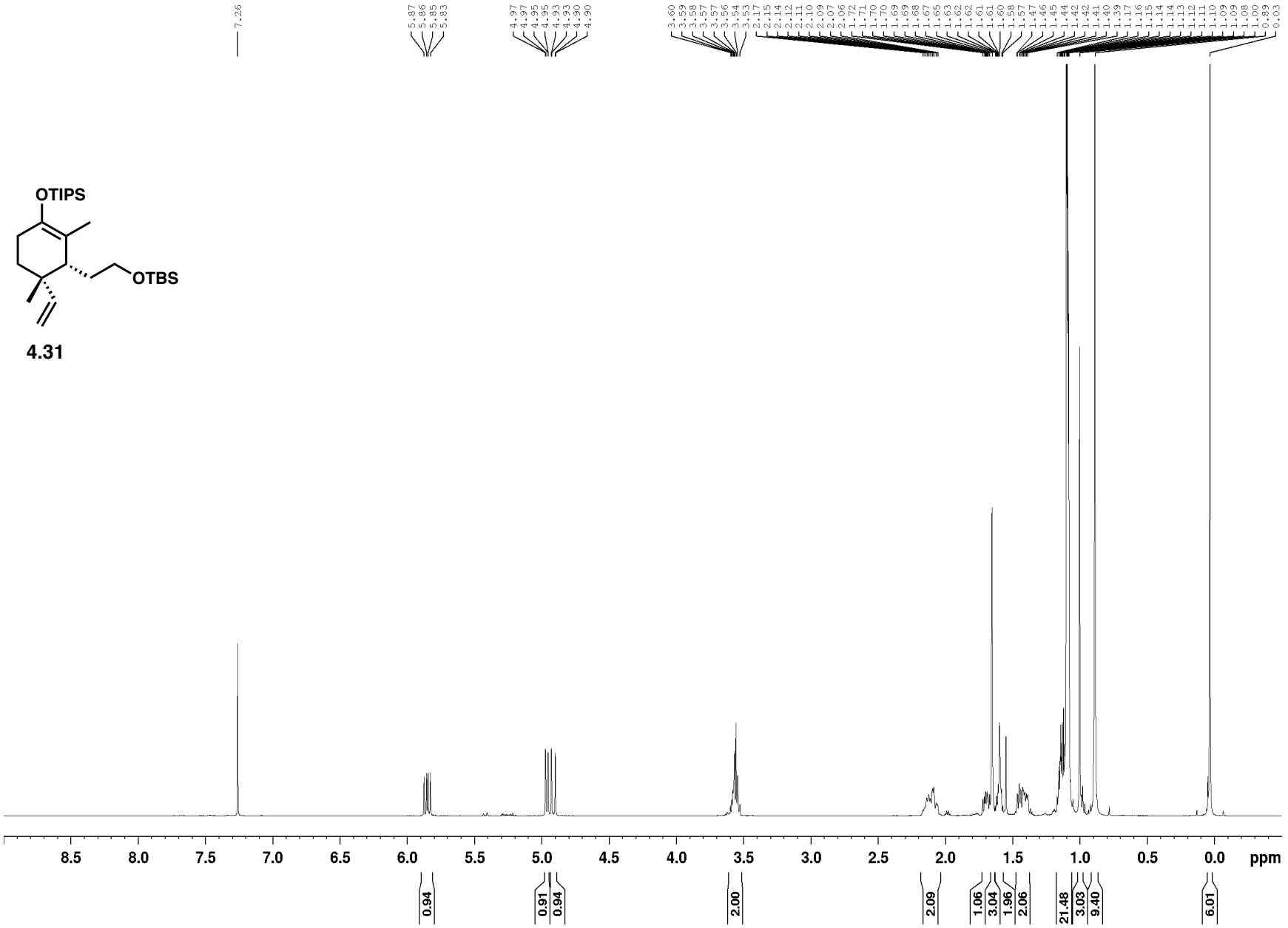
4.17


7.73
7.72
7.72
7.71
7.70
7.70
7.45
7.43
7.42
7.42
7.40
7.40
7.39
7.38
7.37
7.37
7.36
7.26
5.84
3.55
3.54
3.53
3.52
3.50
2.80
2.78
2.40
2.38
2.37
2.36
2.35
2.34
2.33
2.31
1.42
1.25
1.09
0.95
TBDPSO
O
I
4.18
8.5
8.0
7.5
7.0
6.5
6.0
5.5
5.0
4.5
4.0
3.5
3.0
2.5
2.0
1.5
1.0
0.5
ppm
4.04
6.58
0.93
1.04
1.00
1.88
2.89
3.16
9.04
3.00

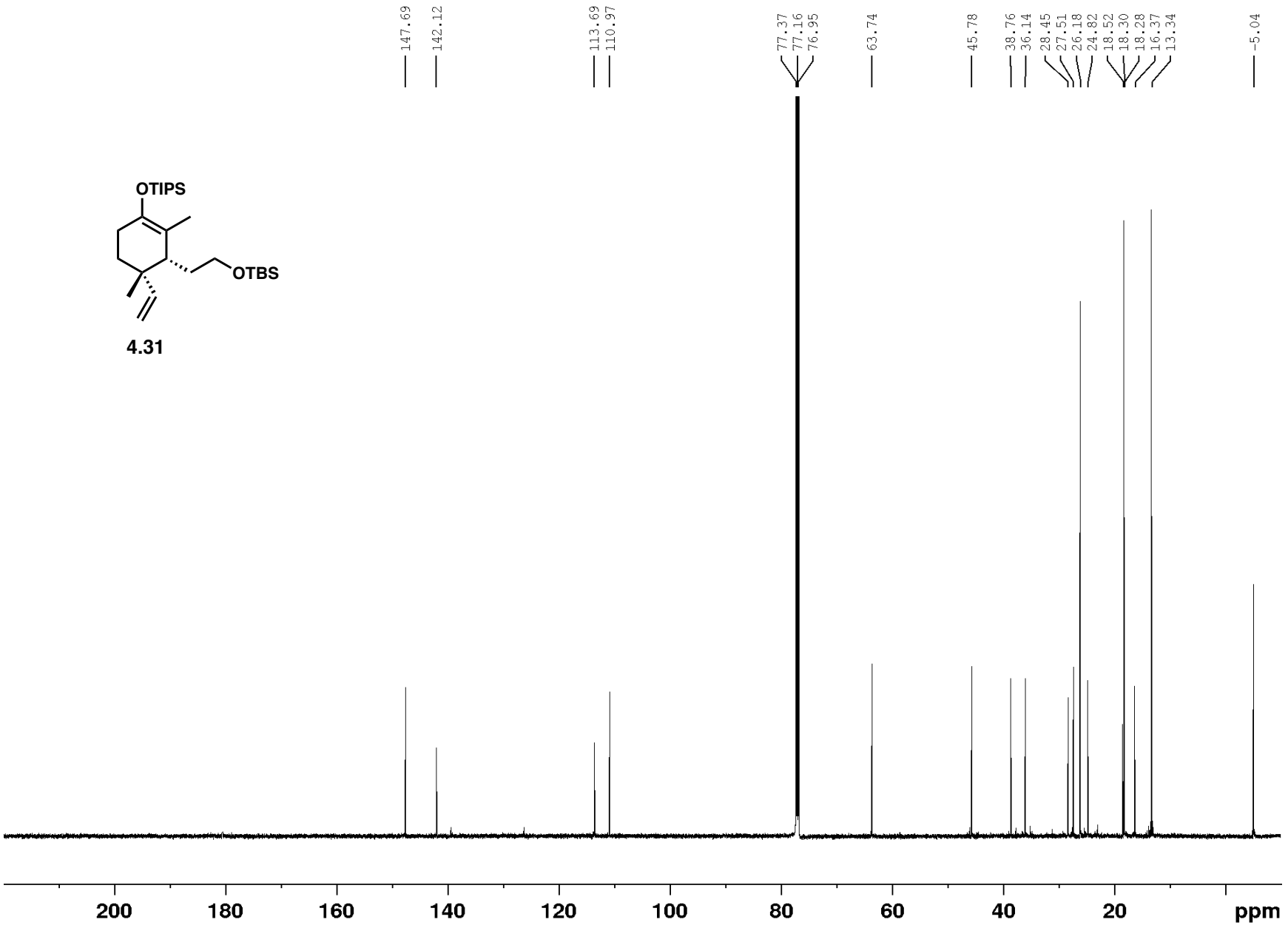

143.36
136.32
136.16
134.22
133.39
129.84
129.80
127.71
127.59
78.11
77.41
77.16
76.90
71.10
67.80
58.86
45.55
27.12
24.90
24.29
19.80
19.50
TBDPSO
O
I
4.18
210 200 190 180 170 160 150 140 130 120 110 100 90 80 70 60 50 40 30 20 10 ppm

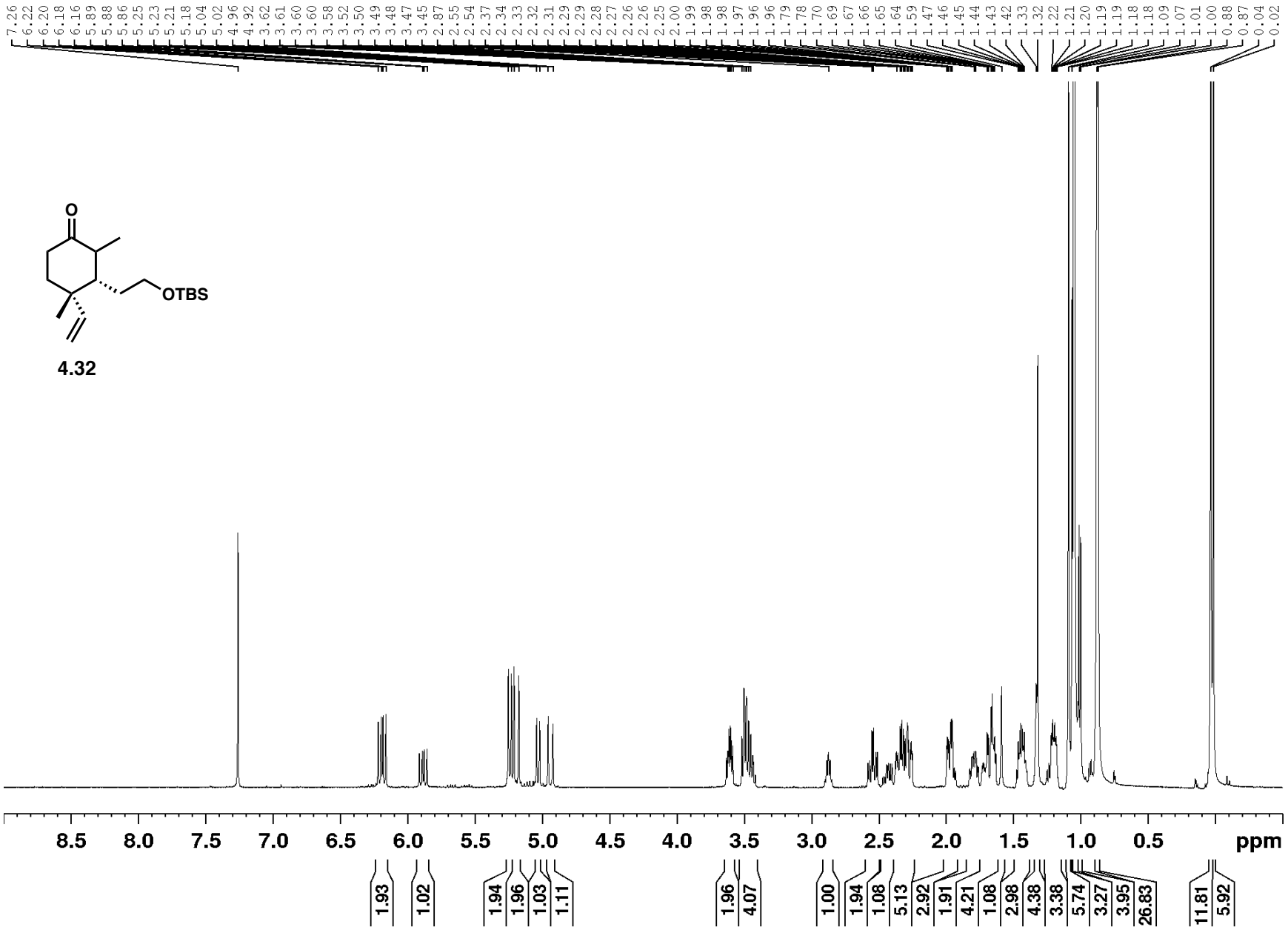

9.59
7.26
3.60
3.59
3.58
3.58
3.57
3.57
3.56
3.55
3.55
3.54
3.54
3.53
2.13
2.12
2.12
2.11
2.11
2.10
1.88
1.87
1.86
1.85
1.85
1.83
1.69
1.58
1.57
1.57
1.56
1.54
1.53
1.52
1.51
1.50
1.49
1.49
1.48
1.47
1.16
1.15
1.14
1.14
1.13
1.12
1.11
1.10
1.09
1.08
1.08
0.89
0.03
OTIPS
OTBS
CHO
4.29
9.5
9.0
8.5
8.0
7.5
7.0
6.5
6.0
5.5
5.0
4.5
4.0
3.5
3.0
2.5
2.0
1.5
1.0
0.5
0.0
ppm
0.93
2.02
2.92
1.00
3.21
3.43
24.18
9.40
6.07

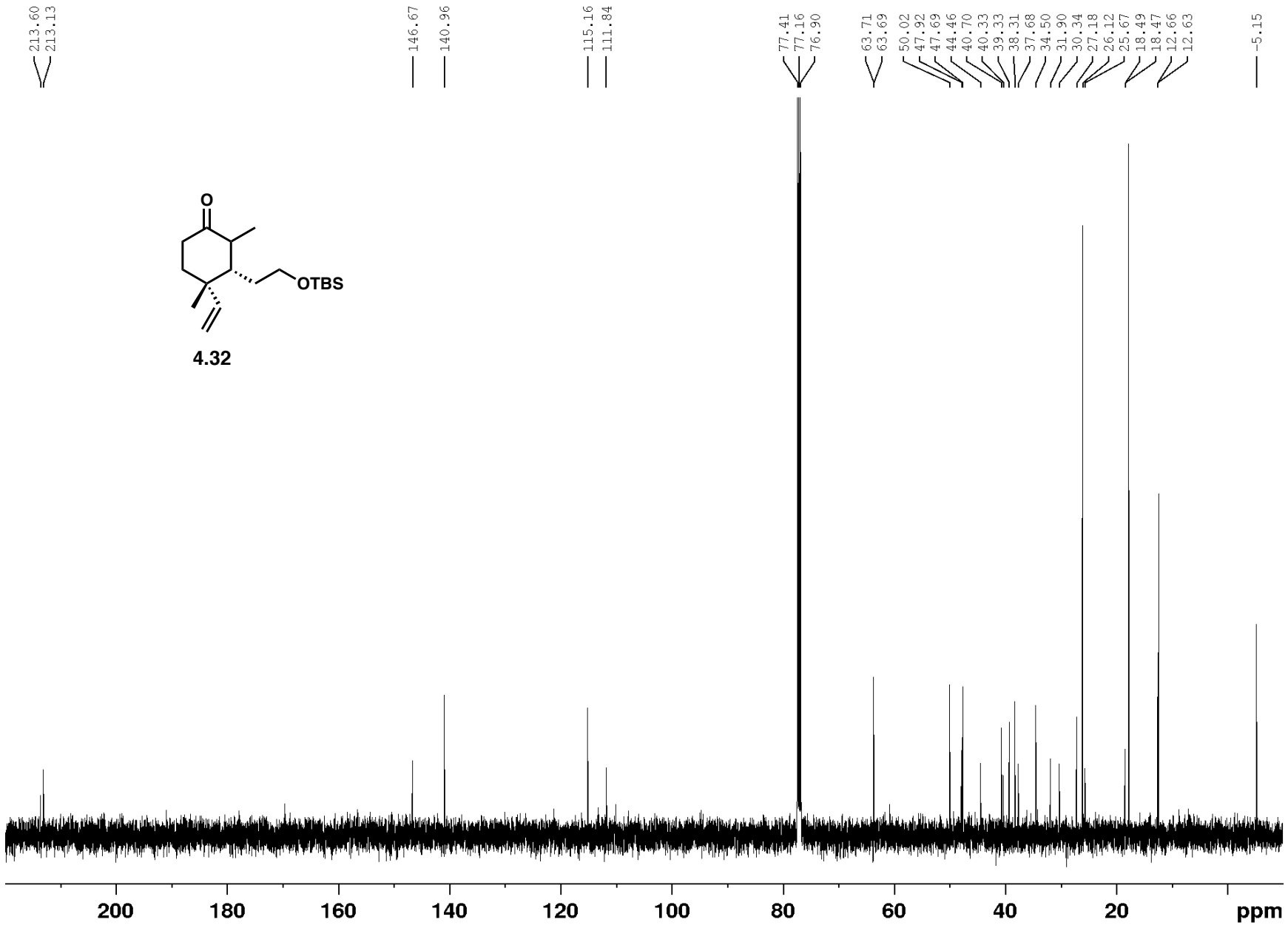

206.52
142.83
112.20
77.37
77.16
76.95
62.38
48.56
42.18
36.61
26.63
26.10
24.07
19.17
18.44
18.26
18.24
16.55
13.33
-5.19
OTIPS
OTBS
CHO
4.29
210 200 190 180 170 160 150 140 130 120 110 100 90 80 70 60 50 40 30 20 10 ppm

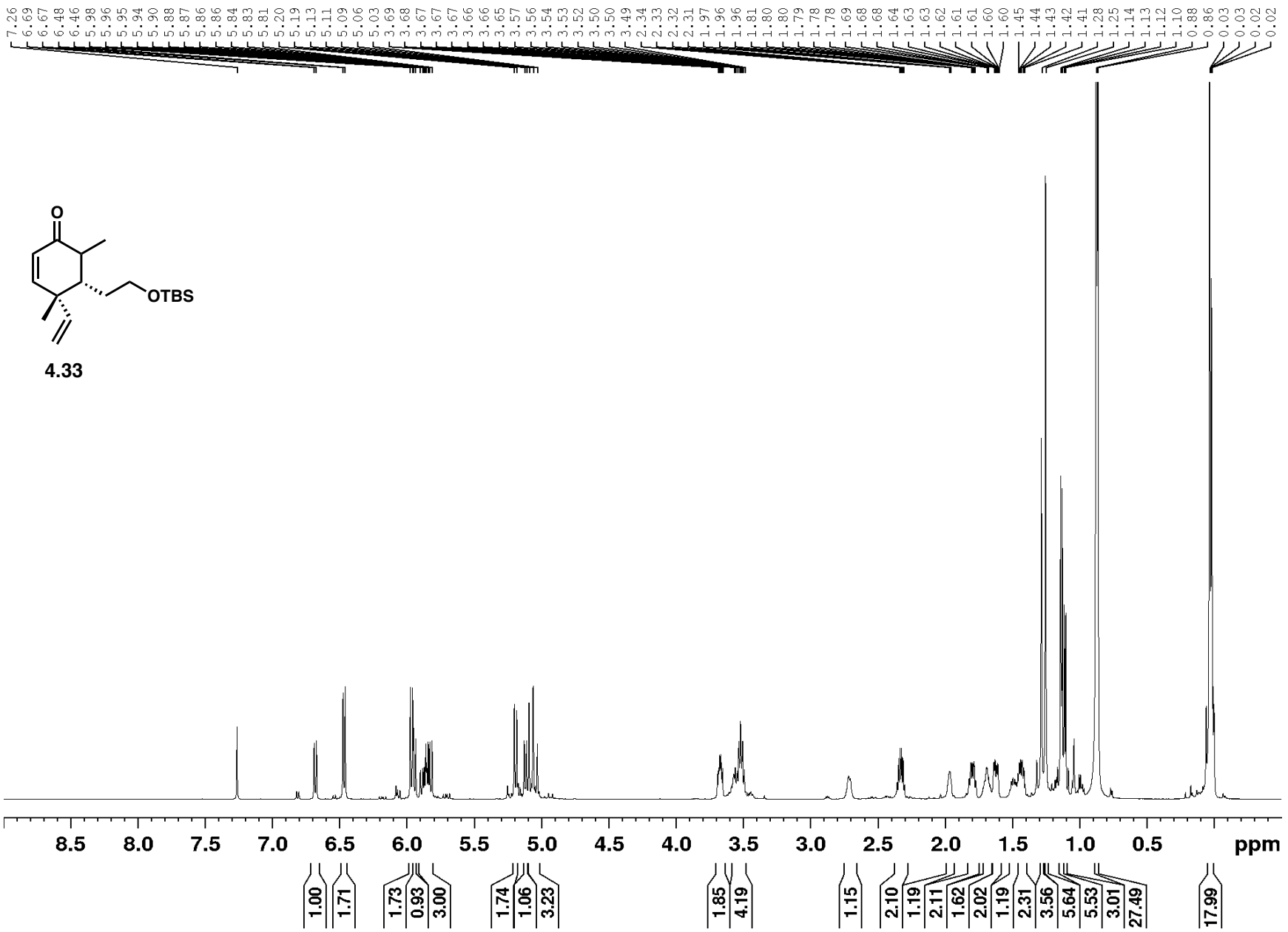

OTIPS
OTBS
7.26
5.87
5.86
5.85
5.83
4.97
4.97
4.95
4.95
4.93
4.93
4.90
4.90
3.60
3.59
3.58
3.57
3.57
3.56
3.54
3.53
2.17
2.15
2.14
2.12
2.11
2.10
2.09
2.07
2.06
1.72
1.71
1.70
1.70
1.69
1.69
1.68
1.67
1.65
1.63
1.62
1.62
1.61
1.61
1.60
1.58
1.57
1.47
1.46
1.45
1.44
1.42
1.42
1.41
1.40
1.39
1.17
1.16
1.15
1.14
1.14
1.13
1.12
1.11
1.10
1.09
1.09
1.08
1.00
0.89
0.03
8.5
8.0
7.5
7.0
6.5
6.0
5.5
5.0
4.5
4.0
3.5
3.0
2.5
2.0
1.5
1.0
0.5
0.0
ppm
0.94
0.91
0.94
2.00
2.09
1.06
3.04
1.96
2.06
21.48
3.03
9.40
6.01

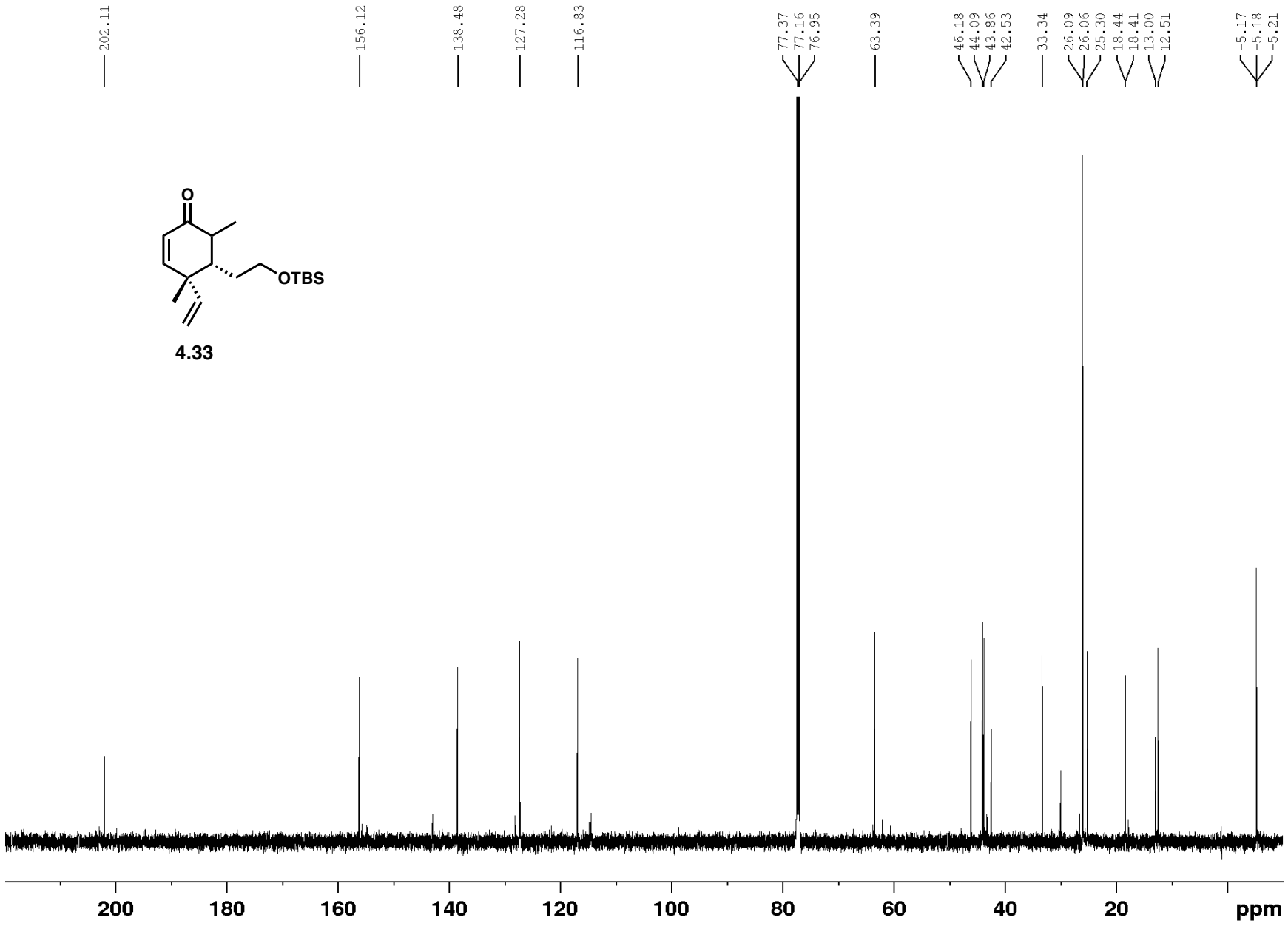
4.31

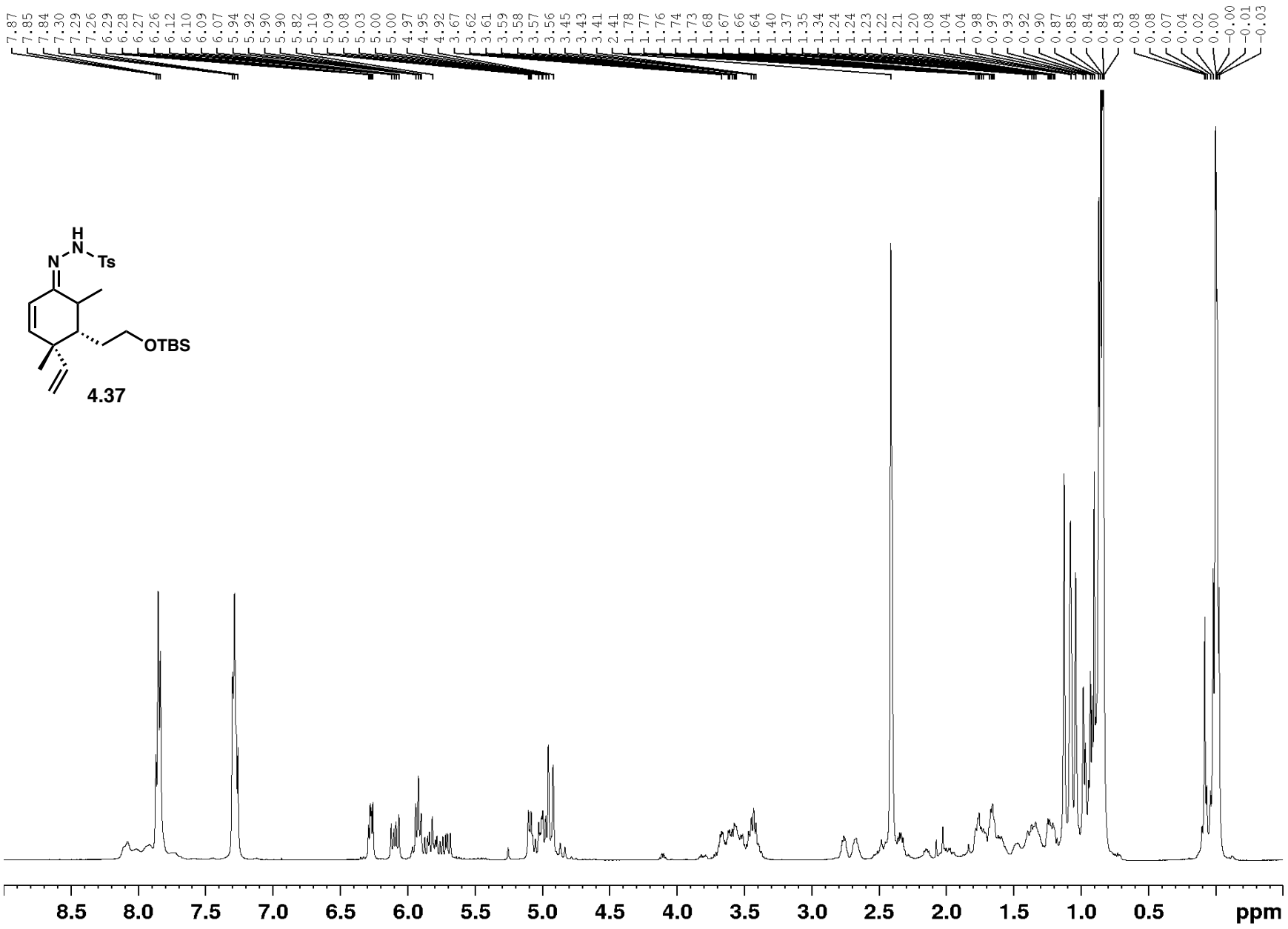

147.69
142.12
113.69
110.97
77.37
77.16
76.95
63.74
45.78
38.76
36.14
28.45
27.51
26.18
24.82
18.52
18.30
18.28
16.37
13.34
-5.04
OTIPS
OTBS
4.31
200
180
160
140
120
100
80
60
40
20
ppm

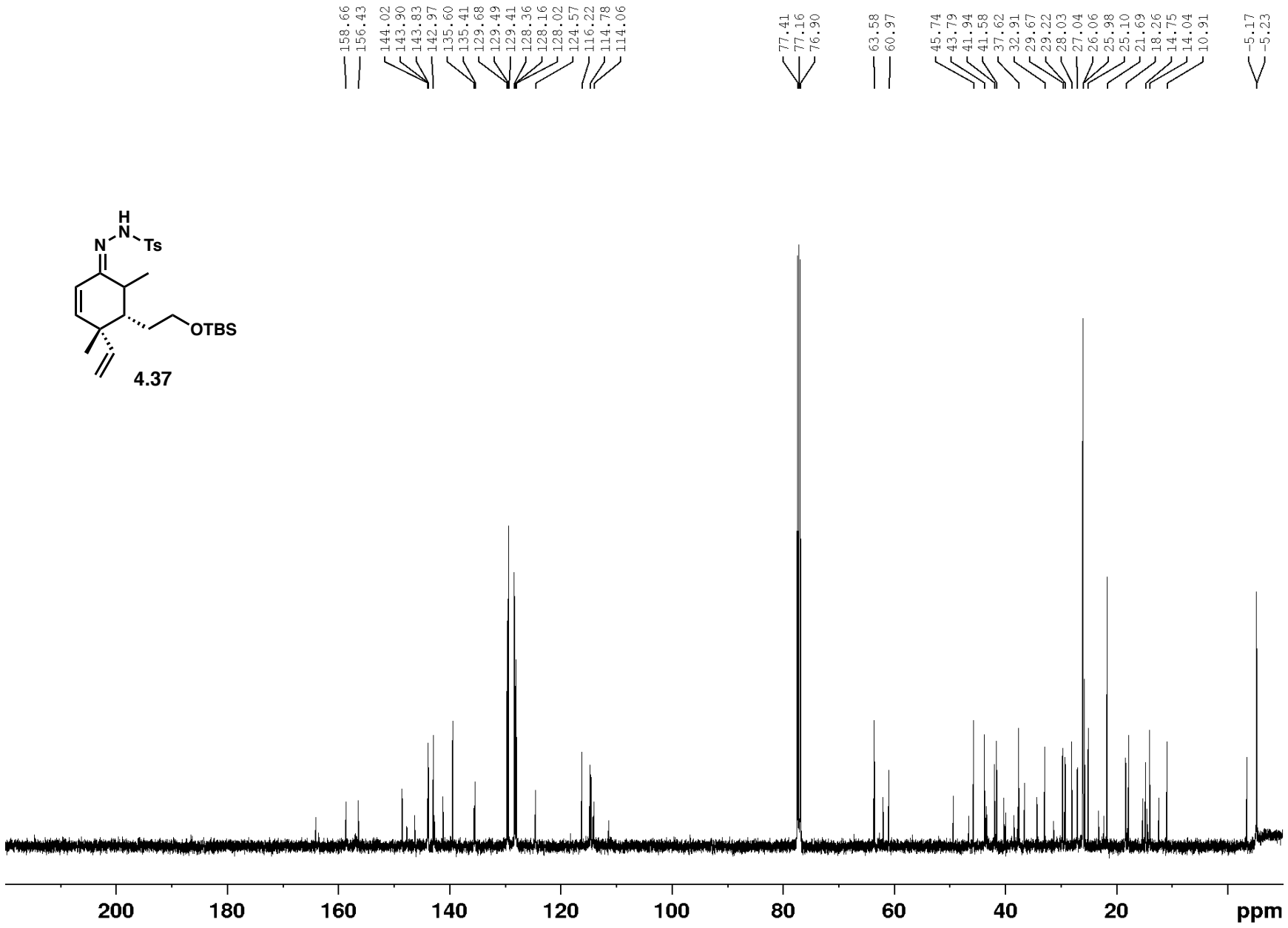

7.26
6.22
6.20
6.18
6.16
5.89
5.88
5.86
5.25
5.23
5.21
5.18
5.04
5.02
4.96
4.92
3.62
3.61
3.60
3.60
3.58
3.52
3.50
3.49
3.48
3.47
3.45
2.87
2.55
2.54
2.37
2.34
2.33
2.32
2.31
2.29
2.29
2.28
2.27
2.26
2.26
2.25
2.00
1.99
1.98
1.98
1.97
1.96
1.96
1.79
1.78
1.70
1.69
1.67
1.66
1.65
1.64
1.59
1.47
1.46
1.45
1.44
1.43
1.42
1.33
1.32
1.22
1.21
1.20
1.19
1.19
1.18
1.18
1.09
1.07
1.01
1.00
0.88
0.87
0.04
0.02
O
OTBS
4.32
8.5
8.0
7.5
7.0
6.5
6.0
5.5
5.0
4.5
4.0
3.5
3.0
2.5
2.0
1.5
1.0
0.5
ppm
1.93
1.02
1.94
1.96
1.03
1.11
1.96
4.07
1.00
1.94
1.08
5.13
2.92
1.91
4.21
1.08
2.98
4.38
3.38
5.74
3.27
3.95
26.83
11.81
5.92

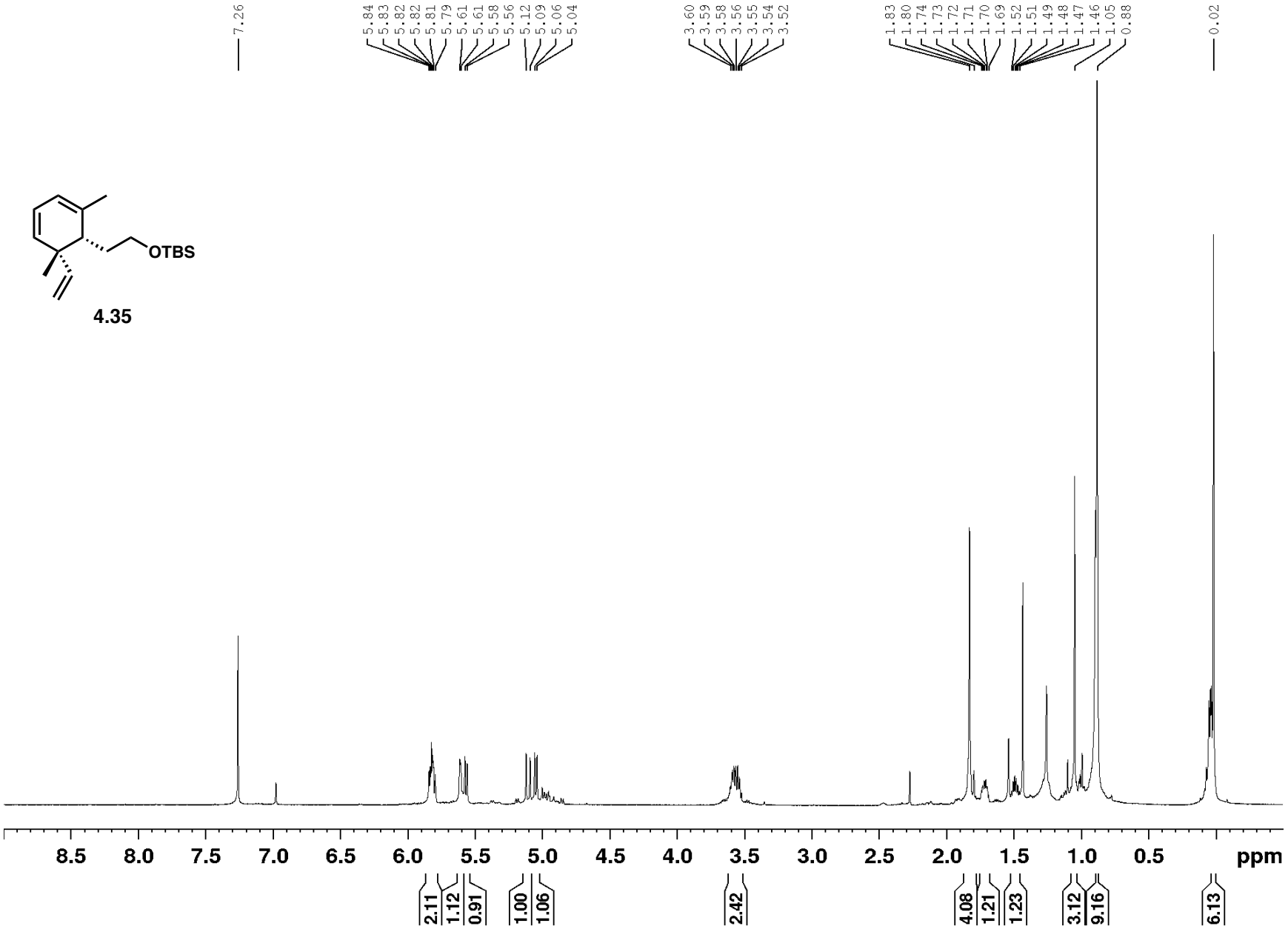

213.60
213.13
146.67
140.96
115.16
111.84
77.41
77.16
76.90
63.71
63.69
50.02
47.92
47.69
44.46
40.70
40.33
39.33
38.31
37.68
34.50
31.90
30.34
27.18
26.12
25.67
18.49
18.47
12.66
12.63
-5.15
O
OTBS
4.32
200
180
160
140
120
100
80
60
40
20
ppm

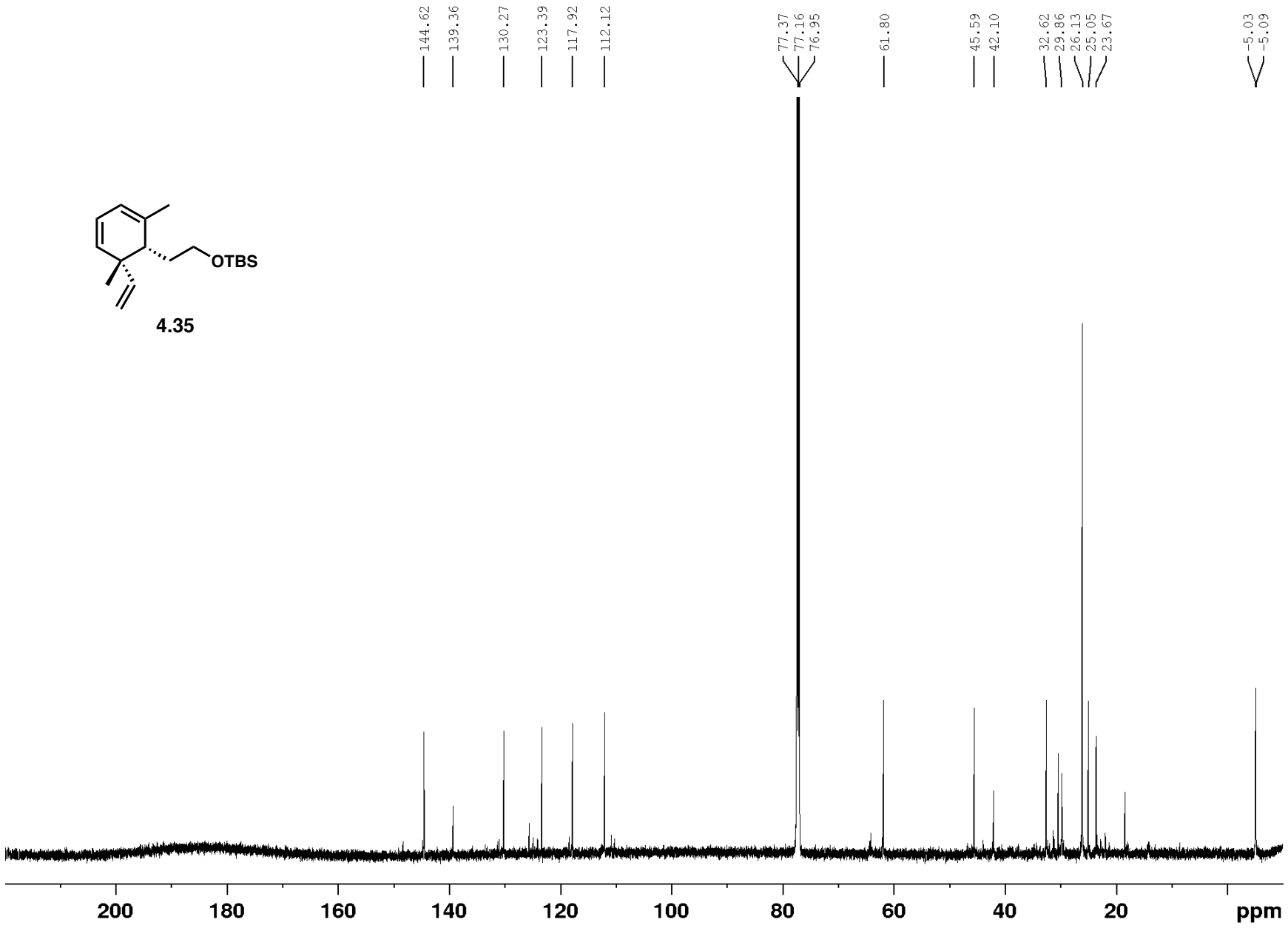

7.26 6.69 6.67 6.48 6.46 5.98 5.96 5.95 5.94 5.90 5.88 5.87 5.86 5.86 5.84 5.83 5.81 5.20 5.19 5.13 5.11 5.09 5.06 5.03 3.69 3.68 3.67 3.67 3.67 3.66 3.65 3.57 3.56 3.54 3.53 3.52 3.50 3.50 3.49 2.34 2.33 2.32 2.31 1.97 1.96 1.96 1.81 1.80 1.80 1.79 1.78 1.78 1.69 1.68 1.68 1.64 1.63 1.63 1.62 1.61 1.61 1.60 1.60 1.45 1.44 1.43 1.42 1.41 1.28 1.25 1.14 1.13 1.12 1.10 0.88 0.86 0.03 0.03 0.02 0.02
O
OTBS
4.33
8.5 8.0 7.5 7.0 6.5 6.0 5.5 5.0 4.5 4.0 3.5 3.0 2.5 2.0 1.5 1.0 0.5 ppm
1.00 1.71 1.73 0.93 3.00 1.74 1.06 3.23 1.85 4.19 1.15 2.10 1.19 2.11 1.62 2.02 1.19 2.31 3.56 5.64 5.53 3.01 27.49 17.99

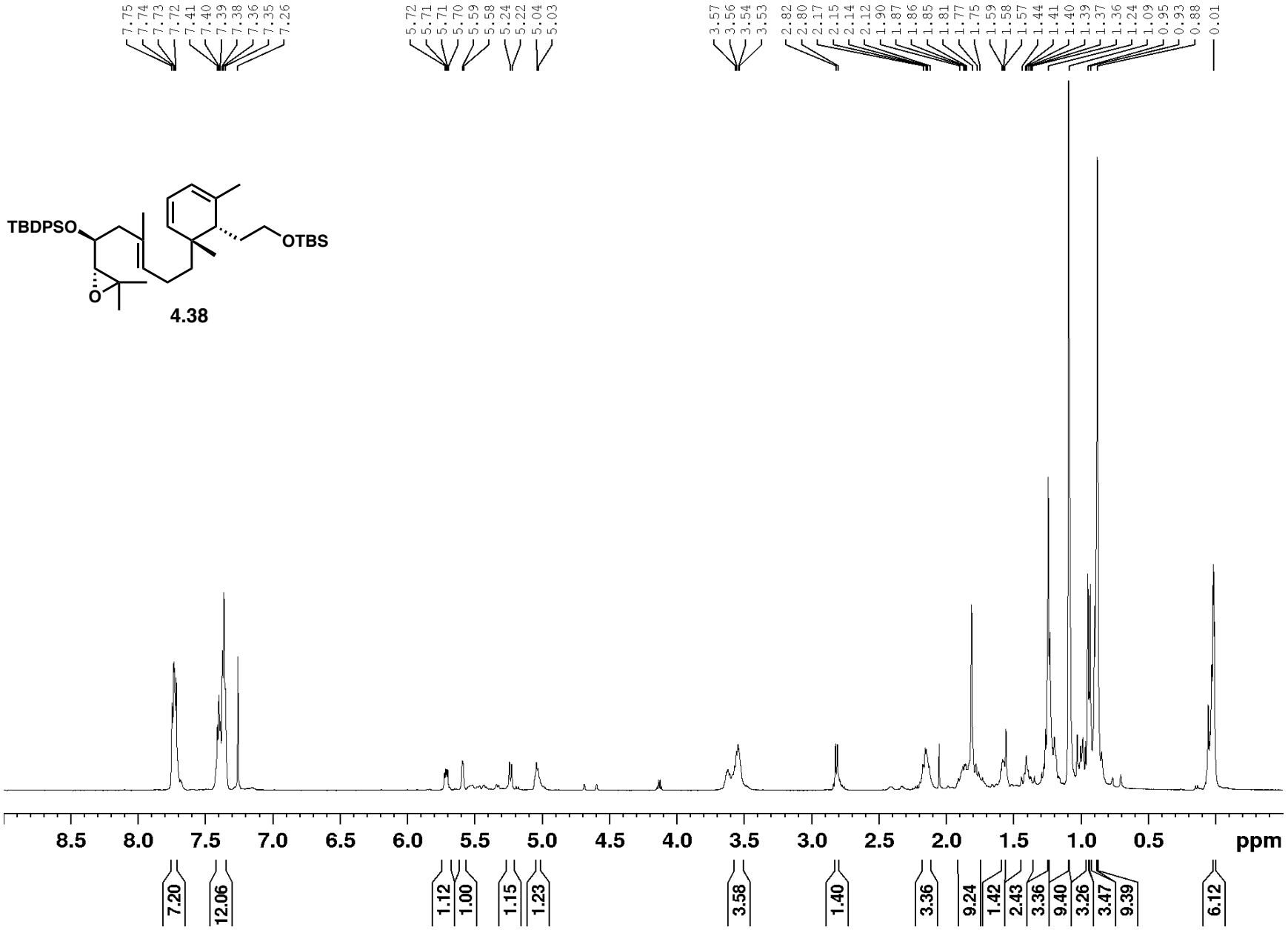

202.11
156.12
138.48
127.28
116.83
77.37
77.16
76.95
63.39
46.18
44.09
43.86
42.53
33.34
26.09
26.06
25.30
18.44
18.41
13.00
12.51
-5.17
-5.18
-5.21
O
OTBS
4.33
200
180
160
140
120
100
80
60
40
20
ppm

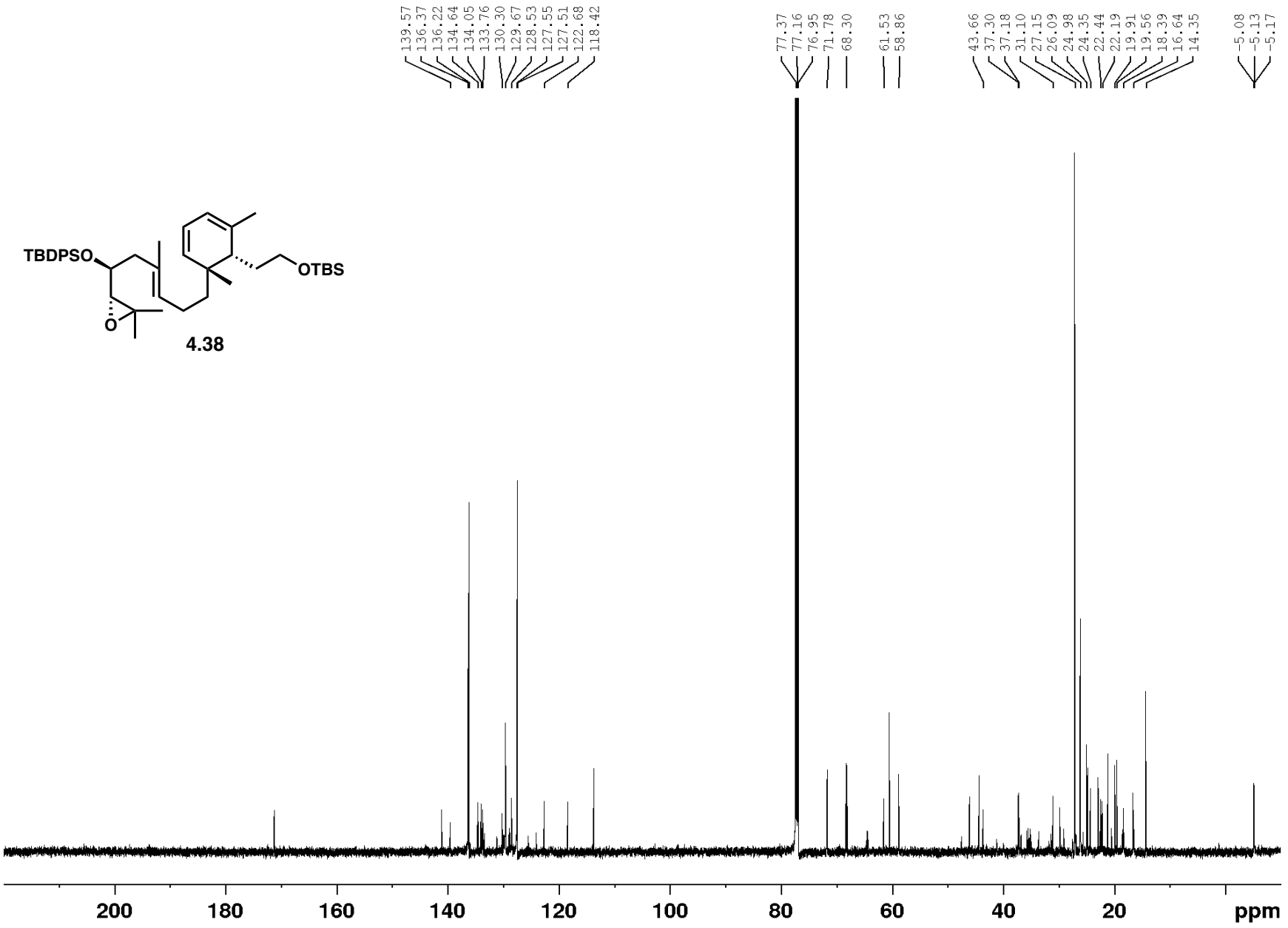

7.87 7.85 7.84 7.30 7.29 7.26 6.29 6.28 6.27 6.26 6.12 6.10 6.09 6.07 5.94 5.92 5.90 5.90 5.82 5.10 5.09 5.08 5.03 5.00 5.00 4.97 4.95 4.92 3.67 3.62 3.61 3.59 3.58 3.57 3.56 3.45 3.43 3.41 2.41 1.78 1.77 1.76 1.74 1.73 1.68 1.67 1.66 1.64 1.40 1.37 1.35 1.34 1.24 1.24 1.23 1.22 1.21 1.20 1.08 1.04 1.04 0.98 0.97 0.93 0.92 0.90 0.87 0.85 0.84 0.84 0.83 0.08 0.08 0.07 0.04 0.02 0.00 -0.00 -0.01 -0.03
H
N
N
Ts
OTBS
4.37
8.5 8.0 7.5 7.0 6.5 6.0 5.5 5.0 4.5 4.0 3.5 3.0 2.5 2.0 1.5 1.0 0.5 ppm

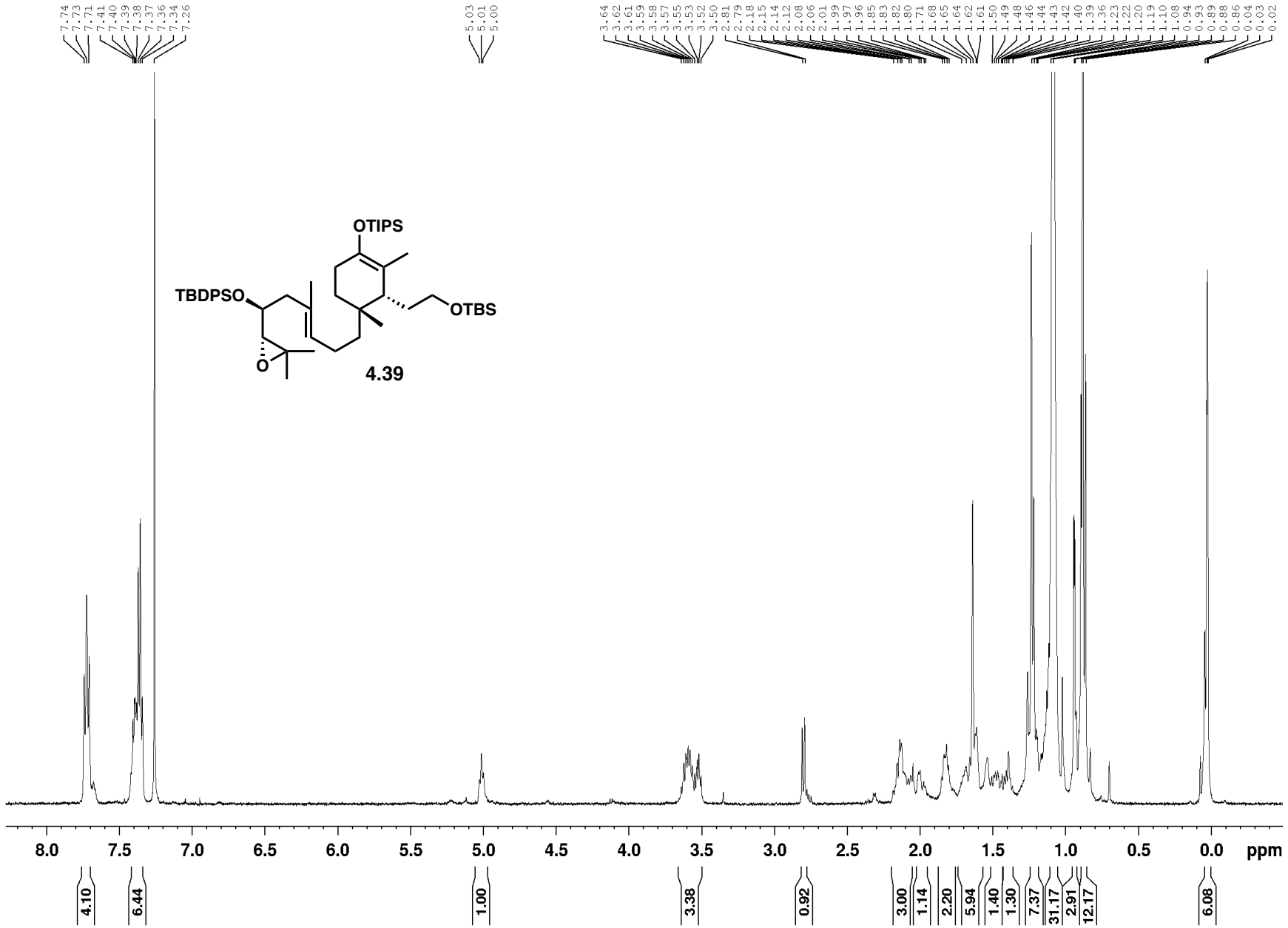

158.66
156.43
144.02
143.90
143.83
142.97
135.60
135.41
129.68
129.49
129.41
128.36
128.16
128.02
124.57
116.22
114.78
114.06
77.41
77.16
76.90
63.58
60.97
45.74
43.79
41.94
41.58
37.62
32.91
29.67
29.22
28.03
27.04
26.06
25.98
25.10
21.69
18.26
14.75
14.04
10.91
-5.17
-5.23
H
N
N
Ts
OTBS
4.37
200
180
160
140
120
100
80
60
40
20
ppm

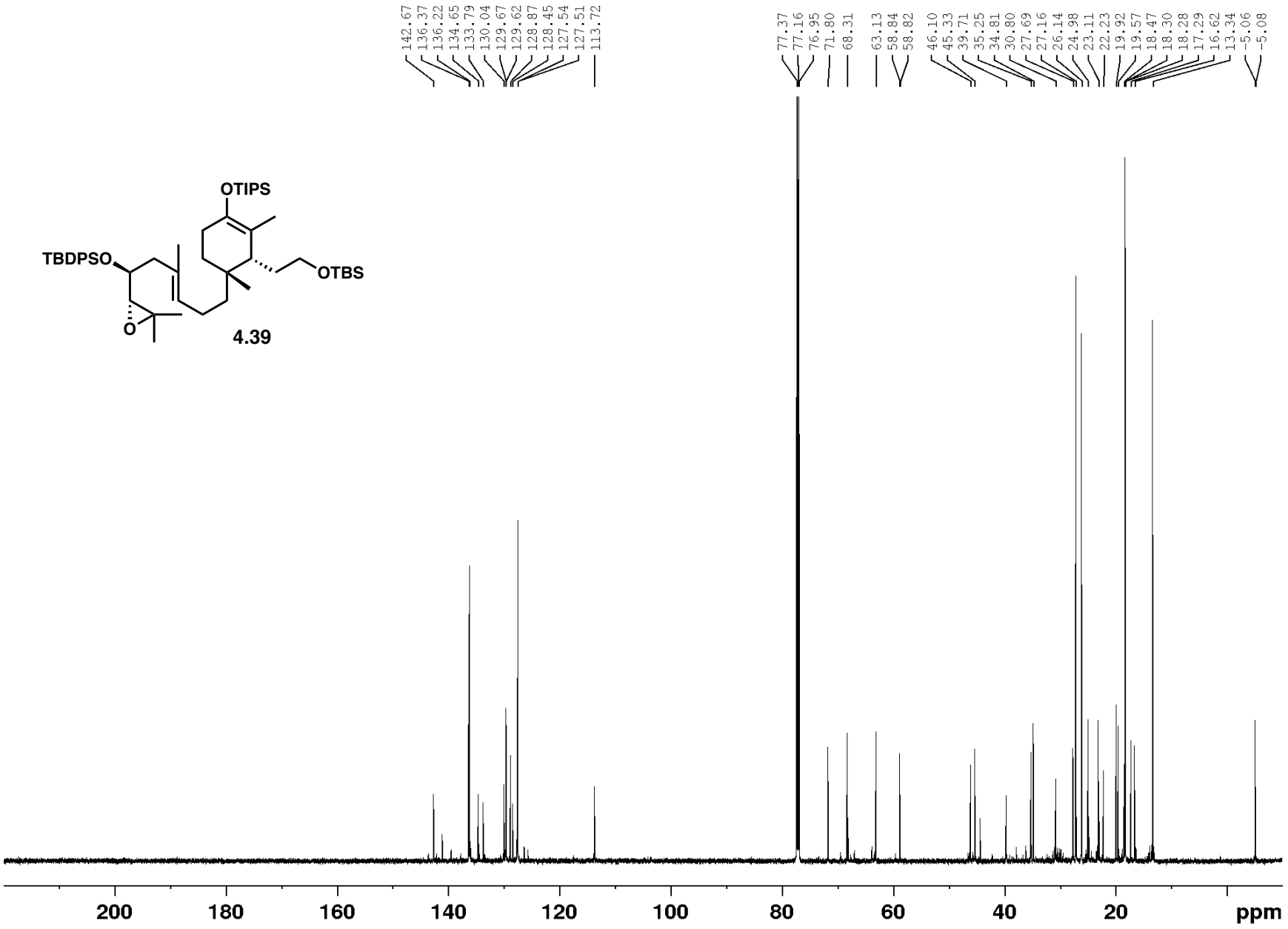

7.26
5.84
5.83
5.82
5.82
5.81
5.79
5.61
5.61
5.58
5.56
5.12
5.09
5.06
5.04
3.60
3.59
3.58
3.56
3.55
3.54
3.52
1.83
1.80
1.74
1.73
1.72
1.71
1.70
1.69
1.52
1.51
1.49
1.48
1.47
1.46
1.05
0.88
0.02
OTBS
4.35
8.5
8.0
7.5
7.0
6.5
6.0
5.5
5.0
4.5
4.0
3.5
3.0
2.5
2.0
1.5
1.0
0.5
ppm
2.11
1.12
0.91
1.00
1.06
2.42
4.08
1.21
1.23
3.12
9.16
6.13

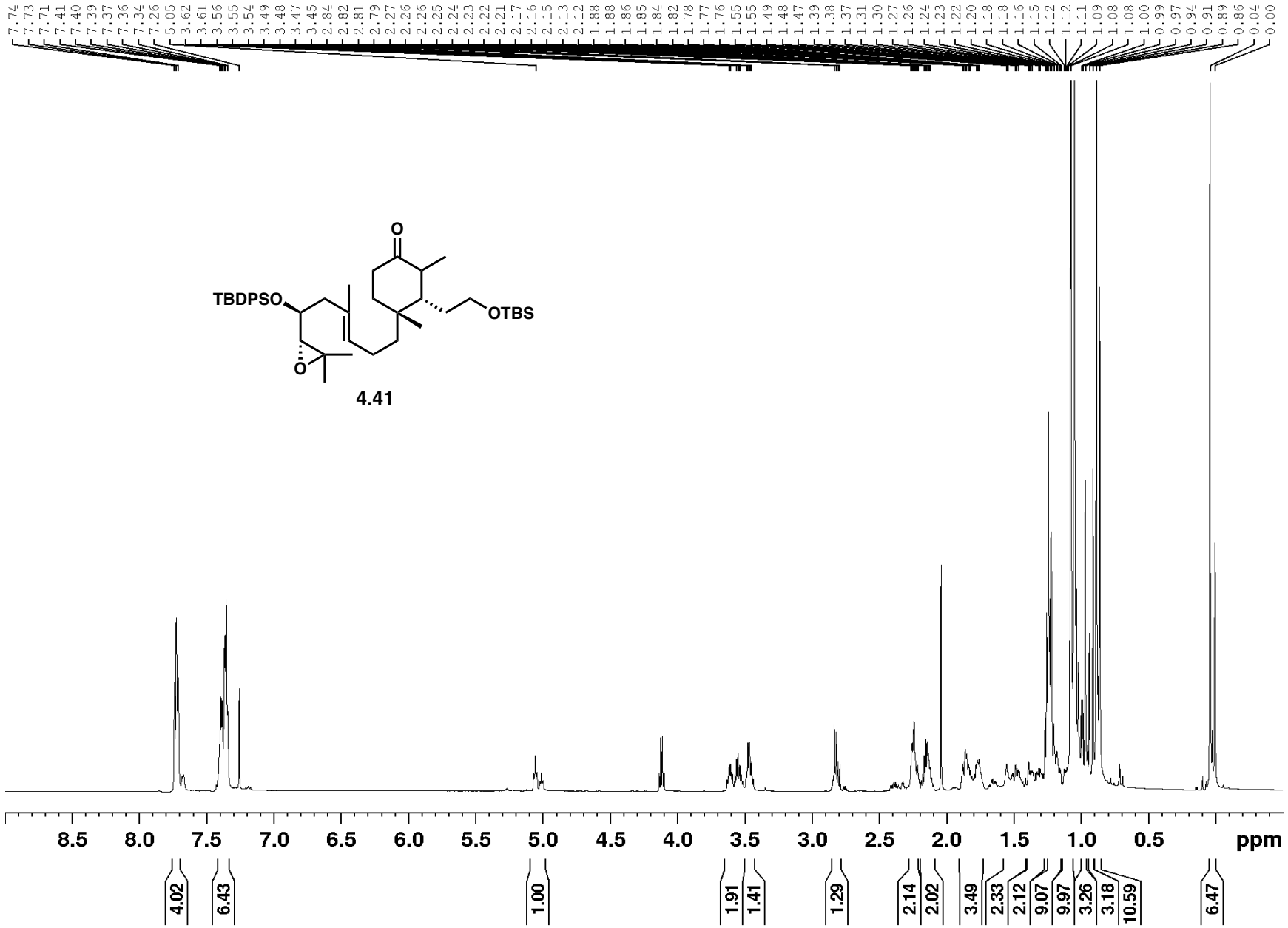

144.62
139.36
130.27
123.39
117.92
112.12
77.37
77.16
76.95
61.80
45.59
42.10
32.62
29.86
26.13
25.05
23.67
-5.03
-5.09
OTBS
4.35
200
180
160
140
120
100
80
60
40
20
ppm

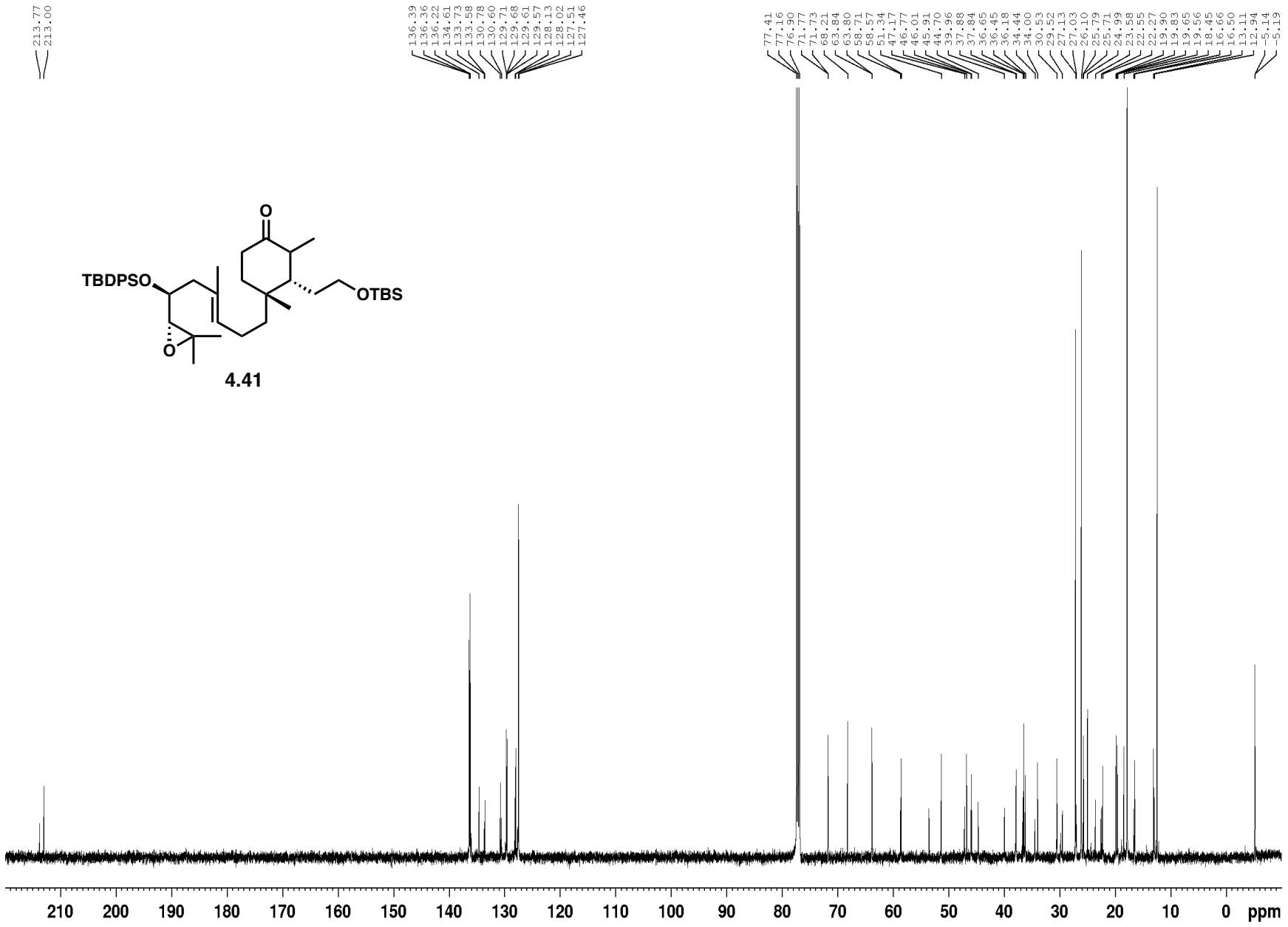

7.75
7.74
7.73
7.72
7.41
7.40
7.39
7.38
7.36
7.35
7.26
5.72
5.71
5.71
5.70
5.59
5.58
5.24
5.22
5.04
5.03
3.57
3.56
3.54
3.53
2.82
2.80
2.17
2.15
2.14
2.12
1.90
1.87
1.86
1.85
1.81
1.77
1.75
1.59
1.58
1.57
1.44
1.41
1.40
1.39
1.37
1.36
1.24
1.09
0.95
0.93
0.88
0.01
TBDPSO
OTBS
O
4.38
8.5
8.0
7.5
7.0
6.5
6.0
5.5
5.0
4.5
4.0
3.5
3.0
2.5
2.0
1.5
1.0
0.5
ppm
7.20
12.06
1.12
1.00
1.15
1.23
3.58
1.40
3.36
9.24
1.42
2.43
3.36
9.40
3.26
3.47
9.39
6.12

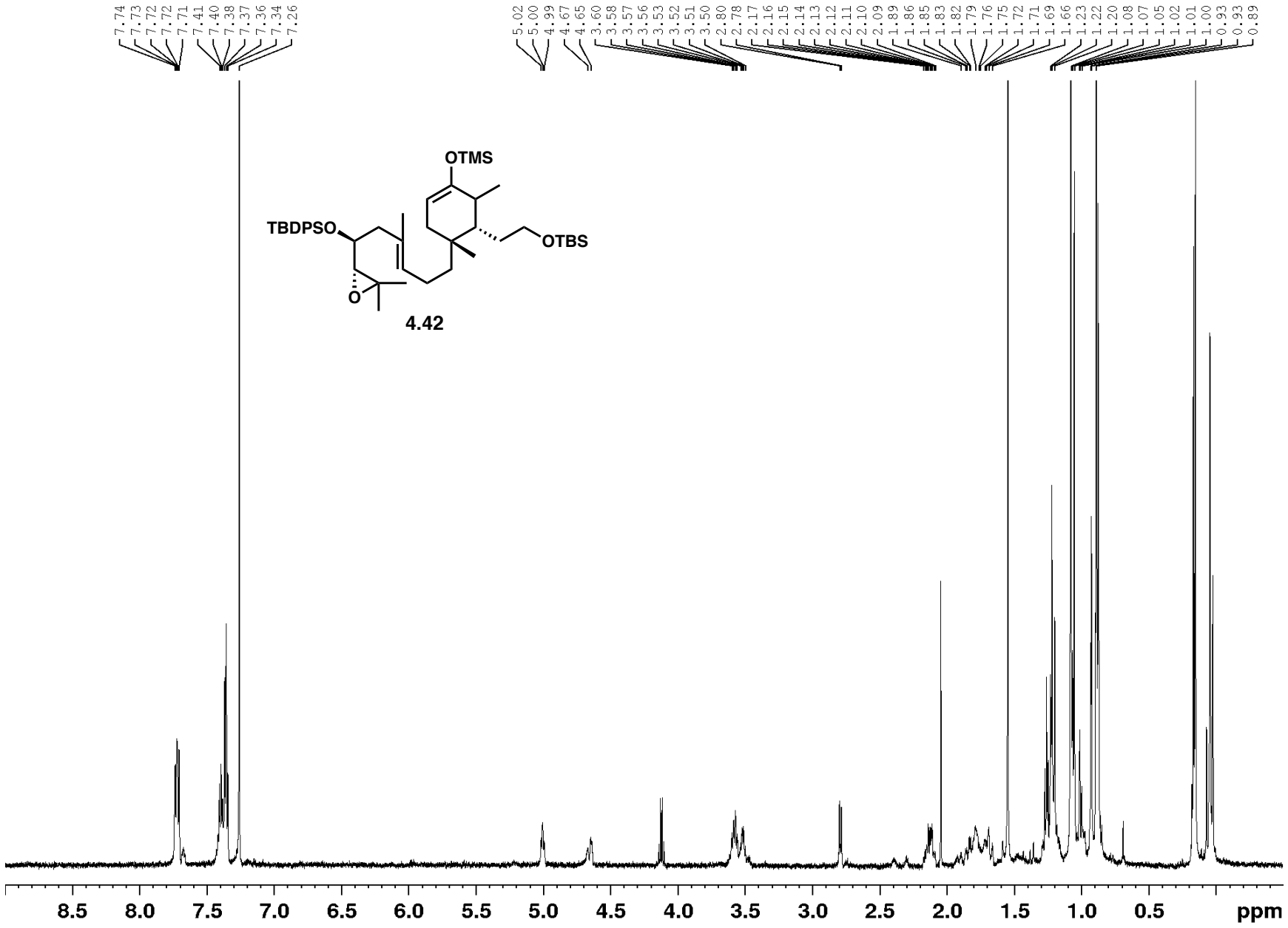

139.57
136.37
136.22
134.64
134.05
133.76
130.30
129.67
128.53
127.55
127.51
122.68
118.42
77.37
77.16
76.95
71.78
68.30
61.53
58.86
43.66
37.30
37.18
31.10
27.15
26.09
24.98
24.35
22.44
22.19
19.91
19.56
18.39
16.64
14.35
-5.08
-5.13
-5.17
TBDPSO
OTBS
O
4.38
200
180
160
140
120
100
80
60
40
20
ppm

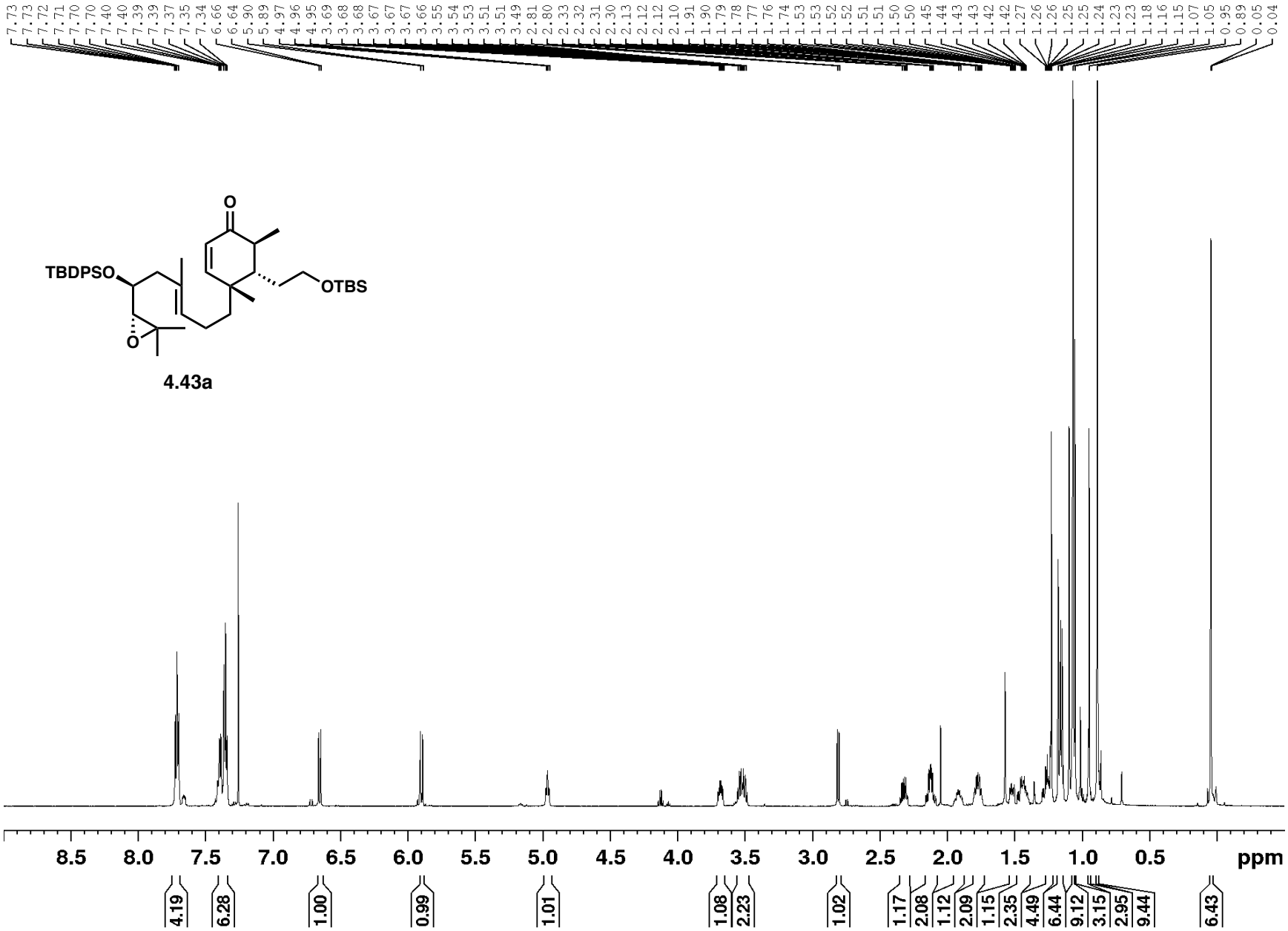

7.74
7.73
7.71
7.41
7.40
7.39
7.38
7.37
7.36
7.34
7.26
5.03
5.01
5.00
3.64
3.62
3.61
3.59
3.58
3.57
3.55
3.53
3.52
3.50
2.81
2.79
2.18
2.15
2.14
2.12
2.08
2.06
2.01
1.99
1.97
1.96
1.85
1.83
1.82
1.80
1.71
1.68
1.65
1.64
1.62
1.61
1.50
1.49
1.48
1.46
1.44
1.43
1.42
1.40
1.39
1.36
1.23
1.22
1.20
1.19
1.10
1.08
0.94
0.93
0.89
0.88
0.86
0.04
0.03
0.02
OTIPS
TBDPSO
OTBS
O
4.39
8.0
7.5
7.0
6.5
6.0
5.5
5.0
4.5
4.0
3.5
3.0
2.5
2.0
1.5
1.0
0.5
0.0
ppm
4.10
6.44
1.00
3.38
0.92
3.00
1.14
2.20
5.94
1.40
1.30
7.37
31.17
2.91
12.17
6.08

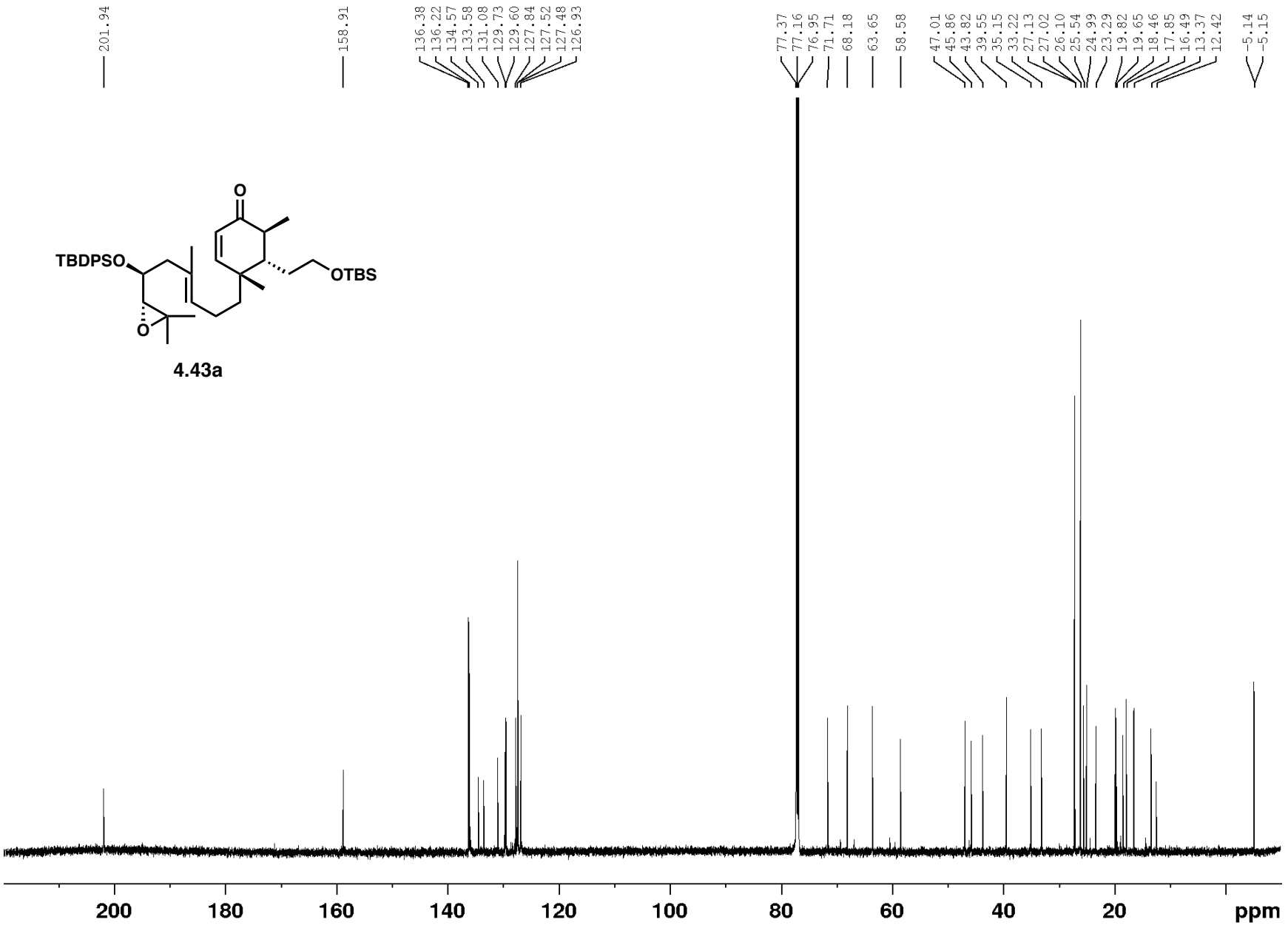

142.67
136.37
136.22
134.65
133.79
130.04
129.67
129.62
128.87
128.45
127.54
127.51
113.72
77.37
77.16
76.95
71.80
68.31
63.13
58.84
58.82
46.10
45.33
39.71
35.25
34.81
30.80
27.69
27.16
26.14
24.98
23.11
22.23
19.92
19.57
18.47
18.30
18.28
17.29
16.62
13.34
-5.06
-5.08
OTIPS
TBDPSO
OTBS
O
4.39
200
180
160
140
120
100
80
60
40
20
ppm


7.74 7.73 7.71 7.41 7.40 7.39 7.37 7.36 7.34 7.26 5.05 3.62 3.61 3.56 3.55 3.54 3.49 3.48 3.47 3.45 2.84 2.82 2.81 2.79 2.27 2.26 2.26 2.25 2.24 2.23 2.22 2.21 2.17 2.16 2.15 2.13 2.12 1.88 1.88 1.86 1.85 1.84 1.82 1.78 1.77 1.76 1.55 1.55 1.49 1.48 1.47 1.39 1.38 1.37 1.31 1.30 1.27 1.26 1.24 1.23 1.22 1.20 1.18 1.18 1.16 1.15 1.12 1.12 1.11 1.09 1.08 1.08 1.00 0.99 0.97 0.94 0.91 0.89 0.86 0.04 0.00
TBDPSO
OTBS
O
O
4.41
8.5 8.0 7.5 7.0 6.5 6.0 5.5 5.0 4.5 4.0 3.5 3.0 2.5 2.0 1.5 1.0 0.5 ppm
4.02 6.43 1.00 1.91 1.41 1.29 2.14 2.02 3.49 2.33 2.12 9.07 9.97 3.26 3.18 10.59 6.47

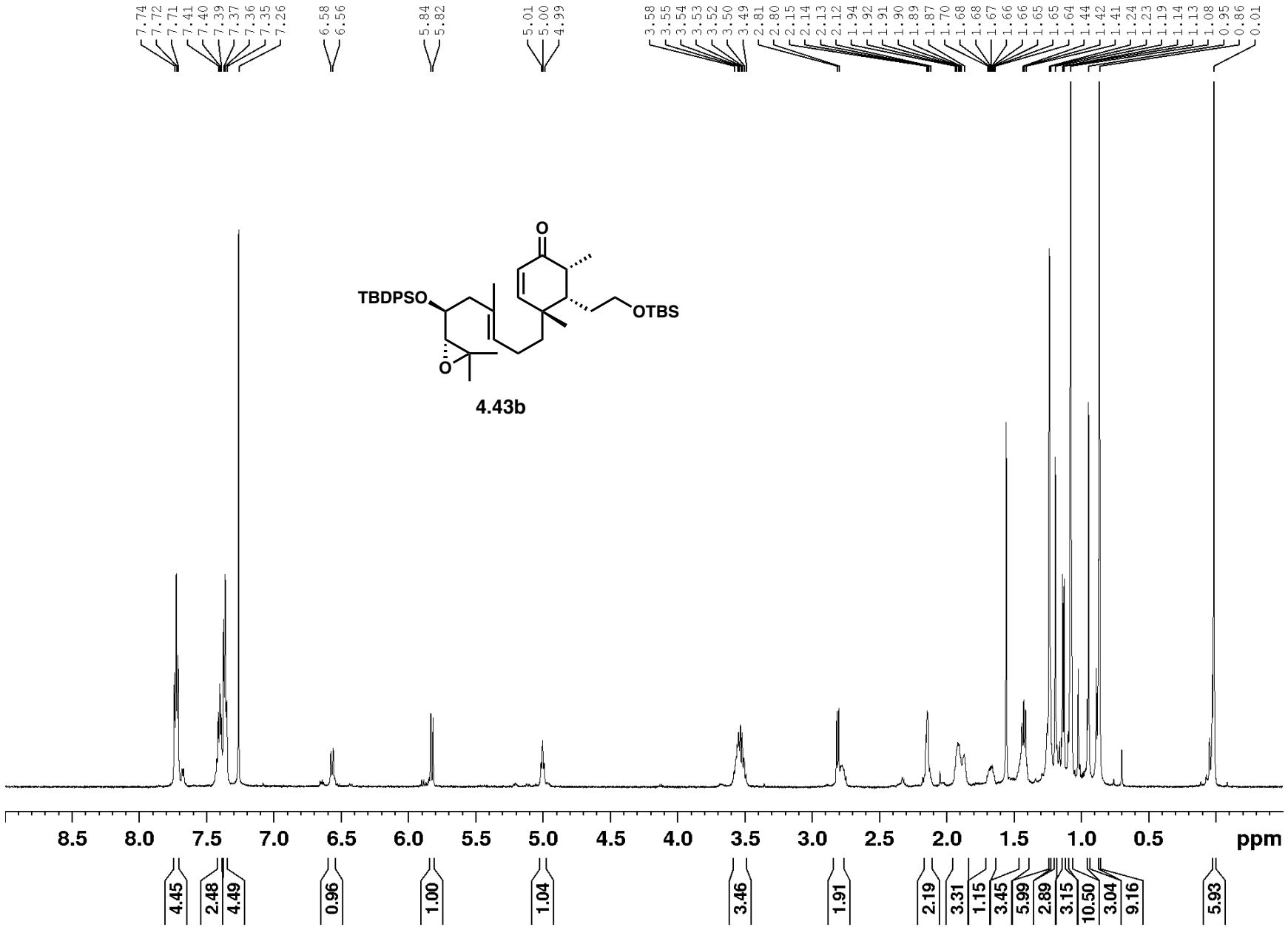

213.77
213.00
136.39
136.36
136.22
134.61
133.73
133.58
130.78
130.60
129.71
129.68
129.61
129.57
128.13
128.02
127.51
127.46
77.41
77.16
76.90
71.77
71.73
68.21
63.84
63.80
58.71
58.57
51.34
47.17
46.77
46.01
45.91
44.70
39.96
37.88
37.84
36.65
36.45
36.18
34.44
34.00
30.53
29.52
27.13
27.03
26.10
25.79
25.71
24.99
23.58
22.55
22.27
19.90
19.83
19.65
19.56
18.45
16.66
16.50
13.11
12.94
-5.14
-5.19
O
TBDPSO
OTBS
O
4.41
210
200
190
180
170
160
150
140
130
120
110
100
90
80
70
60
50
40
30
20
10
0
ppm

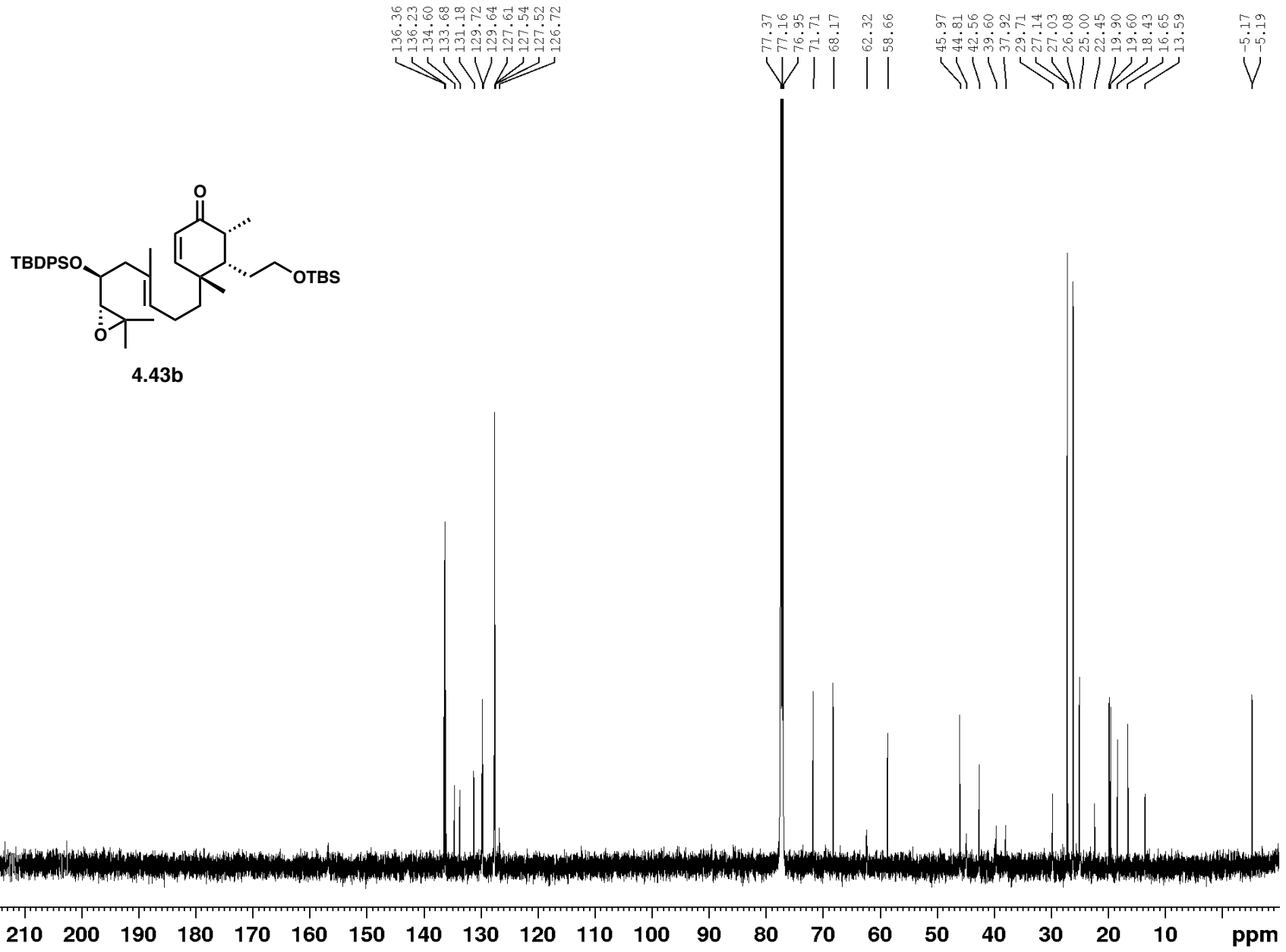

7.74
7.73
7.72
7.72
7.71
7.41
7.40
7.38
7.37
7.36
7.34
7.26
5.02
5.00
4.99
4.67
4.65
3.60
3.58
3.57
3.56
3.53
3.52
3.51
3.50
2.80
2.78
2.17
2.16
2.15
2.14
2.13
2.12
2.11
2.10
2.09
1.89
1.86
1.85
1.83
1.82
1.79
1.76
1.75
1.72
1.71
1.69
1.66
1.23
1.22
1.20
1.08
1.07
1.05
1.02
1.01
1.00
0.93
0.93
0.89
OTMS
TBDPSO
OTBS
O
4.42
8.5
8.0
7.5
7.0
6.5
6.0
5.5
5.0
4.5
4.0
3.5
3.0
2.5
2.0
1.5
1.0
0.5
ppm


7.73
7.73
7.72
7.71
7.70
7.70
7.40
7.40
7.39
7.39
7.37
7.35
7.34
6.66
6.64
5.90
5.89
4.97
4.96
4.95
3.69
3.68
3.68
3.67
3.67
3.67
3.66
3.55
3.54
3.53
3.51
3.51
3.49
2.81
2.80
2.33
2.32
2.31
2.30
2.13
2.12
2.12
2.10
1.91
1.90
1.79
1.78
1.77
1.76
1.74
1.53
1.53
1.52
1.52
1.51
1.51
1.50
1.50
1.45
1.44
1.43
1.43
1.42
1.42
1.27
1.26
1.26
1.25
1.25
1.25
1.24
1.23
1.23
1.18
1.16
1.15
1.07
1.05
0.95
0.89
0.05
0.04
O
TBDPSO
OTBS
O
4.43a
8.5
8.0
7.5
7.0
6.5
6.0
5.5
5.0
4.5
4.0
3.5
3.0
2.5
2.0
1.5
1.0
0.5
ppm
4.19
6.28
1.00
0.99
1.01
1.08
2.23
1.02
1.17
2.08
1.12
2.09
1.15
2.35
4.49
6.44
9.12
3.15
2.95
9.44
6.43

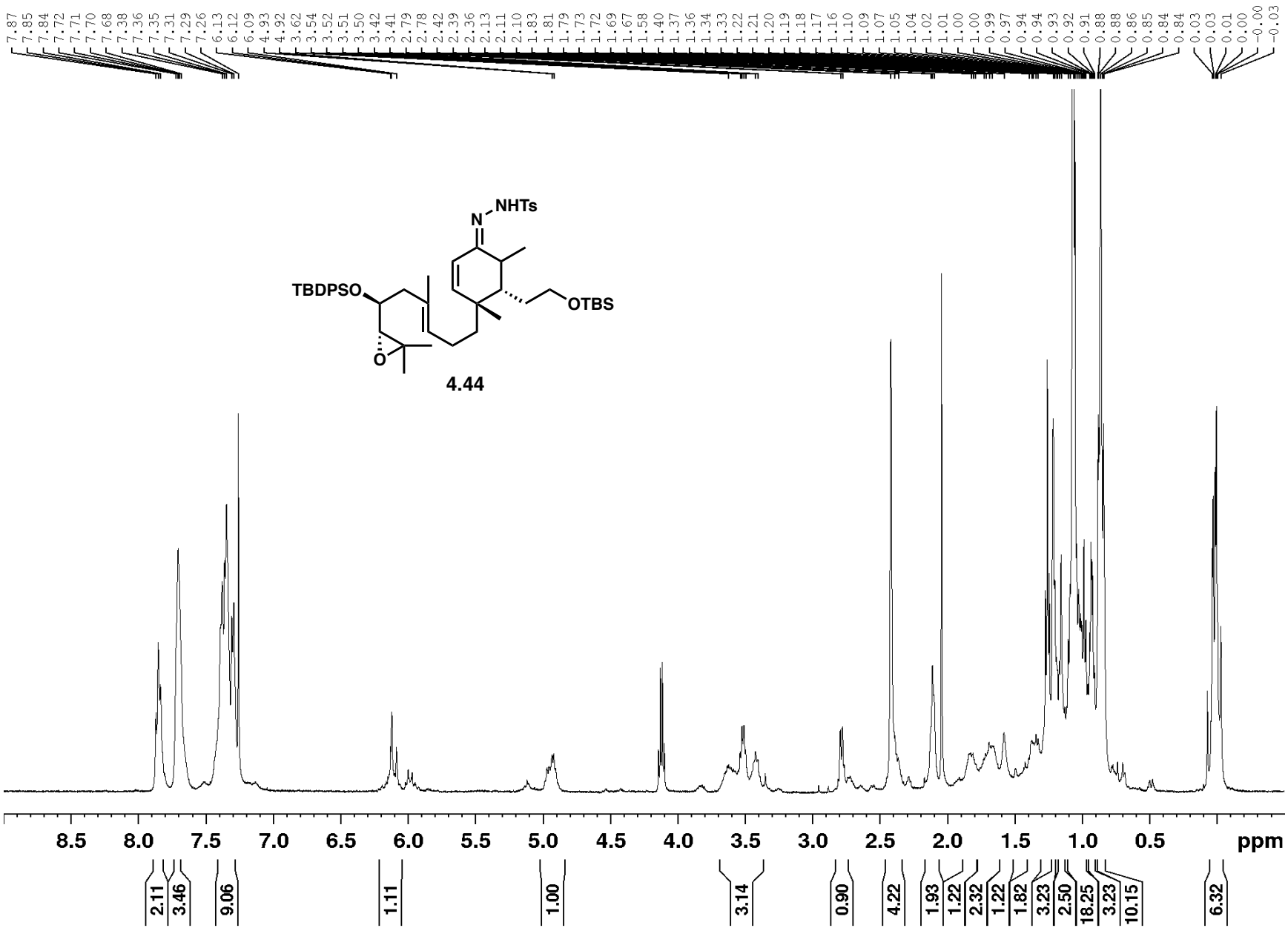

201.94
158.91
136.38
136.22
134.57
133.58
131.08
129.73
129.60
127.84
127.52
127.48
126.93
77.37
77.16
76.95
71.71
68.18
63.65
58.58
47.01
45.86
43.82
39.55
35.15
33.22
27.13
27.02
26.10
25.54
24.99
23.29
19.82
19.65
18.46
17.85
16.49
13.37
12.42
-5.14
-5.15
TBDPSO
OTBS
O
O
200
180
160
140
120
100
80
60
40
20
ppm

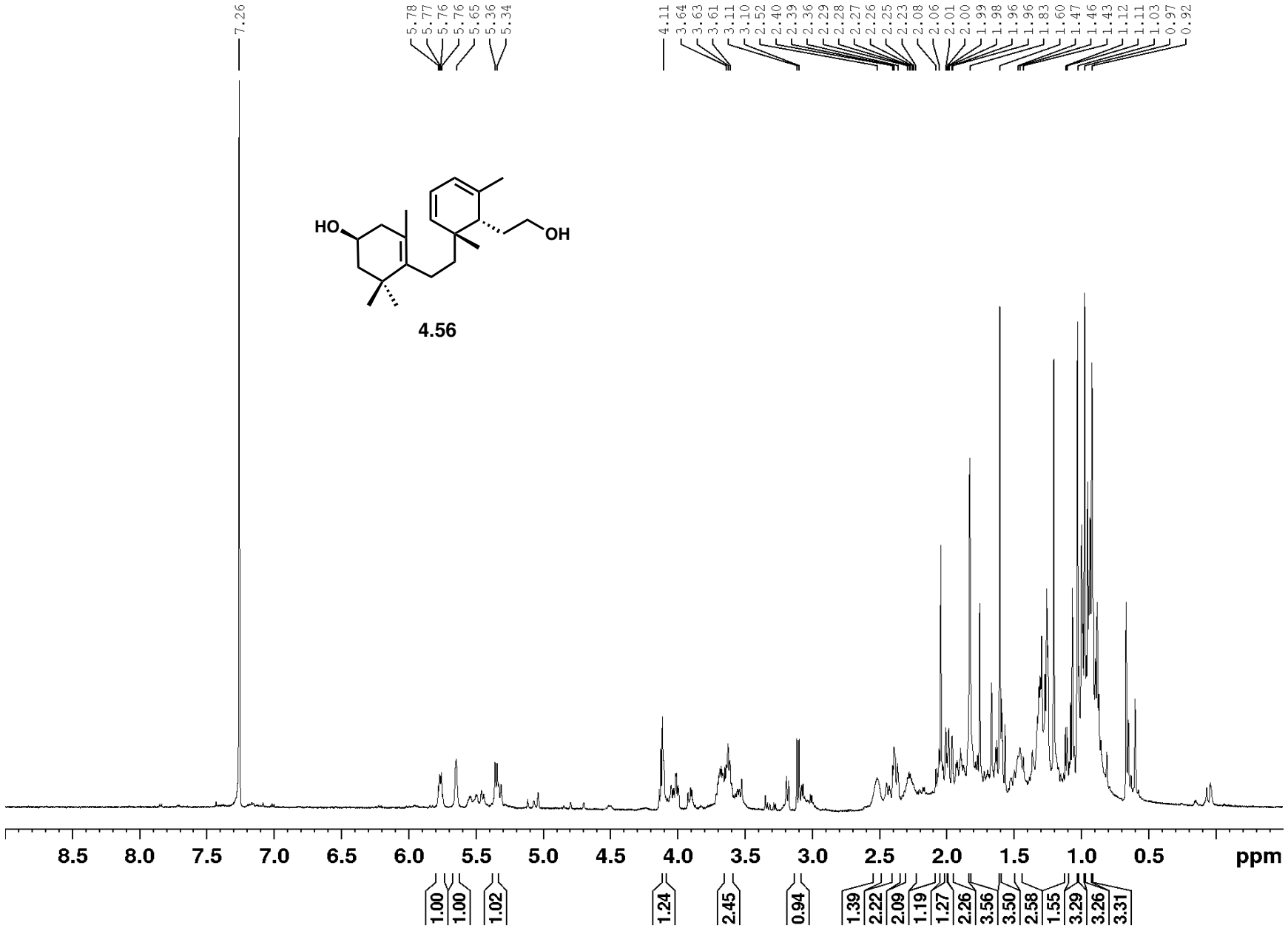
4.43a


7.74
7.72
7.71
7.41
7.40
7.39
7.37
7.36
7.35
7.26
6.58
6.56
5.84
5.82
5.01
5.00
4.99
3.58
3.55
3.54
3.53
3.52
3.50
3.49
2.81
2.80
2.15
2.14
2.13
2.12
1.94
1.92
1.91
1.90
1.89
1.87
1.70
1.68
1.68
1.67
1.66
1.66
1.65
1.65
1.64
1.44
1.42
1.41
1.24
1.23
1.19
1.14
1.13
1.08
0.95
0.86
0.01
O
TBDPSO
OTBS
O
4.43b
8.5
8.0
7.5
7.0
6.5
6.0
5.5
5.0
4.5
4.0
3.5
3.0
2.5
2.0
1.5
1.0
0.5
ppm
4.45
2.48
4.49
0.96
1.00
1.04
3.46
1.91
2.19
3.31
1.15
3.45
5.99
2.89
3.15
10.50
3.04
9.16
5.93

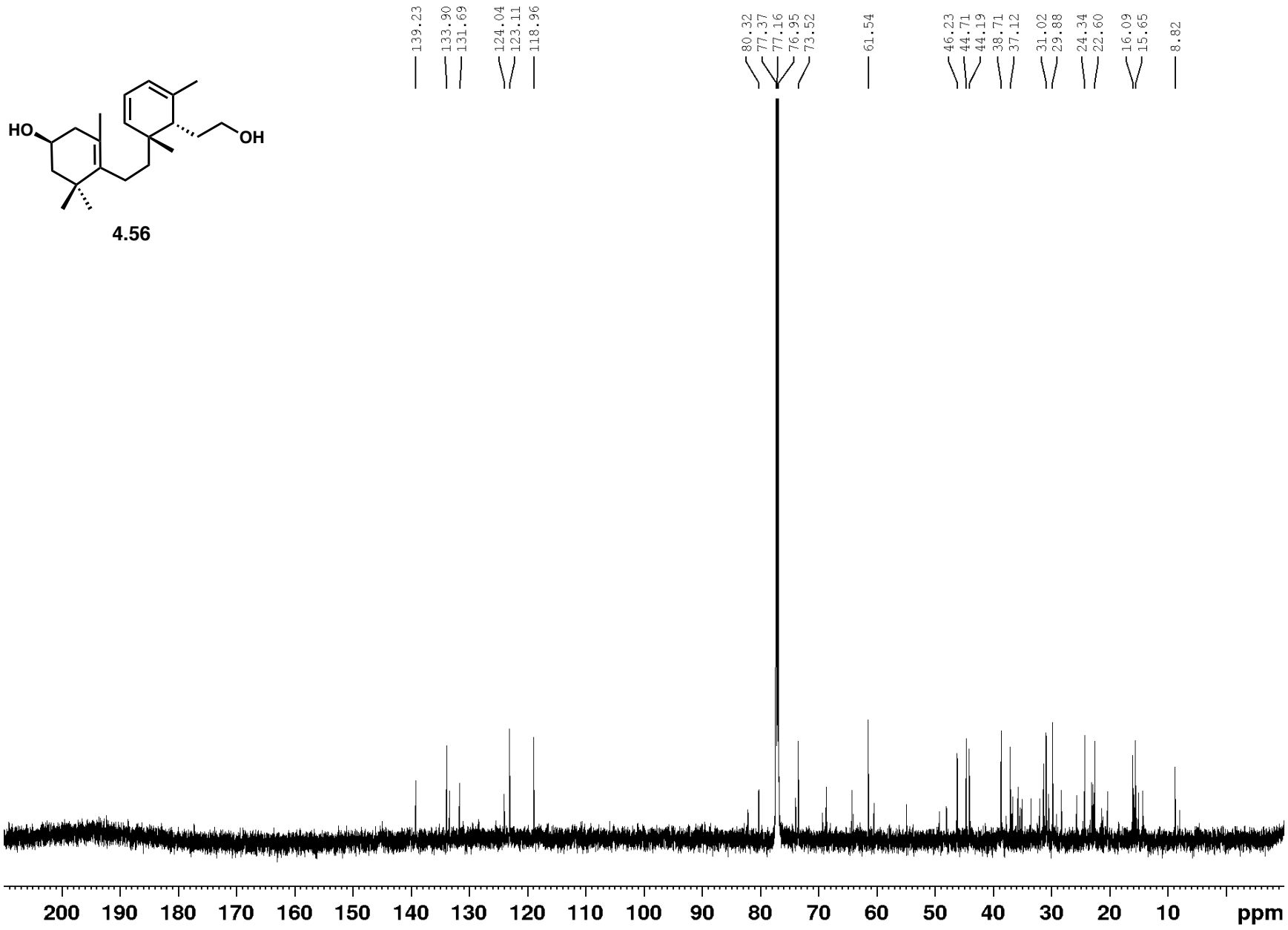

136.36
136.23
134.60
133.68
131.18
129.72
129.64
127.61
127.54
127.52
126.72
77.37
77.16
76.95
71.71
68.17
62.32
58.66
45.97
44.81
42.56
39.60
37.92
29.71
27.14
27.03
26.08
25.00
22.45
19.90
19.60
18.43
16.65
13.59
-5.17
-5.19
TBDPSO
OTBS
O
O
210 200 190 180 170 160 150 140 130 120 110 100 90 80 70 60 50 40 30 20 10 ppm

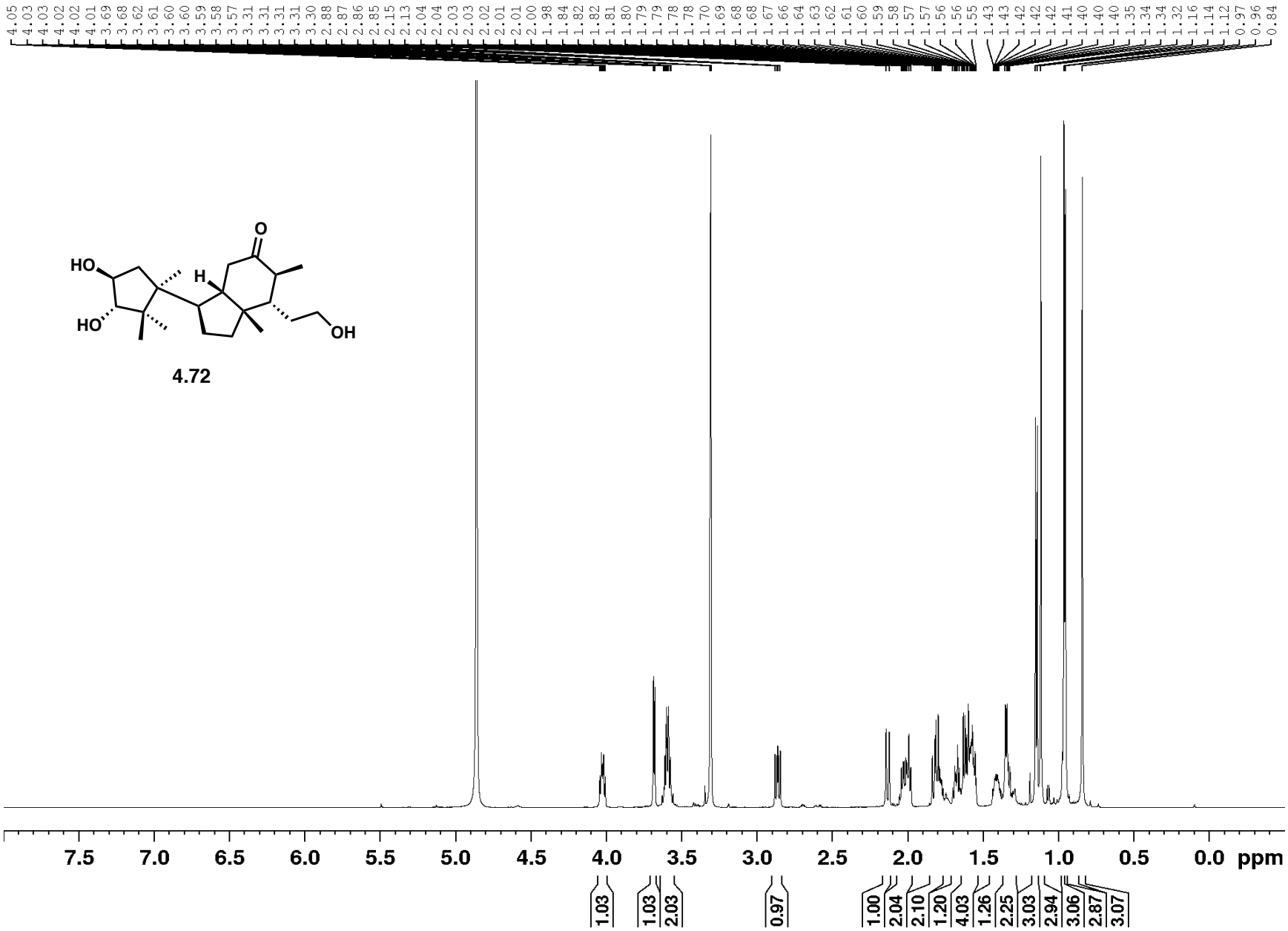
4.43b

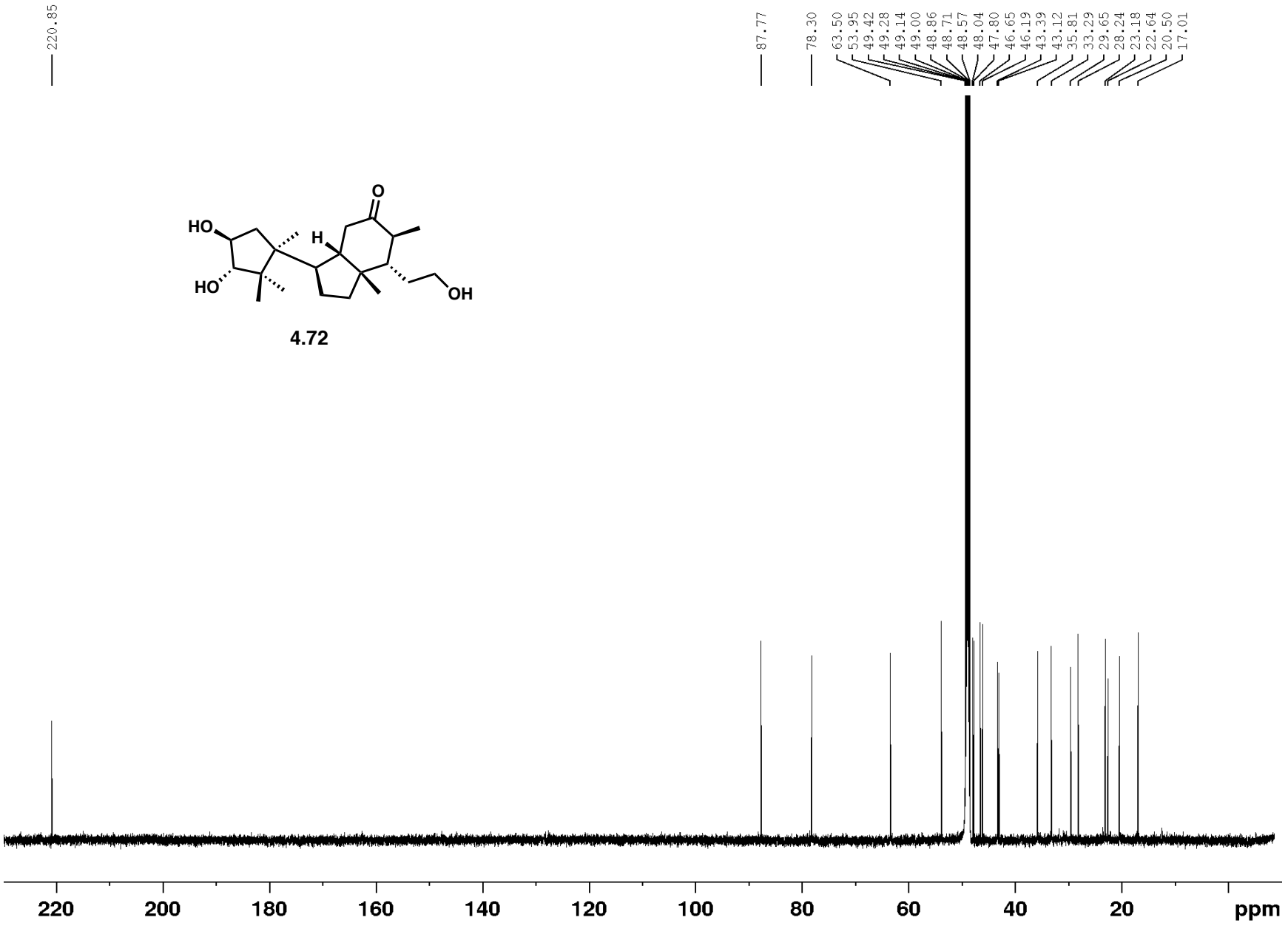

7.87
7.85
7.84
7.72
7.71
7.70
7.68
7.38
7.36
7.35
7.31
7.29
7.26
6.13
6.12
6.09
4.93
4.92
3.62
3.54
3.52
3.51
3.50
3.42
3.41
2.79
2.78
2.42
2.39
2.36
2.13
2.11
2.10
1.83
1.81
1.79
1.73
1.72
1.69
1.67
1.58
1.40
1.37
1.36
1.34
1.33
1.22
1.21
1.20
1.19
1.18
1.17
1.16
1.10
1.09
1.07
1.05
1.04
1.02
1.01
1.00
1.00
0.99
0.97
0.94
0.94
0.93
0.92
0.91
0.88
0.88
0.86
0.85
0.84
0.84
0.03
0.03
0.01
0.00
-0.00
-0.03
NHTs
N
TBDPSO
OTBS
O
4.44
8.5
8.0
7.5
7.0
6.5
6.0
5.5
5.0
4.5
4.0
3.5
3.0
2.5
2.0
1.5
1.0
0.5
ppm
2.11
3.46
9.06
1.11
1.00
3.14
0.90
4.22
1.93
1.22
2.32
1.22
1.82
3.23
2.50
18.25
3.23
10.15
6.32


7.26
5.78
5.77
5.76
5.76
5.65
5.36
5.34
4.11
3.64
3.63
3.61
3.11
3.10
2.52
2.40
2.39
2.36
2.29
2.28
2.27
2.26
2.25
2.23
2.08
2.06
2.01
2.00
1.99
1.98
1.96
1.96
1.83
1.60
1.47
1.46
1.43
1.12
1.11
1.03
0.97
0.92
HO
OH
8.5
8.0
7.5
7.0
6.5
6.0
5.5
5.0
4.5
4.0
3.5
3.0
2.5
2.0
1.5
1.0
0.5
ppm
1.00
1.00
1.02
1.24
2.45
0.94
1.39
2.22
2.09
1.19
1.27
2.26
3.56
3.50
2.58
1.55
3.29
3.26
3.31

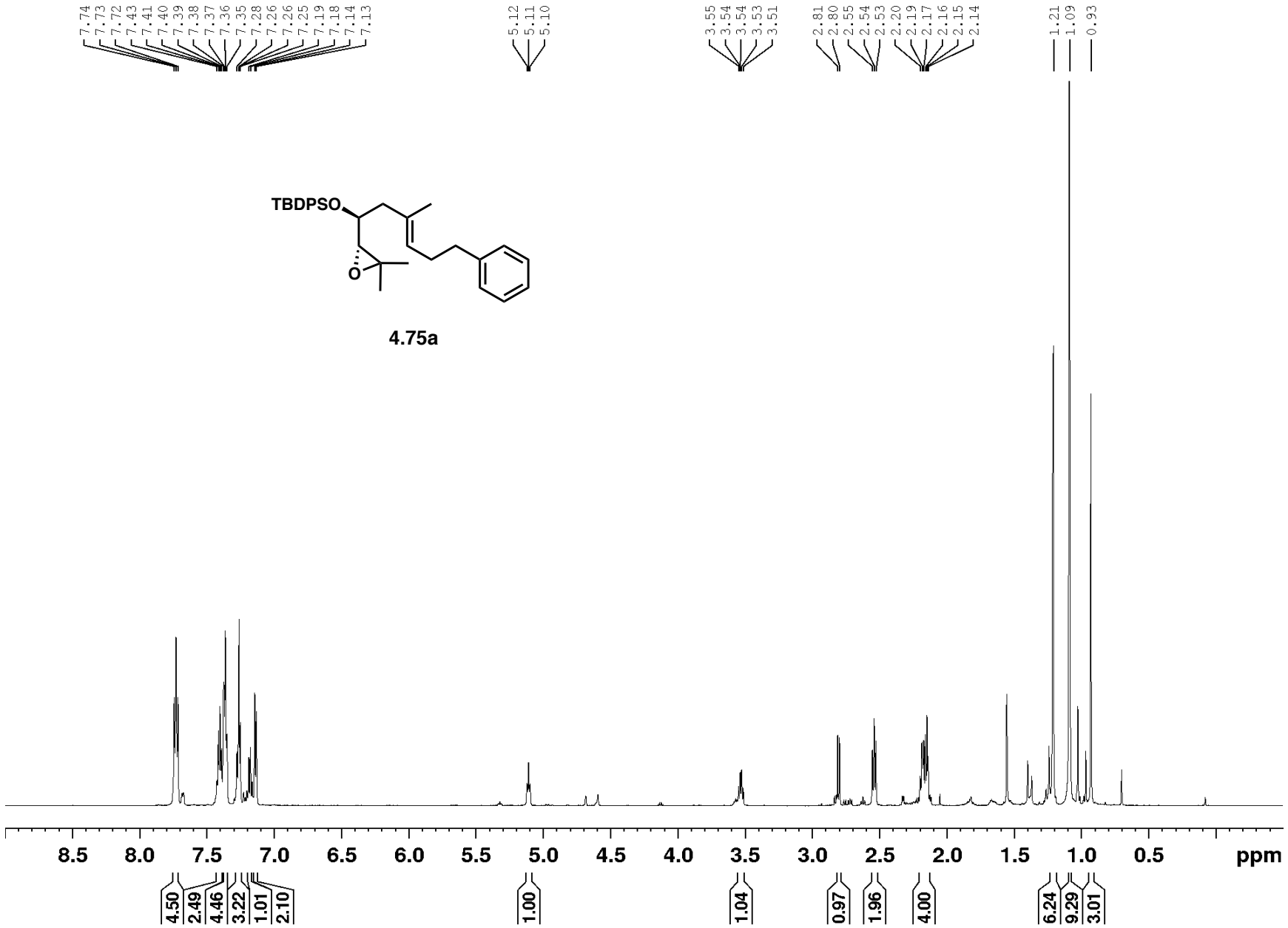
4.56


HO
OH
4.56
139.23
133.90
131.69
124.04
123.11
118.96
80.32
77.37
77.16
76.95
73.52
61.54
46.23
44.71
44.19
38.71
37.12
31.02
29.88
24.34
22.60
16.09
15.65
8.82
200 190 180 170 160 150 140 130 120 110 100 90 80 70 60 50 40 30 20 10 ppm

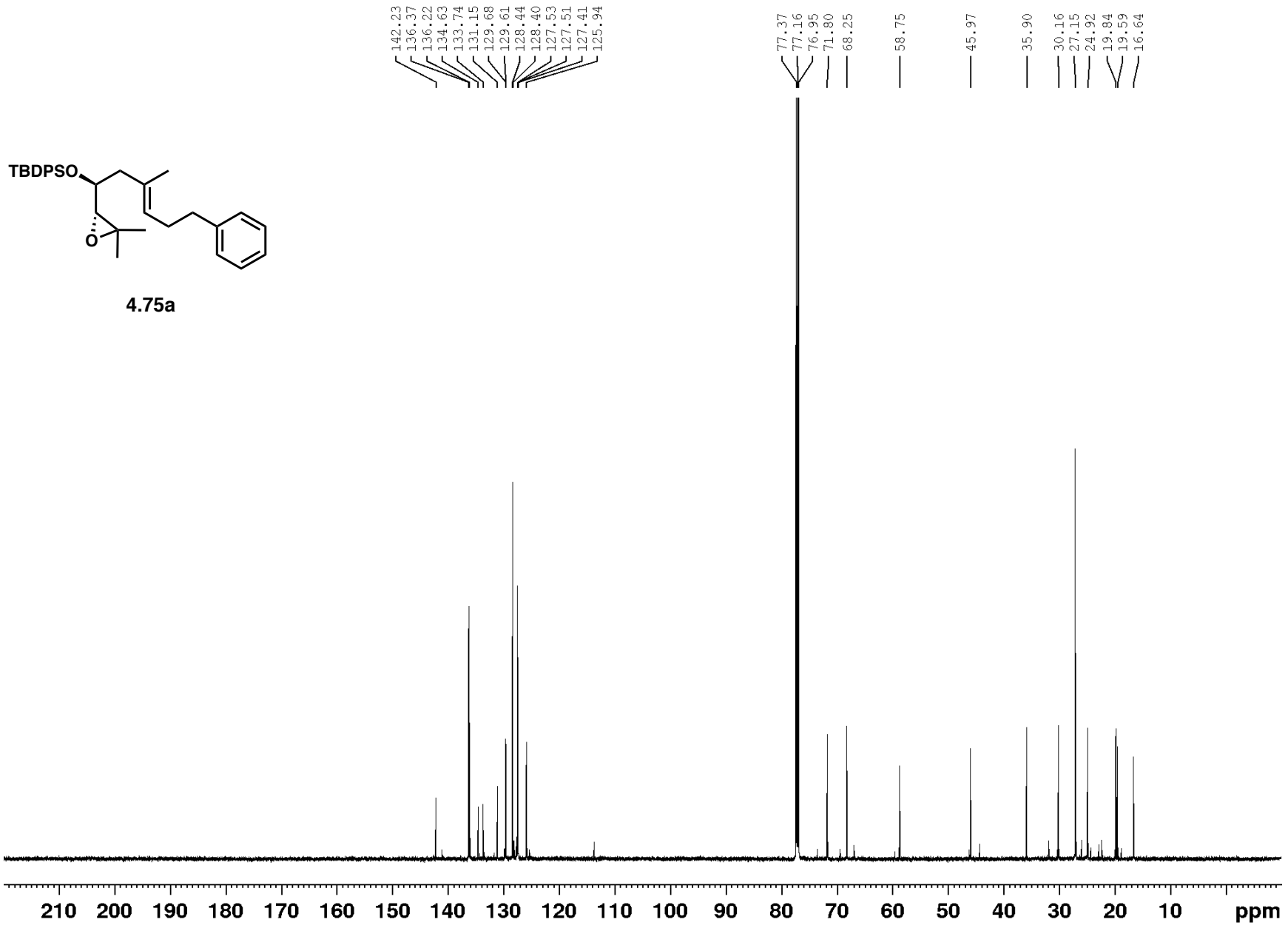

4.05 4.03 4.03 4.02 4.02 4.01 3.69 3.68 3.62 3.61 3.60 3.60 3.59 3.58 3.57 3.31 3.31 3.31 3.31 3.30 2.88 2.87 2.86 2.85 2.15 2.13 2.04 2.04 2.03 2.03 2.02 2.01 2.01 2.00 1.98 1.84 1.82 1.82 1.81 1.80 1.79 1.79 1.78 1.78 1.70 1.69 1.68 1.68 1.67 1.66 1.64 1.63 1.62 1.61 1.60 1.59 1.58 1.57 1.57 1.56 1.56 1.55 1.43 1.43 1.42 1.42 1.42 1.41 1.40 1.40 1.40 1.35 1.34 1.34 1.32 1.16 1.14 1.12 0.97 0.96 0.84
HO
HO
H
O
OH
4.72
7.5 7.0 6.5 6.0 5.5 5.0 4.5 4.0 3.5 3.0 2.5 2.0 1.5 1.0 0.5 0.0 ppm
1.03 1.03 2.03 0.97 1.00 2.04 2.10 1.20 4.03 1.26 2.25 3.03 2.94 3.06 2.87 3.07

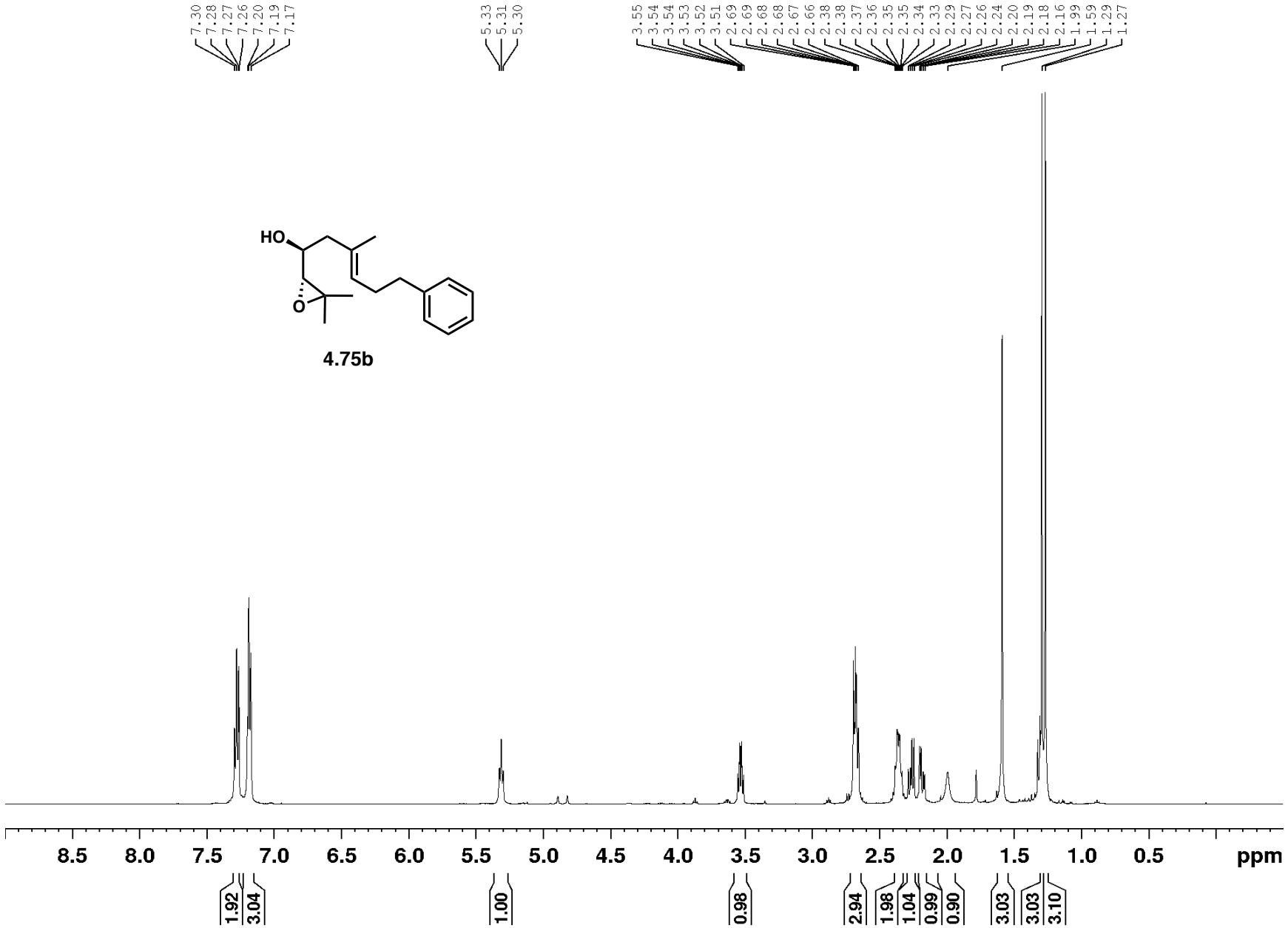

220.85
87.77
78.30
63.50
53.95
49.42
49.28
49.14
49.00
48.86
48.71
48.57
48.04
47.80
46.65
46.19
43.39
43.12
35.81
33.29
29.65
28.24
23.18
22.64
20.50
17.01
HO
HO
H
O
OH
220
200
180
160
140
120
100
80
60
40
20
ppm

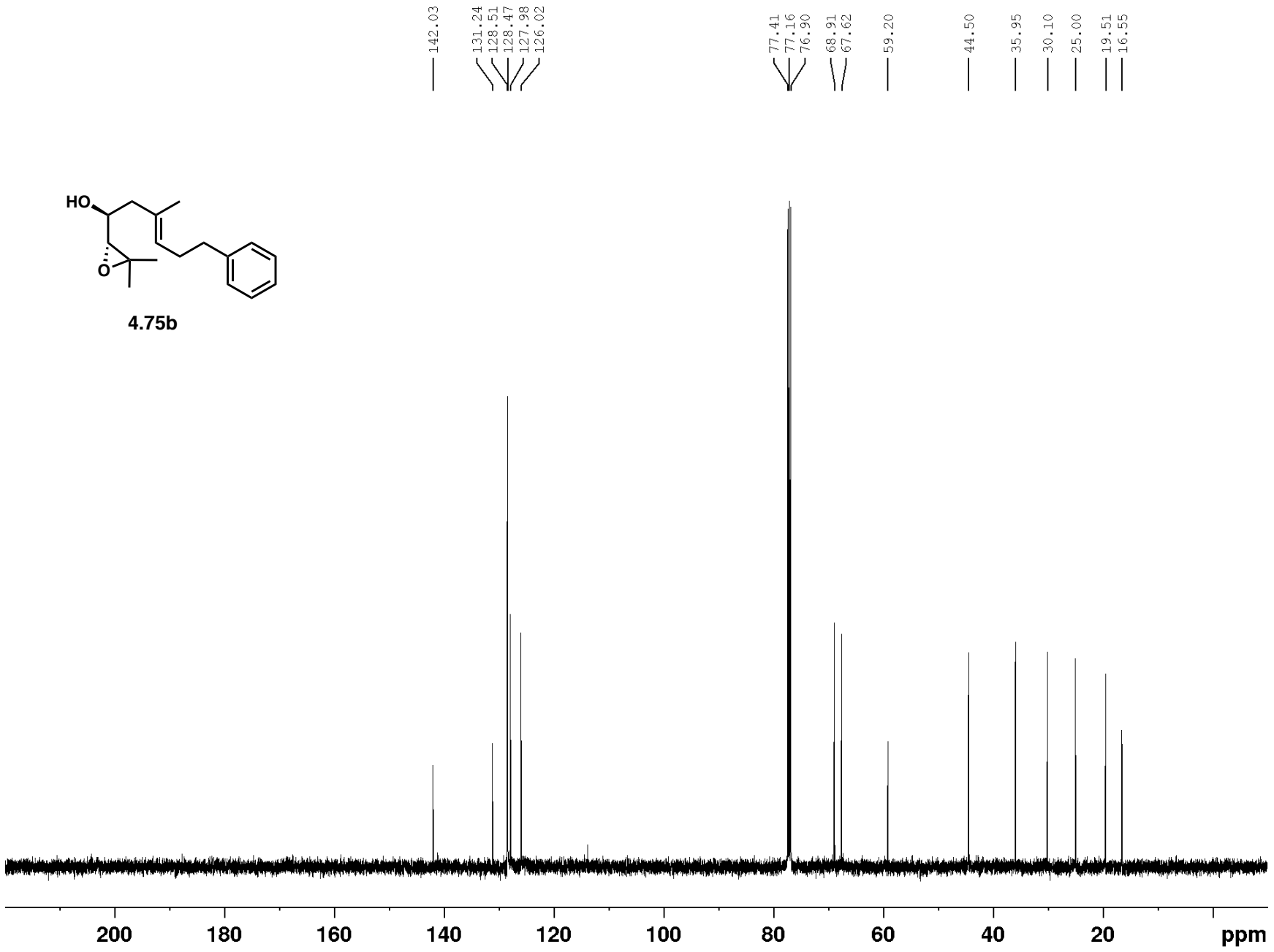
4.72

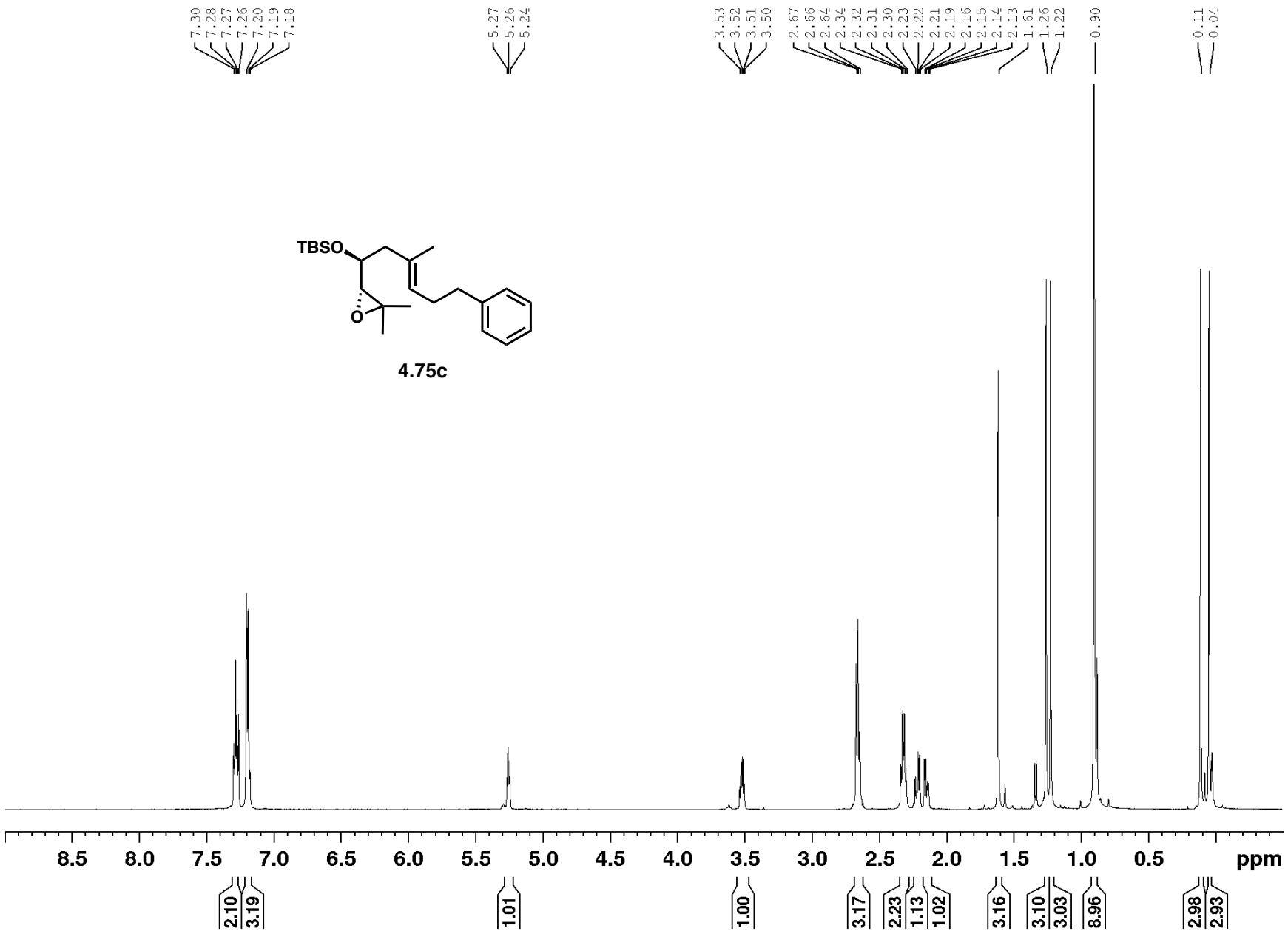

7.74
7.73
7.72
7.43
7.41
7.40
7.39
7.38
7.37
7.36
7.35
7.28
7.26
7.26
7.25
7.19
7.18
7.14
7.13
5.12
5.11
5.10
3.55
3.54
3.54
3.53
3.51
2.81
2.80
2.55
2.54
2.53
2.20
2.19
2.17
2.16
2.15
2.14
1.21
1.09
0.93
TBDPSO
O
8.5
8.0
7.5
7.0
6.5
6.0
5.5
5.0
4.5
4.0
3.5
3.0
2.5
2.0
1.5
1.0
0.5
ppm
4.50
2.49
4.46
3.22
1.01
2.10
1.00
1.04
0.97
1.96
4.00
6.24
9.29
3.01

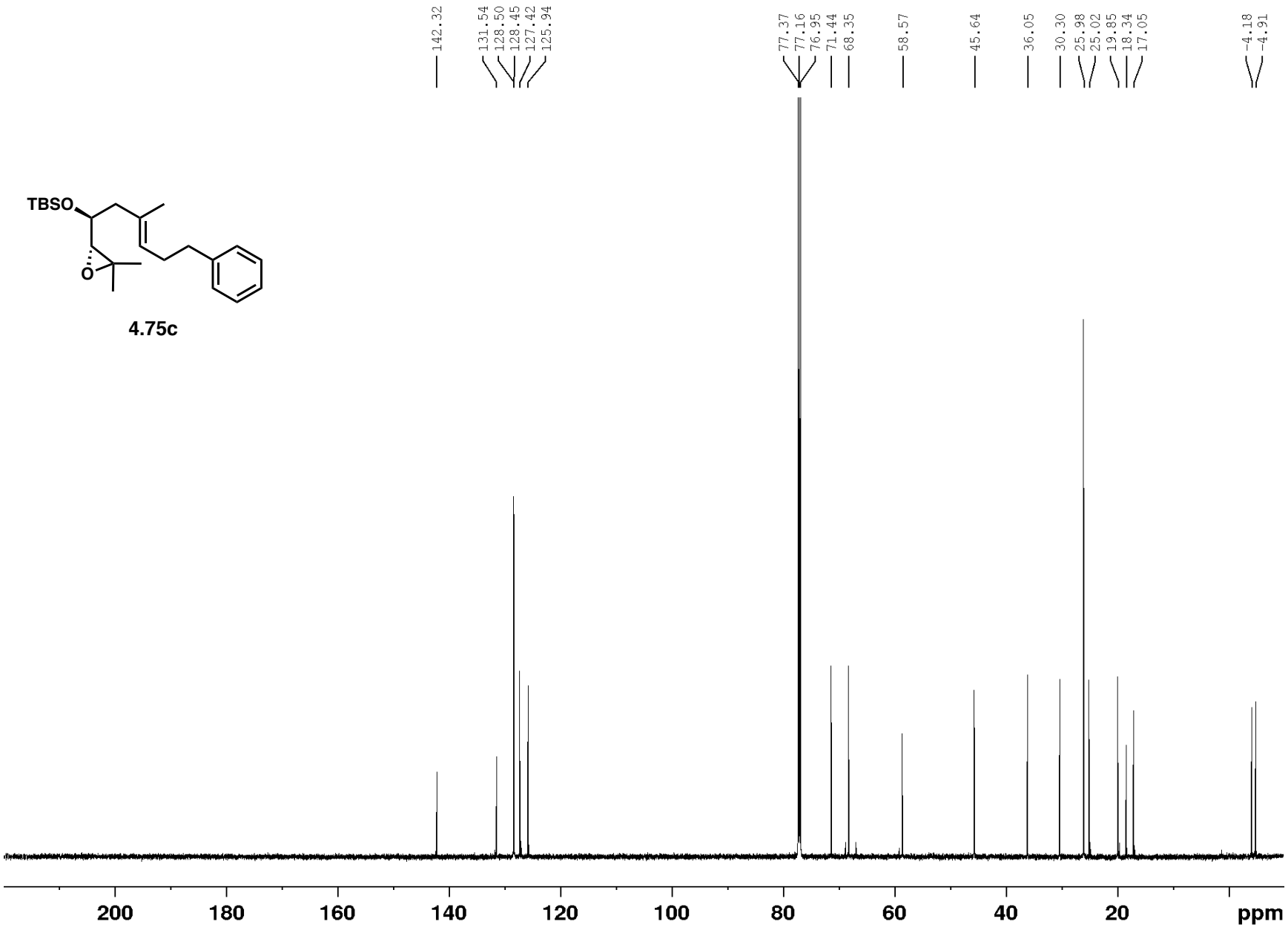
4.75a

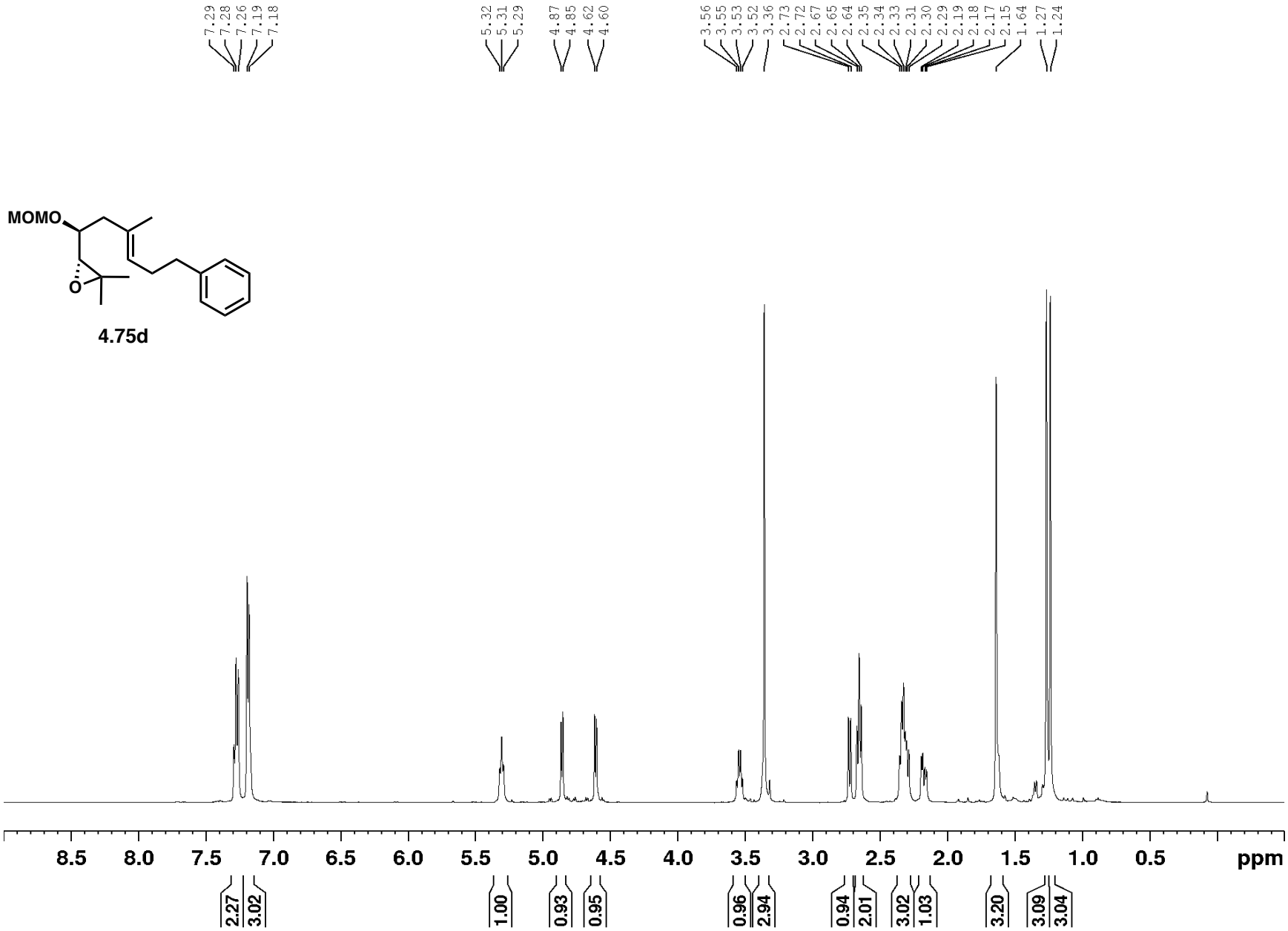

142.23
136.37
136.22
134.63
133.74
131.15
129.68
129.61
128.44
128.40
127.53
127.51
127.41
125.94
77.37
77.16
76.95
71.80
68.25
58.75
45.97
35.90
30.16
27.15
24.92
19.84
19.59
16.64
TBDPSO
O
4.75a
210 200 190 180 170 160 150 140 130 120 110 100 90 80 70 60 50 40 30 20 10 ppm

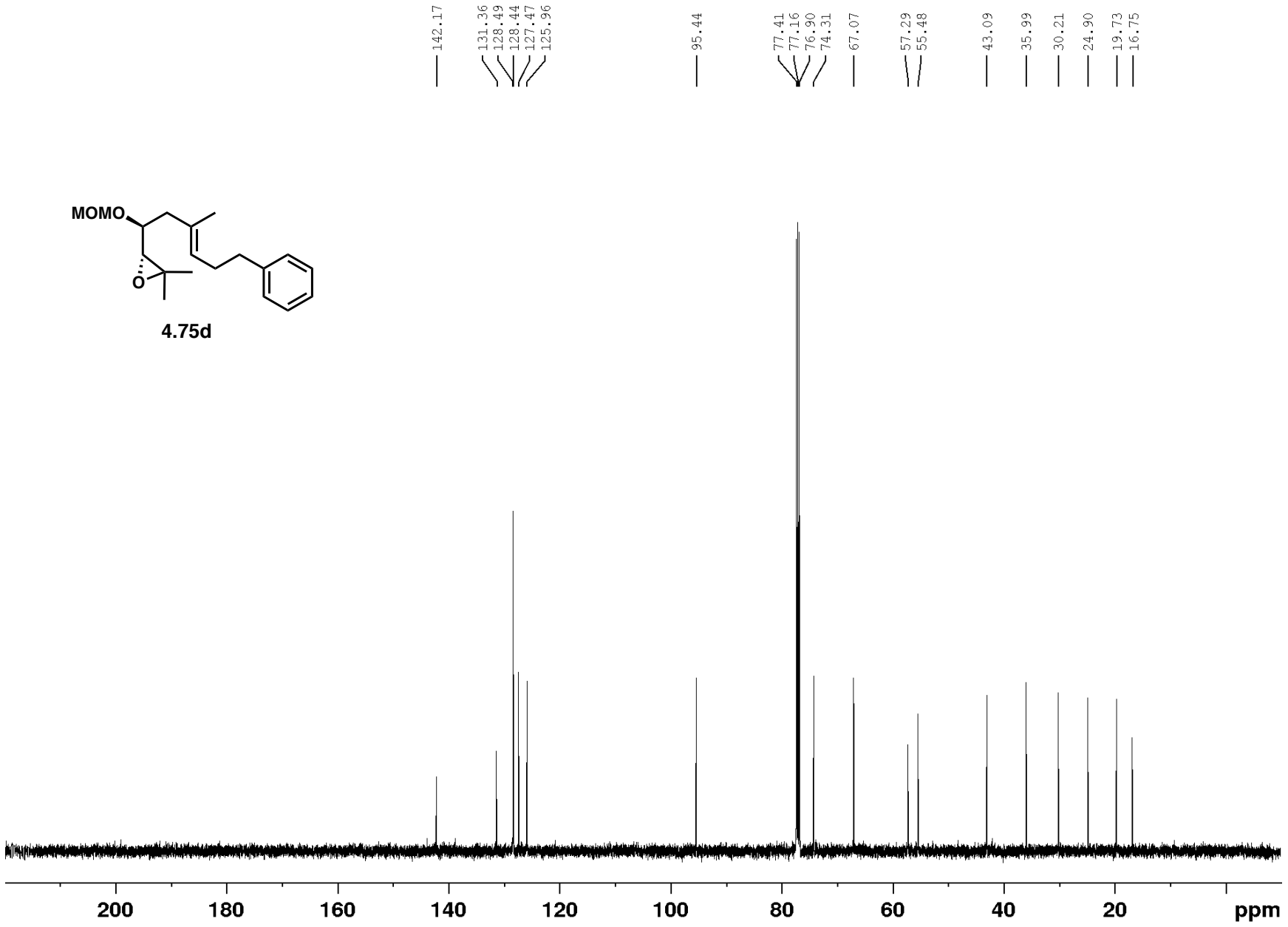

7.30
7.28
7.27
7.26
7.20
7.19
7.17
5.33
5.31
5.30
3.55
3.54
3.54
3.53
3.52
3.51
2.69
2.69
2.68
2.68
2.67
2.66
2.38
2.38
2.37
2.36
2.35
2.35
2.34
2.33
2.29
2.27
2.26
2.24
2.20
2.19
2.18
2.16
1.99
1.59
1.29
1.27
HO
O
4.75b
8.5
8.0
7.5
7.0
6.5
6.0
5.5
5.0
4.5
4.0
3.5
3.0
2.5
2.0
1.5
1.0
0.5
ppm
1.92
3.04
1.00
0.98
2.94
1.98
1.04
0.99
0.90
3.03
3.03
3.10

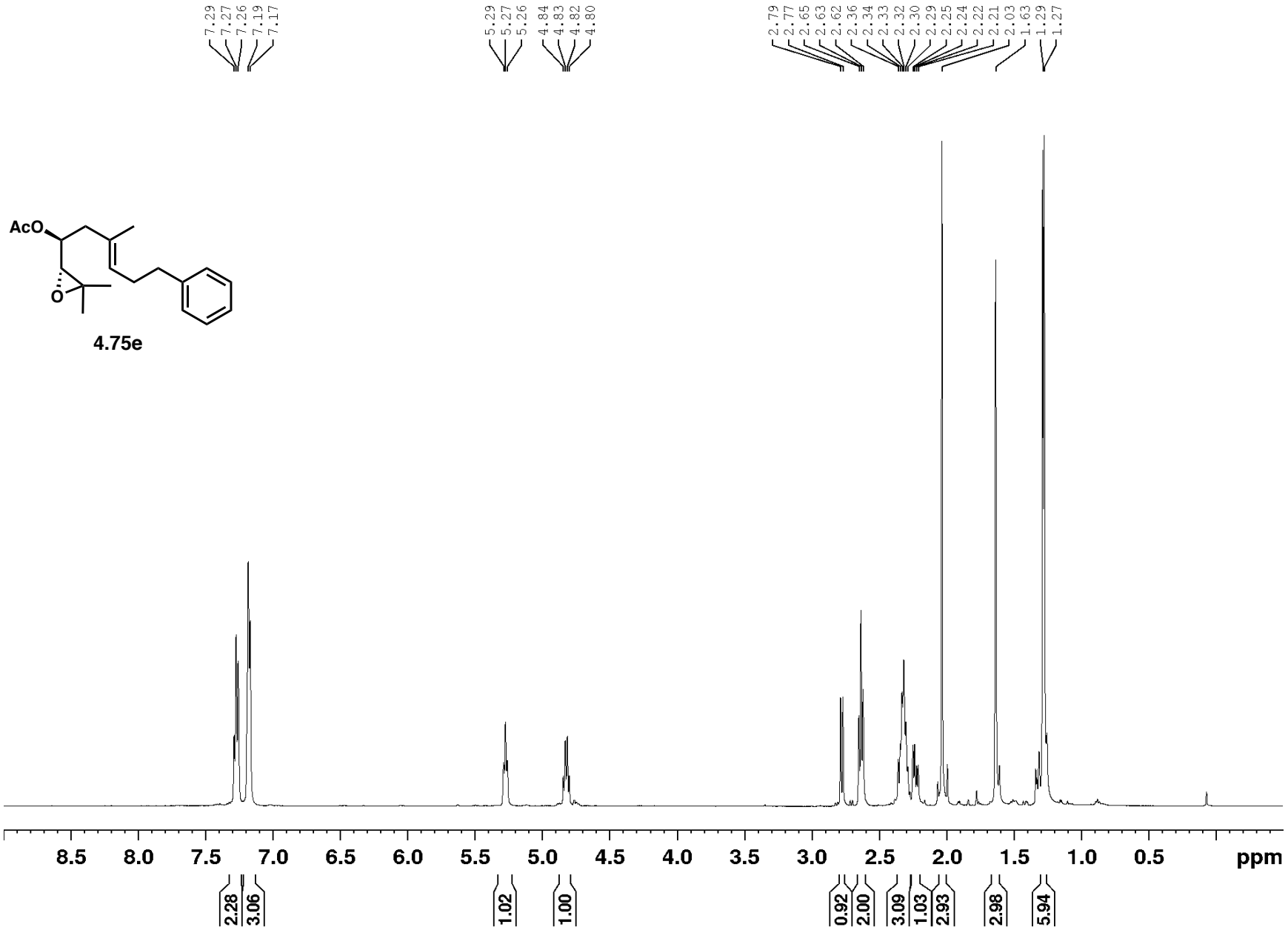

142.03
131.24
128.51
128.47
127.98
126.02
77.41
77.16
76.90
68.91
67.62
59.20
44.50
35.95
30.10
25.00
19.51
16.55
HO
O
4.75b
200
180
160
140
120
100
80
60
40
20
ppm

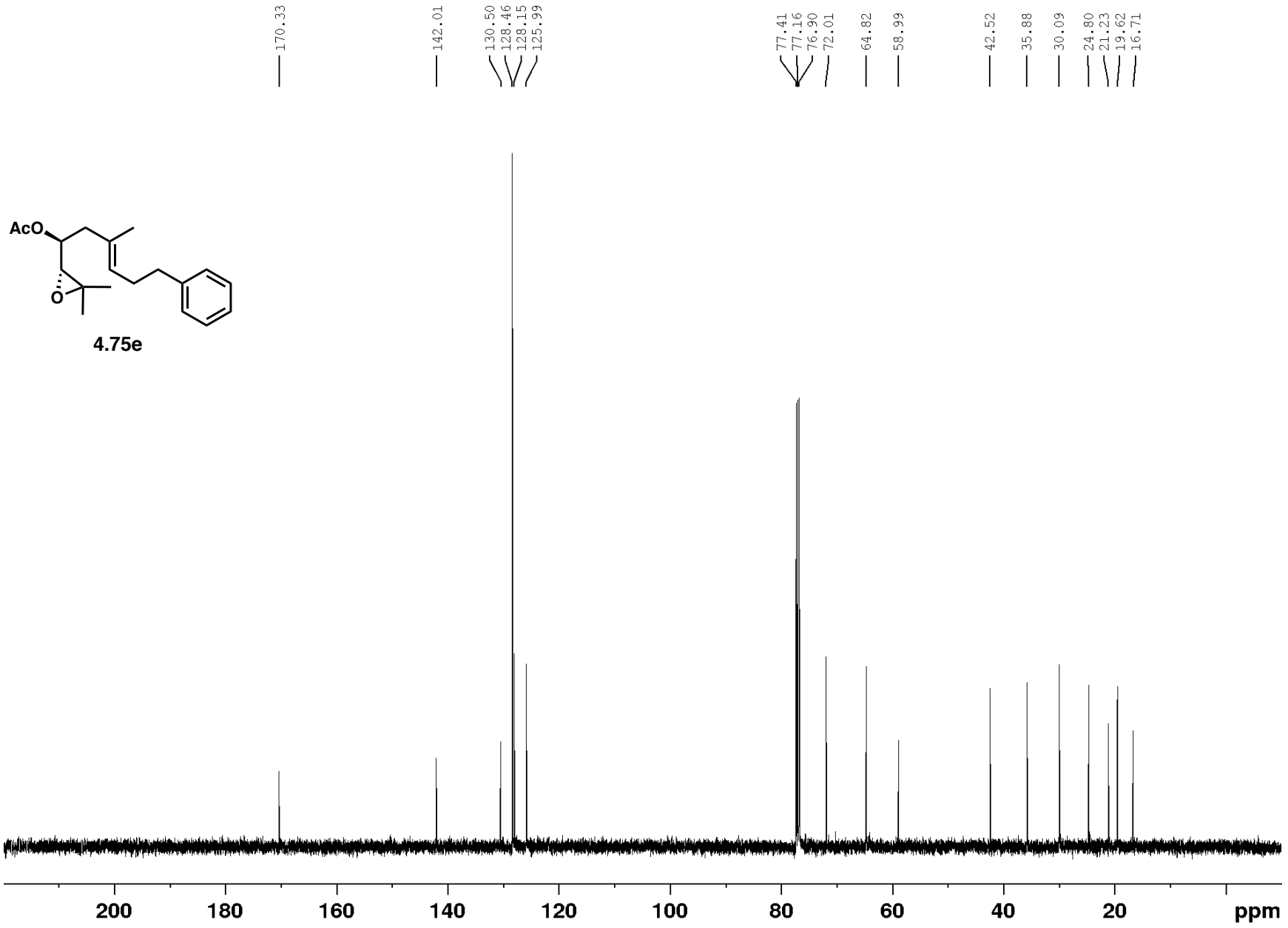

7.30
7.28
7.27
7.26
7.20
7.19
7.18
5.27
5.26
5.24
3.53
3.52
3.51
3.50
2.67
2.66
2.64
2.34
2.32
2.31
2.30
2.23
2.22
2.21
2.19
2.16
2.15
2.14
2.13
1.61
1.26
1.22
0.90
0.11
0.04
TBSO
O
4.75c
8.5
8.0
7.5
7.0
6.5
6.0
5.5
5.0
4.5
4.0
3.5
3.0
2.5
2.0
1.5
1.0
0.5
ppm
2.10
3.19
1.01
1.00
3.17
2.23
1.13
1.02
3.16
3.10
3.03
8.96
2.98
2.93

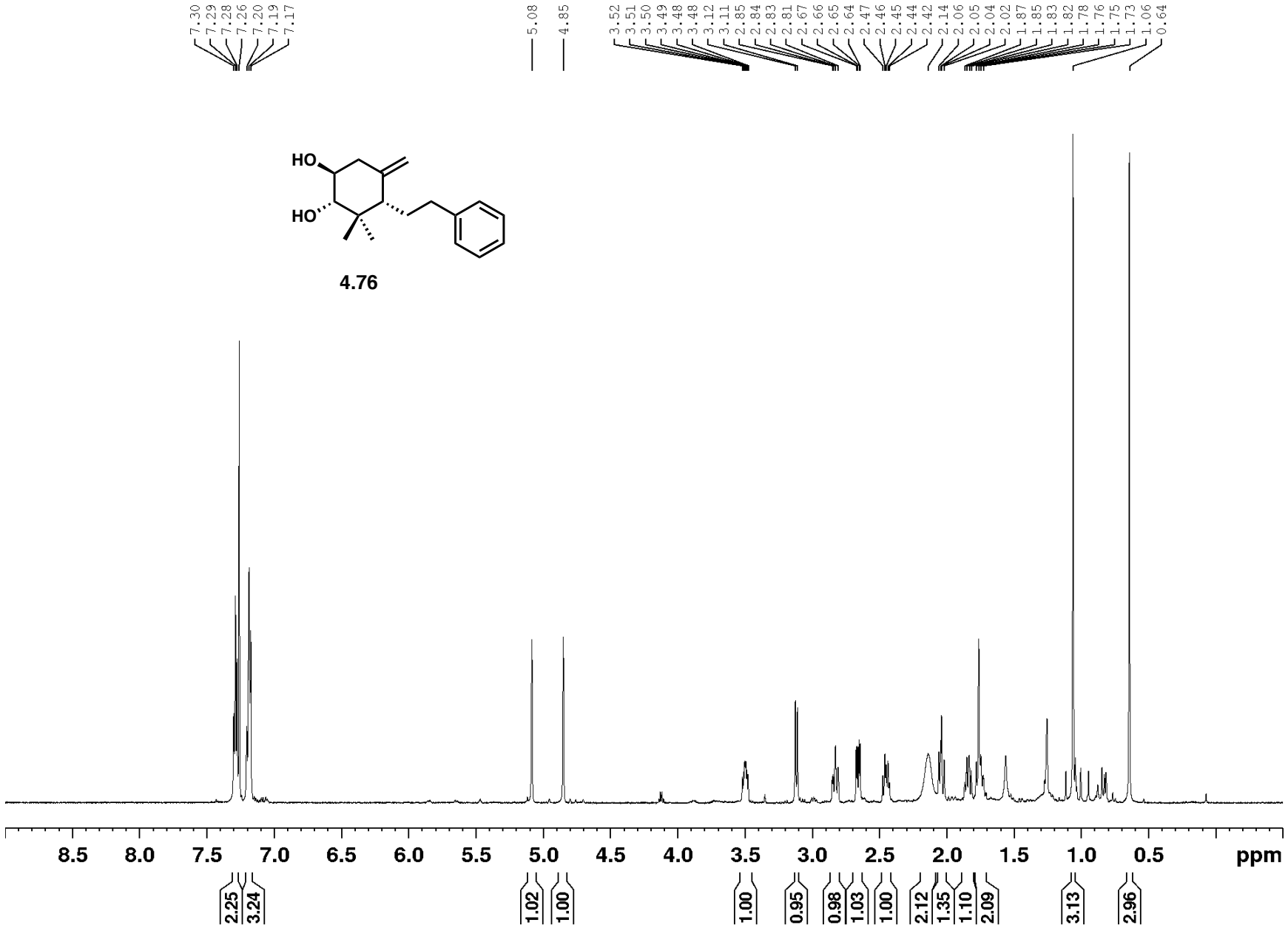

142.32
131.54
128.50
128.45
127.42
125.94
77.37
77.16
76.95
71.44
68.35
58.57
45.64
36.05
30.30
25.98
25.02
19.85
18.34
17.05
-4.18
-4.91
TBSO
O
4.75c
200
180
160
140
120
100
80
60
40
20
ppm


7.29
7.28
7.26
7.19
7.18
5.32
5.31
5.29
4.87
4.85
4.62
4.60
3.56
3.55
3.53
3.52
3.36
2.73
2.72
2.67
2.65
2.64
2.35
2.34
2.33
2.31
2.30
2.29
2.19
2.18
2.17
2.15
1.64
1.27
1.24
MOMO
O
4.75d
8.5
8.0
7.5
7.0
6.5
6.0
5.5
5.0
4.5
4.0
3.5
3.0
2.5
2.0
1.5
1.0
0.5
ppm
2.27
3.02
1.00
0.93
0.95
0.96
2.94
0.94
2.01
3.02
1.03
3.20
3.09
3.04

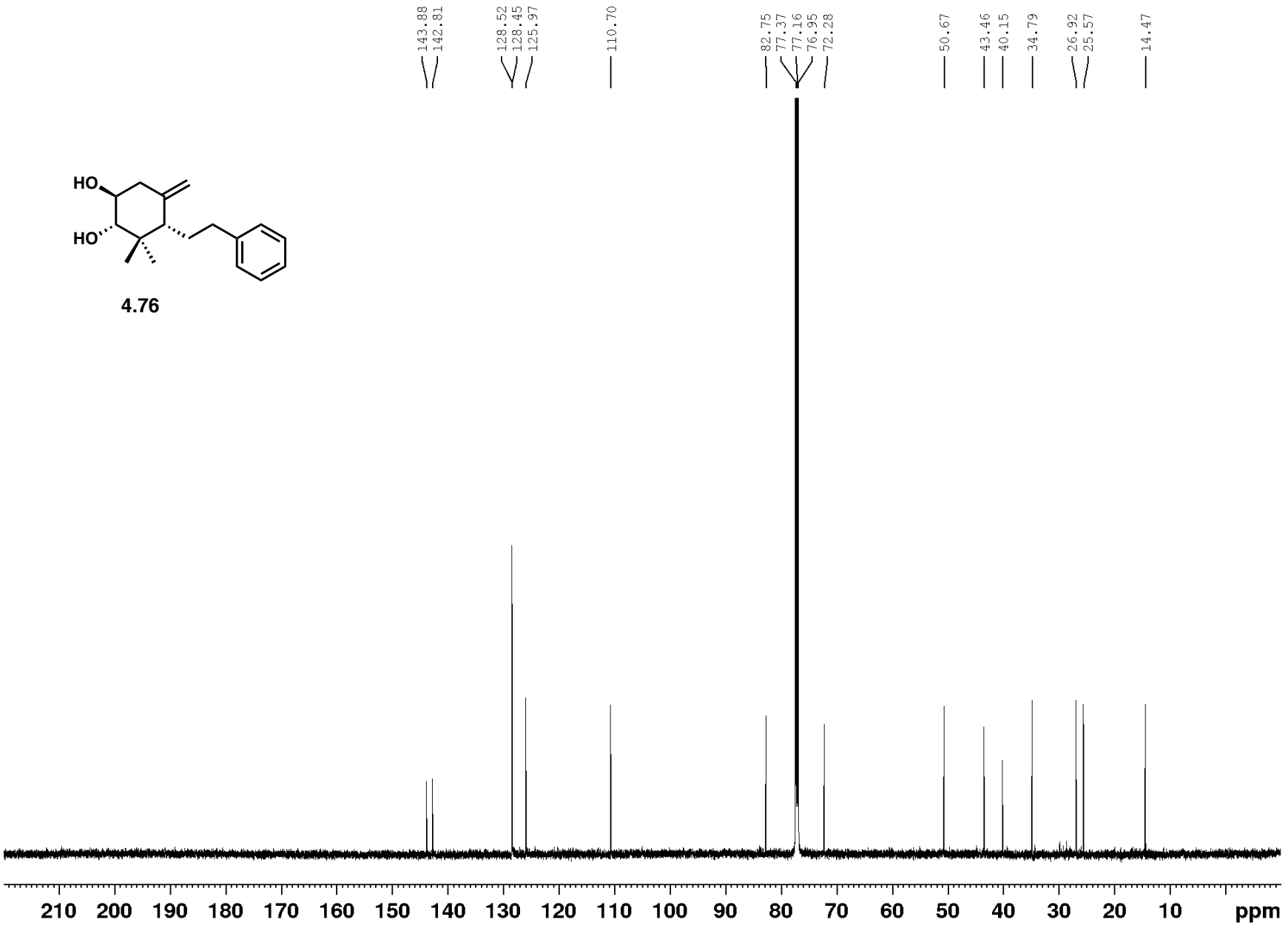

142.17
131.36
128.49
128.44
127.47
125.96
95.44
77.41
77.16
76.90
74.31
67.07
57.29
55.48
43.09
35.99
30.21
24.90
19.73
16.75
MOMO
O
4.75d
200
180
160
140
120
100
80
60
40
20
ppm


7.29
7.27
7.26
7.19
7.17
5.29
5.27
5.26
4.84
4.83
4.82
4.80
2.79
2.77
2.65
2.63
2.62
2.36
2.34
2.33
2.32
2.30
2.29
2.25
2.24
2.22
2.21
2.03
1.63
1.29
1.27
AcO
O
4.75e
8.5
8.0
7.5
7.0
6.5
6.0
5.5
5.0
4.5
4.0
3.5
3.0
2.5
2.0
1.5
1.0
0.5
ppm
2.28
3.06
1.02
1.00
0.92
2.00
3.09
1.03
2.93
2.98
5.94

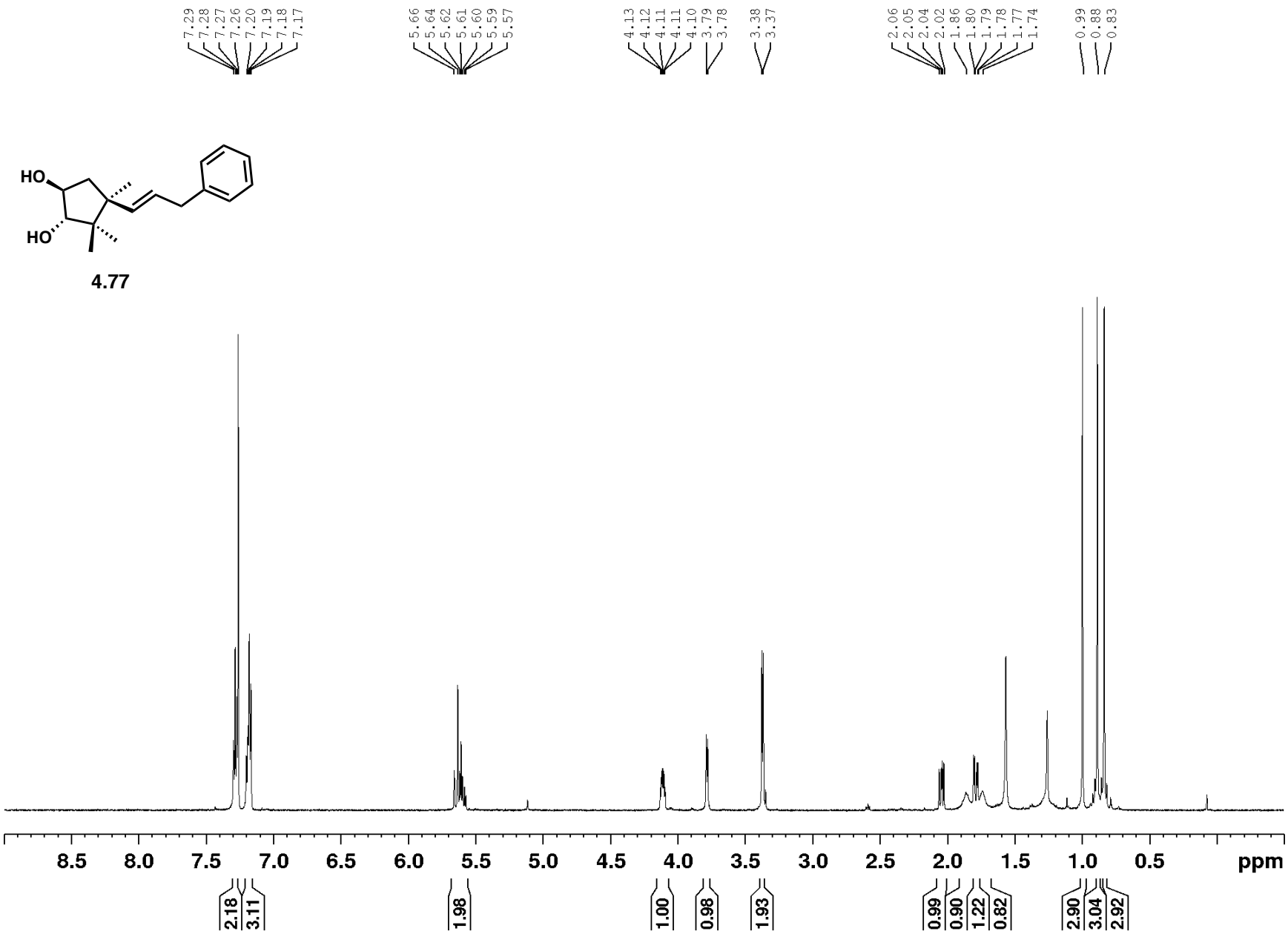

170.33
142.01
130.50
128.46
128.15
125.99
77.41
77.16
76.90
72.01
64.82
58.99
42.52
35.88
30.09
24.80
21.23
19.62
16.71
AcO
O
4.75e
200
180
160
140
120
100
80
60
40
20
ppm

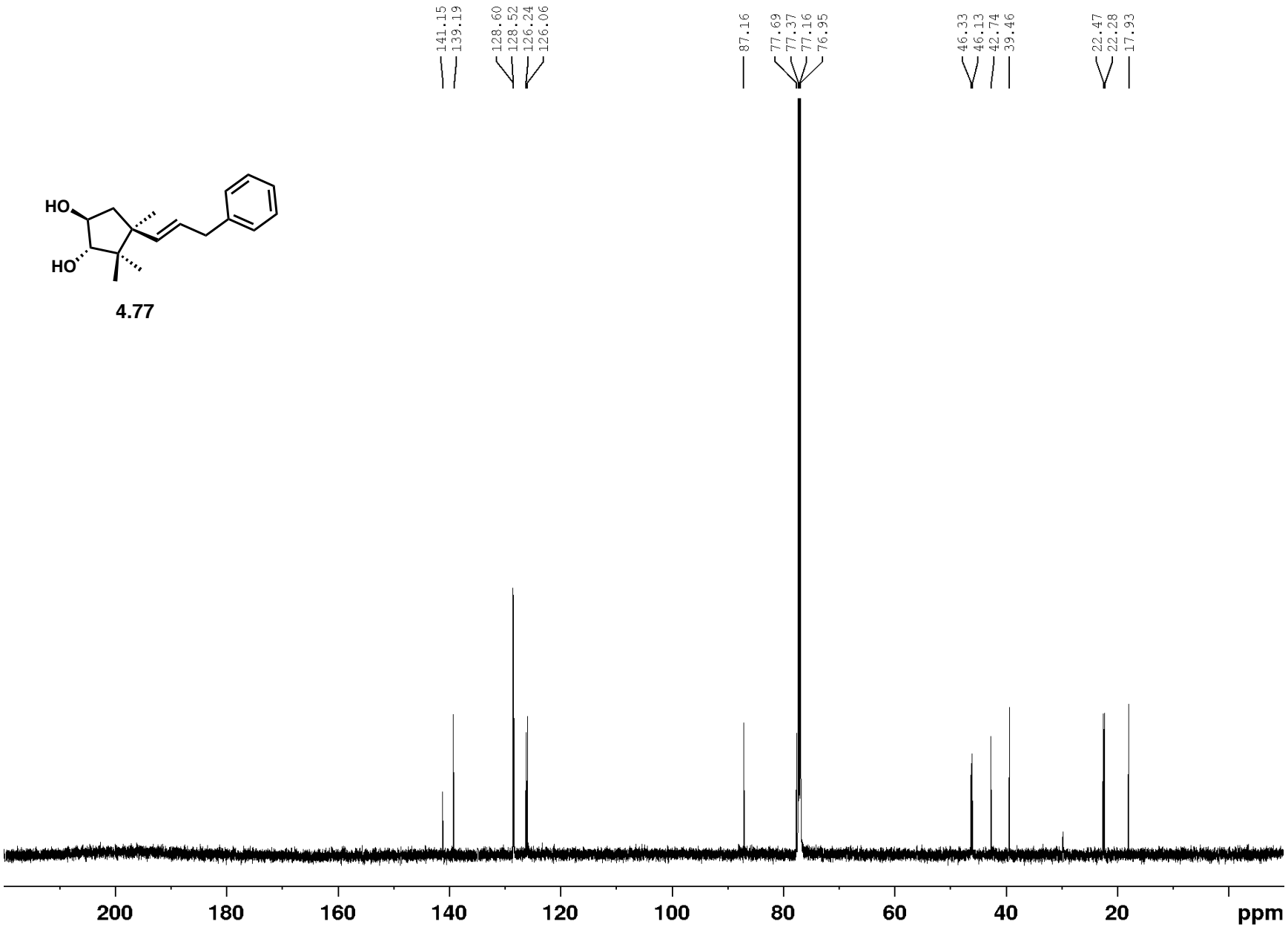

7.30
7.29
7.28
7.26
7.20
7.19
7.17
5.08
4.85
3.52
3.51
3.50
3.49
3.48
3.48
3.12
3.11
2.85
2.84
2.83
2.81
2.67
2.66
2.65
2.64
2.47
2.46
2.45
2.44
2.42
2.14
2.06
2.05
2.04
2.02
1.87
1.85
1.83
1.82
1.78
1.76
1.75
1.73
1.06
0.64
HO
HO
8.5
8.0
7.5
7.0
6.5
6.0
5.5
5.0
4.5
4.0
3.5
3.0
2.5
2.0
1.5
1.0
0.5
ppm
2.25
3.24
1.02
1.00
1.00
0.95
0.98
1.03
1.00
2.12
1.35
1.10
2.09
3.13
2.96

4.76

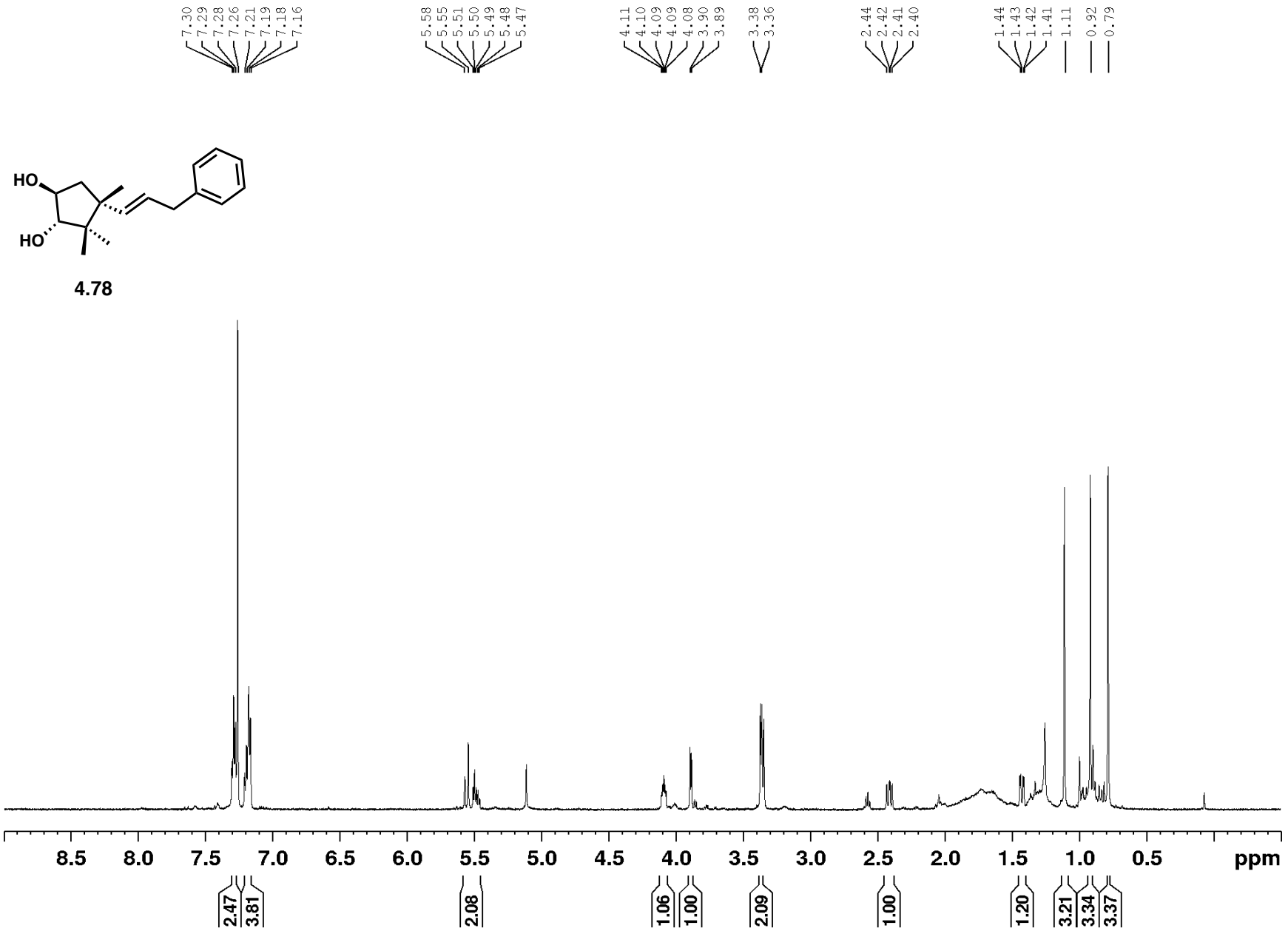

143.88
142.81
128.52
128.45
125.97
110.70
82.75
77.37
77.16
76.95
72.28
50.67
43.46
40.15
34.79
26.92
25.57
14.47
HO
HO
210 200 190 180 170 160 150 140 130 120 110 100 90 80 70 60 50 40 30 20 10 ppm

4.76

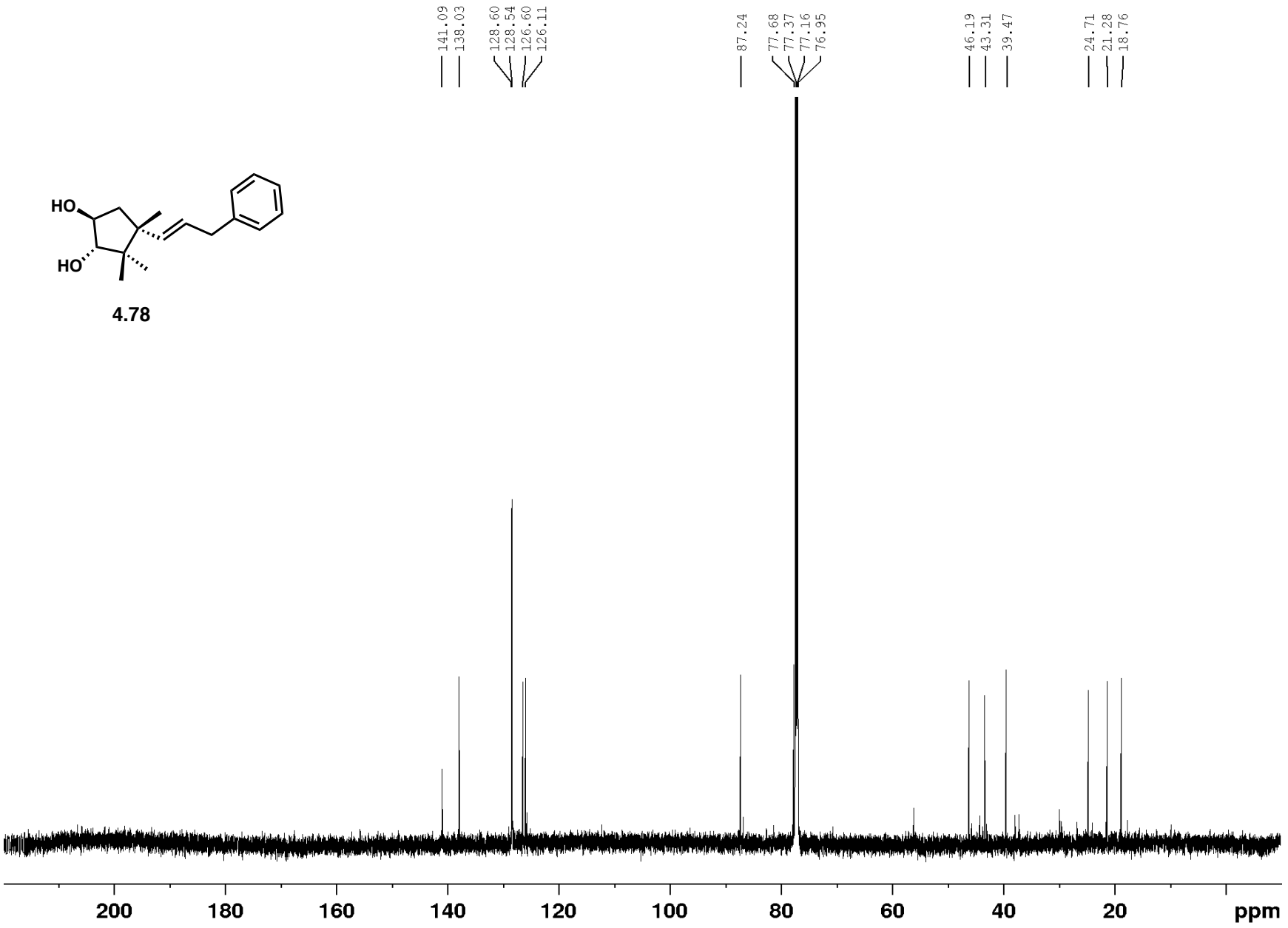

7.29
7.28
7.27
7.26
7.20
7.19
7.18
7.17
5.66
5.64
5.62
5.61
5.60
5.59
5.57
4.13
4.12
4.11
4.11
4.10
3.79
3.78
3.38
3.37
2.06
2.05
2.04
2.02
1.86
1.80
1.79
1.78
1.77
1.74
0.99
0.88
0.83
HO
HO
4.77
8.5
8.0
7.5
7.0
6.5
6.0
5.5
5.0
4.5
4.0
3.5
3.0
2.5
2.0
1.5
1.0
0.5
ppm
2.18
3.11
1.98
1.00
0.98
1.93
0.99
0.90
1.22
0.82
2.90
3.04
2.92


141.15
139.19
128.60
128.52
126.24
126.06
87.16
77.69
77.37
77.16
76.95
46.33
46.13
42.74
39.46
22.47
22.28
17.93
HO
HO
200
180
160
140
120
100
80
60
40
20
ppm

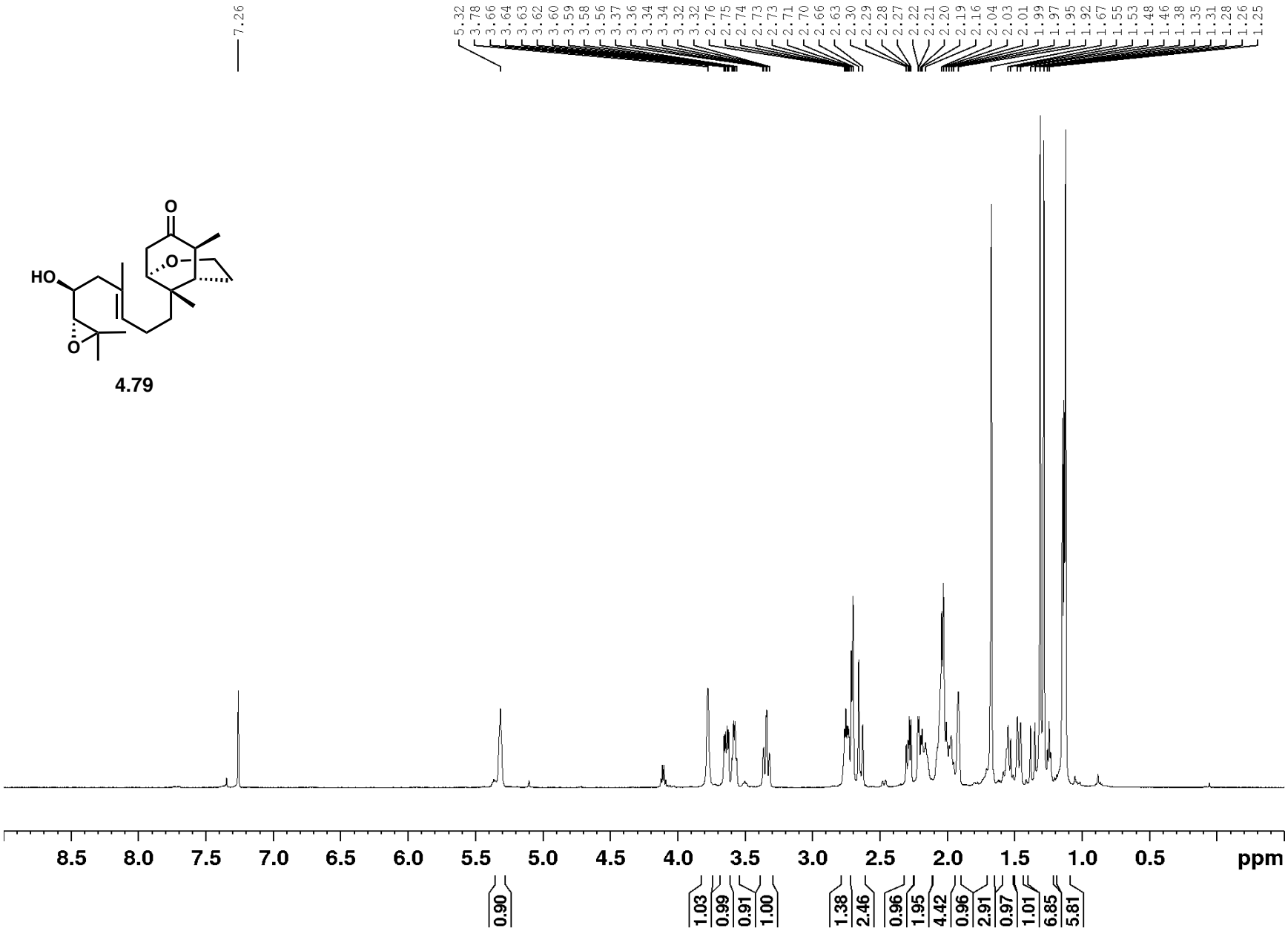
4.77


7.30
7.29
7.28
7.26
7.21
7.19
7.18
7.16
5.58
5.55
5.51
5.50
5.49
5.48
5.47
4.11
4.10
4.09
4.09
4.08
3.90
3.89
3.38
3.36
2.44
2.42
2.41
2.40
1.44
1.43
1.42
1.41
1.11
0.92
0.79
HO
HO
8.5
8.0
7.5
7.0
6.5
6.0
5.5
5.0
4.5
4.0
3.5
3.0
2.5
2.0
1.5
1.0
0.5
ppm
2.47
3.81
2.08
1.06
1.00
2.09
1.00
1.20
3.21
3.34
3.37

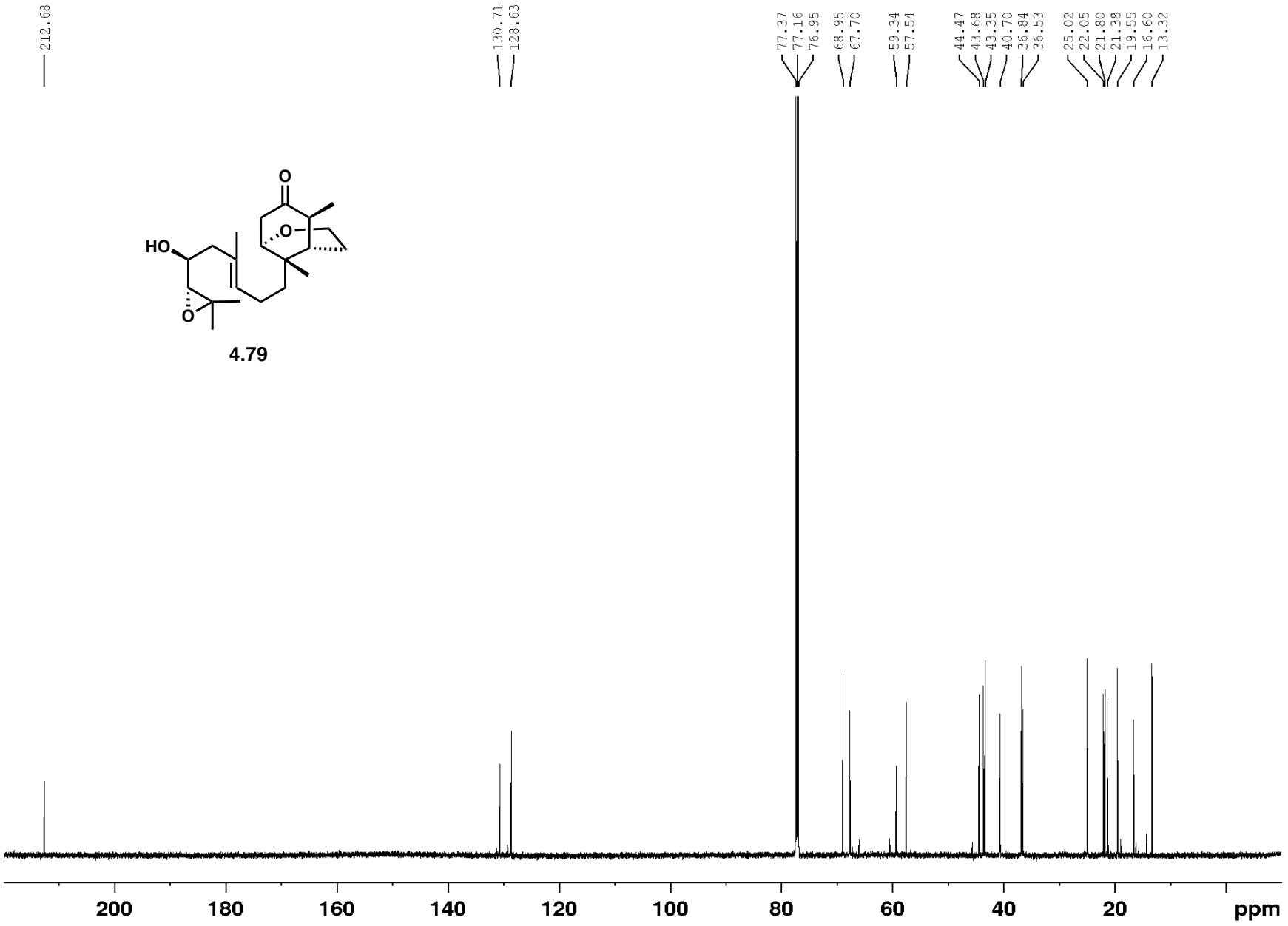
4.78


141.09
138.03
128.60
128.54
126.60
126.11
87.24
77.68
77.37
77.16
76.95
46.19
43.31
39.47
24.71
21.28
18.76
HO
HO
200
180
160
140
120
100
80
60
40
20
ppm

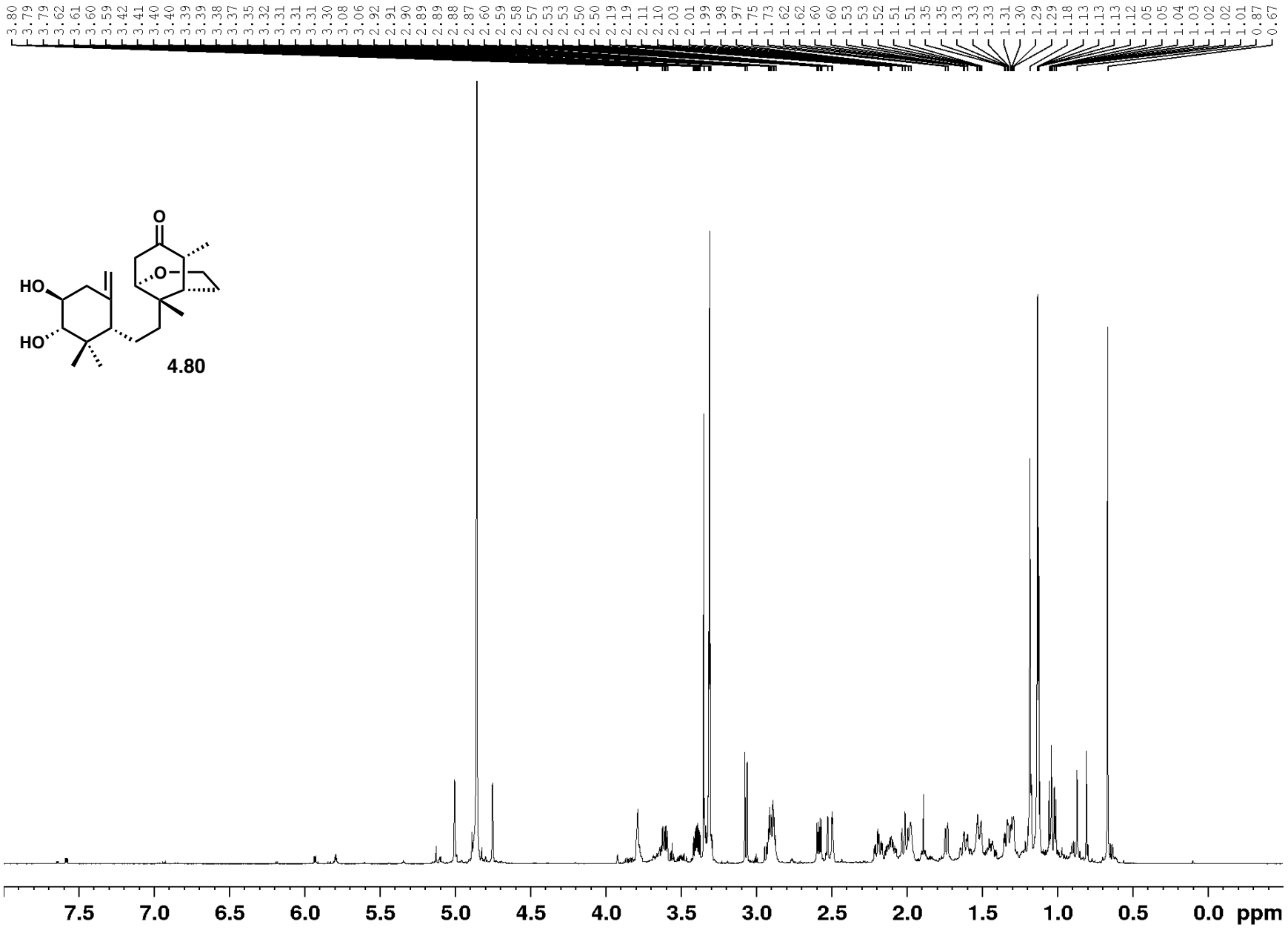
4.78

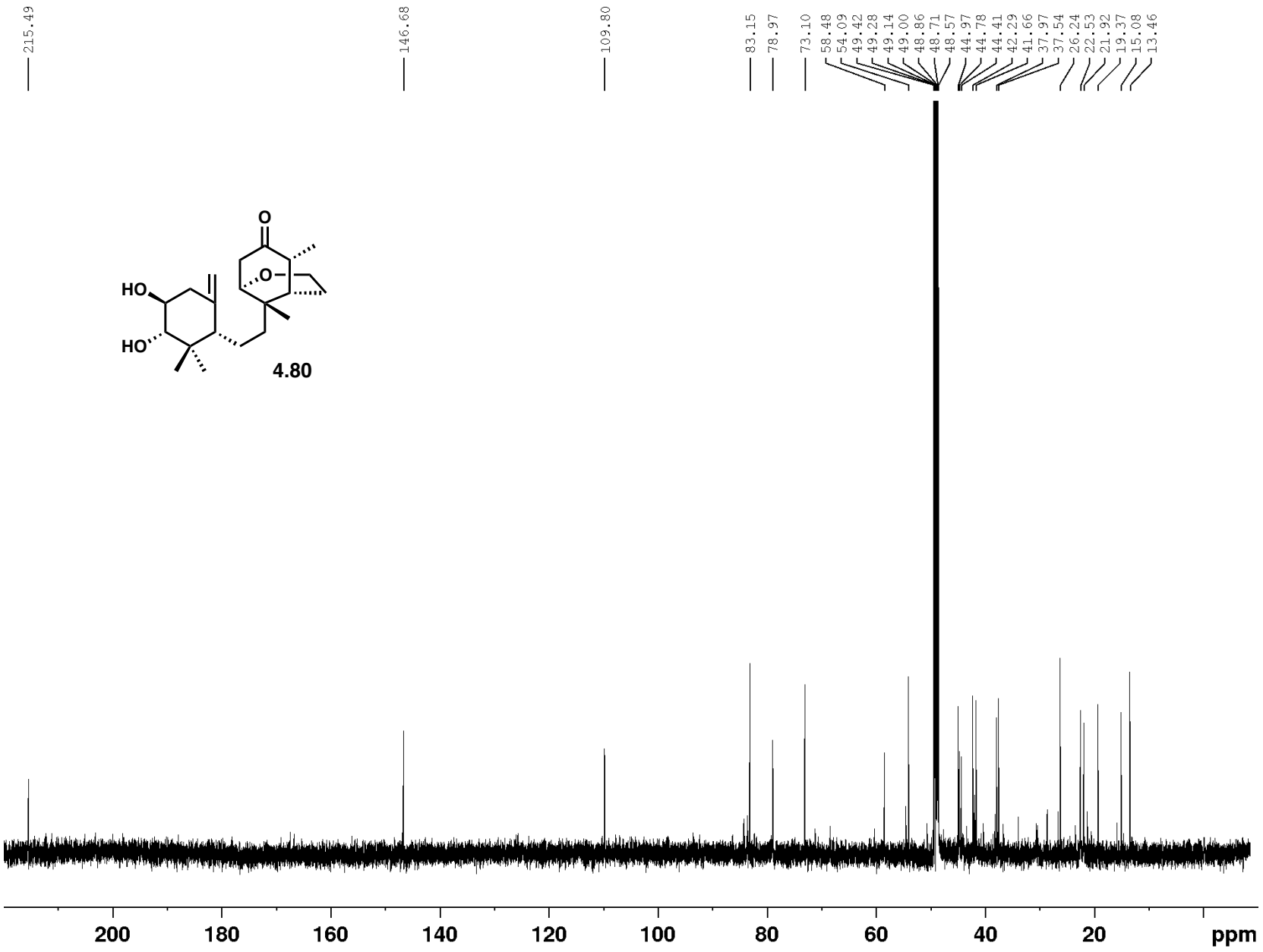

7.26
5.32
3.78
3.66
3.64
3.63
3.62
3.60
3.59
3.58
3.56
3.37
3.36
3.34
3.34
3.32
3.32
2.76
2.75
2.74
2.73
2.73
2.71
2.70
2.66
2.63
2.30
2.29
2.28
2.27
2.22
2.21
2.20
2.19
2.16
2.04
2.03
2.01
1.99
1.97
1.95
1.92
1.67
1.55
1.53
1.48
1.46
1.38
1.35
1.31
1.28
1.26
1.25
HO
O
O
O
8.5
8.0
7.5
7.0
6.5
6.0
5.5
5.0
4.5
4.0
3.5
3.0
2.5
2.0
1.5
1.0
0.5
ppm
0.90
1.03
0.99
0.91
1.00
1.38
2.46
0.96
1.95
4.42
0.96
2.91
0.97
1.01
6.85
5.81

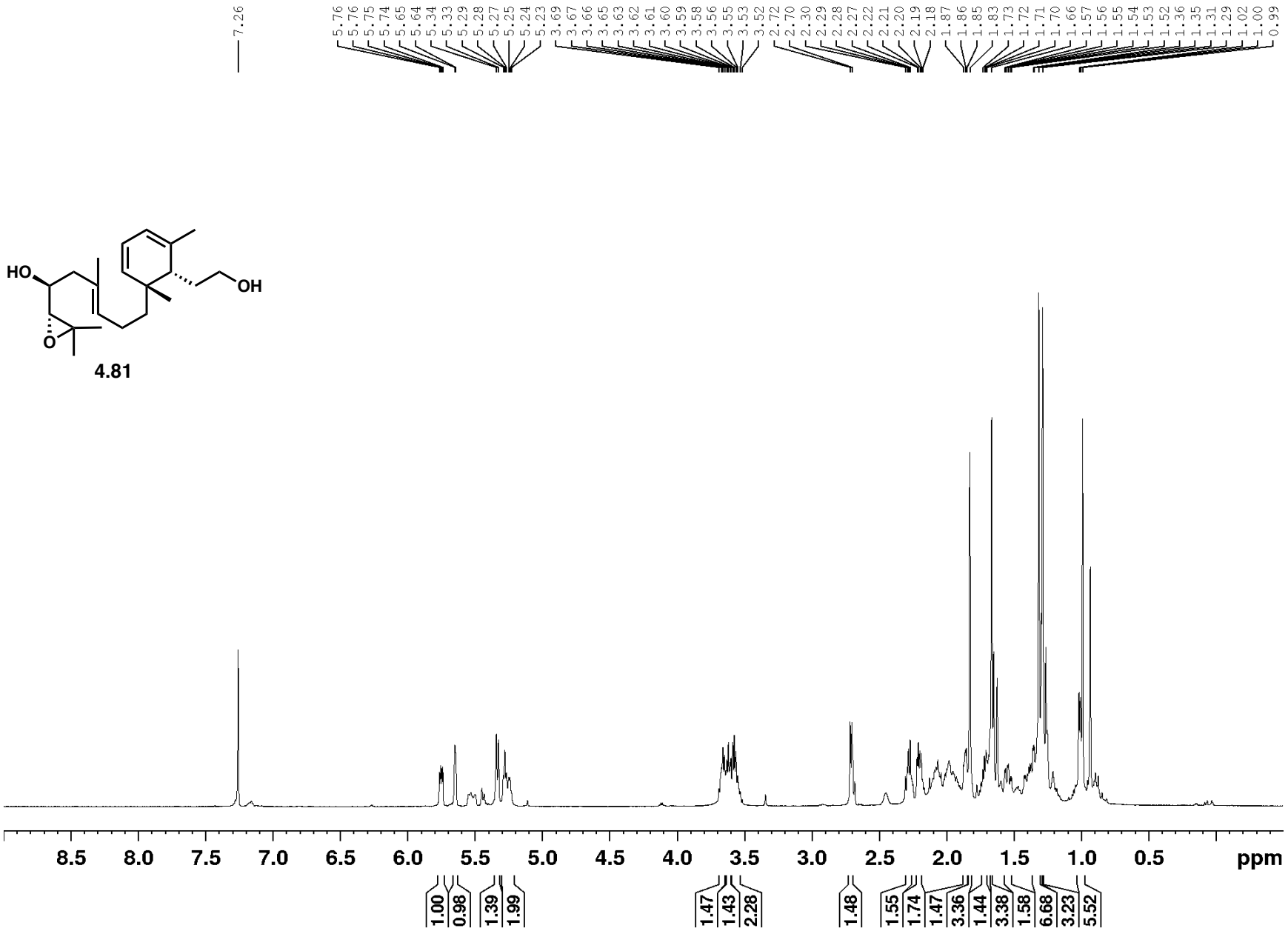
4.79

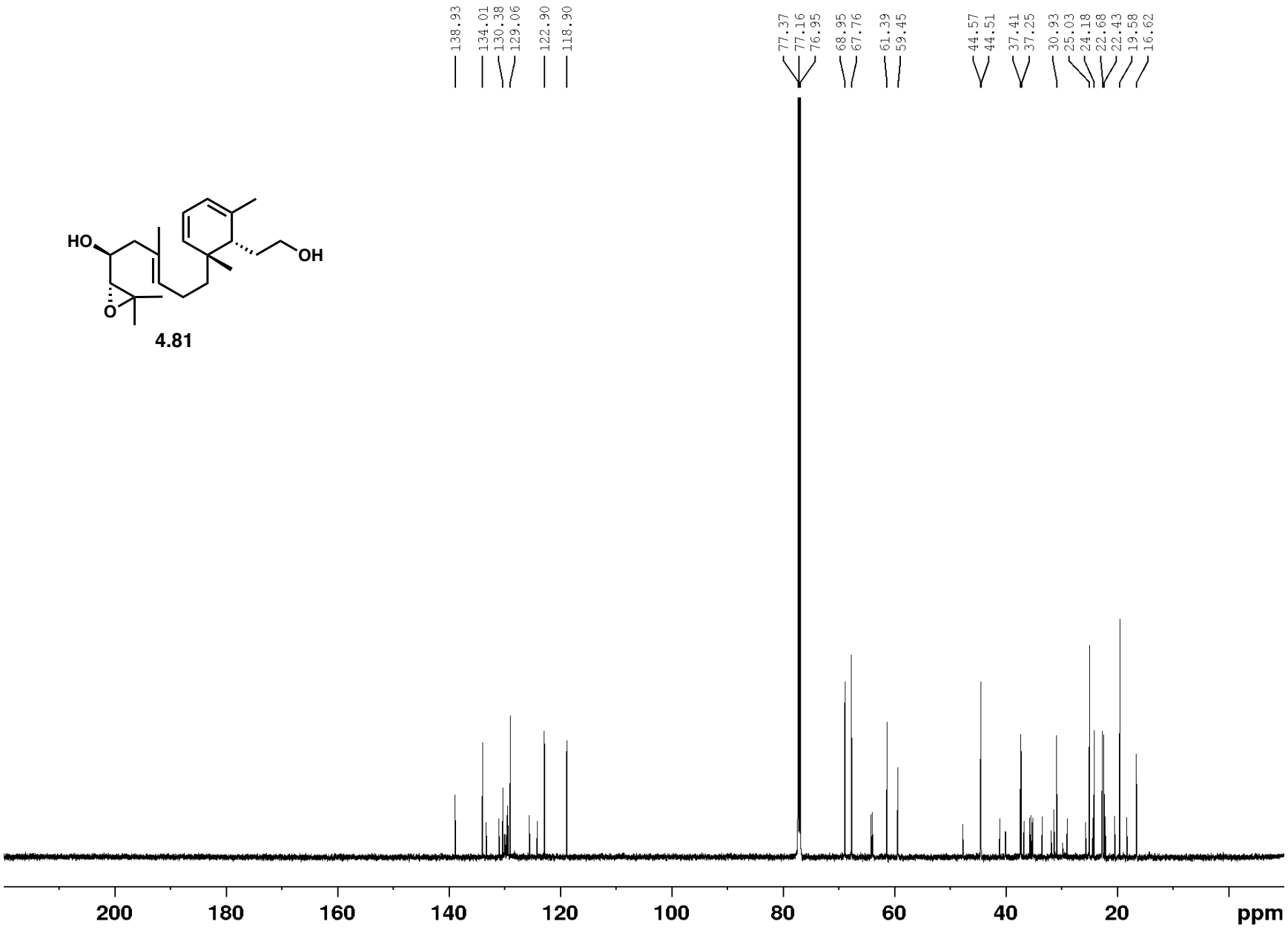

212.68
130.71
128.63
77.37
77.16
76.95
68.95
67.70
59.34
57.54
44.47
43.68
43.35
40.70
36.84
36.53
25.02
22.05
21.80
21.38
19.55
16.60
13.32
HO
O
O
O
200
180
160
140
120
100
80
60
40
20
ppm

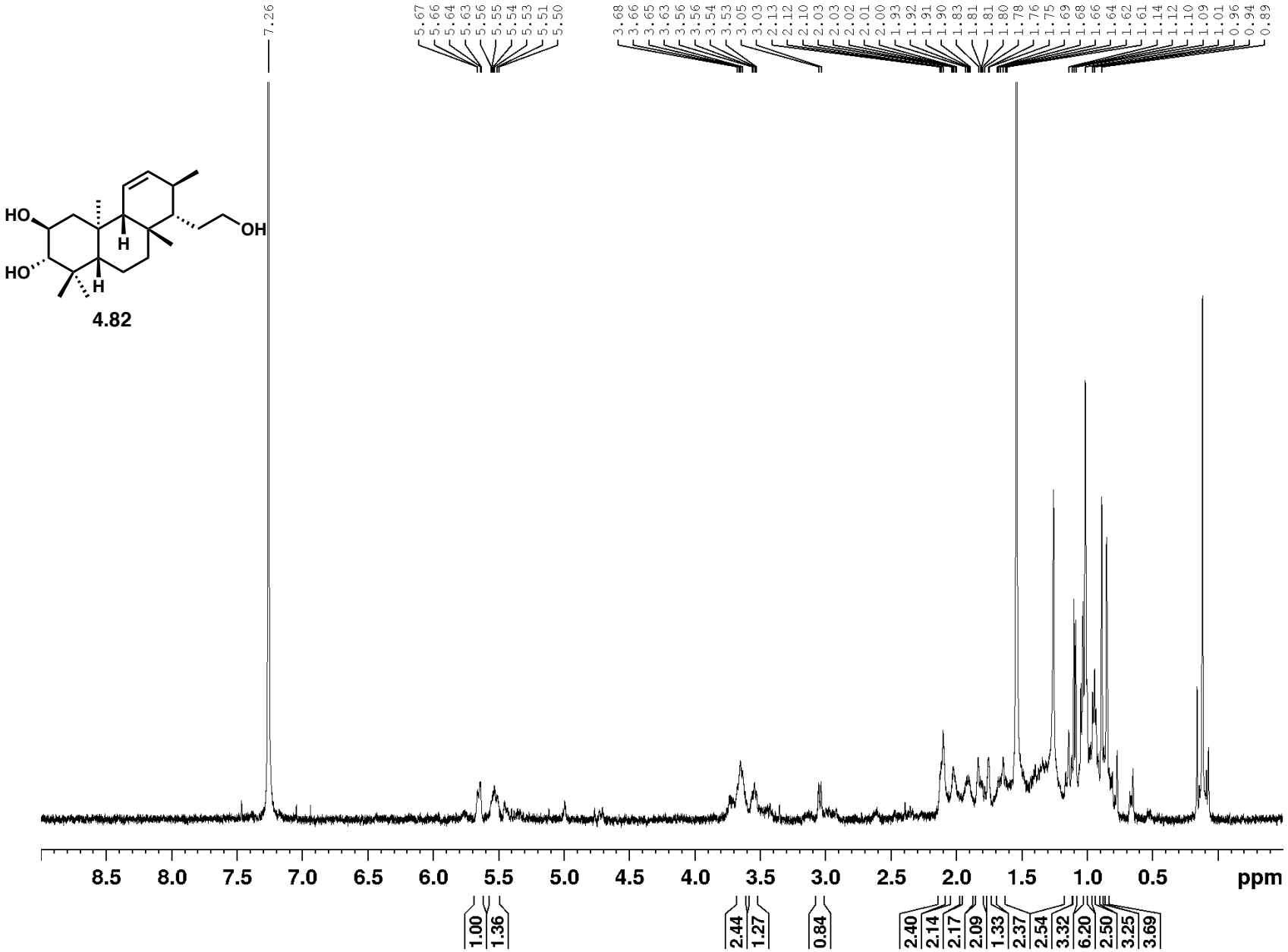
4.79

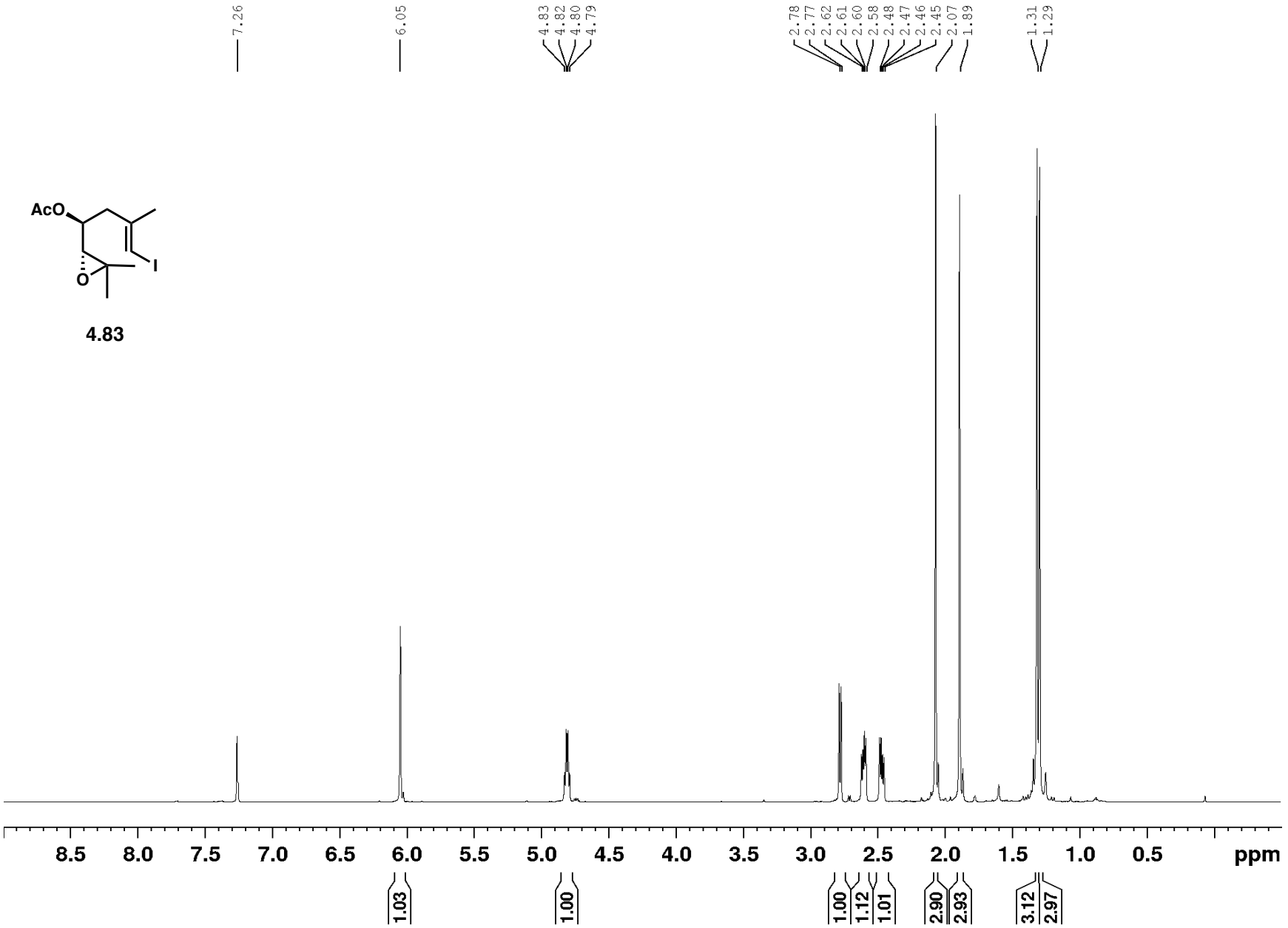

3.80 3.79 3.79 3.62 3.61 3.60 3.59 3.42 3.41 3.40 3.40 3.39 3.39 3.38 3.37 3.35 3.32 3.31 3.31 3.31 3.30 3.08 3.06 2.92 2.91 2.90 2.89 2.89 2.88 2.87 2.60 2.59 2.58 2.57 2.53 2.53 2.50 2.50 2.19 2.19 2.11 2.10 2.03 2.01 1.99 1.98 1.97 1.75 1.73 1.62 1.62 1.60 1.60 1.53 1.53 1.52 1.51 1.51 1.35 1.35 1.33 1.33 1.33 1.31 1.30 1.29 1.29 1.18 1.13 1.13 1.13 1.12 1.05 1.05 1.04 1.03 1.02 1.02 1.01 0.87 0.67
HO
HO
O
O
4.80
7.5 7.0 6.5 6.0 5.5 5.0 4.5 4.0 3.5 3.0 2.5 2.0 1.5 1.0 0.5 0.0 ppm

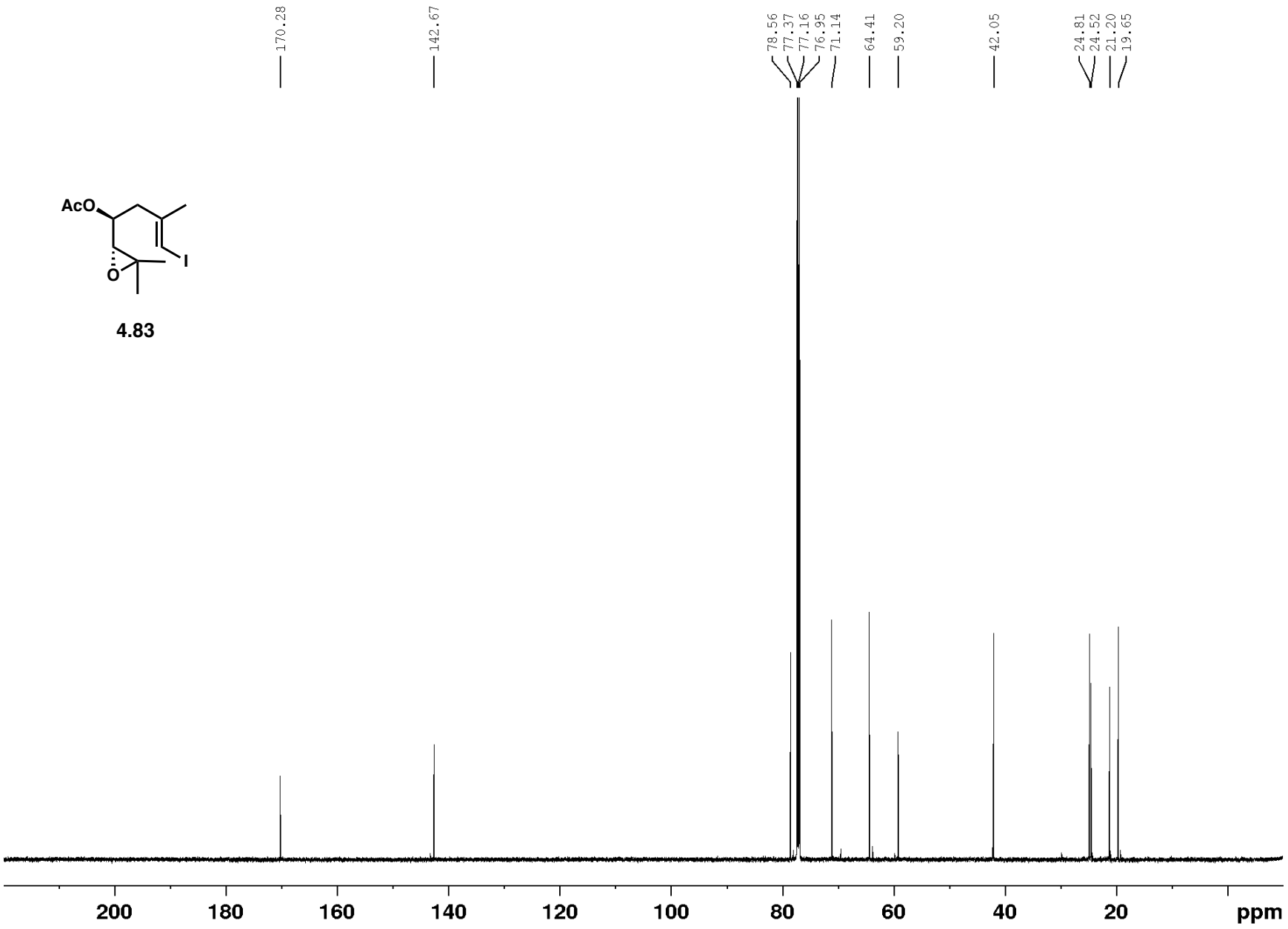

215.49
146.68
109.80
83.15
78.97
73.10
58.48
54.09
49.42
49.28
49.14
49.00
48.86
48.71
48.57
44.97
44.78
44.41
42.29
41.66
37.97
37.54
26.24
22.53
21.92
19.37
15.08
13.46
HO
HO
O
O
4.80
200
180
160
140
120
100
80
60
40
20
ppm


7.26
5.76
5.76
5.75
5.74
5.65
5.64
5.34
5.33
5.29
5.28
5.27
5.25
5.24
5.23
3.69
3.67
3.66
3.65
3.63
3.62
3.61
3.60
3.59
3.58
3.56
3.55
3.53
3.52
2.72
2.70
2.30
2.29
2.28
2.27
2.22
2.21
2.20
2.19
2.18
1.87
1.86
1.85
1.83
1.73
1.72
1.71
1.70
1.66
1.57
1.56
1.55
1.54
1.53
1.52
1.36
1.35
1.31
1.29
1.02
1.00
0.99
HO
OH
O
4.81
8.5
8.0
7.5
7.0
6.5
6.0
5.5
5.0
4.5
4.0
3.5
3.0
2.5
2.0
1.5
1.0
0.5
ppm
1.00
0.98
1.39
1.99
1.47
1.43
2.28
1.48
1.55
1.74
1.47
3.36
1.44
3.38
1.58
6.68
3.23
5.52

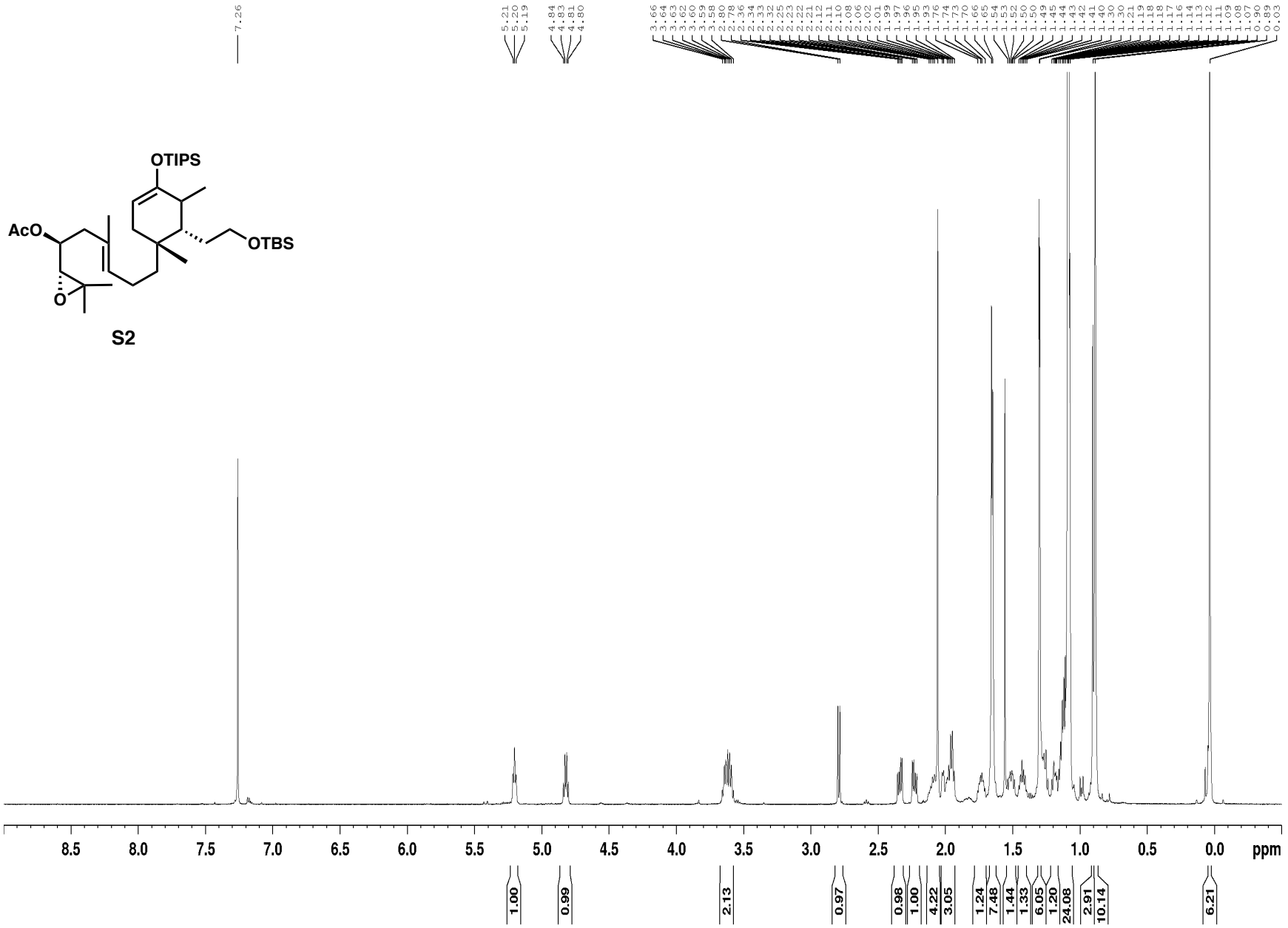

138.93
134.01
130.38
129.06
122.90
118.90
77.37
77.16
76.95
68.95
67.76
61.39
59.45
44.57
44.51
37.41
37.25
30.93
25.03
24.18
22.68
22.43
19.58
16.62
HO
OH
O
4.81
200
180
160
140
120
100
80
60
40
20
ppm

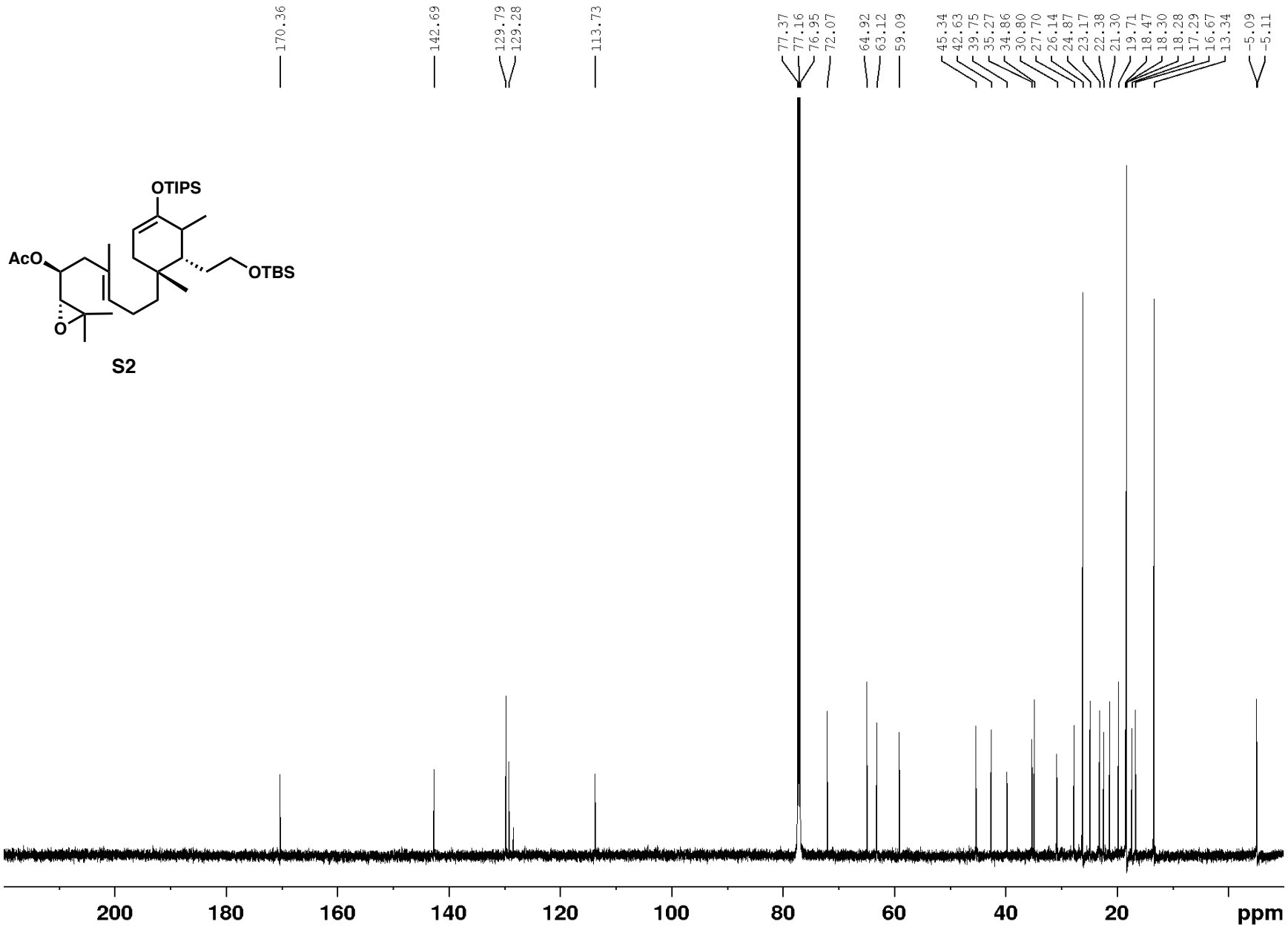

HO
HO
H
H
OH
4.82
7.26
5.67
5.66
5.64
5.63
5.56
5.55
5.54
5.53
5.51
5.50
3.68
3.66
3.65
3.63
3.56
3.56
3.54
3.53
3.05
3.03
2.13
2.12
2.10
2.03
2.03
2.02
2.01
2.00
1.93
1.92
1.91
1.90
1.83
1.81
1.81
1.80
1.78
1.76
1.75
1.69
1.68
1.66
1.64
1.62
1.61
1.14
1.12
1.10
1.09
1.01
0.96
0.94
0.89
8.5
8.0
7.5
7.0
6.5
6.0
5.5
5.0
4.5
4.0
3.5
3.0
2.5
2.0
1.5
1.0
0.5
ppm
1.00
1.36
2.44
1.27
0.84
2.40
2.14
2.17
2.09
1.33
2.37
2.54
3.32
6.20
2.50
3.25
3.69

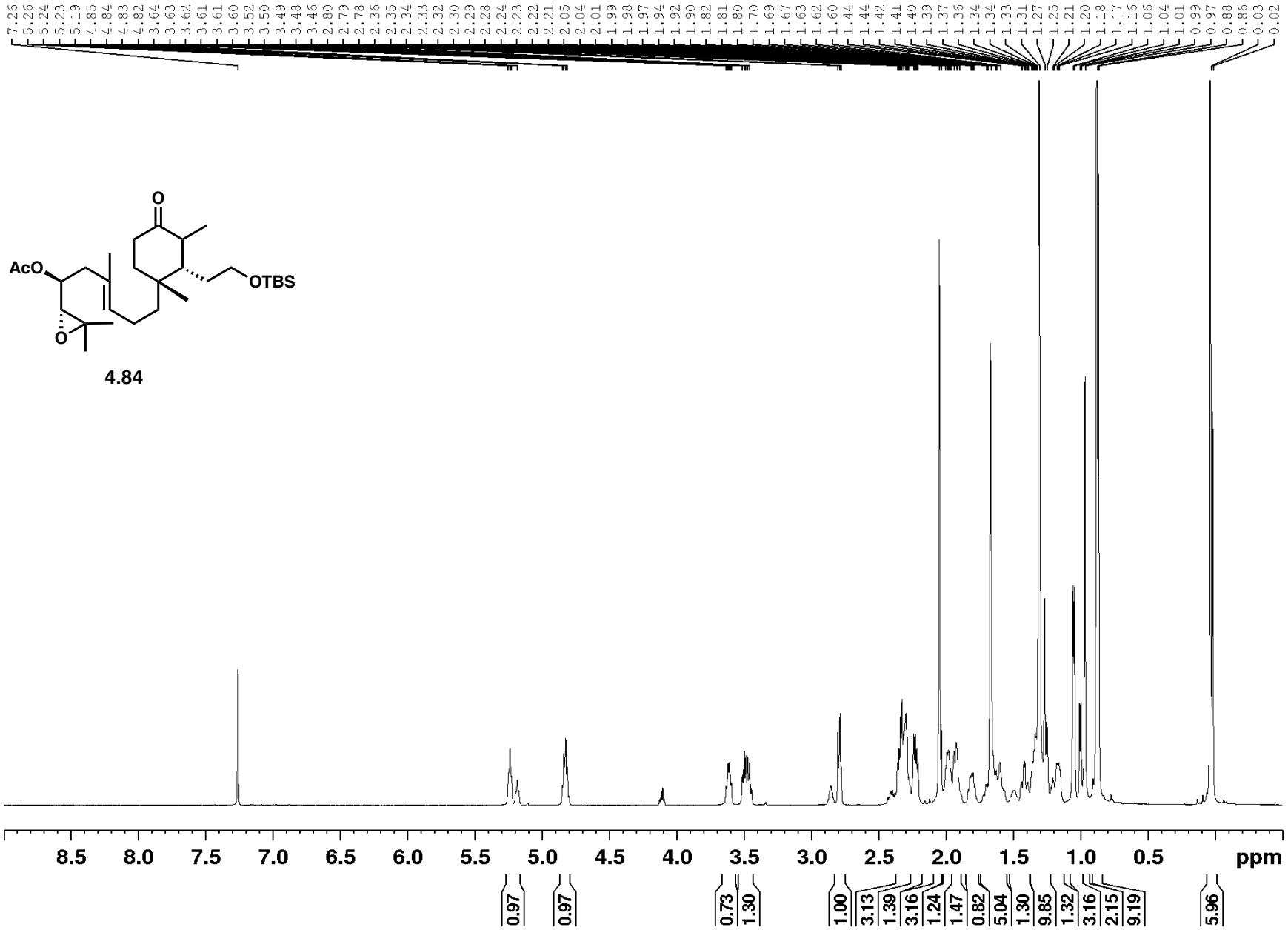

7.26
6.05
4.83
4.82
4.80
4.79
2.78
2.77
2.62
2.61
2.60
2.58
2.48
2.47
2.46
2.45
2.07
1.89
1.31
1.29
AcO
I
O
4.83
8.5
8.0
7.5
7.0
6.5
6.0
5.5
5.0
4.5
4.0
3.5
3.0
2.5
2.0
1.5
1.0
0.5
ppm
1.03
1.00
1.00
1.12
1.01
2.90
2.93
3.12
2.97

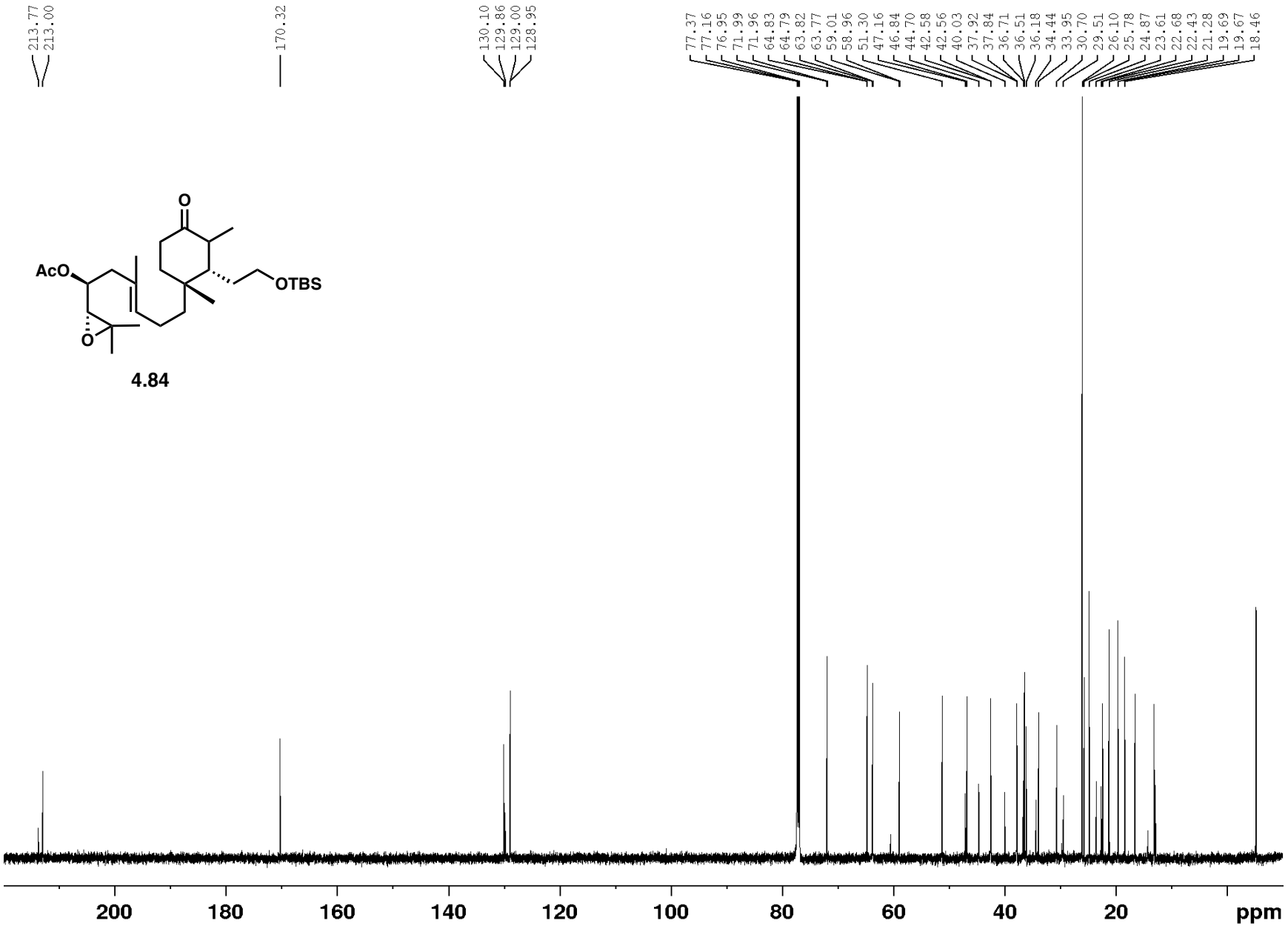

170.28
142.67
78.56
77.37
77.16
76.95
71.14
64.41
59.20
42.05
24.81
24.52
21.20
19.65
AcO
O
I
200
180
160
140
120
100
80
60
40
20
ppm

4.83

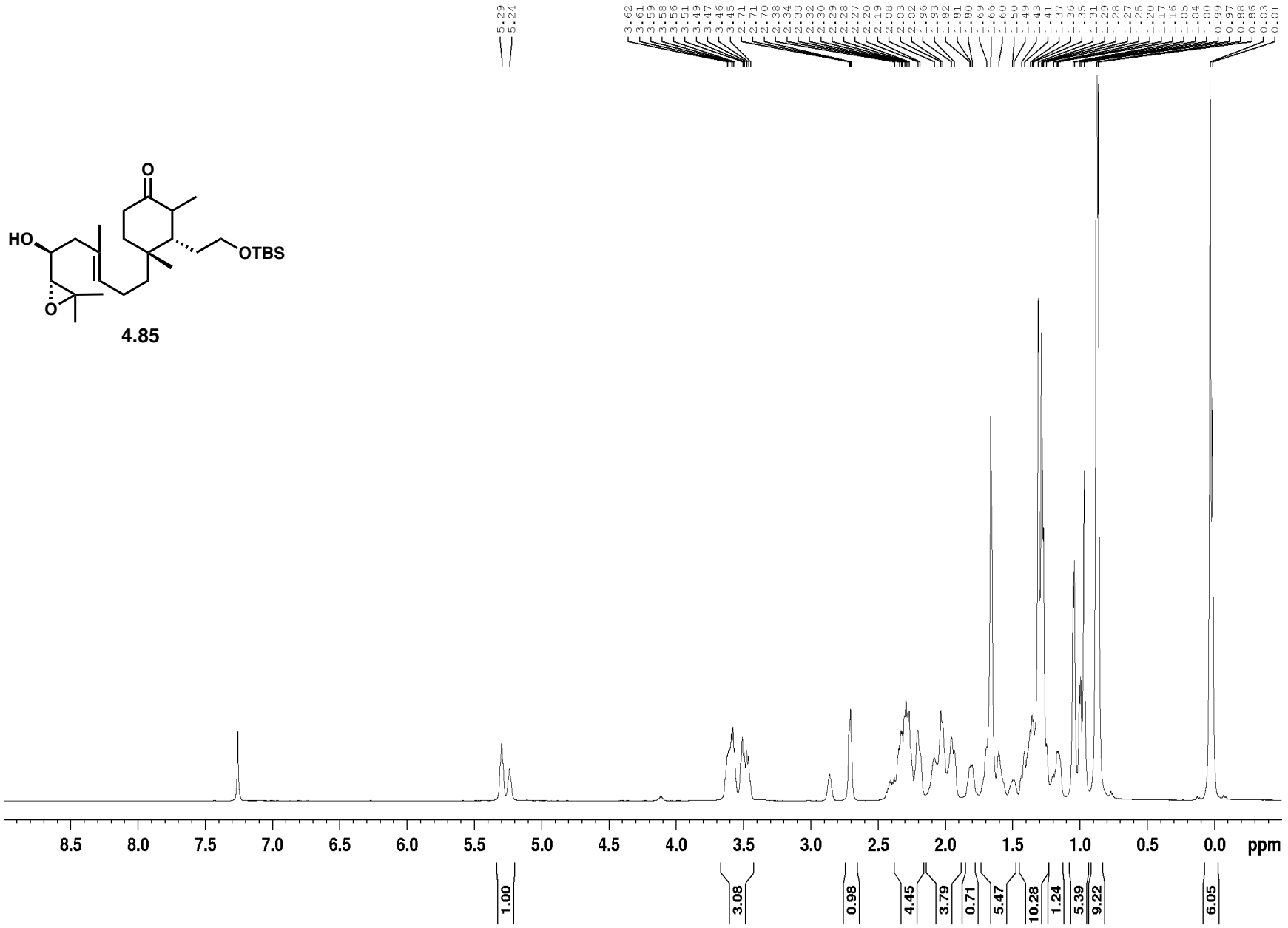

OTIPS
AcO
OTBS
O
S2
7.26
5.21
5.20
5.19
4.84
4.83
4.81
4.80
3.66
3.64
3.63
3.62
3.60
3.59
3.58
2.80
2.38
2.36
2.34
2.33
2.32
2.25
2.23
2.22
2.21
2.12
2.11
2.10
2.08
2.06
2.02
2.01
1.99
1.97
1.96
1.95
1.93
1.76
1.74
1.73
1.70
1.66
1.65
1.54
1.53
1.52
1.50
1.50
1.49
1.45
1.44
1.43
1.42
1.41
1.40
1.30
1.30
1.21
1.19
1.18
1.18
1.17
1.16
1.14
1.13
1.12
1.11
1.09
1.08
1.07
0.90
0.89
0.03
8.5
8.0
7.5
7.0
6.5
6.0
5.5
5.0
4.5
4.0
3.5
3.0
2.5
2.0
1.5
1.0
0.5
0.0
ppm
1.00
0.99
2.13
0.97
0.98
1.00
4.22
3.05
1.24
7.48
1.44
1.33
6.05
1.20
24.08
2.91
10.14
6.21

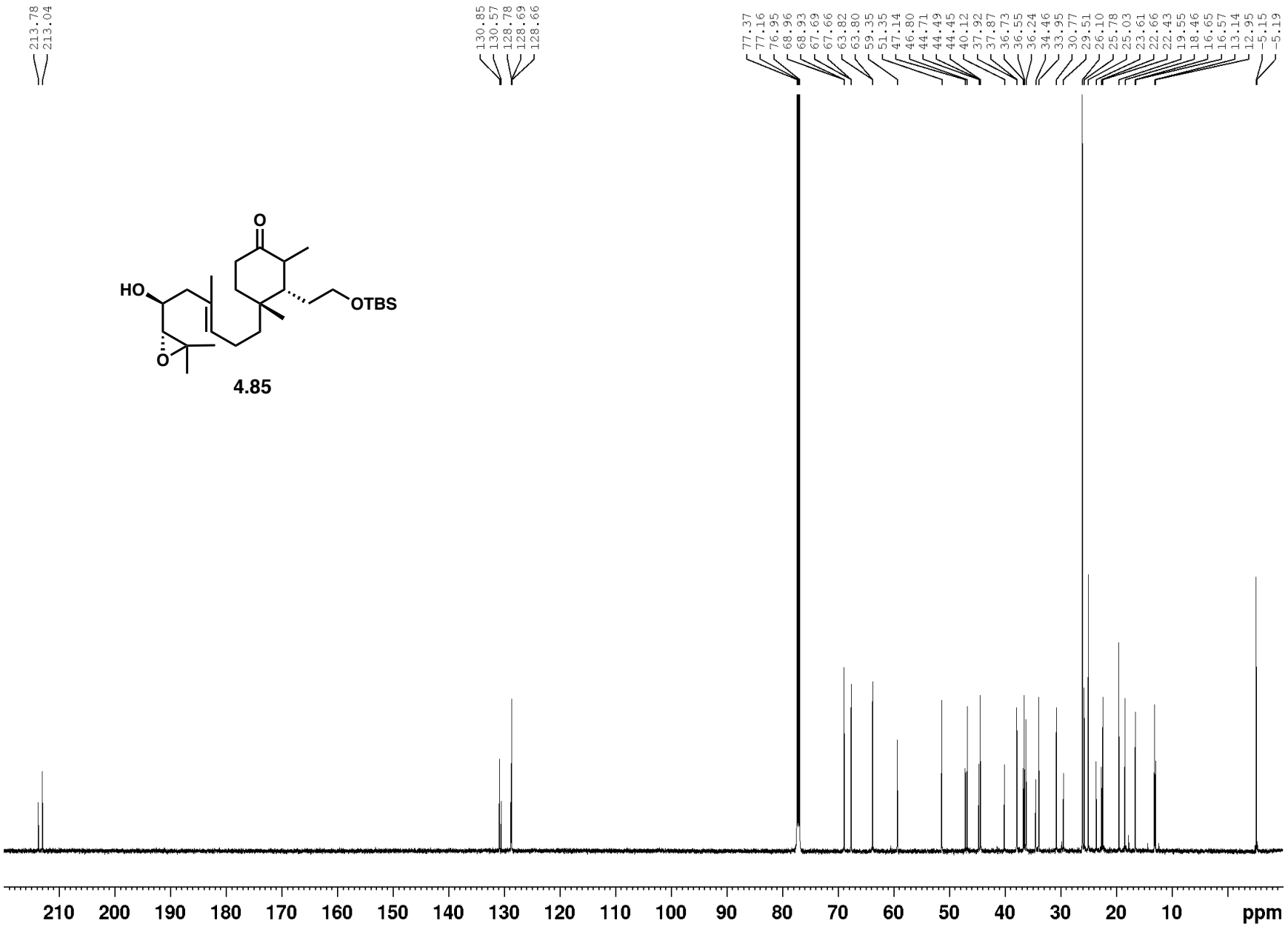

170.36
142.69
129.79
129.28
113.73
77.37
77.16
76.95
72.07
64.92
63.12
59.09
45.34
42.63
39.75
35.27
34.86
30.80
27.70
26.14
24.87
23.17
22.38
21.30
19.71
18.47
18.30
18.28
17.29
16.67
13.34
-5.09
-5.11
OTIPS
AcO
OTBS
O
S2
200
180
160
140
120
100
80
60
40
20
ppm

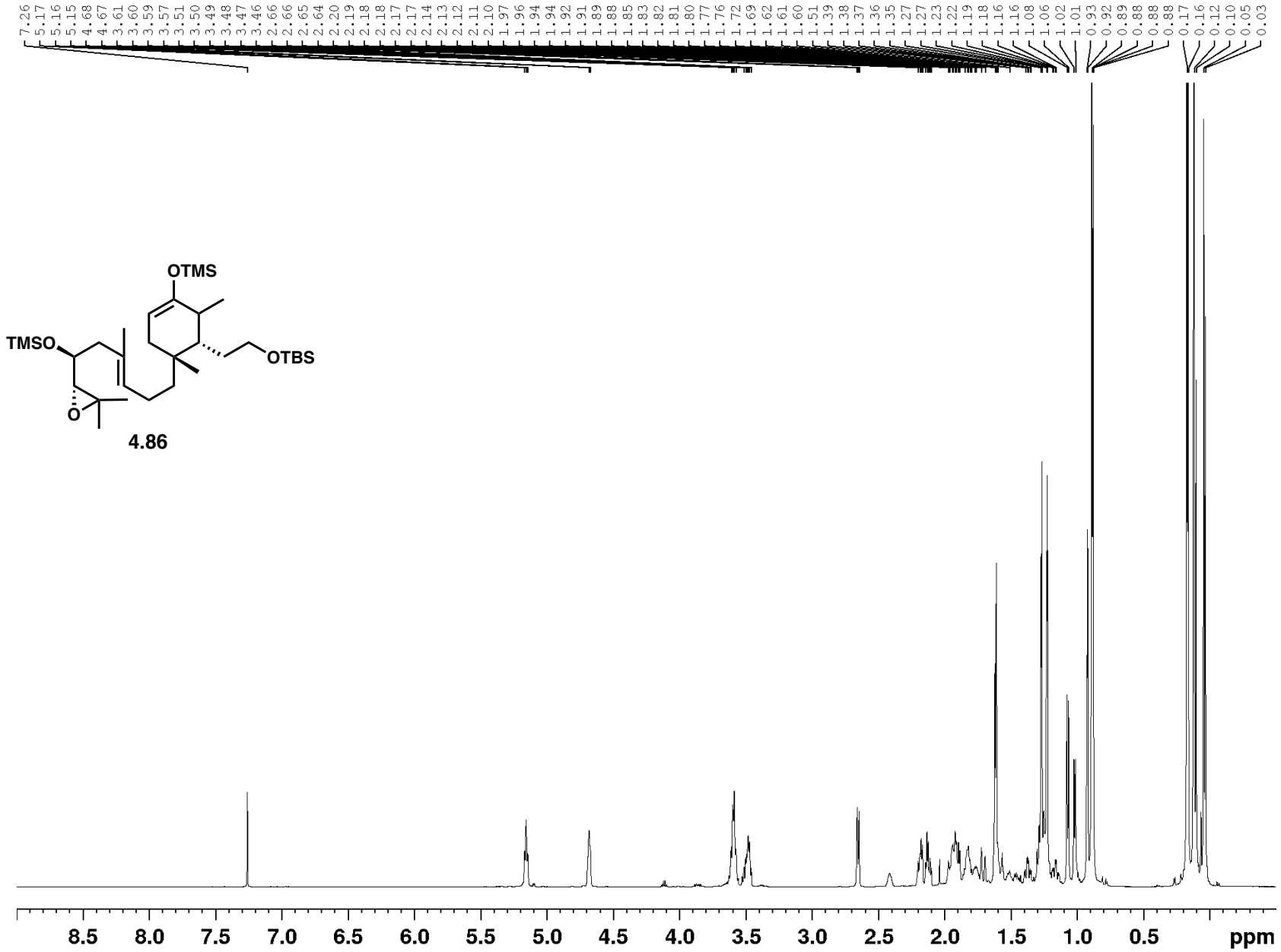

7.26
5.26
5.24
5.23
5.19
4.85
4.84
4.83
4.82
3.64
3.63
3.62
3.61
3.61
3.60
3.52
3.50
3.49
3.48
3.46
2.80
2.79
2.78
2.36
2.35
2.34
2.33
2.32
2.30
2.29
2.28
2.24
2.23
2.22
2.21
2.05
2.04
2.01
1.99
1.98
1.97
1.94
1.92
1.90
1.82
1.81
1.80
1.70
1.69
1.67
1.63
1.62
1.60
1.44
1.44
1.42
1.41
1.40
1.39
1.37
1.36
1.34
1.34
1.33
1.31
1.27
1.25
1.21
1.20
1.18
1.17
1.16
1.06
1.04
1.01
0.99
0.97
0.88
0.86
0.03
0.02
AcO
O
OTBS
O
4.84
8.5
8.0
7.5
7.0
6.5
6.0
5.5
5.0
4.5
4.0
3.5
3.0
2.5
2.0
1.5
1.0
0.5
ppm
0.97
0.97
0.73
1.30
1.00
3.13
1.39
3.16
1.24
1.47
0.82
5.04
1.30
9.85
1.32
3.16
2.15
9.19
5.96

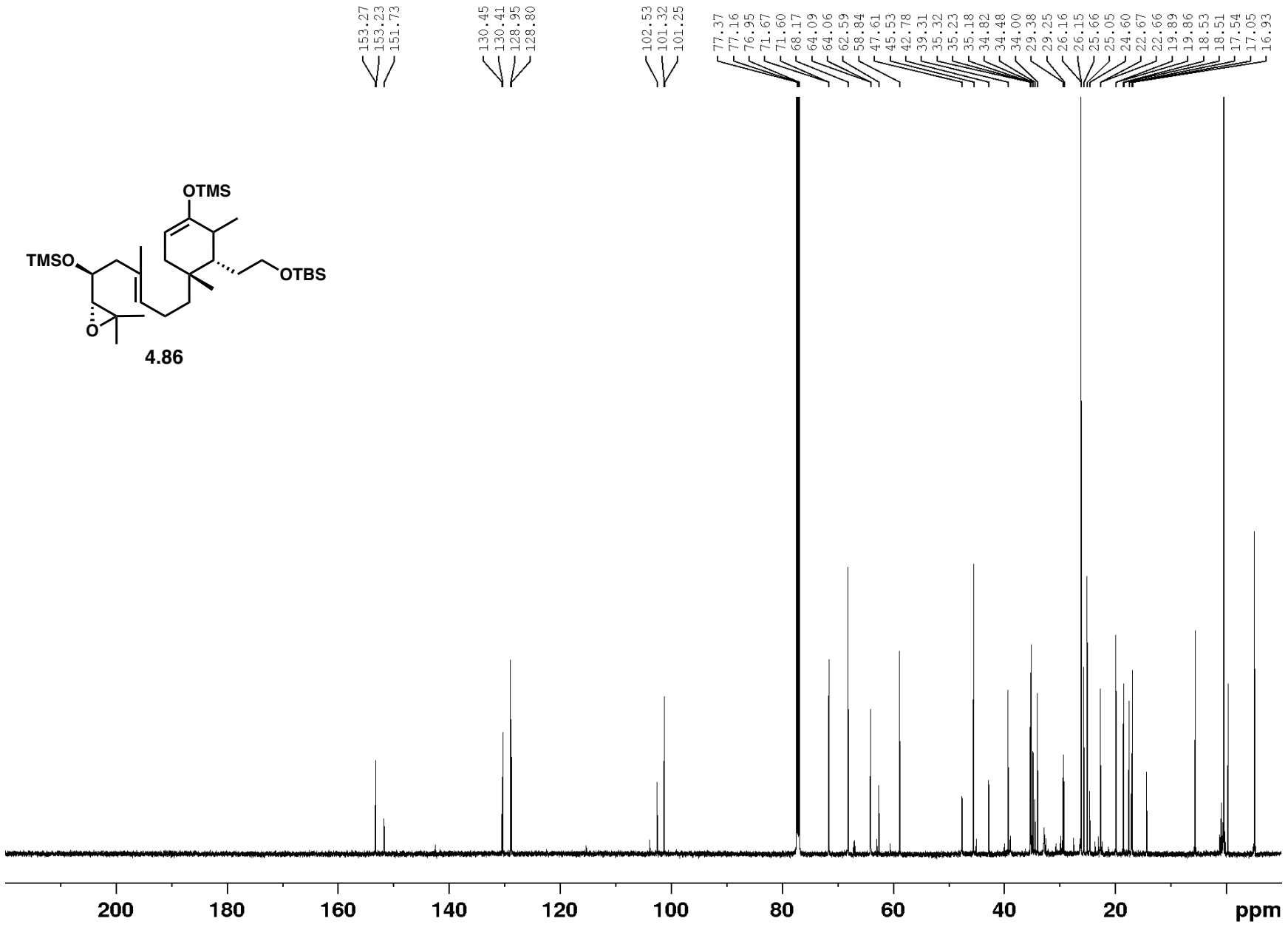

213.77
213.00
170.32
130.10
129.86
129.00
128.95
77.37
77.16
76.95
71.99
71.96
64.83
64.79
63.82
63.77
59.01
58.96
51.30
47.16
46.84
44.70
42.58
42.56
40.03
37.92
37.84
36.71
36.51
36.18
34.44
33.95
30.70
29.51
26.10
25.78
24.87
23.61
22.68
22.43
21.28
19.69
19.67
18.46
AcO
OTBS
O
O
200
180
160
140
120
100
80
60
40
20
ppm

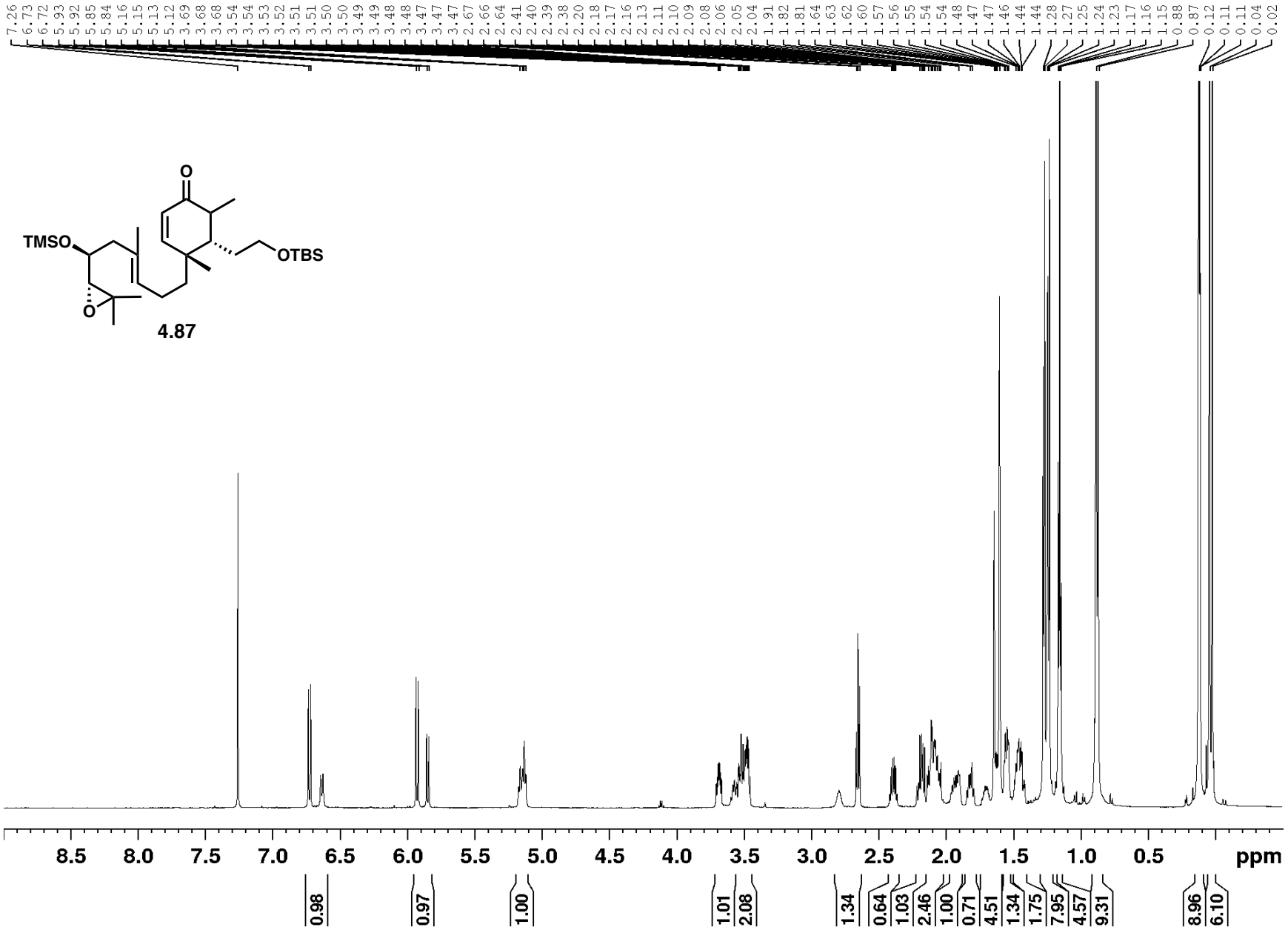
4.84

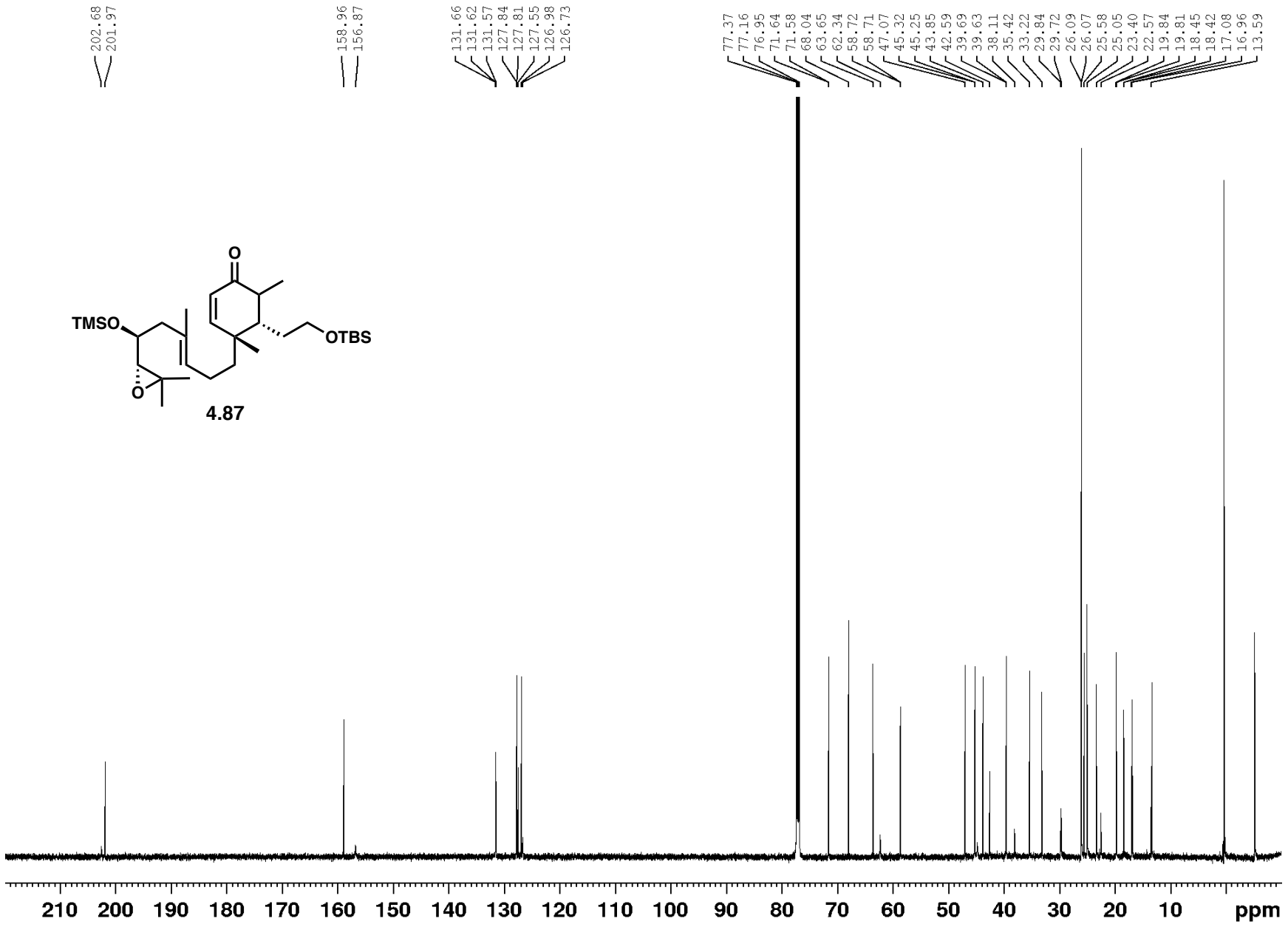

HO
O
O
OTBS
4.85
5.29
5.24
3.62
3.61
3.59
3.58
3.56
3.51
3.49
3.47
3.46
3.45
2.71
2.71
2.70
2.38
2.34
2.33
2.32
2.30
2.29
2.28
2.27
2.20
2.19
2.08
2.03
2.02
1.96
1.93
1.82
1.81
1.80
1.69
1.66
1.60
1.50
1.49
1.43
1.41
1.37
1.36
1.35
1.31
1.29
1.28
1.27
1.25
1.20
1.17
1.16
1.05
1.04
1.00
0.99
0.97
0.88
0.86
0.03
0.01
8.5
8.0
7.5
7.0
6.5
6.0
5.5
5.0
4.5
4.0
3.5
3.0
2.5
2.0
1.5
1.0
0.5
0.0
ppm
1.00
3.08
0.98
4.45
3.79
0.71
5.47
10.28
1.24
5.39
9.22
6.05

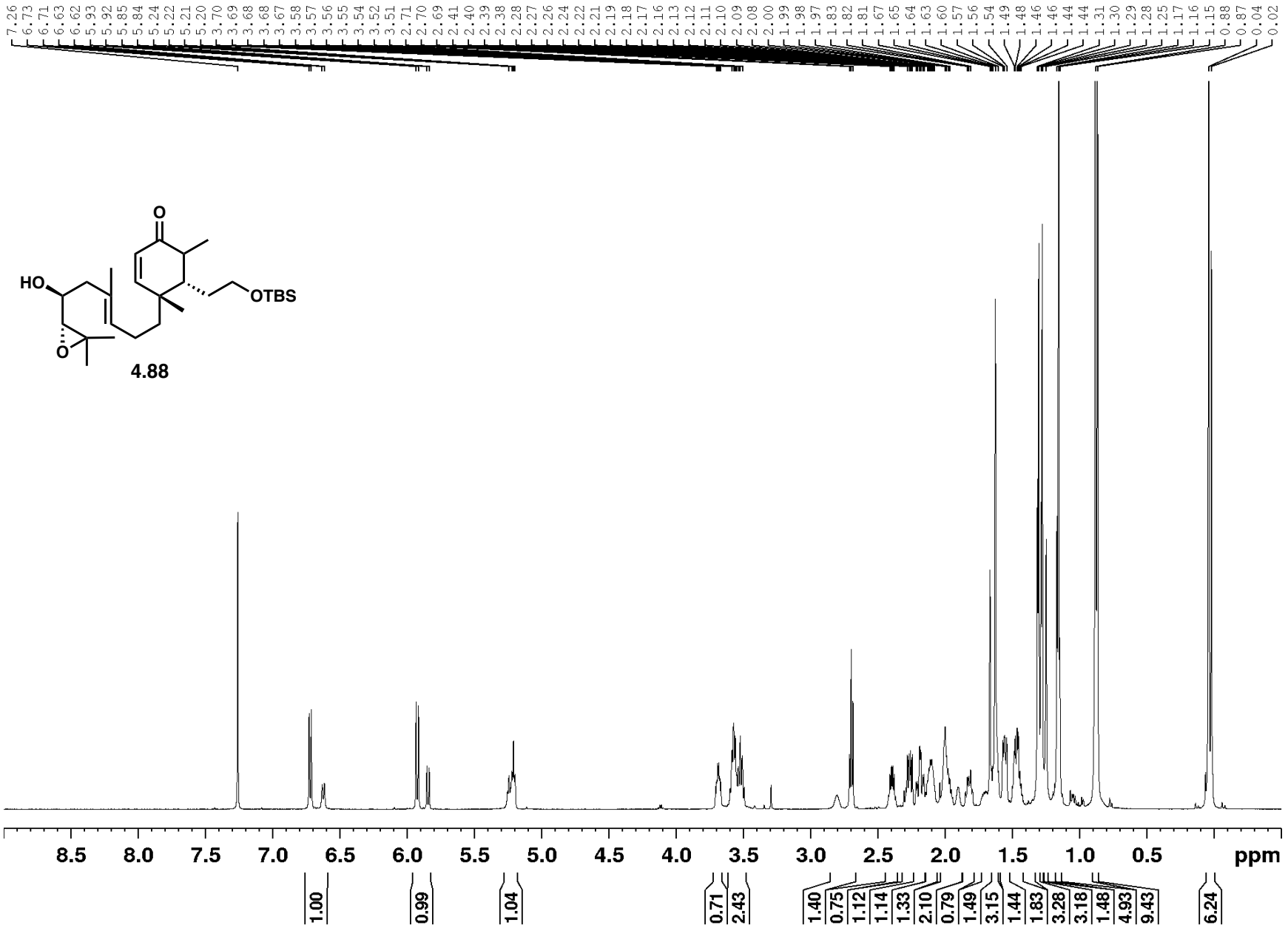

213.78
213.04
130.85
130.57
128.78
128.69
128.66
77.37
77.16
76.95
68.96
68.93
67.69
67.66
63.82
63.80
59.35
51.35
47.14
46.80
44.71
44.49
44.45
40.12
37.92
37.87
36.73
36.55
36.24
34.46
33.95
30.77
29.51
26.10
25.78
25.03
23.61
22.66
22.43
19.55
18.46
16.65
16.57
13.14
12.95
-5.15
-5.19
HO
O
O
OTBS
4.85
210
200
190
180
170
160
150
140
130
120
110
100
90
80
70
60
50
40
30
20
10
ppm

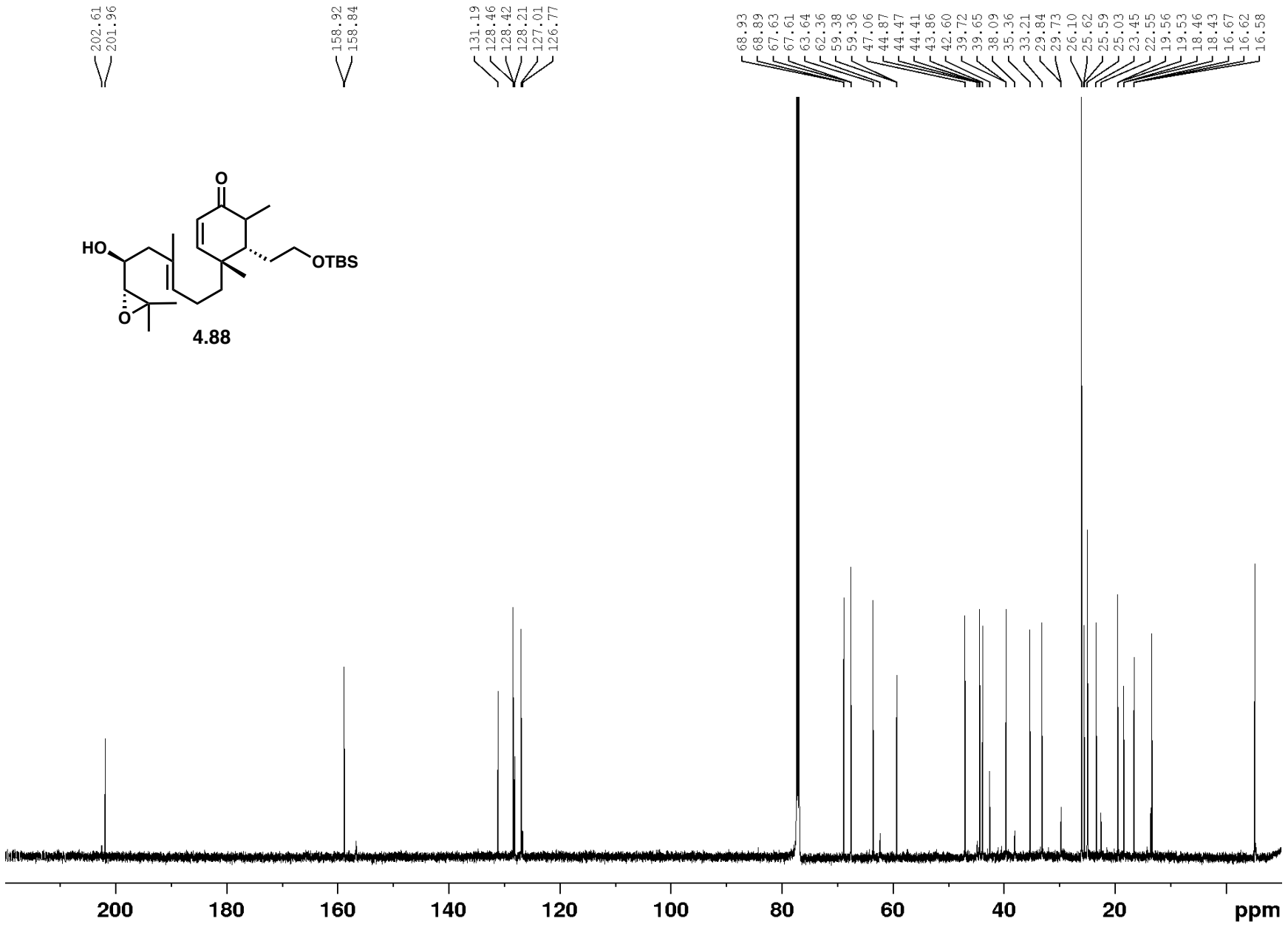

7.26
5.17
5.16
5.15
4.68
4.67
3.61
3.60
3.59
3.57
3.51
3.50
3.49
3.48
3.47
3.46
2.66
2.65
2.64
2.20
2.19
2.18
2.18
2.17
2.17
2.14
2.13
2.12
2.11
2.10
1.97
1.96
1.94
1.94
1.92
1.91
1.89
1.88
1.85
1.83
1.82
1.81
1.80
1.77
1.76
1.72
1.69
1.62
1.61
1.60
1.51
1.39
1.38
1.37
1.36
1.35
1.27
1.27
1.23
1.22
1.19
1.18
1.16
1.08
1.06
1.02
1.01
0.93
0.92
0.89
0.88
0.88
0.88
0.17
0.16
0.12
0.10
0.05
0.03
OTMS
TMSO
OTBS
O
4.86
8.5
8.0
7.5
7.0
6.5
6.0
5.5
5.0
4.5
4.0
3.5
3.0
2.5
2.0
1.5
1.0
0.5
ppm

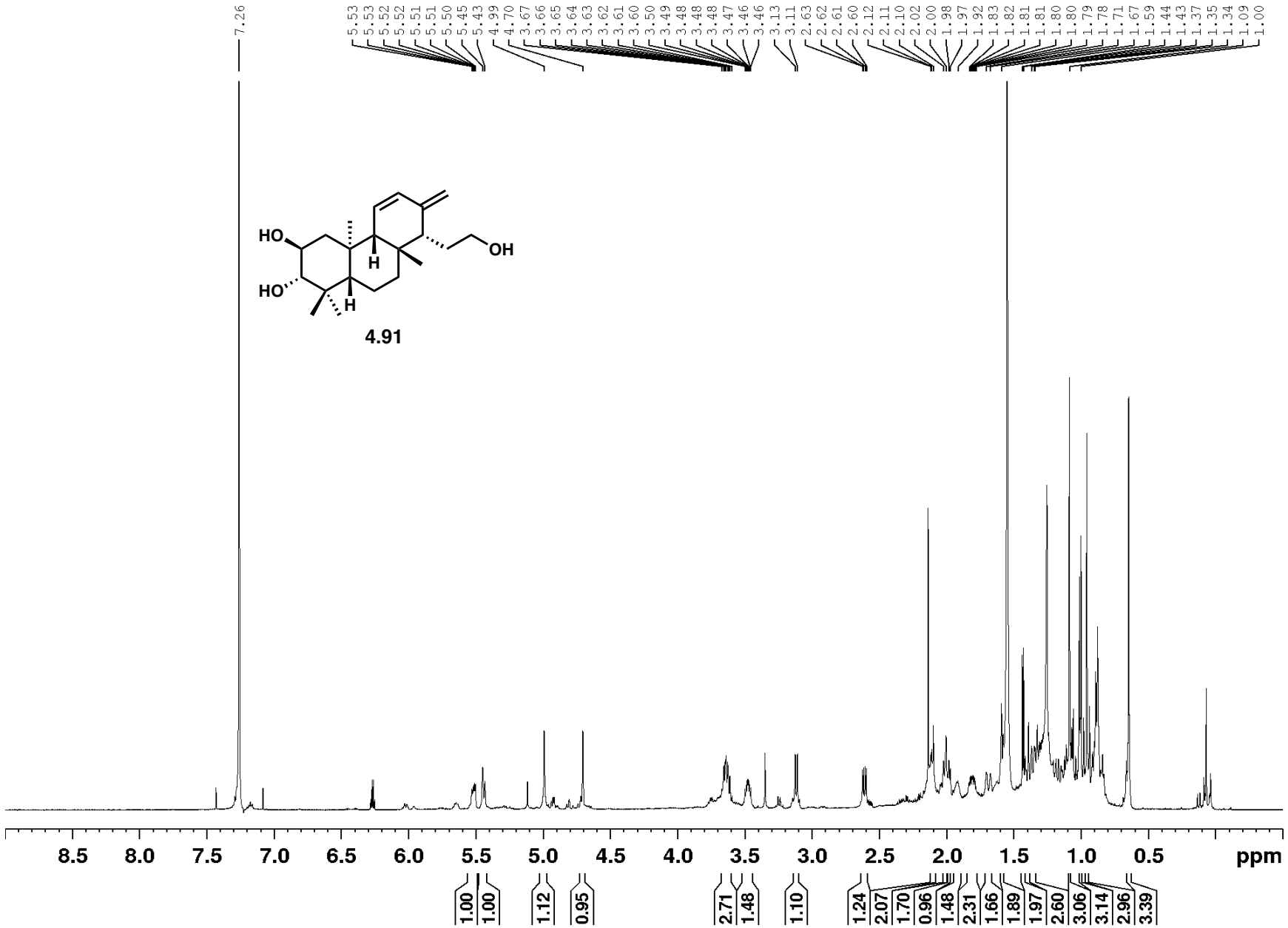

153.27
153.23
151.73
130.45
130.41
128.95
128.80
102.53
101.32
101.25
77.37
77.16
76.95
71.67
71.60
68.17
64.09
64.06
62.59
58.84
47.61
45.53
42.78
39.31
35.32
35.23
35.18
34.82
34.48
34.00
29.38
29.25
26.16
26.15
25.66
25.05
24.60
22.67
22.66
19.89
19.86
18.53
18.51
17.54
17.05
16.93
OTMS
TMSO
OTBS
O
4.86
200
180
160
140
120
100
80
60
40
20
ppm


7.26 6.73 6.72 5.93 5.92 5.85 5.84 5.16 5.15 5.13 5.12 3.69 3.68 3.68 3.54 3.54 3.53 3.52 3.51 3.51 3.50 3.50 3.49 3.49 3.48 3.48 3.47 3.47 3.47 2.67 2.66 2.64 2.41 2.40 2.39 2.38 2.20 2.18 2.17 2.16 2.13 2.11 2.10 2.09 2.08 2.06 2.05 2.04 1.91 1.82 1.81 1.64 1.63 1.62 1.60 1.57 1.56 1.55 1.54 1.54 1.48 1.47 1.47 1.46 1.44 1.44 1.28 1.27 1.25 1.24 1.23 1.17 1.16 1.15 0.88 0.87 0.12 0.11 0.11 0.04 0.02
TMSO
OTBS
O
O
4.87
8.5 8.0 7.5 7.0 6.5 6.0 5.5 5.0 4.5 4.0 3.5 3.0 2.5 2.0 1.5 1.0 0.5 ppm
0.98 0.97 1.00 1.01 2.08 1.34 0.64 1.03 2.46 1.00 0.71 4.51 1.34 1.75 7.95 4.57 9.31 8.96 6.10


202.68
201.97
158.96
156.87
131.66
131.62
131.57
127.84
127.81
127.55
126.98
126.73
77.37
77.16
76.95
71.64
71.58
68.04
63.65
62.34
58.72
58.71
47.07
45.32
45.25
43.85
42.59
39.69
39.63
38.11
35.42
33.22
29.84
29.72
26.09
26.07
25.58
25.05
23.40
22.57
19.84
19.81
18.45
18.42
17.08
16.96
13.59
O
TMSO
OTBS
O
4.87
210
200
190
180
170
160
150
140
130
120
110
100
90
80
70
60
50
40
30
20
10
ppm


7.26
6.73
6.71
6.63
6.62
5.93
5.92
5.85
5.84
5.24
5.22
5.21
5.20
3.70
3.69
3.68
3.68
3.67
3.58
3.57
3.56
3.55
3.54
3.52
3.51
2.71
2.70
2.69
2.41
2.40
2.39
2.38
2.28
2.27
2.26
2.24
2.22
2.21
2.19
2.18
2.17
2.16
2.13
2.12
2.11
2.10
2.09
2.08
2.00
1.99
1.98
1.97
1.83
1.82
1.81
1.67
1.65
1.64
1.63
1.60
1.57
1.56
1.54
1.49
1.48
1.46
1.46
1.44
1.44
1.31
1.30
1.29
1.28
1.25
1.17
1.16
1.15
0.88
0.87
0.04
0.02
HO
O
OTBS
O
4.88
8.5
8.0
7.5
7.0
6.5
6.0
5.5
5.0
4.5
4.0
3.5
3.0
2.5
2.0
1.5
1.0
0.5
ppm
1.00
0.99
1.04
0.71
2.43
1.40
0.75
1.12
1.14
1.33
2.10
0.79
1.49
3.15
1.44
1.83
3.28
3.18
1.48
4.93
9.43
6.24


202.61
201.96
158.92
158.84
131.19
128.46
128.42
128.21
127.01
126.77
68.93
68.89
67.63
67.61
63.64
62.36
59.38
59.36
47.06
44.87
44.47
44.41
43.86
42.60
39.72
39.65
38.09
35.36
33.21
29.84
29.73
26.10
25.62
25.59
25.03
23.45
22.55
19.56
19.53
18.46
18.43
16.67
16.62
16.58
HO
O
OTBS
O
4.88
200
180
160
140
120
100
80
60
40
20
ppm


7.26
5.53
5.53
5.52
5.52
5.51
5.51
5.50
5.45
5.43
4.99
4.70
3.67
3.66
3.65
3.64
3.63
3.62
3.61
3.60
3.50
3.49
3.48
3.48
3.48
3.47
3.46
3.46
3.13
3.11
2.63
2.62
2.61
2.60
2.12
2.11
2.10
2.02
2.00
1.98
1.97
1.92
1.83
1.82
1.81
1.81
1.80
1.80
1.79
1.78
1.71
1.67
1.59
1.44
1.43
1.37
1.35
1.34
1.09
1.00
HO
HO
H
H
OH
4.91
8.5
8.0
7.5
7.0
6.5
6.0
5.5
5.0
4.5
4.0
3.5
3.0
2.5
2.0
1.5
1.0
0.5
ppm
1.00
1.00
1.12
0.95
2.71
1.48
1.10
1.24
2.07
1.70
0.96
1.48
2.31
1.66
1.89
1.97
2.60
3.06
3.14
2.96
3.39